IAEA-TECDOC-872

Progress in design, research and development and testing of safety systems for advanced water cooled reactors

Proceedings of a Technical Committee meeting held in Piacenza, Italy, 16–19 May 1995

INTERNATIONAL ATOMIC ENERGY AGENCY IAEA

The originating Section of this publication in the IAEA was:

Nuclear Power Technology Development Section
International Atomic Energy Agency
Wagramerstrasse 5
P.O. Box 100
A-1400 Vienna, Austria

PROGRESS IN DESIGN, RESEARCH AND DEVELOPMENT
AND TESTING OF SAFETY SYSTEMS FOR ADVANCED
WATER COOLED REACTORS
IAEA, VIENNA, 1996
IAEA-TECDOC-872
ISSN 1011–4289

Printed by the IAEA in Austria
April 1996

FOREWORD

The Technical Committee Meeting on Progress in Design, Research & Development and Testing of Safety Systems for Advanced Water Cooled Reactors was held at the ENEL Training Centre, Piacenza, Italy from 16 to 19 May 1995. The meeting was convened by the International Atomic Energy Agency (IAEA) within the frame of activities of the IAEA's International Working Group on Advanced Technologies for Water Cooled Reactors and was a joint activity of the IAEA's Nuclear Power Technology Development Section of the Division of Nuclear Power and the Engineering Safety Section of the Division of Nuclear Safety. IAEA activities in advanced technology for water cooled reactors serve to provide an international source of objective information on advanced water cooled reactors and to provide an international forum for discussion and review of technical information on research and development activities.

Heat removal systems for evolutionary designs (advanced reactor designs which achieve improvements over existing designs through small to moderate modifications) require at most only engineering and confirmatory testing. Heat removal systems for developmental designs (advanced reactor designs which range from moderate modification of existing designs to entirely new design concepts) in general require more extensive testing and demonstration to verify component and system performance. Key issues are scaling effects for simulated plant configurations, component and system reliabilities, aging, and interactions among different systems. Furthermore, a key activity is validation of the computer codes used for design and safety analyses of advanced water cooled reactors by comparison with experimental test data.

The meeting covered the following topics:

- Developments in design of safety-related heat removal components and systems for advanced water cooled reactors.
- Status of test programmes on heat removal components and systems of new designs.
- Range of validity and extrapolation of test results for the qualification of design/licensing computer models and codes for advanced water cooled reactors.
- Future needs and trends in testing of safety systems for advanced water cooled reactors.

Tests of heat removal safety systems have been conducted by various groups supporting the design, testing and certification of advanced water cooled reactors. The Technical Committee concluded that the reported test results generally confirm the predicted performance features of the advanced designs.

EDITORIAL NOTE

PLEASE BE AWARE THAT
ALL OF THE MISSING PAGES IN THIS DOCUMENT
WERE ORIGINALLY BLANK

CONTENTS

RESULTS OF SAFETY-RELATED COMPONENTS/SYSTEMS TESTS (Session IV) (Part 1)

RESULTS OF SAFETY RELATED COMPONENTS/SYSTEMS TESTS (Session IV) (Part 2)

COMPUTER MODEL DEVELOPMENT AND VALIDATION (Session V)

SUMMARY OF THE TECHNICAL COMMITTEE MEETING

The progress in design, R&D and testing of safety systems for advanced water cooled reactors was addressed in a TCM convened in Piacenza, Italy in May 1995 and organized in cooperation with ENEL SpA (ENEL), Ente per le Nuove Technologie, l'Energia e l'ambiente (ENEA) and Società Informazioni Esperienze Termoidrauliche (SIET). The meeting was attended by 71 participants from 12 countries and two international organizations as follows: Canada (1), Finland (2), France (8), Germany (5), India (1), Italy (37), Republic of Korea (3), Russia (5), Spain (1), Switzerland (1), United Kingdom (2), United States of America (12), World Association of Nuclear Plant Operators, WANO (1), IAEA (2). Thirty four papers were presented and future needs and trends in the field were discussed.

Background

A main focus of reactor design and development efforts in the industrialized countries is on large size water cooled reactor units, with power outputs well above 1000 MW(e), typically aiming at achieving certain improvements over existing designs. The alterations and modifications to a specific design are generally kept as small as possible taking maximum advantage of successful proven design features and components while taking into account feedback of experience from licensing, construction, commissioning and operation of the water cooled reactor plants currently in operation. The design improvements span a wide range but still enhanced safety, increased reliability, more user-friendly systems, and better economics represent rather common denominators for the new designs.

New designs - designs that have not yet been built or operated - are generally called advanced designs. If they do not deviate too much from their predecessors, they are designated evolutionary designs; the designers have retained many proven features of today's plant design, and the evolutionary plant designs therefore require at most engineering, and, possibly, confirmatory testing of some components and systems prior to commercial deployment.

Some evolutionary large size LWR designs are currently under construction, while others are in varying phases of design and regulatory review. The N4 model, a 1400 MW(e) PWR, which is under construction in France, derives directly from the standardized P4 series of 1300 MW(e). The British Sizewell-B, a 1250 MW(e) PWR, is another example of an evolutionary design - an evolution of the WPSS design of Westinghouse. Other examples of large advanced, evolutionary designs are the Westinghouse-Mitsubishi advanced pressurized water reactor APWR (a 1350 MW(e) PWR), the ABB Combustion Engineering System 80+ (a 1300 MW(e) PWR), the Russian V-392 (a 1000 MW(e) PWR of the WWER-1000 type), and the General Electric-Hitachi-Toshiba Advanced Boiling Water Reactor ABWR (a 1350 MW(e) BWR). In this context, it may be noted that two ABWR units are under construction in Japan - at Kashiwazaki Kariwa (No. 6/7) - with grid connections scheduled for 1996 and 1997, and that construction of two APWR units is planned at the Tsuruga site in Japan.

Framatome and Siemens have established a joint company, Nuclear Power International, which is developing a new advanced large PWR of 1500 MW(e) (gross) with enhanced safety features, and they intend to have it reviewed jointly by the French and

German safety authorities. This procedure will provide strong motivation for the practical harmonization of the safety requirements of two major countries, which could later be enlarged to a broader basis. Siemens is also, together with German utilities, engaged in the development of an advanced BWR design, the SWR-1000, which will incorporate a number of passive safety features, for initiation of safety functions, for residual heat removal and for containment heat removal. In Sweden, ABB Atom, with involvement of the utility Teollisuuden Voima Oy (TVO) of Finland, is developing the BWR 90 as an upgraded version of the BWRs of the BWR 75 version operating in both countries.

Smaller advanced LWRs are also being developed in a number of countries, in most cases with a great emphasis on utilization of passive safety systems and inherent safety features. Two typical examples in this context are the Advanced Passive PWR (AP-600) of Westinghouse and the Simplified BWR of General Electric - the mid-size passive units (units in the 600 MW(e) range) of the US ALWR programme. The development of both these designs has been governed by a key guideline: new features should need no more than engineering and confirmatory testing before commercial deployment; they must not lead to a requirement of building and operating a prototype or demonstration plant.

An important programme in the development of advanced light water reactors was initiated in 1984 by the Electric Power Research Institute (EPRI), an organization of US utilities, with financial support from the US Department of Energy, and participation of US nuclear plant designers. Several foreign utilities have also participated in, and contributed funding to, the programme. As a part of the programme, to guide the ALWR design and development, utility requirements were established for large BWRs and PWRs having power ratings of about 1200 MW(e), and for mid-sized BWRs and PWRs having power ratings of about 600 MW(e). In an important related development, a major step forward in licensing of future plants was reached with the ratification of the Energy Policy Act of 1992. The new licensing process allows nuclear plant designers to submit their designs to the US Nuclear Regulatory Commission (US NRC) for design certification. Once a design is certified, the standardized units will be commercially offered, and a utility can order a plant confident that generic design and safety issues have been resolved. The licensing process will allow the power company to request a combined license to build and operate a new plant, and as long as the plant is built to pre-approved specifications, the company can start up the plant when construction is complete, assuming no new safety issues have emerged. In 1994, the two large evolutionary plants which have resulted from the U S programme, ABB-Combustion Engineering's System 80+ and General Electric's (GE's) ABWR, received Final Design Approval, the last step before design certification, from the US NRC. The two smaller 600 MW(e) plants, Westinghouse's AP-600 and GE's Simplified BWR, are expected to receive Final Design Approval in 1996 and 1997 respectively. Today, completion of design certification for advanced light water reactors to assure availability of ALWRs by the end of the decade is a top priority of the Advanced Reactor Programme of the US Department of Energy.

An adaption of the AP600 and SBWR designs in order to meet the European Utility Requirements and to meet the need for a higher net electric power is under progress in Europe. The two programmes are named respectively EPP and ESBWR.

In the Russian Federation, design work on the evolutionary V-392, an upgraded version of the WWER-1000, has been started, and another design version is being developed in cooperation with Finland. The Russian Federation is also developing an evolutionary

WWER-640 (V-407) design along lines similar to those for the AP-600, as well as a more innovative, integral design, the VPBER-600.

In Japan, the Ministry of International Trade and Industry is conducting an 'LWR Technology Sophistication' programme focusing on development of future LWRs and including requirements and design objectives. The Japan Atomic Energy Research Institute (JAERI) has been investigating conceptual designs of advanced water cooled reactors with emphasis on passive systems. These are the JAERI Passive Safety Reactor (JPSR) and the System-Integrated PWR (SPWR). Development programmes for a Japanese simplified BWR (JSBWR) and for a Japanese simplified PWR (JSPWR) are in progress jointly involving vendors and utilities.

In Canada, two advanced CANDU heavy water moderated and cooled reactor designs, the CANDU-3 and CANDU-9, are under development. The CANDU-3 is a 450 MW(e) design which features modular design and construction methods. The 1050 MW(e) CANDU-9 design is based on the proven Darlington and Bruce B large size plants with improvements derived from the design activities of CANDU-3.

In India, development efforts are conducted on an advanced pressure tube AHWR which incorporates passive features including containment cooling and decay heat removal by natural convection.

National and international development efforts presented at TCM:

While current NPPs resulted largely from national design and development activities, advanced LWR programmes are strongly based on international cooperation.

The basic design of the European Pressurized Water Reactor (EPR), an evolutionary PWR with innovative features, has been started in February 1995 under the leadership of Nuclear Power International. The EPR derives from experience gained by EdF, German utilities, Framatome and Siemens during design, licensing construction and operation of current nuclear power plants. The main functions and functional requirements of the EPR safety injection system have been established. The safety injection system design consists of four independent trains, each including an accumulator, a medium head safety injection pump and a low head safety injection pump, both of which inject water from a refuelling water storage tank located in the containment into the reactor coolant system. Analyses have shown that the safety injection system ensures mitigation of all LOCA scenarios and all relevant non-LOCA scenarios.

In the Republic of Korea an effort has been under way since 1992 to develop an advanced design termed the Korean Next Generation Reactor (KNGR) which is an evolutionary large 4000 MW(th) PWR design. The goal is to complete a detailed standard design by the year 2000. KEPCO is the lead organization. KAERI is responsible for NSSS design, with Korean Power Engineering Company (KOPEC) and Korea Heavy Industry Company (KHIC) responsible for architectural engineering and component design respectively. In the first phase, completed in 1994, the design requirements and the design concept were established. In the current phase, the basic design is being developed by KEPCO and the Korean nuclear industry, with financial support by the government, in parallel with licensing review. Phase 3, scheduled to begin in 1997, will establish the detailed standard design.

Many confirmatory component and systems performance tests for mid-sized ALWRs have been completed while others will be completed in 1996. These mid-sized advanced plant designs are the result of an intensive international effort including more than a dozen countries which participate in the US ALWR programme. A key characteristic of these plants is the use of simple passive systems to respond to design basis events. Many tests of these systems are required to satisfy regulatory review leading to design certification. Development of the ALWR designs is supported by both private (including international utility organizations) and government funding, and the programme is carried out in parallel with the design certification review by the US NRC. Test programmes to confirm the predicted safety performance of the Westinghouse AP-600 and the General Electric SBWR are close to completion. Especially in the past two years extensive progress both in testing programmes and in the regulatory review has been made in the US ALWR programme toward the objective of deploying an advanced plant in the United States.

A technical tour to the SIET facilities in Piacenza provided a detailed understanding of the SPES-2 full height, full pressure integral heat transport systems test for the AP-600, and the testing at SIET's PANTHERS test loop of full-scale prototype condensers for both the Passive Containment Cooling System (PCCS) and the Isolation Condenser System (ICS) of the GE-SBWR. A detailed description of the PANDA facility at the Paul Scherrer Institute (PSI) for SBWR heat removal systems tests was provided. These programmes at SIET and PSI support the current design certification activities for AP-600 and the GE-SBWR.

Siemens is developing the SWR-1000, characterized by its use of passive safety systems with the aim of achieving system simplification and reduced capital costs. Passive systems which are incorporated into SWR-1000 include emergency condensers, containment cooling condensers, passive pressure pulse transmitters and gravity driven core flooding lines. The testing programme for the emergency condenser is currently underway in a cooperative effort at the Juelich Research Center (KFA) Germany with funding from the federal government, German utilities, Siemens and KFA.

The French Atomic Energy Commission (CEA) is conducting evaluations of innovative safety systems for ALWRs, in terms of efficiency and reliability in selected accidental sequences. Three kinds of systems are currently evaluated: direct depressurization system designed to control PWR primary pressure to prevent high pressure core melt sequences, passive residual heat removal systems and steam injector systems. A systematic integrated approach for identifying safety objectives and establishing criteria for selecting design options is being developed.

Passive containment cooling by natural convection of air has been proposed for ALWRs. To investigate the phenomena involved, separate effects tests are conducted at KfK, Germany in the PASCO facility. Further, a scaled test facility to investigate integral containment coolability limits by air under coupled convection and thermal radiation conditions is being designed.

Spain's advanced technology for water cooled reactors includes activities to improve performance of its existing reactors, participation in the design of the four ALWRs under development in the US, and involvement in European activities to define user requirements for advanced reactors. The effort is aimed at maintaining and increasing Spain's domestic nuclear industrial capabilities and providing a technical base for choices among electricity supply options in Spain's next National Energy Plan.

In Russia, experimental and analytical efforts are on-going to develop a new type of passive heat removal system which is applicable to all nuclear plants with steam cycle power conversion, i.e. PWRs and BWRs including advanced designs, and for heat removal from the containment as well. The activities are conducted at the Research Institute for Nuclear Power Plant Operation, RINPO (Moscow, Russia) in cooperation with other research centers in Russia, Ukraine and USA. The concept is based on passive heat removal by steam condensation (PAHRSEC) in an ejector-condenser recirculating the condensate to the nuclear heat source. Tests of a full size PAHRSEC system proposed for retrofit for the currently operating WWER-440 plants at Novovoronezh are underway. Probabilistic safety analyses carried out in the USA have indicated that retrofit of the San Onofre nuclear plant with a PAHRSEC system would reduce the probability of core damage from internal events by a factor of about 2.

In Switzerland, in 1991 at the Paul Scherrer Institute, the ALPHA project was initiated with the goal of performing experimental and analytical investigations of long-term decay heat removal from the containment of next generation passive ALWRs. The project is conducted in collaboration with a large international team including design and research organizations from USA, the Netherlands, Japan, Mexico and Italy. Because results of certain tests will be submitted to the USNRC as part of the GE-SBWR design certification process, they are conducted under formal quality assurance procedures. Three major facilities have been constructed including a large scale integral facility (PANDA) to simulate the GE-SBWR containment, a facility (LINX-2) for investigating condensation and buoyancy driven mixing in the containment, and a facility to investigate aerosol transport in the containment. Testing at these facilities is underway.

In Italy, an extensive development programme for safety components and systems for advanced water cooled reactors is conducted in a framework of international cooperation. A comprehensive test and analysis effort to support design confirmation of the safety features of the Westinghouse AP-600 is being completed at the test facilities VAPORE (ENEA Casaccia - full-scale Automatic Depressurization System tests) and SPES-2 (SIET Piacenza - integral systems tests) and involves cooperation between Westinghouse, Ansaldo, ENEA, ENEL and University of Pisa. As a part of General Electric's design certification effort for the SBWR, ANSALDO, ENEA and ENEL in cooperation with GE are conducting a test programme of full scale prototypical condensers for the SBWR passive containment cooling system and the SBWR isolation condenser system in SIET's PANTHERS test facilities. Also, an innovative passive depressurization and safety injection system is under development by ANSALDO and the viability of this system has been demonstrated by testing at SIET.

ENEL is testing an innovative passive containment cooling system from a concrete containment at CISE. ENEL and CISE have developed a high performance steam injector and its operation has been demonstrated by testing at SIET. ENEL is also testing in an international framework the behaviour under severe accidents of the personnel airlock of the abandoned Alto Lazio plant. At University of Pisa, the PIPER-ONE facility, simulating a BWR, was modified to include an out-of-scale Isolation Condenser component. Tests have been performed that demonstrated the facility to be very useful for code assessment.

In Canada, a passive moderator heat rejection system for advanced CANDU reactors is being developed as a diverse emergency heat rejection system. In CANDU reactors, low pressure heavy water moderator surrounds the fuel channels and is available as a heat sink to maintain channel integrity and avoid fuel melting in the unlikely event of a loss of coolant accident with loss of emergency coolant injection. Existing CANDU reactors use pumps to circulate the moderator and the cooling water. The passive moderator heat rejection system involves a natural circulation of heavy water driven by flashing to steam as the heavy water flows to an elevated heat exchanger. The heat exchanger is cooled in turn by a natural circulation flow of light water to a large reservoir. The overall concept has been verified both by analysis and by operation of a full elevation, light water, 1/60th volume scaled test of the natural circulation heavy water loop by AECL.

In Argentina, the CANDU core refill performance of the high pressure accumulator emergency coolant injection system under natural circulation conditions has been investigated for the Embalse nuclear plant for conditions resulting from a small LOCA. Acceptably safe fuel temperatures are predicted even for cases assuming manual initiation of the ECCS.

In India, testing of a passive containment cooling system which is proposed for India's Advanced HWR has been conducted at the Bhabha Atomic Research Centre. The system is designed to provide containment cooling following a LOCA by removing energy through isolation condensers immersed in a pool of water at the top of the containment. The test programme is examining the efficiency of heat transfer and of the removal of non-condensables to a vapour suppression pool.

In summary, arriving at the most advanced point in the realization of the passive safety plants has required extensive component and integral systems effects tests. These tests have been performed by the various groups supporting the design, testing and certification of advanced PWRs and BWRs. The papers presented at the TCM showed results generally confirming the expected performance of the passive safety systems of advanced designs.

Brief description of major components and systems being developed:

Ansaldo Passive Injection and Depressurization System (PIDS)

One of the means to mitigate the consequences of a loss of coolant accident is to inject cold water into the reactor coolant system at low pressure. This requires depressurization of the primary system. A concept of a passive injection and depressurization system which functions without making use of any active component or actuation logic is being developed by Ansaldo (Italy). The system performs the depressurization function by mixing (borated) cold water with the steam present in the reactor cooling system (RCS). The cold water injection is actuated by low RCS water inventory, while the depressurization (down to the containment pressure) is performed by a valve passively actuated by low RCS pressure.

Because of the innovative nature of this concept, before proceeding to the actual system design, an experimental investigation of the physical phenomena has been carried out at SIET and has demonstrated concept viability.

The next steps will consist of:

- separate effect tests aimed to gain information on the attainable depressurization rates and on the associated phenomena;
- integral scoping tests aimed at assessing the PIDS interaction with the other NPP systems.

Steam injector

A steam injector is a device in which steam is used as the energy source to pump cold water from a pressure lower than the steam to a pressure higher than the steam. Heat available from steam condensation can be partly converted into mechanical work useful for pumping the liquid. The steam injector consists of a steam nozzle to partially convert steam enthalpy into kinetic energy, a water nozzle to distribute inlet liquid around the steam, a mixing section for heat, mass and momentum transfer from the steam to the water resulting in condensation at higher pressure than the inlet steam, and a diffuser. Steam injectors are claimed to be useful in advanced light water reactors for high pressure makeup water supply without introduction of any rotating machinery. In particular, steam injectors could be used for high pressure safety injection in BWRs or for emergency feedwater in the secondary side of PWRs. An optimization study has been conducted by CISE in cooperation with ENEL, and steam injectors for advanced water cooled reactor application were tested in 1994 at SIET.

BWR passive containment cooling systems (GE-SBWR and Siemens SWR-1000)

Passive containment cooling systems for BWR application consist of condensers connected to the upper space of the drywell region of the BWR containment. During a loss-of-coolant accident, steam in the drywell is driven into the containment cooling condenser by the pressure difference between the drywell and wetwell in combination with the vacuum produced by condensation in the condenser. The condensate flows down into the gravity-driven cooling system pool in the drywell which provides makeup to the reactor. Non-condensable gases, such as containment nitrogen, are separated in the passive containment condenser and vented to the wetwell. In the General Electric SBWR concept the condensers are located in water pools outside the containment, whereas in the Siemens SWR-1000 concept the condensers are inside the containment. In the GE-SBWR the containment "atmosphere" flows inside the condenser tubes in an expanded containment; in the Siemens SWR-1000 the containment atmosphere is on the outside of the condenser tubes through which water from a pool outside containment flows in natural circulation.

Passive containment cooling system (AP-600)

The passive containment cooling system developed for AP-600 consists of a steel containment shell, inside a shield building, cooled by natural circulation of air, transferring heat from the containment to the environment (as the ultimate heat sink). In order to enhance the heat transfer capability, the system has been provided with large, elevated water storage tanks; when needed valves are opened and water is spread onto the containment shell yielding enhanced heat transfer by water evaporation.

Core make-up tanks, in-containment refuelling water storage tanks, and accumulators

Core make-up tanks and in-containment refuelling water storage tanks contain large volumes of borated water which can be injected into the primary system of PWRs by gravity.

Accumulators are pressurized water storage tanks which passively inject borated water into the primary system of PWRs when the primary system pressure falls below the design selected value.

Isolation condenser (GE-SBWR)

The main purpose of the isolation condenser is to limit the pressure in the reactor system to a value below the set-point of the safety relief valves, in the event of a main steam line isolation. The condensers are submerged in a pool of water located in the reactor building above the reactor containment. The primary side of the three isolation condensers is connected by piping to the reactor containment. Closed valves in each condensate return line prevent flow through the condenser during normal power operation of the plant. When operation of the isolation condenser system is required, the valves are opened, the steam flows directly from the reactor to the condensers and the condensate is returned to the reactor vessel by gravity. The rate of flow is determined by natural circulation. Vent lines are provided to remove non-condensable gases (radiolytic hydrogen and oxygen) which may reduce heat transfer rates during extended periods of operation.

Emergency condenser (Siemens SWR-1000)

Emergency condensers are heat exchangers consisting of a parallel arrangement of horizontal U-tubes between two common heads. The top header is connected via piping to the reactor vessel steam space, while the lower header is connected to the reactor vessel below the reactor vessel water level. The heat exchangers are located in a pool filled with cold water. The emergency condensers and the reactor vessel thus form a system of communicating pipes. At normal reactor water level, the emergency condensers are flooded with cold, non-flowing water. If there is a drop in the reactor water level, the heat exchanging surfaces are gradually uncovered and the incoming steam condenses on the cold surfaces. The cold condensate is returned to the reactor vessel. The condenser pool is located at a rather low level - with the return lines to the reactor vessel connected about 2m above the top of the core. System function does not require opening of valves, but requires a drop in the reactor water level.

Ejector-condenser

The principle of the ejector-condenser is based on the dynamic form of natural convection utilizing inertial forces instead of gravity for fluid circulation. The process develops in a loop combining an ejector specifically designed for dynamic natural convection and a heat exchanger for condensation. Since the motive power does not depend on gravity, heat can be rejected from a high elevation to a lower level. The condensate is recirculated to the nuclear steam supply system.

Passive pressure pulse transmitters (Siemens SWR-1000)

Passive pressure pulse transmitters function in a similar manner as the emergency condensers. The pressure generated in a heat exchanger secondary circuit is used to actuate pilot or main valves.

(In-vessel) residual heat removal system

The in-vessel residual heat removal system consists of in-reactor vessel heat exchangers located above the core, removing heat by natural convection to an external heat sink. To integrate the heat exchangers the size of the reactor pressure vessel has to be increased with respect to current PWR reactor vessel sizes.

Secondary condensing system

The secondary condensing system consists of a heat exchanger in a condensing pool located above the steam generator and connected to the steam generator by piping, with heat removal to the pool by natural convection. Condensate flow is returned to the steam generator by gravity. It might be useful to add that the development of operating procedures is interesting for transient conditions such as start-up and shutdown and is best pursued using the larger facilities.

Computer model development and validation:

A number of papers dealt with the computer code modelling of components, separate systems and integral systems and generally it appeared that after careful "tuning" the codes have been successfully applied to the thermalhydraulics of passive systems - especially problematic at low pressure. A point that should be kept in mind in these circumstances is that phenomena and components should be modeled individually, and that these models should be combined into the systems code rather than modifying the code by "tuning" or "biasing" to obtain agreement between code predictions and experimental results.

Future needs in development and testing of safety systems for advanced water cooled reactors:

Because of the intensive international cooperation in ALWR development and certification several suggestions for future cooperative activities resulted.

The issues discussed at the meeting ranged from the fundamental choice of advanced approaches to safety through the analysis and testing of selected approaches, to the results of tests in direct support of the safety systems proposed in the designs of those reactors in the most advanced stages of certification. As for future information exchange meetings in this area, it would seem appropriate to focus on individual areas. Topics could include: national advanced reactor programmes, methodology in selecting and testing advanced safety systems, initiation and reliability of passive systems including analysis approaches to examine passive system reliability, testing and analysis of component and system performance, quantification of uncertainties in computer codes, testing to address new thermohydraulic phenomena which are being incorporated into these codes and the results of test programmes in support of advanced reactor designs undergoing regulatory review.

Another topic of interest would be accident management especially for accidents beyond design basis including in-vessel retention of corium in the event of a core melt accident by flooding the reactor cavity.

It was the general consensus that testing of heat removal safety systems at large scale integral test facilities should continue to provide an extensive experience base in system behaviour and data for validation of computer codes. Importantly, these integral facilities could also be used to develop operating procedures for ALWRs.

While proof of predicted performance to satisfy safety requirements in support of design certification is the major goal of such testing, more complete understanding of the basic heat transfer phenomena, including the influence of non-condensable gases, would be very worthwhile for thorough understanding of the phenomena. This is especially important for passive heat transport systems which rely on small driving forces at low pressure thereby requiring comprehensive testing to assure that conditions resulting in system initiation and conditions affecting system reliability are thoroughly understood.

The question of extrapolability of the test results to larger sized plants which rely on the same phenomena should be addressed, as such larger plants could bring economic advantages. Existing facilities with some modification may be useful in examining performance and systems interaction (a concern for extrapolation) for such larger sized plants. Development of operating procedures is important for transient conditions such as start-up and shutdown and is best pursued using the larger facilities. PRA could be used to examine the need for additional testing with regard to potential systems interactions and the sequences to be examined.

Regarding code validation, predicting the performance of passive components and systems represents a new challenge to existing codes. New models are being developed in the following areas in order to qualify the codes:

- nonequilibrium mixtures involving subcooled and saturated water, saturated and superheated steam
- low velocity natural circulation
- initiation of passive systems
- effects of non-condensables on steam condensation
- water circulation in pools
- rapid condensation caused by interfacing steam and subcooled water.

Code benchmarking activities on an international level could be useful to assure proper modelling of passive components and systems.

Peer reviews by international experts would be worthwhile on topics such as, for example

- ejector condenser and other passive safety components mentioned above
- review of test results - both integral systems and safety components
- computer code qualification and approaches for uncertainty analysis.

In summary, the meeting provided a timely forum for review of design, R&D and testing of safety systems for advanced water cooled reactors, and for identification of key activities for future international cooperation in advanced technology for water cooled reactors.

OPENING ADDRESS

L. Noviello
ENEL-ATN, Rome, Italy

Three decades have passed from the inception of the peaceful use of nuclear energy. If I had to characterize those three decades I would say that:

-The 1960s were the years during which most of the safety and the industrial rules were established.
-The seventies were the years during which those rules were tested and a lot of experience feedback was obtained.
-The eighties were the years during which many corrective actions were put in place.

In the sixties the safety authorities had to develop a lot of regulations to obtain the safety level in the plants that they wanted.

In the seventies the industry, especially the utilities, had the heavy task of managing the nuclear power plant projects in this complex licensing environment.

The first years of the 1980s were the years of a joint reflection: nuclear energy would have not survived if the industrial and licensing environment did not stabilize and become more predictable.

The successful French experience became the example to follow. The concepts of construction in series, efficient project management and extensive pre-agreements with the safety authorities became the prerequisites to any new initiative.

As a consequence in the first years of the 1980s the government research bodies, the utilities, the vendors and the safety authorities jointly coordinated their roles and found new agreements.

The 1980s were also the years of a large research effort to address the safety problems posed by the TMI accident. The results of those researches have provided the basis for many modifications to the operating plants and have caused an ample debate about the design basis and the environmental impact objectives for the next generation of nuclear power plants.

The utilities are playing a major role in this redefinition. In the USA, in 1986, EPRI launched a program to develop the Utilities Requirement Document (URD). At the same time, in strong cooperation with DOE and the vendors, development was initiated on four new plant designs.

A few years later, actually in a more difficult environment, a similar initiative has been launched by a group of European Utilities, which have already issued the Revision A of the European Utilities Requirements (EUR). In this case too, the development of some plant designs is foreseen. The program for a large evolutionary design (EPR) is well underway, a program for a passive PWR (EPP) has just started, while programs for passive BWRs are under discussion.

Similar approaches have been taken in other countries, as for instance the Republic of Korea.

For the first time all the conceivable accident scenarios have been considered in the designs from their inception while, at the same time, the radioactivity release limit objectives have been decreased. This evolution of the overall safety objectives of the next generation of nuclear power plants (NPPs) has posed to the new designs very difficult, but also very fascinating problems: the new plants had to have a reduced core melt probability and to warrant the leak tightness of the containment for all the conceivable accident scenarios.

In a short time the easiest way was identified. Today, at the middle of the 1990s, we can say that the next generation of NPPs will be characterized by the following features:

- Reduced core melt probability, based on improved safety systems;
- Lower sensitivity to the operator's actions, based on advanced man-machine interface;
- Elimination by design of the most challenging sequences by the adoption of a primary circuit depressurization system, of advanced reactor cavity design and of advanced hydrogen control systems;
- Elimination of the slow overpressurization of containment by the introduction of ad hoc heat removal systems.

The development of many new systems has caused extensive test programs. During this meeting we will have the opportunity to discuss the results of those programs and I am sure that this TCM will help to improve the confidence on the new systems, in particular on those based on the natural circulation.

The above are the areas where the improvements are already well established. There are other areas where additional work is still needed to reach a consensus. I refer, in particular to the in-vessel coolability of , but perhaps intend to improve it further or intend to go from a design to a family of designs in terms of plant size.

the corium. Unfortunately not very much will be presented in this TCM on the effectiveness of heat transfer through the vessel wall and on the related design features. I hope that the next opportunity, that is the TCM on severe accidents to be held in Vienna in October, will allow to look at those areas.

The last remark I want to make is on the possibility to extrapolate the developmental work already done to different conditions and to different plant sizes. The investigation of this subjecit during this TCM would be very beneficial to those who intend to maintain the basic phlosophy of a specific design

STATUS AND PLANS OF DEVELOPMENT AND TESTING PROGRAMMES

(Session I)

Chairman

L. NOVIELLO
Italy

THE PROGRAMME OF ADVANCED LIGHT WATER REACTORS IN SPAIN

M. MALAVÉ
Consejo de Seguridad Nuclear,
C/Justo Dorado, Madrid,
Spain

Abstract

Spain's programme in advanced technologies for water cooled reactors has the objectives to (1) improve performance of currently operating plants, (2) participate in establishment of user requirements, and (3) be informed of advances to support future governmental choices.

Spain has **nine water reactors in operation**, such as two of them are of "3rd generation" reactors: a Westinghouse PWR at Vandellos II, and a KWU PWR at Trillo I. In addition, Spain has two modern BWR's at Valdecaballeros (GE BWR-6's) and two modern PWR's at Lemoniz which are partially completed, but which were halted in construction by the **Energy Plan's moratorium** of 1983 such as have been confirmed recently by a new bill on December 31, 1994 that will make sweeping changes to the country's national electricity supply sector (Ley de Ordenamiento del Sistema Eléctrico).

At the beginning of the nuclear programme in Spain, a major effort was made **to invest in domestic capabilities**, including new machinery, new quality assurance practices, and training of engineers. As a result, domestic participation in the civil work and manufacture has risen from 24% in the first generation (1969 with Zorita start up) to 78-80% in the third generation (1988 with Vandellós II). Spanish utilities intend to maintain and increase this participation in the future.

Spain has a **very active applying of advanced water reactor technologies** aimed at achieving performance from their operating reactors. Their R&D programmes are supported by the 0.3% fund of electric utilities income, and include:

- Improvements in control room, man machine interface and post accident monitoring systems
- Probabilistic safety assessments
- Steam generator and secondary side improvements
- BWR integrated corrosion programme
- Life extension
- Advanced fuel design and fabrication
- Source term.

Spain actually also participates **in multinational programmes** such as PHEBUS-FP, HALDEN, RASPLAV, CAMP, Post-ACE, ISA, MCAP, Several code validations and benchmarkings, CSAR Programme, IV Framework Programme of the EU, Assistance to Eastern countries and others contributions.

Spain has an effort underway **in the participation to design and build Evolutionary and Passives LWR's plants** as AP-600 of Westinghouse, ABWR and SBWR of GE and SYSTEM 80+ of ABB-Combustion. Nothing at longer term of concerning Inherent Safety Reactors is being made.

Spain is also participating **in projects to define objectives and requirements of advanced water reactors** to be built in the near future in the European Union (EU). We can extract from the 1991 Spanish Energy Plan as pattern of the institutional interest on it the following:

> "...Spain must participate in an active way in the consecutions of EU goals, with the aim of reach the harmonization of rules in the nuclear field, giving place to the opening of exportation of technology, equipments and engineering services and to cause the colaboration in the EU for the development of advanced reactors clearly european".

However, Spain **is not only following closely the development** of others advanced water reactor designs in other countries and intends to be in a position to apply these, but it is actively participating in the EPRI's ALWR Programme and others, both within Spain and for possible export, should circumstances permit. On this regard, the anticipated demand growth within Spain should call for the commissioning of new facilities as from approximately year 2000. Two alternatives being considered to meet this demand growth are: new gas thermal plants and developing and installing advanced light water reactors. When a decision is made among these alternatives, it will be included in the pertinent Energy Plan to be submitted by the Spanish Government for approval by the Legislative Assembly. To explain the position of Spain I choosed seven different topics to be analized:

Underlying Rationale For Advancements

Spain has five reasons for pursuing advanced light water reactors:

- It would be extremely difficult to maintain Spain's existing technological capacity in the nuclear field without new nuclear power projects. Monitoring international efforts to develop advanced light water reactors will assure that Spain's technological capacity is up-to-date and available to benefit the safety and operation of existing reactors as well as those to be built in the future.

- Improved water reactors would result into improved availability factors, decreased operating costs, improved nuclear safety and radiological protection.

- Positive impact on Spanish R&D activities in areas such as robotics, expert systems, welding, etc.

- Obtaining a high degree of technology transfer from multinational firms well recognised in the nuclear field, with the ultimate objective of enabling the future independent development in Spain of competitive designs of nuclear power plants.

- The eventual prospect of exporting the design and equipment of advanced nuclear power plants to developing countries. This might include fuel cycle services as well.

The **Spain's Electricity Supply Industry** has decided to pursue an Advanced Water Reactor Programme. The **Nuclear Safety Council (NSC)** is getting involved in the revision "C" of the European Utility Requirements -in whose redaction the Electricity Sector is participating- and until present moment NSC has presented to a document study of state-of-art of basically the most important designs of Future Reactors, enhacements of design objectives, nuclear trends, new NRC's Licensing, European Requirements and Conclusions.

Relevance to Operating Water Reactors

Should Spain decide to go forward with a programmme of Advanced Water Reactors, initially using imported technology and later becoming more self-sufficient, they would not see any conflict with continuing operation and reliance on existing operating light water reactors, as indeed, the completion of four units is presently cancelled. There is a very active programme of research and applying advanced technology to operating plants that continue to assure these plants operate safely, reliably and economically. The fact that advanced water reactors have even greater capability in the areas of safety, reliability and aconomics, does not in any way detract from the conclusion that those in operation are completely satisfactory in each one of these areas.

Approach to Obtaining Advancements

The most probable systems of future reactors are considered to be the Advanced Pressurised Water Reactor (APWR), the Advanced Boiling Water Reactor (ABWR), with a potential capacity of about 1000 MWe and Passives Plants (AP-600 and SBWR). This is largely due to the vast experience obtained by the Spanish nuclear industry in the design and construction of reactors from which these types have originated.

Selection of Plant Size

Should the National Energy Plan call for new nuclear power plants, Spain is interested in advanced nuclear power plants. The size will be based on utility-specific considerations such as demand growth, grid size and economics.

Prospects for Success

The main ingredient influencing the prospects for success of advanced water reactors in Spain is the decisions made on electricity supply choices to be included in the National Energy Plan. In the medium term, the possible further lowering of the price of crude oil, and the dollar would favour continued reliance on gas fuel plants in Spain.

A further consideration in choosing among electricity supply choices is the existence of various current nuclear projects (e.g. Valdecaballeros I and II and Lemoniz I and II) authorized for construction and in different stages of progress, affected by the nuclear moratorium of 1983 and finally cancelled.

In the event that Spain does undertake on a programme for future advanced water reactors in Spain, the following are important ingredients for success:

1) Cooperation agreements between Spanish firms, or groups of firms and foreign companies that are leaders in their field, with a view towards assimilating and transferring technology.

2) The decisive support of the administration to these agreements, either directly or through the official bodies in R&D and regulation.

3) Support of investing community.

Prospects for Cooperative Efforts

Spanish organisations are participating in various multinational nuclear research programmes such as PHEBUS-FP, HALDEN, RASPLAV, CAMP, MCAP, CSAR Programme, EPRI-ALWR Programme, etc, as we've seem before. With respect to advanced reactors, there are some groups of companies all of them integrated in a common company, called Agrupación Eléctrica para el Desarrollo Tecnológico Nuclear (DTN), that are participating in the development of advanced reactors, for possible future application in Spain and also in the redaction of the European Utility Requirements (EUR) and in the European Pressurized Passive Reactor (EPP Project) wich main objective is to assess compliance with the EUR by the AP-600 concept and to present alternatives. Utilities have a great interest in having any design of advanced water reactors pre-licensed, so that licensing effort needed to construct the plant in Spain would be limited to site specific aspects only.

Economics of Advanced Water Reactors

Spain indicates that economics will be a very important consideration in choosing among electric supply options in Spain's next National Energy Plan. Emphasis for nuclear power would be a reduction of construction periods, reduction of capital costs, and stabilization of the licensing process.

PROGRESS IN DESIGN, RESEARCH AND DEVELOPMENT AND TESTING OF SAFETY SYSTEMS FOR THE KOREAN NEXT GENERATION REACTOR

YOUNG SANG CHOI, BYONG SUP KIM
KEPCO Research Center, Taejeon,
Republic of Korea

Abstract

Korean Next Generation Reactor Development Project has been launched to develop the advanced design which has the potential to become a safe, economical and environmentally sound energy source in Korea.

The target of the project is to develop the whole plant design to the sufficient level of detail to be built in the early 2000's.

This paper provides development program and design concept overview of the KNGR.

1. Introduction

Korea has launched next generation reactor development project, so called the KNGR project, in 1992 to complete a detailed standard design by 2,000.

This project aims at developing the advanced design which has the potential to become a safe, economical and environmentally sound energy source for the early 2000's in Korea.

To develope the KNGR, an integrated project team has been setup to incorporte the specialized institutes and companies of Korea nuclear industry. KEPCO is the leading organization in this project and Korea Atomic Energy Research Institute (KAERI) is responsible for the NSSS design, Korea Power Engineering Company (KOPEC) is for architecture engineering and Korea Heavy Industry Company (KHIC) is for component design.

For the basic research, the Center for Advanced Reactor Research (CARR), an university association, is participating in this project and for the early interaction of licensing issues, Korea Institute of Nuclear Safety (KINS), regulatory agency is also participating in the project.

This project consists of three phase in developmental activities from 1992 to 2000.
The phase I which has already been finished was a two year program from 1992 to 1994 and its major activities were the development of top tier design requirements and design concept for the next generation nuclear plant. The phase II is 3 year program from 1995 to 1998 and its major activities are the development of basic design for the licensing review. The phase III will start from 1997 to 2000 and its main activities are the development of detailed standard design to the level which will enable the accurate cost estimation and investment assurance.

2. Phase I Program Summary

The main focus of the first phase was to establish design concept of the Korean next generation reactor.

Several studies have been performed to establish the design concept such as the top-tier requirement development, comparative study on evolutionary versus passive type plant and case studies for adapting hybrid design concept, etc.

The top-tier requirements have been developed to specify the utility goal of safety and economics that will give a guidence in the second phase design activities.

The comparative study has been performed to select the reactor type suitable and desirable for Korea by comprehensively reviewing the available design options.

In parallel with the comparative study, case studies have been performed to examine the possibility of uprating of passive type plants and the feasibility for adapting passive design features in evolutionary plants.

In this series of studies, the KNGR team outlined design requirements and the KNGR design concept for the future PWR in Korea.

3. Top-tier Design Requirement

As the primary design requirements, an evolutionary type pressurized water reactor (PWR) with a capacity of 4000MWth and 60 year design life have been selected. Major considerations for this selection were the level of maturity of technology, the economy of scale and the availability of new nuclear sites, etc.

As the safety goal of the KNGR, the core damage and containment failure frequencies are required to be less than 10^{-5}/RY and 10^{-6}/RY respectively, which are, to our thought, in the world-wide consensus as seen in the EPRI URD, EUR and IAEA recomendations. In addition to the above safety goals, the limits to the whole body dose and to the concentration of long lived Cs_{137} at the site boundary have been placed in order to provide technical soundness for possible reduction of emergency planning boundary in the future and to prevent land contamination in case of postulated accidents.

The economic goal of the KNGR is to accomplish cost advantage over the coal by at least 20%. To achieve this goal, adoption of new technology as well as the introduction of advanced management systems will be necessary. Standardization policy is emphasized again and the improvement of regulatory systems is continuously pursued. The 48 months of constuction period and maximization of modular construction are the subset of the requirements, and also the reliability assurance program and configuration management system are required to be applied systematically.

The design of the KNGR shall be standardized, and so site parameters were determined to bound all potential nuclear sites in Korea. The seismic value of 0.3g is specified as the safe shutdown earthquake(SSE).

4. Design Concept of KNGR

Nuclear Steam Supply System (NSSS)

The KNGR core design consists of 241 fuel assembilies and utilizes uranium dioxide fuel which is operated at a power density (95.9 KM/ℓ) lower than conventional large PWRs. The uranium-235 enrichment of the fuel has been selected to achive 18 month or 24 month operation cycle.

The KNGR Reactor Coolant System (RCS) is configured in two seperate loops with the core power density of 95.9 KW/ℓ and water inventory of 322.1 ℓ/MWe which is a 3.5% increase over existing reactors.
The primary coolant flow is set to give a conservative thermal margin of approximately 15% to improve response to a variety of performance transients.

The reactor vessel is fabricated by steel forging with controlled copper, nickel, phosphorus, and sulfur content. By using these materials, the change nilductility transition temperature (RT_{NDT}) can be minimized resulting in the longer life of a reactor vessel.
Two U-tube, vertical steam generators provide the means to transfer heat from the primary RCS to the secondary feed water. The resistance stress corrosion cracking in the S/G tubes will be improved by using In-690 tube material.
A tube plugging margin of 10% will be required to provides a longer life of steam generators.
The volume of pressurizer, which provide a means of maintaining the RCS pressure by compensating volumetric fluctuation in RCS, will be increased to 2400 ft^3.

Safety Features

KNGR safety features are designed to follow the defence in-depth approach.

The one feature of the defence-in-depth design is the reactor core protection with the protection systems.
Protection systems include four independent trains in the Safety Injection

System, Shutdown Cooling System which can be used to backup the containment spray pumps, and a four-train dedicated Emergency Feedwater System.
Four independent trains of safety injection system discharge borated water directly into the reactor vessel. This direct vessel injection method eliminates complicated interconnection pipes and ensures more water to reach the core. The IRWST is employed for the suction to the safety injection system which simplifies operation and increases reliability. The safety injection function of shutdown cooling system has been removed for simplicity. In stead, shutdown cooling pumps can be used for cotainment spray when spray pumps fail. The design pressure of the SCS is increased to minimize intersystem LOCA.

The other features of the defence-in-depth is the mitigation of the consequences of a severe accident.
This level of defense is accomplished through design features such as the Safety Depressurization System, the Hydrogen Mitigation System, the Cavity Flooding System, and a reactor cavity designed to mitigate the consequences of the steam explosions and molten core-concrete interaction.

The containment is of particular importance within the safety concept of accident consequences. It is the final barrier in the defence-in-depth concept.
A double, cylinderical, and concrete containment design has been selected for the KNGR taking into account the severe accident. It consists of a prestressed concrete inner wall designed to withstand post accident pressure buildup with significant margin and a reinforced concrete outer wall designed to withstand external hazards. The annulus between the inner containment and the outer wall is maintained at a pressure below ambient atmospheric pressure in order to collect any leak through the inner containment of penetrations and filter them before release to the environment.

In addition, we have studied feasibility to apply passive design features as a supplemental function to enhance the safety. Currently we are implementing the conceptual design to apply the following passive features to KNGR, :

- Fluidic device in safety injection tank
- Passive Cavity Flooding System
- Secondary Condensing System
- Catalytic hydrogen igniter

Man-Machine Interface System (MMIS)

The KNGR MMIS employs digital I&C and advanced man-machine interface technology to improve the operational reliability, plant safety, and economy. The KNGR control room is implemented through the systematic human factor engineering process and provides the primary interaction with the plant via computer based interfaces, such as CRT, ELD. Large wall mimic is employed in the MCR to promote the plant situation awareness of operators. Functional information such as SPDS and task information such as procedures are extensively provided to address the information necessary for operators. A mockup of control room with plant simulation models will be used to verifiy the suitability of the design.

Open architecture digital I&C technology such as PLC, mutiplexing, fiber optic comunication is employed for safety and non-safety systems. Diverse digital technologies are used for safety system and non-safety system to prevent the common mode failure of digital I&C. Commercial I&C equipment and software are evaluated and adopted according to commercial item dedication criteria which will be approved by regulation.

General Arrangement

General arrangement of the KNGR has been developed based on the twin unit concept and slide-along arrangement with common facilities such as radwaste building. The schematic for twin units is depicted in figure 1.

The auxiliary and fuel buildings which accomodate the safety related systems and components are located adjacent to the reactor building and

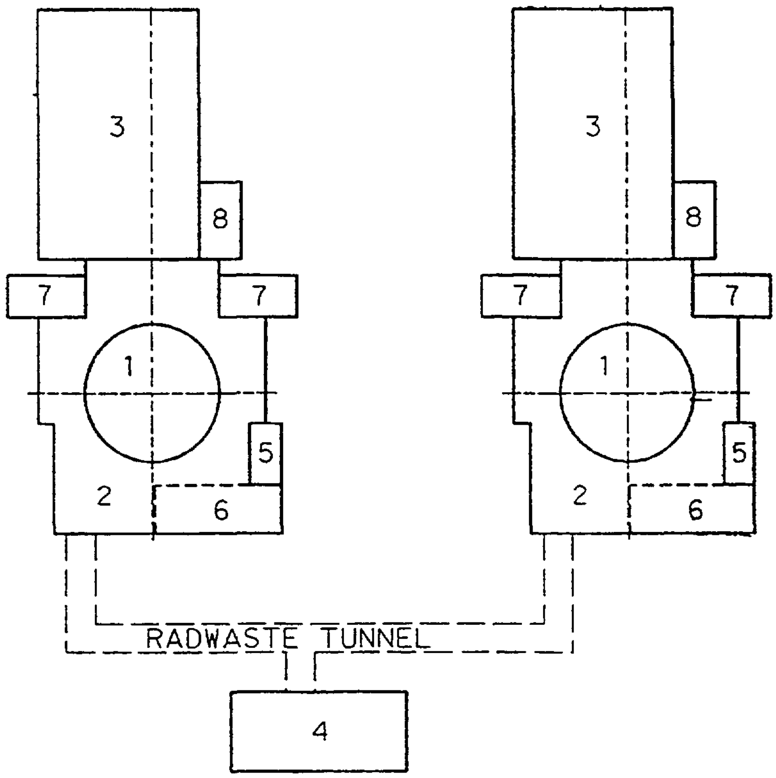

1. CONTAINMENT BUILDING
2. AUXILIARY BUILDING
3. TURBINE BUILDING
4. RADWASTE BUILDING
5. ACCESS CONTROL BUILDING
6. FUEL HANDLING AREA
7. DIESEL GENERATOR
8. SWITCHGEAR BUILDING

Fig. 1 : Dual Unit Arrangement

they are seated on a common basemat with the reactor building in lieu of separate basemats. common basemat will improve the resistance against seismic event. It also allows to reduction of the number of walls between buildings so that rebar and form work cost can be reduced compared to the separate basemat of current plant.

As mentioned earlier, the KNGR adopts four train safety injection system. The safety injection pumps are located in the aux. building near the containment structure and each pump is located in each of four quadrants surrounding containment. This arrangement maximizes physical separation of the pumps to provide protection against damage due to fire, sabotage, and internal flooding. The vertical plan view is depicted in figure 2.

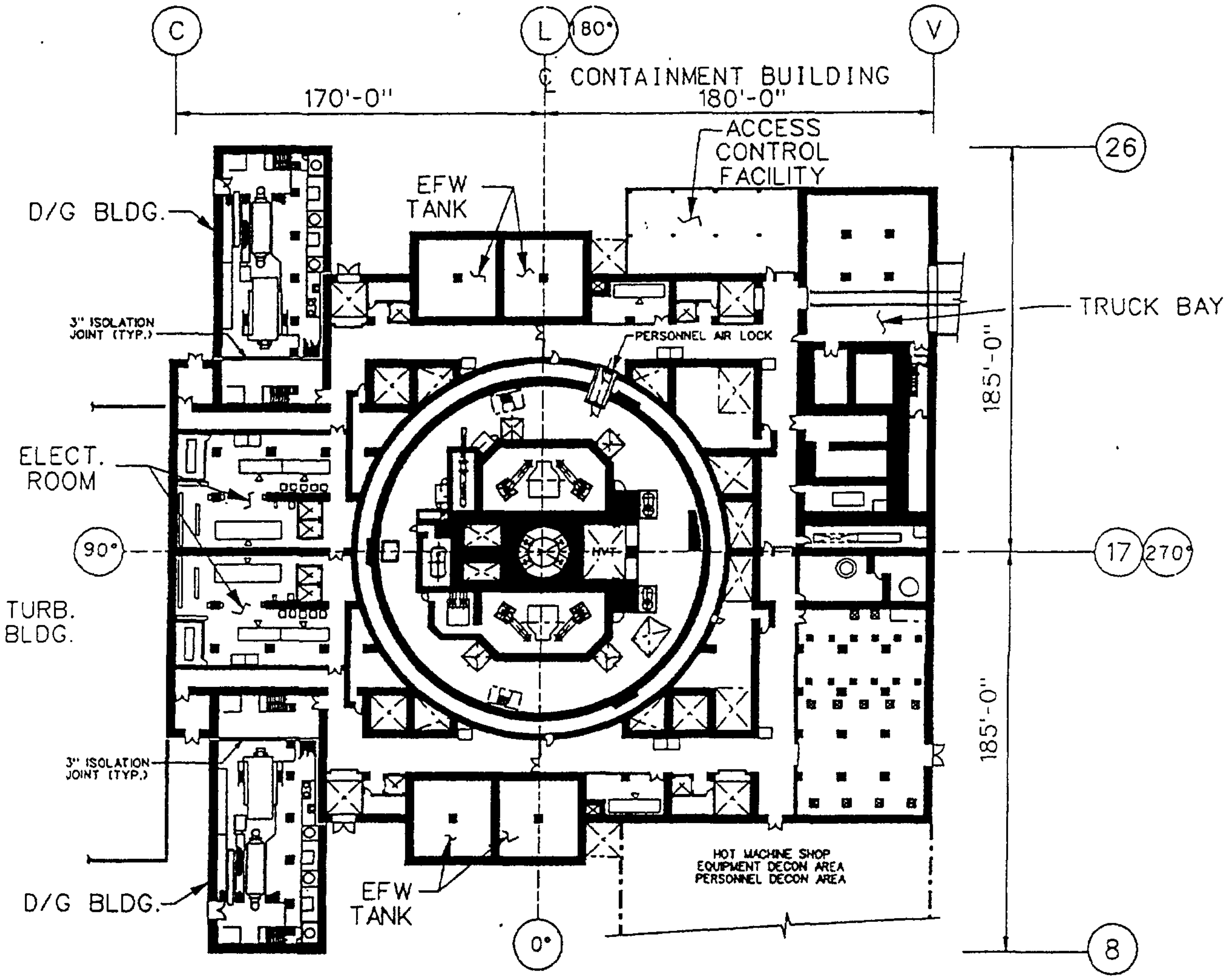

Fig. 2 : Vertical View of the KNGR

5. Phase II Program Outline

The objectives of the Phase II program are to complete engineering for the KNGR in sufficient detail to assess safety, economic and contructability and prepare for construction of KNGR from the 2000.

To achieve these objectives, the scope of the KNGR phase II program will encompass the work necessary to provide design detail, along with the work necessary to support the success of the design activities.

The major activities in Phase II program can be categorized such as basic studies, detailed URD development, regulatory research, information magement system development and basic design activities.

The scope of the phase in design development is to complete the basic design. It should provide the total power block information necessary to make a decision in building the 1st unit. This will accomplish the design details comparable to the Standard Safety Analysis Report as in the U.S.A for the design certification.

The degree of design finality is difficult to quantify but the KNGR team outline that the basic design will meet around 20% of all the necessary works to complete the plant design.

The KNGR design work will be conducted to assure the design of the highest quality and to meets all applicable requirements through the project quality program and implementation of periodic evaluation of the design. This evaluation will be performed three times in the second phase.

Licensing stabilization is one of the main concerns to the development of new design.
In the KNGR development, regulatory agency is directly involved in the KNGR team to establish the licensing requirement as early as possible to guide the designers.
Licensing interactions with the Korea Institute of Nuclear Safety (KINS) on the issues identified in the preapplication review will be continued.
As required by the top-tier requirement, the KNGR design team will develop and operate Information Management System (IMS) in the Phase II.

For the design process, the IMS will be used as a single central, logical data base of storing, securing and providing access to the wide variety of information necessity associated plant design and to utilize configuration management.

In addition to the above activities, some supportive research and development will be conducted to enhance in-house engineering capability, design alternatives study and extension of top-tier requirement to detailed requirements to support system, structure and component design in the second phase.
Also, major advanced and passive safety features such as IRWST, Fluidic Device, Secondary Condensing System will be tested to verify it's function and the design.

6. Conclusion Remark

With the KNGR concept outlined in this paper, KEPCO and the Korean nuclear industry with the support of government will jointly develop basic and detailed design.

The KNGR design will meet the enhanced safety requirements and economic goal for future nuclear power plants in Korea, in particular, for the protection of investment and prevention of severe accidents.

Nuclear energy will remain as essential energy source for the 21st century in Korea.
Accordingly, KNGR will play animportant role by satisfying the requirements of enhanced safety, improved economics and environmental protection.

Finally, it is anticipated that the Korean nuclear industry improves dramatically its basic nuclear technology through the completion of the KNGR project.

THE STATUS OF THE ALPHA-PROJECT

G. YADIGAROGLU, G. VARADI, J. DREIER,
F. DE CACHARD, B. SMITH S. GŰNTAY,
Th. BANDURSKI
Paul Scherrer Institute Wűrenlingen & Villigen,
Villigen , Switzerland

Abstract

A review of the ALPHA project is presented, including a summary of progress and current status. The project comprises the experimental and analytical investigation of the long-term decay heat removal phenomena from the containment of the next generation of "passive" Advanced Light Water Reactors. The effects of aerosols that may result from hypothetical severe accidents are also considered. The construction of the major ALPHA experimental facilities, PANDA, LINX-2 and AIDA, has been completed. First steady-state tests have been performed on PANDA. The other facilities are now in their commissioning phases. Scaling studies have guided the design of the experimental facilities. Several small-scale experiments and studies have already produced valuable results which can be used to direct the experimental work, as well as the design of the passive ALWRs.

1. INTRODUCTION

In 1991, PSI initiated the major new project ALPHA [1]. The central goal of this project is the experimental and analytical investigation of the long-term decay heat removal from the containment of the next generation of "passive" Advanced Light Water Reactors (ALWR). The dynamic containment response of such systems, as well as containment phenomena, are investigated. Two such passive ALWR systems are presently being designed and engineered in the United States. The projects are led by the US Department of Energy (DOE) and the Electric Power Research Institute (EPRI). Both projects are for reactors in the 600 MWe range. The research and development (R&D) efforts will lead to the generic "certification" of the reactor designs by the US regulatory authorities (the US Nuclear Regulatory Commission, US NRC). These efforts are conducted with broad international cooperation and the participation of institutions from several American, European and Far-Eastern countries.

The first passive ALWR concept is a Pressurized Water Reactor (PWR), the AP-600, while the second is the Simplified Boiling Water Reactor (SBWR) shown in Fig. 1. Both make use of large passive systems for the transfer of decay heat following an assumed depressurization of the primary system, from the containment building to either evaporating water pools, or to convectively air-cooled structures. These systems should be able to remove the decay heat for at least three days without any intervention. Simple measures, such as the refilling of an open water pool, may be needed after this period. Similar passive systems are also under consideration in other countries including Germany, Italy and Japan.

In all passive ALWRs, the energy removal from the reactor containment involves the condensation of the steam produced by the evaporation of water in the core. This takes place in the presence of some of the non-condensable gases that initially constituted the containment atmosphere. It is the efficiency of this condensation process and the distribution of the gases in the various containment volumes that determine overall containment behavior. These are the main containment phenomena of interest for the ALPHA project. The project has been, so far,

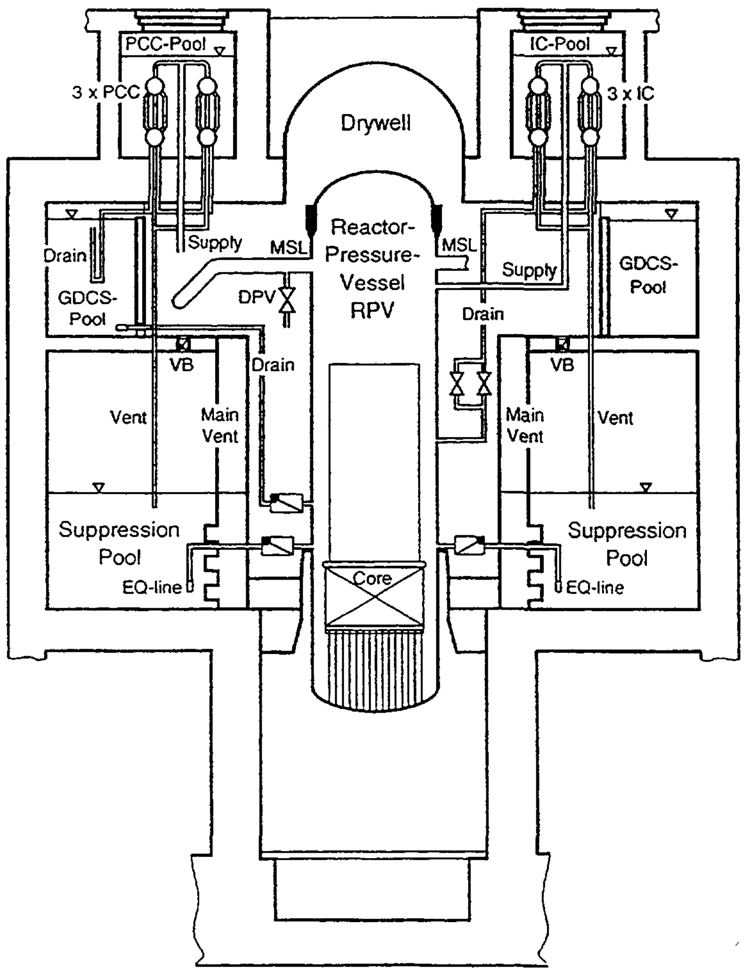

Fig. 1: Schematic Representation of the SBWR Showing the Various Containment Components.

directed to the investigation of the SBWR Passive Containment Cooling System (PCCS) and related phenomena.

The ALPHA Project at PSI is conducted in collaboration with a large, truly international R&D team. The main PSI partners in this team have been so far EPRI, the General Electric Company and the University of California-Berkeley in the US, KEMA and ECN in the Netherlands, Toshiba in Japan, the IIE in Mexico, and ENEL, ENEA SIET and Ansaldo in Italy. The project includes four major items:

- PANDA is a large-scale, integral system test facility, presently configured to simulate the containment of the SBWR on a volumetric scale of 1:25 and a height scale of 1:1.
- LINX is an experimental and analytical investigation of condensation and buoyancy-driven mixing and stratification phenomena of importance to containment performance. LINX-2 is the major facility related to this part of the project.
- AIDA is a program set up to investigate aerosol transport and behavior in the SBWR Passive Containment Cooling System (PCCS) during core destructive accidents.
- Analytical model development, code validation, system analyses, and the extension and application of three-dimensional Computational Fluid Dynamics (CFD) tools to large scale mixing problems complement the experimental studies and complete this program.

The purpose of this paper is to review progress to date and to outline certain recent achievements.

Although the ALPHA results were initially expected to bring only "confirmatory" information for the generic "certification" of the SBWR, recent developments have made the first series of experiments to be conducted in the PANDA facility the essential experimental element in the certification process. Thus, the results of the first series of PANDA experiments will be formally submitted to the US NRC as part of the SBWR Design Certification Process. As a consequence of the "formalization" of these tests, they are performed according to the US NRC Quality Assurance procedure NQA-1.

The PANDA data will be used for the development and validation of models for computer codes such as TRACG [2], RELAP5 [3], etc.

Other elements of the international program closely linked to ALPHA and the SBWR are:

- Single-tube condensation experiments at the University of California-Berkeley [4] and at MIT [5].
- The smaller scale (1/400) containment integral test facility GIRAFFE, located at Toshiba in Japan [6].
- The full-scale PCCS condenser qualification experiments (PANTHERS) performed by SIET in Italy [7].

In addition to the work which is focused directly on the PCCS for the SBWR, there is a great deal of other work already in progress at both small and large scale: for example, towards understanding the long-term behavior of the SBWR Pressure Suppression Pool, including its possible thermal stratification, and potential heat-up and pressurization of the Wetwell. Certain phenomena of generic interest to all passive containment concepts are also being investigated, and tests directly related to the development of alternative concepts are also being conducted.

2. STATE OF THE ALPHA PROJECT AT PSI

The major project activities within the period 1991-94 have concentrated on the design, scaling and construction of the three major experimental facilities, namely PANDA, LINX-2 and AIDA. The detailed conceptual design of all three was completed in 1992, together with ordering of the major components. Significant work has also been carried out on the development of the required instrumentation and data acquisition systems. Construction of all the facilities is now complete, and commissioning is underway or completed. First steady-state tests have been performed on PANDA. Tests in the other major facilities will start in 1995.

In addition, small-scale experiments and numerous analyses were conducted within the LINX framework (LINX-1 and LINX-1.5) to better understand basic phenomena, and to provide preliminary experimental data for the development of computational models for thermal mixing in open pools: specifically, plume development, mixing and stratification [8,9,10]. To understand SBWR system behavior and to support both facility design and the definition of instrumentation, extensive computer calculations have been performed using the TRACG, FLOW3D and ASTEC codes [11,12].

3. THE PANDA FACILITY

The PANDA general experimental philosophy, facility design, scaling, and measurement concepts were defined in early 1991 [13]. On-site construction began in 1993 with the delivery of the major PANDA components. The facility is now complete and fully instrumented. The instrumentation includes numerous temperature sensors (including "floating thermocouples" capable of measuring the temperature of the surface of water pools), pressure as well as differential pressure and water level difference sensors, flow rate measurements (over wide ranges), non-condensable fraction sensors (oxygen probes), phase (liquid or gas) detectors, electric power measurement, and sensors detecting the positions of valves; a total of some 620 channels. The computer-based data acquisition system (DAS) is capable of sampling all channels continuously with a frequency of 0.5 Hz. For short periods of time, sampling with a "burst" frequency of 5 Hz is also available. The DAS displays the data in a variety of "screens" representing schematics of various parts of the facility [14]. The time histories (trends) of selected channels can be displayed at will. The facility is operated and controlled remotely and interactively by a computer-screen-based system.

The very first series of PANDA experiments have been steady-state tests of PCCS condenser performance. These have been counterpart tests to similar tests conducted at the PANTHERS facility in Italy [7]. Extensive facility characterization tests will follow: the heat losses from the facility, as well as the actual pressure-drop-flowrate characteristics of the various lines will be obtained. These are needed for the accurate description of the facility by computer codes. The actual transient system behavior tests will follow.

In relation to the SBWR certification effort, the PANDA facility was primarily designed to examine system response during the long-term containment cooling period. The overall objectives of the transient PANDA tests are to demonstrate that:

- The containment long-term cooling performance is similar in a larger scale system to that previously demonstrated with the GIRAFFE tests.
- Any non-uniform spatial distributions in the Drywell or Wetwell do not create significant adverse effects on the performance of the PCCS.
- There are no adverse effects associated with multi-unit PCCS operation and interactions with other reactor systems.
- The tests will also extend the database available for computer code qualification.

The initial test series at PANDA will include two Main Steam Line Break (MSLB) tests. One test will be similar to a GIRAFFE MSLB test with uniform Drywell conditions, while a second is planned in a manner maximizing the influence of Drywell asymmetries on the operation of the PCCS condensers. Uniform and asymmetric Drywell conditions can be created in PANDA via the capability to vary the fraction of steam flow which is injected into each of the interconnected Drywell vessels, Fig. 2. The steam condensing capacity directly connected to each vessel (i.e., the number of condenser units) can also be varied. Such tests and several systematic variations of the experimental conditions will help identify any scale and multi-dimensionality effects that may not have been present in the smaller scale facilities. The test matrix for further tests is dictated by the needs of certification and code assessment and is still evolving. Steam and/or non-condensables can be injected at various locations in the Drywell vessels to study mixing phenomena and to provide envelope information for the corresponding SBWR conditions.

3.1. Scaling Considerations

A rigorous scaling study [15] covering all the SBWR related tests describes the scaling rationale and details of the PANDA facility. Other documents cover particular aspects of scaling [10,16,17,18].

The SBWR containment is particularly complex and thermal-hydraulically coupled to the primary system. In addition to the complexity of the usual BWR pressure suppression system and its various components, such as the main vents, one must now also consider the operation of the particular PCCS system and its components. Both "top-down" and "bottom-up" scaling considerations [19] and criteria were developed.

According to the "top-down" approach, general scaling criteria are derived by considering the processes controlling the state of classes of containment sub-systems (e.g., containment volumes, pipes, etc.). Close examination of the specific phenomena governing the operation of certain system components (e.g., vents immersed in the Pressure Suppression Pool of the SB-WR) leads to "bottom-up" scaling rules.

3.1.1. Top-Down Scaling

Generic scaling criteria for thermal-hydraulic facilities, such as those proposed by ISHII and KATAOKA [20], are not specific to the combined thermodynamic and thermal-hydraulic phenomena taking place inside containments. Thus, specific scaling criteria for the design of facilities simulating the dynamic operation of BWR containments such as PANDA were derived [15]. For example, mass and energy transfers take place between containment volumes through their junctions. Heat may also be exchanged between volumes by conduction through the structures connecting them. These exchanges lead to changes in the thermodynamic condition of the various volumes; this, in particular, leads to changes of the volume pressures. The junction flows (flows between volumes) are driven by the pressure differences between volumes. Thus, the thermodynamic behavior of the system (essentially, its pressure history) is linked to its thermal-hydraulic behavior (the flows of mass and energy between volumes).

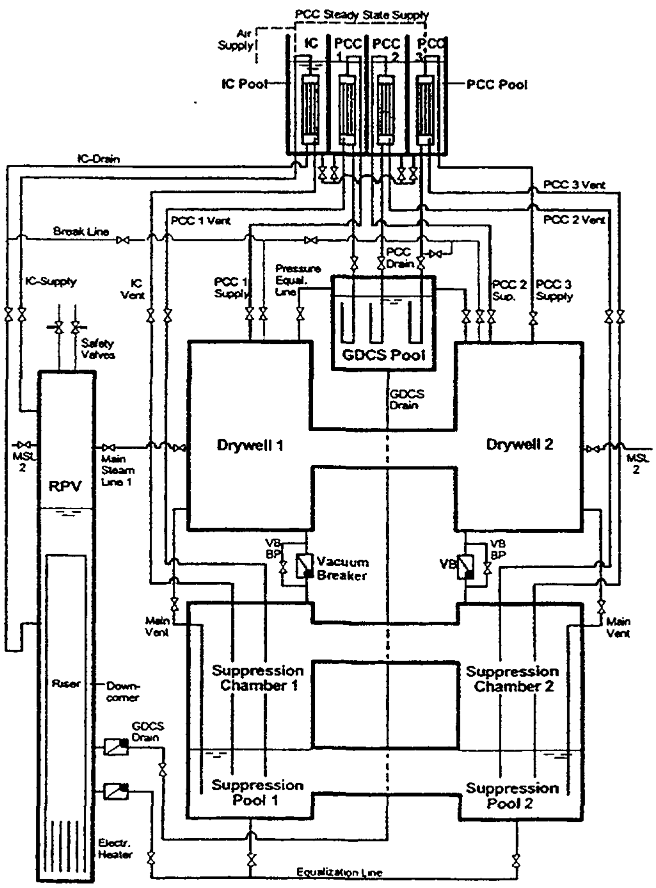

Fig. 2: Schematic Representation of the PANDA Facility.

The "top-down", generic scaling criteria were derived by considering generic processes, including:

(1) The effects of the addition of heat and mass to a gas or liquid volume (namely, the resulting rates of change of the pressure).

(2) The rates of phase change at interfaces such as pool surfaces.

(3) Flows of mass between volumes.

Prototypical fluids, i.e. those pertaining to the actual reactor system, under prototypical thermodynamic conditions, are used in PANDA. The fact that the fluids are expected to be in similar thermodynamic states, and have similar composition in the prototype and the model, can be used to simplify the analysis and scaling of the facility. The first two processes listed above (1 and 2) confirm the validity of the (familiar) scaling of all the following variables with the "system scale", R:

$$(\text{power})_R = (\text{volume})_R = (\text{horizontal area in volume})_R = (\text{mass flow rate})_R = R$$

where the subscript R denotes the ratio between the corresponding scales of prototype and model. Although other choices are also possible, the system scale R can be defined as the ratio of prototype to test facility power input. For PANDA, R = 25. A time scale of 1:1 between prototype and model has been adopted for the presently planned PANDA tests; however, this is not a necessity. Under certain conditions, the choice of a scale for the volumes different from the system scale R will lead to accelerated (or decelerated) tests in time.

Process (3) leads to the determination of the pressure drops and of the hydraulic characteristics of the junctions between volumes. In the BWRs, certain pressure drops and the corresponding junction flows are controlled by the submergence depth of vents in the Pressure Suppression Pool. The analyses of these processes justify the choice of 1:1 scaling for the vertical heights in general and for the submergence depths in particular [15].

The pressure evolution resulting from the thermodynamics of the system and the pressure drops between volumes must clearly scale in an identical fashion. Considering the fact that prototypical fluids are used, this requirement links the properties of the fluid (in particular the latent heat and the specific volumes of water and steam) to the pressure differences between volumes (and to the submergence depths of vents), resulting in 1:1 scaling for pressure drops. Thus, the above considerations result in:

1:1 scaling for pressure differences, elevations and submergences.

This scaling rule determines the pipe diameters, lengths and hydraulic resistances, and the transit times between volumes. These transit times should, in principle, have the same (1:1) time scale as the inherent time constants of the system considered in the analysis of process (1). This matching cannot be perfect, but is shown not to be important [15].

The criteria derived are combined to arrive at general scaling laws for the PANDA model of the prototype SBWR. Several non-dimensional numbers, three time scales and certain geometric ratios must be matched.

The three time scales produced by the analysis are the scales for the rates of volume fill, of inertial effects, and of pipe transfers. Clearly, the systems considered here are made of large volumes connected by piping of much lesser volumetric capacity. The pressure drops between these volumes are not expected to be dominated by inertial effects. Thus, the inertia and transit times, which are of the same order of magnitude, are much smaller than the volume fill times. Consequently, the important time scale that must be considered in scaling is the volume fill time scale. The other two time scales are clearly of lesser importance. In relation to this conclusion, the lengths of piping connecting containment volumes and the velocities in these pipes do not have to be scaled exactly. Usually (and fortunately), the total pressure drops in the piping are dominated by local losses, so that the total pressure drops in the scaled facilities end up being somewhat smaller. They can therefore be matched by introducing additional losses by local orificing.

3.1.2. Scaling of Specific Phenomena - Bottom-Up Approach

Bottom-up scaling for phenomena that were selected as being of particular importance by a Phenomena Identification and Ranking Table (PIRT) exercise were examined in detail to arrive at their proper simulation in the PANDA facility [15]. Several documents cover in detail such particular aspects of scaling [10, 16, 17, 18, 21], as already noted.

The scaling of thermal plumes, mixing and stratification phenomena in the pool, as well as in the Drywell volume, heat and mass transfers at liquid-gas interfaces, the heat capacity of containment structures, and heat losses were examined in detail in [15]. Of particular importance is the scaling of the various vents, discharging mixtures of steam and non-condensable gases into the Pressure Suppression Pool. This is important in relation to the possibility of steam "bypassing" this pool and entering directly into the Wetwell gas space. Heat and mass transfer in the PCCS condensers must also be properly scaled, considering both condensation inside the tubes and heat transfer on the secondary pool side [21]. The latter may be affected by any induced natural circulation.

4. THE LINX PROGRAM

The LINX Program (Large-Scale Investigation of Natural Circulation, Condensation and Mixing) aims at a better understanding of the most important physical processes taking place in passive ALWR containments. Small-scale experiments (LINX-1 and LINX-1.5) addressing certain issues encountered in the SBWR have already been conducted [8,9,10]. The main effort in this program includes medium-scale, highly instrumented experiments in the LINX-2 facility which are described below. These will look at natural circulation, mixing and condensation phenomena in pressure suppression pools and containment volumes in the presence of non-condensable gases. This work will also support the application of Computational Fluid Dynamics (CFD) tools for single- and multi-phase flow to mixing and natural circulation problems.

4.1. The LINX-2 Facility

The LINX-2 facility has been designed to study condensation and mixing phenomena encountered in passive ALWRs, such as direct-contact and surface condensation in the presence of non-condensables and pool thermal mixing induced by single and two-phase plumes. The experiments are to be conducted at a fairly large scale and under prototypical pressure and temperature conditions. Some issues relevant to the SBWR and to a European version of the AP-600 are being addressed in the present phase of this program.

The facility, Fig. 3, consists of a pressure vessel (rated at 10 bar and 250°C), steam and nitrogen (or air) supply lines, and a water conditioning loop. The vessel is very carefully insulated (35 cm insulation thickness) to minimize heat losses and allow the performance of accurate heat balances. Heat losses are monitored using thermocouples on the vessel wall and penetrations, and within the insulation itself. The vessel pressure is regulated. Constant (regulated) steam and nitrogen flow rates can be injected from either the bottom or the top of the vessel. The steam and nitrogen flow-rate ranges can be adjusted from 10 to 120 kg/h (± 1.3% of the Measured Value) and 0.1 to 75 kg/h (± 3% MV), respectively. The gas injection temperature (up to 180°C) is also regulated. The water conditioning loop is a multi-purpose heating and cooling system. Outside the vessel, either heating or cooling power is provided by steam or cold water, respectively. Inside the vessel, water can be circulated at constant (regulated)

Fig. 3: Schematic of the LINX-2 Facility.

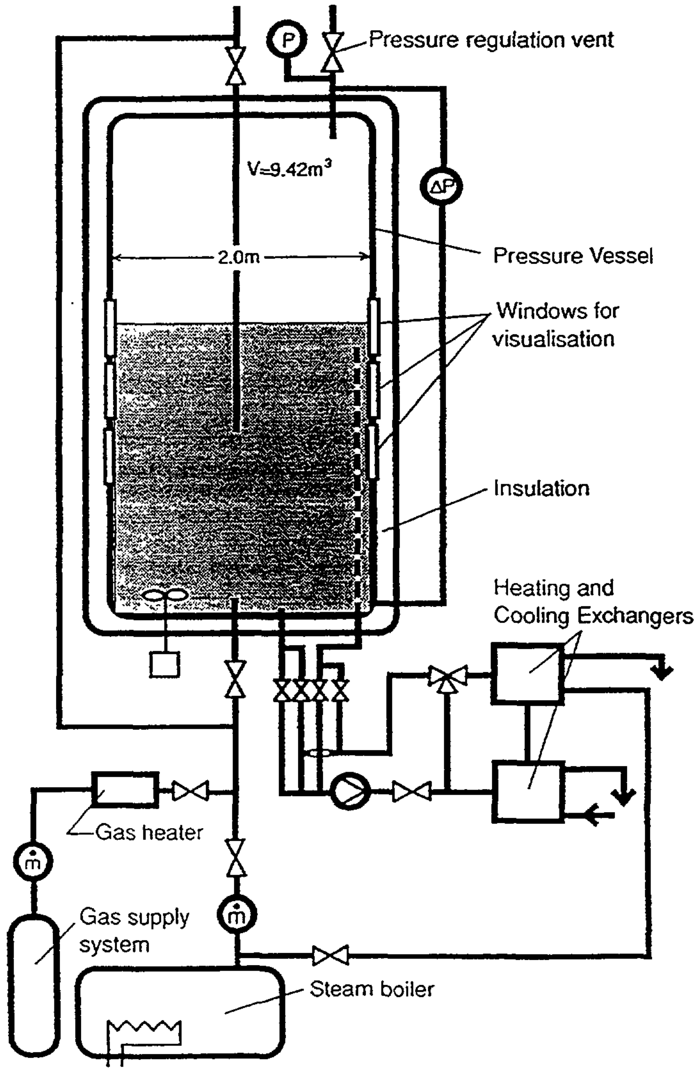

flow rate in a closed loop, and can be brought to the required temperature. This flow rate may be set between 0 and 10 m^3/h (± 40 l/h) and the water temperature between 15 and 180°C (±1°C). The maximal heating and cooling powers are about 140 and 120 kW, respectively.

In the SBWR, following primary system depressurization, a steam/air mixture flows into the Pressure Suppression Pool. The efficiency of the condensation and mixing processes there affects the Wetwell, and consequently the whole containment pressure level. The LINX-2 facility will be used to study PCCS venting in the Pressure Suppression Pools and the three-dimensional velocity and temperature fields created in the pool by the two-phase flow plume emerging from the vent. The experiments will give a better understanding of the physical phenomena and allow the development of ad-hoc models. Three-dimensional, multi-phase, multi-component CFD models, as well as simpler models intended for the system codes, will be proposed and assessed against the results and/or further developed.

The three-dimensional temperature field within the vessel may be investigated, without significant disturbance, using up to 273 thermocouples attached to 1 mm wires by miniature pinch-screw clips. A number of wires are mounted on a swinging arm, which allows radial scanning of the temperature field during an experiment. Six high-precision sensors are also available inside the vessel. Impeller-type anemometers will be used for velocity measurements, and double optical probes for two-phase flow investigations. A customized data acquisition system, together with a PC-based, multi-tasking software package, will provide the data acquisition needs.

A cooperation agreement was concluded in 1994 between ENEL (the Italian national electric utility) and PSI on ALWR thermal-hydraulics; a first common project has been defined and is underway. This concerns a PCCS proposed as a European alternative to the Westinghouse AP-600 passive containment cooling design. The purpose is to substitute a double concrete containment for the original AP-600 metallic envelope. Due to the high thermal resistance of concrete, the proposed PCCS needs a steam condensing heat exchanger placed inside the containment and an intermediate loop extracting the heat from the containment and taking it to an external atmospheric heat exchanger. The intermediate loop is a water-steam thermosiphon. The internal heat exchanger is a compact, finned tube bundle; non-condensable gases and steam circulate by natural draft. The external heat exchange takes place in a hybrid cooling tower, combining a water pool with a natural draft cooling tower.

Internal heat exchanger and intermediate loop mock-ups of this system will be tested in the LINX-2 facility. The use of finned tubes in a condensing heat exchanger allows the device size to be reduced. Accumulation of non-condensable gases and condensate in the spaces between fins could, however, take place, thus degrading heat transfer. Predictive computational models of this system are being developed and the experimental results will be used to assess and improve them.

For the passive PWR-related tests, in addition to the components depicted in Fig. 3, the facility is equipped with a closed gas (steam/air) recirculating loop. The recirculated gas flow rate (up to 0.5 kg/s) and its humidity are measured.

5. THE AIDA PROGRAM

The AIDA program examines the behavior of the PCCS system when aerosols are present in the containment, following a hypothetical severe accident. Under such conditions, aerosols present in the Drywell will be entrained into the PCCS condensers. This may degrade condenser performance. The condensers may, however, also act as scrubbers and help reduce the aerosol concentration in the Drywell.

The possible formation of an aerosol layer at the condenser tube entrance (reduction of tube-inlet free flow area) and inside the tubes (reduction of the tube cross-section) may cause a new flow distribution among the tubes; it will also affect their heat transfer performance. Flow redistribution among the tubes may change the heat removal characteristics of the entire PCCS system; such changes may appear as a result of a reduction in the number of tubes that are properly active, leading to a situation in which some tubes continuously receive more steam than they can condense. Thus, it is clear that, under hypothetical severe accident conditions, the long-term pressure history of the SBWR containment depends on the behavior of the PCCS units in the presence of aerosols. Consequently, the goals of the AIDA program are to:

- Experimentally determine the degree of PCC condensation degradation in the presence of aerosols.

- Investigate aerosol behavior in the upper header of the condenser units.
- Investigate aerosol behavior under strong condensation in condenser tubes.
- Investigate the aerosol retention capability of the condenser units.
- Provide the basis for the development of a physical model for aerosol behavior in the condensers and its effects on the thermal-hydraulics within the PCC units.

5.1. The AIDA Facility

A versatile, multiple-purpose aerosol testing facility was constructed at PSI [22] and is also being used for the AIDA tests. Two plasma torches, two reaction chambers, a mixing tank, and steam and non-condensable supply systems are the main components of the facility. The system is computer controlled and can produce aerosol particles at a desired steady mass flow rate and concentration. The particles are entrained by a carrier gas, composed of steam and non-condensable gas at a desired composition. The plasma torches used for aerosol generation produce aerosol mixtures of up to three components (CsI, CsOH and MnO or SnO_2) with a maximum concentration of 20 g/m^3. Experiments can be performed with the following boundary conditions:

- steam fraction ranging from 0 to 95%,
- steam flow rate up to 250 kg/hr,
- non-condensable gas flow rate up to 280 kg/hr,
- system pressure up to 5 bar..

For the AIDA experiments, a slice of the SBWR PCCS condenser unit containing eight full-height tubes and connected to full-diameter lower and upper headers, was constructed. Both glass and steel tubes can be tested. The glass tubes are intended mainly for visualization of the phenomena. The tubes are heavily instrumented with thermocouples to measure the gas and wall temperatures, and estimate the heat flux across the tube wall. The secondary coolant channel surrounding the tubes is made of glass to facilitate visualization of the aerosol deposition and transport phenomena within the glass tubes, Fig. 4. The secondary cooling water, flowing upward at a desired small velocity and at a predefined temperature (up to 80°C), can properly simulate the heat transfer conditions expected in the prototype.

The condensed water is collected in a Condensate Tank simulating the Gravity-Driven Cooling System (GDCS) pool, Fig. 5. The non-condensable gas and uncondensed steam flow into a Scrubber Tank that condenses the steam and scrubs the aerosol particles carried out of the condenser unit. The condensate that is produced in the Scrubbing Tank is collected in a second Collection Tank. The Scrubbing and Collection Tanks simulate the behavior of the Wetwell. The pressures in the Condensate and Collection Tanks are regulated to obtain the pressures expected in the Drywell and Wetwell.

The facility is instrumented with several devices to provide information on: a) energy transfer and steam mass balance related to steam condensation in the condenser, as well as in other parts of the experiment, and b) aerosol mass balances. The instruments provide on-line data that is displayed via a special data acquisition system on a computer screen to continuously monitor the system response. The aerosol instrumentation comprises: a) off-line devices like filters, impactors and deposition coupons, and b) on-line devices like photometers and ion detectors.

5.2. Aerosol Particle Trajectories

Certain knowledge about the behavior of the aerosols in parts of the PCCS system can be obtained by CFD calculations. Such information can later be integrated in aerosol behavior models, including their deposition and re-entrainment behavior. As a first step in this direction, aerosol tracking calculations with the ASTEC and FLOW3D codes were performed to examine aerosol behavior in the upper header of the AIDA condenser [12].

An aerosol-tracking model has been specially written for this application and interfaced with the ASTEC and FLOW3D codes. The calculations were conducted for the expected typical aerosol and flow conditions; they considered the deposition of the aerosols on a deflector plate placed below the steam-inlet tube in the upper header of the condenser unit, Fig. 6. The purpose of this deflector plate is to distribute the flow to the condenser tubes as well as possible; both the SBWR prototype condenser and the AIDA mockup have such plates installed.

The first calculations conducted assumed, in a simplistic manner, that all particles reaching a surface will be deposited and remain on the surface. With such a deposition "model", the results show that 98% of the aerosols which enter the drum with the inlet steam jet are deposited on the deflector plate. The remainder circulate in the upper part of the drum and finally deposit on its inner surface. To go a step further in the simulation and consider re-entrainment of the aerosols from the impact plate, calculations were performed assuming that particles could "spill-over" from the edges of the impact plate; this constitutes a very crude re-entrainment model. It was found that any particles that are subsequently dislodged from the plate have a 15% probability of entering one of the condenser tubes. The rest are deposited, more or less uniformly, in the upper drum. Clearly, the first steps taken in this direction must be supplemented and completed with more realistic aerosol deposition and re-entrainment models. The possibility of re-entrainment of aerosol agglomerations will also have to be addressed.

6. PANDA PRE-TEST CALCULATIONS

As part of the SBWR certification process, calculations to predict the outcomes of the experiments that will be conducted later in the PANDA facility are being performed and formally submitted to the US NRC. These "blind" pre-test calculations are done in collaboration with other SBWR international partners using the official SBWR safety analysis tool (the TRACG code). The pre-test calculations will be used as part of the validation data base for the application of TRACG to the SBWR. Following the experiments, post-test calculations will be performed, as needed, to resolve any outstanding issues.

Pre-test calculations for the steady-state PANDA PCCS condenser tests have been completed and submitted already. During 1994, the TRACG input model of PANDA was updated in a formal manner to satisfy the Quality Assurance (QA) requirements needed for such formal submissions. This included an independent design review of the model, an independent verification of all the numbers used against the facility data base (the as-built drawings), formal exchanges of comments and replies, and formal documentation of the entire procedure.

Two fully verified models were produced: The first is a partial model of the PCCS system used to predict the steady-state PANDA condenser performance tests; the second is a model of the entire PANDA facility, with initial and boundary conditions applicable to the first PANDA system test M3. The initial and boundary conditions for PANDA test M3 are based upon TRACG calculations of the state of the SBWR containment one hour after reactor scram. A counterpart GIRAFFE test will be carried through using the same initial boundary conditions.

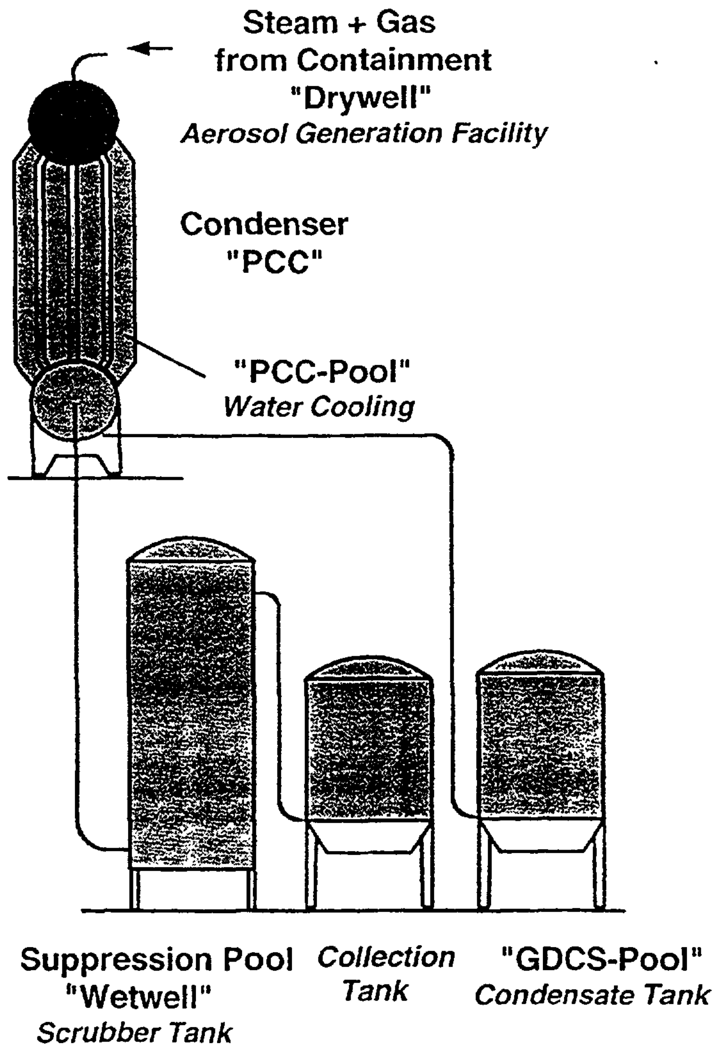

Fig. 4: The AIDA PCCS Mockup.

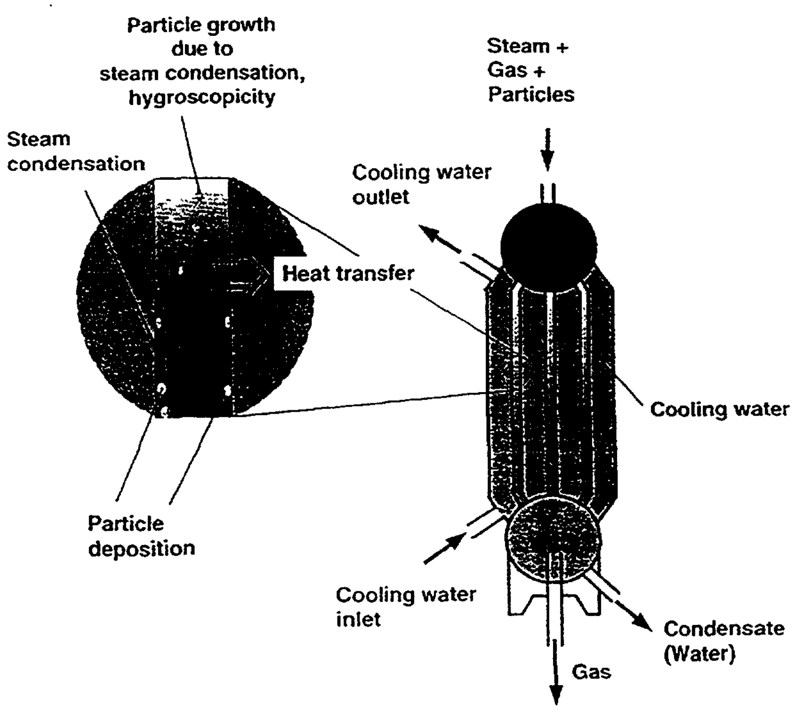

Fig. 5: The AIDA Facility Schematic.

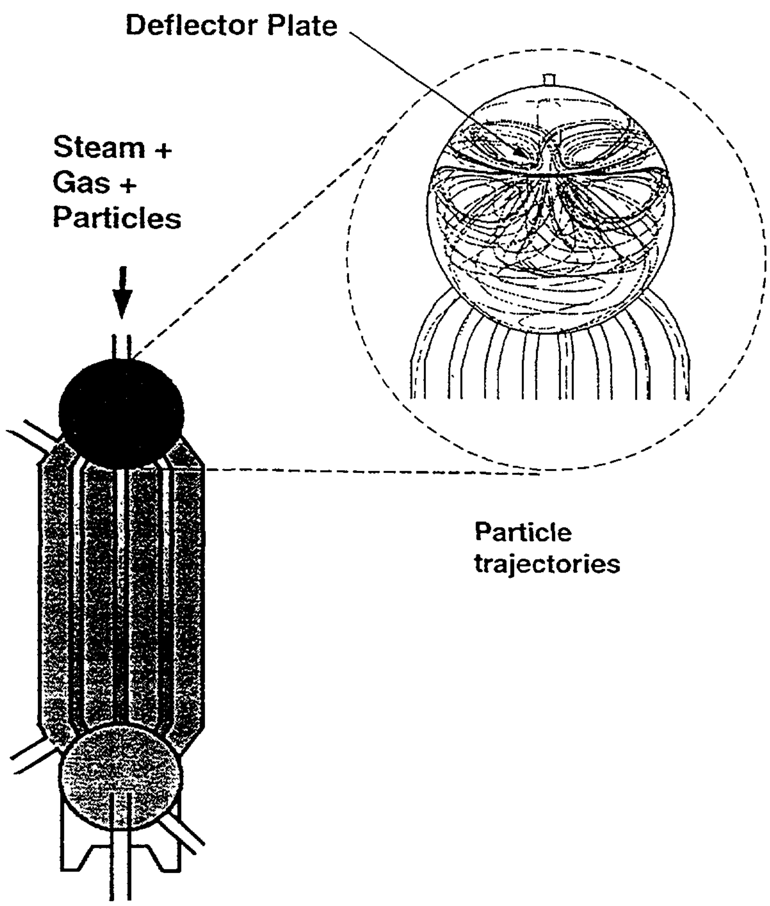

Fig. 6: Calculated Paths of Aerosol Particles in the Upper Header of the AIDA Condenser.
Top: most of the aerosols entering the header impact the deflector plate.
Bottom: aerosols are allowed to "spill over" from deflector plate.

Facility characterization tests will be performed, e.g. heat loss and pressure drop tests, and the models will be further improved using the information obtained from these tests.

The partners of this international collaboration have so far included PSI, which had the technical lead and produced the TRACG PANDA model and transient calculations, the IIE in Mexico, which provided model verification; KEMA in the Netherlands, which performed the condenser performance calculations, and the General Electric Company (GE) that provided overall coordination and the "Design Record File".

7. OTHER ACHIEVEMENTS

In addition to the main project activities outlined above, several scientific achievements that helped better understanding of system behavior and containment phenomena also took place. These include:

ALPHA staff members have made significant contributions to the understanding of the modes of passive operation of the SBWR. Contributions include, for example, detailed modeling of the condensation of steam in the presence of non-condensables in the PCCS units used to remove the decay heat from the containment [21].

An example of sophisticated but small-scale experiments and analytical modelling are the study of plumes in small-scale water pools (LINX-1) [8,9] and of two-phase flows of mixtures of air and steam bubbles in water (LINX-1.5) [10].

Development and testing of instrumentation has also taken place, triggered by the needs of the PANDA and LINX experiments (e.g., floating thermocouples for water surface temperature measurement, testing of non-condensable fraction sensors [23], etc.).

8. CONCLUSIONS

In several countries, there is a general move towards the introduction of more passive systems for emergency core cooling and containment decay heat removal in future reactors. In the US, this trend has materialized with the certification effort related to the AP-600 and the SBWR. In Europe, certain recent concepts for new BWRs and PWRs also include long-term passive decay heat removal systems. In Japan, Canada, and other countries there is interest in adding such passive systems to either existing reactor designs or to new ones. The ALPHA project is situated in this international framework. Its long-term objectives are to contribute at the forefront of this research area worldwide, but in Europe in particular.

As stated, future reactor systems are likely to include some form of passive containment cooling systems. Although the designs of such systems may vary from one reactor concept to another, there is a need to provide basic scientific understanding of their performance under fairly large-scale prototypical conditions. The PANDA and LINX-2 facilities provide the ideal environment for long-term international collaboration in this area. For example, the LINX-2 facility will be used in the near future to test, in collaboration with the Italian ENEL, the design of an advanced PWR containment building condenser.

Although the present PANDA experiments constituted initially "confirmatory" research, the data that they will deliver has now become an essential part of the "certification" process for the SBWR.

ACKNOWLEDGMENTS

All the members of the ALPHA team in the Thermal-Hydraulics Laboratory and of the AIDA team at the Safety and Accident Research Laboratory have contributed to the progress of the ALPHA project and, therefore, indirectly to this article. Their particular contributions are too numerous to mention here but are gratefully acknowledged by the authors.

The ALPHA project receives financial support from the Nuclear Power Committee of the Swiss Utilities (UAK), the (former) Swiss National Energy Research Foundation (NEFF) and the General Electric Company. Particular contributions from international collaborations are mentioned in the text.

The authors wish to acknowledge the Toshiba Corporation for permission to use data from the GIRAFFE facility.

REFERENCES

[1] CODDINGTON P., HUGGENBERGER M., GÜNTAY S., DREIER J., FISCHER O., VARADI G. AND YADIGAROGLU G., "ALPHA: The Long-Term Decay Heat Removal and Aerosol Retention Programme", 5th International Topical Meeting on Nuclear Reactor Thermal Hydraulics (NURETH-5), pp 203-211, Salt Lake City, USA, Sept. 1992.

[2] ANDERSEN J.G.M., ET AL., (1993b), "TRACG Qualification", Licensing Topical Report, NEDE-32177P, Class 3 (February 1993).

[3] CARLSON K.E., ET AL., "RELAP5/MOD3 Code Manual. Vol. I: Code Structure, System Models, and Solution Methods", NUREG/CR-5535, EGG-2596 (June 1990).

[4] VIEROW K.M. AND SCHROCK V. E.,"Condensation in a Natural Circulation Loop with Non-Condensable Gases, Part I Heat Transfer", Proc. Int. Conf. Multiphase Flows, Tsukuba, Japan, September 1991.

[5] SIDDIQUE M., GOLAY M.W. AND KAZIMI M.S., "Local Heat Transfer Coefficients for Forced Convection Condensation of Steam in a Vertical Tube in the Presence of a Non-condensable Gas", Nucl. Technol. 102 (1993) 386.

[6] YOKOBORI S., NAGASAKA H., TOBIMATSU T., "System Response Test of Isolation Condenser Applied as a Passive Containment Cooling System", 1st JSME/ASEM Joint International Conference on Nuclear Engineering (ICONE-I) Nov. 1991 Tokyo.

[7] BOTTI S. ET AL., "Tests on Full Scale Prototypical Condensers for SBWR Application", European Two-Phase Flow Group Meeting, SIET, June 6-8, 1994.

[8] SMITH B.L., DURY T.V., HUGGENBERGER M. AND NÖTHIGER H., "Analysis of Single-Phase Mixing Experiments in Open Pools", ASME Winter Annual Meeting, HTD-Vol. 209, pp 101-109, Anaheim, CA, USA, Nov. 1992.

[9] HUGGENBERGER M., NÖTHIGER H., SMITH B.L. AND DURY T.V., "Single-Phase Mixing in Open Pools", NURETH-5, pp 547-555, Salt Lake City, USA, Sept. 1992.

[10] CODDINGTON P. AND ANDREANI M. "SBWR PCCS Vent Phenomena and Suppression Pool Mixing", paper submitted to NURETH-7, 10-15 September 1995, Saratoga Springs, NY, USA.

[11] CODDINGTON P., "A TRACG Investigation of the Proposed Long-Term Decay Heat Removal Facility PANDA at the Paul Scherrer Institute", NURETH-5, pp 192-202, Salt Lake City, USA Sept. 1992.

[12] DURY T.V., "Pre-Test Thermal-Hydraulic Analysis in Support of the AIDA Testing Design Using the ASTEC Code", PSI internal report TM-42-94-10, ALPHA-409.

[13] HUGGENBERGER M., "PANDA Experimental Facility Conceptual Design", PSI internal report AN-42-91-09, ALPHA-105.

[14] DREIER J., "PANDA-Versuchsanlage; Pflichtenheft für Messung, Steuerung und Regelung", PSI internal report TM-42-92-21, ALPHA- 217.

[15] YADIGAROGLU G., "Scaling of the SBWR Related Tests", GE Nuclear Energy report NEDC-32288 (July 1994).

[16] CODDINGTON P., "A Procedure for Calculating Two-Phase Plume Entrainment and Temperature Rise as Applied to LINX and the SBWR", PSI internal report TM-42-94-01, ALPHA-401.

[17] CODDINGTON P., "A Review of the SBWR PCCS Venting Phenomena", PSI internal report TM-42-94-02, ALPHA-402.

[18] ANDREANI M., "Study of the Horizontal Spreading of Rising Two-Phase Plumes and its Effects on Pool Mixing", PSI internal report TM-42-94-05, ALPHA-404.

[19] ZUBER N., (1991), "Hierarchical, Two-Tiered Scaling Analysis" Appendix D to "An Integrated Structure and Scaling Methodology for Severe Accident Technical Issue Resolution", Nuclear Regulatory Commission Report NUREG/CR-5809, EGG-2659 (November 1991).

[20] ISHII M. and KATAOKA I., (1983), "Similarity Analysis and Scaling Criteria for LWR's Under Single-Phase and Two-Phase Natural Circulation," NUREG/CR-3267 (ANL-83-32).

[21] MEIER M., "SBWR-PCCS Numerical Integration Programme and Test Results", PSI in ternal report TM-42-94-08, ALPHA-406.
[22] S. GÜNTAY, G. VARADI, J. DREIER, "ALPHA- The Long-Term Passive Decay Heat Removal and Aerosol Retention Program", IAEA Advisery Group Meeting on the Technical Feasibility and Reliability of Passive Safety Systems, November 21-24,1994, Jülich, Germany.
[23] LOMPERSKI S., "High Temperature and Pressure Humidity Measurement Using an Oxygen Sensor", PSI internal report TM-42-94-03, ALPHA-403.

PREDICTED PERFORMANCE AND ANALYSIS OF ADVANCED WATER COOLED REACTOR DESIGNS

(Session II)

Chairman

G.D. MCPHERSON
United States of America

EVALUATION OF THE DESIGN OPTIONS FOR FUTURE POWER PLANTS: IDENTIFICATION OF THE SAFETY RELATED CRITERIA AND EVALUATION OF THE DECAY HEAT REMOVAL OPTIONS

G.L. FIORINI
Centre d'études de Cadarache,
France

Abstract

The Nuclear Reactor Division (DRN) of CEA is in charge of the evaluation of the design options for the future power plant. The objective of this report is the identification of the safety related concerns (criteria) that must be used to fulfil this task. Starting from the main levels of Defence in Depth, and taking into account the recommendations for future Nuclear Power Plants, these criteria are obtained using a functional approach (⇦What for ; What is to be done⇨). After the identification of these criteria, the exercise is performed, as a matter of example, for three options among those suggested for the Decay Heat Removal (DHR).

1. INTRODUCTION

The design options for future fission plant (systems, design features, materials) must be evaluated by the Nuclear Reactor Division (DRN) of CEA on the basis of several types of concerns : operation, safety, fuel cycle, economics, etc.

A task of which the Innovative Reactor Concept Service (CEA/DRN/DER/SIS) is in charge is the contribution to the evaluation of the design options on safety level and licensing. The final goal is the assessment of the **coherence between the design choices and the Defence in Depth principles**. The first objective of the task is to help formulate the **top level interim safety criteria** essentials to perform this evaluation. This is why, within the frame of this task, it is requested to develop a **standard ad-hoc methodology to identify such a criteria (safety concerns)**.All the design **safety related objectives** already formulated by the safety authorities and/or by the international advisory groups for the future power plants must be taken into account. The need for a systematic integrated approach, useful to select the design options, is justified because of number and complexity of the issues involved.

The main goal of the report is to suggest such a pragmatic approach for the identification of these safety related objectives and consequently for the selection of the criteria needed for the final evaluation.

2. RECALL ON THE SAFETY APPROACH FOR NUCLEAR PLANTS

2.1 Safety objectives and approach

An **high safety level** is advocated for future power plants.

To fulfil this objective the key recommendation is to design future fusion plants implementing the strategy of **Defence in Depth** (D. in D.). This approach, can be summarized as follows :

1. Priority to the **prevention** efforts to avoid incidents and accidents.
2. Design effort for an easier management of abnormal situations (**protection**).
3. Design effort to take into account and to mitigate the consequences of major accidents (**mitigation**).

Moreover, to cope with general requirements for future plants and still within the frame of a correct D. in D. implementation, it is essential to design the safety systems and their architecture in order to achieve :

1. an **extended defence** with an effort to prevent systematically potential accident initiators and take severe accidents into account; the aim is to tentatively reduce, at the prevention level, their potential consequences,
2. a **balanced defence** to avoid singularities among the different accident families contributing to the plant degradation,
3. a **gradual defence** to avoid short sequences and to allow the operator back-up at intermediate accident stages.

The interest of the proposed design options (and so their evaluation) must be judged on the basis of their coherence when compared to **all above objectives**.

2.2 Technical guide-lines

Following the reference /1/ the technical guidelines (principles) to concretize the above objectives cover the following items: ⇨General technical principles;⇨Specific principles: •Siting; •Design; •Manufacturing and construction; •Commissioning; • Operation; •Accident management; •Emergency preparedness

The reference /2/ recognizes the previous items as mandatory, and recommend the adoption of some complementary generic principles

- ⇨ The concept of plant design should be extended to include the operating and maintenance procedures required for it
- ⇨ Design should avoid complexity
- ⇨ Plants should be designed to be "user friendly"
- ⇨ Design should further reduce dependence on early operator action
- ⇨ The design of the system provided to ensure confinement of radioactive materials after a postulated accident should take into account the values of pressure and temperature encountered in severe accident analysis
- ⇨ Accidents that would be large contributors to risk should be designed out or should be reduced in probability and/or consequences
- ⇨ The plant should be adequately protected by design against sabotage and conventional armed attack
- ⇨ Design features should reduce the uncertainty in the results of probabilistic safety analysis
- ⇨ Consideration should be given to passive safety features

As a complement of these international guide-lines, French safety authorities ask explicitly for the reduction of common mode failures /3/ The implementation of functional redundancies capabilities (two or more systems to realize the same safety function) is recommended to fulfil this objective Those recommendations have been confirmed within the frame of the European Pressurized Reactor (EPR) activities A common **French and German safety authorities** report /4/ precognize the evolutive appproach for the future EPR. The role of the defence in depth is stressed and a significant reduction of radioactive releases due to all conceivable accidents -including core melt accidents- is explicitely requested. Among the suggested technical principles it is interesting to recall the following

- ⇨ **Quality of design, manufacturing, construction and operation** to point out the importance for the inspectability and the testability of equipments
- ⇨ **Reduction of frequency of initiating events** to reduce the frequency of occurrence of accidents (including core melt accidents)
- ⇨ **Improved plant transient behaviour** to avoid unnecessary safety systems actions
- ⇨ **Redundancy and diversity** to be consistent with the general objective of reducing the probabilities of occurrence of accidents
- ⇨ **Active and passive systems** in order to identify the advantages and the disadvantages of passive systems
- ⇨ **Integrity of primary circuit** as well as the integrity of the other safety related high energy components and piping within the containment systems to reduce the potential containments loads
- ⇨ **Man-machine interface** to take advantage of the human abilities, while minimizing the possibilities for human erors and making the plant less sensitive to these errorsi
- ⇨ Qualification of computerized systems **to obtain the necessary high reliability for instrumentation and control systems**

The use of **probabilistic safety assessment** is suggested to support the design options, a well balanced safety concept and the valuation of expected deviations from present French and German safety practices

The reference /4/ also recommend that accident situations which would lead to large early releases have to be **"practically eliminated"** (when they cannot be considered as physically impossble, design provisions have to be taken to design them out) reactivity accidents, high pressure core melt situations, global Hydrogen detonation **Low pressure core melt accidents have to be "deal with"**, so that the associated conceivable releases would necessitate only **very limited protective measures in area and in time** The objective of significant reduction of the radioactive releases implies a substantial improvement of the containment function To do this, among others, the residual heat must be removed from the containment without venting device For this function, a last-resort heat removal system must be installed this system should be **preferably passive** with respect to its primary circuit inside the containment

2.3 Defence in Depth (D. in D.) implementation

As stated above, the design effort must be coherent with the D in D approach through the implementation of three generic goals prevention, protection and mitigation These goals can be expanded to obtain five levels of D in D

Prevention	1st	conservative design, quality assurance, safety culture
Protection	2nd	**control** of abnormal operations and detection of failures
	3rd	**protection** and safeguard systems
Mitigation	4th	**major accident management** including containment protection
	5th	off-site emergency response **(consequences mitigation)**

NOTE It is essential to note that through the fourth and fifth levels, the Defence in Depth approach requires an ultimate demonstration of the plant safety, taking into account, as a matter of routine, the plant degradation (severe accident) The reasons of this last requirement can be interpreted as follows

a. *to cover the eventual **lack of exhaustivity** of the selected deterministic sequences,*
b. *to demonstrate the **potential of the concept for mitigating severe accidents**,*
c. *to demonstrate the **avoidance**, by design, **of any cliff edge effect**.*
(The cliff edge is a discontinuity in the relationship between the frequencies and the consequences that defines the risk : Risk = frequency x consequences).

3. SAFETY CONCERNS

The section 2.2 presents some generic recommendations and the technical guide-line that must be taken into account for future nuclear plants. Starting from the Defence in Depth levels (see section 2.3) all these indications are integrated and developed following a **functional analysis approach**. This approach, currently used for the **value analysis**, details generic specifications (**what for**) suggesting more and more detailed technical solutions (**what is to be done**).

The methodology allows to identify:
- the generical criteria for the evaluation of the main plant design options,
- the specific safety concerns (or specific criteria) for the evaluation of the safety function related system, subsystems or components.

The first steps are presented on Table 1 (left hand). After the generical criteria (level 1 (⇨)) applicable to the future reactors, the identified safety concerns (or design safety related objectives - level 2 (•)) are still generic and **must be applied to all safety related design options**. A further step is presented still on Table 1 (left hand). As a trial measure, the methodology is applied to the decay heat removal identifying the design specifications (safety function related objectives - level 3 (*)) proper to the corresponding systems, subsystems or components.

4. OPTIONS FOR THE DECAY HEAT REMOVAL

4.1 Options
Several options for the decay heat removal coolant have been proposed for the implementation on future NPP. Three among them are choosen to present and discuss the suggested methodology.

OPTION	System	Comments
1	PRHR	Passive Decay Heat Removal system implemented on the primary circuit of the AP600 concept. Studies have been performed at the CEA to implement similar system on a 900 MW PWR (see diagram).
2	RRP	Passive/active Decay Heat Removal system. Heat exchangers installed within the primary vessel Studies have been performed at the CEA to design the system for a 900 MW PWR (see diagram; /5/ for the performances).
3	SCS	Passive Decay Heat Removal system implemented on the secondary circuit of the SIR concept. Studies have been performed at the CEA to implement similar system on a 900 MW PWR (see diagram; /5/ for the performances).

4.3. Qualitative evaluation of the heat removal

The different options are evaluated using the safety concerns identified and listed on table 1. The appreciation is expressed in term of **Favourable** ⇧; **unfavourable** ⇩; **unaffected** ⇨. The preliminary evaluation results are tentatively (and not completly) summarized on tables 1 (right hand). This allows to identify the pro and cons of each option. Those results are essential to identify, motivate and prioritize the R & D efforts that support the system design activities.

The details of these results are not commented here. The main objective of the report is to present the methodology. The design objectives presented on table 1 are **open for discussion** to improve their coherence versus the claimed goals. The system qualitative evaluations are also preliminary and **must be discussed in detail**.

5. CONCLUSIONS

The discussion of the recommendations already available for future nuclear plants provide clear guidelines directly applicable for the design. The Defence in Depth approach remains the reference. Its correct implementation leads to take care of all the levels (prevention, protection, mitigation) and provide an extended, gradual and well balanced defence.

The development of these levels following a functional approach (what for ↔ what is to be done) allows to identify a series of technical generic design objectives for future nuclear plant. The development can be pursued to define the objectives/criteria needed for the evaluation of the systems, subsystems or components, related to a safety function. The report provides a first proposal for the methodology and identifies, as a matter of example, the evaluation criteria useful for a comparative qualitative evaluation among different design options for Decay Heat Removal. Similar approach can easily be applied for the evaluation of the design options in charge of the other important safety functions e.g. Reactivity Control and Fission Products Containment.

It is important to point out that the results of this approach are essential to **identify, motivate and prioritize the R & D efforts** that support the system design activities.

TABLE 1

FUTURE PWR

DECAY HEAT REMOVAL (DHR) FUNCTION - COMPARATIVE EVALUATION AMONG DIFFERENT DHR SYSTEMS

Implementation of a PRHR system, or a RRP system; or a SCS system for the Decay Heat removal of a future standard PWR.

Identification of the **favourable (⇧)**, **unfavourable (⇩)**, **indifferent (⇨)** contributions linked to the systems implementation

PRHR system; or RRP system, or SCS system for the Decay Heat Removal of a future standard PWR. Identification of the contribution linked to the implementation of each system **Favourable ⇧; unfavourable ⇩; indifferent ⇨**				
SYSTEMS	PRHR	RRP	SCS	Comments
1st level : PREVENTION conservative design, quality assurance, safety culture				
⇨ Elaborate a simplified design				
• Elaborate a simplified neutronic design				
• Elaborate a simplified thermohydraulic design				
• *Simplify the vessel internals*	⇨	⇩	⇨	RRP - Increased complexity within the vessel
• *Simplify the thermohydraulic for the normal DHR*	⇧	⇧	⇧	
• *Simplify the thermohydraulic for the safeguard DHR*	⇩ ⇧	⇧	⇧	PRHR ⇩ Steam generator thermally isolated RRP - The DHR function efficiency is still guaranted with low primary water inventory
• *Separe the normal operating DHR function from the safeguard DHR*	⇧	⇧	⇧	Systems for normal and/or safeguard DHR ?
• *Increase the range covered by normal DHR systems (forced conv., natural conv)*	⇧	⇧	⇧	(→must be defined after accurate design)
• *Reduce the number of components per system*	⇧	⇧	⇧	
• *Standardize the components among normal operating DHR and safeguard DHR*	⇧	⇧	⇧	
• Elaborate a simplified thermomecanic design				
• *Simplify the vessel internals*	⇨	⇩	⇨	RRP - Increased complexity within the vessel
• *Reduce the number of systems connected to the primary circuit*	⇩	⇧	⇧	PRHR implemented as an extension of the P C
• *Reduce the impact of transients*	⇩ ⇧?	⇧	⇩ ⇧	PRHR(⇧?), SCS ⇧ with thermal valve
• *Minimise the thermomechanical loads (pressure versus geometry, ΔP)*	⇩	⇧	⇧	The risk for overcooling in case of complete system
• *Reduce the number of components per system*	⇧	⇧	⇧	intervention must be evaluated
⇨ Satisfy the design rules				
• Elaborate a design consistent with all the plausible situations				
• *Take into account the Passive Single Failure criterion for the short term*	⇩	⇧ ⇩	⇧	PRHR - Primary LOCA, RRP ⇩ in case of internal heat
• Qualify the materials (mechanical, electrical, etc.)				exchangers (IHX) tubes rupture
• *Qualify the materials for the planned function (performances)*	⇧	⇧	⇧	
• *Qualify the materials versus the requested reliability*	⇧	⇧	⇧	
• *Qualify the materials versus the requested availability*	⇧	⇧	⇧	
• *Qualify the materials for the espected environmental conditions*	⇧	⇧	⇧	
• *Plan the possibility for representative tests*	⇧	⇧	⇧	
• *Standardize the components among systems (improve the feedback experience)*	⇧	⇩	⇧	RRP - Ad hoc in vessel exchangers
⇨ Simplify the reactor operations and the maintenance procedures for normal conditions (human factor for operation and shut down)				
• Improve the quality of the information (operational data)				
• *Implement adequate control on systems behaviour and status*	⇧	⇩?	⇧	RRP - Difficulties for IHX instrumentation? (anyhow reduced needs)
• Improve the man-machine interface	⇧	⇧	⇧	Systems easy to operate
• Simplify and automatize the procedures for the operation	⇧	⇧	⇧	Systems easy to operate
• Simplify and automatize the procedures for the inspection	⇧	⇩	⇧	RRP - Difficulties for IHX inspection
• Simplify and automatize the procedures for the maintenance and preventive repair	⇧	⇩	⇧	RRP - Difficulties for IHX maintenance and repair

TABLE 1 (cont.)

PRHR system; or RRP system; or SCS system for the Decay Heat Removal of a future standard PWR. Identification of the contribution linked to the implementation of each system **Favourable ⇧; unfavourable ⇩; indifferent ⇨**				
SYSTEMS	PRHR	RRP	SCS	Comments
1st level :PREVENTION conservative design, quality assurance, safety culture (follows)				
⇨ Integrate the principles of the defence in depth : balanced, gradual and extended defence				All the systems can be considered as indipendent LOD Their correct implementation leads to improve the Defence in Depth principle
• Take care to the balanced character of the implemented defence				
• *Implement an homogeneous number of Lines of Defence (LOD) for each operating condition (OC : PIE applied to an Initial plant status)*	⇧	⇧	⇧	
• Take care to the gradual character of the implemented defence				
• *Implement functional redundancies: indipendent LOD*	⇧	⇧	⇧	
• Take care to the extensive character of the implemented defence				
• *For each operating condition, implement an number of Lines of Defence (LOD) coherent with the probabilistic objectives →(2a+b)*	⇧	⇧	⇧	
⇨ Minimize the personnel exposure during normal operation				
• Minimize the contact dose				
• *Reduce the corrosion phenomena and the radioactive products transport*	⇩?	⇩?	⇧	PRHR, RRP Increased surfaces of the second barrier
• Limit the length of circuits which carry activated fluid				Negligible versus the SG?
• *Reduce the portions of circuits that carries primary coolant*	⇩	⇧	⇧	PRHR implemented as an extension of the P C
• Minimize the maintenance times for normal conditions				
• *Improve the accessibility*	⇩	⇩	⇧	PRHR implemented as an extension of the P C
• *Foresee equipments and robots*	⇧	⇩	⇧	RRP - Difficulties for IHX accessibility
⇨ Minimize radioactive waste during normal operation	⇨	⇨	⇨	Globally indifferent
• Simplify the chemistry of the primary circuit				
• Reduce the self -generation of radioactive waste				
• Reduce the corrosion phenomenon	⇩?	⇩?	⇨	PRHR, RRP Increased surfaces of the second barrier
• Ensure the good materials behaviour under irradiation				Negligible versus the SG?
⇨ Minimize the frequency for the Postulated Initiating Events (PIE - abnormal situations; during normal operation and shut down) :				
▫ Control rod withdrawal				
▫ Uncontrolled boron dilution				
▫ LOFA - Sequences initiated by loss of primary coolant flow				
▫ Loss of charge / turbine trip				
▫ Loss of normal feedwater				
▫ Loss of external electrical power supply				
▫ LOCA - Sequences initiated by a leakage of primary coolant	⇩	⇧⇩	⇨	PRHR, RRP Increased surfaces of the second barrier
• *Reduce the number of chipping on primary loops*				Negligible versus the SG?
• *Minimise the length of the loops which carry primary fluid*				RRP tubes 0 external loads (pressure outside) are
• *Minimise the fluids internal energy (primary pressure)*				favourable
• *Reduce the corrosion phenomenon*				
▫ Sequences initiated by loss of secondary coolant or heat sink	⇨	⇩	⇩	RRP, SCS increased lenght of secondary loops
• *Minimise the length of the loops which carry secondary fluid*				(RRP - small inertia in case of loop rupture)
• *Minimise the fluids internal energy (secondary pressure)*				
• *Reduce the corrosion phenomenon*				
▫ Steam Generator tubes rupture	⇨	⇩⇨	⇨	RRP - IHX tubes equivalent to the SG ones,
• *Minimise the fluids internal energy (ΔP primary/secondary pressure)*				nevertheless the external loads (pressure outside) are
• *Reduce the corrosion phenomenon*				favourables

TABLE 1 (cont.)

PRHR system; or RRP system; or SCS system for the Decay Heat Removal of a future standard PWR.
Identification of the contribution linked to the implementation of each system
Favourable ⇧; unfavourable ⇩; indifferent ⇨

SYSTEMS	PRHR	RRP	SCS	Comments
1st level :PREVENTION conservative design, quality assurance, safety culture (follows)				
⇨ Minimize the potential for Common Modes (Initiators)				
• Separate and diversify the systems				
• *Diversify the components*	⇧	⇩	⇧	RRP - Difficult to diversify the IHX
• *Keep segregate the single loops*	⇧	⇧	⇧	
• Minimize the potential for flooding	⇨	⇨	⇨	
• *Put out of water the compnents important for safety*				
• Minimize the potential for fires	⇨	⇨	⇨	
• *Implement incombustible materials*				
• Qualify the material for the earthquake	?	?	?	The earthquake response must be carefully analysed
⇨ Minimize the inherent potential consequences for the PIE (oper. and shut down) :				
○ Control rod withdrawal				
○ Uncontrolled boron dilution				
○ LOFA Sequences initiated by loss of primary coolant flow				
• *Foresee an adequate pump inertia*	⇨	⇨	⇨	
• *Foresee the natural convection behaviour*	⇧	⇧	⇧	
○ Loss of charge / turbine trip				
• *Foresee the natural convection behaviour*	⇧	⇧	⇧	
○ Loss of normal feedwater				
• *Foresee the natural convection behaviour*	⇧	⇧	⇧	
○ Loss of external electrical power supply				
• *Foresee the natural convection behaviour*	⇧	⇧	⇧	
○ LOCA Sequences initiated by a leakage of primary coolant				
• *Minimise the primary depressurisation effects (on the three barriers)*	⇨	⇨	⇨	
• *Ensure the DHR with reduced primary water inventory*	⇨	⇧	⇨	RRP - The DHR function efficiency is still guaranted with low primary water inventory
○ Sequences initiated by loss of secondary coolant or heat sink				
• *Minimise the secondary depressurisation effects (on the three barriers)*	⇨	⇨	⇨	
○ Steam Generator tubes rupture				
• *Confine the secondary discharges*	⇨	⇨	⇨	
⇨ Avoid by design (prevent) the sequences that can leads to unacceptable consequences and early releases. Reject the risk for the cliff edge effect				
• Avoid by design the reactivity excursions				
• Avoid by design the core melting under high primary pressure conditions				
• *Participate efficiently to the primary circuit depressurisation*	⇩ ⇧	⇧	⇧	The systems can actively participate to the primary circuit depressurisation. PRHR ⇩ - SG thermally isolated : primary circuit still pressurized
• Avoid by design the core melting concomitant to the loss of the containment (bypass).	?	?	?	The systems potential for DHR in case of severe accident is not clearly established
• *Foresee an ultimate passive DHR system within the containment*	⇧	⇧	⇧	
• *Set up within the containment all the loops that carry primary coolant*	⇧	⇩ ⇧	⇩ ⇧	RRP ⇧ what internal heat exchanger SCS ⇧ With internal pool
• *Foresee the isolation of all intermediate loops at the containment level*				
• Avoid by design the risks for the steam explosions				
• Avoid by design the risks for the Hydrogen detonation				

TABLE 1 (cont.)

PRHR system; or RRP system; or SCS system for the Decay Heat Removal of a future standard PWR. Identification of the contribution linked to the implementation of each system **Favourable ⇧; unfavourable ⇩; indifferent ⇨**				
SYSTEMS	PRHR	RRP	SCS	Comments
★ **2nd level :CONTROL** control of abnormal operations and detection of failures				
⇨ Detect the Postulated Initiating Events (PIE - operation and shut down) -	⇨	⇨	⇨	Globally indifferent
▫ Control rod withdrawal				
▫ Uncontrolled boron dilution				
▫ LOFA Sequences initiated by loss of primary coolant flow				
▫ Loss of charge / turbine trip				
▫ Loss of normal feedwater				
▫ Loss of external electrical power supply				
▫ LOCA Sequences initiated by a leakage in primary coolant				
▫ Sequences initiated by loss of secondary coolant or heat sink				
▫ Steam Generator tubes rupture				
⇨ Minimize the uncertainties about the plant conditions				
• Implement an adequate instrumentation (for automatic and manual devices)				
• *Foresee an instrumentation able to identify without ambiguity the systems configurations and the consequences on the control parameters*	⇧	⇧	⇧	Passive systems reduced need for instrumentation and control
• Implement a design that simplify the abnormal sequences				
• *Dispose of the natural convection within the primary circuit*	⇧	⇧	⇧	These advantages arise from the passive character of the
• *Dispose of the natural convection within the secondary loops*	⇧	⇧	⇧	systems
⇨ Simplify the plant inherent behaviour under abnormal conditions (operation and shut down)				
▫ Control rod withdrawal				
▫ Uncontrolled boron dilution				
▫ LOFA - Sequences initiated by loss of primary coolant flow				
• *Foresee an adequate pump inertia*	⇨	⇨	⇨	
• *Foresee the natural convection behaviour*	⇧	⇧	⇨	Easy natural convection on the primary circuit
▫ Loss of charge / turbine trip				
• *Implement passive and efficient functional redundancy*	⇧	⇧	⇧	
▫ Loss of normal feedwater				
• *Implement passive and efficient functional redundancy*	⇧	⇧	⇧	
▫ Loss of external electrical power supply				
• *Implement passive and efficient functional redundancy*	⇩ ⇧	⇧	⇧	PRHR ⇩ - SG thermally isolated
▫ LOCA - Sequences initiated by a leakage in primary coolant				
• *Foresee the passive cooling of the primary coolant still within the vessel*	⇨	⇧	⇨	RRP - The DHR function efficiency is still guaranted
• *Foresee the passive coolant injection to guarantee the primary coolant inventory*	⇨	⇨	⇨	with low primary water inventory
• *Foresee the passive cooling of the primary coolant rejected in the containment (Control the containment temperature and pressure)*	⇨	⇨	⇨	
▫ Sequences initiated by loss of secondary coolant or heat sink				
• *Foresee the passive cooling of the primary coolant*	⇩ ⇧	⇧	⇧?	PRHR ⇩ - SG thermally isolated
	⇨	⇨	⇨	SCS - efficient if the secondary breach is isolated
• *Foresee the passive cooling of the secondary coolant rejected in the containmen (Control the containment temperature and pressure)*				
▫ Steam Generator tubes rupture				
• *Avoid the activation of the secondary overflow valves*	⇧?	⇧	⇧	The systems can contibute to depressurize the primary
• *Confine the secondary discharges*	⇨	⇨	⇨	circuit (PRHR ?)

TABLE 1 (cont.)

PRHR system, or RRP system, or SCS system for the Decay Heat Removal of a future standard PWR. Identification of the contribution linked to the implementation of each system **Favourable ⇧, unfavourable ⇩; indifferent ⇨**				
SYSTEMS	PRHR	RRP	SCS	Comments
★ **2nd level :CONTROL** control of abnormal oper and detection of failures (follows)				
⇨ Elaborate a forgiving design				
• Ensure appropriate physical margins				
• *Improve the system efficiency*	⇧	⇧	⇧	RRP The DHR function efficiency is still guaranted with low primary water inventory
• *Increase the common range covered by complementary systems*	⇧	⇧	⇧	The risk for overcooling in case of complete system intervention must be evaluated
• Ensure appropriate grace period	⇧	⇧	⇧	
• *Increase the process internal inertia*				
• *Provide the passive access to adequate external inertia*				
• Limit the intervention of safeguard functions (unnecessary safety systems actions)	⇧	⇧	⇧	Potentially favourable The role of the systems must be
• *Foresee control and limitation devices*				clearly defined
⇨ Take into account aggravating situations (coherently with the PIE category)				
• Take into account the corrective functions unavailability for maintenance				
• *Foresee an internal redundancy*	⇧	⇧	⇧	Separate loops for all the systems
• Take into account the PIE with cumulative system failures				
• *Take into account the Operating Conditions (OC) with the Loss of Offsite Power*	⇧	⇧	⇧	
• *Take into account the OC considering the Single Failure Criterion*	⇧	⇧	⇧	
• *Take into account the OC with internal and external hazards*	?	?	?	PRHR and SCS are perhaps more sensible to the external hazards must be verified
⇨ Simplify the reactor operations and maintenance procedures under abnormal conditions (human factor for operation and shut down)				
• Improve the quality of the information (operation data)				
• Simplify and automatize the procedures for the plant oper under abnormal cond				
• *Improve the man machine interface*	⇧	⇧	⇧	Easily operate
• *Limit the interactions among systems that perform the same function*	⇧	⇧	⇧	Dedicated systems
• *Implement safety system automatisation*	⇧	⇧	⇧	Passive systems
• Simplify and automatize the procedures for the plant inspection, maint. and repair				
• *Improve the accessibility*	⇩	⇩	⇧	PRHR, RRP difficult to access SCS 0 if the pool is
• *Foresee equipments and robots*	⇩	⇩	⇧	outside the containment
⇨ Minimize the personnel exposure under abnormal conditions (oper and shut down)				
• Strengthen the first barrier				
• Strengthen the second barrier				
• *Reduce the portions of circuits that carries primary coolant*	⇩	⇧	⇧	RRP SCS favourable except in case of
• Reduce the time for the intervention under abnormal conditions				primary/secondary breach
• *Improve the accessibility*	⇩	⇩	⇧	PRHR, RRP difficult to access SCS 0 if the pool is
• *Foresee equipments and robots*	⇩	⇩	⇧	outside the containment
⇨ Minimize the radioactive waste under abnormal conditions (oper and shut down)				
• Strengthen the first barrier				
• Strengthen the second barrier				
• *Conceive the circuits connected to the primary*				
- permanently → installed within the containment	⇧	⇧	⇨	RRP with intermediate heat exchanger within the
- temporarely → eventually outside but isolable	⇨	⇨	⇨	containment (internal heat exchanger)
• *Conceive the circuits connected to the secondary*				
→ designed to the maximum injection pressure	⇨	⇧	⇧	
→ in order to confine the discharge within the containment	⇨	⇨	⇨	
• Strengthen the third barrier				
• *Limit the number of containment penetrations*	⇧	⇧⇩	⇧⇩	PRHR 0 for the AP600 configuration RRP 0 with external heat exchanger SCS 0 if the pool is inside the containment

TABLE 1 (cont.)

PRHR system; or RRP system; or SCS system for the Decay Heat Removal of a future standard PWR. Identification of the contribution linked to the implementation of each system **Favourable ⇧; unfavourable ⇩; indifferent ⇨**				
SYSTEMS	PRHR	RRP	SCS	Comments
★3rd level : PROTECTION <u>safety systems and protection systems</u>				
⇨ Minimize the uncertainties about the plant conditions under accidental conditions (operation and shut down)				
• Implement an adequate instrumentation (for automatic and manual devices)	⇧	⇧	⇧	Passive systems reduced need for instrumentation and control
• *Foresee an instrumentation able to identify without ambiguity the systems configurations and the consequences on the control parameters*				
• Implement a design that simplify the accidental sequences	⇧	⇧	⇧	These advantages arise from the passive character of the systems
• *Reduce the number of possible systems response configurations*				
• *Dispose of a primary circuit natural convection configuration*				
• *Dispose of a primary circuit natural convection configuration*				
⇨ Simplify the reactor management under accidental conditions (oper. and shut down)				Due to the degraded situation, the systems favourable contibution is due to the passive character of their intervention
▫ Control rod withdrawal				
▫ Uncontrolled boron dilution				
▫ LOFA - Sequences initiated by loss of primary coolant flow	⇧	⇧	⇧	
▫ Loss of charge / turbine trip	⇧	⇧	⇧	
▫ Loss of normal feedwater	⇧	⇧	⇧	
▫ Loss of external electrical power supply	⇧	⇧	⇧	
▫ LOCA - Sequences initiated by a leakage in primary coolant	⇨	⇧	⇨	RRP - The DHR function efficiency is still guaranted with low primary water inventory
▫ Sequences initiated by loss of secondary coolant or heat sink	⇧	⇧	⇧	SCS - efficient only if the secondary breach is isolated
▫ Steam Generator tubes rupture	⇧	⇧	⇧	
⇨ Take into account aggravating situations (coherently with the PIE category)				
• Take into account the safeguard functions unavailability for maintenance				
• *Foresee a functional redundancy*	⇧	⇧	⇧	
• Take into account the PIE with cumulative safeguard system failures (multiple failure situations)				
• *Take into account the Operating Conditions (OC) with the Loss of Offsite Power*	⇧	⇧	⇧	
• *Take into account the OC considering the Single Failure Criterion*	⇧	⇧	⇧	
• *Take into account the OC with internal and external hazards*	?	?	?	PRHR and SCS are perhaps more sensible to the external hazards - must be verified
• Take into account the loss of the redundant systems (complementary situations)				
• *Foresee an ultimate passive DHR within the containment*	⇨?	⇨?	⇨?	A systems contribution can perhaps be envisaged
⇨ Minimize the potential for Common Modes (mutual agressions, internal or external hazards)				
• Separate and diversify the safety systemes				
• *Avoid any physical interaction between the systems in case of failure*	?	?	?	The contribution can be effectively appreciated only after accurate design analysis
⇨ Simplify the accidental intervention procedures under accidental conditions (human factor for operation and shut down)				
• Ensure an adequate information (abnormal situation)				
• Simplify and automatize the procedures for the accident management				
• *Improve the man-machine interface*	⇧	⇧	⇧	Easy to operate
• *Limit the interactions among systems that perform the same function*	⇧	⇧	⇧	Dedicated systems
• *Implement safety system automatisation*	⇧	⇧	⇧	Passive systems
• Simplify and automatize the procedures for the plant inspection, and repair				
• *Improve the accessibility*	⇩	⇩	⇧	PRHR, RRP difficult to access, SCS ⇧ if the pool is outside the containment
• *Foresee equipments and robots*	⇩	⇩	⇧	

TABLE 1 (cont.)

PRHR system; or RRP system; or SCS system for the Decay Heat Removal of a future standard PWR. Identification of the contribution linked to the implementation of each system **Favourable ⇧; unfavourable ⇩; indifferent ⇨**				
SYSTEMS	PRHR	RRP	SCS	Comments
★3rd level : PROTECTION safety systems and protection systems				
⇨ Reduce the core melt frequency				
• Improve the availability of the safeguard systems	⇧	⇧	⇧	These generic favourable contributions must be
• Implement an adequate functional redundancy for the important safety functions	⇧	⇧	⇧	quantified through probabilistic safety assessment
⇨ Minimize the offsite accidental release (without core melt)				
• Conceive the plant in order to guarantee no necessity for protective measures				
• *Strengthen the third barrier*	⇧	⇧⇩	⇧⇩	PRHR ⇧ for the AP600 configuration RRP ⇧ with internal heat exchanger SCS ⇧ if the pool is inside the containment

PRHR system; or RRP system; or SCS system for the Decay Heat Removal of a future standard PWR. Identification of the contribution linked to the implementation of each system **Favourable ⇧; unfavourable ⇩; indifferent ⇨**				
SYSTEMS	PRHR	RRP	SCS	Comments
★ 4th level : MAJOR ACCIDENT MANAGEMENT accident management including the confinement protection				
⇨ Take into account the severe accident configurations				
• Ensure the safety function accomplishment under severe accident conditions				
• *Foresee the DHR with severe accident configurations:*				
- *Corium within the primary vessel*	⇧?	⇧	⇧?	RRP - The efficiency versus the DHR function is still guaranted with low primary water inventory For the PRHR and SCS the efficiency must be demonstrated
- *Corium within the containment (core catcher)*	⇧?	⇧?	⇧?	
• Protect the material against the potential hazards (steam explosion, H2 deflag., etc.)				
• *Protect the material against the following hazards: corium, H_2 deflagration, temperature, pressure, etc*	⇧	⇩	⇧	RRP - More sensible to the potential in-vessel agressions
⇨ Minimize the uncertainties about the plant conditions under severe accidental conditions (operation and shut down)				
• Implement an adequate instrumentation				
• Elaborate a design that simplifies the inherent plant accidental scenarii	⇧?	⇧?	⇧?	Internal containment natural convection configurations the systems efficiency must be demonstrated
⇨ Simplify the reactor operations procedures under severe accident conditions				
• Improve the grace delay				
• *Implement an ultimate passive DHR for the corium cooling*	⇧?	⇧?	⇧?	Internal containment natural convection configurations the systems efficiency must be demonstrated
⇨ Minimize the offsite accidental release (low pressure core melt situations)				
• Conceive in order to need only very limited protective measures in area and in time				
• *Qualify the third barrier to the configurations with the low pressure core melt· guarantee its cooling*	⇨?	⇨?	⇨?	The systems contribution to the third barrier strenght must be evaluated

TABLE 1 (cont.)

PRHR system; or RRP system; or SCS system for the Decay Heat Removal of a future standard PWR. Identification of the contribution linked to the implementation of each system **Favourable ⇧; unfavourable ⇩; indifferent ⇨**				
SYSTEMS	PRHR	RRP	SCS	Comments
★ **4th level : MAJOR ACCIDENT MANAGEMENT** accident management including the confinement protection				
⇨ Avoid by design (prevent) the sequences that can leads to unacceptable consequences and early releases. Reject the risk for the cliff edge effect. **(For recall → must be realized at the prevention level.)**				
• Avoid by design the reactivity excursions				
• Avoid by design the core melting under high primary pressure conditions				
• *Participate efficiently to the primary circuit depressurisation*	⇩⇧	⇧	⇧	The systems can actively participate to the primary circuit depressurisation. PRHR ⇩ - SG thermally isolated primary circuit still pressurized
• Avoid by design the core melting concomitant to the loss of the contain. (bypass).				
• *Foresee an ultimate passive DHR system within the containment*	?	?	?	The systems potential for DHR in case of severe accident is not clearly established
• *Set up within the containment all the loops that carry primary coolant*	⇧	⇧	⇧	
• *Foresee the isolation of all intermediate loops at the containment level*	⇧	⇩⇧	⇩⇧	RRP ⇧ whit internal heat exchanger SCS ⇧ With internal pool
• Avoid by design the risks for the steam explosions				
• Avoid by design the risks for the Hydrogen detonation				

PRHR system; or RRP system; or SCS system for the Decay Heat Removal of a future standard PWR. Identification of the contribution linked to the implementation of each system **Favourable ⇧; unfavourable ⇩; indifferent ⇨**				
SYSTEMS	PRHR	RRP	SCS	Comments
★ **5th level : CONSEQUENCES MITIGATION** offsite emergency response				
⇨ Delay the offsite release				
⇨ Minimize the offsite radioactive release				

Passive Residual Heat Removal - Heat exchanger

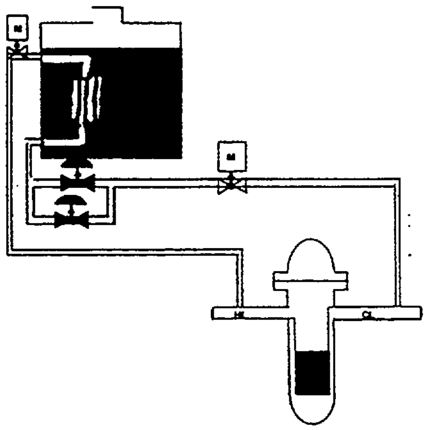

Secondary Condensing System

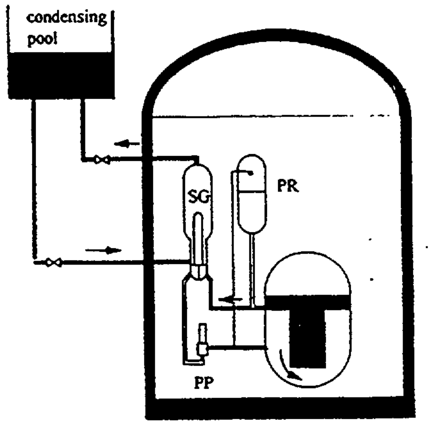

RRP in reactor vessel

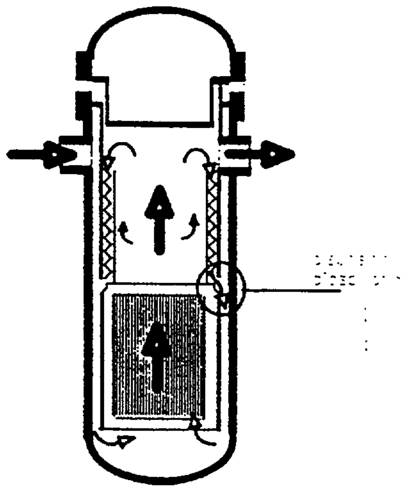

ECHANGEUR INTEGRE EN [illegible]

RRP diagram

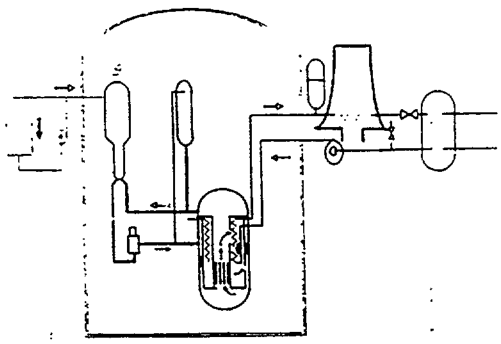

DECAY HEAT REMOVAL SYSTEMS DIAGRAMS

REFERENCES

/1/ Nuclear Safety Advisory Groups: Basic Safety Principles for nuclear Power Plants
IAEA Safety Serie n°75-INSAG3

/2/ Nuclear Safety Advisory Groups: The Safety of Nuclear Power
IAEA Safety Serie n°75-INSAG5

/3/ Letter from the DSIN Director (M. Laverie - Direction de la Sûreté des Installations Nucleaires) to the CEA General Manager on the Pressurized Water Reactors for the future; DSIN 984/91

/4/ Letter from the DSIN Director (M. Lacoste - Direction de la Sûreté des Installations Nucleaires) to the EDF General Manager on the Pressurized Water Reactors for the future; DSIN 1394/93
+ the joined report : GPR/RSK Proposal for a common Safety Approach for Future Pressurized Water Reactors; adopted during the GPR/RSK meeting on May 25, 1993

/5/ P.Aujollet CEA/DRN/DER/SIS - Efficiency Studies of Future PWR Safety Systems
Presentation to the same conference

POSTULATED SMALL BREAK LOCA SIMULATION IN A CANDU TYPE REACTOR WITH ECC INJECTION UNDER NATURAL CIRCULATION CONDITIONS

G. BEDROSSIAN, S. GERSBERG
Comisión Nacional de Energía Atómica-Avda,
Buenos Aires, Argentina

Abstract

This paper presents a thermalhydraulic analysis of the simulation of a postulated 55 kg/s inlet header break (very small LOCA) in the primary heat transport system of Embalse Nuclear Power Plant, coincident with a loss of Class IV Power Supply, on the assumption that the Emergency Core Cooling System action is not automatic but it must be performed manually.
The main objective of this work was to evaluate the refill performance of a high-pressure accumulator tank emergency coolant injection system under natural circulation conditions.
It is proposed a multiple channel model approach to study the response of the broken loop on the basis that it is expected that the behaviour will not be the same for all the channels in the critical core pass. The intact loop was represented by an average channel model.
The emergency coolant was injected in all the headers of the primary system and in the inlet headers only. The system was activated at 630 sec. and 1000 sec. after the beginning of the event.
Stagnation and flow reversal phenomena were observed in the broken loop, before the emergency coolant injection or because of it. This condition is known as bidirectional flow, that is, flow in some channels in the same pass continues in the normal direction while flow in the other parallel channels is in the reverse direction. This may be attributed to changes in the hydrostatic forces in the loop.
In every case, single phase flow was established by the end of the transient, associated with low fuel temperature.
However, it was seen that core cooling is improved whenever the injection is directed to the inlet headers only, since nominal direction flow is reestablished in all the channels.
On the other hand, even though the results for the later injection showed a fuel temperature decrease, it is recommended not to delay the initiation of the emergency coolant injection beyond 600 sec. because it was seen that void would reach the critical pass inlet header, denoting an insufficient heat removal by the boilers.

1. INTRODUCTION

This paper presents a thermalhydraulic analysis of the simulation of a postulated 55 kg/s inlet header break (very small break) in the primary heat transport system of Embalse Nuclear Power Plant, coincident with a loss of Class IV Power Supply, on the assumption that the Emergency Core Cooling System action is not automatic but it must be performed manually.

The main objective of this work was to evaluate the refill performance of a high-pressure accumulator tank emergency coolant injection system under natural circulation conditions.

A multiple channel representation was proposed to study the broken loop response since previous simulations demonstrated that emergency coolant injection under natural circulation conditions causes low flow periods, even temporary stagnation and flow reversal. [1]

In these cases, it is thought that density gradients are the driving forces of coolant flow. So, it is expected that all the channels in the critical core pass will not have the same behaviour, as they differ in power, elevation and hydraulic resistance.

Therefore, a multiple channel representation for the critical pass of the broken loop would account for these spatial phenomena.
The accident scenario included a loss of Class IV Power because a reactor trip can result in a sudden loss of generation which in some cases results in a grid disturbance that may lead to a loss of Class IV Power. [2]

2. MODELS AND ASSUMPTIONS

The study postulated a very small inlet header break (6.41 10^{-4} m^2) in the Primary Heat Transport System of Embalse Nuclear Power Plant (fig. 1) which produces an initial flow dicharge of 55 kg/s. The area corresponds to 0.32% of twice the cross-sectional area of the inlet header.

For this break size it is assumed that:

- the Emergency Core Cooling System action is not automatic. [2]
- the Reactivity Control System is fast enough and has enough negative reactivity to compensate for the increased reactivity. Therefore the reactor power stays constant up to the trip. [3]

High reactor building pressure trip was credited; this would take place -according to the Safety Report- around 25 seconds after the event initiation.
Forty seconds after reactor trip, Class IV Power Supply was supposed to be lost, and reestablishment of Class III Power was not credited.
The major consequence of a loss of electrical power is the loss of power to the heat transport system pumps. Without these pumps the effectiveness of the steam generators as a heat sink and the speed with which the Emergency Core Cooling System can refill fuel channels is quite different than for a loss of coolant with the pumps running.
After a loss of Class IV power, other functions are also lost. These include the steam generators feedwater pumps, the medium and low pressure emergency coolant injection pump, the moderator circulation pump, the heat transport feed pumps and the heavy water recovery pumps.

Both circuits of the Heat Transport Primary System were modelled, which isolate when pressure falls below 56.2 kg/cm^2 in two of the three instrumented reactor headers, interrupting coolant flow from the intact loop to the broken one.

The system representation [4] considered the 380 core channels as shown in Figure 1.

For the intact loop: two identical passes were modelled, each one representing 95 channels considered as a single average channel (fig. 2)

For the broken loop: the model considered a critical pass (downstream the break) and a non-critical pass (upstream the break) (fig. 3). The former was represented by 5 channel groups with the following features:

Group	Number of channels	Channel power [MW]	Initial channel flow [kg/s]	Initial group flow [kg/s]	Elevation [m]
1	24	6.29	26.4	633.7	5.66
2	24	6.33	26.2	628.1	7.63
3	16	3.97	17.2	275.8	4.27
4	16	4.39	19.9	317.7	6.46
5	15	4.03	17.5	262.1	8.79

The non-critical pass was modelled identical to both passes of the intact loop, that is, as a single average channel representing 95 channels.
The power of each one of these channels is 5.23 MW and their flow 22.3 kg/s.

The transient thermohydraulic computer program FIREBIRD III, Mod. 1.0 was used to calculate the response of the system. [5]

3. RESULTS AND DISCUSSION

The system was allowed to operate simulating no corrective actions to mitigate the accident effects.
It was observed that the break produces system depressurization and loss of inventory, which would result in reactor building pressure increase that causes a reactor trip and then a loss of Class IV Power, as it was postulated.
The sequence of events is the following:

t = 0 sec	Inlet header break, with an initial discharge of 55 kg/s.
t = 25 sec	Reactor trip on high reactor building pressure signal.
t = 65 sec	Loss of electrical power.
t = 360 sec	Loops isolation on low primary system pressure.

After 600 seconds the system cooling was due to the mechanism of double phase thermosyphoning in both circuits, with the following flows:

	Pass		Flow [kg/s]
Intact loop	1		142.0
	2		142.0
Broken loop	Critical	Group 1	38.8
		Group 2	48.3
		Group 3	16.4
		Group 4	24.3
		Group 5	25.2
	Non critical		167.5

The Emergency Core Cooling System action was initiated manually around 630 seconds, together with the steam generators crash cool down.
In the simulation the emergency coolant injection was directed:
- to all the headers.
- to inlet headers only.

Summary of results

The results of the emergency coolant injection at 630 seconds are presented in Table I, comparing the effects of injecting in the two modes described above.
Figures 4 and 5 show inlet and outlet temperatures for the broken loop.
For thermosyphoning mechanism circulation there must be an important temperature difference between both headers.
Between 800 and 900 seconds, near to zero temperature difference was observed in the broken loop, denoting that core cooling would be temporary endangered. The intact loop always exhibited an appreciable difference.
Figures 18 and 19 show these temperature differences for the case when injection is directed to inlet headers. A clear difference existed between inlet and outlet headers, anticipating nominal direction flows for all the groups.
In every case, the emergency coolant injection produces a transitory flow oscillation (fig. 6 to 10 and fig. 20). This is more accentuated when the coolant is directed to all the headers, predicting periods of very low flow and even momentary flow reversals. In particular, the channel representing Group 3 reverses definitely. On the other hand, when the emergency coolant injection is initiated to inlet headers only, all the channels remain with nominal direction flow.
In spite of these differences, all the channels exhibit an adequate fuel cooling (fig. 11 to 15), with single phase flow (fig. 16, 17 and 21 for example).

Afterwards, the possibility of delaying the Emergency Core Cooling System action was analyzed.
The injection was carried out around 1000 seconds after the initiation of the accident. It was also directed to all the headers and to inlet headers only.
The results are shown in Table II again comparing the two possible scenarios.

By 1000 seconds we find a degraded core cooling. The steam generators are not able to condensate all the vapor produced, and we find void in the broken loop inlet headers (fig.32).
The high void fraction in the core causes a sheath temperature increase.
At the moment of the injection, the coolant is practically stagnant in Groups 1, 2 and 5 and has reversed in Groups 3 and 4.
Figures 22 and 23 show that in the broken loop inlet and outlet headers temperatures are practically equal in the critical pass, and in the non-critical pass outlet header is cooler than inlet header. This would anticipate stagnation or flow reversal.
When emergency coolant is directed to inlet headers the injection keeps a positive temperature difference between outlet and inlet headers.
The entrance of the emergency coolant to all the headers leads again to a transitory flow oscillation (fig. 24 and 25); but finally, all the channels remain with nominal direction, except Group 3, that continues reversed.
When the emergency coolant injection is supplied to inlet headers only a more definite tendency to reach nominal direction flow was observed in all the channels (fig. 28 and 29). Finally, the coolant in every group flows in nominal direction by the end of the transient.
When the emergency coolant injection is initiated to all the headers, the simulation predicted long periods of low flow for Groups 1, 2 and 4, which results in a considerable void increase (fig. 26 and 27), with the consequent sheath temperature increase.
Injecting to inlet headers only, this was not observed (fig. 30 and 31), except for Group 2 where coolant stagnation causes vapor generation and temporary increase of sheath temperature.
However, the calculated temperatures did not show values high enough to produce fuel damage.

As mentioned at the begining, during low flow periods the driving forces are the density gradients in each channel. We considered useful to estimate this driving forces in order to compare them with pressure differences between headers (inlet and outlet to that channel) to have an adequate measure of the circulation conditions through the core in the critical pass.
As long as the hydrostatic height between inlet and outlet feeders is greater than pressure difference between inlet and outlet headers of the critical pass, coolant will flow in nominal direction. Otherwise, it will reverse.
This analysis confirmed the results described above: supplying emergency coolant injection to all the headers, all the channels stay with nominal direction flow, except Group 3; injecting to inlet headers only, all the channels remain with flow in nominal direction.

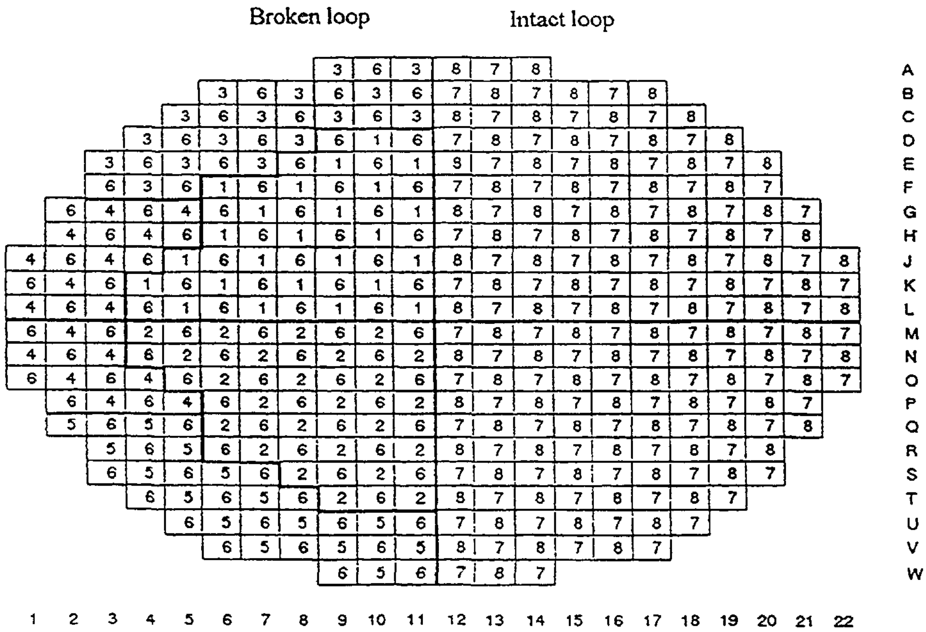

Figure 1 Core channel groups representation

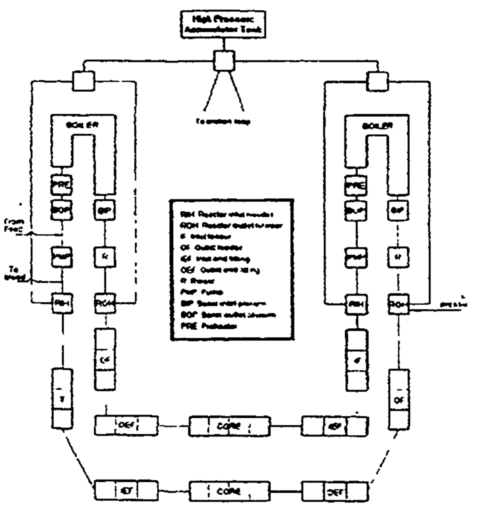

Figure 2 Intact loop representation

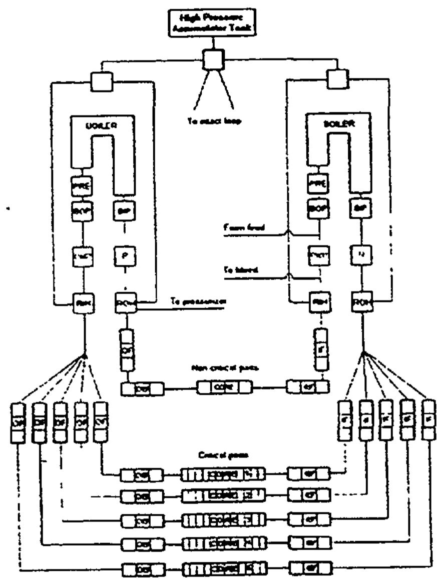

Figure 3 Broken loop representation

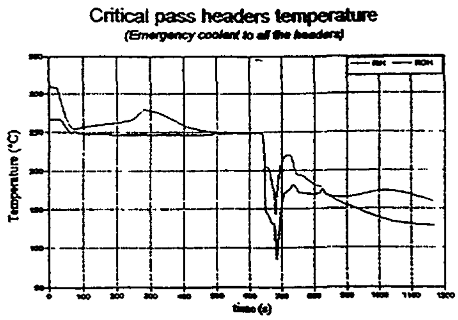

Figure 4

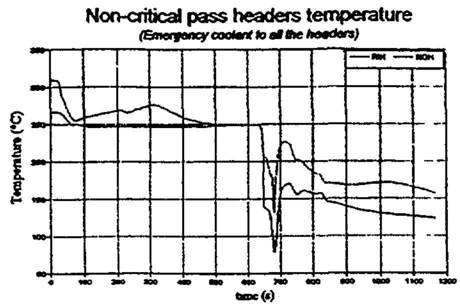

Figure 5

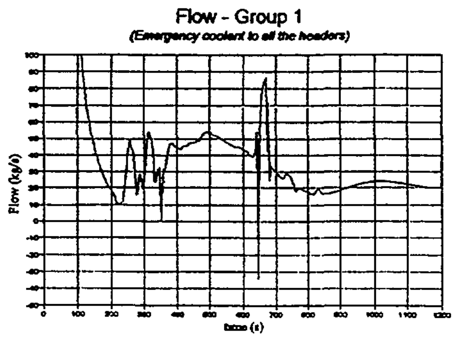

Figure 6

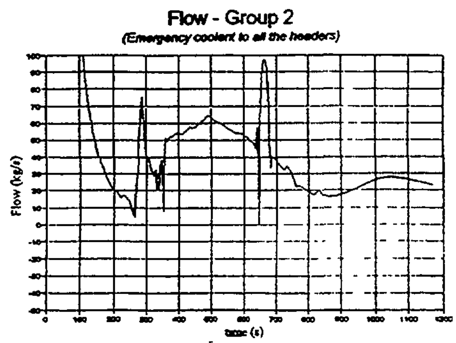

Figure 7

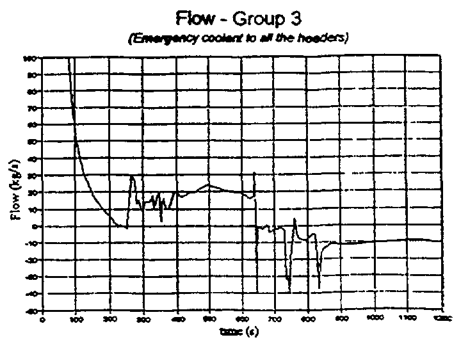

Figure 8

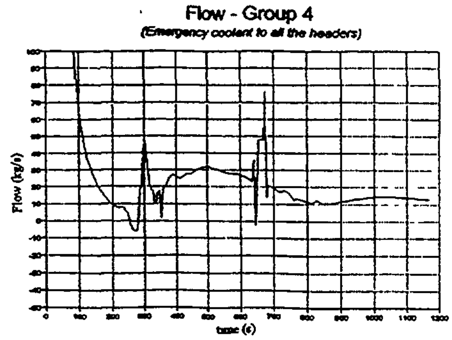

Figure 9

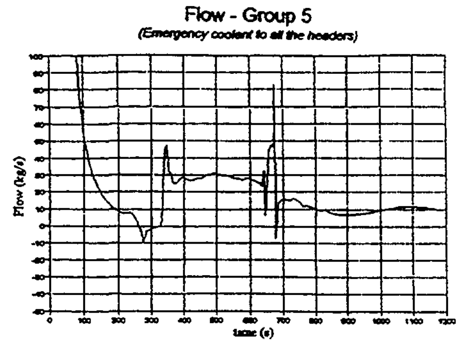

Figure 10

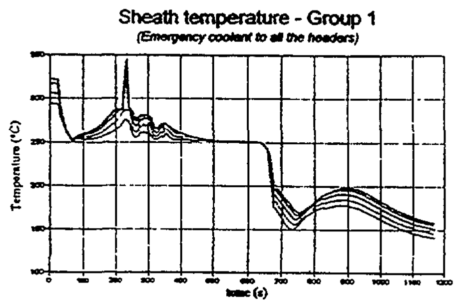

Figure 11

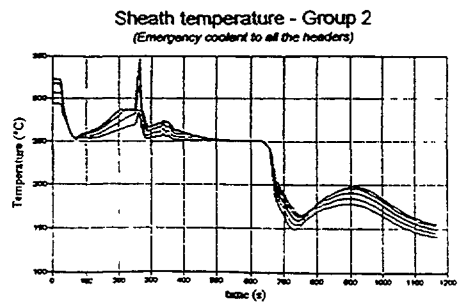

Figure 12

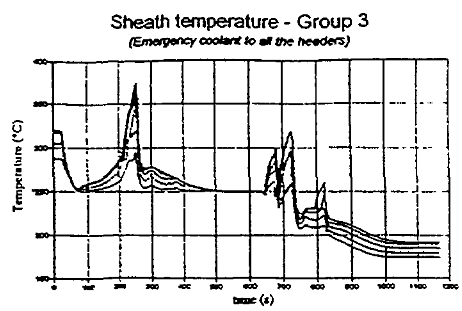

Figure 13

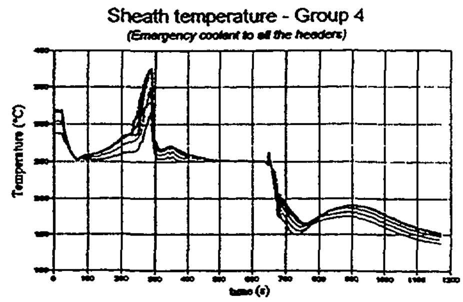

Figure 14

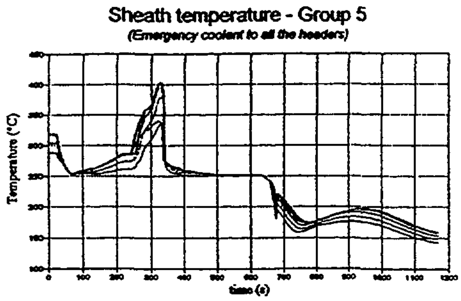

Figure 15

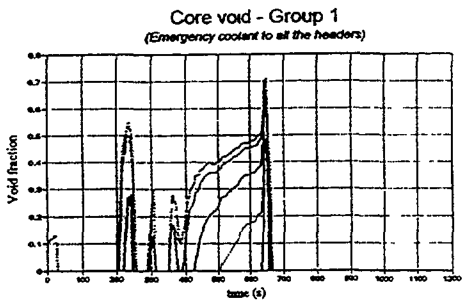

Figure 16

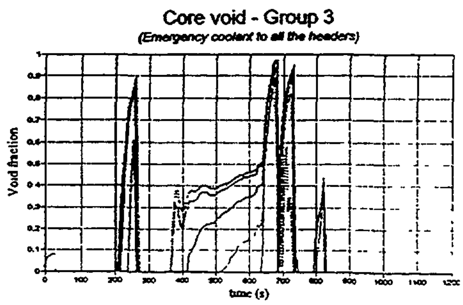

Figure 17

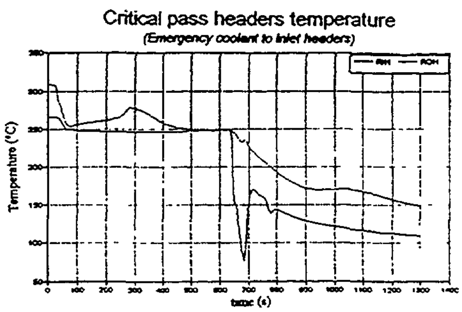

Figure 18

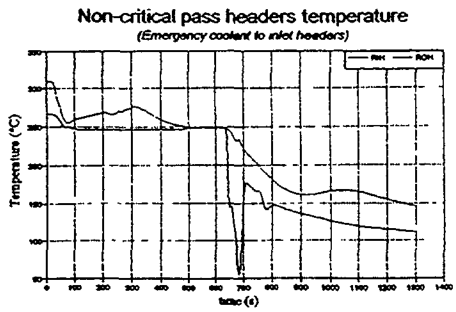

Figure 19

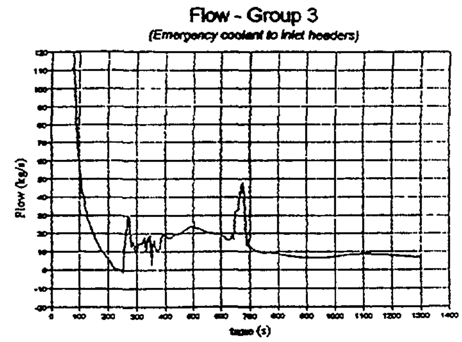

Figure 20

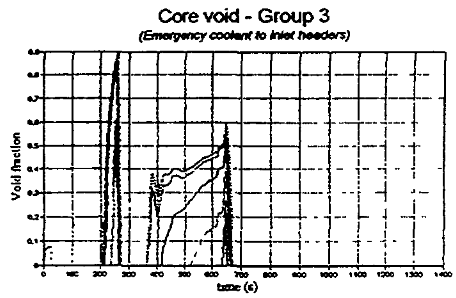

Figure 21

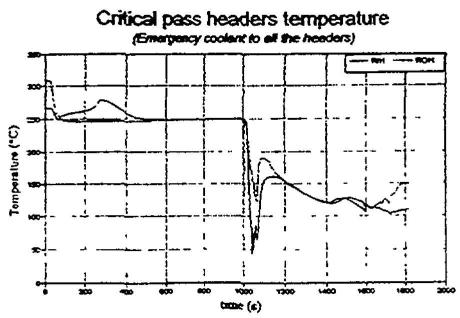

Figure 22

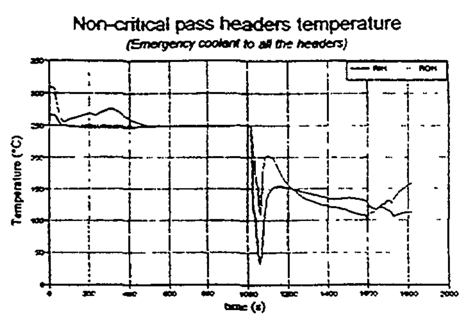

Figure 23

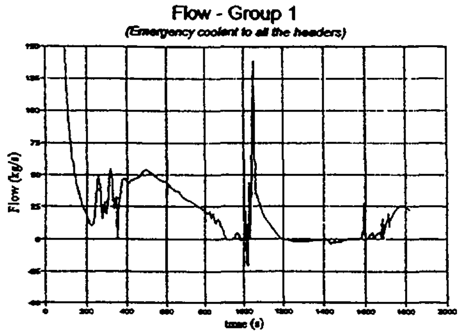

Figure 24

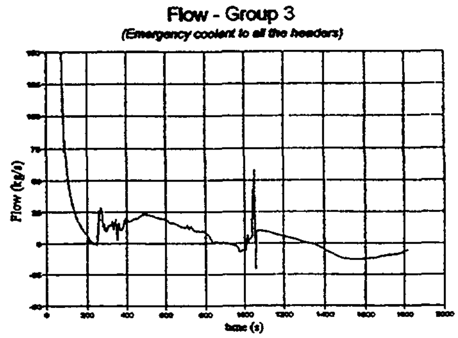

Figure 25

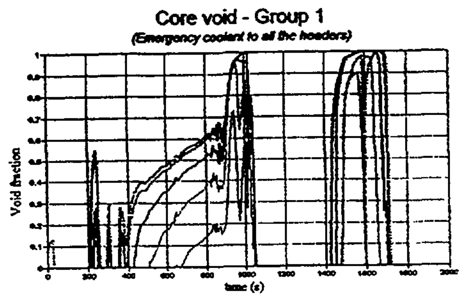

Figure 26

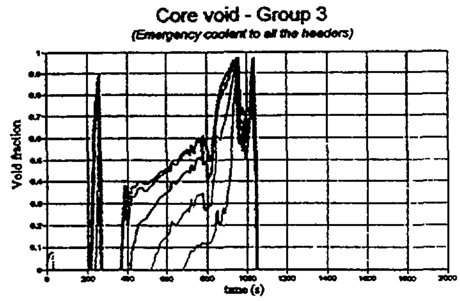

Figure 27

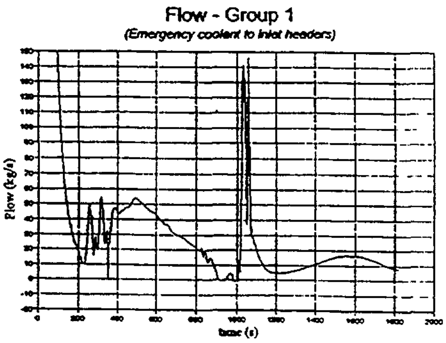

Figure 28

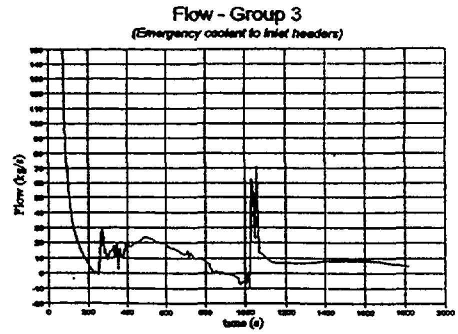

Figure 29

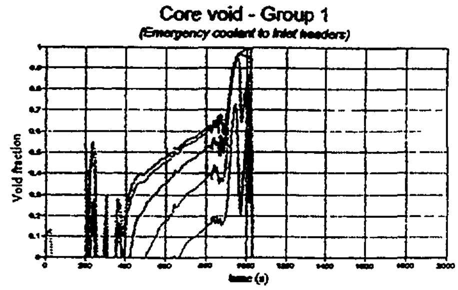

Figure 30

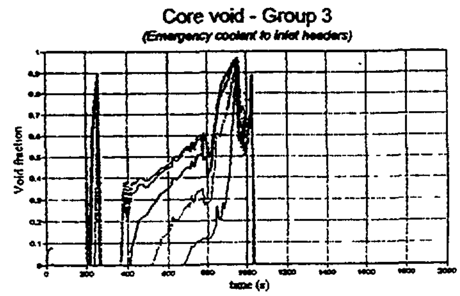

Figure 31

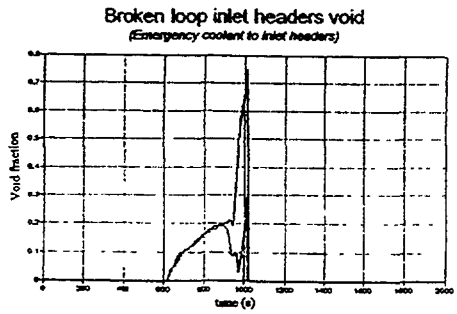

Figure 32

TABLE I: EFFECTS OF EMERGENCY COOLANT INJECTION

Injection time: 632 sec.

In every case:

- Coolant flow was in nominal direction at injection time.
- The injection causes a transitory flow oscillation.

Variable		Emergency coolant to all the headers	Emergency coolant to inlet headers
		End of simulation: 1170 sec.	End of simulation: 1300 sec.
Flow	Group 1	A momentary flow reversal during the oscillation period was observed. Then it continues in nominal direction.	No flow reversal was observed. It keeps nominal direction.
	Group 2	After the oscillation period, flow continues in nominal direction.	It keeps nominal direction.
	Group 3	During the oscillation (which is longer in time than in other channels) stagnation was observed and then a definitive flow reversal.	Neither stagnation nor flow reversal were observed. It keeps nominal direction.
	Group 4	After the oscillation period, flow continues in nominal direction.	Idem Group 2.
	Group 5	A momentary flow reversal during the oscillation period was observed. Then it continues in nominal direction.	No flow reversal was observed. It keeps nominal direction.
	non critical pass	After the oscillation period, flow continues in nominal direction.	Idem Group 2.
Sheath temperature	Group 1	The prompt effect is a great decrease. The final value is less than 160°C.	In all the channels the prompt effect is a great temperature decrease. The final value is always less than 140°C.
	Group 2	Idem Group 1.	
	Group 3	Because of the stagnation caused by the injection some peaks no greater than 320°C were observed. However the final value is less than 200°C.	
	Group 4	Idem Group 1.	
	Group 5	Idem Group 1.	
	non critical pass	Idem Group 1.	

TABLE II: EFFECTS OF EMERGENCY COOLANT INJECTION

Time injection: 1007 sec.

- Coolant flow at injection time:
  a) **Is stagnant** in Groups 1, 2, 5 and in the non-critical pass.
  b) **Is reversed** in Groups 3 and 4.

- In every case:
  a) Emergency coolant injection causes a **transitory flow oscillation.**
  b) Prior to the injection sheath temperatures begin to increase because of the low flows.
  c) The prompt effect of the injection is a great sheath temperature decrease.

Variable		Emergency coolant to all the headers	Emergency coolant to inlet headers
		End of simulation: 1820 sec.	End of simulation: 1820 sec.
Flow	Group 1	A momentary flow **reversal** was observed during the oscillation period. Then it was seen a long **stagnation**, but finally flow is reestablished in **nominal direction.**	Neither reversal nor stagnation were observed during the oscillation period. **Nominal direction** flow is reestablished.
	Group 2	Similar behaviour as Group 1 was observed.	Neither reversal nor stagnation were observed during the oscillation period. Then there is a transitory flow reversal, but finally **nominal direction flow is** reestablished.
	Group 3	Momentary **stagnations** were observed during the oscilation period, after which **nominal direction** flow is reestablished. However, it decreases and finally **reverses** definitively.	After the oscillation period **nominal direction** flow is reestablished.
	Group 4	Similar behaviour as Group 1 was observed.	Similar behaviour as Group 1.
	Group 5	A very accentuated oscillation was observed with successive **stagnations and flow reversals**, after which **nominal direction** flow is reestablished.	Similar behaviour as Group 1.
	non critical pass	Emergency coolant injection reestablishes **nominal direction** flow.	Similar behaviour as Group 1.
Sheath temperature	Group 1	The low flow causes an important transitory increase. The final value is less than 130°C.	The pronounced peak was not observed. The final value is less than 130°C.
	Group 2	Similar behaviour as Group 1. The final value is less than 150°C.	A peak was observed, although not as pronounced as when the emergency coolant enters to all the headers. The final value is less than 130°C.
	Group 3	A transitory increase was observed here also, but not so important. The final value is less than 130°C.	Non important increase was observed. The final value is less than 120°C.
	Group 4	Similar behaviour as Group 3, although the peak is more pronounced. The final value is less than 130°C.	Idem Group 3.
	Group 5	The better circulation conditions prevent the temperature peak. The final value is less than 130°C.	Idem Group 3.
	non critical pass	A slight transitory increase was observed. The final value is less than 150°C.	Idem Group 3.

4. CONCLUSIONS

The refill performance of a high -pressure accumulator tank emergency coolant injection system under natural circulation conditions was evaluated. The scenario consisted of a 55 kg/s reactor inlet header break coincident with a loss of electrical power supply.
The emergency core cooling system action was initiated manually, supplying injection to all the headers and to inlet headers only.
This was performed at 630 seconds and at 1000 seconds after the header break.

The results showed a better performance of the mentioned system whenever the injection is directed to inlet headers only.
The code accounted for some experimental tests carried out at RD-14M loop:

- core cooling may be satisfactory even with reversed flows.
- emergency coolant injected to inlet headers reestablishes nominal direction flows.

Although the results for the later injection showed a fuel temperature decrease, it is recommended not to delay the initiation of the emergency coolant injection beyond 600 seconds because it was seen that void would reach the critical pass inlet header, denoting an insufficient heat removal by the boilers

REFERENCES

[1] BEDROSSIAN, G. - GERSBERG, S. - *Simulación de una rotura pequeña en colector de entrada del sistema primario de transporte de calor de la Central Nuclear de Embalse con pérdida de suministro eléctrico normal* - Comisión Nacional de Energía Atómica, 1025 (1993).
[2] ATOMIC ENERGY OF CANADA LIMITED - *Small loss-of-coolant accident and emergency core cooling operation* - 59 SDM-7 Second Edition (1982).
[3] ATOMIC ENERGY OF CANADA LIMITED - 600 MWe CANDU-PHW, Central Nuclear en Embalse, Córdoba, for Comisión Nacional de Energía Atómica - Safety Report (1985)
[4] CALABRESE, R. - GERSBERG, S. - *Sistema de cálculo de accidentes por pérdida de refrigerante con acoplamiento neutrónico-termohidráulico para reactores tipo CANDU. Informe preliminar* - Comisión Nacional de Energía Atómica 1046 (1992)
[5] LIN, M. R. et al. - *FIREBIRD III Program Description* - AECL 7542 (1984)

A RISK-BASED MARGINS APPROACH FOR PASSIVE SYSTEM PERFORMANCE RELIABILITY ANALYSIS

N.S. SALTOS, A. EL-BASSIONI
US Nuclear Regulatory Commission,
Washington

C.P. TZANOS
Argonne National Laboratory

USA

Abstract

Passive safety systems (e.g., those used in Westinghouse's AP600 and General Electric's SBWR designs) rely on natural forces, such as gravity, to perform their functions. Such forces are relatively small compared to pumped system driving forces, their magnitude varies from one scenario to another and they are subject to large uncertainties. These uncertainties affect the passive system thermal-hydraulic (T-H) performance reliability (for short, T-H reliability). For this reason, the T-H unreliability of the passive systems must be assessed and accounted for in the Probabilistic Risk Assessment (PRA). The quantification of T-H unreliability involves a prohibitively large number of computations. This paper presents a conservative risk-based "margins" approach which eliminates the need to quantify T-H unreliability for most, if not all, accident sequences. With this approach the issue of T-H unreliability is addressed by linking it to the passive safety system success criteria and, thus, to core damage frequency (CDF). This is achieved by assuring that the adopted success criteria for safety systems and operator actions are conservative enough so that the contribution to a sequence CDF from T-H uncertainties is significantly smaller than the contribution from hardware failures and human errors.

INTRODUCTION

Current advanced "passive" reactor designs, such as Westinghouse's AP600 and General Electric's SBWR designs, have a number of unique features that distinguish them from both operating and advanced evolutionary light water reactor designs. Although, they use both active and "passive" systems for accident prevention and mitigation, only the "passive" systems are classified as safety related by the vendor. The word "passive" is in quotation marks because these systems are not purely passive. Active components, such as motor operated valves and check valves, are used for system actuation. The mission of the active systems is to provide a first line of defense and reduce the challenge rate for the safety-related "passive" systems.

The passive safety systems in these designs rely on natural forces, such as gravity and stored energy, to perform their accident prevention and mitigation functions once actuated and started. These driving forces are not generated by external power sources (e.g., pumped systems), as is the case in operating and evolutionary reactor designs. Because the magnitude of the natural forces which drive the operation of passive systems is relatively small, counter-forces (e.g., friction) can be of comparable magnitude and cannot be ignored as is usually done with pumped systems. This requires more accuracy in estimating "net" driving forces. Moreover, there are considerable "knowledge-based" uncertainties associated with factors on which the magnitude of these forces and counter-forces depends (e.g., values of heat transfer coefficients and pressure losses). In addition, the magnitude of such "natural" driving forces depends on the specific plant conditions and configurations which could be existing at the time a system is called upon to perform its safety function. For these reasons, the reliability of the thermal-hydraulic (T-H) performance of the "passive" systems must be assessed.

The United States Nuclear Regulatory Commission (U.S. NRC) is currently reviewing the AP600 design. The assessment of the T-H reliability of passive safety systems is a major issue in the review of the AP600 design PRA because it can have a large impact on the success criteria for systems and operator actions as well as on the structure of the event trees themselves (e.g., by underestimating pressures which would cause safety relief valves to open and potentially stick open or by not modeling human actions that would change the course of an accident).

ASSESSMENT OF THERMAL-HYDRAULIC PERFORMANCE UNRELIABILITY

The quantification of T-H unreliability for all accident sequences involves statistical evaluations which require a prohibitively large number of computations. The conservative risk-based "margins" approach, presented in this paper, eliminates the need to quantify the T-H unreliability for most, if not all, accident sequences.

The T-H unreliability of a sequence for which a best estimate T-H analysis predicts no core damage (success sequence) is defined as the probability that this sequence will actually lead to core damage because of uncertainties in the predicted T-H performance of passive systems. With this definition, the problem of assessing the T-H unreliability of passive systems becomes equivalent to assessing the impact of uncertainties on the predicted value of the variable used in the core damage criterion, such as peak cladding temperature (PCT) or water level in the reactor vessel. Through the core damage criterion, the T-H unreliability is linked to the success criteria of the passive systems and, thus, to the core damage frequency. In the following discussions, a PCT value equal or greater than 2200 °F is assumed to lead to core damage. However, in the margins approach, presented in this paper, any other core damage criteria can be used.

The value of the PCT predicted by a T-H computer code can significantly differ from its actual value because of uncertainties, approximations and errors in the calculation, which are driven by:

- uncertainties in the values of code input variables,
- approximations and uncertainties in modeling the physics of the process,
- approximations in modeling the system geometry,
- the use of numerical methods to solve the system equations.

The code input variables include:

- initial and boundary conditions, such as initial plant temperatures, pressures, water inventories (levels), and reactor power
- forcing functions, such as decay heat and flow rates of active systems
- physical properties, such as densities, conductivities, viscosities, and specific heats
- dimensions, such as clad diameter and thickness and fuel-cladding gap
- thermal-hydraulic parameters, such as heat transfer coefficients, friction factors and gap conductance
- timing of human actions (e.g., manual actuation of core makeup tanks or manual depressurization in the AP600 design).

Examples of approximations and uncertainties in modeling the process physics are: (1) the treatment of a liquid steam mixture as a homogeneous fluid, (2) the assumption of thermodynamic equilibrium, (3) the use of correlations (e.g., correlations for heat transfer coefficient, pressure drop coefficient and critical heat flux) and simple models (e.g., models for slip, flooding, entrainment and critical flow).

To avoid excessive computational times, approximations in modeling the system geometry are necessary. These involve simplification of complex geometry features and approximation of a three-dimensional system by a two or one-dimensional system. In numerical approximations derivatives are replaced by finite differences and the resulting error depends on grid structure and time step size.

To assess the impact of uncertainties on the predicted value of the PCT, a large number of calculations is needed. This number can be reduced by: (a) concentrating on sequences that contribute significantly to core damage frequency, (b) grouping (binning) the accident sequences and selecting a "bounding" sequence for each group (bin), and (c) performing sensitivity analyses to determine the "large impact" variables, i.e., those variables whose uncertainty has a significant impact on the T-H performance of passive systems. The effort can be significantly reduced if a conservative bounding analysis can be used. A very conservative bounding analysis can be based on values for all variables that can be justified as bounding (as defined by their range of uncertainty). For sequences where conservative bounding is not successful, a statistical approach can be used to assess the probability that the limiting value of the PCT will be exceeded. Even for these sequences, the effort to assess the T-H unreliability of passive systems can be reduced if a combination of conservative bounding and statistical analysis can be used, where the statistical evaluation is performed for a very small number of "large-impact" parameters, while a bounding approach is used for the remaining (larger) number of parameters.

The statistical evaluation can be based on the generation of random samples (where dependent variables are properly treated) of the "large-impact" variables by using a Monte-Carlo method. The PCT can be computed for each sample, and the resulting values can be used to assess the probability that the limiting value of 2200 °F will be exceeded due to T-H uncertainties. Depending on the size of the problem under consideration (number of "large-impact" variables) and the information available about the problem, direct Monte-Carlo, Latin Hypercube, or Monte-Carlo Importance sampling can be used. Direct Monte-Carlo can be inefficient if the number of "large-impact" variables is not small. Similar statistical approaches have been discussed extensively in the literature. This includes early work performed by Westinghouse for EPRI (Ref. 1), work performed at national laboratories (Refs. 2 and 3), and work performed for the CSAU (Code Scaling, Applicability and Uncertainty) evaluation methodology (Refs. 4 and 5).

Differences between code predictions and actual values due to geometry simplifications (one or two-dimensional), coarse spatial grids and large time steps can be assessed by comparing predictions of simplified computational models with those of more detailed models (e.g., two or three-dimensional, finer spatial grids, smaller time steps). Differences due to approximations of the process physics should be evaluated by comparing predictions of simple codes with those of more mechanistic codes and with experimental measurements. Analyses must show that there are no surprises due to multi-dimensional effects, system asymmetries, two phase flow instabilities, oscillatory system behavior, and the presence of noncondensible gasses.

RISK-BASED MARGINS APPROACH

The risk-based margins approach is a graded approach which consists of four basic steps. In step 1, the accident sequences are grouped into "bins" and a "bounding" sequence for each bin is selected. In step 2, sources of uncertainty associated with the T-H performance of passive systems are identified. In step 3, sensitivity analyses are performed to identify those variables (such as T-H parameters) whose uncertainty has significant impact on the predicted PCT. In step 4, for each of the "bounding" sequences identified in step 1, the available "margin" to core damage is explored and this information is used to determine success criteria for passive systems and operator actions or to decide on an appropriate resolution path (e.g., need for more detailed analyses, need for regulatory oversight or design changes). These basic steps of the margins approach are described in more detail below.

1. Accident sequence grouping and selection of "bounding" sequences

The effort of assessing the T-H unreliability is drastically reduced if the success accident sequences, modeled in the event trees, are grouped into bins and, for each bin, a "bounding" sequence is selected. This is done using a combination of probabilistic and deterministic arguments (e.g., considering sequences initiated by the same event with a frequency above a certain cutoff and using similarity and bounding arguments to select a "bounding" sequence). Analyses are then performed only for these "bounding" sequences since the results are good (i.e., "bounding") for all the other sequences. To reduce the number of T-H computations, several conservative assumptions can be made. For example, if the initiating event is a break, the most limiting break in terms of size and location can be determined and used in subsequent analyses.

When the T-H unreliability of passive systems is taken into account, some success sequences (i.e., sequences for which a best estimate T-H analysis predicts no core damage) could actually lead to core damage. Thus, additional cut sets could be generated which would contribute to an increased core damage frequency (CDF). These new cut sets are the product of three terms: (1) the initiating event frequency; (2) a non-T-H unavailability term, which is the product of unavailabilities of all failed systems due to hardware failures and human errors; and (3) a T-H unreliability term.

The magnitude of these three terms provide important clues about the risk importance of the T-H unreliability term in a certain sequence. For example, if the product of the first two terms is very small in a certain sequence (e.g., smaller than 1E-9/year), then the T-H unreliability for this sequence is not risk important and can be ignored. This implies that success sequences with frequency below a certain cutoff can be ignored. Among the remaining sequences, the lower the product of the first two terms, the higher the T-H unreliability term must be to have a significant impact on CDF. This implies that success sequences with many redundant system (and train) failures, such as those close to the bottom of an event tree, will not become significant risk contributors unless the T-H unreliability is very high. This is an important observation since such sequences are the most likely candidate "bounding" sequences. If the margins approach fails to show margin for such sequences, a combination of this approach with statistical analysis can be used. Since it must only be shown that the T-H unreliability is not higher than a rather large number, the computational effort will not be extensive. On the contrary, it is likely that an approach that uses statistical analysis with only one variable (preferably having the largest impact on PCT) will be successful. Statistical analyses with only one variable pose minimal computational effort.

2. Identify Sources of Uncertainty

For each "bounding" sequence, determined in the previous step, sources of uncertainty associated with the T-H performance of passive systems must be identified. A systematic process is necessary to ensure that uncertainties in code input variables as well as in software correlations and models are considered. This process could start with the review of models and parameters of a best estimate computer code in conjunction with available information from existing studies to concentrate on the modeling of phenomena that dominate plant behavior. For example, available information from the Code Scaling, Applicability, and Uncertainty (CSAU) program [Ref. 6] could be used.

Since the computer codes used to predict the T-H behavior of a nuclear power plant are approximate simulators of complex phenomena, the code predicted values of important plant variables differ from the actual values of these variables. Typically, large T-H system codes model 100 to 200 parameters associated with mass and energy transfer processes. Although the value of all of them is known or is predicted with some uncertainty, for any given accident sequences a small subset of these parameters dominate plant response.

To guide the code assessment (validation) effort and associated experimental programs for computer codes to be used for audit calculations in the certification of Advanced Reactor designs, the U.S. NRC is using the Code Scaling, Applicability, and Uncertainty (CSAU) evaluation methodology, which was developed in the late 80's [Ref. 6]. The CSAU methodology is based on the Phenomena Identification and Ranking Process (PIRT); i.e., the identification of phenomena and their ranking in terms of their relative importance in determining plant response during a given accident sequence. PIRTs provide assurance that all phenomena having some significance to plant behavior have been identified and the effort to assess uncertainties in computer code predictions is concentrated on the modeling of phenomena that dominate plant behavior.

Based on preliminary computer code calculations and expert judgement, detailed PIRTs have been formulated, documented, and peer reviewed for five postulated accident categories. They are: (1) small loss of coolant accidents (LOCAs), (2) main steam-line break accidents with depressurization, (3) main steam-line break accidents without depressurization, (4) steam generator tube rupture accidents with depressurization, and (5) steam generator tube rupture accidents without depressurization. These results have been directed towards the assessment of RELAP5 and CONTAIN computer codes.

Future activities planned include validation of the PIRTs, first with sensitivity calculations and later by the use of the experimental data as they become increasingly available. Refined PIRTs will be used as the foundation for determination of the uncertainty in computer code predictions, when these codes will be applied to audit safety analyses involving the transients used in the development of PIRTs. The results that have been generated, as well as those that will be generated in the future, by the PIRT process can provide very useful information in the identification of "large-impact" variables and in assessing computer code biases for the evaluation of passive system T-H unreliability.

3. Identify "Large Impact" Variables

Once the sources of uncertainty are determined and the various parameters (variables) whose uncertainty contributes to the T-H unreliability of the passive systems are known, sensitivity analyses can be performed to identify "large-impact" variables (i.e., variables whose uncertainty has a significant impact on the value of the PCT. In these analyses, the change in the value of the PCT per unit change of the variable under consideration (i.e., $\partial PCT/\partial v$, where PCT = peak clad temperature, v = variable under consideration) as well as the uncertainty range of the variable should be considered. For some parameters the derivative may be large while the uncertainty range is small, for others the derivative may be smaller while the range of uncertainty is larger. Since such variables are the most important contributors to T-H unreliability, their identification is needed for efficient implementation of the margins approach. Particular attention should be paid in selecting the range of uncertainty for these variables. If more refined uncertainty analyses are needed to show that the success criteria are conservative, analyses which would narrow the variation range of some "large impact" variables would be the most beneficial.

4. Explore Available "Margin" to Core Damage

Results from the first three steps of the margins approach, described above, contain all the information that is needed to explore the available "margin" to core damage (for each "bounding" sequence). A very conservative bounding analysis is performed first to determine whether the assumed success criteria for passive systems and operator actions are conservative. If this analyses fails to show that the success criteria are conservative, then several options can be investigated to ensure conservative success criteria. Such options include more detailed analyses of the variation range of some "large impact" variables and/or use of experimental information and/or commitment by the vendor to perform pre-operational tests and show that certain assumed values of variables are indeed bounding. If such options are exercised but still cannot be shown that the success criteria are conservative, then the option of quantifying the T-H unreliability and properly incorporating it into the PRA can be exercised. This option may not be as demanding in computational effort if a combination of conservative bounding and statistical analysis can be used, where the statistical evaluation is performed for a very small number of "large-impact" parameters, while a bounding (margins) approach is used for the remaining (larger) number of parameters. Quantification of the T-H unreliability can be avoided if changes are made in either the design or the success criteria which make the bounding analysis successful (i.e., with these changes the margins approach shows that the success criteria are conservative).

The various steps that are used to explore the "margin" to core damage are listed below.

1. Each "bounding" sequence should be analyzed first with values of (all) variables that can be justified as bounding, to determine whether the assumed success criteria are conservative (i.e., whether the predicted value of the PCT is less than its limiting value of 2200 °F after the computer modeling error has been accounted for).

2. If the analyses of previous step fail to show margin for one or more "bounding" sequences, then more refined analyses can be used to show that the safety system success criteria for such sequences are conservative (e.g., perform more refined uncertainty analyses on the variation range of some "large impact" variables and/or use experimental information and/or commit to perform pre-operational tests and show that certain assumed values are indeed bounding).

3. If for some sequences the analyses of the previous two steps would fail to show that the success criteria are conservative, i.e., the peak cladding temperature determined from these analyses exceeds the limiting value of 2200°F), then one or more of the following options should be considered:

   - Quantify the probability that these sequences would lead to core damage because of T-H performance uncertainties, and properly incorporate this probability in the PRA analysis.

   - Consider regulatory oversight of active nonsafety-related systems. This would increase the reliability of such systems and, in turn, would decrease the challenge rate of the safety-related passive systems.

   - Consider design <u>and/or</u> success criteria changes which make the analyses of either one of the first two steps successful (i.e., with these changes the analyses show that the new success criteria are conservative).

SUMMARY AND CONCLUSIONS

The T-H unreliability of passive safety systems, such as those used in Westinghouse's AP600 design, must be assessed and accounted for in the PRA. However, the quantification of T-H unreliability involves a prohibitively large number of computations. A conservative risk-based "margins" approach was developed which eliminates the need to quantify T-H unreliability for most, if not all, accident sequences. With this approach the issue of T-H unreliability is addressed by linking it to the passive safety system success criteria and, thus, to core damage frequency (CDF). This is achieved by assuring that the adopted success criteria for safety systems and operator actions are conservative enough so that the contribution to a sequence CDF from T-H uncertainties is significantly smaller than the contribution from hardware failures and human errors.

The margins approach is currently being implemented for the analysis of the passive system performance reliability of the AP600 design. This analysis, which is performed in support of the AP600 design certification, has so far indicated that the conservative margins approach can be a very efficient tool for addressing the issue of passive system T-H reliability in advanced passive reactor designs. In addition, such an approach can drastically reduce the effort needed to address this issue. Preliminary indications (no complete results are available yet) are that there is adequate margin to core damage for most AP600 design accident sequences. However, the success criteria for a few sequences may have to be changed.

REFERENCES

1. M. Mazumdar, J.A. Marshall, and S.C. Chay, "Methodology Development for Statistical Evaluation of Reactor Safety Analyses," EPRI-NP-194 (1976).

2. J.K. Vaurio and C.J. Mueller, "Probabilistic Analysis of LMFBR Accident Consequences with Response Surface Techniques," Nuclear Science and Engineering 75, 401-413 (1978).

3. E.E. Morris, C.J. Mueller, J.E. Cahalan, and H. Komortya, "A Comparison Study of Reactor Surface Methodology and Differential Sensitivity Theory in Core Disruptive Accident Analysis," Proc. 1981 International ANS/ENS Topical Meeting on Probabilistic Risk Assessment, September 1981.

4. NUREG/CR-5249, "Quantifying Reactor Safety Margins," 1989

5. M.G. Ortiz and L.S. Ghan, "Uncertainty Analysis of Minimum Vessel Liquid Inventory During a Small-Break LOCA in a B&W Plant - An Application of the CSAU Method Using the RELAP5/MOD3 Computer Code,"NUREG/CR-5818, 1992.

6. C.D. Fletcher, G.E. Wilson, C.B. Davis, and T.J. Boucher, "Interim Phenomena Identification and Ranking Tables for Westinghouse AP600 Small Break Loss-of-Coolant Accident, Main Steam Line Break, and Steam Generator Tube Rupture Scenarios," INEL-94/0061 (Draft Report), October 1994.

FEASIBILITY AND EFFICIENCY STUDIES OF FUTURE PWR SAFETY SYSTEMS

P. AUJOLLET
Commissariat à l'Energie Atomique,
Cadarache, France

Abstract

The French Atomic Energy Commission (CEA) has initiated evaluation studies of innovative safety systems, in terms of efficiency and reliability in selected accidental sequences. Three kinds of systems are currently evaluated : direct depressurization system designed to control PWR primary pressure to prevent in-pressure core melt down, passive residual heat removal systems and steam injector systems.

The feasibility and performance of each system is assessed through the analyses of accidental transients in a reference three loops PWR, making use of the Probabilistic Risks Analysis (PRA) method and the CATHARE 2 thermal hydraulic code.

These studies are conducted in four steps : sizing of each system using one or more reference transients, insertion of each new system ; modification of accidental procedures and event-trees, calculation of fuel damages probabilistic risk values during selected accidental transients and ranking of core damages probabilistic risk values.

In particular, a high pressure single stage steam driven injector which was tested at SIET laboratories was modelled with the thermal hydraulic code CATHARE.

INTRODUCTION

The present article summarizes some features of the PWR innovative safety systems wich are currenly studied at CEA Innovative Safety Systems Department mainly with Cathare 2 code:

- direct depressurization system sizing and opening setpoint value adjustment
- passive residual heat removal: Secondary Condensing System and In-vessel Heat Exchangers studies
- Safety Injection System or Auxiliary Feedwater Systems with Steam injector. ENEL/SIET Steam injector Mock up tests results (2) studies with Cathare 2 code

Beyond the specificities of these particular systems, current studies objectives are to verify the ability of the concept to fullfill its function, to determine its physical generic limits, to foresee code developments and experimental code assessment programs, to eventually improve the systems and determine complementary safety systems.

DEPRESSURIZATION SYSTEM

This system must permit a direct control of the primary circuit pressure in extreme conditions. Its objectives are to prevent a in-pressure core melt down by discharging primary circuit to a low pressure value (fixed at 1 MPa in that case).

System description.

A valve system is located at the top of the pressurizer, the discharging system is connected to a pool (IRWST : In-Reactor Water Storage Tank) located inside the containment. These studies are performed with Cathare Safety code reactor data set to simulate standart 900 PWR.

Applications and Objectives.

This system has to achieve a fast (hundred secondes) depressurization of the primary circuit to reach and to maintain it at a pressure value lower than 1 MPa.

Method.

After a first sizing of the valve, opening setpoint value adjustment is achieved by simulation with Cathare code of anticipated transients with multiple failures leading to extreme conditions with uncovered core and primary circuit at a high pressure value.

The first transient chosen was a total loss of Auxiliary Feedwater Systems event with only accumulators and LPIS available, during this transient the system has to remove heat from nuclear core primary and secondary circuits.

Then several transients were tested. Among them, a small break Steam Generator tube rupture event with only accumulators and LPIS available, gave a sizing point at low pressure as the depressurization system with a decreased flowrate had to remove heat coming from the core, the primary circuit and from the broken Steam Generator.

The current signal for valve opening is based on reactor vessel water level measurement with an opening of the valve at hot and cold legs uncovering. CATHARE simulations results show the efficiency of the depressurization system during these transients.

It was also verified that an inadvertant opening of the valve during reactor normal operating conditions do not lead to core damages.

The size of the discharging pool was determined by considering the subcooled liquid water mass needed to condensate the entire primary coolant mass in vapor phase.

Studies current status

Additional calculations are currently performed to verify the efficiency of the system during other transients such as multiple Steam Generator tubes ruptures, or small break with primary pumps kept on.

All these results are to be compared with a fast depressurization valve opening test experimental results which is to be performed on BETHSY integral test facility in 1996.

These studies are completed by a definition work of an experimental program on CEA Super Claudia facility to modelize direct condensation of water/steam jets in a pool. Super Claudia experimental activities will be focused on separate effect tests in order to measure fixed physical parameters influence on condensation process.

RESIDUAL HEAT REMOVAL SAFETY SYSTEMS

Two kinds of passive systems are currently assessed :

- At primary circuit level (Refroidissement du Réacteur au Primaire system RRP from CEA/DER/SIS)
- At secondary circuit level (Secondary Condensing System SCS)

Reacteur Refroidissement Primaire system [1].

Usually the residual power is removed in an active way in two steps : first by the Steam Generators (SG) at high primary side pressure, second by Residual Heat Removal System (RHRS) at low primary side pressure and temperature.

A new passive system supplying similar functions is described and analysed. This studies have been performed with a standart 900 MWe PWR reactor Cathare 2 data set.

Description and principle. RRP system includes three in-reactor vessel heat exchangers. A layout of reactor vessel internal structures to allow forced or natural convection and of the external heat sink are shown in Fig. 1.

A suction system (Fig. 2) allows forced or natural convection around the integrated heat exchangers.

The heat sink introduced into the reactor vessel is placed above the core so natural convection can occur inside the reactor vessel.

The size of the reactor vessel has to be increased with respect to current PWR reactor vessel sizes, to integrate the heat exchangers.

Functional analysis and efficiency.

RRP system can work in a large range of conditions.

• In normal operating conditions, convection in the intermediate circuit is available as primary pumps are working, the suction system establishes convection around the heat exchangers; the heat removal capacity of the system is about 80 MW. A cold shutdown can be conducted using only RRP system

• If primary pumps are off, a short natural circulation loop between the core and the heat exchanger is established . Primary water is circulating only inside the reactor vessel Under these conditions, it has been shown that with only natural circulation heat exchanges in the intermediate circuit 30 MW can still be extracted. These last results have been evaluated by CATHARE 2 calculation in the cases of a small break or a total blackout with in both cases Auxiliary Feedwater System (AFS) unavailable These accidental sequences were conducted in a totally passive way by the RRP system

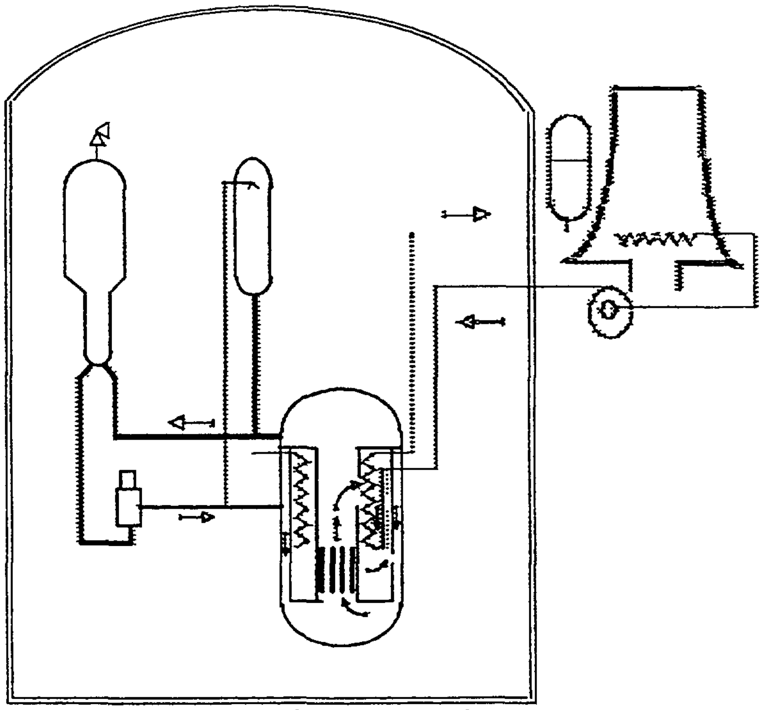

Figure 1. RRP System

It must be noticed that RRP system still works with a primary low water level (under hot and cold leg level)

System advantages.

Cold shutdown can be achieved without any extra system.

RRP system can work totally passively with no time limit (atmosphere as heat sink) at hot shutdown.

The primary fluid is always confined in reactor vessel.

RRP is always effective even if vessel water level is at primary hot and cold legs level

For small breaks and blackout kind of accidents, RRP system allows a significant increase of the intervention delay and only low pressure safety systems needed

System drawbacks.

The inspection and maintenance operations are obviously more difficult to perform

It implies additive penetrations in the reactor vessel

Reactor vessel dimensions must be significally increased.

The system needs additive penetrations in the containment

Intermediate circuit water flows from the core vessel to the outside of the containment during accidental transients

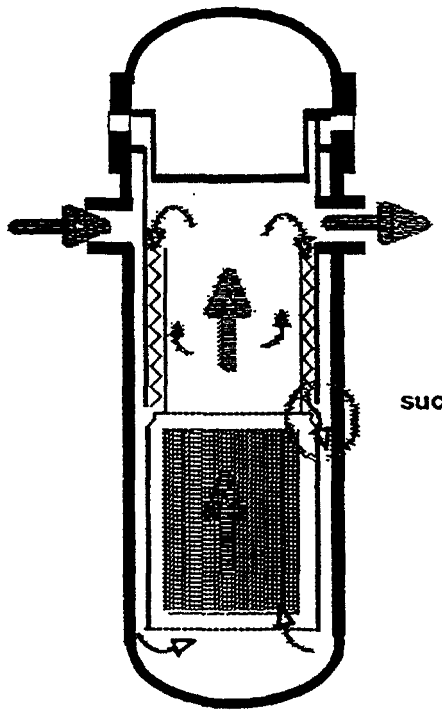

Figure 2. Reactor Vessel with RRP System

Current studies

_Linked to the drawbacks last point mentionned a RRP system with an intermediate circuit heat sink created by a in-pool heat exchangers system located in the containment is currently studied

Secondary Condensing System.

Description and principle.

SCS is a passive system using natural convection. It has to fullfill the safety function of the classical Auxiliary Feedwater System.

After closure of the main steam valves and opening of the SCS valves steam coming from the three Steam Generators · is condensed in heat exchangers immersed in three pools located outside the containment, condensed water is driven back by gravity to Steam generator inlets. Fig. 3 shows a scheme of this system.

Heat exchangers sizing is based on ability to remove residual heat during a loss of feedwater transient with the application of the single failure criterion (that means roughly 45 Mw for one heat exchanger), cooling rate limits, low steam temperature at low load and degraded steam generator mass inventorie. The calculations were performed with the two phase flow COPIE code to get an optimized couple tubes number-tubes length.

Efficiency.

In the case of blackout sequence with all AFS unavailable, CATHARE 2 simulations have been performed. Cathare results shows that, after opening of the SCS steam valves, elapsed time value to reach the SCS liquid water maximum flowrate value seems to be convenient (less than 20 sec.), stationnary flowing conditions inside the SCS are established after 40 sec.allowing heat removal from the primary circuit untill standard low pressure decay heat removal system can be started.

Extra CATHARE calculations with degraded Steam Generator mass inventory or with one or two SCS systems unavailable were performed, the results show that safe conditions are maintained as far as natural circulation is maintained in the pools (water level)

Steam Generator Tube Rupture (SGTR) simulations have shown that an automatically started SCS on Scram signal is particularly efficient even with a one hour delayed operator action.

Current studies status

. They are focused on pool characteristics adjustment with 3 D.two phase flow code calculations and on EPICE experimental program definition to improve and validate Cathare in-pool (or low pressure) heat exchangers modelling .

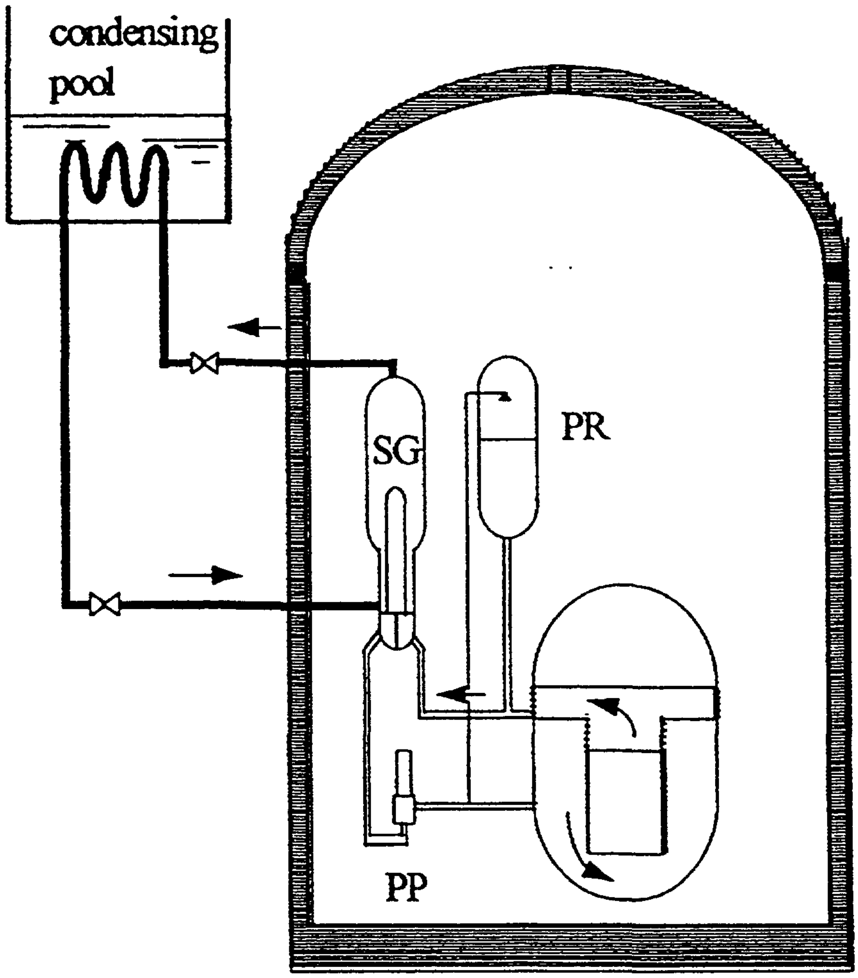

Figure 3. SCS

STEAM INJECTOR SYSTEM

A Steam Injector (SI) is a device without moving part, in which steam is used as the energy source to pump cold water from a pressure lower than the steam to a pressure higher than the steam. In SI all thermodynamic processes rely on direct contact transport phenomena (mass, momentum and heat transfer) between fluids, not requiring any moving mechanism. Schemes of both real [2] and modelled SI are shown in Fig. 4.

SI Description(2).

SI can be divided in four parts :

• a steam nozzle, producing a nearly isentropic expansion and partially converting steam enthalpy into kinetic energy,

• a water nozzle, producing a moderate acceleration and distributing the liquid all around the steam,

• a mixing section, where steam and water come into contact. Steam transfers to water heat (because of temperature difference), mass (because of the related condensation) and momentum (because of velocity difference). The final result is the complete steam condensation, with a liquid outflow at relatively high pressure.

• diffuser, where the liquid kinetic energy at mixing section outlet is partially recovered

A numerical model has been developed using CATHARE 2.

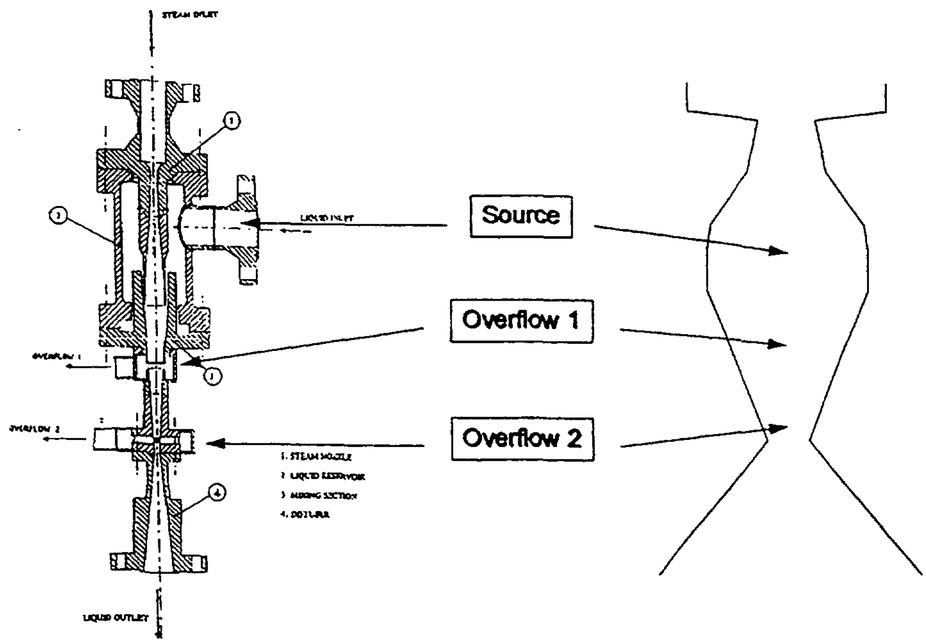

Figure 4. Real and Modelled Steam Injector

Results of the numerical simulation.

Several experimental tests have been reproduced with CATHARE. And some unexperimented situations have also been simulated. In particular, SI have been shown to still work even with very degraded steam quality. Later, a similar case has been experimented by CISE, and it has confirmed our observation.

First, a standard case will be shown. Table 1 shows the conditions that have been used.

TABLE 1. Test conditions

water tank temperature (°C)	12.7
water tank pressure (MPa)	0.2
inlet steam pressure (MPa)	5.14
inlet steam temperature (°C)	275.3
discharge pressure (MPa)	5.58

Fig. 5 shows the pressure profile that has been calculated

In steam nozzle part, steam flow passes from a subsonic to a supersonic flow

At water source location, pressure is low enough to allow liquid water injection from water tank

In mixing section, a supersonic two-phase flow is observed, until complete condensation of steam into water

At that full condensation point, a sharp pressure rise occurs, it corresponds to a supersonic-subsonic transition

In the last diverging part, pressure is recovered from kinetic energy

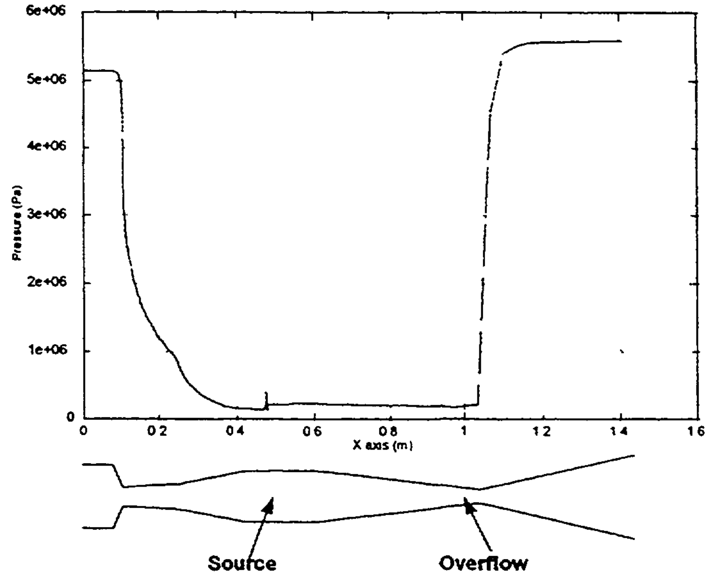

Figure 5. Pressure Profile in SI

SI Systems applications.

Several kinds of safety injection systems using SI can be considered.

Primary Side Safety Injection System. For that kind of systems, the most interesting source of steam is the pressurizer. Indeed, it seems very attractive during an accidental transient to condense steam coming from the core vessel through the pressuriser with subcooled water coming from a safety tank and re-injecte the water liquid flow in the primary system. It is obviously a very efficient way to depressurize primary circuit. It must be noticed that, with an optimal adjustment, it could be possible to continuously replace a steam mass by the same mass of subcooled water. With such a kind of systems, SGTR management could be particularly eased.that sharp steam quality and inlet pressure variations due to the pressuriser two phase flow would not stall SI.

The main problems to solve are coming from steam injector unstability (it cannot be restarted after stalling) and, from overflows control during Steam Injector starting procedure (it is not proved that SI would start with two phase flow) and, when running, as the overflow has to remain open

It has to be mentionned also that CATHARE simulations results indicated that non consable gas presence seems to affect SI functionning.

An other point to be explored by experimental means is the behaviour of diluted boron in a supersonic SI and, in general, the boron concentration control with a steam injector.

Auxiliary Feedwater System. Systems using SI for secondary safety injection seem, a priori,easyer to built. as there is no diluted boron to inject and no uncondensable gas (at least in unbroken steam generators in the case of steam generator tube rupture transient)

But the main point is : can SI systems be more reliable than existing systems? . More complete studies are necessary to answer that question.

Current studies status

They are in two directions:

Steam Injector Cathare 2 modelling improvments to adapt the heat exhanges model (gas phase at a supersonic velocity) as there are still discrepencies between experimental data results and Cathare results

Auxiliary Feedwater System using several Steam Injectors Cathare 2 PWR data set, coupling of the steam injector data set with a 900 Mw PWR Cathare 2 data set in the way of accidental transient (Loss of Feedwater) numerical simulation.

ABBREVIATIONS

AFS : Auxiliary Feedwater System
IRWST : In-Reactor Water Storage Tank
LPSIS : Low Pressure Safety Injection System
PWR : Pressurized Water Reactor
PRA : Probabilistic Risks Analysis
RHRS : Residual Heat Removal System
RRP : Refroidissement du Réacteur au Primaire
SCS : Secondary Condensing System
SG : Steam Generator
SGTR : Steam Generator Tube Rupture
SI : Steam Injector

REFERENCES

[1] Gautier, G-M., **Dispositif d'Evacuation de la Puissance Résiduelle du Coeur d'un Réacteur Nucléaire à Eau Pressurisée**, Patent n° 92 05220, April 28, 1992.

[2] Cattadori, G., Galbiati, L., Mazzocchi, L., Vanini, P., **A Single-Stage High-Pressure Steam Injector for Next Generation Reactors : Test Results and Analysis**, European Two-Phase Flow Group Meeting, University of Hannover, Germany, June 7-10, 1993.

RISK REDUCTION POTENTIAL OF JET CONDENSERS

A.W. REINSCH, T.G. HOOK
Southern California Edison Co., San Clemente,
California, USA

K.I. SOPLENKOV, V.G. SELIVANOV, V.V. BREDIKHIN
Research Institute of Nuclear Power Plant Operation,
Moscow

I.I. SHMAL, Y. FILIMONOV, Y.N. PAVLENKO
Electrogorsk Research Engineering Center,
Electrogorsk

Russian Federation

Abstract

Ejectors serving as high-pressure condensers produce a self-controlling heat removal process induced by the dynamic form of natural convection. The simplicity of passive heat removal systems with ejector condenser (PAHRSEC or jet condenser) reduces the likelihood of component failures and human errors. Designed for a heat removal rate exceeding the decay heat, the system has the capability for internal depressurization of the reactor coolant system without loss of primary or secondary coolant. In the event of a small loss-of-coolant accident (LOCA), jet condensers reduce the reactor system pressure to the point where the shutdown cooling system can operate. Simulations of the response of the 1,100 MW_e pressurized-water reactors at San Onofre with two PAHRSEC loops to transients and small LOCAs determined the success criteria for the system. Jet condensers designed for internal depressurization can cope with more than 99% of all initiating events in terms of frequency. Based on a probabilistic safety assessment, the system would reduce the frequency of core damage at the San Onofre Plant by a factor of 2. This value applies to internal initiating events only. If external events are included in the evaluation, the risk reduction factor would increase significantly. In the event of a steam generator leak or tube rupture, a release of fission products to the atmosphere would be prevented by the closed jet condenser loop.

1. INTRODUCTION

In the early phase of the advanced reactor program, some aspects of nuclear safety were defined in absolute terms: Passive systems were considered "inherently" safe and, therefore, essential for advanced reactor safety. The increased use of probabilistic safety assessment in the design and operation of nuclear power plants has led to a more balanced approach, replacing qualitative terms with quantitative measures.

While physical effects utilized in passive systems tend to increase system reliability because of the absence of moving parts and support systems, the reliability of core cooling is not necessarily improved significantly by the increased system reliability itself. A more effective way to reduce the core damage frequency (CDF) is to develop systems with the capability to respond to the majority of initiating events and, consequently, terminate a broad spectrum of accident sequences.

Another important aspect in the development of advanced reactor systems is cost. From the beginning of the nuclear era, attention had been focused on safety at any price. As a result, nuclear power became too expensive. Electric power generated by recent light-water reactors in the United States costs currently twice as much as power from combined-cycle gas turbine plants. Wall Street analysts predict now that the competitive pressure developing in the U.S. utility industry since the passage of the National Energy Policy Act will lead to the permanent shutdown of 20 to 25 nuclear power plants in the next 10 years. In this economic environment, the objective for advanced safety systems must be a significant risk reduction at the lowest possible cost.

2. PRINCIPLE

2.1 PAHRSEC flow scheme

The essential feature of the concept is the utilization of the reactor decay heat to produce pumping power for coolant circulation [1,2]. Although comprehensive computer analyses and large-scale testing of the concept is of relatively recent origin, considerable experience in the design, analysis and performance verification of the system has been gained in the last years [3].

A high-pressure jet condenser (Figure 1) converts about 5% of the decay heat into kinetic energy by expanding steam from the steam generator in a convergent nozzle. For a heat removal rate of 75 MW_t, the kinetic energy of the steam jet at sonic velocity is about 4 MW. The steam mixes in the ejector with water at lower temperature from a heat exchanger and condenses. Kinetic energy of the mixture is converted at the increased density into a pressure rise of the fluid sufficient to return the condensate to the steam generator and recirculate coolant through the heat exchanger serving as heat sink. Most of the kinetic energy in the steam jet is converted into heat during mixing with water at low velocity. Less than 10% of it produces pumping power for fluid circulation and heat removal. The overall ejector efficiency in converting the decay heat into pumping power is less than 1% which reflects the simplicity and ruggedness of the component.

One important characteristic of the concept is that the whole loop including the heat exchanger is at the same pressure as the steam, supplying high-pressure water to the "suction" side of the ejector. This characteristic extends the operating range of the PAHRSEC ejector to a much higher pressure level than that of conventional single-stage ejectors whose maximum discharge pressure is about 2.5 MPa.

2.2 Dynamic natural convection

Fluid circulation in jet condensers can be considered the dynamic form of natural convection. Unlike the static form of natural convection which is driven by hydrostatic pressure differences, dynamic natural convection uses inertial forces to

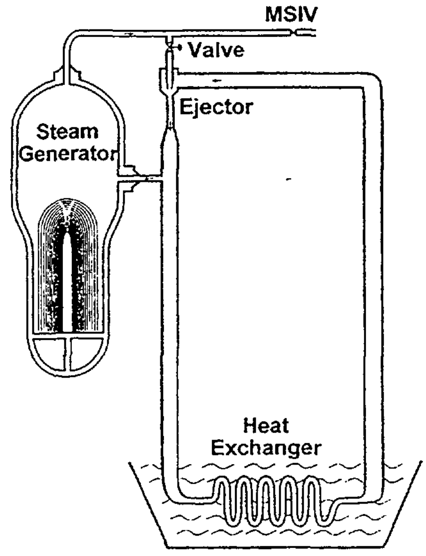

Figure 1: Principle of jet condenser (PAHRSEC) as heat removal and depressurization system

generate flow [4]. The system's process-inherent control function regulates the steam pressure and the mass flow rate depending on the decay heat generated in the core.

Two-phase hydrostatic natural convection is susceptible to flow oscillations since condensation phenomena affect the steam flow to the condensation surfaces. This feedback between the process and its power supply leads to instabilities such as chugging. In the jet condenser, critical flow in the ejector steam nozzle separates the mixing and condensation process downstream of the nozzle from the steam supply upstream, preventing feedback between condensation and steam flow. Flow perturbations originating downstream of the ejector steam nozzle cannot travel through the critical flow region at the nozzle exit into the steam pipe upstream of the nozzle. This characteristic ensures smooth and stable operation under all transient conditions.

3. SAFETY-RELATED SYSTEM CHARACTERISTICS

3.1 Internal depressurization

The risk reduction potential of jet condensers is determined by the combined safety functions of heat removal and internal depressurization. Designed for a heat removal rate exceeding the reactor decay power, the system has the capability to depressurize the reactor without coolant blowdown by lowering the reactor coolant system temperature.

The effect of the internal depressurization is similar to steam relief through atmospheric dump valves or an automatic depressurization system. However, the coolant is not discharged from the closed PAHRSEC loop into the atmosphere or a suppression pool at low pressure. Rather, it is returned to the heat source at high pressure, conserving coolant and preventing the release of fission products to the environment. Current active designs compensate for the loss of coolant through the relief valves by coolant injection with feedwater pumps.

3.2 Spectrum of initiating events mitigated

Jet condensers can cope with a broad spectrum of initiating events. Passive heat removal protects the reactor against all transients including loss of offsite power and station blackout. The additional capability of internal depressurization provides protection against LOCAs with an equivalent diameter of up to 5 cm. This increases the spectrum of events covered by jet condensers to over 99% of all initiating events in terms of frequency. In a typical pressurized-water reactor population, initiating events that exceed the mitigation capability of PAHRSEC loops would occur only about every 500 reactor-years.

3.3 Reduced human error potential

A single response - opening of the startup valve - is required from PAHRSEC for all initiating events to function. Thermal equilibrium between decay power and heat removal from the reactor coolant system is established rapidly after reactor shutdown. The water returned to the steam generator by the ejector is heated by mixing with high-pressure steam, reducing thermal stresses significantly. Because of these operational characteristics, automatic PAHRSEC actuation is recommended after plant trip, obviating the need for human interaction. Human errors during maintenance and testing are unlikely owing to the system's simplicity. Inadvertent actuation of a jet condenser caused by operator error or a spurious signal results in a reduction of the steam pressure by less than 5%. This pressure reduction would not trip the plant.

3.4 Process-inherent control

Utilizing the reactor decay heat as power source for the heat removal process provides process-inherent control of the coolant flow to match the decay heat. Less decay heat means also reduced pumping power for fluid circulation, keeping the temperature distribution relatively stable. With decreasing decay heat, the pressure in the system decreases, lowering the density of the steam in the ejector nozzle and, consequently, the steam and water flow rates.

The controlling phenomenon of the process is critical flow at the exit of the ejector steam nozzle. The sonic velocity of steam remains almost constant over a wide pressure range. Therefore, a constant volume flow of steam is discharged by the ejector steam nozzle into the ejector mixing section. If the decay heat decreases requiring less coolant flow, a reduced saturation pressure in the steam generator (and a lower steam density) satisfy the energy balance by reducing the mass flow rate in the ejector steam nozzle.

3.5 Prevention of initiating events

The heat removal rate of a PAHRSEC loop is designed to be approximately equal to the decay heat following reactor trip. Since the flow and heat removal rates depend on the geometry only and are not influenced by outside parameters such as valve alignment, control systems, pump speed, electric power and operator actions, a quasi-equilibrium is reached rapidly after startup of the system. The capability to reduce pressure and temperature transients after reactor trip can prevent certain initiating events. For example, the lifting of a pressurizer relief valve led to the accident at Three Mile Island. An instant balance between decay heat generation and heat removal after reactor trip reduces the potential for initiating events such as pressure transients, pressurized thermal shock, cooldown transients, pump seal failure and water hammer.

3.6 Dose reduction

Similar to a condenser driven by hydrostatic forces, the jet condenser forms a closed loop with the steam generator, condensing high-pressure steam and returning the condensate to its source. Heat is rejected to the environment by heat conduction through the heat exchanger walls without mass exchange between the closed jet condenser loop and the environment. Fission products carried by the steam into the loop are returned with the condensate to the steam generator. In contrast to hydrostatic natural convection, however, the condenser surfaces are not exposed to two-phase flow, preventing flow oscillations, erosion and heat exchanger leaks.

3.7 Removal of non-condensibles

The liquid state of the coolant in the heat exchanger loop makes the separation of non-condensibles (for example, H_2 or N_2) feasible. Connected to the pressurizer steam space of a pressurized water reactor or the steam line of a boiling-water reactor, PAHRSECs would remove gases from the primary system during a severe accident exceeding the core design limits. This capability eliminates the failure mode of hydrostatic condensers caused by accumulation of gases blocking heat transfer.

3.8 Passive accident management

Two of the most effective actions in accident management are heat removal and depressurization. Both functions are immediately available upon PAHRSEC actuation after reactor trip and would prevent core damage. However, if the startup of the system would be delayed until the onset of core damage, the system would provide passive accident management by reducing pressures, temperatures and the hydrogen concentration in the reactor coolant system without operator action or support systems. At high steam pressure, the heat removal and depressurization rates would be high. The rates would decrease with the decay heat and system pressure.

3.9 Reliability of jet condenser

Only one valve has to be actuated to start the system. Its independence from electric power and support systems increases the reliability, resulting in a low number of failure modes and high system reliability. However, the reliability of the system contributes only little to the increased reliability of core cooling. The type of safety function and the safety-related system characteristics are more important in enhancing reactor safety than the system reliability. These characteristics of the jet condenser concept have been discussed in Sections 3.1 through 3.7.

During normal operation of the reactor, the startup valves to the PAHRSEC loops are closed. After reactor trip, the valves are opened to start the heat removal process. The pressure in the system before startup is essentially the same as the steam generator pressure. Only a small pressure difference across the closed startup valve exists which is created by a water column of about 5 meter in the jet condenser. Owing to the small load on the valve disc, little force is necessary to open the valve for startup, increasing the reliability of the valve.

4. SUCCESS CRITERIA AND SYSTEM SIMULATION

The jet condenser success criterion for decay heat removal and depressurization following a small break LOCA was determined by transient system analysis using the Computer Code MAAP 3B (Modular Accident Analysis Program). The code had been used to establish the system success criteria for San Onofre's probabilistic safety assessment, the Individual Plant Examination, mandated by the U.S. Nuclear Regulatory Commission. MAAP simulates the effects of a wide range of accident scenarios and phenomena including the effect of engineered safety features, operator actions and changes in geometry during a severe accident.

The code was used to analyze the response of a pressurized-water reactor with 3,390 MW thermal power (2 steam generators, 4 reactor coolant pumps, San Onofre Unit 2/3) to a 5cm LOCA using two 75MW jet condensers as heat sinks. A failure of all coolant injection pumps and feedwater pumps was postulated.

During a small LOCA, heat removal from the reactor coolant system by the two PAHRSEC loops competes with the heat loss through the break by coolant leakage. The energy removed by the systems is not available for forcing coolant out the break. The net effect is a continuous reduction of the saturation temperature and pressure in the reactor coolant system, reducing the density of the two-phase flow discharged through the leak and, therefore, the leakage flow significantly.

Results of the transient MAAP analysis of a 5cm LOCA are shown in Figure 2. Temperature, pressure, flow and leak rates decrease gradually. The core is never uncovered during the transient. Without any active safety system available, the water inventory in the reactor coolant system decreases initially. However, the accumulator tanks supply coolant at the same rate as the decreasing leakage rate, maintaining a nearly constant coolant inventory after the first hour of the accident. After the first hour, the pressure of the reactor coolant system has been sufficiently lowered to allow the use of the shutdown cooling or low-pressure injection system.

5. PROBABILISTIC ASSESSMENT OF RISK REDUCTION

An evaluation of the impact of passive heat removal and depressurization effected by two jet condenser loops on the core damage frequency of a 1,100 MW_e pressurized-water reactor has been performed. The analysis is based on the models of the Individual Plant Examination (IPE) for San Onofre Units 2 and 3. The IPE was mandated by the Nuclear Regulatory Commission as a plant-specific probabilistic safety assessment for all U.S. nuclear power plants.

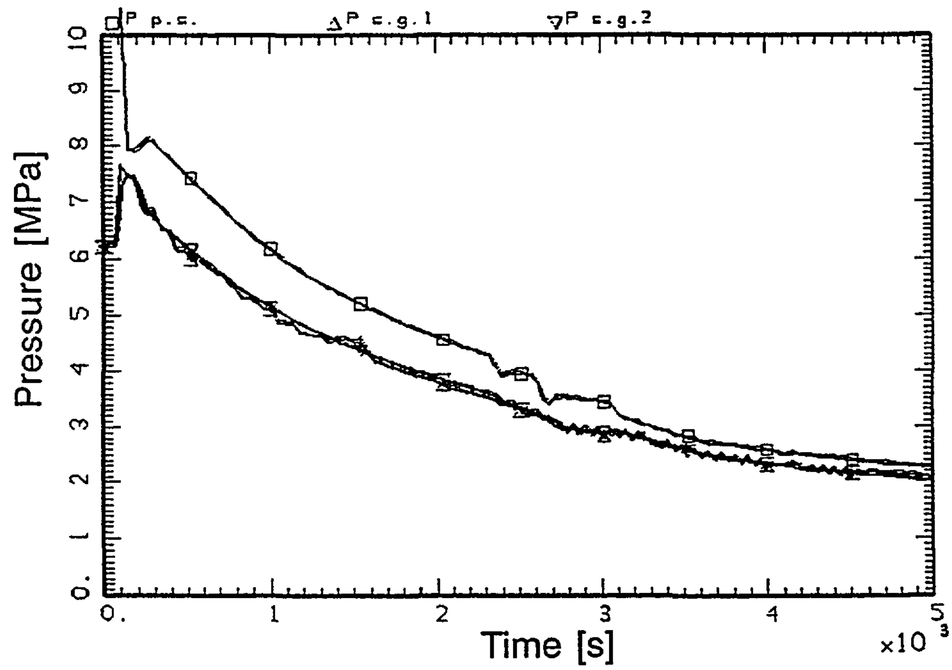

Figure 2a: Primary system pressure and steam generator pressure as a function of time after reactor trip

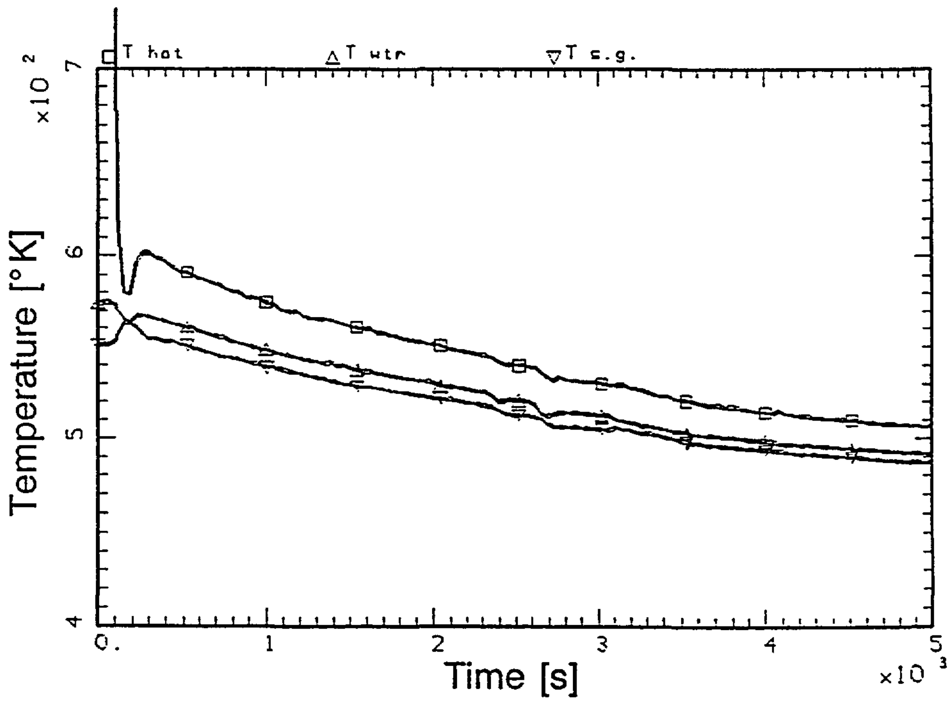

Figure 2b: Peak clad temperature, core water temperature and steam generator temperature as a function of time after reactor trip

The code QUIKRISK was used to compute the reduction in core damage frequency resulting from heat removal/depressurization by jet condensers. QUIKRISK was developed to determine the impact of changes in the configuration of a nuclear power plant on the core damage frequency. QUIKRISK cuts the time for the solution of probabilistic models significantly, allowing the analyst to investigate various plant configurations in a limited time. The code uses existing fault tree models of San Onofre 2 and 3 developed for the Individual Plant Examination. The input for the code consists of configuration changes caused by maintenance, repair and testing as well as design changes or component failures.

A base case without any plant changes was quantified with QUIKRISK first. The core damage frequency of the plant design configuration (without jet condenser) was computed by QUIKRISK as 2.8E-5 per year. Subsequently, the fault tree models of the auxiliary feedwater system and LOCAs with less than 5 cm diameter were changed to incorporate the jet condenser safety function. After adding the jet condenser to the models, the core damage frequency decreased to 1.4E-5 per year.

These results do not take into account the safety characteristics discussed in Section 3.5. In addition, the consequences of core damage would be significantly reduced by the system characteristics discussed in Sections 3.6 through 3.8. External initiating events are not expected to cause LOCAs with diameters larger than 1 cm. Medium and large LOCAs are, therefore, not part of the external initiating event spectrum. Consequently, jet condensers can cope with all external initiating events. Including external events in a probabilistic safety assessment increases the system's risk-reduction potential significantly.

6. EXPERIENCE AT U.S. NUCLEAR POWER PLANTS

Current risk assessment techniques use plant-specific failure probabilities where available and generic numbers for rare events. In order to gather information on rare events, the experience with safety-related incidents in the entire population of U.S. nuclear power plants has to be reviewed.

Cable fires, cooldown transients, steam generator tube ruptures, loss of offsite power, station blackout and one small LOCA were the events with the highest impact on public safety at commercial nuclear plants. In areas with frequent seismic activity, the nuclear risk is increased significantly by potential earthquakes.

A review of these initiating events indicates that jet condensers can prevent core damage following all of these events and keep transient pressure and temperature changes in the reactor coolant system within safe limits. For loss of offsite power and station blackout, core damage is prevented since the safety function of the passive heat removal system is independent from electric power. Fire affects automatic control systems and electric power supply which are not required for PAHRSEC operation.

A cooldown transient in a nuclear power plant is highly unlikely if the decay heat is removed by jet condensers. The fixed geometry of the system makes a sudden imbalance between decay power and heat removal impossible, maintaining a quasi-equilibrium with a steady temperature distribution.

Small LOCAs with up to 5 cm diameter have been discussed in Section 5. The analysis using the MAAP Code proved that core temperatures and leakage from the reactor coolant system are continually decreasing with 2 PAHRSECs operating. The core remains covered throughout the transient. A window of several hours is available for switching from the PAHRSEC loops to shutdown cooling or low-pressure injection.

In the event of a steam generator tube rupture, fission products leaking into the steam generator would be retained in the closed PAHRSEC loop. Both steam generators would be effective for heat removal and depressurization. Identification of the leaking steam generator and/or operator decisions are not required. Similar to a small LOCA, depressurization of the primary and secondary sides reduces the leakage flow continually. The loss of reactor coolant inventory is made up by coolant injection from the accumulator tanks.

Earthquakes contribute significantly to the core damage frequency of nuclear power plants in seismically active regions. Although the interaction of numerous minor malfunctions such as relay chatter causes a large increase in risk, no major structural damage to the nuclear system such as a large LOCA or a vessel failure is expected. Since PAHRSEC loops are independent from electric power and control systems, they have the capability to mitigate all consequences of seismic events and effect a safe shutdown.

7. SUMMARY

The core damage frequency of light-water reactors can be reduced significantly by passive heat removal using jet condensers. Utilizing the decay heat to induce coolant circulation and system depressurization, jet condensers have the capability to terminate the majority of potential accident sequences in light-water reactors. The simplicity of the system lowers the likelihood of human errors significantly. Cost reductions during construction and operation are anticipated.

REFERENCES

[1] SOPLENKOV, K. I., NIGMATULIN, B., Passive heat removal system with ejector-condenser, American Nuclear Society Winter Meeting, San Francisco, California, November 10 - 14, 1991.

[2] Reinsch, A. W., Process-inherent operational safety through jet condensers, Second International Conference on Thermal Hydraulics and Nuclear Power Plant Operation, Tokyo, May 14 - 16, 1986.

[3] Soplenkov, K.I., Selivanov, V.G., BREDIKHIN, V.V. et. al., Design and testing of passive heat removal system with ejector-condenser, IAEA Technical Committee Meeting, Piacenza, Italy, May 16 - 19, 1995.

[4] REINSCH, A.W., Static versus dynamic natural convection, American Nuclear Society Annual Meeting, Nashville, Tennessee, June 10 - 14, 1990.

DIVERSIFIED EMERGENCY CORE COOLING IN CANDU

P.J. ALLEN, N.J. SPINKS
Atomic Energy of Canada Ltd.,
Canada

Abstract

The CANDU low pressure heavy water moderator surrounds the fuel channels and is available as a heat sink to maintain channel integrity and avoid fuel melting in the unlikely event of a loss of coolant accident with loss of emergency coolant injection. Existing CANDU reactors use pumps to circulate the moderator and the cooling water.

A passive moderator heat rejection system is being developed to diversify the emergency heat rejection paths to the environment. The moderator heat rejection system, as described in reference 1, incorporates a natural circulation of heavy water driven by flashing to steam as the heavy water flows to an elevated heat exchanger. The heat exchanger is cooled in turn by a natural circulation flow of light water to a large reservoir.

Analysis has shown that this system can reject the moderator heat in a stable manner. As further confirmation, a full elevation, light water, 1/60th volume scaled test of the natural circulation heavy water loop has been carried out to verify the overall concept and the analysis. In particular, the stability of the flashing driven flow has been confirmed and will be reported in reference 2.

With careful attention to eliminating common mode failures in the shutdown systems, the heat transport system, the emergency core cooling system and the moderator system, the core melt frequency can be reduced to the point that core melt mitigation for events internal to the plant ceases to be a design concern. These same design provisions will form additional lines of defence for all but the most extreme external events as well.

Introduction

As in other pressurized water reactors, the primary accidents of concern for CANDU are those that involve a loss of coolant (LOCA), or failures in systems that could induce a LOCA (such as a loss of flow, loss of heat sink). For these accidents, the requirements of shutdown, cool, contain and monitor apply.

Where CANDU differs from standard pressurized light water reactor technology is primarily the design of the reactor core. The CANDU core design offers some unique possibilities for design of mitigating measures that are diverse in concept from the traditional technology. These differences have been exploited to a degree in existing CANDU designs. For future designs, concepts are being developed to enhance system diversity to the point that core melt mitigation for internally caused events ceases to be a design concern.

Diversity in Current CANDU Designs

Contemporary CANDU reactor designs employ redundancy and a considerable level of diversity in the safety systems. Thus redundancy and diversity exist in the two shutdown systems. Both shutdown systems make use of the low-pressure moderator environment (the calandria) but shutoff rods enter the calandria from above whereas the poison injection system enters the calandria from the side, as shown in figure 1. Each system has its own initiating signals. For every postulated accident, there are normally two diverse signals on each shutdown system to trip the reactor for the complete range of initial operating conditions. Note that the two shutdown systems are passive in that no operator action and no external power are needed for shutdown action to occur.

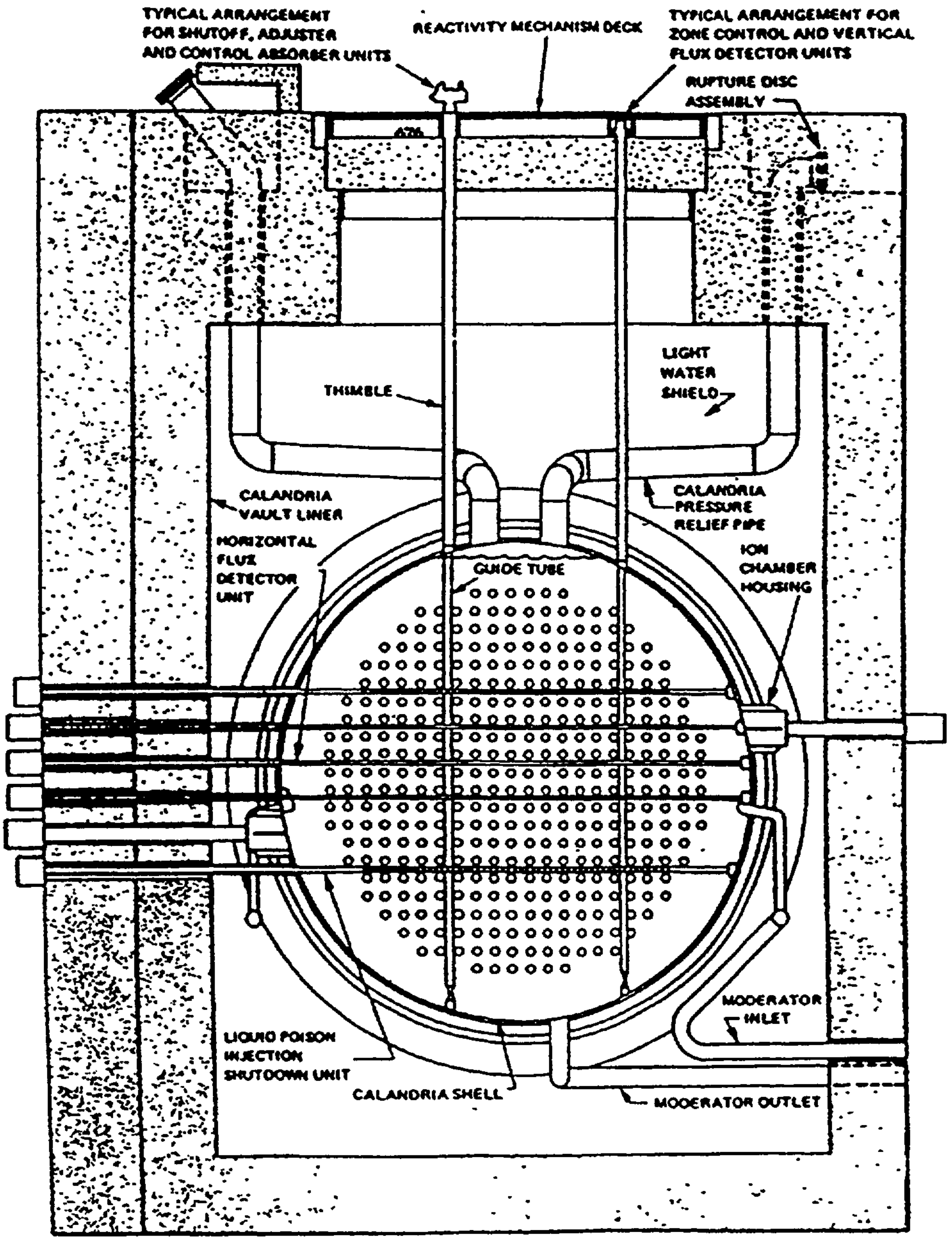

FIGURE 1
CANDU CORE SHOWING SHUTDOWN SYSTEM ARRANGEMENT

Redundancy also exists in the emergency-core-cooling systems. In the event of a loss-of-coolant accident, the Emergency Core Cooling (ECC) system uses pressurized gas (or pumps in some plants) to inject light water into the heat transport system. The water is eventually recovered from a sump in the reactor building, cooled in a heat exchanger and pumped back into the heat transport system.

The low-pressure low-temperature moderator serves as a redundant and potentially diverse emergency-core-cooling system. Its availability during normal operation is apparent and it acts passively to accept heat from the fuel channels in an accident involving loss of coolant with loss of ECC. However moderator heat rejection is currently done with electrically powered pumps and pumped cooling water. The electrical supply and cooling water system also serve the ECC. The common electrical supplies and cooling water limit the combined reliability of the emergency core cooling systems.

Core melt in CANDU can occur only with a loss of coolant (whether caused by pipe failure or a support system failure that induces loss of coolant by system overpressure and relief) with loss of ECC plus loss of the moderator heat sink. Common failures in these systems, e.g. loss of service water or electrical power to both the moderator and the ECC systems, are the main contributors limiting the core-melt frequency for internal events to about $4x10^{-6}$ per year (ref. 3). While this core melt frequency meets targets set for advanced designs, the ability of the moderator to act as a heat sink provides the opportunity to progress further by eliminating common links between the moderator and other systems.

A conceptual CANDU design is under study which employs a conventional ECC system with a passive moderator heat rejection system. Thus passive design techniques are used to advantage in enhancing the diversity in the two core cooling systems.

Passive Moderator Heat Rejection

Progress on the passive moderator system development was last given in reference 1. Figure 2 illustrates the concept.

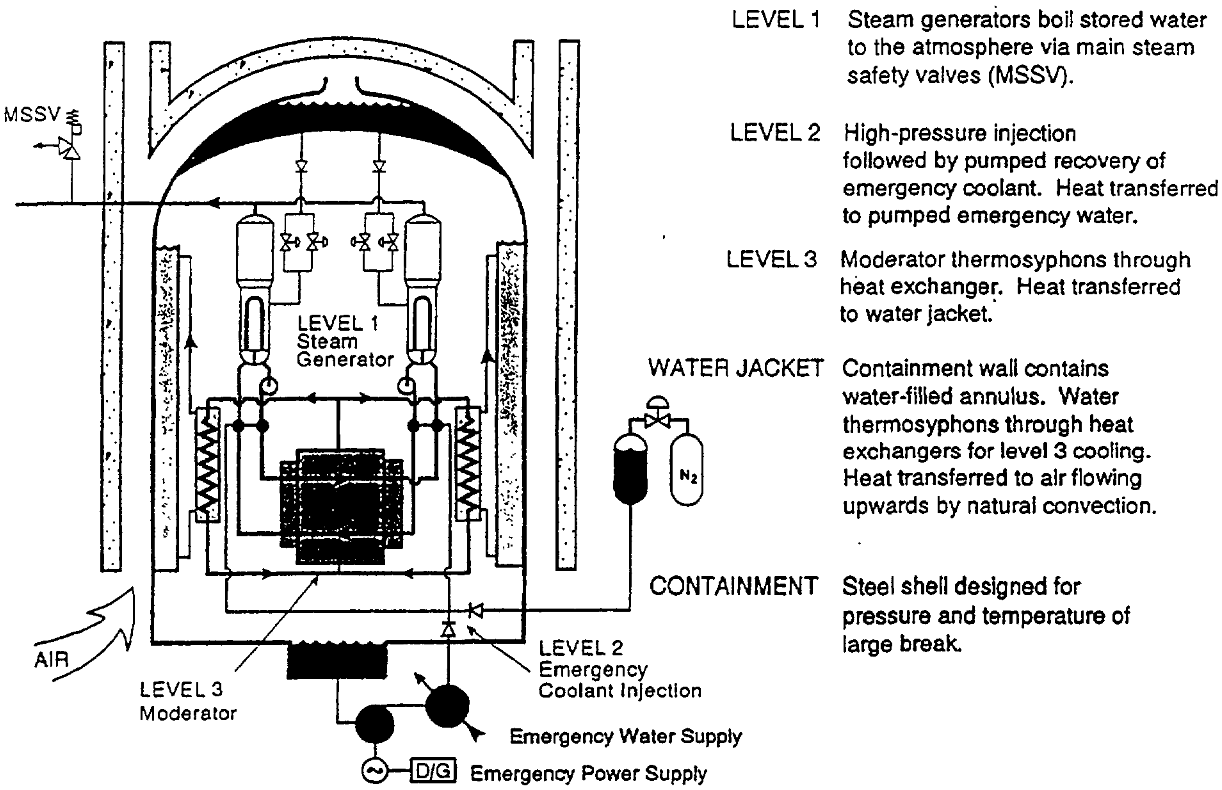

FIGURE 2
CANDU EMERGENCY COOLING

The idea is to run the heavy water in the calandria at a temperature near the boiling point but to allow the water to flash to steam as it rises in a pipe from the calandria to an elevated heat exchanger. Subcooled heavy water would be returned to the calandria. The difference in density between the two-phase flow in the riser and the liquid in the downcomer would provide the buoyancy force to drive the flow.

Reference 1 gives results of simulations using the CATHENA transient thermalhydraulics code which demonstrates that the normal full power heat load to the moderator can be transferred in a stable manner with such a design. Note that the heat load to the moderator during a loss of coolant accident, with the reactor at decay power, is only 30% of normal full power moderator heat load.

More recently, further CATHENA simulations have been done at reduced powers. They show a flow oscillation at low power. Also tests have been done in a full elevation loop having a scale of about 1/60 in power, volume and flow area. They confirm the CATHENA predictions. The tests will be reported in more detail in reference 2.

As power is increased, flashing is first observed in the transparent glass riser at upper elevations. The flow is oscillatory with the riser being liquid filled after the high-flow part of a cycle. No untoward effect of the oscillations is evident. As the power is increased, the oscillation amplitude decreases and the flow becomes stable. During a rapid increase of power, only one or two oscillations are seen as the flow overshoots before returning to the steady-state value. Thus the feasibility of the flashing-driven design is considered to be established both for the normal operating condition and for accidents.

Loss of Shutdown

As in other reactors, the CANDU reactor must be shutdown following an accident so that the mitigating systems can deal with the consequences. The unique CANDU geometry has allowed the implementation of a second shutdown system which is diverse from the shutdown system using rods and equally capable in terms of speed and more capable in terms of reactivity depth. Both shutdown systems are totally independent of the control system (no rods or controls are shared) and each shutdown system has independent instrumentation and trip circuitry. Both shutdown systems make use of the low-pressure moderator environment (the calandria) but shutoff rods enter the calandria from above whereas the poison injection system enters the calandria from the side, as shown in figure 1. For every postulated accident, two diverse signals are normally provided on each shutdown system to trip the reactor for the complete range of initial operating conditions.

The careful attention given to diversity in the design of CANDU and its two safety shutdown systems has led to common mode failures being reduced to a very low probability. This fact means that a simple product of the failure frequency of events leading to overpower (beyond the capability of the reactor control system) and the unavailabilities of the two shutdown systems reflects properly the order of magnitude for loss of shutdown events. Based on the 200 unit-year CANDU operating record, improvements made to earlier reactor control systems and more recent operating experience, the frequency of challenges to the shutdown systems is now about 10^{-2} per year. Also the two shutdown systems are each required to have an unavailability of 10^{-3} and continued operation requires testing to ensure that this figure is met. Thus the frequency of loss of shutdown is of order

$$10^{-2} \times 10^{-3} \times 10^{-3} = 10^{-8} \text{ per unit-year.}$$

See also the figure of 2.5×10^{-8} per unit-year calculated in more detail in reference 3.

Core Melt

Core melt can occur in CANDU only with a loss of heat transport system inventory (whether caused by pipe failure, valve failure or loss of heat sink), a loss of ECC and a loss of the moderator as a heat sink. Reference 3 gives a detailed account of the accident sequences leading to core-melt for CANDU 6. The sequences are dominated by common cause events such as loss of service water and loss of electrical power. These contribute most of the core-melt frequency of 4.4×10^{-6} per unit-year. The triple failure events involving LOCA with loss of ECC and loss of the moderator heat sink contribute only 0.6×10^{-6} per unit year and this figure is dominated by the continuing need to keep moderator and ECC pumps running in the longer term.

With diversity in the heat transport system, the ECC system and the moderator system, the core melt frequency reduces to a simple product of the failure frequency of the heat transport system and the unavailabilities of the ECC and the moderator systems. From the 200 unit-year operating record for CANDUs, and the single event (Pickering unit 2, 1994) which required actuation of ECC, the failure frequency is order 10^{-2} per unit year. Also the ECC system is required to have an unavailability of 10^{-3} and in-service testing is done to ensure that this figure is met. However the ECC pumps have to keep running for an extended period and an unreliability of 10^{-2} has been calculated (reference 3) over the mission period.

A passive moderator heat rejection system which does not rely on continued operation of pumps should be more reliable than a pumped system and is likely more reliable than the ECC system. Also it is possible to operate the moderator system continuously so that its availability is assured. It follows that an unavailability better than 10^{-3} is achievable and given a low probability of cross link failures, the frequency of core melt becomes on the order of

$$10^{-2} \times 10^{-2} \times 10^{-3} = 10^{-7} \text{ per unit-year.}$$

The key issue is the probability of crosslink failures between the mitigating systems (ECC and the moderator) and the initiating accidents. Given the diverse nature of ECC and the moderator, the probability of crosslinks between these two systems is low. The remaining question is whether the initiating accidents can cause failures in either mitigating system.

As in other water cooled reactors, the ECC system is designed to be independent, to the degree possible, from events that could lead to a loss of coolant. Standby equipment is provided to support the ECC function that is also independent of the normally operating process equipment used to cool the fuel.

The proposed arrangement for cooling the moderator is also independent of the normal process fuel cooling and the ECC cooling. The main interface with either system is due to the physical arrangement of the calandria. If a fuel channel failure is the initiating event, then the LOCA discharge is into the moderator fluid. Calculations have been done (reference 1) for this situation and the results show that the heat load from the discharge can be accommodated by the moderator cooling system.

The remaining issue is calandria leakage following a LOCA event. Loss of the moderator fluid would disable the moderator as a emergency heat sink. Two mechanisms exist which could lead to calandria leakage. They are addressed in existing designs by pumping makeup water to the calandria. For the passive design, reliance on pumps is to be avoided.

One mechanism is a fuel channel failure which leads to ejection of the channel endfitting. For a passive design, there needs to be a restraint to limit end fitting movement following a channel failure. The other mechanism is a inlet feeder pipe break which, with the reactor at high power, diverts sufficient flow from the channel to cause overheating and channel failure. Eventually the moderator water could drain through the failed channel and broken feeder. For the passive design, early reactor trips which can prevent channel failure will be installed.

Development programs are ongoing to address these issues.

External Events

Given that the passive moderator equipment is inside the containment/shield building, it can be protected from most external hazards by the surrounding structure. Well tested engineering design approaches can be used to protect the containment contents from flood, high wind, tornado missiles, etc. This situation is different than for more conventional core cooling systems that depend on power and cooling water coming from outside the containment. Such sources of power and water are more vulnerable to effects from external events.

In addition, seismic qualification would not seem to be problematic for a passive cooling system of this type.

Since survival of the passive moderator system can be assured for foreseeable external events, core melt frequency will also be reduced for external events.

Conclusion

A passive moderator heat rejection system is being developed for CANDU which, combined with a conventional emergency-coolant injection system, will provide the diversity to reduce core-melt frequency to order 10^{-7} per unit-year. This is similar to the approach used in contemporary CANDU designs in the shutdown systems which results in a frequency of loss of shutdown on the order of 10^{-8} per unit-year.

Testing of a full height 1/60 power-and-volume-scaled passive-moderator-heat-rejection system has demonstrated its feasibility for removal of heat during normal operation and during accidents.

With the frequency of severe accidents caused by internal events reduced to order 10^{-7} per unit year by these measures, no need should exist for consideration of core damage states more severe than the moderator acting as a heat sink. Providing a reliable and diverse alternate emergency heat sink reduces the severe accident challenge to containment integrity and provides more assurance of the release to the public and the environment being limited.

REFERENCES

1. W.P. Baek and N.J. Spinks, "CANDU Passive Heat Rejection Using the Moderator", International Conference on New Trends in Nuclear System Thermohydraulics, Pisa, May 1994.

2. H.F. Khartabil and N.J. Spinks, "An Experimental Study of a Flashing-Driven CANDU Moderator Cooling System", for CNS Conference, Saskatoon, 1995 June.

3. Report AECL-9607,"CANDU 6 Probabilistic Safety Study Summary", 1988 July.

MITIGATION OF TOTAL LOSS OF FEEDWATER EVENT BY USING SAFETY DEPRESSURIZATION SYSTEM

YOUNG M. KWON, JIN H. SONG, SANG Y. LEE,
SANG K. LEE
Korea Atomic Energy Research Institute
Taejon, Republic of Korea

Abstract

The Ulchin 3&4, which are 2825 MWt PWRs, adopted Safety Depressurization System (SDS) to mitigate the beyond design basis event of Total Loss of Feedwater (TLOFW). In this study the results and methodology of the analyses by CEFLASH-4AS/REM for the determination of SDS bleed capacity are discussed.

To verify the results of CEFLASH-4AS/REM simulation a comparative analysis has also been performed by more sophisticated computer code, RELAP5/MOD3. The TLOFW event without operator recovery and TLOFW event with feed and bleed (F&B) were analyzed. The predictions by the CEFLASH-4AS/REM of the transient two phase system behavior are in good qualitative and quantitative agreement with those by RELAP5/MOD3 simulation. Both of the results of analyses by CEFLASH-4AS/REM and RELAP5/MOD3 have demonstrated that decay heat removal and core inventory make-up can be successfully accomplished by F&B operation during TLOFW event for the Ulchin 3&4.

1. Introduction

Following the Three Mile Island accident, the potential ability of Power Operated Relief Valves (PORVs) to provide an alternate method to remove decay heat from the primary system was identified and considered to be beneficial in dealing with severe accidents. Recent studies [1, 2, 3, 4] have concluded that F&B can be a viable alternate means of decay heat removal, but successful use of F&B is contingent upon the implementation of proper procedures, as well as upon the specific plant design. ABB-CE's latest plant design, System 80+[5], includes manual bleed valves to provide the F&B capability according to the USNRC's Severe Accident Policy.

The Korea Atomic Energy Research Institute (KAERI) is performing detailed design of the SDS similar to that of System 80+. In particular, manually-actuated bleed valves are designed to provide a capability to rapidly depressurize the Reactor Coolant System (RCS) for TLOFW event. Presented in Reference 6 are the preliminary results of thermal-hydraulic analyses of TLOFW for the Ulchin 3&4, which were performed by CEFLASH-4AS/REM [7]. In this study provided are the final results and methodology of the thermal-hydraulic analyses to determine the Ulchin 3&4 SDS bleed capacity. Also an alternate analysis by more sophisticated computer code RELAP5/MOD3[8] is performed to verify the results and methodology used for Ulchin 3&4 SDS design.

2. Plant description and initial conditions

The Ulchin 3&4 are two loop 2825 MWt PWRs. The Ulchin 3&4 are designed with two cold legs per loop and thus contain four reactor coolant pumps. The SDS consists of two separate lines connected to the top head of the pressurizer and the flow through each line discharges to the containment atmosphere through a rupture disc as shown in Figure 1. The two bleed paths consist of an isolation valve and control valve in series per path, and provide redundant paths. The plant nodal diagrams for CEFLASH-4AS/REM and RELAP5/MOD3 are provided in Figure 2.

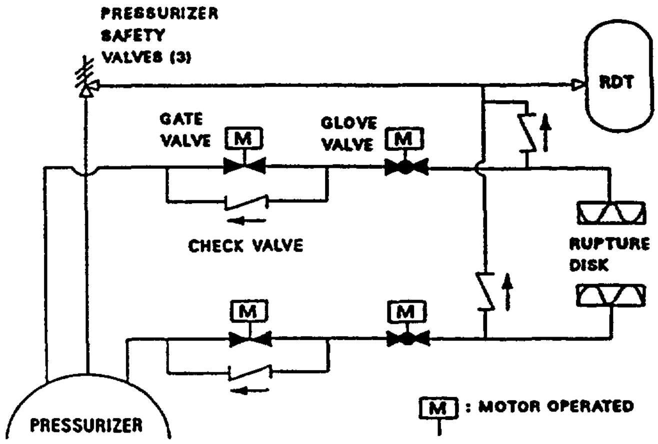

Fig.1 A Schematic Diagram of UCN 3&4 SDS

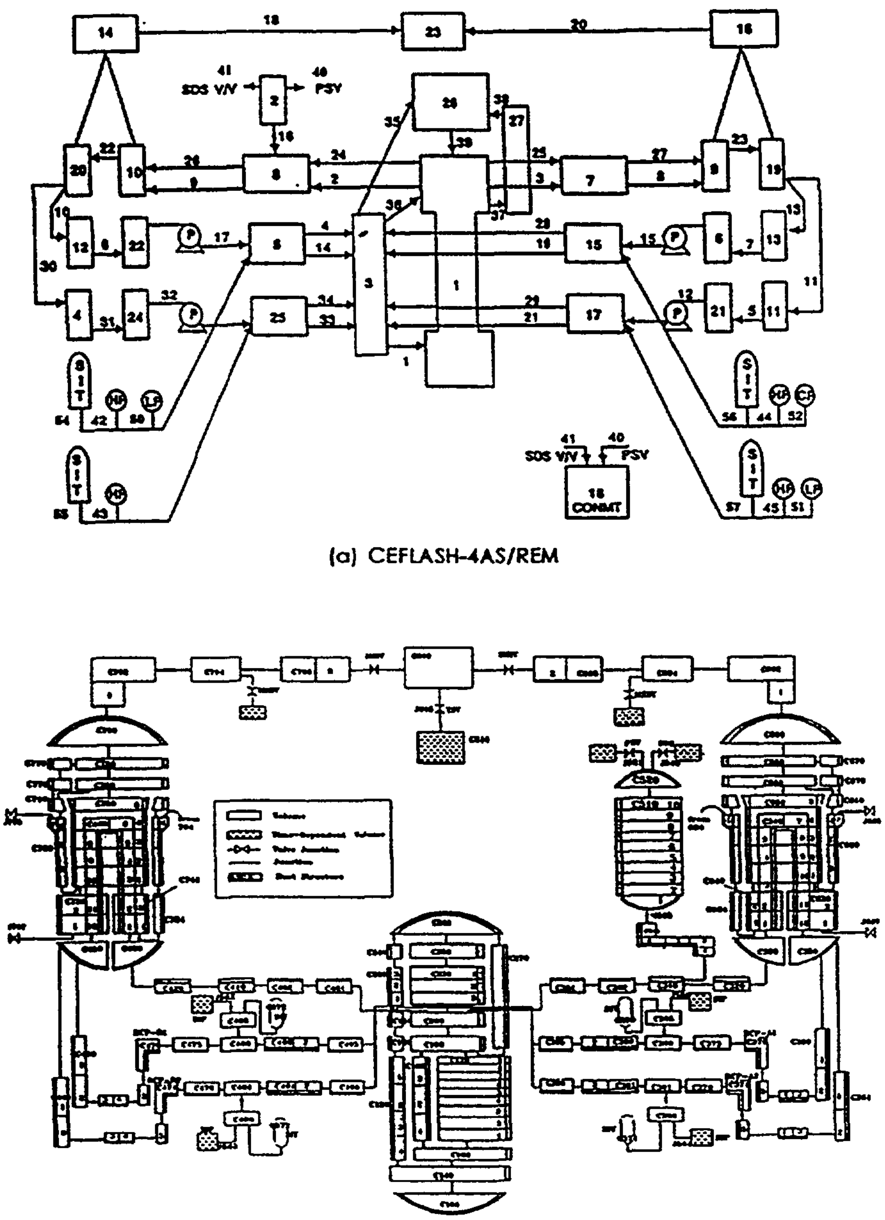

(a) CEFLASH-4AS/REM

(b) RELAP5/MOD3.1

Fig.2 The Nodalization Scheme of UCN 3&4

The plant initial conditions are assumed at full power steady state nominal conditions. Table 1 provides major plant parameters. Also provided are steady state initial conditions obtained by two computer codes. The results of initialization indicate that the two initial conditions are essentially same.

Table 1. Plant Initial Conditions and Major Plant Parameters

a. Plant Initial Conditions and Steady State Value

Parameter	Design Value	Steady State: CEFLASH/RELAP5
Core power (MWt)	2815	2815 / 2815
RCS pressure (MPa)	15.5	15.5 / 15.48
RCS flowrate (ton/hr)	55113	55113 / 55113
Cold leg temperature (°C)	295.8	295.8 / 296.7
Hot leg temperature (°C)	327.3	327.3 / 327.7
SG pressure (MPa)	7.5	7.2 / 7.27
RCS Inventory (Kg)	N/A	211000/ 216200
SG Inventory at Rx trip(Kg)	N/A	41400 / 41100

b. Major System Parameters

Primary side volume (m^3)	329.4
Pressurizer volume, liquid/total (m^3)	25.5/51.4
Low SG level reactor trip setpoint (% WR)	38.5
SIAS setpoint (MPa)	12.6
HPSI pump shutoff head (MPa)	12.65
PSV setpoint (MPa)	17.2
PSV capacity (steam at 17.2 MPa), per valve (Kg/hr)	247517
Number of PSVs	3
Analytical bleed area (m^2)	0.0026

3. Analyses methodology

3.1 Design criteria

The use of F&B is a trade-off between allowable time before operator action and the bleed capacity of the system. The longer the time, the larger the system capacity must be. A shorter allowable time before operator action increases the possibility of inadvertent actuation and resultant containment contamination. Therefore, appropriate design criteria are required. Followings are design criteria selected for the Ulchin 3&4: 1) Each SDS flow path, in conjunction with one of two HPSI pumps, is designed to have a sufficient capacity to prevent core uncovery following a TLOFW if one SDS path is opened simultaneously with the opening of the PSVs. 2) Both SDS bleed paths are designed to have sufficient total capacity with both HPSI pumps operating to prevent core uncovery following a TLOFW event if the feed and bleed initiation is delayed up to thirty minutes from the time of the PSVs lift.

The analysis procedure for the bleed capacity starts with a base case in which the bleed paths are not available, i.e., no operator action is assumed. This base case yields the time of PSVs lift and core uncovery. The duration between PSVs lift and core uncovery is the maximum theoretical allowable time for the operator to open the bleed paths to prevent the core uncovery. All subsequent cases are analyzed with F&B operation. The analytical bleed path area required to prevent core uncovery were investigated in conjunction with operator action time for each F&B cases.

3.2 Differences in analytical models

This analysis employs two analytical models, CEFLASH-4AS/REM computer code developed by ABB-CE and RELAP5/MOD3 computer code version 3.1 developed by INEL. CEFLASH-4AS/REM has been improved from the CEFLASH-4AS[9] which is used for licensing analysis of small break LOCAs. Reference 10 provides the validation of the CEFLASH-4AS/REM against experimental data to verify the capability of the code for use in the analysis of a TLOFW event with F&B. The CEFLASH-4AS/REM (simply, CEFLASH) employs two mass, two energy, and one mixture momentum equations. Since the CEFLASH solves only mixture momentum equation, various constitutive relations using drift flux model are employed. RELAP5/MOD3 (simply, RELAP5) employs two-fluid, nonequilibrium, nonhomogeneous, hydrodynamic model (six equations) for the transient simulation of the two-phase system behavior.

Like all other computer codes, RELAP5 and CEFLASH are limited by the phenomenological models built into the codes. In addition, RELAP5 and CEFLASH have different nodalization scheme; RELAP5 permits the user to vary the nodalization. On the other hand, the CEFLASH has a customized nodalization scheme as shown in Fig.2-(a).

4. Simulation results and discussions

4.1 Determination of bleed capacity

CEFLASH is used for the simulation of TLOFW event without operator recovery and TLOFW event with F&B. The assumptions used in the simulation of these transients are: 1) The plant initial conditions are at steady state full power condition. 2) A reactor trip occurs due to low steam generator level 30 seconds after event initiation. 3) The Reactor Coolant Pumps(RCPs) are tripped 10 minutes after the reactor trip per Emergency Procedure Guidelines[14]. The 10 minutes operator action time is based on the fact that the operator should trip the all RCPs in the Optimal Recovery Guideline(ORG) for the Loss of All Feedwater. For the TLOFW event like scenarios the operator can diagnose the event as Loss of All Feedwater easily, since the system pressure will increase rapidly in couple of minutes after reactor trip due to heat transfer degradation. Since the operator can trip the RCPs in the main control room, the 10 minutes operator action time can be justified. 4) The operator actions are considered according to the design criteria discussed in section 3.1.

For the F&B cases the single failure case and no failure case are considered, where single failure implies operation of only one HPSI pump and opening one SDS bleed path and no failure means operation of two HPSI pumps and opening of two bleed paths. The analytical bleed capacity to prevent core uncovery are investigated by varying the analytical bleed area in TLOFW simulations. The operator actions coincident with PSVs lift and 10 minutes after the PSVs lift are considered for the single failure case. For the no failure case 2 minutes, 10 minutes, 30 minutes, and 40 minutes are considered. Figure 3 shows analytical bleed area required to prevent core uncovery for various operator action times for the single failure case and no failure case determined by CEFLASH.

Since the analytical bleed area to meet the second design criterion (28 cm^2) is smaller than twice the analytical area to satisfy the first design criterion (40 cm^2) as can be seen in Figure 3, the first design criterion is more restrictive with respect to bleed capacity. Theses results are in the same trend as the preliminary analyses results presented in Reference 6. However, current analysis does not assume charging pumps operation, since Chemical and Volume Control System (CVCS) including charging pumps is not credited as safety system. The design bleed capacity is selected as 26 cm^2 by accounting for the various uncertainties, such as, valve stroke time, decay heat curve, and code uncertainties.

To verify the results and methodology of CEFLASH analyses, comparative analyses have also been performed by RELAP5. The cases selected for presentations are TLOFW without recovery and single failure case. In the next sections discussions are focused on the results of simulations using 26 cm^2 bleed capacity.

4.2 TLOFW without recovery

Table 2 provides major chronology of the event predicted by CEFLASH and RELAP5. Fig.4 shows pressurizer pressures predicted by the CEFLASH and RELAP5. Following reactor trip the RCS pressure drops due to a sudden decrease in heat generation from

Table 2. Chronology of the TLOFW Event

	TLOFW w/o Recovery (REM/RELAP5)	TLOFW with F&B (REM/RELAP5)
Bleed Area (m^2)	0	0.0026
Feed flow	No HPSI	1 HPSI
Event	**Time (seconds)**	
Total loss of feedwater	0/0	0/0
Reactor trip	30/30	30/30
RCP trip, manual	630/630	630/630
Steam generator dryout	1360/1600	1360/1600
PSVs open	1389/1345	1389/1345
SDS bleed path(s) opens	N/A	1389/1345
HPSI flow on	N/A	1511/1385
Hot leg saturation	2923/2875	1510/1420
Core uncovery begins	5296/ -	N/A
or		
Minimum RV inventory, Kg		47300/44300
occurred at, sec		3280/3600

the core. After a short time period, the RCS pressure starts to rise in response to the power-to-flow mismatch and reaches to a new steady state. After the RCP trip at 630 seconds, the pressurizer pressure increases more rapidly due to RCP coast down. Fig.5 shows steam generator inventory. When both steam generators dry out at about 1360/1600 seconds (The dryout time can be determined from the liquid inventory in the RELAP simulation. Since only mixture inventory has physical meaning in the CEFLASH simulation, the time when the mixture inventory flattens out corresponds to dry out time in the CEFLASH simulation), the RCS volume expansion and pressurization is accelerated. Then the pressurizer pressure reaches the PSVs opening setpoint. Since the PSVs have enough capacity to accommodate the increased volumetric expansion, the pressurizer pressure is maintained around PSVs setpoint during the whole transient. It is shown that the pressurizer pressures are in good agreement between two simulations. The primary temperature rises until it reaches the saturation temperature corresponding to the pressurizer safety valve setpoint as shown in Fig. 6. From that time on, the primary temperature stays constant while void is generated in the RCS.

Pressurizer goes solid at about 2500 seconds as shown in Fig.7, and the discharge flow becomes single phase liquid. After the RCS reaches saturation condition around 3000 seconds, steam generated in the core due to decay heat flows from the core to pressurizer via hot leg and surge line. Once the surge line begins to draw vapor, the net inventory in the pressurizer drops rapidly because low quality mixture is still flowing out of safety valves. Fig.8 shows the integrated surge flow and PSV discharge flow. The integral surge flows predicted by CEFLASH and RELAP5 are in good agreement before hot leg is highly voided. After that, two predictions deviate slightly, which might be due to the absence of countercurrent flow model for the surge line in the REM.

Core uncovery begins at around 5300 seconds into the transient, when the RCS inventory becomes so low that the void fractions in the top three nodes of the core reaches 1.0 in the RELAP5 (refer to Fig.9 for Reactor Vessel(RV) liquid inventory and Fig.10 for core void fraction). At that time, the collapsed water level in the core begins to decrease rapidly and the cladding and core outlet temperatures begin to rise. It is observed that the vapor fractions in the core region tend to hang up in the 25-40% range for extended period of time as shown in Fig.10. When core inventory decreases, it frequently takes place in such a manner that the local vapor fraction jumps from 0.4 to 1.0 over a very brief time interval as shown in Fig.10. This is purely a result of the flow regime map change in RELAP5. As shown in Fig.9 the RV inventory behavior is quite different between two predictions after the RCS starts to void. This difference in RV inventories is judged to be from the difference in inventory distribution among various RCS components including RV upper head, pressurizer, hot legs, cold legs and SG U-tubes. It is observed that the drainage of RV upper head inventory after hot leg voiding predicted by RELAP5 is much faster than that predicted by CEFLASH.

4.3 TLOFW with feed and bleed

Presented in this subsection are the results of the case where F&B operation is utilized to attempt to cool the core and make up the RCS inventory. The assumptions used in the simulation of this transient are: 1) Operator opens one train of SDS bleed path and aligns one train of HPSI pump for injection at the time of PSVs' lift. 2) The SDS is modeled by an orifice located on the top of the pressurizer whose analytical bleed *area corresponds to 26 cm^2.*

This case is identical to TLOFW without recovery case until PSVs lift. Table 2 provides chronology of major event scenarios predicted by CEFLASH and RELAP5. Soon after the bleed path is opened the RCS pressure decreases rapidly as shown in Figure 11, and hence HPSI injection flow is initiated at 1511/1385 seconds. A significant amount of energy is removed through the SDS bleed path when the discharge flow is a single phase steam. However, as the flow leaving the SDS path becomes two-phase, the energy removal slows down. Hence the RCS pressure decrease also slows down. And the RCS pressure briefly begins to repressurize when the discharge flow becomes single phase liquid. At that point the pressurizer becomes solid (refer to Fig.11,12 and 13). The pressurizer behavior during repressurization is generally in good agreement between CEFLASH and RELAP5. CEFLASH shows rather smooth pressurizer pressure transient. The pressurizer inventory keeps increasing after 4200/5400 seconds as can be seen in Fig.12.

The RCS becomes saturated quickly after the bleed valves open. The steam generated in the core migrates from the core to the pressurizer, which increases the amount of steam bubbles in the pressurizer and consequently increases break flow quality. As the quality of bleed flow increases, the energy removal rate increases. This results in the decrease in the pressurizer pressure. Therefore, the HPSI injection flow is reinitiated (See Fig.14). As the RCS depressurizes, HPSI flow with low temperature at 50 °C also increases, which contributes to further reduction of RCS pressure as shown in Fig.11. The combination of opening the SDS bleed path, which results in loss of RCS inventory, and the HPSI injection of cold fluid, which lowers the RCS average temperature and therefore leads to contraction of RCS fluid, eventually causes voiding in the RCS. Void formation is evident in the core as early as 2000 seconds into the transient. However the void fraction at the top of the core is maintained below 40% due to increased HPSI injection flow (See Fig.15). The reactor vessel inventory reaches minimum at 3600 seconds in RELAP5 predictions and continuously increases as shown in Fig.16. The CEFLASH prediction shows that core mixture level is always maintained above the top of the core as shown in Fig.17. This result indicate that the selected SDS bleed capacity meets the first design criterion discussed in section 3.1.

As shown in Fig.16 the reactor vessel inventory behavior is quite different between two predictions after RCS starts to void. This difference in RV inventories is judged to be from the differences in inventory distribution among various RCS components. Therefore, further study on the nodalization scheme of RV upper head is recommended. However, this difference does not affect the conclusion of this analysis, since the event scenarios before the time of minimum RV inventory are almost the same for both cases and both predictions show that core is covered two-phase mixture.

The peak cladding temperature is calculated to evaluate the impact of core voiding. As shown in Fig.18 the cladding temperature is well below acceptance criteria, which assures core to coolant heat transfer is well maintained.

5. Summary and conclusions

The SDS bleed capacity is determined by numerical simulation of TLOFW event without operator recovery and TLOFW event with F&B by CEFLASH computer code. The analytical bleed capacity to prevent core uncovery are investigated by varying the analytical bleed area and number of operating HPSI pumps.

To verify the results of CEFLASH simulation a comparative analysis has also been performed by more sophisticated computer code. The predictions by the CEFLASH simulation of the transient two phase system behavior is found to be in good agreement with those by the RELAP5 simulation, except the RCS water inventory distribution which shows small difference after the hot leg voiding.

In conclusion, the results of analyses for TLOFW event with F&B by CEFLASH and RELAP5 have demonstrated that decay heat removal and core inventory make-up can be successfully accomplished by F&B operation for Ulchin 3&4 Nuclear Power Plants.

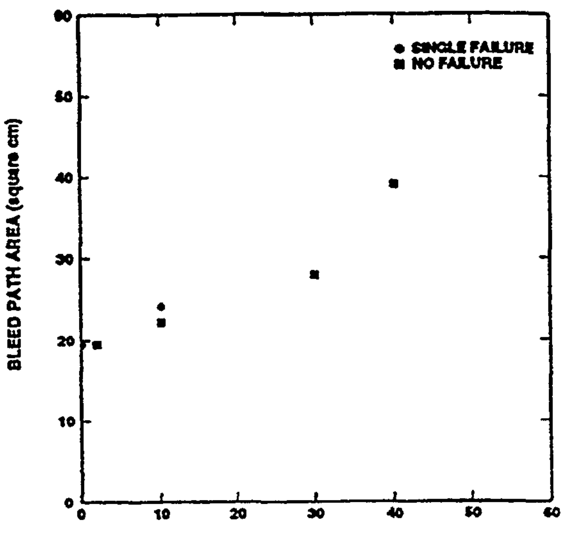

Fig. 3 Analytical Bleed Areas Required to Prevent Core Uncovery for Various Operator Times

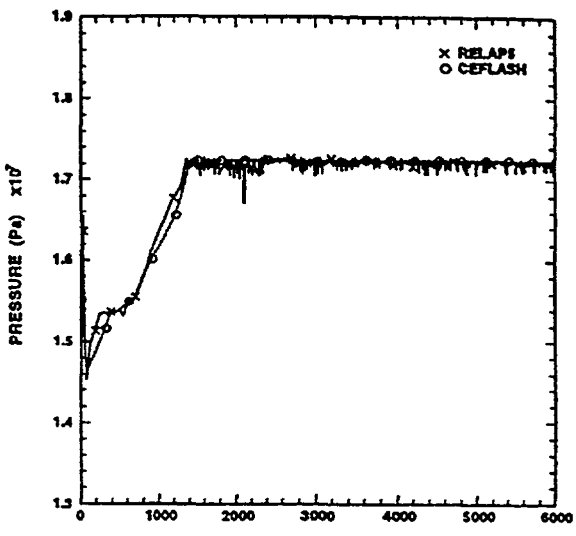

Fig. 4 Pressurizer Pressure (TLOFW w/o Recovery)

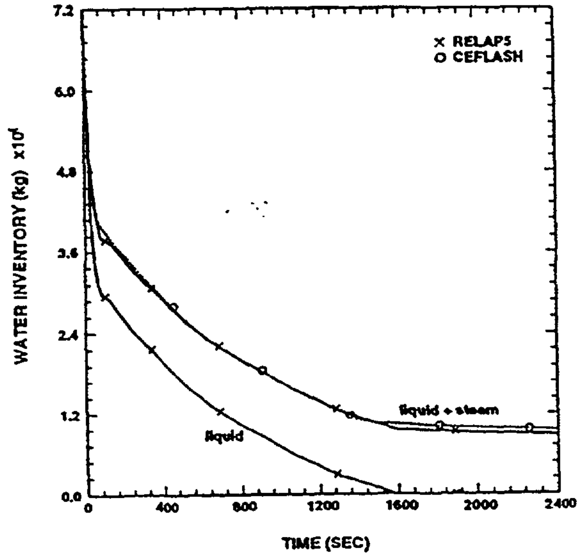

Fig. 5 SG Inventory (TLOFW w/o Recovery)

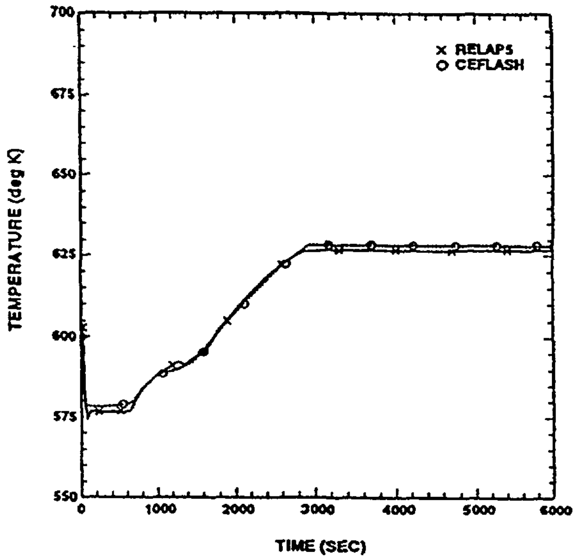

Fig. 6 Hot Leg Temperature (TLOFW w/o Recovery)

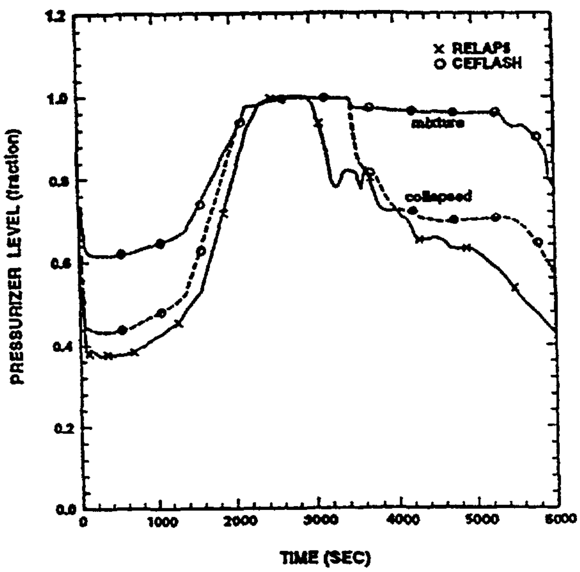

Fig. 7 Normalized Pressurizer Level (TLOFW w/o Recovery)

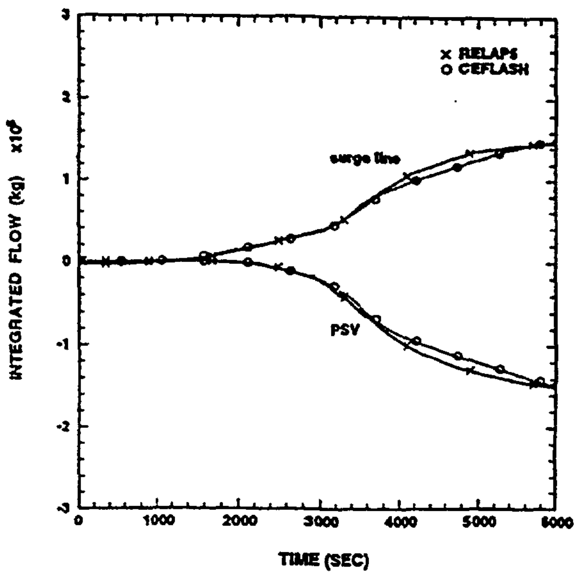

Fig. 8 Integrated Surge and PSV Flows (TLOFW w/o Recovery)

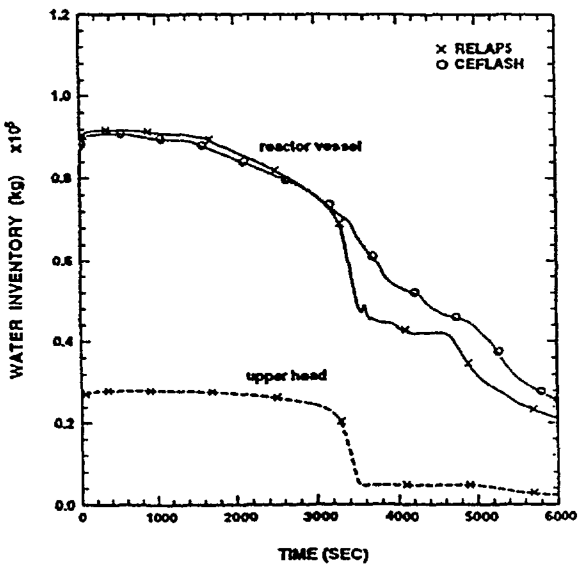

Fig. 9 Reactor Vessel Inventories (TLOFW w/o Recovery)

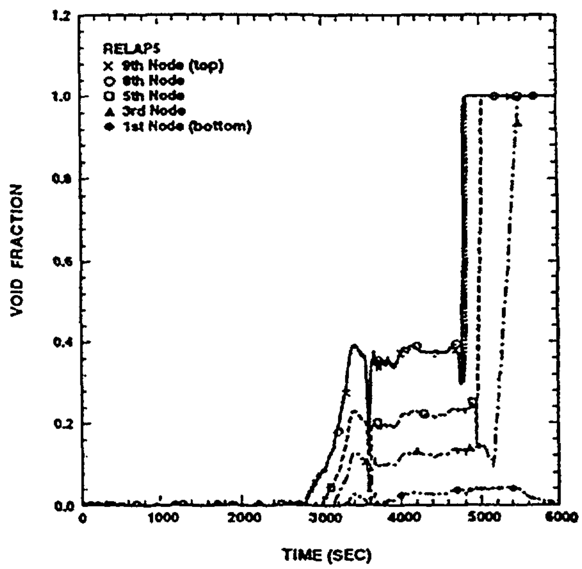

Fig. 10 Core Void Fraction (TLOFW w/o Recovery)

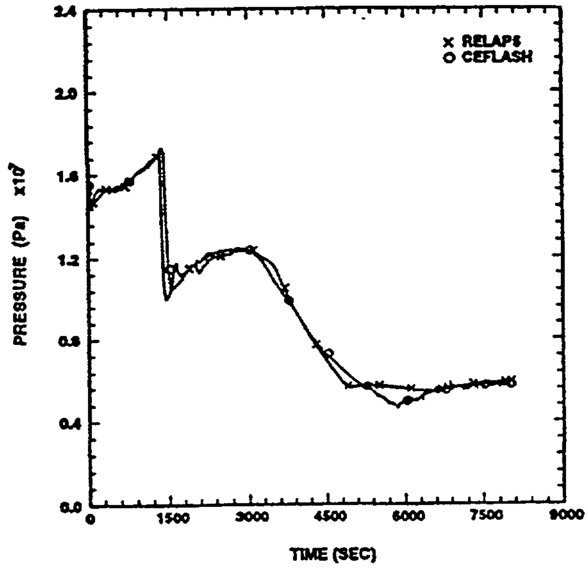

Fig. 11 Pressurizer Pressure (F & B)

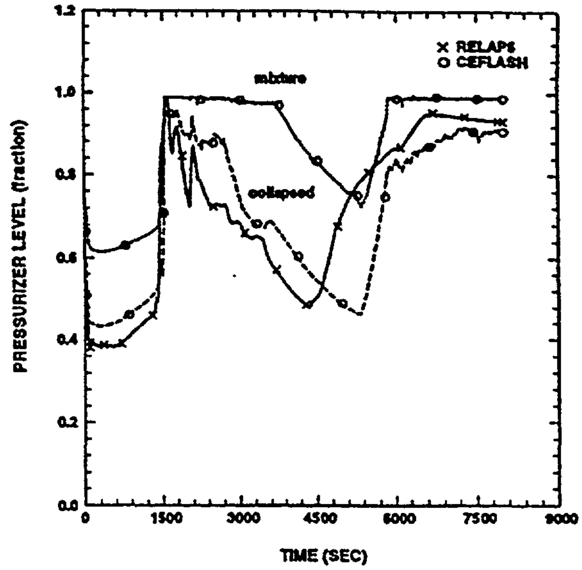

Fig. 12 Normalized Pressurizer Level (F & B)

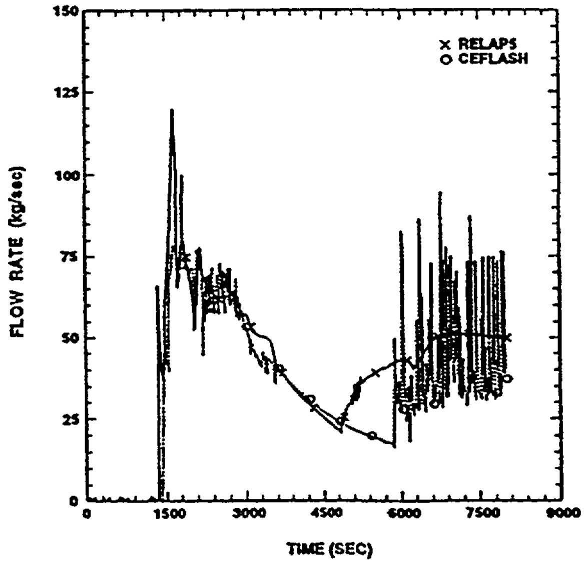

Fig. 13 Bleed Path Discharge Flow Rate (F & B)

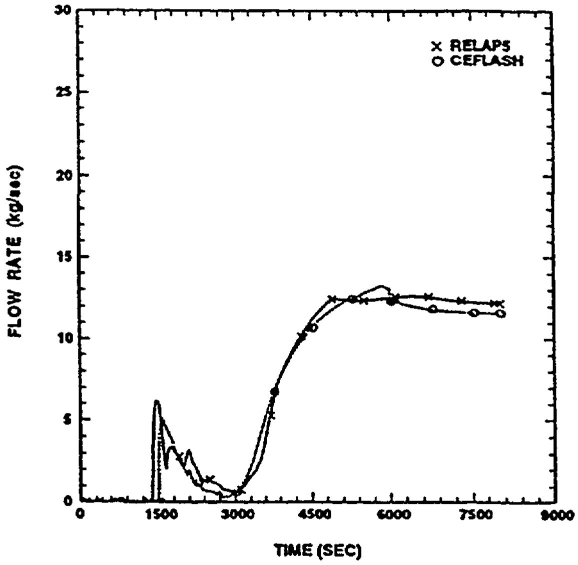

Fig. 14 HPSI Injection Flow (F & B)

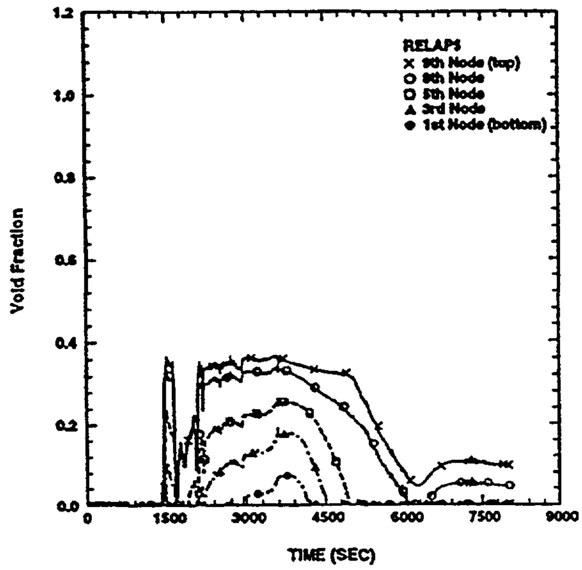

Fig. 15 Core Void Fraction (F & B)

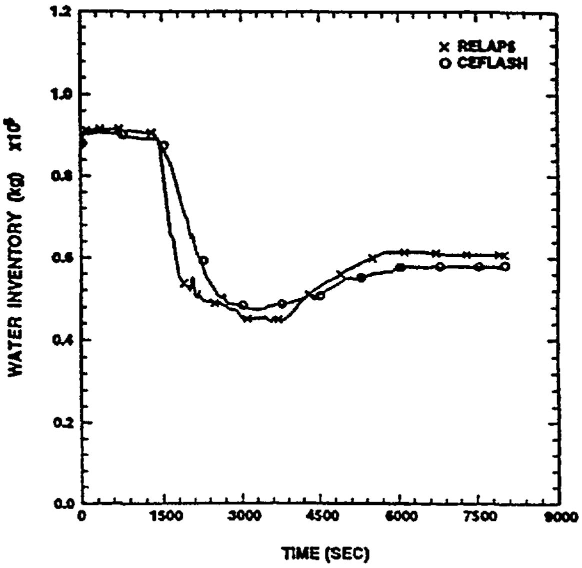

Fig. 16 Reactor Vessel Inventory (F & B)

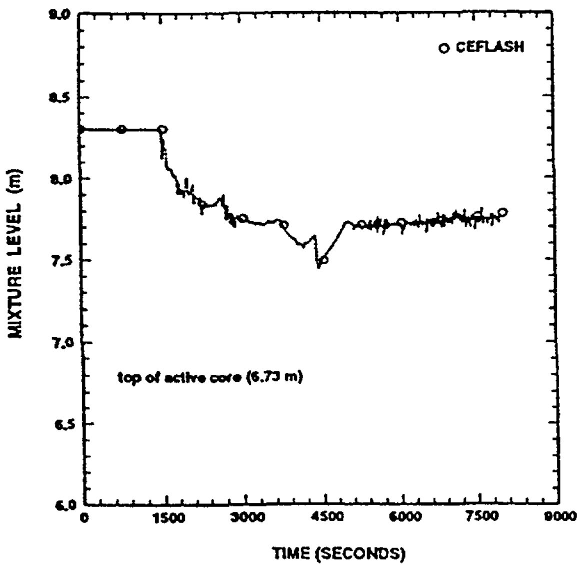

Fig. 17 RV Core Mixture Level (F & B)

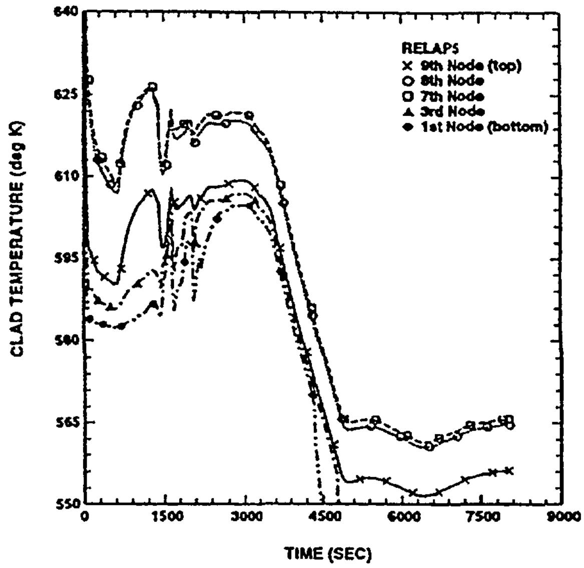

Fig. 18 Fuel Cladding Temperature (F & B)

REFERENCES

1. H. Komoriya and P. B. Abramson, "Decay Heat Removal During a Total Loss of Feedwater Event for a C-E System 80 Plant," ANL/LWR/NRC 83-6, Argonne National Laboratory, 1983.
2. Boyack, B. E. et al., Los Alamos PWR Decay Heat Removal Studies Summary Results and Conclusions, NUREG/CR-4471, Los Alamos Laboratory (1985).
3. Loomis, G. G. & Cozzuol, J. J., Decay Heat Removal Using Feed-and-Bleed for U.S. PWR, NUREG/CR-5072, Idaho National Engineering Laboratory, 1988.
4. Young Seok Bang, Kwang Won Seol and Hyo Jung Kim, "Evaluation of Total Loss of Feedwater Accident/Recovery Phase and Investigation of the Associated EOP, Journal of the Korean Nuclear Society, Vol. 25, Number 1, March 1993.
5. Asea Brown Boveri - Combustion Engineering, CESSAR-DC Chapter 5, 1989.
6. Kwon, Y. M., Song, J. H., & Ro, T. S., Decay Heat Removal Capability of Safety Depressurization System for Total Loss of Feedwater Event, Proc. 5th International Topical Meeting on Reactor Thermal Hydraulics, Salt Lake City, Vol. 6, 1992.
7. C-E Power Systems, Realistic Small Break LOCA Evaluation Model, CEN-373-P, 1987.
8. K. E. Carlson et al., "RELAP5/MOD3 Code Manual Volume I: Code Structure, System Models, and Solution Methods (DRAFT), " June 1990.
9. C-E Power Systems, "CEFLASH-4AS, A Computer Program for the Reactor Blowdown Analysis of the Small Break Loss of Coolant Accident," CENP-133P, 1974.
10. C-E Nuclear Power Systems, Software Verification and Validation Report for CEFLASH-4AS/REM, VV-FE-0063, 1992.
11. J. A. Trapp and V. H. Ransom, "A Choked-Flow Calculation Criterion for Nonhomogeneous, Nonequilibrium, Two-Phase Flows," International Journal of Multiphase Flow, 8, 6, 1982.
12. T. M. Anklam and M. D. White, "Experimental Investigation of Two-Phase Mixture Level Swell and Axial Void Fraction Distribution under High Pressure, Low Heat Flux Conditions in Rod Bundle Geometry," Proceedings of ANS Small Break Specialist Meeting, 1981.
13. Wallis, G., One Dimensional Two-Phase Flow, McGraw-Hill Book Company, 1969.
14. C-E Power Systems, Combustion Engineering Emergency Procedure Guidelines, CEN-152, 1987.

DESIGN AND ANALYSIS OF ADVANCED WATER COOLED REACTOR SAFETY COMPONENTS AND SYSTEMS

(Session III)

Chairman

J. LILLINGTON
United Kingdom

EUROPEAN PRESSURIZED WATER REACTOR CONFIGURATION, FUNCTIONAL REQUIREMENTS AND EFFICIENCY OF THE SAFETY INJECTION SYSTEM

F. CURCA-TIVIG
Siemens AG (KWU), Erlangen,
Germany

J.L. GANDRILLE
Framatome, Cedex,
France

Abstract

The paper presents the thermal-hydraulic behavior of the European Pressurized Water Reactor (EPR) under LOCA conditions and demonstrates the efficiency of EPR's Safety Injection System (SIS). Safety criteria as well as performance of the SIS - i.e., main functions, functional requirements, design and emergency core cooling mode - are discussed. The thermal-hydraulic response of the EPR to various LOCAs was analyzed by performing best-estimate or conservative LOCA-calculations with the advanced computer codes CATHARE, RELAP5/MOD2 and SPC-RELAP5. A large spectrum of leak sizes, from small leaks ($\phi \leq 25$ mm) up to double ended guillotine breaks, was simulated. The calculation results demonstrate the efficiency of the SIS: a) In case of LOCAs caused by very small breaks ($\phi \leq 25$ mm) the EPR's SIS is capable - in conjunction with the automatic partial cooldown of the secondary side - to prevent loop draining, even when only two Medium Head Safety Injection (MHSI) trains are effective. In case of small and intermediate leaks ($\phi \leq 150$ mm) the SIS ensures sufficiently high injection rates for preventing core uncovery, again even when only two MHSIs are effective. For leaks within the range $150 \leq \phi \leq 350$ mm, the SIS is able to limit the core uncovery. b) In case of large break LOCAs the SIS ensures a fast reflood of the core within approximately 120 s; the peak cladding temperature is 810°C. Reflood of the core is achieved by the accumulator injection.

1. INTRODUCTION

The paper presents the thermal-hydraulic behavior of the European Pressurized Water Reactor (EPR) under Loss-of-Coolant Accidents (LOCAs) conditions and demonstrates the efficiency of EPR's Safety Injection System (SIS). Safety criteria as well as performance of the SIS - i.e., main functions, functional requirements, design and emergency core cooling mode - are discussed.

The EPR is a PWR which synthesises the experience gained by EdF, German Utilities, Framatome and Siemens during the design, manufacturing, construction and operation of numerous nuclear power plants with a total capacity of 100 000 MWe and an operation time of 900 years. The EPR is an evolutionary reactor; additionally, it has innovative features in technical areas such as prevention and mitigation of severe accident scenarios. The EPR Basic Design is performed under the leadership of Nuclear Power International (NPI), which is a joint company formed by Framatome and Siemens.

2. SAFETY INJECTION SYSTEM DESIGN

The design of the EPR is based on the defence in depth principle. The choice of the events to be considered for EPR design and safety assessment is firstly done deterministically. They consist of the normal operational states and are enlarged by systematically looking for events having the potential of disturbing the reactivity or power control, the heat removal from the fuel elements and the confinement of radioactivity.

A number of representative initiating events is derived from this systematic approach, which lead to bounding cases for design and assessment of safety-classified systems, components and structures. The deterministic design basis is in full compliance with the approach which was already followed in France and Germany in the past. According to their expected frequencies, the events are divided in four Plant Condition Categories (PCC): normal operation (PCC 1), anticipated operational occurrences (PCC 2), infrequent accidents (PCC 3) and limiting accidents (PCC 4).

Probabilistic targets have been set up for the EPR too. They comprise two safety objectives: firstly, integral Core Melt Frequency (CMF) considering all plant states and all types of events < 10^{-5} y^{-1}, and secondly, integral large release frequency < 10^{-6} y^{-1}. In order to meet the safety objectives, the following design targets are defined: a) integral CMF for internal events, reactor in power state: 10^{-6} y^{-1}, b) shutdown states shall contribute to CMF less than power states, and c) integral CMF for internal events associated with early loss of containment: 10^{-7} y^{-1}.

In order to meet the probabilistic targets, the deterministic design basis is extended. In this design extension, a limited number of accidents with multiple failures and coincident occurrences including the total loss of some safety-grade systems will be selected by probabilistic assessment. This assessment will permit to design a limited number of additional systems or to adapt existing systems for additional backup functions. The accidents are divided in two Risk Reduction Categories: firstly, prevention of core melt (RRC-A) and secondly, prevention of large releases (RRC-B).

The present section gives an overview of the SIS design; safety and operational functions, functional requirements and a brief description are included.

2.1. Safety Functions

The safety functions of the EPR's SIS are the following:

- Rapid reflood of Reactor Pressure Vessel (RPV) and reactor core following a LBLOCA.
- Provision for long-term injection of water to the core for small, intermediate and LBLOCA.
- Cooling of the injected water in case of LOCA, in order to terminate the release of steam to the containment atmosphere as early as possible.
- Provision for water injection to the Reactor Coolant System (RCS) for small to intermediate break LOCA or Steam Generator Tube Rupture (SGTR), at any pressure less than the discharge pressure of Steam Generator (SG) safety valves.
- Provision for cooling of the In-containment Refueling Water Storage Tank (IRWST), in case of LOCA.
- Mixing of water recirculated during the long term core cooling after LOCA to ensure homogeneous boron concentration and temperature.
- Boration of the RCS for PCC 3 and PCC 4 accidents.
- In conjunction with discharge from the RCS via the pressurizer safety valves, provision for injection of water in order to ensure residual heat removal (RHR) from the RCS and cooldown to a cold condition, in case of loss of RHR via the SGs.
- Provision of backup to RHR system, as a different means of ensuring RHR, with the capability for cooling of the RCS when the temperature is < 100 °C and the pressure is low.
- Provision for emergency makeup to the RCS in case of loss of water inventory during cold shutdown or refueling shutdown.

2.2. Functional requirements

The functional requirements of the EPR's SIS are the following:

- For large and intermediate break LOCA the SIS shall be capable of ensuring that acceptable core damage limits (see Section 2.3) are not exceeded even assuming a single failure (SF).
- The cooling capability of the SIS shall be sufficient to ensure termination of steam release to the containment following a LBLOCA, without exceeding a mean temperature of 110 °C in the IRWST, even assuming a single failure.

- For small break LOCA of PCC 3, the SIS shall be capable, if necessary in conjunction with secondary-side heat removal, of ensuring that acceptable core heatup limits (as defined below) are not exceeded, even assuming a single failure.
- Boration of the RCS in accidents of PCC 3 or PCC 4 shall be ensured at a rate such that cold shutdown boron concentration can be reached, assuming a single failure and assuming, in parallel, cooldown by the secondary side at a cooldown-rate not exceeding the temperature limit that corresponds to an acceptable core shutdown margin.
- SIS capability shall be sufficient to ensure that, following a total loss of secondary side heat removal, a time delay for operator actions of approximately one hour is adequate to avoid exceeding acceptable core damage limits. It is assumed that, in conjunction with SIS operation, discharge of the RCS via pressurizer valves will be initiated (feed and bleed operation).
- The cooling capability of the SIS shall be sufficient to maintain in case of SBLOCA the mean temperature in the IRWST < 110 °C (for "feed and bleed" transients, this limit may be exceeded).
- In case of loss of the RHR system, the SIS is used in a RHR mode as a functional backup.
- Provision shall be taken to ensure that, during all plant initial conditions where SIS operation might be required, the operational readiness of SIS equipment for automatic and/or manual initiation of safety injection is maintained.

2.3. Description

The SIS consists of four separate and independent trains, each providing injection capability by an accumulator (ACCU), a Medium Head Safety Injection (MHSI) pump, and a Low Head Safety Injection (LHSI) pump (see Fig. 1). Both the MHSI and the LHSI pumps take suction from the IRWST and inject into the RCS loops via nozzles located on the upper part of the loops. The pumps are located in the Safeguard Buildings, close to the containment. The LHSI pumps inject simultaneously into both the hot and the cold legs of RCS. The MHSI pumps inject into the cold legs. The accumulators are located inside containment and inject into the hot legs, using the same injection nozzles as the hot leg injection of the LHSI. A heat exchanger is located downstream of each LHSI pump. These heat exchangers are also installed in the Safeguard Buildings and are cooled by the Component Cooling Water System (CCWS).

TABLE I: CHARACTERISTICS OF EPR'S SAFETY INJECTION SYSTEM

Medium Head Safety Injection	
- Location	cold leg
- No. of pumps	4
- Shutoff head	8.0 MPa
- Maximum injection rate	64 kg/s
Accumulators	
- Location	hot leg
- No. of accumulators	4
- Injection pressure	4.5 MPa
- Water/ Nitrogen volumes	32 m^3 / 15 m^3
Low Head Safety Injection	
- Location	combined (cold and hot leg)
- No. of pumps	4
- Shutoff head	2.0 MPa
- Maximum injection rate	125 kg/s

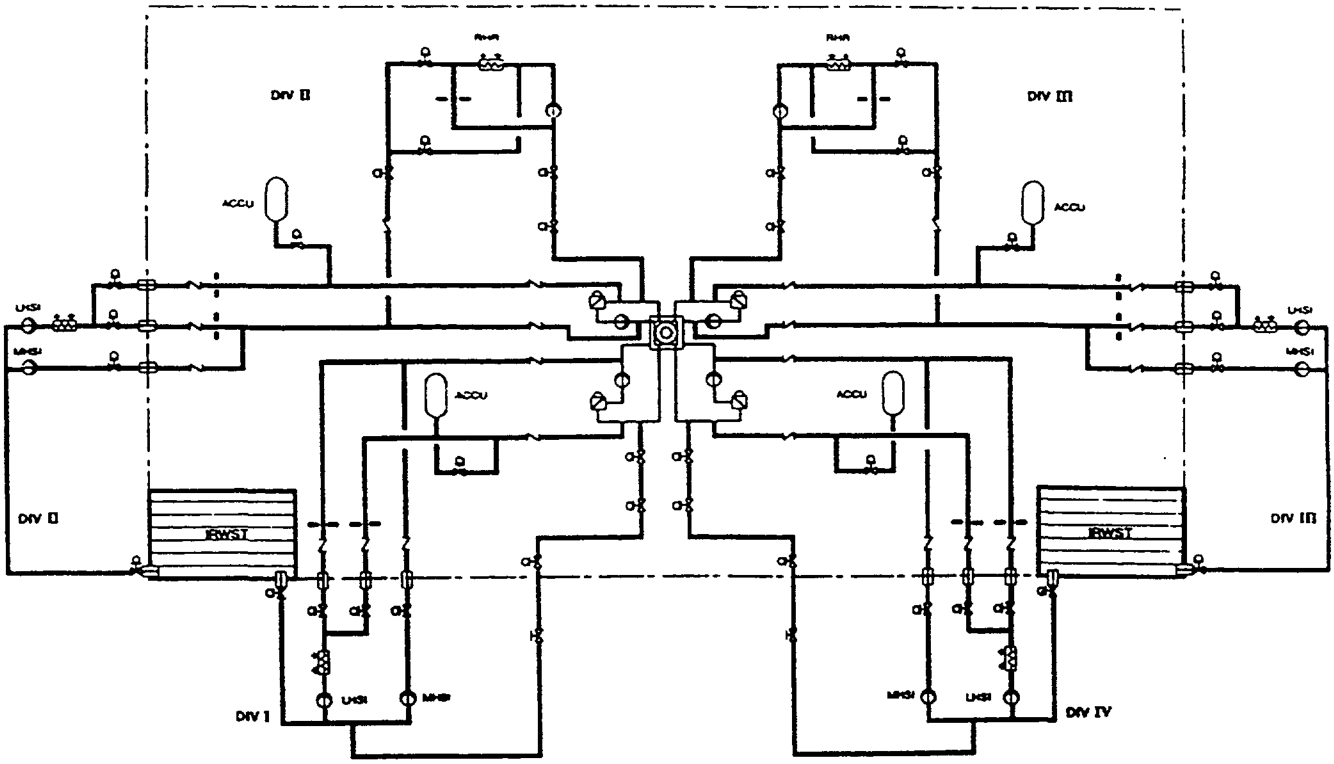

FIG. 1: EPR SAFETY INJECTION SYSTEM CONFIGURATION

2.4. Emergency core cooling mode

The emergency core cooling (ECC) mode includes the first four safety functions of the SIS, as described in Section 2.1. The most important new features of EPR's SIS which have been evaluated in particular with respect to SBLOCA scenarios are the shut-off head of only 8 MPa for the Medium Head Safety Injection (MHSI), and the secondary side partial cooldown to about 6 MPa, which is necessary in order to enable MHSI.

With implementation of a partial automatic secondary side cooldown the SIS configuration ensures appropriate mitigation of all types of primary side break (LOCA) in terms of location and size as well as all relevant NON-LOCA scenarios. The preliminary SIS configuration and characteristics are summarized in Table I. The design and safety criteria to be fulfilled by the SIS under LOCA-conditions are listed in Table II. The criteria have to be fulfilled under consideration of the single failure criterion.

2.5. Rationale for the selected emergency core cooling mode

2.5.1. MHSI

The reduced head of the MHSI has been selected in order to clearly improve the mitigation of SGTR. There is no need for variable set points of the secondary-side safety valves (less risk of human error).

The cold leg injection of the MHSI complies best with the requirements resulting from both SBLOCA (≤200 cm^2) and NON-LOCA mitigation. For SBLOCA the cold leg and hot leg injections are practically equivalent from the point of view of ECC-efficiency. However, for severe NON-LOCA scenarios (e.g. overcooling transients or those resulting in "feed and bleed") the cold leg injection is advantageous in terms of core cooling and boration.

TABLE II: DESIGN AND SAFETY CRITERIA FOR THE SIS

Design criteria	complete core quenching time for 2A LBLOCA ≤ 3 min no core uncovery for break sizes $\phi \leq$ 150 mm (≤ 180 cm^2) no loop draining for break sizes $\phi \leq$ 25 mm (≤ 5 cm^2)
Safety criteria	peak cladding temperature < 1200 °C local cladding oxidation < 17% of cladding thickness core geometry integrity: no prevention of core cooling Zirconium-water reaction < 1% of total cladding material

2.5.2. Accumulators

The hot leg injection has been selected because it provides major advantages in the mitigation of large and intermediate break LOCA:

- faster core reflood and lower peak clad temperature (PCT) because of high steam condensation in the upper plenum and the hot legs,
- pressurized thermal shock concerns are excluded.

2.5.3. LHSI

The combined injection, i.e. the simultaneous injection into both the hot leg and the cold leg of the main coolant line is favorable for mainly three reasons:

- during LBLOCA the hot leg contribution supports the accumulators by minimizing the quenching time and consequently the steam release to the containment,
- the combined injection ensures an uniform boron concentration distribution, and
- makes any valve switching unnecessary (e.g. from cold leg to hot leg injection) and thus increases the reliability of the procedure.

3. SAFETY INJECTION SYSTEM EFFICIENCY UNDER LOCA CONDITIONS

A large number of SBLOCA and LBLOCA analyses have been carried out by Framatome and Siemens within the aim of SIS sizing. The CATHARE, SPC-RELAP5 and RELAP5/MOD2 computer codes have been used. Certain scenarios have been defined as benchmark calculations and have been simulated with both codes in parallel; comparison of the results allowed the adaptation of model options as well as of various modeling methods in order to get similar predictions with both codes.

Results of preliminary LOCA analyses are discussed in this section. Conclusions with respect to the sizing of the SIS-components (i.e. MHSI, LHSI and accumulators) are drawn

3.1 Computer codes used and EPR modeling

The thermal-hydraulic response of the EPR to LOCA-conditions was analyzed with the advanced computer codes CATHARE [1, 2], RELAP5/MOD2 [3] and SPC-RELAP5. The well known French code CATHARE was developed by CEA, Framatome and EdF; it is used by Framatome for both SB and LBLOCA analysis. Siemens used RELAP5/MOD2 for SBLOCA-and SPC-RELAP5 for LBLOCA-calculations. SPC-RELAP5 was developed by Siemens Power Corporation (Richland, WA) for performing realistic analysis of accident thermal-hydraulics in PWRs. It is a RELAP5-based system code incorporating features of RELAP5/ MOD2 and RELAP5/MOD3 [4], and company improvements. In general, the improvements and modifications included are those required to provide congruency with the unmodified literature correlations and those to obtain adequate simulation of key LBLOCA experiments. For LBLOCA-analysis SPC-RELAP5 was coupled with the containment code COCO. Thus, both the RCS response and the containment response are simultaneously calculated; this allows more accuracy in the accident simulation. The coupling method is described in [5].

Depending on the simulated LOCA-scenario, different CATHARE and RELAP5 nodalizations of the EPR have been used. Two representative models are presented below.

3.1.1. EPR Modeling for CATHARE Calculations

The CATHARE nodalization is depicted in Fig. 2 for the RCS; it is composed of an arrangement of 1-D components (pipes), 0-D components (volumes), tees, junctions between components, and boundary conditions. The RCS model features three primary loops: one broken loop, one intact loop, with the pressurizer, and one double loop lumping the two remaining intact loops. It comprises 12 volumes, 5 in the reactor vessel (upper region of the downcomer, lower plenum, upper plenum, guide tubes, upper head), 6 for the SG inlet and outlet plena, 1 for the pressurizer. It also comprises 12 pipes for the core, downcomer lower region, hot legs (3), SG tubes (3), cold legs (3) and pressurizer surge line, amounting to more than 400 hydraulic meshes. All hydraulic components are thermally linked to meshed walls or fuel rods.

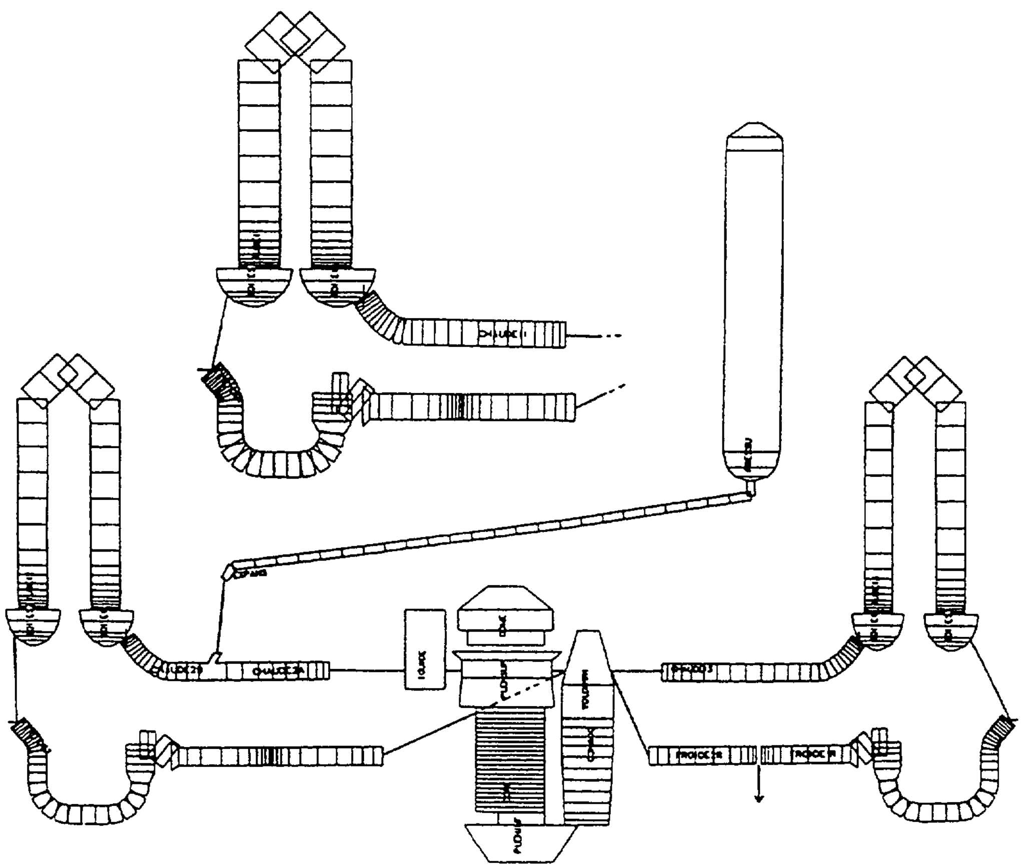

FIG. 2: EPR 1400 MW. CATHARE 2 NODALIZATION OF REACTOR COOLANT SYSTEM

The secondary side model is depicted in Fig. 3 and features 3 SG and connected pipes; it is also described by volumes and pipes, amounting to more than 200 hydraulic meshes. The secondary side is an axial preheater type SG. The downcomer is split into two regions; normal feedwater is delivered to the region which supplies the axial preheater zone of the riser. Heat exchange between preheater and the lower part of the downward cold U-tubes is modeled. The fluid of the axial preheater zone mixes above the partition plate with the mixture of the opposite riser zone. The resulting mixture is then boiled above that plate

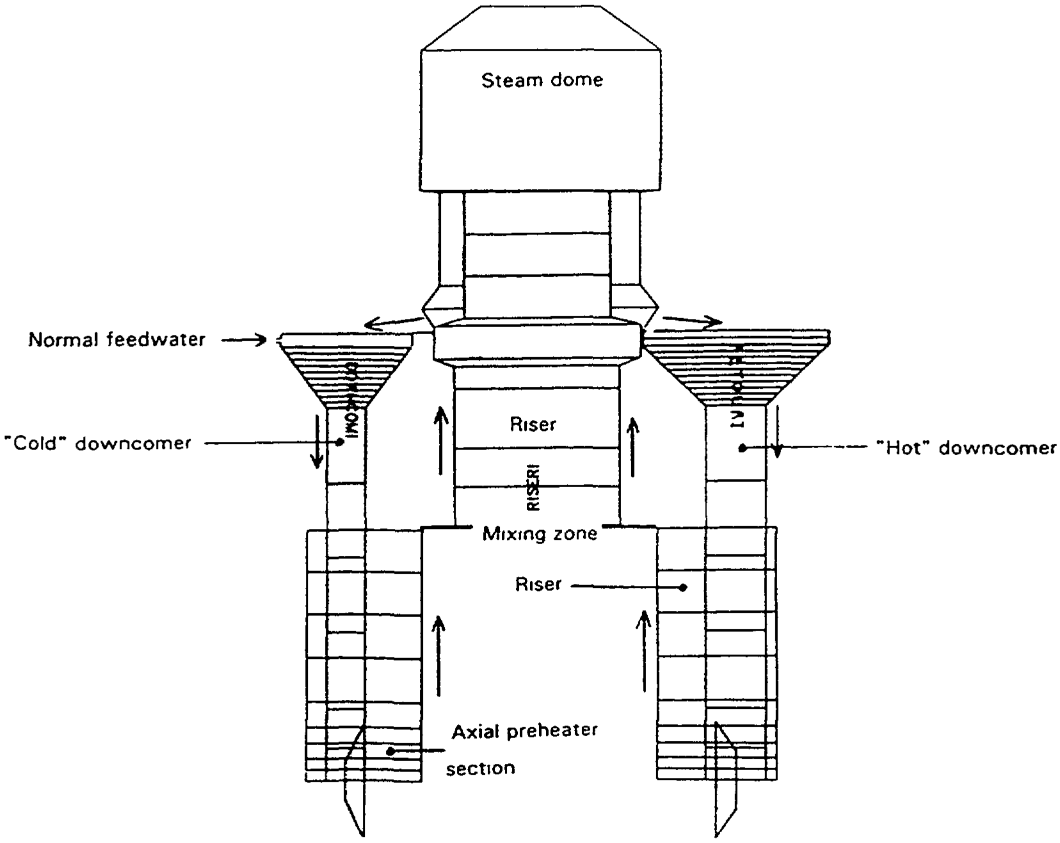

FIG. 3: EPR 1400 MW. CATHARE 2 NODALIZATION OF SG SECONDARY SIDE

by the heat exchange with the upper part of the U-tubes, both upward and downward parts; the CATHARE model allows to describe these processes.

3.1.2. EPR Modeling for SPC-RELAP5 Calculations

Very similar plant models have been used for RELAP5/MOD2 and SPC-RELAP5 calculations. The SPC-RELAP5 nodalization is depicted in Fig. 4. The EPR model consists of 620 control volumes, 660 junctions and 640 heat structures (HS) with more than 4000 HS mesh points. All RCS components - primary and secondary side - are modelled in detail; this way the model can be used without major modifications for the simulation of various scenarios (e.g. small, intermediate and large breaks, feed & bleed, etc.). Special attention was paid to the RPV-model. The active core is represented by three channels: a breakthrough channel which represents 20% of the fuel assemblies (FAs), a hot channel (1 FA), and a main channel - also called up-flow channel - including the rest of FAs. The breakthrough and main channels are connected by cross flow junctions, whereas the hot channel is isolated. Every channel is axially sub-divided into 15 axial nodes. The upper plenum (UP) is also divided into a 20% breakthrough region and a 80% upflow region. This nodalization is based on UPTF test data and enables the best-estimate simulation of hot leg injection.

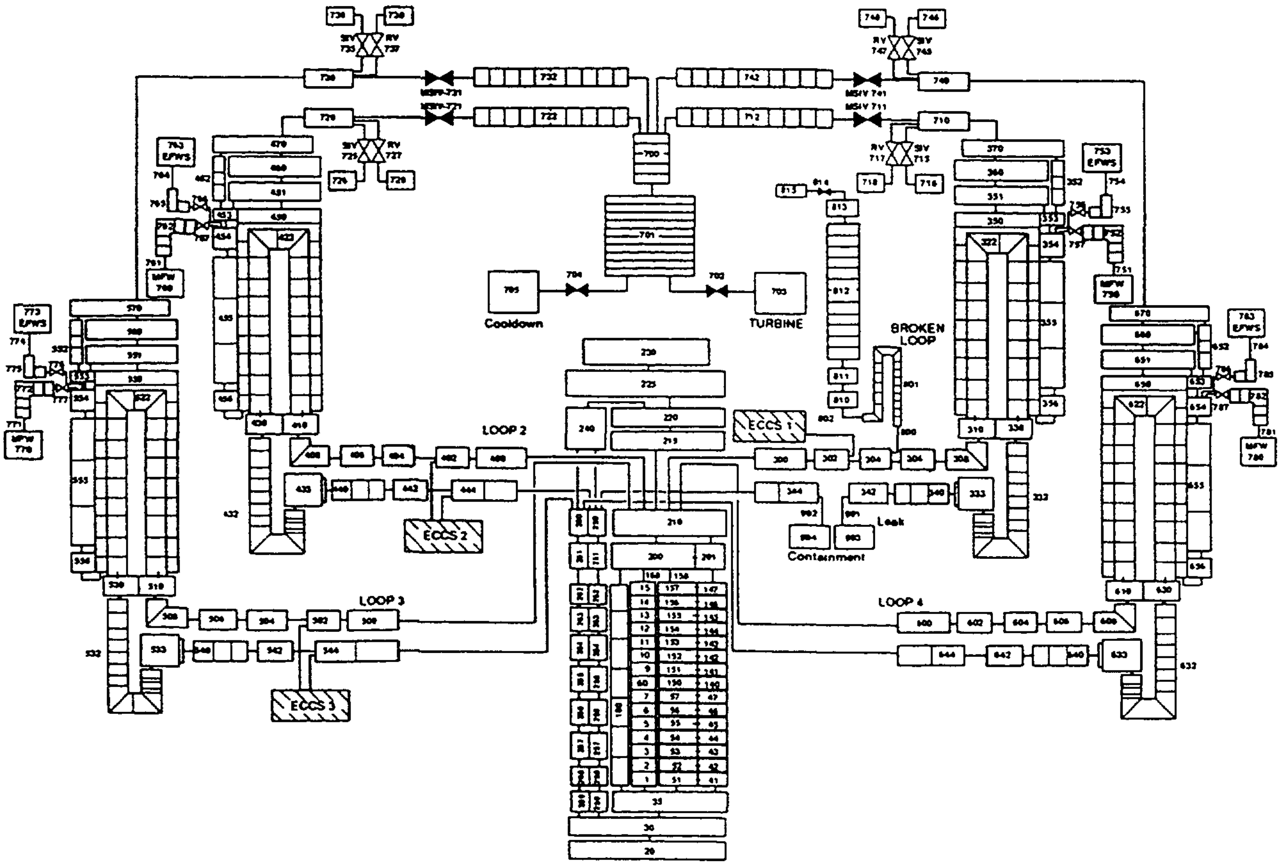

FIG. 4: EPR 1400 MW. SPC-RELAP5 NODALIZATION OF REACTOR COOLANT SYSTEM

TABLE III: EPR STEADY-STATE AT 100% REACTOR POWER

STEADY STATE CHARACTERISTIC	VALUE
Reactor power	4250 MW
Primary pressure (hot leg)	15.5 MPa
Secondary pressure (steam dome)	7.25 MPa
Coolant temperature at core outlet	328.6 °C
Coolant temperature at core inlet	291.3 °C
Temperature difference SG inlet/outlet	35 K
Mass flow rates	
- Loop	5263 kg/s
- Core inlet total	21050 kg/s
- Core reflector (5%)	1052 kg/s
- Upper head bypass (2%)	421 kg/s
Reactor coolant pump velocity	155.5 rad/s
Reactor coolant pump head	1030 kPa
Main steam flow rate	601 kg/s
MFWS injection rate	601 kg/s
MFWS water temperature	230 °C
Pressurizer water volume	42 m^3
SG water volume secondary side	100 m^3
RCS water volume (PRZ included)	412 m^3

3.2. Initial and boundary conditions for LOCA-analysis

The initial thermal-hydraulic state of the reactor coolant system at 100% reactor power is summarized in Table III. The main boundary conditions assumed are:
- reactor power 103% of the nominal power,
- 3% of the reactor power are generated directly in the moderator,
- axial reactor power distribution with chopped cosine shape,
- average Linear Heat Generation Rate (LHGR) 159 W/cm, maximum LHGR 450 W/cm,
- peaking factor 1.45 for the average rod and 2.83 for the hot rod,
- primary system pressure increased by 0.2 MPa,
- conservative decay heat, i.e. ANS 71 + 20% or DIN 25463 + 2σ,
- containment back-pressure either set constant (SBLOCA) or calculated on-line (LBLOCA).

Concerning the availability of SIS, single failure of the diesel generator of one SIS train is assumed, i.e. one MHSI and one LHSI are not available. Because of this SF, one train of the Emergency Feed Water System (EFWS) is also not available, since it is connected to the same diesel generator. Additionally, the cold leg injection of the SIS which belongs to the broken loop is supposed to be lost directly into the containment. It is furthermore assumed that the LHSI is distributed 50% to 50% between the cold and hot legs. The resulting SIS effectiveness is summerized in Table IV.

TABLE IV: ASSUMPTIONS ABOUT SIS AVAILABILITY FOR LOCA ANALYSIS

	MHSI PUMPS	ACCUMULATORS	LHSI PUMPS
HOT LEG	-	4 out of 4	1.5 out of 2
COLD LEG	2 out of 4	-	1.0 out of 2

3.3 Calculation's results

3.3.1. SBOCA; MHSI-sizing

RELAP5 and CATHARE 2 calculations were performed for different break sizes in order to assess the required injection rates to be delivered by the MHSI pumps in compliance with the design criteria specified in Tab. II:

a) "No loop draining for break sizes $\phi \leq$ 25 mm". Strict accomodation of the Moody liquid critical flow model results in a requirement of 40 kg/s at 7.5 MPa RCS pressure for the 25 mm break. However, a limited loop draining, consistent with maintaining the two-phase natural circulation all around the entire RCS loop, with large margin to the RCS residual mass corresponding to the transition towards reflux condensation, results in a requirement of 22 kg/s only at 6.5 MPa.

b) "No core uncovery for break sizes $\phi \leq$150 mm". According to increasing break sizes, i.e. for break equivalent diameters of 50, 75, 115 and 150 mm, the requirements to the MHSI flow rate versus RCS pressure are roughly 20 kg/s at 6 MPa, 45 kg/s at 6 MPa, 80 kg/s at 4.5 MPa and 90 kg/s at 4.5 MPa, respectively. The results rely upon the following assumptions:
- most conservative core decay heat, according to ANS 71+ 20% margin,
- secondary side partial cooldown from 8.5 MPa to 6 MPa at 100 K/h rate, actuated upon pressurizer low pressure signal (11 MPa),
- main coolant pumps trip upon fluid saturation signal.

The required flow rates must be delivered by 2 out of 4 MHSI, since one MHSI is lost because of assumed single failure of the corresponding diesel generator (see Section 3.2) and a second one is connected to the broken loop and spills directly into containment.

The compatibility between these requiremetns and the preliminary design of EPR's MHSI system was verified: the MHSI effective flow rate injected by 2 out of 4 MHSI pumps comply with all a.m. requirements.

3.3.2. LBLOCA; accumulator sizing

A double-ended (2A) guillotine break in the cold leg piping system between the ECC injection nozzle and the reactor vessel was simulated. SPC-RELAP5 calculation results are presented below. Main events are listed in Table V.

The system behavior during the blowdown phase is independent on the SIS configuration until ACCU injection starts. The pressures in the primary system and the containment equalize 36 s after break initiation at a pressure of 320 kPa. The ACCU injection starts at 15 seconds, when the primary system pressure has decreased below 4.5 MPa. A few seconds later highly subcooled ECC-water from the hot legs is delivered to the UP and penetrates through the tie plate to the core. The water breakthrough occurs only within a defined area of approximately 20% - 25% of the total core flow area. While a significant portion of the steam in the hot legs and the UP is condensed by the hot leg injection, ECC-water which penetrates through the tie plate is still highly subcooled.

Water downflow from the UP initiates core cooling during end-of-blowdown (Fig. 5). Some of the water downflow is vaporized and steam flows out of the top and bottom of the core; however, most of the water downflow is heated to near saturation and flows to the LP. Within the breakthrough region, the core is quenched from the top down by the water downflow from the UP at the end of blowdown. The LP inventory starts to increase about 10 s before the end of blowdown. This level increase is exclusively due to the hot leg injection which penetrates through the tie plate and core; the cold leg injection (LHSI + MHSI) only starts at 40 s (Fig. 6).

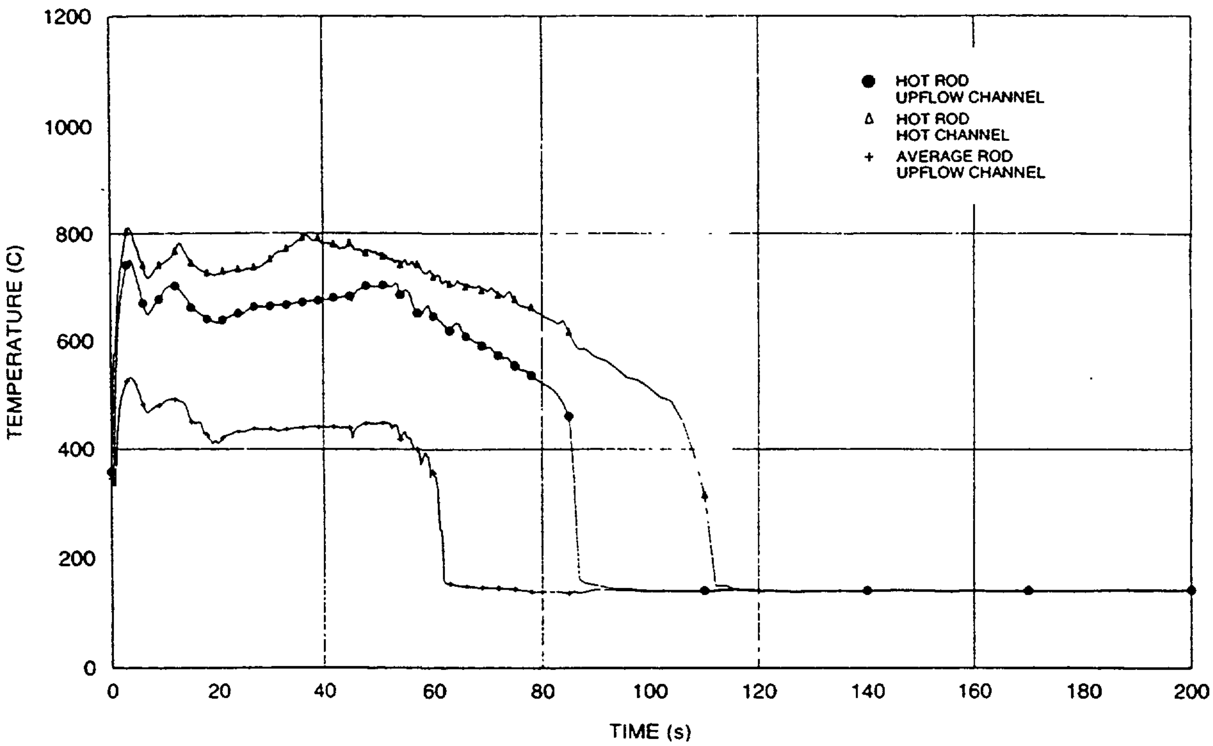

FIG. 5: 2A COLD LEG BREAK ANALYSIS. PEAK CLADDING TEMPERATURES

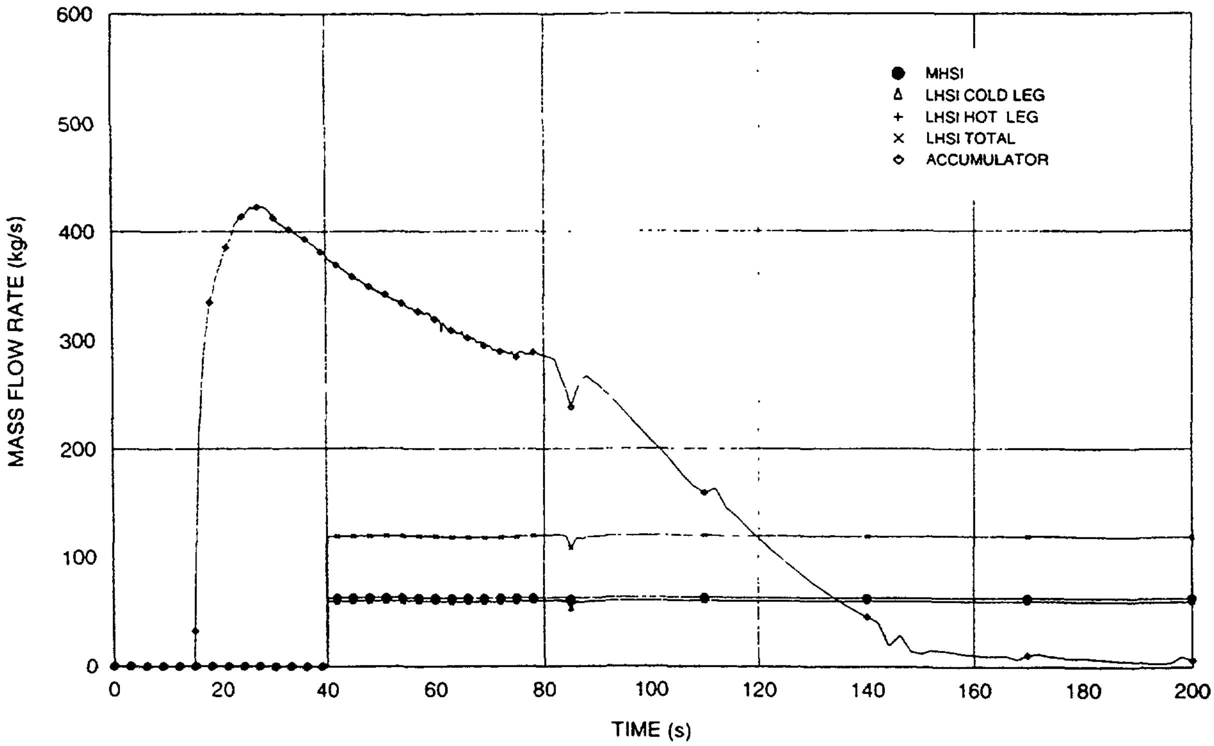

FIG. 6: 2A COLD LEG BREAK ANALYSIS. SIS INJECTION RATES (ONE TRAIN)

By the completion of blowdown, the LP is filled to the bottom of core barrel. A few seconds later (i.e. 45 s after break initiation), the vessel fills to the core inlet and refill is complete. Hence, the end-of-blowdown and refill are overlapping which reduces the time to core reflood and therefore the heat-up period of the non-downflow regions of the core; consequently, the cladding temperature is relatively low: < 800 °C.

The reflood phase begins at approximately 36 s after break initiation. Initially, the DC water level increases rapidly as ECC-water injected into the cold legs is delivered to the DC and ECC-water injected into the hot legs penetrates through the core to the LP and flows into the DC. When, at 70 s, the DC water level reaches the cold leg elevation, water spills out the broken cold leg and the water level stabilizes.

Table V: 2A COLD LEG BREAK ANALYSIS: SEQUENCE OF EVENTS

EVENT	TIME [seconds after break opening]
Break opening, reactor trip, turbine trip and reactor coolant pump trip	0
Beginning of ACCU injection	15
Beginning of refill phase	26
End of blowdown phase	36
MHSI and LHSI start	40
End of refill phase	45
Quenching of average rod in up-flow channel	60
Quenching of hot rod in up-flow channel	90
Quenching of hot rod in hot channel	115
Accumulators empty	150

During refill/reflood the hot leg injection condenses efficiently most of the steam produced in the core. The uncondensed steam flows through the loops. However, since most of the steam is condensed in the UP and hot legs, the loop steam flows are minimal and the corresponding pressure drop is small; thus the core flooding rate is high.

Hot rods located in the up-flow channel (which represents 80% of the FA) are quenched 90 s after break initiation; the hot rod included in the hot channel is quenched within 115 s. The peak cladding temperature (PCT) is reached within the blowdown phase; the PCT is 810 °C. The second peak reached at 35 s is only 800 °C (metal-water reaction and eventual fuel rupture are not taken into account in the present analysis).

The ACCUs empty 150 s after break initiation, i.e. the ACCU injection has a duration of approximately 135 s. The ACCU injection rate is in maximum 430 kg/s or, averaged over the time between injection start and total core quenching, approximately 330 kg/s. There is a delay of approximately 30 s between core quenching and ACCU emptying. This injection characteristic was achieved by optimizing the water/nitrogen volumes and by throttling the ACCU injection line in an adequate way.

4. CONCLUSIONS

The most important new features of EPR's SIS have been evaluated with respect to SBLOCA scenarios: they are firstly, the shut-off head of only 80 bar for the MHSI and secondly, the secondary side partial cooldown to about 60 bar. With implementation of a partial automatic secondary side cooldown the SIS configuration ensures appropriate mitigation of all types of primary side breaks (LOCA) in terms of location and size as well as all relevant NON-LOCA scenarios.

Preliminary results of analyses performed with the best-estimate codes CATHARE, RELAP5/MOD2 and SPC-RELAP5 demonstrate the efficiency of the SIS:

a) In case of LOCAs caused by very small breaks ($\phi \leq 25$ mm) the EPR's SIS is capable - in conjunction with the automatic partial cooldown of the secondary side - to prevent loop draining, even when only two MHSIs are effective. In case of small and intermediate leaks ($\phi \leq 150$ mm) the SIS ensures sufficiently high injection rates for preventing core uncovery, again even when only two MHSIs are effective. For leaks within the range $150 < \phi \leq 350$ mm, the SIS is able to limit the core uncovery.

b) In case of double-ended break LOCAs the SIS ensures the fast reflood of the core within approxi-mately 120 s; the peak cladding temperature is 810°C. The reflood of the core is achieved by the accumulator injection, which lasts about 135 s and ensures a relatively large time delay of 30 s between core quenching and accumulator emptying.

REFERENCES

[1] BARRE, F., BERNARD, M., "The CATHARE Code Strategy and Assessment", Nuclear Eng. and Design 124 (1990) 257-284

[2] BESTION, D., "The Physical Closure Laws in the CATHARE Code", Nuclear Eng. and Design 124 (1990) 229-245

[3] RANSOM, V.H., et al., RELAP5/MOD2 Code Manual, Volumes 1 and 2, NUREG/CR-4312, Rev. 1, (1987)

[4] CARLSON, K.E., et al., RELAP5/MOD3 Code Manual, Volumes 1 and 2, NUREG/CR-5535, EGG-2596 (Draft), (1990)

[5] CURCA-TIVIG, F., KÖHLER M., "A Code System for Coupled Analysis of Reactor Coolant System and Containment Thermal-hydraulics", New Trends in Nuclear System Thermal-hydraulics (Proc. Int. Conf., Pisa, 1994), Vol. 2, 293-301

SWR-1000: THE DIMENSIONING OF EMERGENCY CONDENSERS AND PASSIVE PRESSURE PULSE TRANSMITTERS

C. PALAVECINO
Power Generation Group (KWU) of Siemens AG,
Offenbach am Mein, Germany

Abstract

The Power Generation Group (KWU) of Siemens AG and the German electrical power utilities - particularly those operating boiling water reactor plants - are together developing a new reactor type which is characterized in particular by its passive safety systems.

These passive safety systems are the emergency condensers, the containment cooling condensers, the passive pressure pulse transmitters, the gravity-driven core flooding lines, the rupture disks arranged in parallel to the safety-relief valves, and the scram systems.

This presentation constitutes a report on the emergency condensers and the passive pressure pulse transmitters.

The most important reasons for introducing passive safety systems are to increase the safety of future nuclear power plants, to simplify reactor safety systems and to reduce capital costs.

The emergency condensers are heat exchangers consisting of a parallel arrangement of horizontal U-tubes between two common heads. The top header is connected via piping to the reactor vessel steam space, while the lower header is connected to the reactor vessel below the reactor vessel water level. The heat exchangers are located in a pool filled with cold water. The emergency condensers and the reactor vessel thus form a system of communicating pipes. At normal reactor water level, the emergency condensers are flooded with cold, non-flowing water. No heat transfer takes place in this condition. If there is a drop in the reactor water level, the heat exchanging surfaces are gradually uncovered and the incoming steam condenses on the cold surfaces. The cold condensate is returned to the reactor vessel.

The design of the emergency condensers must meet the requirements dictated by the given thermal and hydraulic conditions.

The effects of the thermal condition parameters are relatively well known to us from the evaluation of emergency condenser testing conducted at Gundremmingen Nu-

clear Power Station. As we have altered the elevation conditions in the radial direction in comparison to Gundremmingen Unit A, new sizing calculations have been performed. An emergency condenser test rig was constructed at the Jülich nuclear research center in order to provide experimental verification of our calculations.

Taking into consideration a redundancy degree of N + 2, a specific thermal rating of 63 MW per emergency condenser results for a reactor with an output of 2778 MW. The total performance of the emergency condenser system is thus 252 MW, or 9.1 % of reactor output.

Given this emergency condenser rating, accident control of some transients becomes very interesting:

- The heat removal capacity in the lower pressure range corresponds to that of 2 to 3 relief valves.
- In the event of a stuck-open relief valve with simultaneous failure of all reactor vessel injection possibilities, the core will not become uncovered until some 24 hours after the onset of accident conditions.

The following can be said of this component:

a) It is more reliable than components designed for comparable functions.

   The probability of failure of the emergency condenser of Siemens' BWR 1000 is approximately 10^{-4} per demand, while that of older emergency condenser designs such as at Gundremmingen Unit A is approximately 2 to 3 x 10^{-3} per demand, and that of the active residual heat removal systems of Siemens advanced boiling water concept about 2 to 3 x 10^{-2} per demand.

b) It is considerably less expensive than the residual heat removal systems implemented to date, which comprise a primary circuit, a component cooling system and a final cooling system, each equipped with pumps, valves and heat exchangers, etc. These latter systems are provided with a diesel generator as a redundant power supply system. The cost of one train (without considering infrastructure elements such as the building, etc.) can be assumed to amount to some DM 100 million. In contrast to this, the cost for an emergency condenser system (comprising four emergency condensers) is estimated to cost between somewhere between DM 10 and 20 million.

The reliability of the electrically-operated reactor protection system represents a limitation to achieving a higher degree of safety. It was therefore necessary to duplicate the functions of the reactor protection system in a different way. These efforts successfully culminated in the development of the passive pressure pulse transmitter.

Passive pressure pulse transmitters function in the same manner as the emergency condensers. The pressure generated in a heat-exchanger secondary circuit is used to actuate pilot or main valves. These passive pressure pulse transmitters allow the scope of reactor protection systems requiring electric power to be reduced considerably, while plant safety and reliability are increased through the combination of electrically-operated reactor protection systems with passive safety equipment.

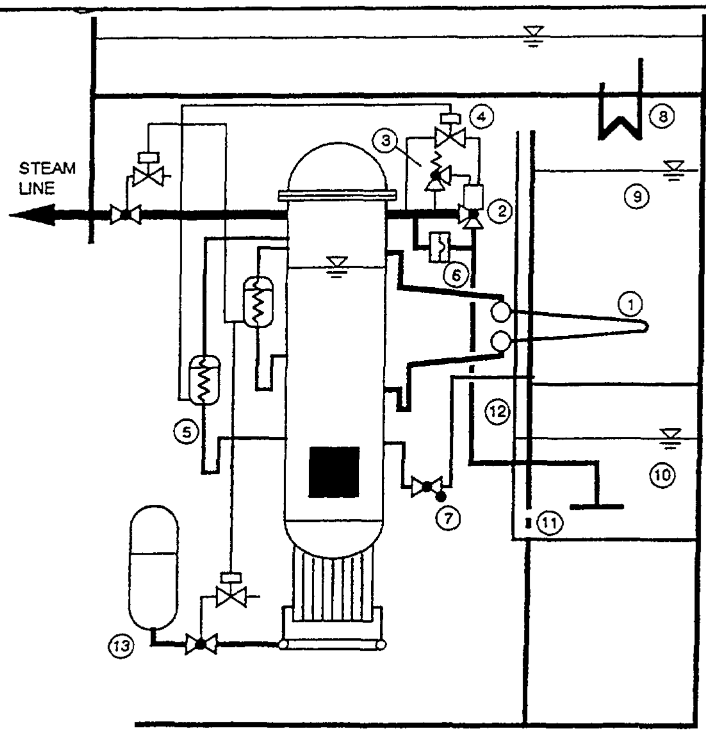

No		Quantity
1	Emergency condenser	4
2	Safety-relief valve	8
3	Spring-loaded pilot valve	8
4	Diaphragm pilot valve	8
5	Passive pressure pulse transmitter	4
6	Rupture disk	8
7	Flooding line	4
8	Containment cooling condenser	4
9	Core flooding pool	
10	Pressure suppression pool	
11	Horizontal discharge vent	42
12	Vertical discharge shaft	12
13	Scram system	4

Fig. 1. SWR 1000 Passive Safety Systems

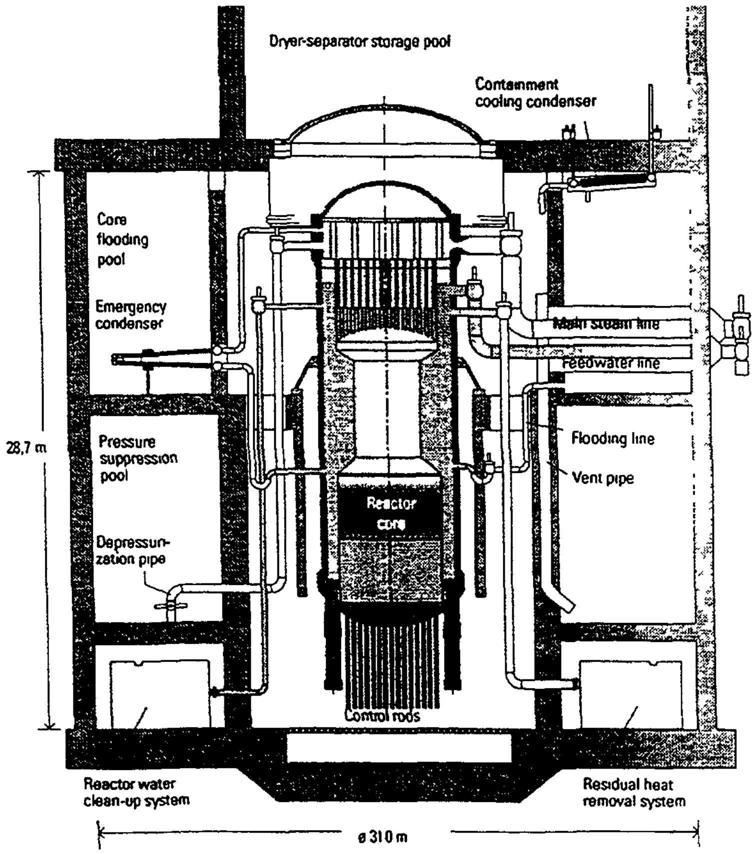

Fig. 2. SWR 1000 - Containment

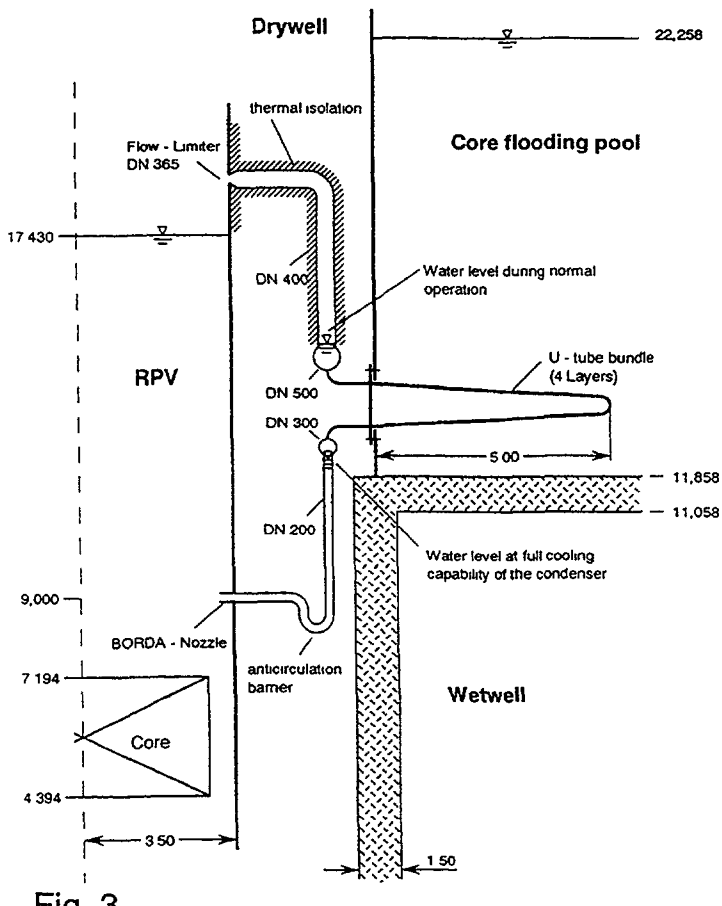

Fig. 3.
SWR 1000 - Isolation condenser (schematic)
(Height in m above ± 0.0 elevation in RPV)

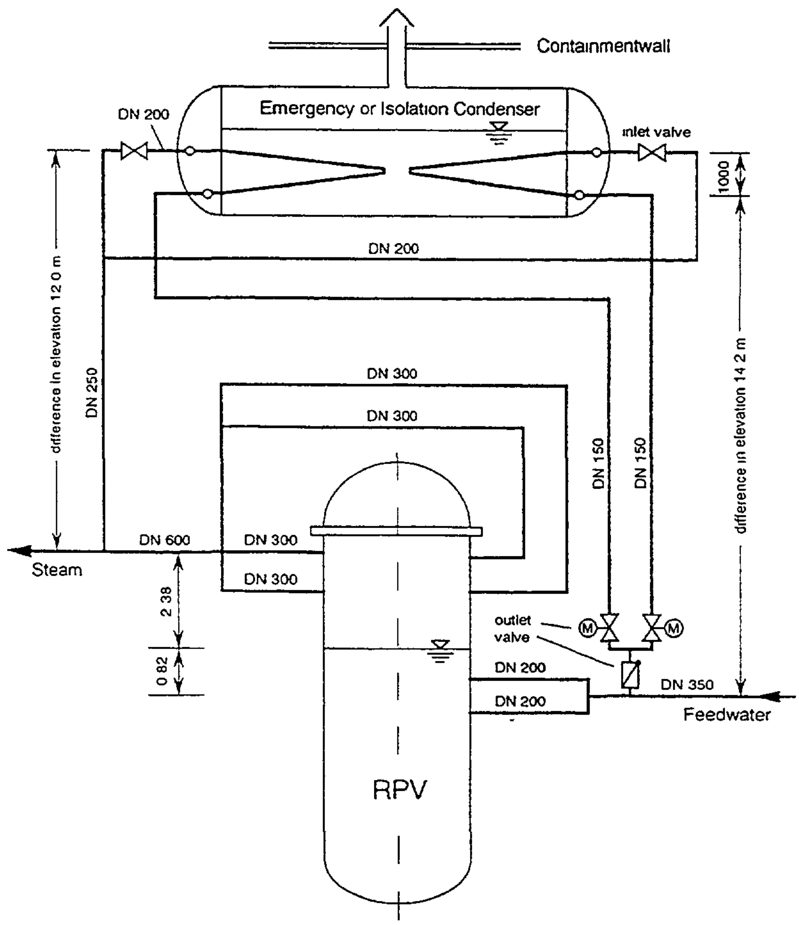

Fig. 4.
KRB - A Emergency condenser diagram

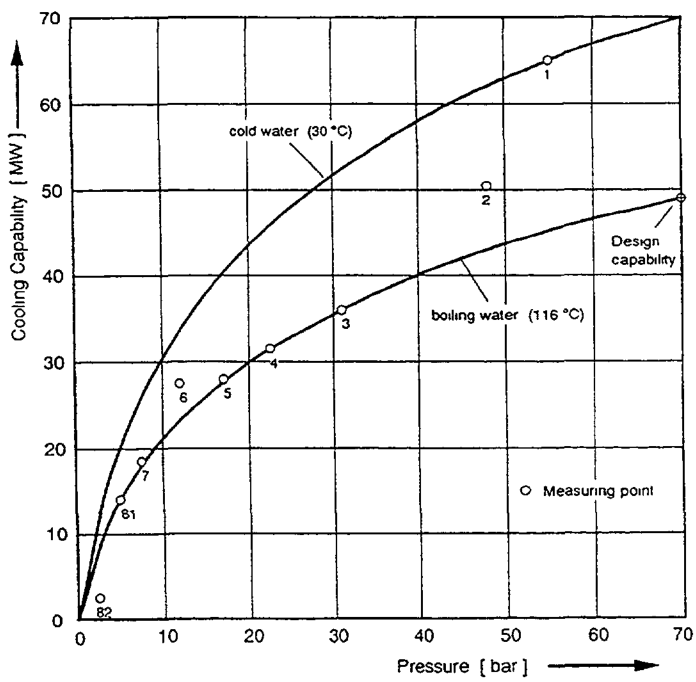

Fig. 5.
KRB - A
Cooling capability of the emergency condenser
Measurement on May 10, 1975

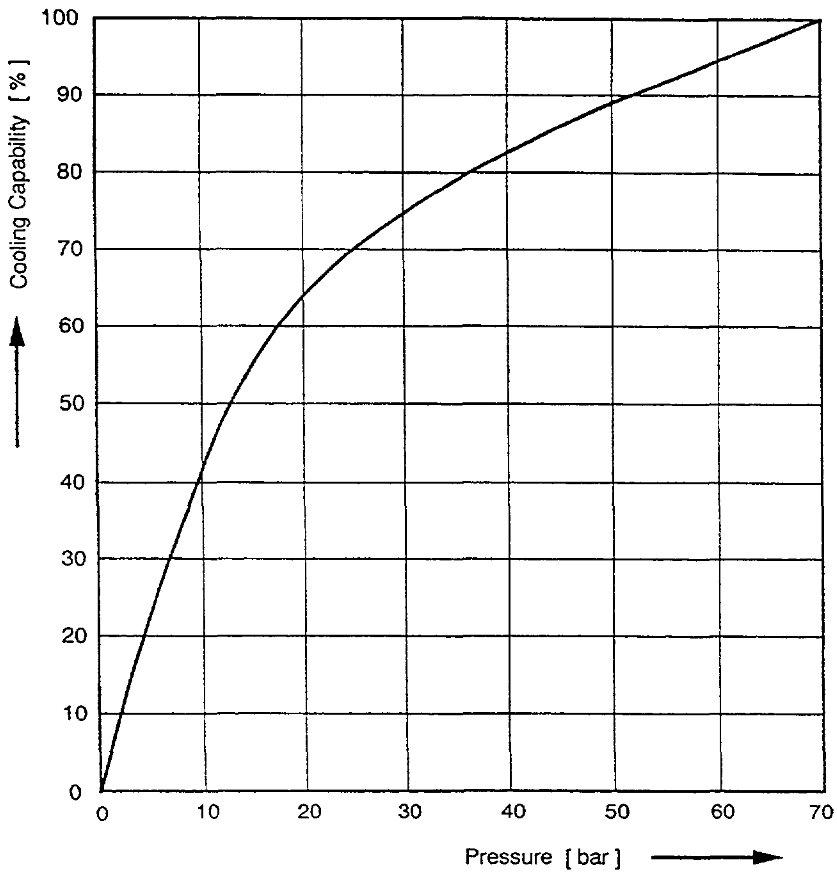

Fig. 6.
SWR 1000 - Emergency condenser.
Cooling capability as a function of the pressure in the RPV

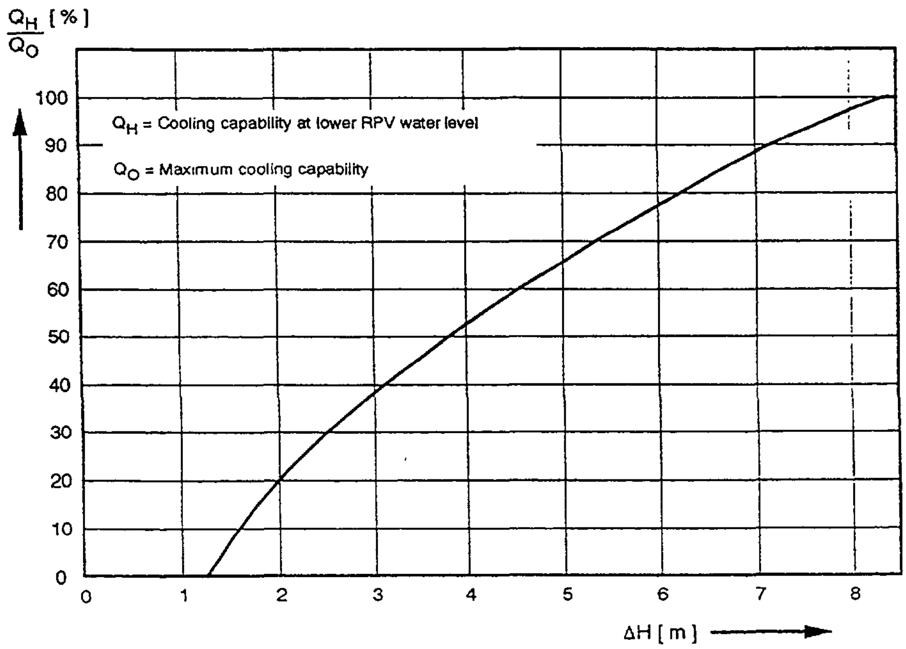

Fig. 7.
SWR 1000 - Emergency condenser.
Cooling capability as a function of loss of water level in the RPV. (ΔH in m)

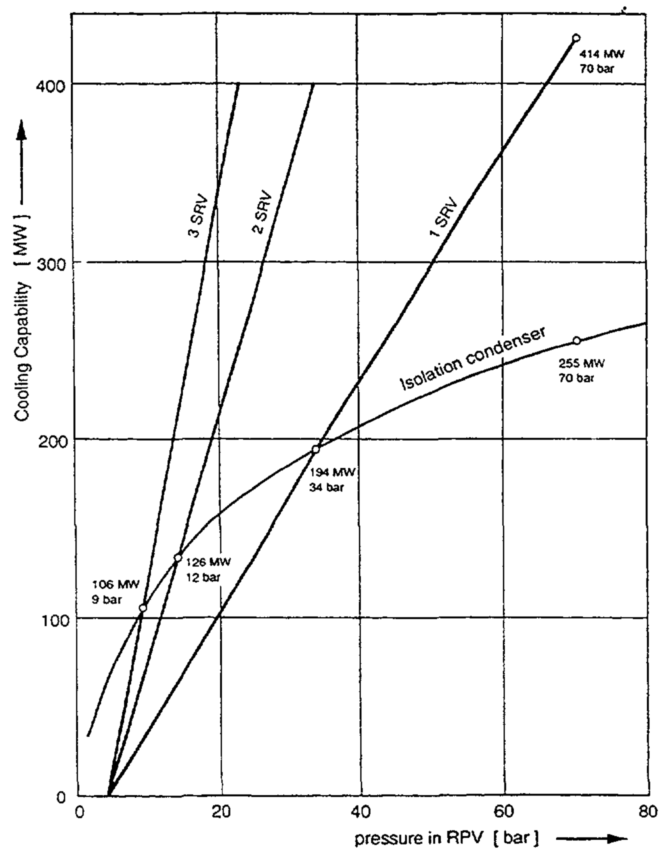

Fig. 8.
SWR 1000 - Comparison between the cooling capability of the isolation condenser and those of the safety relief valves

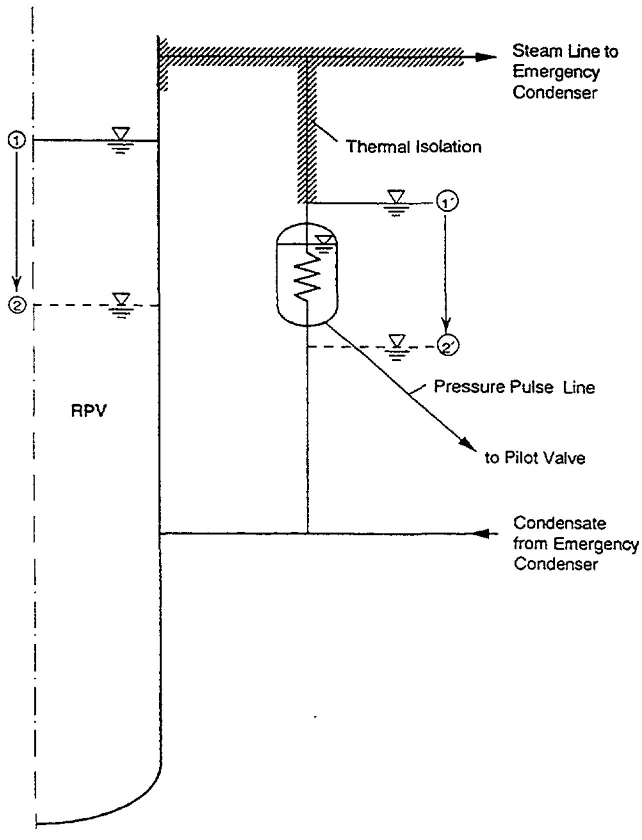

Fig. 9.
SWR 1000 - Passive Pressure Pulse Transmitter

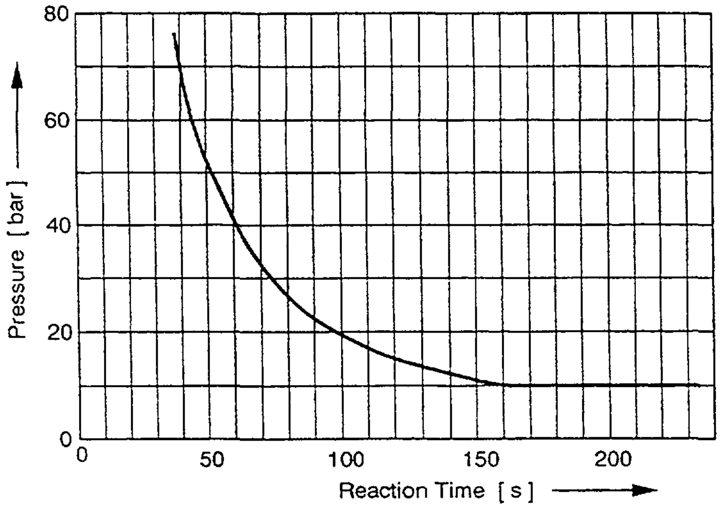

Fig. 10. SWR 1000 - Reaction Time of PPPT

Table 1: Principal Data of Emergency Condenser System

Number of emergency condensers	4
Design	1 tube bundle comprising a four-pass U-tube configuration, with connection to two common headers
Performance of each emergency condenser	63 MW given a primary system pressure of 70 bar, a core flooding pool temperature of 40 °C, and a reactor vessel water level drop of 8.20 m
Heat transfer area per condenser	138 m², comprising 104 tubes; tube diameter: 44.5; wall thickness: 2.9 mm
Design conditions:	
- Primary side	88 bar, saturated water
- Secondary side	0 - 10 bar
Temperature:	
- Primary side	300 °C
- Secondary side	40 - 180 °C
Size (diameter) of connected piping	- Supply steam line: 400 mm - Condensate discharge line: 200 mm - Headers o steam side: 500 mm o condensate side: 300 mm

Table 2: Comparison of Magnitude of Failure Probabilities per demand of Various Residual Heat Removal Systems

Failure Probability / System	BWR 1000 Emergency Condenser	Gundremmingen A Type Emergency Condenser	Siemens-KWU Series ABWR Active RHRS
Signal acquisition and processing	-	1 E - 3	1 E - 4
Startup failure (valves, pumps, etc.)	-	1 E - 3	1 - 3 E - 2
Failure during accident (7 days)	-	1 E - 4	1 E - 2
Failure of piping and heat exchanger tubing	1 E - 4	1 E - 4	1 E - 3
Failure of power supply (from this, failure of emergency power supply)	-	1 E - 5	2 E - 5 (2 E - 2)

Table 3: Principal Data of Passive Pressure Pulse Transmitter

Type	Dimensions	Heat-Exchanger Tube				Volume of water	Exchanger Area	Ratio Volume/Area
	Diameter x Heigth	Diameter	Thickness	Length	Number			
	mm	mm	mm	mm	--	l	m^2	l/m^2
1	555 x 650	25	1,5	3250	1	4,05	0,24	17
2	555 x 650	20	1,2	860	7	17,60	0,36	50
3	430 x 560	20	1	383	30	4.,33	0,69	6

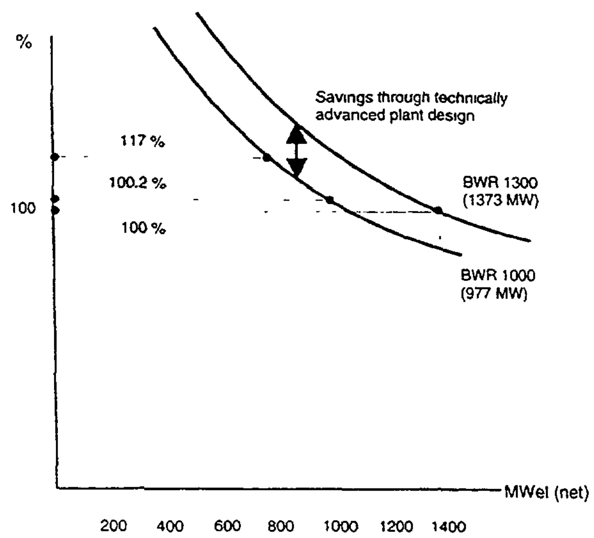

BWR - Degression of Specific Plant Costs as Fuction of Output and Technical Design

DESIGN, FABRICATION AND TESTING OF FULL SCALE PROTOTYPE FOR PASSIVE COOLING APPLICATIONS

P. GIRIBALDI, F. MAGRIS, M. ORSINI, FL. RIZZO
ANSALDO, Genova, Italy

Abstract

The paper presents the ANSALDO main activities performed during Design, Fabrication and Site Assembly of the full-scale prototypes of two essential components for the G.E. Simplified Boiling Water Reactor, i.e. the Passive Containment Cooler (PCC) and the Isolation Condenser (IC).

The PCC and IC are two safety related components

The reference Design provides the following advantages:

1) New safety features i.e. the use of natural circulation
2) Decreased operator burden: i.e passive safety approach

2. INTRODUCTION

An essential feature of the SBWR, the advanced BWR developed by General Electric is the presence of two safety related and passive systems, the IC and PCC which enhance the overall plant safety.
They perform their functions (control of reactor and containment pressure) for 72 hours without operator actions.
The key components of these systems are two natural circulation condensing heat exchangers immersed in a pool water vented to atmosphere, i.e. the Isolation Condeser (I.C.) and the Passive Containment Cooler (PCC).
The design analysis methodology and the main structural problems faced during the design development have been already described in detail in doc. [1].
After a brief summary of the main design aspects focused in this document, emphasis will be given to the manufacturing methodology of the prototypes.
The on-site activities in order to assembly the components coming from the Manufacturer shop are described.
Finally being recently completed the test campaign on the PCC, some preliminary evaluations about its structural integrity are given.

3. COMPONENT DESCRIPTION

3.1 Isolation Condenser

Following is a summary of the main functional and design requirements of the Isolation Condenser (IC).

*	Function:	Remove decay heat from RPV following isolation events, to control the RPV pressure and water level
*	Heat removal capacity	30 MW per unit
*	No of units	3
*	Code Classification	ASME Section III Class 2
*	Design Pressure	8.62 MPa , 1250 psi
*	Design Temperature	302 °C, 575 °F

* Corrosion Resistant Material
* Low susceptibility to Intergranular Stress Corrosion (IGSC)
* Reliability for 60 years design life
* Easy In Service Inspection, maintenance, repair and removal
* Fouling and plugging margin included in the design
* Continuous operation at RPV pressure, 10 °C
* 135 severe thermal transients, 10 to 302 °C in a few seconds
* Periodic venting of small volumes of non-condensable gases

The Isolation Condenser, see fig. 1, is made of two identical modules, each consisting of a upper header, a vertical tube bundle and a lower header. Each header is closed at both ends by flanged dished covers; the upper one is fed by two lines connected to the main steam line from the R.V. and the lower one is drained by a condenste line to the R.V.

The system is operated by simple automatic opening of a redundant valve placed on the condensate return line to the R.V., the connection between the R.V. steam area and the condenser upper headers being always opened.
The Isolation Condenser is started into operation by draining the condensate to the Reactor thus causing steam from the Reactor to fill the tubes which transfer heat to the cooler pool water.

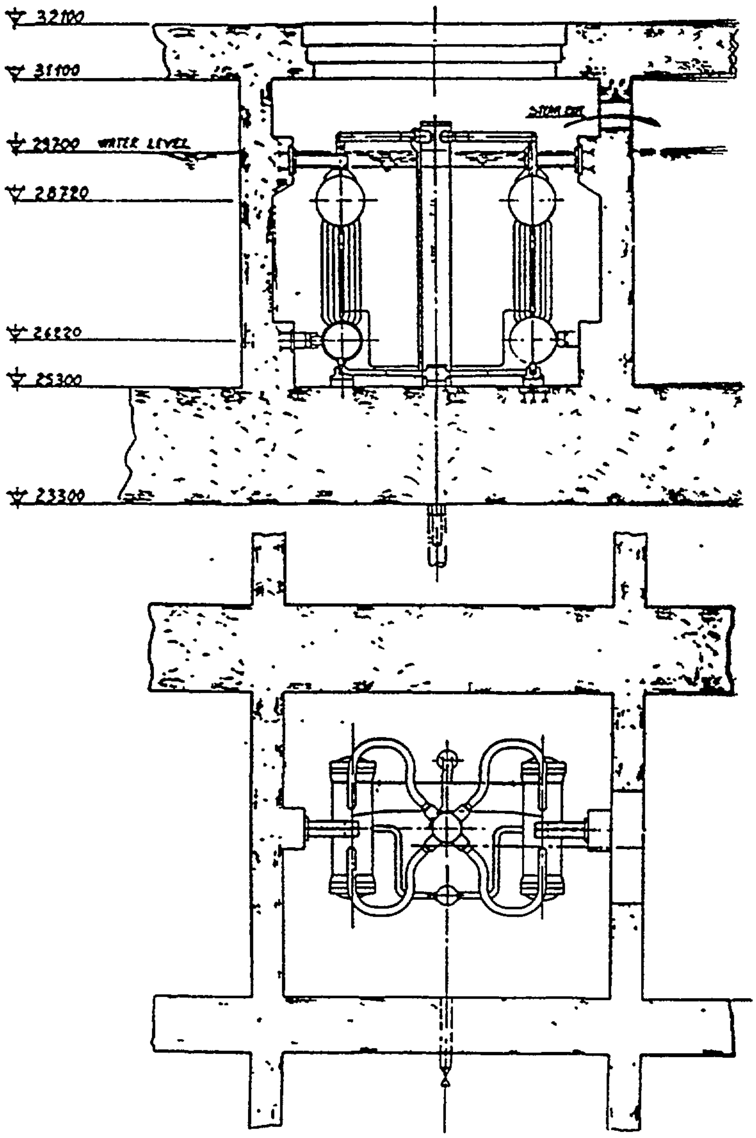

FIG. 1 ISOLATION CONDENSER CONFIGURATION

- Two modules per unit (horizontal steam inlet upper header, 120 vertical condensing tubes 50.8 mm OD * 2.30 mm, horizontal condensate outlet lower header).
- Main steam line enclosed in a guard pipe and one-piece steam distributor with built-in Venturi flow limiters to provide protection against potential breaks outside containment.
- Two feed lines/one drain line per module
- Upper support allowing tubes thermal expansion free downward.
- Horizontal dynamic restraints on lower header
- Headers removable bolted covers allowing access to the tubes for all required operations.

3.2 Passive Containment Cooler

Following is a summary of the main functional and design requirements of PCC

*	Function:	Remove decay heat from RPV following LOCA/SA, to control the containment pressure
*	Heat removal capacity	10 MW per unit
*	No of units	3
*	Code Classification	ASME Section III Class 2
*	Design Pressure	0.76 MPa , 110 psi
*	Design Temperature	171 °C, 340 °F

* Corrosion Resistant Material
* Reliability for 60 years design life
* Easy In Service Inspection, maintenance, repair and removal
* Fouling included in the design
* Continuous operation at Drywell pressure, 10 °C
* 2 thermal transients, 10 to 150 °C
* Venting of large volumes of non-condensable gases

The PCC has basically the same geometry of the IC: upper and lower header connected by vertical tubes.
The PCC general arrangement is shown in fig. 2

The system is operated in a completely passive way, the connection between the PC and the Condensers being always opened.
The PCCS loops are initially driven by the pressure differences created between the containment drywell and the suppression pool during a LOCA and then by gravity drainage of steam condensed in the tubes, so they required no sensing, control logic or power - actuated devices to function.

- Two modules per unit (horizontal steam inlet upper header, 248 vertical condensing tubes 50.8 mm OD * 1.65 mm, horizontal condensate outlet lower header).
- One feed line per module
- Single bottom nozzle, including concentric pipes for both condensate drainage and non-condensible venting.
- Lower header support, allowing tubes thermal expansion free upward.

- Horizontal dynamic restraints on upper header
- Headers removable bolted covers allowing access to the tubes for all required operations.
- Disc shaped deflector in upper header to prevent flow maldistribution inside tubes.

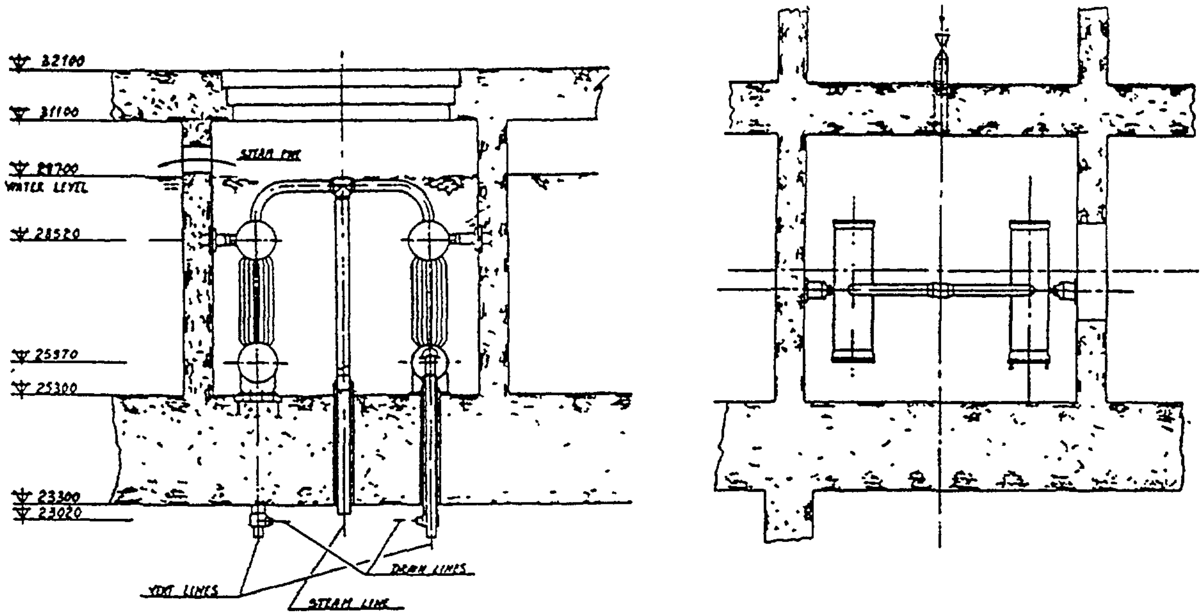

FIG. 2 PASSIVE CONTIANMENT COOLING CONDENSER CONFIGURATION

4. DESIGN PHILOSOPHY

The sizing loads are those associated with the thermal transients on calling in service of the system.
In fact both the equipments are subjected to a shock transient when the stagnant cold water or gas mixture is replaced by hot condensing steam.
As a result the component structures will experience temperature distributions evolving with time, leading to significant temperature differences between parts of different thermal capacities, as well to important in wall thermal gradients, due to high external heat transfer coefficient. Furthermore high pressure loads are present for the IC.

These very high stresses are not related to an accident condition, but to a level B operating transient and to steady state conditions.

Facing the level B requirements expecially on stress ratcheting and fatigue was the big design challenge.

The design approach was:

* Use of a modular design which minimizes the required thickness and hence the thermal gradients.

* Keep the primary stresses low in order to avoid the risk of cyclic progressive incremental deformation caused by very high thermal stresses.

All the peculiar aspects of the design were investiagated (see ref. (1)) from steam distribution to nozzles, tubes risk of instability due to the imposed displacements resulting from the header shell thermal behaviour during transients. Results are always within the Code allowable limits.

5. FABRICATION OF THE PROTOTYPES

Because of their geometry the two prototypes were shop fabricated as separate pieces which were assembled directly at site

The following subassemblies related both to the PCC and the IC have been manufactured at the ANSALDO GIE - MILANO shop in Milan

a) Exchanging modules consisting of the two headers and the tube bundle.
b) Steam line complete with its diffuser
c) Feed lines
d) Drain lines

The most interesting aspects are related to:

a) Extensive use of forgings
b) Module assembling with particular attention to the Tube-header junction welding.
c) Instrumentation installation on the exchange tubes.

Hereafter these technical features are discussed

5.1 Extensive use of forgings

To satisfy the requirement of minimal in service inspection, the design makes extensive use of forgings, in particular the headers and the covers are made by single-piece forgins, without any welding.

For the headers the nozzles where obtained by extrusion and then machining to final dimensions.
For the IC cover, the curved shape was obtained by drop-forging, then the component was machined to final size.

5.2 Module assembly

While the lines assembly has followed a quite classic proceedings (cutting, calking, welding and non destructive examinations) the module one may present a particular interest.

The assembling methodology has followed the following steps

a) The drilling of the cylindrical wall in order to seat the exchange tubes, This operation has been performed at the boring machine by a special tool which created at the same time the hole and the external circular groove.

b) Vertical positioning of the two headers within a solid structure for assembling in order to avoid deformations caused by the contraction of the welding between tubes/headers

c) Following a geometrical survey, the exchange tubes cutting consistent with the measuring, in order to obtain the edge overlapping required by the tube/header welding.

d) Positioning of the exchange tube between the headers

e) Welding execution and non destructive examinations.

The tube/header welding is an automatic orbital TIG type without weld material obtained by melting the overlapped edges of tube and the welding bath was produced by a pulsating and rotating current.
A typical weld result is shown in Fig. 3.

The welding machine is automatic and programmable for each of its functions.
The hardest effort has been spent to identify all the parameters and the related tolerances (current intensity, voltage, overlapping of the joint edges,

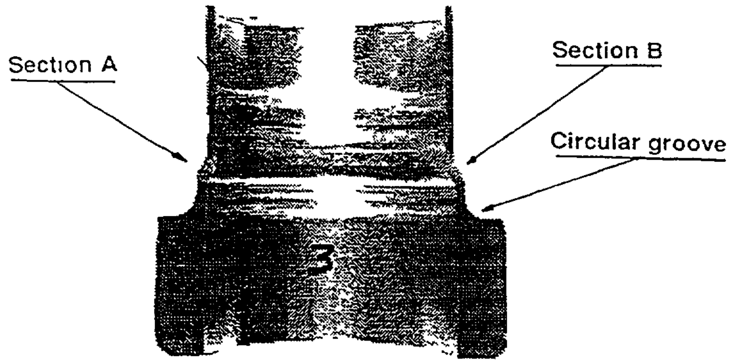

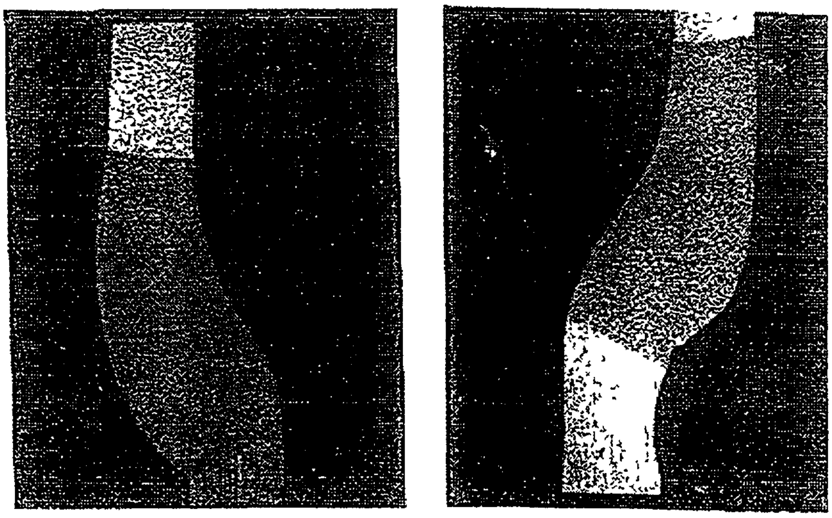

Section A Welding blow-up

Section B Welding blow-up

Fig.3 Tube-header junction

rotation speed of the plasma torch, number of the qualified remeltings and the related variations of parameters).

The specification of all these parameters has required long proof compaignes completely repeated for both the prototypes, since manufactured with different materials and different tubes thickness.

It must be remarked that the definition of the procedure for the IC has been more laborious than for the PCC, due to the material (INCONEL 600) greater fluidity in the melted state.

It has been also set a repair proceeding by manual TIG with weld mateiral to be used during manifacturing if some welding accident, had occurred.

5.3 Instrumenation installation on the exchange tubes

As a special application, the installation of the thermocouple for reading the PCC tubes inner wall tempeature must be pointed out.
The procedure consists in creating a very precise groove on the tube external by a circular milling cutter, leaving only 1/10 mm thickness at the tube inner surface, then the thermocouple was put in the cavity and the recess was filled by brazing.

Samples were subjected to pressure tests, up to 4 times greater than the design one, and to corrosion tests in Na Cl solution, showing a very good behaviour.

6. ON-SITE ASSEMBLY

All the subassemblies manufactured at the ANSALDO GIE shops have been delivered to Piacenza site where they have been assembled in the pools assigned to the thermohydraulic tests.

The moduls final positioning has been completed and then they have been connected to the steam and condensate lines

Following the covers were installed with the metallic O rings and the unit hydrotest was performed.
After resolution of a very small leak from one PCC flange, the prototype was ready for starting the test compaign.

7. FINAL EXAMINATIN OF THE COMPONENTS

While the tests on the IC prototype will start soon the test campaign has been completed on the PCC.

The unit has undergone

*	5	Hydrostatic test at 1.5 x Design Pressure, i.e	11.4 bar, rel
*	10	Pneumatic test with air	7.6 bar, rel
*	1	Stream flushing (empty pool) at 143 °C	3.0 bar, rel
*	2	Shakedown hot tests	4.9-6.9 bar, rel
*	40	Thermal hydraulic tests	3.8-6.9 bar, rel
*	10 + 4	LOCA pressure/temperature transients	4.0

The complete "structural" instrumentation results are not available yet (post processing the large amount of date related to strain gauges, thermocouples, accelerometers etc is very lows) and therefore the detailed comparison between analytical and experimental results has not been made yet.

Nevertheless there is great evidence that the component has survived all the tests - equivalent to more than 300 years of life - without any damage.

REFERENCE

1) I. Micheli, M. Orsini
Design by analysis of SBWR key components
SMIRT August 1993.

RESULTS OF SAFETY-RELATED COMPONENTS/SYSTEMS TESTS

(Session IV)
Part 1

Chairman

S. FRANKS
United States of America

INVESTIGATION ON PASSIVE DECAY HEAT REMOVAL IN ADVANCED WATER COOLED REACTORS

F.J. ERBACHER
Forschungzentrum Karlsruhe, Institut für Angewandte Thermo- and Fluiddynamik

X. CHENG
Technische Universität Karlsruhe,
Institut für Strömungslehre und Strömungmaschinen

H.J. Neitzel
Forschungzentrum Karlsruhe, Institut für Angewande Thermo- und Fluiddynamik

Karlsruhe, Germany

Abstract

For future advanced water cooled reactor designs passive safety systems should be investigated in respect of their feasibility and functional performance. The Research Center Karlsruhe and the Technical University of Karlsruhe have proposed a composite containment concept which copes with severe accidents. One essential of this concept is the decay heat removal from the containment by natural air convection and thermal radiation in a passive way. To determine the coolability of such a passive cooling system and to study the physical phenomena involved, experimental separate-effects investigations are under way in the PASCO test facility which is a one-sided heated rectangular channel. In addition numerical calculations are performed by using the one-dimensional code PASCO and the three-dimensional thermal-hydraulic code FLUTAN. Experimental results in respect to the distribution of the fluid velocities, fluid temperatures and wall temperatures are presented. Based on the experimental data the essential contribution of thermal radiation to the total heat transfer is illustrated. A comparison is made between the experimental data and code predictions. The deficiencies and needs for further research are being discussed. From the results achieved so far it has been found that the passive containment cooling by natural air convection coupled with thermal radiation is very promising. A medium-scale integral test facility MOCKA is presently under design and will serve to study the integral performance of the passive decay heat removal system proposed and to investigate the coolability limits by natural air convection coupled with thermal radiation under all conceivable boundary conditions.

1. INTRODUCTION

For future advanced water cooled reactors the use of passive safety features should be encouraged and expanded whenever they can provide an adequate level of functional performance. Passive safety systems rely on naturally available sources of motive power, such as natural convection. The use of passive safety features in a nuclear power plant is a desirable method of achieving simplification and increasing the reliability of the performance of essential safety functions, e.g. reactor control and shutdown, core and containment cooling, and retention of fission products. In this way passive systems can also promote an improved public acceptance of nuclear energy [1], [2].

Passive containment cooling by natural air convection has been proposed in the past for several innovative reactor concepts e.g. MHTGR, PRISM, AP-600 [3], [4]. A review of the experimental and analytical studies performed show the need for further experimental and theoretical research work concerning natural air convection and thermal radiation. It became evident that due to the complexity of the thermalhydraulic processes involved in passive systems with their inherent small driving forces by temperature and pressure differences, experiments have to be performed for each specific design. Validated computer codes must be developed to support the expected operational performance. Also, proper attention should be given to system reliability and to possible failure mechanisms which do not arise with active components and systems.

2. CONTAINMENT CONCEPT

The composite containment proposed by the Research Center Karlsruhe and the Technical University Karlsruhe is to cope with beyond-design basis accidents. It pursues the goal to restrict the consequences of severe core meltdown accidents to the reactor plant without any noticeable release of radioactivity impairing the public [5].

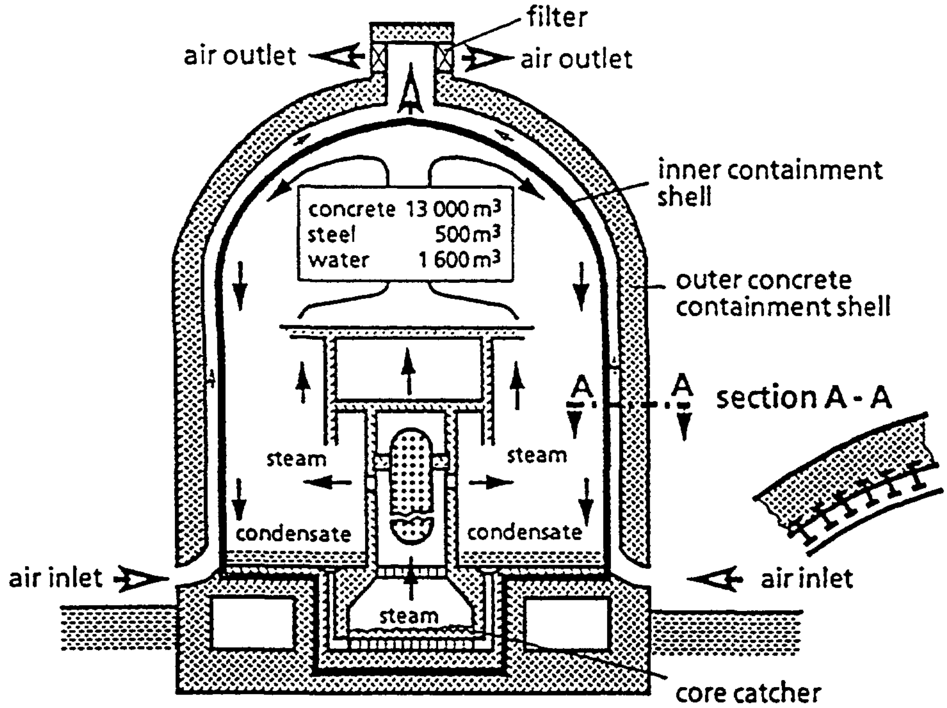

Fig.1 New containment concept with passive decay heat removal

Figure 1 illustrates schematically the composite containment proposed. It consists of an inner steel shell of about 60 m diameter and 38 mm wall thickness and an outer reinforced concrete shell of approx. 2 m wall thickness. The annulus of approx. 80 cm radial gap width is bridged by longitudinal support ribs fixed in the concrete shell. The ribs are placed on the circumference with approx. 50 cm spacing and transfer the load of the expanding and deflecting steel containment to the reinforced concrete wall (composite containment) in a potential hydrogen detonation. With this concept the two individual containment shells of the present design remain essentially unchanged and the capability of withstanding higher loads is achieved by the composite structure which can cope with a maximum static pressure of 1.5

MPa. Such a containment concept has been investigated with respect to its feasibility [6]. The higher costs for this improvement of the containment compared to the present-day design is estimated at approx. 5 % of the overall plant investment costs.

A core catcher is an integral part of this new design proposal. In a core meltdown accident the decay heat is converted into steam by direct contact of the melt with the water. The steam produced condenses on the inner surface of the externally cooled containment shell. By reflux of the condensate to the core catcher a passive self-circulating steam/water flow is established. One essential of this new containment concept is its potential to remove the decay heat by natural air convection in a passive way. The increase in the temperature of the steel shell results in natural convection of air in the individual chimneys formed by the support ribs in the annular gap. Moreover, radiative heat transfer takes place between the steel shell, the support ribs and the concrete shell. Decay heat is thus removed by natural air convection coupled with thermal radiation to the ambient atmosphere in a passive way.

On the basis of containment calculations with the TPCONT code, which was especially developed for the given purpose, it can be assumed that due to the high heat storage capacity of the internal structures of the containment (approx. 13000 m^3 concrete, 500 m^3 steel) the maximum heat flow through the containment wall to the air is reached in a 1300 MWe reactor after about 10 days and amounts to approx. 8 MW [7]. Figure 2 illustrates the heat flow rates in the containment.

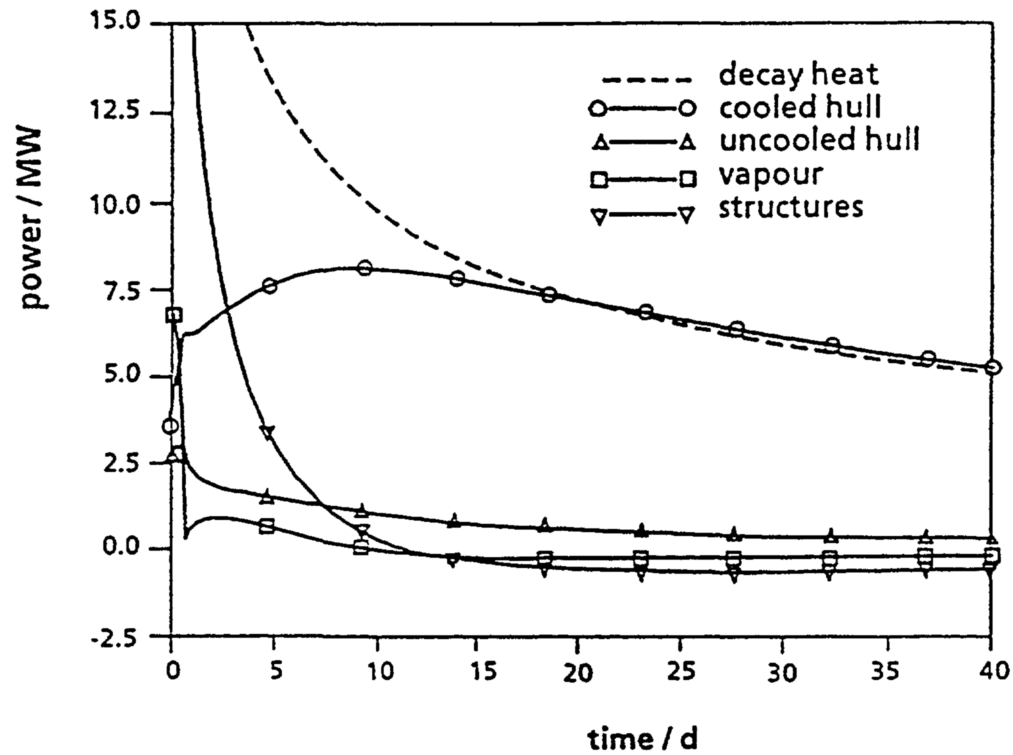

Fig.2 Heat flow rates in the containment

A preliminary analysis of the heat removal capability of the composite containment proposed has been performed using the one-dimensional PASCO computer code [8]. All calculations performed have shown that the contribution of radiant heat transfer to the total heat transfer in the chimneys is considerable. With high emissivities of 0.9 of the walls the heat transferred by radiation equals approximately the amount transferred by convection [9]. Figure 3 illustrates the removable heat as a function of the steel containment temperature for different emissivities of 0.1 and 0.9, respectively. The calculations have been performed for an inlet temperature of 30°C and no filtering of the cooling air. The following dimensions have been assumed: diameter of the steel containment 60 m, height of the steel containment 40 m, depth of the annulus 80 cm, thickness of the steel containment 38 mm, thickness of the support ribs 10 cm, circumferential distance of the support ribs 50 cm. It becomes evident from figure 3 that with an emissivity of 0.9 which corresponds approximately to the technical surfaces involved a decay heat of 8 MW can be removed at a steel containment temperature of approx. 150 °C . With the additional pressure increase due to the non-condensable gases released in a core meltdown accident this corresponds to a maximum containment pressure of about 0 8 MPa. The figure underlines also the significant contribution of the radiant heat transfer which in the past was often neglected in evaluating passive air cooled systems

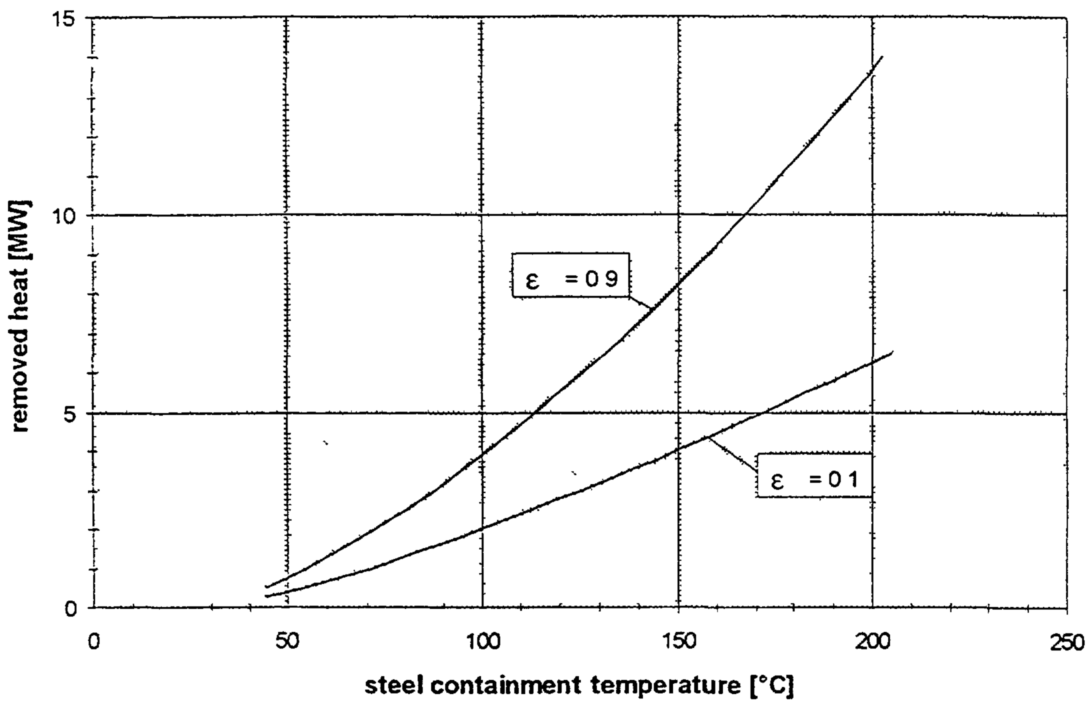

Fig 3 Heat removal with different emissivities ε of the wall

All preliminary evaluations performed show that the composite containment concept with its passive containment cooling by natural air convection is a very promising alternative for future advanced water cooled reactors. However, additional experimental and theoretical research work needs to be done for the given conditions: large channel geometry and strong interaction between convective and radiative heat transfer. To investigate the basic phenomena involved in natural convection coupled with thermal radiation the separate-effects test program PASCO is under way. The MOCKA test facility serves to finally prove the operational performance of the passive cooling system under all conceivable conditions. This integral test facility is presently in the process of a design study.

3. PASCO TEST PROGRAM

The test program PASCO (acronym for passive containment cooling) is presently under way at the Institute of Applied Thermo- and Fluiddynamics (IATF) of the Research Center Karlsruhe (previously Nuclear Research Center Karlsruhe, KfK) The general aim of this separate-effects test program is to investigate passive containment cooling by natural air convection and thermal radiation

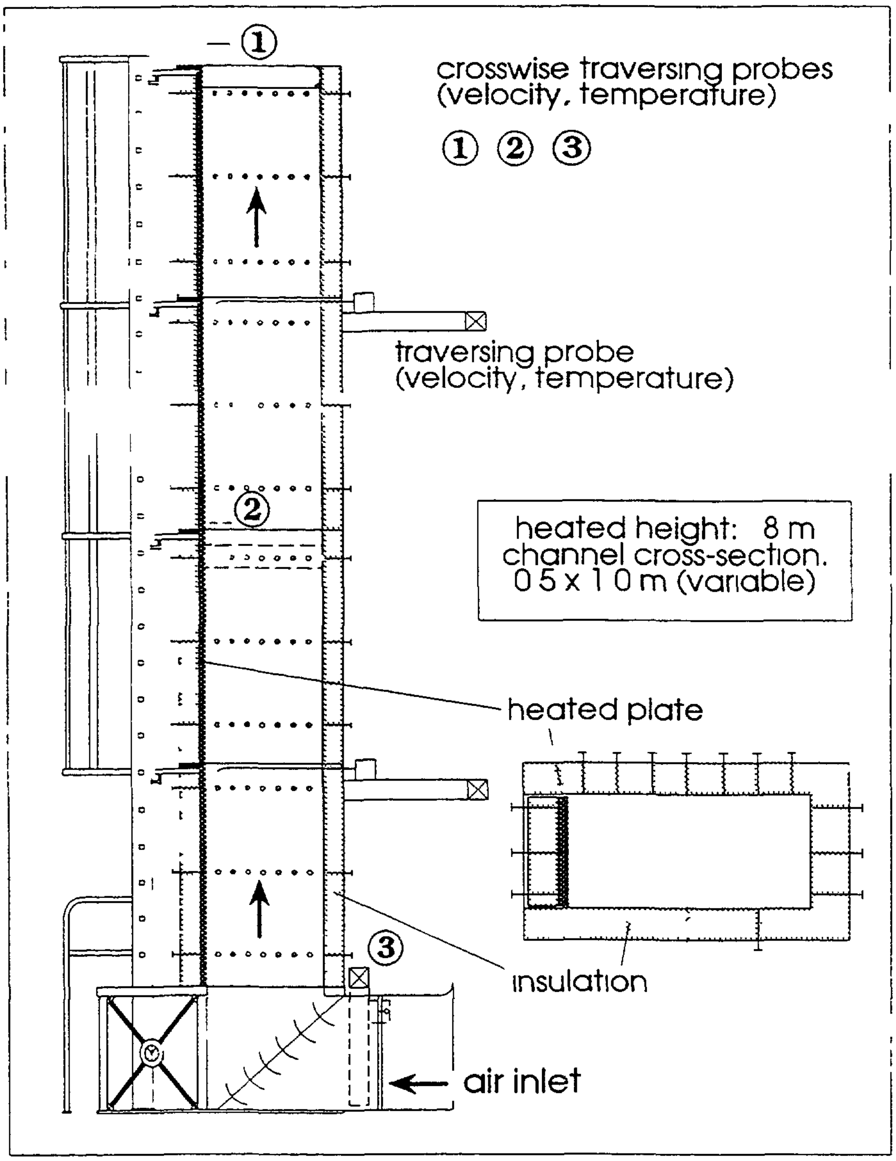

Fig 4 PASCO test facility

The PASCO test facility shown in fig 4 simulates one cooling channel in the annular gap of the composite containment proposed The test section consists of a vertical rectangular channel of which one wall is electrically heated The other three walls are thermally insulated from the ambient surrounding The maximum channel cross-section is 500 mm x 1000 mm, the heated height is 8000 mm with four individually heatable zones By changing the channel depth and the heated height the effect of the channel geometry on heat transfer will be studied The wall emissivity is varied over a wide range, so that the influence of thermal radiation on the total heat transfer can be investigated To study the methods of enhancing the heat transfer, different internal structures (e g inclined repeated fins) will be used Table I summarizes the test matrix

Table I: Test matrix

Heated wall temperature T_h, °C	100 - 175
Wall emissivity ε	0 2 - 0.9
Heated height H, m	2 0 - 8.0
Channel depth L, m	0 25 - 1.0

The test facility is equipped among others with approx 170 thermocouples to measure the distribution of wall temperatures Traversing probes for recording the temperature and velocity of the air are installed at five different elevations Cross-wise traversing probes at the inlet, in the mid-plane and at the outlet measure the temperature- and velocity distributions over each individual channel cross-section Moreover, the pressure at the channel inlet, the air humidity and the heating power are recorded With this comprehensive instrumentation data are generated for the validation and development of multi-dimensional computer codes.

4. EXPERIMENTAL RESULTS

Up to now steady-state experiments have been performed under the following boundary conditions: channel width 500 mm, channel depth 250 - 1000 mm, heated height 8000 mm, wall emissivity 0 9, heated wall temperature 100 - 175 °C

Figure 5 illustrates the wall temperatures measured at the heated plate and the channel walls for the channel cross-section 500 mm x 1000 mm. The boundary conditions of the test (M019) are given in Tab.II. It is evident from the figure that with a nominal temperature of the heated plate of 150 °C the uniformity of temperature can be considered as sufficiently good The temperatures measured at the back wall and the side walls that are heated by radiation underline the great influence of radiative heat transfer

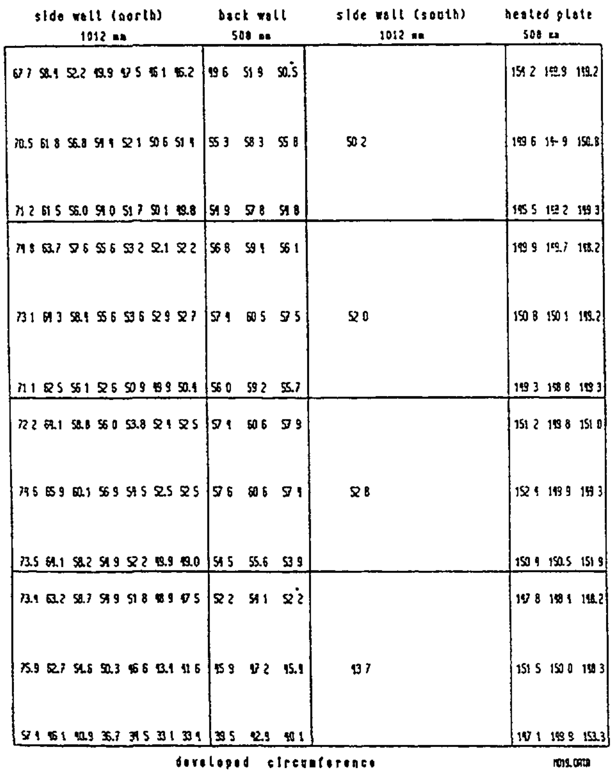

Fig 5 PASCO test results. Wall temperatures (channel cross-section 500mm x 1000mm)

Figure 6 shows the profiles of the air temperature and of the air velocity measured at the test channel outlet for the channel cross-section 500 mm x 1000 mm. The nominal temperature of the heated plate was 150 °C, the emissivity of the channel walls 0.9. It can be clearly seen in which way the profiles are affected by the side and back wall temperatures induced by thermal radiation.

The experimental data generated by the present PASCO tests represent an important data base for the validation and further development of multi-dimensional computer codes, mainly in respect to a proper modeling of the radiative heat transfer and the mixed convection turbulent flow. Such 3D codes (e.g. FLUTAN, TRIO-EF), if verified, will finally be used to evaluate and design the containment cooling system.

channel cross-section: 500 mm x 1000 mm

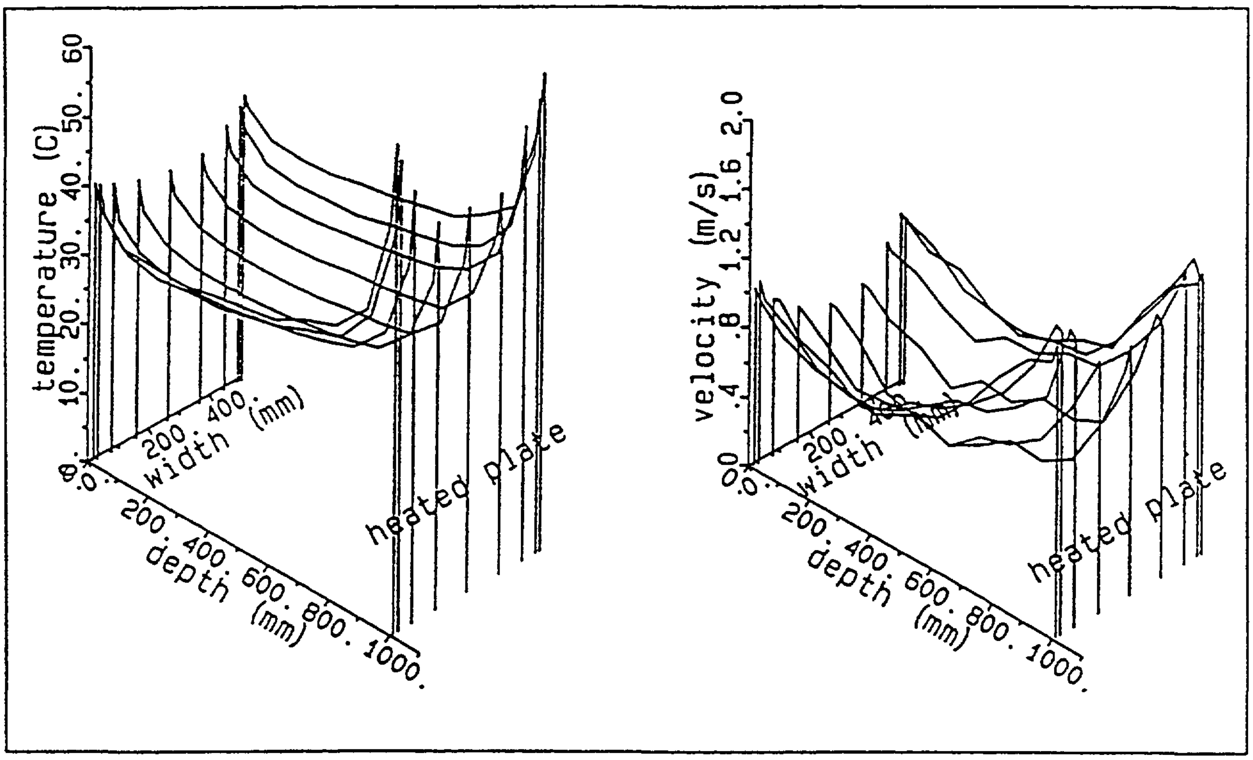

Fig.6: PASCO test results: Temperature and velocity profiles at the channel outlet

5. CODE- / TEST EVALUATION

Calculations are being performed by using the one-dimensional code PASCO and the three-dimensional computer code FLUTAN. The PASCO code has been developed to predict the global thermal-hydraulics of the containment cooling and to assess the experimental data of the PASCO test facility. The more time-consuming code FLUTAN is primarily used for detailed analyses.

5.1 Test evaluation by the PASCO code

The PASCO code [8, 9] is based on the heat balances at the individual walls and the enthalpy- and momentum balances for the air. The heat transfer from the walls to the air takes place by natural convection. Between the individual walls of the chimney radiative heat transfer occurs.

For the convective heat transfer at each wall the following Nusselt-correlation has been used:

$$Nu = C \cdot Ra^{1/3}$$

Here Nu stands for Nusselt number and Ra for Rayleigh number. The coefficient C of the Nusselt-correlation needs to be determined for all individual walls of the chimney by the experiments for the given conditions, i.e. non-symmetrical heated confined channel geometry.

Up to now 16 experiments have been evaluated in order to determine the coefficients C of the Nusselt-correlation for the individual walls. In the experiments four different channel depths were employed, i.e. 250 mm, 500 mm, 750 mm and 1000 mm. For each test four various temperatures of the heated plate were adjusted, i.e. 100 °C, 125 °C, 150 °C and 175 °C. The coefficients evaluated from all these tests resulted in the following C-values: 0.112 for the heated plate, 0.215 for the back wall and 0.160 for the side walls.

Table II summarizes the measured and calculated values for all temperatures investigated and for the channel cross-section 1000 mm x 500 mm. In the experiments flow diverters were installed at the inlet, the emissivity of the walls was 0.9. It is evident that the agreement is rather good for all experiments even when adopting the same coefficients C in the Nusselt-correlation.

Table II: PASCO, comparison between experiment and calculation

	TPI [°C]	Phi [%]	TE [°C]	TU [°C]	TR [°C]	TS [°C]	QPI [kW]	ML [kg/s]
Experiment (MO14)	100.0	58.1	23.31	25.37	41.6	40.3	3.33	0.34
Calculation					42.8	43.5	3.23	0.34
Experiment (MO18)	124.9	42.9	23.56	25.34	47.8	45.9	4.79	0.41
Calculation					49.5	50.6	4.77	0.42
Experiment (MO19)	149.8	42.8	22.36	24.79	54.0	51.1	6.58	0.44
Calculation					56.0	57.5	6.60	0.46
Experiment (MO22)	175.3	45.7	23.01	25.04	62.9	59.5	8.23	0.54
Calculation					64.8	66.6	8.63	0.53

Given conditions of the experiments:

TPI = temperature of the heated plate
Phi = relative humidity of the air
TE = inlet temperature of the air
TU = environment temperature of the air (averaged over the height)

Results:

TR = temperature of the back wall (averaged)
TS = temperature of the side wall (averaged)
QPI= heat removal from the heated plate
ML = mass flow rate of the air

5.2 Test evaluation by the FLUTAN code

The advanced 3D thermal-hydraulic code FLUTAN available at the Research Center Karlsruhe is a finite-difference code for single-phase steady-state and transient analyses of single- and multi-component systems in Cartesian or in cylindric coordinates [10, 11].

In the FLUTAN code of the present version four turbulence models are available, i.e. constant turbulent viscosity model, mixing length model, one equation (k-equation) model and two-equations (k-ε) model. All the models are based on the turbulent diffusivity concept and take a constant value for the turbulent Prandtl-number. For models with transport equations (k-, and k-ε-model) logarithmic wall functions for velocity- and temperature-distribution near the wall are used.

To extend the application of the FLUTAN code to the PASCO test channel, a thermal radiation model has been developed with the following simplications [12]:

- *Air is radiatively nonparticipating.*
- *Wall surfaces are gray and diffuse.*
- *Cartesian coordinate system.*

For flow channels in a Cartesian coordinate system where boundary walls are either parallel or perpendicular to each other, view factors have been derived analytically [12]. In addition the so-called macro-element method is introduced, to reduce storage need and computing time [12].

Figure 7 shows the distribution of air temperature and air velocity along the mid-line at the channel outlet as function of the distance from the heated plate y for the channel cross-section 500 mm x 1000 mm. The temperature of the heated wall is 150 ^{0}C and the wall emissivity is 0.9. The curves are the results calculated with the FLUTAN code and the symbols are the data obtained in the PASCO experiments. The temperature distribution is well reproduced by the FLUTAN code, whereas the FLUTAN code overpredicts the air velocity in the near wall region and underpredicts it in the central region. This discrepancy emphasizes the need of improving turbulence-modeling in the FLUTAN code.

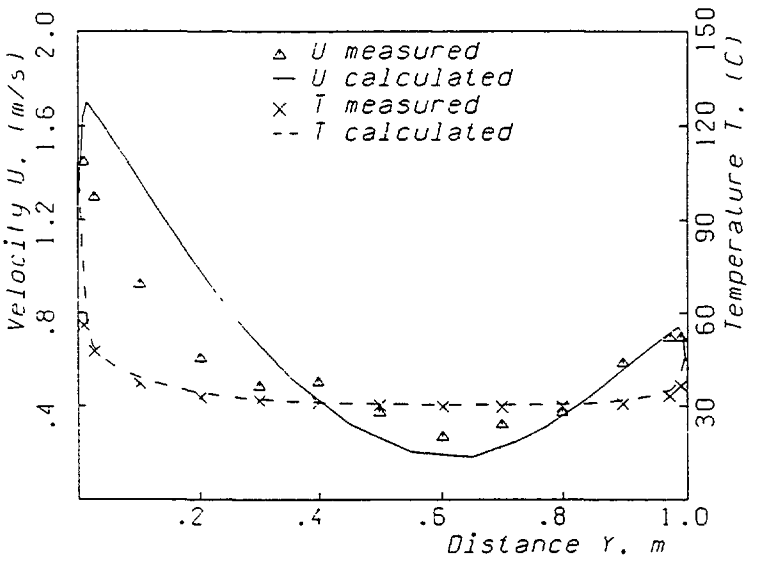

Fig.7: Measured and calculated distribution of air temperature and air velocity at the test channel outlet

Figure 8 shows the temperature distribution on the side wall and on the back wall at the middle elevation for the following conditions: channel cross-section 500 mm x 1000 mm, temperature of the heated wall 150 ^{0}C and wall emissivity 0.9. The curves represent the calculated results and the symbols are the experimental data. A good agreement is found between the experimental and the calculated results. On the side wall the maximum temperature appears close to the heated wall. It decreases rapidly with increasing distance from the heated wall. Towards the corner where the side wall connects the back wall the temperature increases again because of higher temperature of air in this region.

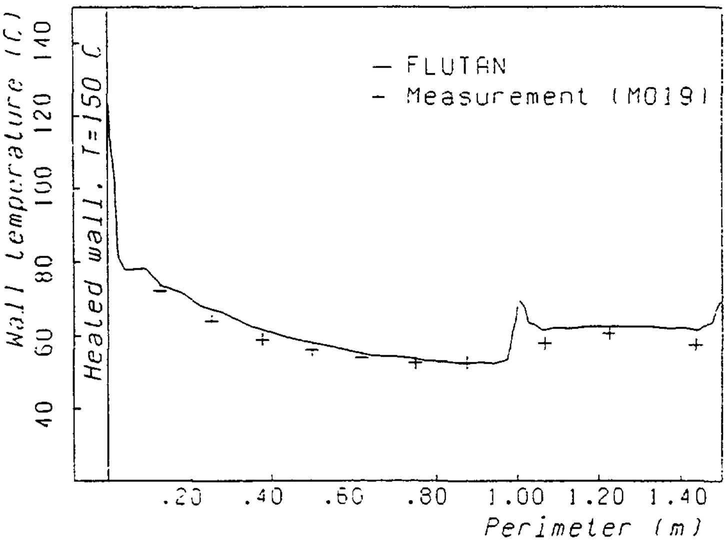

Fig.8: Temperature distribution on the side wall and on the back wall curves: FLUTAN calculation, symbols: PASCO measurements

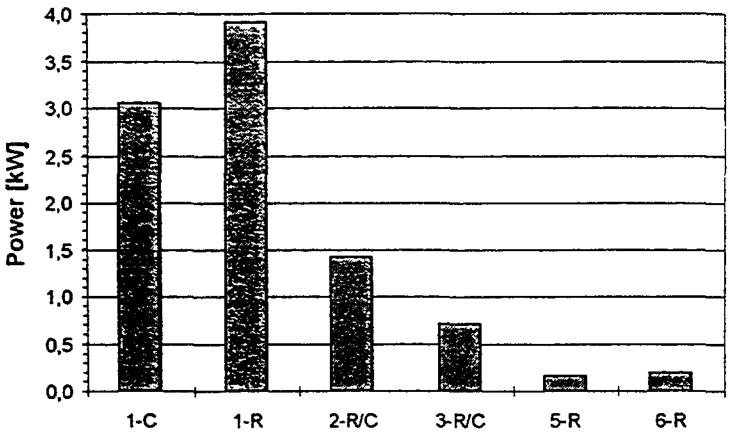

Fig.9: Heat power transferred at different walls and by different heat transfer modes
1 - heated plate, 2 - side wall, 3 - back wall, 5 - inlet, 6 - outlet
C - convection, R - radiation

Figure 9 shows the transferred heat power at different surfaces and by different heat transfer modes under the following conditions: channel cross-section 500 mm x 1000 mm, temperature of the heated wall 150 ^{0}C and wall emissivity 0.9. From the heated wall a heat power of about 3 kW is transferred directly to air by natural convection. About 4 kW heat power is transferred from the heated wall via thermal radiation. The results show a considerable enhancement of total heat transfer due to thermal radiation.

Additional numerical calculations with the FLUTAN code show that a strong influence of thermal radiation on total heat transfer is obtained for the entire range of wall temperature. Even at low temperature of the heated wall, e.g. 100 ^{0}C, the heat power transferred by thermal radiation equals to that transferred by natural convection.

6. FUTURE WORK

Future test series in the PASCO separate-effects program deal mainly with studies using a test channel with low emissivity surfaces and also with different channel insertions to investigate means to enhance the heat transfer Also tests with different heated heights and additional hydraulic resistances are being performed

To finally prove the integral operational performance of the passive decay heat removal system proposed and to investigate its coolability limits under all conceivable boundary conditions a medium-scale integral test facility MOCKA is presently under design Figure 10 illustrates schematically the test facility The main objectives of MOCKA (acronym for Model Containment Karlsruhe) are

- To study local condensation behaviour in different types and different parts of containment
- To examine the influence of non-condensable gases on condensation behaviour
- To investigate the consequences of non-symmetric / local release of steam and gas
- To examine the effects of containment wall structure and internal structures
- To study the effects of water sprays
- To study the effect of cooling channel structure (e g geometry, filter, fins)
- To investigate coolability limits by natural air convection and thermal radiation
- To demonstrate the operational performance under various conditions
- To produce a data base for validation and development of advanced multi-dimensional computer codes for advanced containment designs

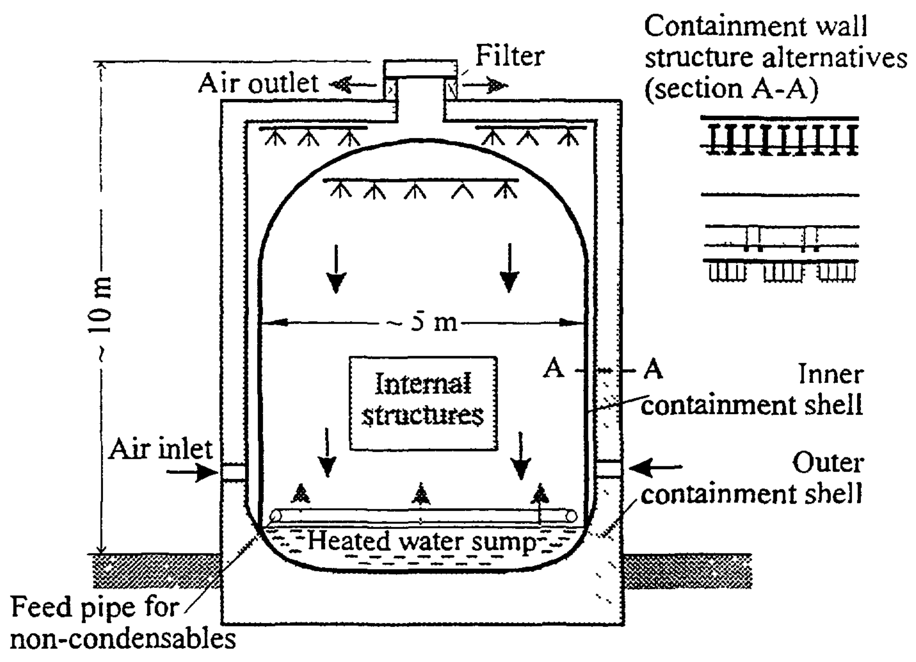

Fig 10 MOCKA test facility

The MOCKA test facility will be designed as a flexible equipment to investigate also containment issues of present-day reactors and the European Pressurized Water Reactor EPR

7. CONCLUSIONS

The present experimental and analytical research work within the PASCO program have shown that passive containment cooling in natural air convection coupled with thermal radiation is a promising concept. The tests performed have generated a broad and detailed data base for the validation and improvement of different computer codes.

The following specific main conclusions can be drawn:

- With high emissivities of the walls the decay heat of a 1300 MWe pressurized water reactor can be removed by natural air convection in a passive way with maximum steel containment temperatures not exceeding 150 °C.
- At intermediate and high wall emissivities thermal radiation contributes significantly to the total heat transfer by natural air convection, even at relatively low temperatures of the heated wall.
- A radiation model has been developed and implemented in the FLUTAN-code.
- The numerical results agree well with the experimental data concerning the distribution of the wall temperatures.
- The prediction of the velocity- and temperature profiles of the air within the cooling channel emphasizes the need of improving the turbulence modeling in natural air convection.
- Additional larger scale integral experiments in the MOCKA test facility must prove the containment coolability under all conceivable conditions.

ACKNOWLEDGMENTS

This work is partially supported by the "Bundesministerium für Bildung, Wissenschaft, Forschung und Technologie" under the Project Grant 15NU 0961.
The authors greatly acknowledge the contributions of W. Just, H. Schmidt and E. Arbogast in preparing and performing the experiments.

REFERENCES

[1] INTERNATIONAL ATOMIC ENERGY AGENCY, The Safety of Nuclear Power: Strategy for the Future, Proceedings of a IAEA-Conference, Vienna, September 2 - 6, 1991

[2] INTERNATIONAL ATOMIC ENERGY AGENCY, The Safety of Nuclear Power, INSAG-5; A report by the International Nuclear Safety Advisory Group, IAEA, Vienna, 1992

[3] PEDERSEN, D.R., et al., "Experimental and Analytical Studies of Passive Shutdown Heat Removal from Advanced LMRs", International Topical Meeting on Safety of Next Generation Power Reactors, Seattle, USA, 1992

[4] KENNEDY, M.D., et al., "Advanced PWR Passive Containment Cooling System Testing", International Topical Meeting on Advanced Reactors Safety, Pittsburgh, Pennsylvania, USA, April 17-21, 1994

[5] HENNIES, H.H., KESSLER, G., EIBL, J., "Improved Containment Concept for Future Pressurized Water Reactors", International Workshop on Safety of Nuclear Installations of the Next Generation and Beyond, Chicago, IL, USA, August 28-31, 1989

[6] EIBL, J., "Zur bautechnischen Machbarkeit eines alternativen Containments für Druckwasserreaktoren -Stufe 3-", KfK 5366, August 1994

[7] SCHOLTYSSEK, W., ALSMEYER, H., ERBACHER, F.J., "Decay Heat Removal after a PWR Core Meltdown Accident", International Conference on Design and Safety of Advanced Nuclear Power Plants (ANP 92), Tokyo, Japan, October 25-29, 1992

[8] NEITZEL, H.J., "Abschätzung der Wärmeabfuhr durch Naturkonvektion bei einem alternativen Containmentkonzept", KfK 5005, Juni 1992

[9] ERBACHER, F.J., NEITZEL, H.J., "Passive Containment Cooling by Natural Air Convection for Next Generation Light Water Reactors", NURETH-5, Salt Lake City, Utah, USA, September 21-24, 1992

[10] SHAH, V.L., et al., "COMMIX-1B: A Three-Dimensional Transient Single-Phase Computer Program for Thermal Hydraulic Analysis of Single and Multicomponent Systems", NUREG/CR-4348 Vol.1 and Vol.2, 1985

[11] BORGWALDT, H.A., "CRESOR, A Robust Vectorized Poisson Solver Implemented in the COMMIX-2(V)", Proc. of the Int. Conference on Supercomputing in Nuclear Applications, Mito City, Japan, pp.346-351, 1990

[12] CHENG, X., ERBACHER, F.J., NEITZEL, H.J., "Thermal Radiation in a Passive Containment Cooling System by Natural Air Convection", International Symposium on Radiative Heat Transfer, Kusadasi, Turkey, August 14-18, 1995

SPES-2, AP600 INTEGRAL SYSTEMS TEST RESULTS

L.E. CONWAY, R. HUNDAL
Westinghouse Electric Corporation,
Pittsburgh, Pennsylvania, USA

Abstract

The SPES-2 test program was performed to obtain data to validate safety analysis computer codes used to analyze the performance of the Westinghouse AP600 reactor and passive safety system designs. The test matrix included nine simulated loss-of-coolant-accidents (LOCAs) and four non-LOCA transients. The nine LOCAs were performed at three different break locations; and at each location, two different break sizes were simulated. The simulated breaks ranged from a 1-in. diameter break, up to the double-ended break of an 8-in. pipe. Non-LOCA tests included three steam generator tube ruptures (SGTRs) and a large steam line break (SLB). In all tests, the passive safety systems performed as expected and mitigated the simulated accidents with no heatup of the reactor heater rods. Test results, test-to-test comparisons, and passive safety system performance are discussed.

INTRODUCTION

SPES-2 is a full-height, full-pressure integral systems test of the Westinghouse AP600 reactor design. The SPES-2 test was performed as part of the Advanced Light Water Reactor (ALWR) program sponsored by the U.S. Department of Energy (DOE) and the Electric Power Research Institute (EPRI). Westinghouse, in cooperation with SIET (Società Informazioni Esperienze Termoidrauliche), ENEL (Ente Nazionale per l'Energia Elettrica), ENEA (Ente per le Nuove Technologie, l'Energia e l'ambiente), and Sopren-Ansaldo, performed the SPES-2 tests to obtain data on the integrated behavior and performance of the AP600 passive safety systems to validate the computer codes used to perform the licensing safety analyses for the AP600.

The AP600 is a 600 MWe reactor designed to increase plant safety. It has accident mitigation features that, once actuated, depend only on natural forces such as gravity and natural circulation to perform all required safety functions. These "passive" safety features can also significantly simplify plant systems, equipment, and operation.

The AP600 primary system is a two-loop design. Each loop has one hot leg, two cold legs, and one steam generator with two canned reactor coolant pumps (RCPs) attached directly to the steam generator outlet channel head. The passive safety systems, shown in Figure 1, are comprised of the following:

- Two core makeup tanks (CMTs) that can provide borated makeup water to the primary system by gravity at any pressure.
- Two accumulators that provide borated water to the reactor vessel when/if primary pressure $\leq$ 700 psia.
- A passive residual heat removal (PRHR) heat exchanger (HX), comprised of a C-shaped tube bundle submerged inside the in-containment refueling water stor-age tank (IRWST), that can remove heat from the primary system by natural circulation at any pressure.
- The automatic depressurization system (ADS), which is comprised of a set of valves connected to the pressurizer steam space and the two hot legs. These valves are opened sequentially to provide a controlled depressurization of the primary system, if the CMT water level significantly decreases.
- An IRWST that provides a large source of core cooling water, which drains by gravity after the ADS has actuated.
- A passive containment cooling system (PCS) that utilizes the AP600 steel containment shell to transfer heat to the environment (ultimate heat sink) by natural circulation of air and water evaporation. The PCS was not included in the SPES-2 experiments.

The SPES-2 test facility was designed to model the AP600 at full-scale elevation and full pressure, simulating the full AP600 plant range of power with a volume scaling factor of 1/395. Portions of the reactor vessel, all main coolant loop piping and passive safety systems have been expressly designed and constructed for SPES-2 to model the AP600 plant.

SPES-2 Test Matrix

The SPES-2 test matrix examines the performance/capability of the AP600 passive safety systems in mitigating the effects of postulated DBEs, and provide useful data for computer code development and validation. The initial and boundary test conditions challenge the passive safety systems, provide direct comparisons between selected tests, and/or match the limiting assumptions used in safety analysis computer codes including the worst single failure. The resulting test matrix is discussed below.

Loss of Coolant Accidents

The passive safety systems are required to provide sufficient water for LOCA mitigation over a long period of time; thus CMT draindown, ADS actuation, accumulator delivery, and primary system depressurization to IRWST delivery all occur. Therefore, eight different LOCA simulations varying in size and location were tested to observe the integrated operation of the passive system over a wide range of conditions. All LOCA tests, with one exception, were performed without operation of the active, nonsafety pumped injection/heat removal. All tests were initiated from full-power operating conditions and used the minimum Standard Safety Analysis Report (SSAR) pressure setpoints for reactor trip and safety system actuations.

Test 1 (S00401). A 1-in. diameter break simulation was selected as the smallest LOCA. This was based on analyses that showed that complete heatup of the CMT water occurred prior to ADS actuation, so that any effect of CMT water flashing during depressurization could be observed.

Test 3 (S00303). A 2-in. diameter break simulation in the bottom of a cold-leg loop pipe (containing a CMT balance line) was performed as the base case LOCA to which other LOCAs would be compared.

This 2-in. diameter, base case break simulation was repeated at the end of the test program and demonstrated the repeatability of the SPES-2 facility operation and passive safety system performance (S01703).

Test 4 (S00504). The 2-in. LOCA simulation with operation of the active, nonsafety systems was performed to observe the interaction of the passive safety and nonsafety systems compared with the base case 2-in. LOCA (Test 3).

Tests 5 & 7 (S00605 & S01007). A 2-in. break simulation in the DVI line and in the cold-leg to the CMT balance line were performed to observe the effect of break location on the passive safety system mitigation capability as compared to the base case 2-in. LOCA (Test 3).

Test 6 (S00706). A DEG break simulation of one of two DVI lines was performed to minimize the amount of safety injection flow delivered to the reactor vessel (only one of two CMTs, accumulators, and IRWST injection lines deliver). This was the largest break that could be reasonably simulated in the SPES-2 facility.

Test 8 (S00908). A DEG break simulation of one 8-in. cold-leg to CMT balance line was performed to observe the effect on the faulted CMT and provide a comparison LOCA with the DEG DVI LOCA.

Test 13 (S01613). The 1-in. diameter break simulation (Test 1) was repeated with the number of PRHR HX tubes increased from one to three tubes to maximize the primary system cooling and better simulate two PRHR HXs in operation in the AP600 plant.

Steam Generator Tube Ruptures

The mitigation of an SGTR consists of reducing the pressure of the primary system to be equal to or less than the faulted steam generator pressure to terminate primary to secondary flow and to prevent overfill of the faulted generator. At the same time, heat removal from the primary system must be provided to remove core decay heat and keep the primary pressure less than secondary pressure. In current PWR designs, recovery from an SGTR requires operator actions to identify and isolate the faulted generator, establish primary system heat removal using the intact steam generator, and manually depressurize the primary system. Three SGTRs were performed at SPES-2. All these tests modeled a full rupture of a single steam generator tube. All were initiated from full-power operating conditions and used low-low pressurizer level to initiate reactor trip and safety system actuations.

Test 9 (S01309). An SGTR with operator action and nonsafety systems operating was performed to observe the combined effect of manual SGTR recovery actions (used in current plants) and passive system operation.

Test 10 (S01110). An SGTR without operator actions and without operation of active, nonsafety, pumped injection/heat removal was simulated to observe the capability of the passive systems to terminate the event without intervention.

Test 11 (S01211). An SGTR without operator actions or nonsafety system operation but with the inadvertent actuation of the ADS was performed to observe the effect of backflow from the faulted steam generator on ADS depressurization capability and to obtain data for determining primary system boron concentration versus time.

Steam Line Break

This test simulated a large single-ended SLB. It provided a rapid primary system cooldown transient and demonstrated the ability of the CMT to provide primary system mass addition without requiring ADS actuation.

Test 12 (S01512). This test was performed at AP600 hot, zero power conditions, and no core decay heat was used. This test was performed with three PRHR HX tubes to maximize primary system cooling and better simulate two PRHR HXs operating in the AP600. The break size was scaled to simulate a 1.388 ft^2 AP600 break area (full steam generator outlet area) and was performed with no operator actions or active, nonsafety system operation.

Note: Tests 8, 11 and 12 have been designated as blind tests. The SPES-2 facility responses for the tests will be compared to analysis predictions without prior knowledge of actual test results, therefore, these test results cannot be discussed at the present time.

SPES-2 TEST RESULTS (BLIND TESTS RESULTS EXCLUDED)

The passive safety systems mitigated consequences of the design basis events tested in an orderly and predictable manner. Therefore, LOCA tests followed the same sequence of primary and passive safety system responses. For example, as shown in Figure 2, in Matrix Test 3 (Test Run S00303) primary system pressure decreases rapidly when the break occurs and results in reactor trip and safety system actuation. Primary pressure is stabilized by flashing when pressure decreases to the saturation pressure corresponding to the temperature of the water in the rod bundle region, upper plenum, and hot legs. The CMTs and PRHR HX begin operation and after RCP trip they operate by natural circulation. Primary pressure slowly decreases as water is lost through the break with the PRHR HX and CMTs removing heat. When the cold legs begin to drain, the CMTs transition from their natural circulation mode of operation to a draindown mode, greatly increasing their net injection rate and effective cooling; increasing the rate of primary system pressure decrease. The draining CMTs result in ADS Stage 1, 2, and 3 actuation, which rapidly decreases primary pressure and results in accumulator delivery. When the accumulator injection has been completed, the CMTs continue to drain which results in actuation of ADS Stage 4. ADS Stage 4 completes depressurization of the primary system below the elevation head of the water in the IRWST, and injection flow from the IRWST begins. The IRWST flow subcools and refills the primary system to the ADS Stage 4 elevation.

Figure 3 illustrates the net change in primary system (PZR not included) water inventory during the course of Matrix Test 3. After break initiation, primary system inventory steadily decreases due to mass loss through the break. When the primary system inventory loss reaches ~400 lbs in SPES-2, the cold legs begin to drain causing the CMTs to transition to draindown operation, and the rate of inventory decrease lessens. In fact, the CMTs draindown injection rate is sufficient to almost match break flow. When the CMT has partially drained, ADS Stage 1 is actuated and is shortly followed by Stage 2 and 3 actuation. After ADS actuation, the accumulators provide injection at a high flow rate, offsetting water lost into the PZR and out through ADS Stages 1, 2 and 3, and primary system inventory is restored. When accumulator delivery is completed, the CMTs continue to drain, but primary inventory steadily decreases until CMT low level actuates ADS Stage 4 and IRWST injection begins. IRWST injection steadily increased the primary system water inventory until the SPES-2 power channel was completely refilled.

Figure 4 illustrates the collapsed liquid level in the heated portion of the rod bundle and in the lower portion of the upper head just above the heated rods, during the course of Matrix Test 3. The rod bundle region collapsed level measurement shows that two periods of high steam fraction occur in the rod bundle. The first period occurs during the early portion of the transient and is due to flashing of the water in the rod bundle resulting from decay heat and the rate at which primary pressure is decreasing. The steam fraction reached ~45 percent at the time the CMTs begin draindown. The increase in CMT net injection flow rate causes the stream fraction to decrease and subsequent accumulator injection rapidly refills the rod bundle region with subcooled water. The second period of high steam fraction occurs after accumulator injection, when the steam fraction of the water/steam mixture in the rod bundle steadily increases to 25 percent until IRWST injection begins. IRWST injection refills the rod bundle with subcooled water. The collapsed liquid level measurement in the region above the heated rods provides a good indication of the steam/water fraction of the fluid exiting the top of the rod bundle. This parameter indicates that the two phase fluid cooling the rod bundle, reaches a maximum steam fraction of ~50 percent just prior to IRWST injection.

Comparison of LOCA Test Results

Figure 5 shows the rod bundle region fluid steam fraction estimated from collapsed liquid level. This occurs just prior to CMT draindown—ADS—accumulator delivery, for all the LOCA tests. The fluid steam fraction is plotted vs. the rate of primary system pressure decrease. The steam fraction is directly related to the rate of depressurization, indicating that flashing is a major contributor to the two-phase fluid steam fraction in the rod bundle at this time, in addition to boiling. Since the primary system inventory is the same for most tests when the CMTs begin to drain, the flow to the rod bundle, as dictated by the water elevation on the cold-leg side of the power channel, are also similar and the rod bundle fluid steam fraction is break size dependent.

Figure 6 shows the relationship between steam fractions in and above the rod bundle with the minimum downcomer level just prior to the IRWST injection. Figure 6 shows that the high rod bundle fluid steam fraction, occurring prior to IRWST injection, corresponds to the downcomer water level at that time. This water level results from the primary system water inventory at the end of the accumulator delivery, and the net fluid losses during the subsequent time delay until ADS-4 actuation. This time delay is relatively fixed by the CMT draindown rate. Note that the downcomer water level is below the elevation of the top of the rod bundle for many events; however, the rod bundle remains fully covered with a two-phase mixture due to its lower density.

Comparison of LOCA Locations

The effect of break location can be examined by comparing Baseline Test S00303 with Tests S00605 and S01007.

These tests demonstrate two important characteristics of break location: the elevation of the break and the affected line. The break elevation affects the amount of coolant lost through the break, while the line in which the break occurs can directly affect the CMT performance.

In all three tests, primary fluid at the break is initially single-phase water and, therefore, the break flow is initially at a high mass flow rate. When the primary system water level drains to the break elevation, the fluid at the break converts to two-phase fluid or steam and break mass flow rate decreases. The DVI line break is at the lowest elevation in the primary system, and the break flow continues to be high until the primary system fluid level decreases into the annular downcomer and reaches the DVI nozzle elevation. As seen in Figure 7, more water is lost from the primary system before the break flow converts to two-phase fluid for the DVI line break than for the two other breaks. Similarly, more water is lost in Test S00303 than in Test S01007, since the break for S01007 is effectively from the top of the cold leg.

Figure 7 shows a decrease in the slope of the S01007 breakline catch tank curve first, when water level in the primary system has decreased to the top of the cold-leg. This change in slope indicates the conversion of breakflow from single-phase water (from a full cold-leg pipe) to two-phase fluid. In Test S00303 the decrease in break flow occurs later. In Test S00605 no change in break flow is indicated until after ADS actuation.

Since the break flows for all three breaks are initially similar, the water level decreases to the top of the loop-B cold legs at similar times for all three tests. This is important for CMT draindown initiation.

In all three tests, CMT transition to the draindown operating mode began at similar times. In the DVI line break test, CMT-A and -B transitioned simultaneously. In the Cold Leg Break Test, the cold leg with the break (CL-B2) drained prior to the intact cold leg; since CMT-B connected to B2 transitioned slightly earlier than CMT-A. In the balance line break test, CMT-A transitioned at approximately the same time as the other tests; however, both CMT-B recirculation and draindown modes of operation were affected. Natural circulation was initially suppressed by the dP caused by the single-phase flow from the cold leg to the break. When two-phase flow to the break started, some flow to the top of CMT-B occurred where the steam was condensed by the cold CMT water. This resulted in wide variations in CMT flow until full transition to draindown operation occurred after ADS actuation.

In all three tests, ADS initiation occurred at similar times, since the transition to draindown for at least one of the two CMTs occurred at similar times in all tests.

Figure 5 shows the rod bundle steam fraction just prior to accumulator injection is higher for the DVI line break than for the cold-leg and balance-line breaks (Tests S00605, S00303, and S01007, respectively). This indicates that flow through the rod bundle and the fluid inventory is lowest for S00605 (DVI line), and highest for S01007 (balance line). Also the downcomer level for S00605 rapidly decreases to the DVI nozzle level before accumulator injection starts while the annular downcomer is full for S00303 and S01007 prior to accumulator injection.

Prior to IRWST injection the rod bundle steam fractions for Test S00303 (cold leg break) and Test S01007 (balance line break) are very similar, as are the minimum downcomer levels. In test S00605 (DVI line break) the rod bundle fluid steam fraction, and minimum level in the tubular downcomer is lowest (Figure 6). Lower water inventory in Test S00605 is due in part to the fact that there is less downcomer and power channel water inventory after accumulator injection than in S00303 and S01007. During the accumulator injection for the cold leg and the balance-line breaks, the rod bundle is subcooled and completely refilled, as seen in the increasing collapsed level for the rod bundle shown in Figure 4. However for the DVI line break, the collapsed level in the rod bundle indicates two-phase flow still exists at the end of accumulator injection.

In summary, break location had a significant impact on the simulated 2-in. LOCAs. Break elevation affected the amount of reactor coolant loss through the break, which significantly influences the power channel coolant inventory prior to start of IRWST injection. Also, a 2-in. break in the cold leg to CMT balance line will initially prevent CMT recirculation and delay transition to draindown of the affected CMT. However, this did not greatly affect overall coolant inventory or the ADS-4 timing since it is actuated by the level of the unaffected CMT.

Comparison of LOCA Sizes

The SPES-2 LOCA tests included four break sizes: 1-in., 2-in., and two DEGs. The 2-in. and DEG breaks were performed at two or more break locations.

The effect of break size can be comparing the baseline test S00303 (2-in. LOCA in the bottom of CLB-2) with test S00401 (1-in. LOCA in the bottom of the CLB-2).

Figure 8 shows the coolant inventory for the primary system (except pressurizer) during Test S00303 and Test S00401. For the 2-in. break, the coolant inventory rapidly decreases to the ~400 lbm level (corresponding to the elevation of the top of the cold-leg) and CMT draindown mode is initiated. Since the CMT draindown flow rate is less than the break flow rate, the CMT draindown is uninterrupted and ADS-1 is actuated. The primary system pressure decreased to just below the accumulator gas pressure when ADS-1 actuated, so there was very little injection from the accumulators. When ADS-1 occurred, essentially all of the accumulator water inventory was still available for refilling the power channel.

Test S00401, the 1-in. break, is four times smaller than the 2-in. break, and therefore, the inventory decreased at a slower rate. When the cold legs finally began to void, causing the CMT balance lines to drain, the CMTs started a period of intermittent short draindowns followed by refill and natural circulation, which increased their overall injection rate sufficiently to keep the water level in the cold leg. In fact, the CMT draindown injection capability at this time, exceeds the break flow. The intermittent CMT draindown and refill extended the time for draindown and delayed ADS-1 actuation. Primary system pressure had decreased below the accumulator gas pressure and the accumulators injected ~25 percent of their water inventory prior to ADS-1. Therefore, the coolant inventory after accumulator injection just prior to IRWST injection is less for the 1-in. break than the 2-in. break and resulted from the expenditure of accumulator inventory prior to ADS-1; so less water was available for injection between ADS-1 and ADS-4. The lower inventory is also reflected in the higher rod bundle steam fraction prior to IRWST injection for the 1-in. break, as compared to the 2-in. break.

Test S00706 (DEG of the DVI-B line) is very different from the 1-in. and 2-in. breaks.

In Test S00706, there is a complete loss of injection from CMT-B, accumulator-B, and one of two IRWST injection lines. This, in addition to the high break flow, results in a very low minimum coolant inventory. The minimum coolant inventory in the power channel still provided adequate cooling although the two-phase fluid flow in the rod bundle had a much higher steam fraction. Figure 9 shows the difference between the temperature of Heater Rod 87 at the highest elevation in the bundle (TW020P87) and the saturation temperature corresponding to primary system pressure for S00706 and S00303. The Test S00706 rod temperature followed the saturation pressure as in the Reference Test S00303, despite the higher void fraction in the rod bundle.

Effects of Nonsafety Systems

The effect of nonsafety systems operation on the passive safety system response and overall plant response can be assessed by comparing Baseline Test S00303 with Test S00504. S00504 is a 2-in. break in the bottom of cold leg B-2, with the CVCS and NRHR pumped injection and SFWS addition to the steam generators simulated. The CVCS injection started on the safety systems actuation (S) signal, and the NRHR started to inject coolant after ADS-3 when the primary system pressure was reduced to less than the NRHR pump discharge pressure.

Test S00504 is very similar to S00303 until ADS-1 was actuated. The reactor trip (R) and the S signals occurred at nearly identical times, and the pressure decrease vs. time were similar. The rod bundle steam fraction prior to ADS were very similar for the two tests. The CVCS injection did not have significant impact on the initial part of the test since break flow greatly exceeds the maximum possible flow from two CVCS pumps. The NRHR flows started when primary pressure was ~160 psia and had a significant effect on the test. The CMTs' draindown stopped when the NRHR flow started due to the backpressure NRHR flow imposes on the CMT discharge line. ADS-4 never occurred since CMT draindown stopped before reaching the ADS-4 trip level.

Figure 10 shows the coolant inventory for Tests S00504 and S00303. The CVCS injection helped to maintain coolant inventory during the first part of Test S00504 until ADS-1 occurred. The inventory losses after accumulator delivery are similar for the two events until the NRHR injection matched the primary system inventory loss out the break, then the primary system started to refill. The minimum inventory for Test S00504 was higher than in Test S00303 since refill was not delayed until ADS-4 and IRWST injection.

Comparison of PRHR Performance

The effect of additional PRHR capability on the LOCA mitigation can be assessed by comparing Test S00401 (performed with one PRHR tube) with Test S01613 (performed with 3 PRHR tubes). Both of these tests are 1-in. breaks in the bottom of cold leg-B2.

The PRHR performance measured for Test S01613 was slightly higher than for S00401, and showed that the 200 percent increase in heat transfer area for the PRHR HX yielded some additional heat transfer. The PRHR flow is slightly higher for S01613; however, the biggest difference is that the PRHR HX exit temperature was lower for S01613 than for S00401.

Figure 11 shows the coolant inventory for Tests S00401 and S01613. Both tests spend an extended time period at the -400 lbm inventory level. In S01613, the CMTs expended less inventory maintaining the coolant inventory, due to extra PRHR HX return flow and additional injection from the accumulators caused by the lower system pressure. ADS-1 was therefore delayed for S01613 relative to S00401. When ADS occurred, less fluid was discharged through ADS due to the lower initial system pressure at the start of ADS. Therefore, S01613 had more coolant inventory than S00401 after the accumulator delivery. The net coolant losses from the end of accumulator delivery until the start of IRWST injection were very similar for the two events. However, since S01613 started this period with more coolant inventory, it also ended with more inventory than S00401, at the point of minimum coolant inventory in the vessel.

The greater PRHR heat removal in S01613 increased the primary system pressure decrease relative to S00401 prior to ADS-1. The overall effect of the lower system pressure mitigated the severity of the test.

Comparison of Steam Generator Tube Rupture

Two steam generator tube rupture events were performed (S01110: SGTR without nonsafety systems and S01309: SGTR with nonsafety systems and operator actions). There were significant differences between the two tests and these are attributable to the effects of nonsafety systems operating for S01309. Specifically the use of the SFW system and the steam generator-A PORV to maintain the primary system cooldown rate provided sufficient heat removal to maintain single-phase flow conditions in the primary system. Also, two of the six pressurizer external heaters were operated in S01309.

In Test S01110, the primary to secondary flow through the SGTR was quickly terminated with no operator action, as shown in Figure 11.

Figure 12 shows primary system pressure for the two tests. The S01309 pressure is lower than S01110 due to the additional cooling provided by CVCS injection, SFWS addition, and steam generator-A PORV actuation. The primary system pressure was actually higher than steam generator-A pressure throughout the test for S01309. The steam generator-A provided heat removal from the primary system to maintain the primary system at single phase flow conditions. The dP measured in the steam generator-A U-tubes, showed that primary system natural circulation flow was maintained through steam generator-A.

Figure 13 compares the rod bundle differential pressure for the two transients, showing that two-phase flow conditions eventually occurred in the primary system in Test S01110, while S01309 maintained single phase flow through the core until test termination.

Figure 14 shows pressurizer levels differed greatly between the two tests. In S01110 the pressurizer refills completely. In S01309, the pressurizer only partially refilled in response to venting through the ADS-1 flow path by operator action, and a low level was maintained for the rest of the test. Measured temperatures in the pressurizer in S01110 indicated that the pressurizer was subcooled, at which time the pressurizer completely filled. In S01309, the top of the pressurizer remained superheated throughout the test, so it never refilled completely. This occurred because two pressurizer external heaters were kept on. In Test S01110, the heat losses were sufficient to reduce pressurizer pressure and temperature. In both of these tests the ADS was not actuated since the CMTs remained in their natural recirculation mode throughout the test.

These tests demonstrate that the primary-to-secondary flow due to the SGTR can be terminated by the passive safety systems with no operator actions, or by the operators using the non-safety systems in a manner similar to current PWRs.

Conclusions/Observations

1. The passive safety systems mitigated the consequences of the design basis events tested in an orderly and predictable manner.

2. The passive safety systems were able to prevent dryout or heater rod temperature increase for all LOCA's up to and including a DEG of an 8-in.. DVI line.

3. Stable long term cooling of the rod bundle was established by IRWST water injection, through the rod bundle and out through the ADS Stage 4 flowpaths.

4. Following a single, double-ended SGTR, the passive systems provided primary system boration and heat removal, and terminated primary- to secondary-side leakage with no operator action, no operation of non-safety systems, and no actuation of non-safety systems, and no actuation of ADS.

5. Non-safety system operation improved overall performance.

REFERENCES

1. SPES-2 Test Final Data Report, WCAP-14309, Rev. 0, March 1995.

2. SPES-2 Facility Description, WCAP-14073, Rev. 0, May 1994 (SIET Document 00183R192, Rev. 0, April 1994).

3. AP600 Standard Safety Analyses Report, AP600 Doc. GWGL021, Rev. 2, March 1995.

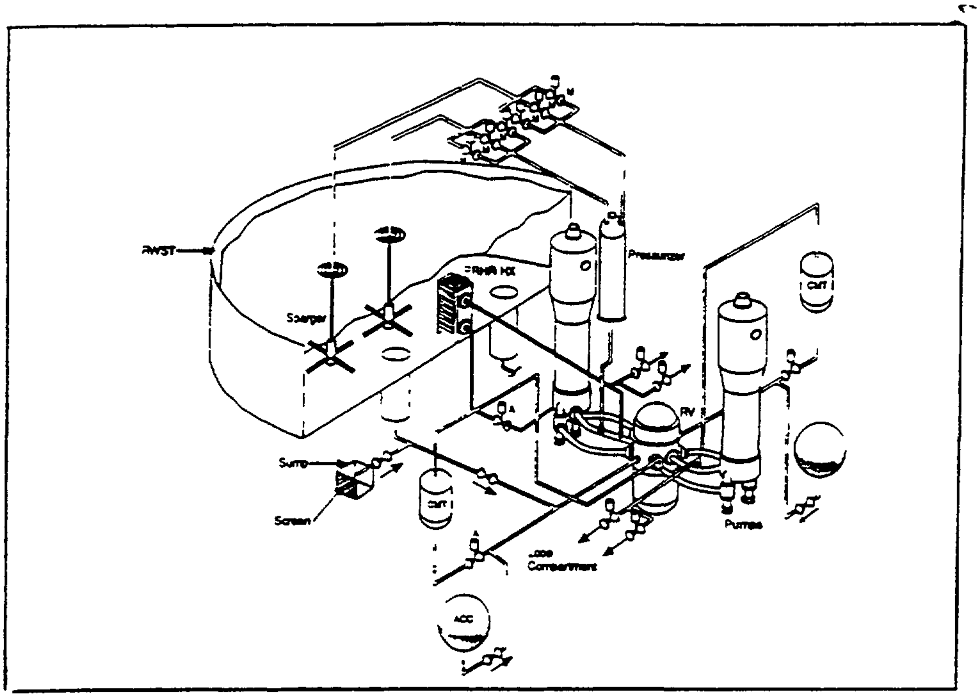

FIG. 1. *AP600 passive safety systems configuration*

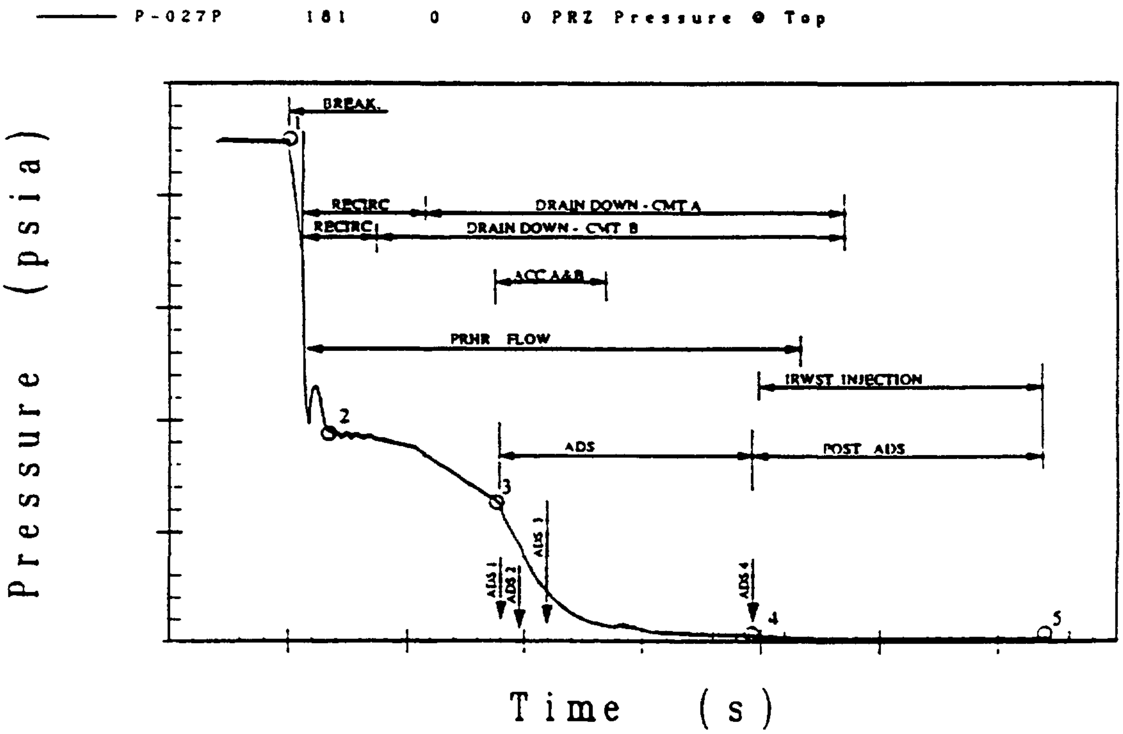

FIG. 2. *Facility response summary for S00303*

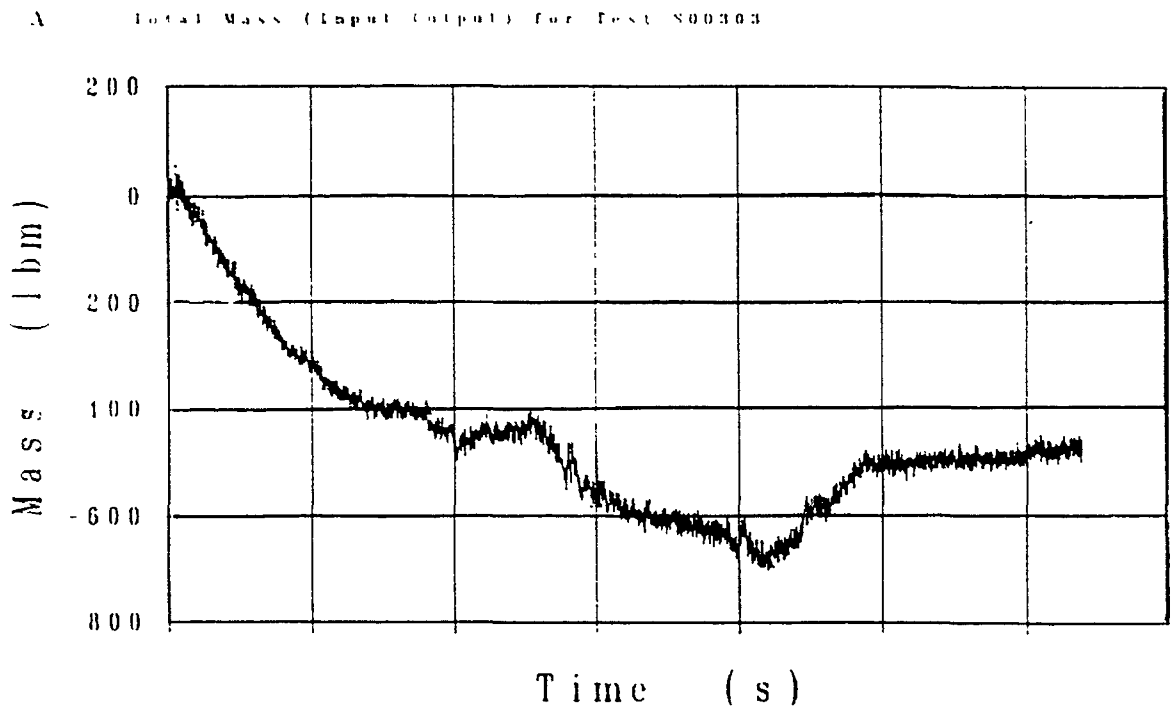

FIG. 3. Comparison of break locations
Change in system mass inventory

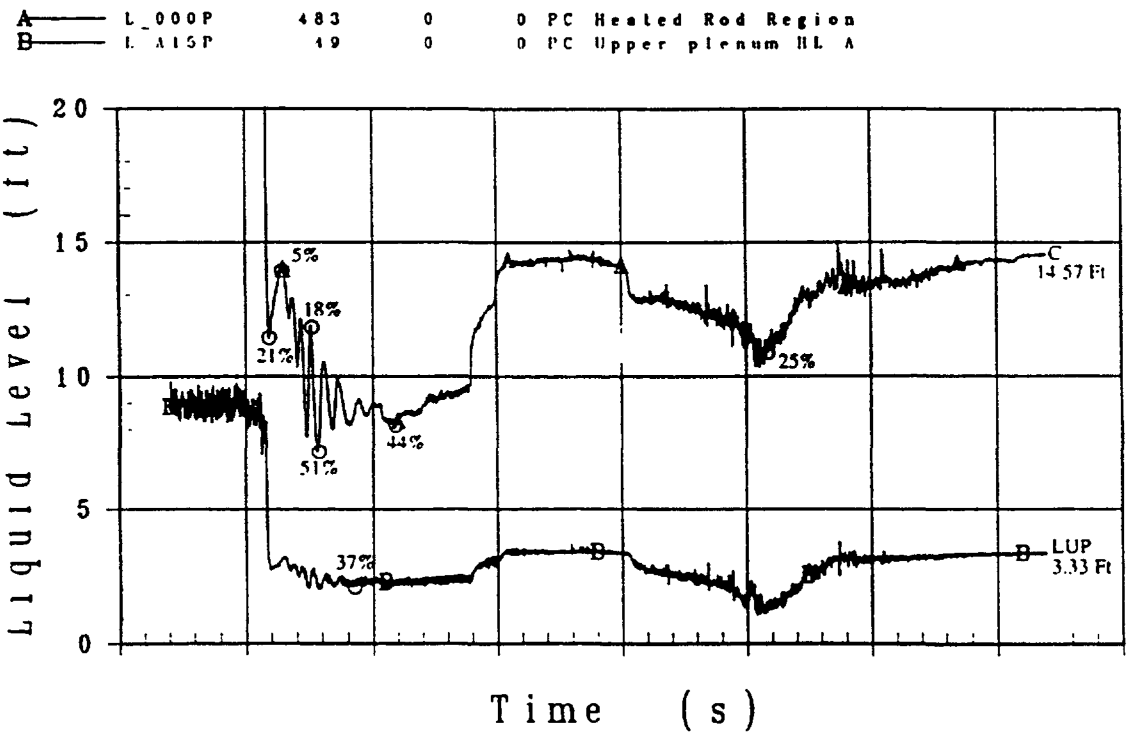

FIG. 4. SPES - 2 Test: S00303

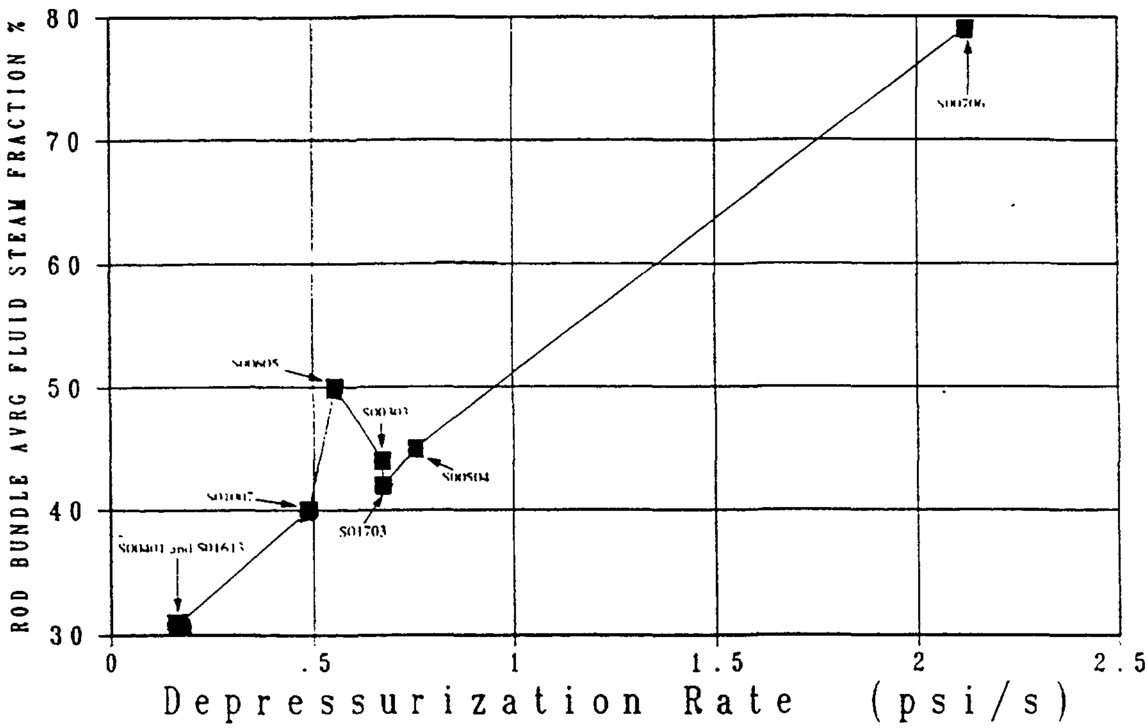

FIG. 5. Rod bundle steam fraction before ADS actuation

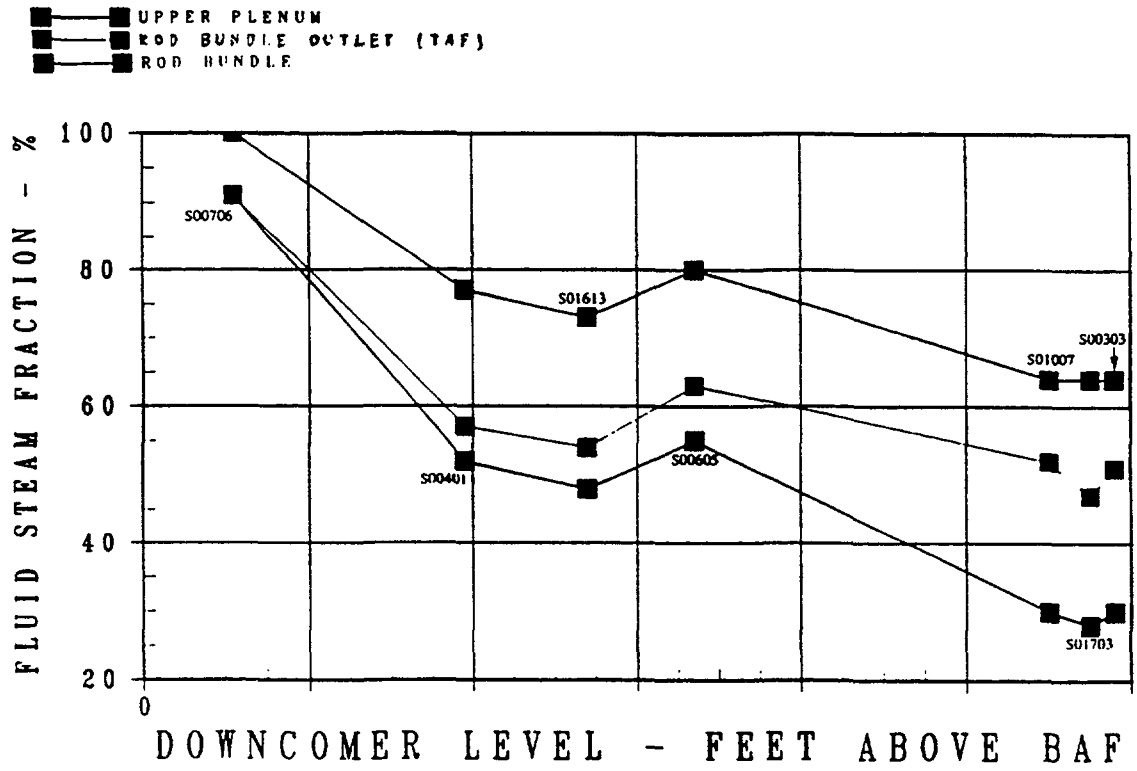

FIG. 6. Fluid steam fraction in core at minimum coolant inventory

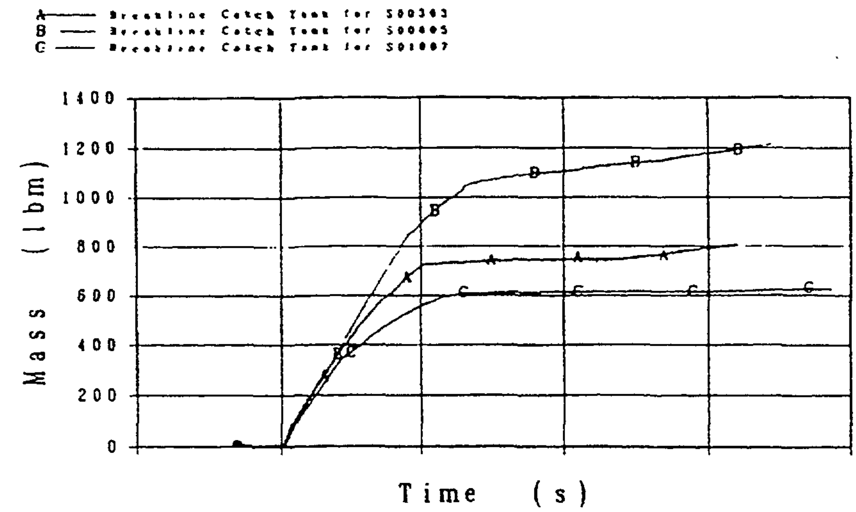

FIG. 7. Total break flow

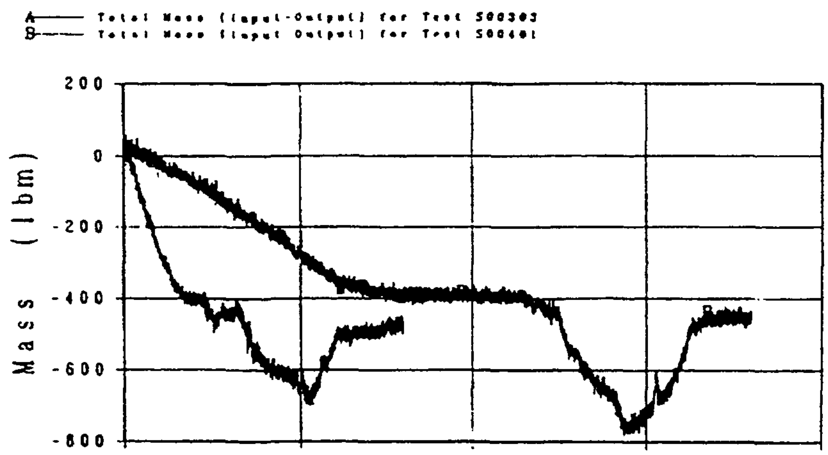

FIG. 8. Comparison of break sizes
Change in system mass inventory

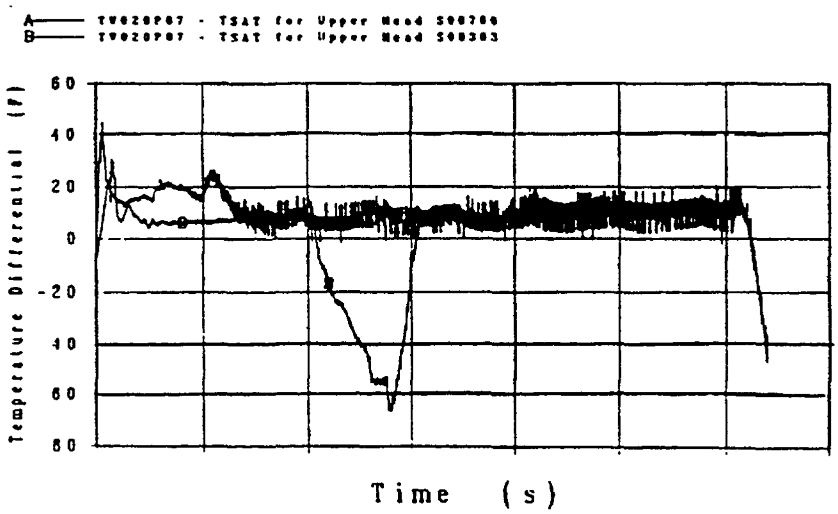

FIG. 9. Comparison of break sizes
Rod temperature relative to saturation temperature

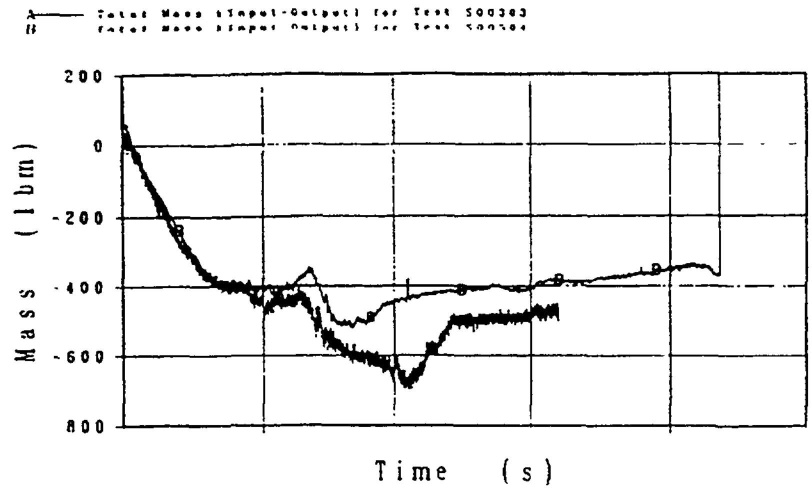

FIG. 10. Effects of non-safety systems
Change in system mass inventory

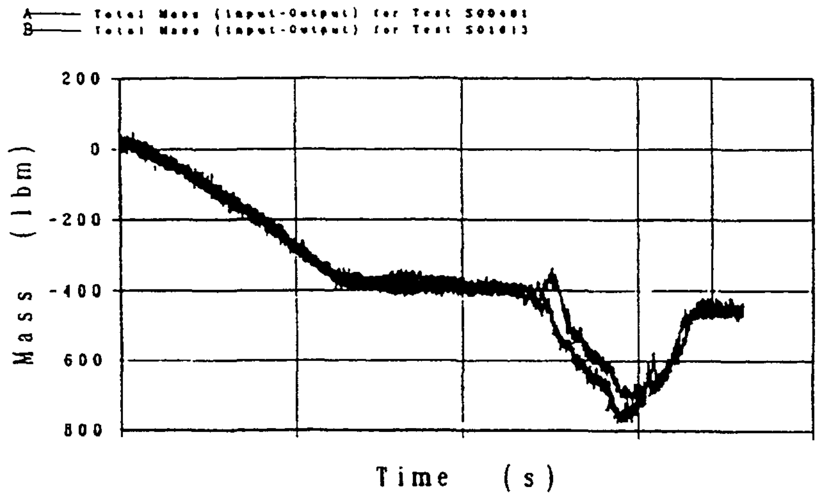

FIG. 11. Comparison of PRHR performance
Change in system mass inventory

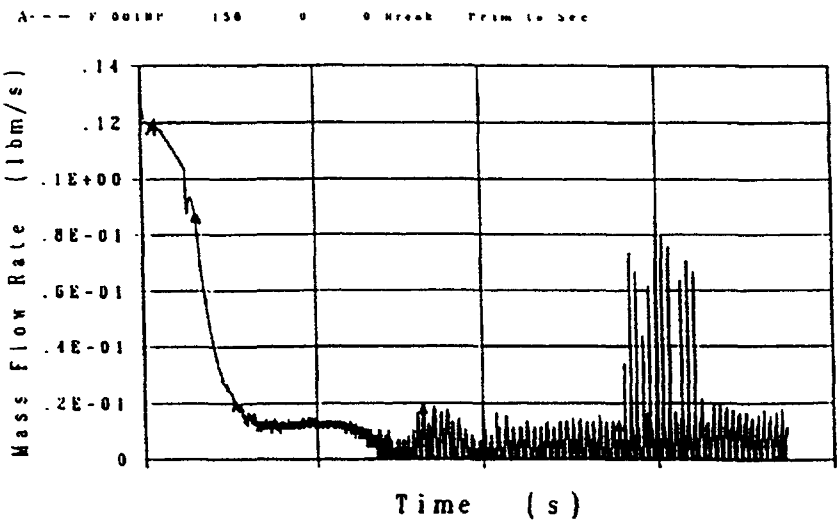

FIG. 12. Primary to secondary SGTR flow rate for S01110

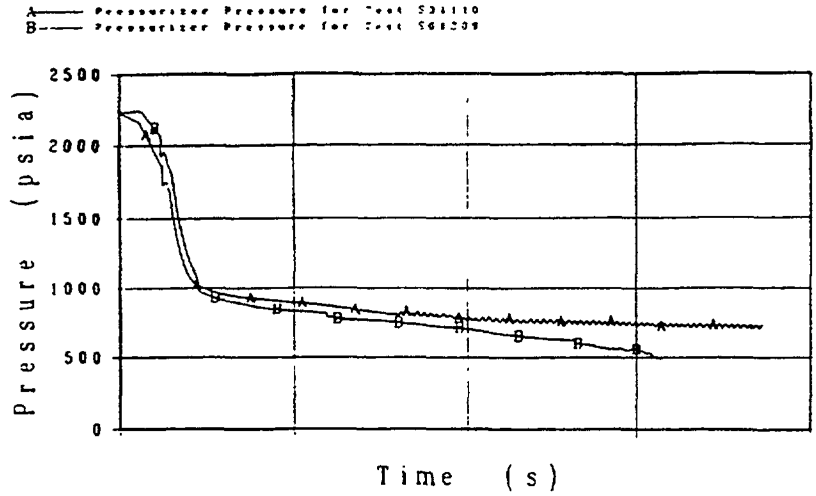

FIG. 13. *Comparison of steam generator tube rupture*
Primary system pressure

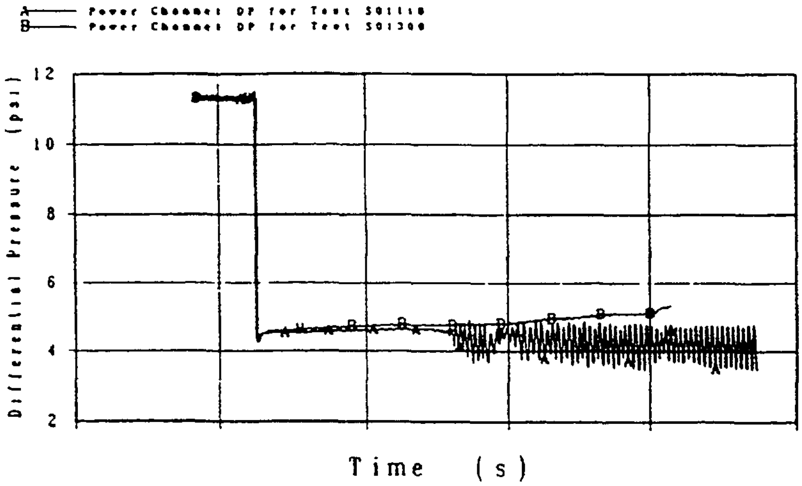

FIG. 14. *Comparison of steam generator tube rupture*
Rod bundle differential pressure

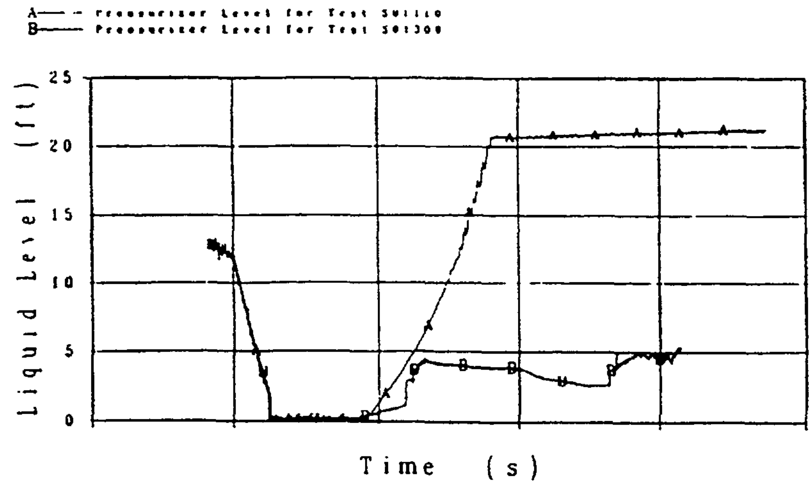

FIG. 15. *Comparison of steam generator tube rupture*
Pressurizer level

EXPERIMENTAL INVESTIGATION ON AN INHERENTLY ACTUATED PASSIVE INJECTION AND DEPRESSURIZATION SYSTEM

L. MANSANI, L. BARUCCA
ANSALDO Nuclear Division,
Genova

G.P. GASPARI
SIET, Piacenza

Italy

Abstract

ANSALDO has conceived an inherently actuated Passive Injection and Depressurization System (PIDS) to be used in Nuclear Power Plants (NPP).
The adoption of the PIDS would allow to enhance the reliability of the Safety Systems, with the additional advantage of a simplification of the NPP current designs.
Due to the innovative concept of this system, an experimental investigation has been performed at SIET Laboratory aimed at exploring the physical phenomena governing the behavior of the system, with the basic goal to demonstrate the concept viability.
After a brief description of the PIDS concept, the paper presents the experimental tests matrix and some results.
The obtained experimental data confirm the validity of the concept, justifying and encouraging the continuation of the activities and calling for a further development and the execution of related experimental activities.

INTRODUCTION

In a Nuclear Power Plant (NPP) one of the means to mitigate the consequences of a Loss of Coolant Accident (LOCA) is to inject cold water into the Reactor Coolant System (RCS) at low pressure. This requires RCS depressurization. The larger effort finalized to work out design solutions for the next generation of NPPs, capable to obtain a step ahead with respect to the already satisfactory safety standards as well as a simplification of current design, has produced the concept of an innovative inherently actuated Passive Injection and Depressurization System (PIDS). The PIDS is a system, conceived by ANSALDO, to perform the depressurization function without making use of any active component or actuation logic. ANSALDO, conscious of the innovative concept, before proceeding to the actual system design, committed SIET to perform an experimental investigation aimed at exploring all the physical phenomena and demonstrating the concept viability.

The paper gives a PIDS concept short description and presents the main experimental results. The final experimental data report is still in progress.

CONCEPT AND WORKING PRINCIPLE DESCRIPTION

ANSALDO conceived a completely Passive Injection and Depressurization System which does not make use, to perform its function, of any active component, actuation logic or operator action.

The basic concept is to perform the required depressurization function by mixing (borated) cold water with the steam present in the RCS. The cold water injection is inherently actuated on low RCS water inventory, with the depressurization (down to the containment pressure) completed by a valve passively actuated on low RCS pressure. The approach of depressurizing by adding mass, is of interest for a NPP in which the current Automatic Depressurization Systems intervention causes, in most cases, a large mass depletion due to the level swell in the RCS while depressurizing.

Figure 1 shows a PIDS basic configuration. A tank of (borated) cold water, connected to the RCS steam space, is equipped with a syphon shaped discharge line. The syphon ascending leg connects the tank bottom and overcomes the top of the tank by some meters, the descending leg connects an ejector. The ejector has two additional connections: upstream with the RCS steam space and downstream with a horizontal small condenser. The condenser outlet line terminates in the RCS. The elevation of the condenser is determined according to a predefined RCS level set point for system actuation. An injection spray line connects the line downstream the ejector to the RCS location chosen for cold water injection.

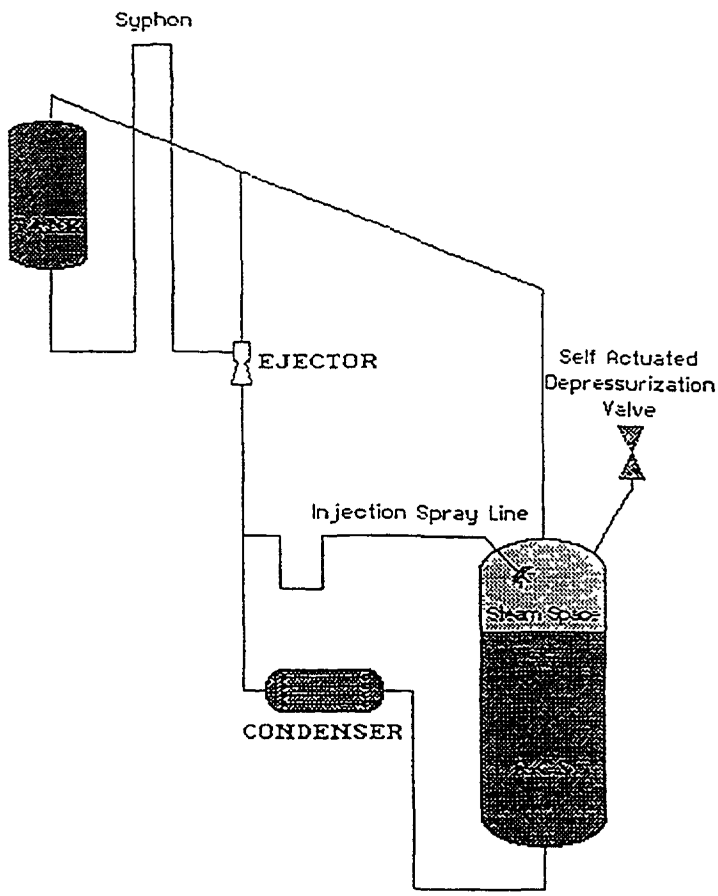

Fig 1 - PIDS BASIC CONFIGURATION

In normal conditions, the system can be seen as constituted by two communicating, water filled, vessel subsystems: the first one being the tank and syphon ascending leg, the second one being the pipe downstream of the ejector, the condenser and the RCS water space. When the water level in the RCS decreases below the condenser elevation, the condenser starts to condense the steam coming from the RCS steam space through the ejector. The resulting pressure reduction in the ejector throat will clear the vapour space over the syphon hydraulic seal and will trigger the syphon. From now on, the cold water injection will be stable until the tank empties.

The cold water may be sprayed into any vapour space of the primary system available at the syphon triggering time, thus causing the RCS depressurization up to a pressure value well below the minimum pressure reached under any operational transient. The remaining depressurization down to the containment pressure, will be completed by pilot operated Passive Depressurization Valves (PDV) passively actuated on low RCS pressure.

EXPERIMENTAL TESTS

In principle, the PIDS is applicable both to Boiling and Pressurized Water Reactor designs. However the PIDS developed so far has been conceived for application to a PWR design. It is composed of two subsystems: a) the high pressure subsystem, which consists of the ejector, the condenser, the water tank and the connection lines to/from the RCS, b)the low pressure subsystem, which consists of a Passive Depressurization safety Valve (PDV). The two subsystems operate in sequence: the former is required to depressurize the RCS below the PDV actuation set point, the latter is required to continue the system depressurization from the PDV set point down to the containment pressure.

An experimental campaign has been undertaken on a properly scaled test facility, designed by ANSALDO and constructed by SIET, with reference to a medium size PWR (like for instance the Westinghouse AP600), to test the PIDS high pressure subsystem. The specified tests are "conceptual" tests and therefore the quantitative results (such as depressurization rate and depth) are not intended nor expected to be representative of the real PWR system ones.

The goals of the experimental tests are:

- to confirm that the system is actuated as soon as the water level uncovers the condenser;
- to confirm that, for sufficiently small breaks (less than 3" equivalent diameter) wherever located, the system is not activated by any spurious effect until the water level uncovers the condenser;
- to confirm that following the syphon triggering the injection water flowrate is stable until the tank empties;
- to asses the PIDS performance in presence of non-condensable gases.

TEST FACILITY DESCRIPTION

The test facility has three tanks simulating in a 1:30 volume and full height scale, the volume of an AP600 Core Make-up Tank (CMT), Pressurizer (PRZ) and Reactor Vessel (Fig. 2). Water can be heated up to 300°C at a pressure of 8 MPa by means of steam circulating through dedicated U-tubes bundles inside the RV and PRZ.

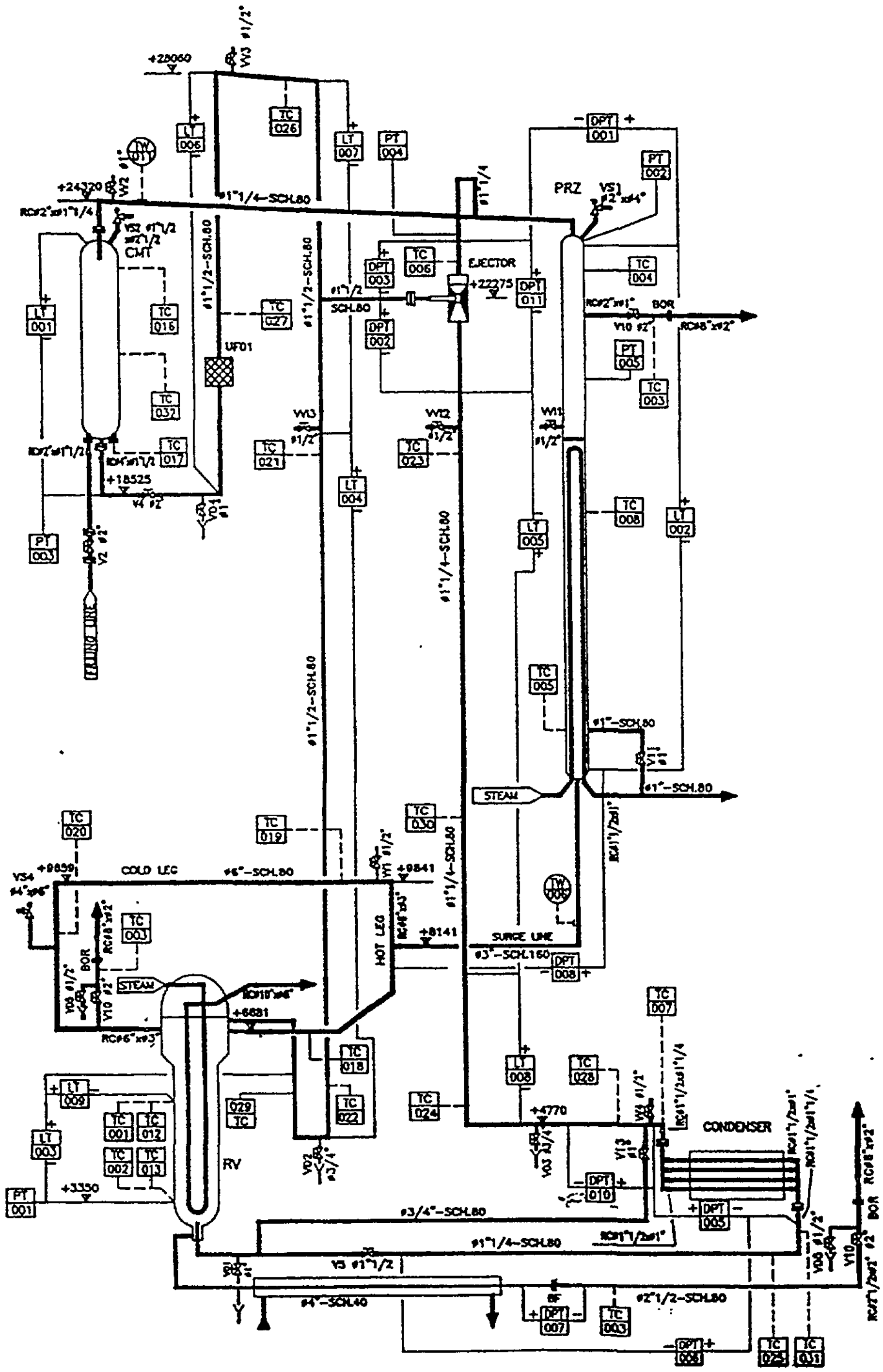

Fig. 2 - SKETCH OF THE TEST FACILITY AND INSTRUMENTATION

Table 1 gives the major geometrical data of the main facility components which, in addition to the above mentioned tanks (CMT, PRZ and RV) include a Condenser, an Ejector and related piping. The facility includes a device to simulate the break at various locations. The facility is thermally insulated, except the upper portion of the pipes normally filled with steam, so that the heat losses are reduced. The reason for not insulating the mentioned portions of lines is to prevent an excessive water temperature decrease in the line downstream the ejector, which might generate a spurious system actuation during RCS level decrease before the condenser is uncovered. The test facility is sketched in Fig. 2.

Table 1 - GEOMETRICAL DATA OF THE MAIN PIDS COMPONENTS AND PIPES

SCALE		
	Elevation	1:1
	Volume	1:30
OVERALL ELEVATION (m)		28
PRESSURIZER (PRZ)		
	Inner diameter (m)	0.363
	Height (m)	11.50
	Volume (m^3)	1.2
REACTOR VESSEL (RV)		
	Inner diameter (m)	0.98
	Height (m)	4.2
	Volume (m^3)	2.1
COLD WATER TANK		
	Inner diameter (m)	0.69
	Height (m)	4.20
	Volume (m^3)	1.5
HOT LEG / COLD LEG		
	Inner diameter (m)	0.146 (6" sch 80)
SURGE LINE		
	Inner diameter (m)	0.067 (3" sch 160)
INJECTION LINE		
	Inner diameter (m)	0.038 (1.5" sch 80)
BALANCE, EJECTOR - CONDENSER LINES		
	Inner diameter (m)	0.032 (1.25" sch 80)

Thermalhydraulic instrumentation is installed for measuring the parameters of interest. The following types of instrumentation are provided:

- 34 thermocouples to measure the fluid temperature in the pipes and components;
- one flowmeter to measure the injection mass flowrate;
- 8 pressure transducers to record the absolute pressure within the various tanks;
- 18 differential pressure transducers to record pressure drops and liquid levels in tanks and pipes.

All instruments were calibrated in laboratory before their installation on the plant. The instruments overall accuracy resulted ± 1.1 °C for thermocouples, ± 20 kPa for absolute pressure transducers, ± 0.15÷0.30 kPa for differential pressure transducers. The maximum estimated error of the main interesting quantities (error analysis is underway) is ± 1.5 °C for the fluid temperature, ± 50 kPa for the fluid pressure, ± 0.3 ÷ 0.5 kPa for the ejector pressure drops and ± 0.05 ÷ 0.10 m for the water level.

The test facility has digital data acquisition systems to record all the instrument signals.

TEST MATRIX AND TEST PROCEDURE

Several tests are included in the test matrix given in Tab.2 with different break sizes and locations. For all the tests, but #12, the initial pressure is 8 MPa while the RV water temperature is set 250 °C, for RV and cold leg breaks, and 275 °C for the top PRZ breaks. LOCA analyses /4/ /5/, performed on the reference NPP, highlighted that:

- the RV water flashes and, as a consequence, the system pressure stabilizes at a constant value (≈ 6 MPa);
- for breaks in the RCS water region, the PRZ empties before the RV flashing;
- for breaks in the RCS steam region (i.e. in the top PRZ) a water level still remains inside the PRZ also after the RV flashing.

Table 2 - PIDS TEST MATRIX

RUN #	BREAK SIZE	BREAK LOCATION	INITIAL CONDITIONS P (MPa)	INITIAL CONDITIONS RV Temp (°C)	NOTES
1	1"	RV bottom	8	250	
2	1"	Cold Leg	8	250	
3	2"	Cold Leg	8	250	
4	3"	Cold Leg	8	250	
5	1"	Cold Leg	8	250	0.4 kg of Nitrogen injected under water N_2 in equilibrium at transient start
6	1.5"	PRZ top	8	275	Transient limitations due to CCFL in surge line
7	1.25"	PRZ top	8	275	Transient limitations due to CCFL in surge line
8	1 81"	PRZ top	8	275	Transient limitations due to CCFL in Hot Leg nozzle Modified surge line geometry
9	3"	PRZ top	8	275	Transient limitations due to CCFL in Hot Leg nozzle Modified surge line geometry
10	1"	RV bottom	8	250	0 2 kg of Helium plus 0 7 kg of Nitrogen both injected under water He and N_2 in equilibrium at transient start
11	1"	RV bottom	8	250	Test 1 repetition
12	3"	RV bottom	4 5	250	0 23 kg of Helium plus 0 52 kg of Nitrogen injected into PRZ steam space He and N_2 not in equilibrium at transient start
Cold water injection was into RV for all runs but #1 which was into Hot Leg					

In the experimental facility, due to limitation in the maximum operating pressure, the above behavior is reproduced by setting 250 °C the RV water temperature for RV and cold leg break tests and 275 °C for top PRZ break tests.

The amount of non-condensable gases used in the tests is a conservative upper bound which takes into account the RCS hydrogen content in normal operation as well as the hydrogen and oxygen produced by radiolysis after the LOCA (a period of three hours has been considered). Helium and nitrogen have been used in the tests instead of hydrogen and oxygen.

The tests have been conducted using the following procedure. Initial steady state conditions were established by heating the PRZ and RV with steam circulating inside dedicated tubes, then the break valve was opened. As soon as saturation conditions were reached in the RV the system pressure was automatically kept constant until the tank water injection started by heating the RV. During the water injection the power to the RV (supplied by steam) was maintained at the same value as at the system triggering instant.

TEST RESULTS

Among the performed tests, the 1" and 3" cold leg break results are here summarized.

For both tests, when the initial conditions were reached (system pressure 8 MPa, RV temperature 250°C and nominal water level in the PRZ) the break valve was opened.

<u>1" cold leg break</u>

The system pressure decreased down to 4 MPa in approximately 1000 s, at which time the RV water started to flash, (Fig. 3). From this time on the pressure was kept constant by heating the RV until the condenser uncovered (4615 s) and hence water injection started, from the tank to the RV. The water level continuously decreased in the PRZ, ejector and injection lines due to the loss of mass inventory. As soon as the condenser has been uncovered (4615 s), Fig. 4, the condensation rate was enhanced, with steam supplied from the PRZ through the steam ejector. The resulting pressure reduction in the steam ejector throat, Fig. 5, cleared the vapour space over the syphon hydraulic seal and triggered the syphon. The water injection started and, from this time on, the system was depressurized by the cold water injected into the RV, Fig. 3.

<u>3" cold leg break</u>

The same transient events as for 1" cold leg break were observed, of course, in shorter times. The system pressure decreased down to 4 MPa in approximately 190 s, Fig. 7, and then kept constant (the pressure peak being caused by a mismatch in the RV heating control). The condenser uncovered 645 s after the break, Fig. 8, at which time the cold water injection started, Figs. 9 and 10.

The above behavior was observed, though with different time histories, also in all the remaining tests, including those with non-condensable gases.

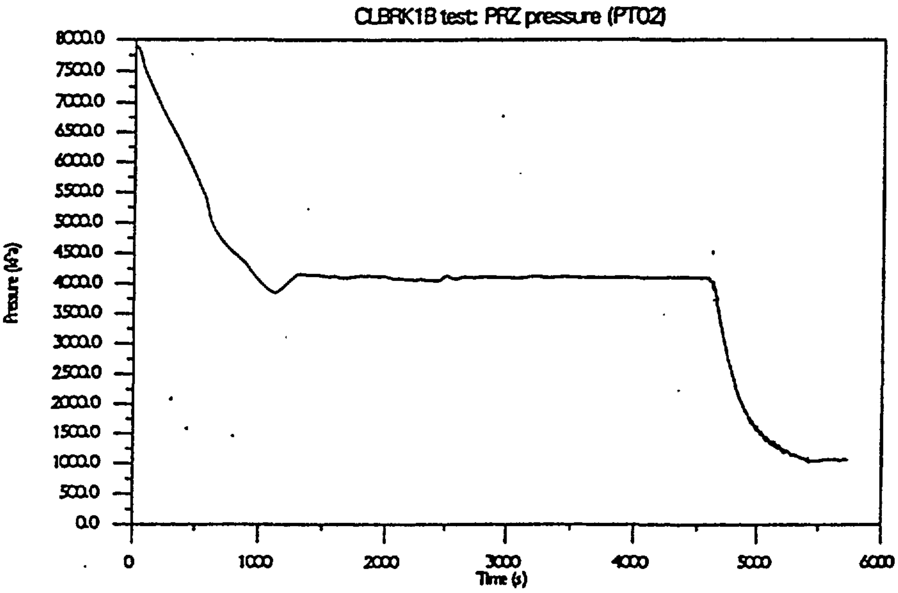

Fig. 3 - 1" COLD LEG BREAK - PRZ PRESSURE VERSUS TIME

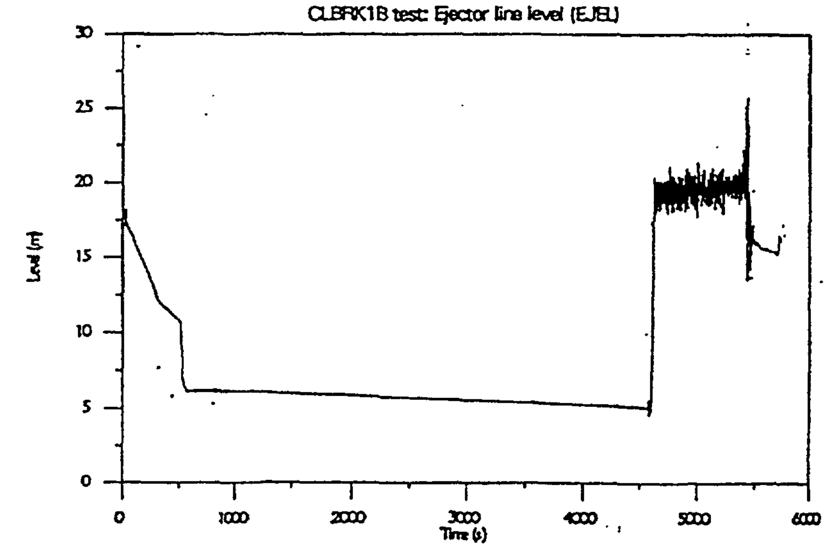

Fig. 4 - 1" COLD LEG BREAK - EJECTOR LINE LEVEL VERSUS TIME

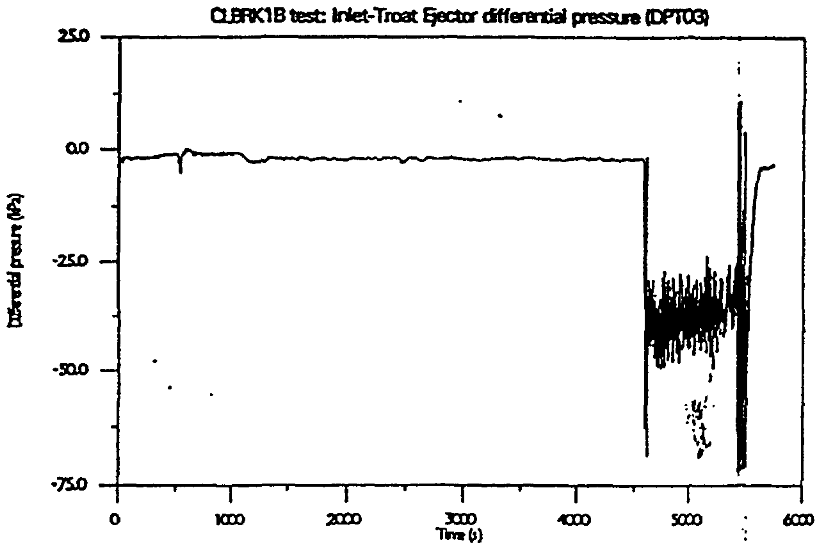

Fig. 5 - 1" COLD LEG BREAK - INLET-THROAT EJECTOR DIFFERENTIAL PRESSURE VERSUS TIME

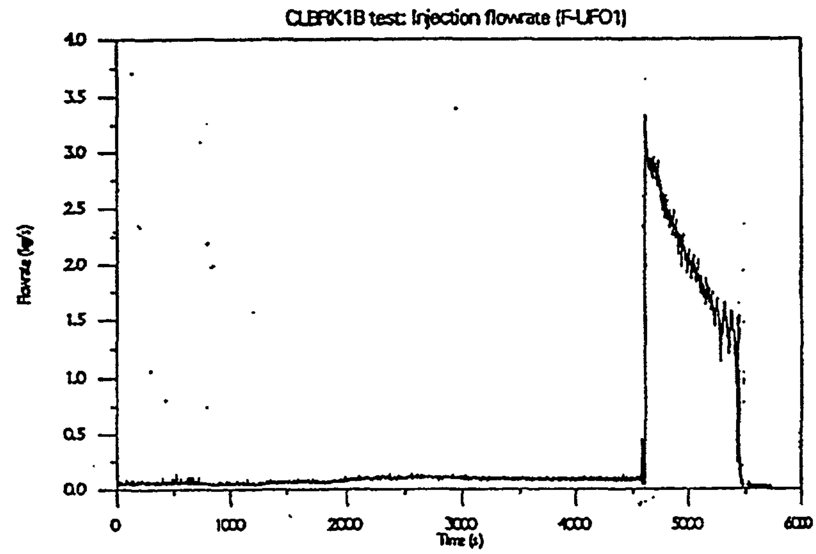

Fig. 6 - 1" COLD LEG BREAK - COLD WATER INJECTION FLOWRATE VERSUS TIME

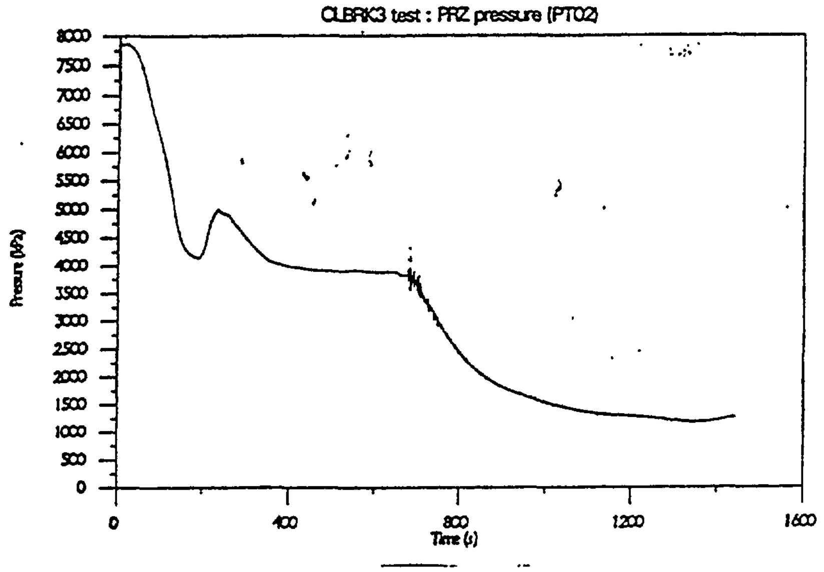

Fig. 7 - 3" COLD LEG BREAK - PRZ PRESSURE VERSUS TIME

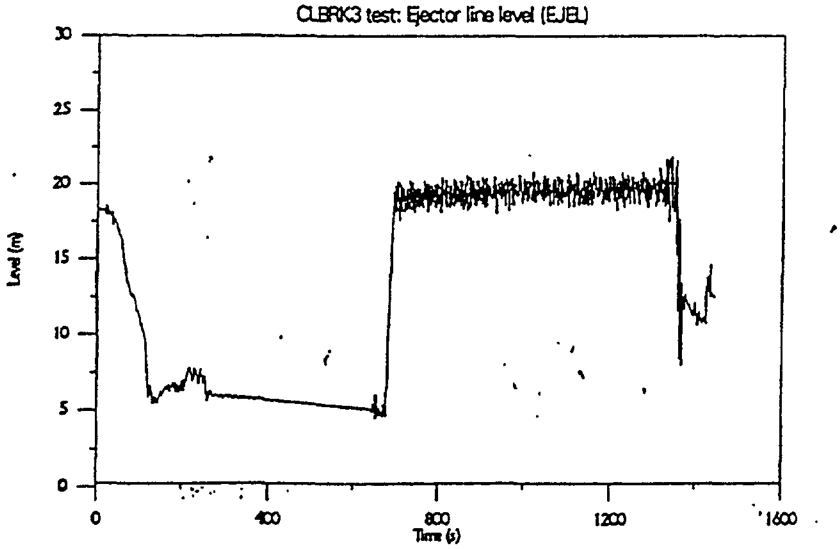

Fig. 8 - 3" COLD LEG BREAK - EJECTOR LINE LEVEL VERSUS TIME

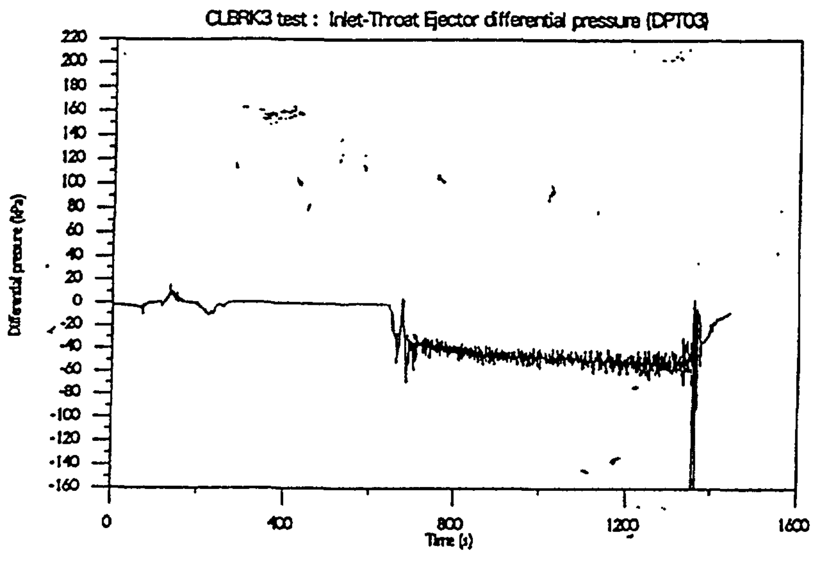

Fig. 9 - 3" COLD LEG BREAK - INLET-THROAT EJECTOR DIFFERENTIAL PRESSURE VERSUS TIME

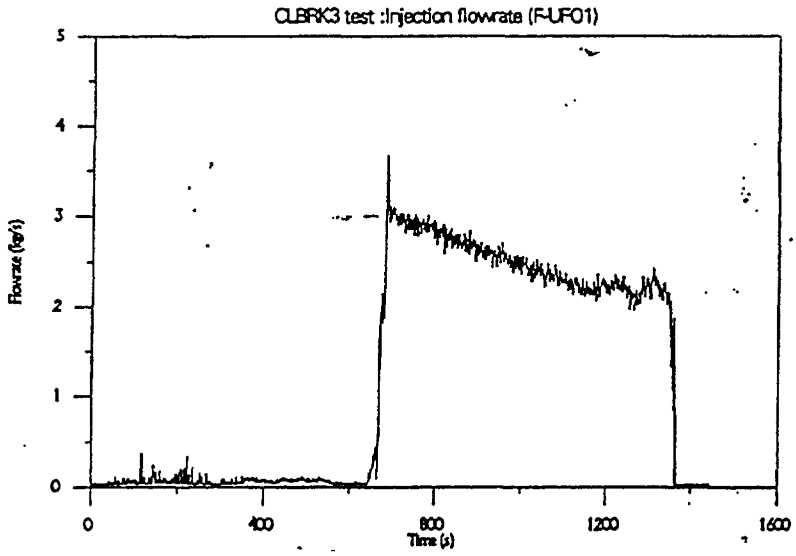

Fig. 10 - 3" COLD LEG BREAK - COLD WATER INJECTION FLOWRATE VERSUS

CONCLUSIONS

The performed tests have demonstrated the PIDS concept viability. In particular the tests have confirmed that:

- the system is actuated as soon as and every time the water level uncovers the condenser. The system actuation has always occurred at about the same RV level;
- no spurious effects, capable to actuate the system before the water level uncover the condenser, has been experienced. A wide margin against early actuation has been evidenced;
- the injected flowrate has resulted stable;
- the presence of non-condensable gases, even at very high concentration, had no adverse effect on PIDS actuation and did not reduce its performances;
- although the test objective was not to get information of RCS depressurization rate, a very fast depressurization was observed in all the tests during the water injection phase.

The successful test results strongly encourage to continue the PIDS investigation program activity. The next steps will consist in:

- separate effect tests aimed to gain information on the attainable depressurization rates and on the associated phenomena;
- integral scoping tests execution aimed at assessing the PIDS interaction with the other NPP systems.

REFERENCES

/1/ Patent No. PCT/EP94/03162 "Depressurization System for Plants Operating with Pressurized Steam", September 22, 1994.

/2/ L. Mansani, "Passive depressurization system large scale test specification". ANSALDO STU 5100 SMEX 0020000 , January, 1994

/3/ G.P. Gaspari, "Passive injection and depressurization system - Test facility description", SIET 00324 RI 94, May, 1995

/4/ L. Mansani, R. Lenti, G. Saiu, "Preliminary accident analysis to support a passive depressurization system design". Proceeding of the Int. Conf. New trends in nuclear system thermohydraulics, Pisa, May 30 - June 2, 1994

/5/ Westinghouse, 1992 - AP600 Standard Safety Analysis Report (Chapter 15: Accident Analysis)

DESIGN AND TESTING OF PASSIVE HEAT REMOVAL SYSTEM WITH EJECTOR-CONDENSER

K.I. SOPLENKOV
Research Institute for Nuclear Power Plant Operation,
Moscow, Russian Federation

V.G. SELIVANOV
Kharkov Aeronautical Institute,
Kharkov, Ukraine

Yu.N. FILIMONTSEV
Research Institute for Nuclear Power Plant Operation,
Moscow, Russian Federation

B.I. NIGMATULIN
Electrogorsk Research Engineering Center,
Russian Federation

V.V. BREDIKHIN
Kharkov Aeronautical Institute,
Kharkov, Ukraine

E.I. TRUBKIN
Electrogorsk Research Engineering Center,
Russian Federation

E.Z. EMELJANENKO
Odessa Polytechnic Institute,
Odessa, Ukraine

A.W. REINSCH
Southern California Edison
California, USA

Abstract

The objective of the analysis, design, and testing of a new type of passive heat removal system is the development of a concept with the capability to terminate a broad spectrum of postulated accident sequences. Its principle is based on the dynamic form of natural convection utilizing inertial forces instead of gravity for fluid circulation. The process develops in a loop combining an ejector specifically designed for dynamic natural convection and heat exchanger in a fixed geometry. This simple configuration, independent of electric power and automatic controls, is capable of coping with the majority of initiating events occurring in light water reactors. Since motive power does not depend on gravity, heat can be rejected from a high elevation to a lower level, reducing capital costs by locating the heat sink at the ground level.

A broad analytical and experimental development program for a passive heat removal system with ejector-condenser (PAHRSEC) has been conducted at [1] in cooperation with [2], [3], [4]. Various ejector types and PAHRSEC flow schemes were tested. The most

promising one removes heat from steam generator, and has been tested in a 3.5 MW PAHRSEC facility at [2]. The system starts up rapidly and maintains stable operation over a wide range of thermohydraulic parameters and transient conditions. Based on the results from these comprehensive tests, PAHRSEC loops have been proposed as retrofits for the currently operating WWER-440 nuclear power plants at Novovoronezh. The analysis of a station black-out at a WWER-440 plant equipped with 4 PAHRSEC of 10 MW each was performed with the integral codes DYNAMICA (Russia) and TRAC-PF1/MOD2 (USA). The results prove consistently that heat removal from the reactor core was ensured for extended time with only two out of four PAHRSECs operating. The last phase of validation effort, the construction and adjustment of a full-scale test loop of the PAHRSEC designed for a WWER-440 plant, is proceeding swiftly. Completion of the facility and first tests are scheduled for the second quarter of 1995.

The concept of heat removal by steam condensation in an ejector recirculating the condensate to the nuclear steam supply system is applicable to all nuclear plants with a steam cycle power conversion system. A modified PAHRSEC can serve as passive heat sink in the containment under severe accident conditions.

1. Principle of Dynamic Natural Convection

Since the PAHRSEC process functions within a fixed geometry, flow developing within the system boundaries is a form of natural convection which, in this particular application, is based on inertial forces. In contrast, natural convection induced by hydrostatic or aerostatic pressure differences is caused by gravitational forces. Most of the natural fluid phenomena such as wind, ocean currents, rivers and fire are controlled by static natural convection depending on gravity essentially. A common feature of static and dynamic natural convection is that density differences resulting from energy exchange in a fixed geometry generate the flow.

For steady compressible flow in a streamline, the equation of motion without viscous effects in differential form is

$$\rho\, g\, dz + \rho\, w\, dw + dP = 0$$

The integral of the first term represents the hydrostatic or aerostatic pressure difference between two elevations. Static natural convection develops if heat is added at low elevation to a fluid and removed at high elevation. In an analogous way, dynamic forces for fluid propulsion are developed if heat is added at low fluid velocity and removed at high fluid velocity. The second term in the differential equation of motion represents dynamic pressure gradients. Accelerating and decelerating flow in dynamic natural convection correspond to ascending and descending flow in static natural convection. In the PAHRSEC concept, heat is added, for example, in the steam generator at low flow velocity and removed in the ejector at high flow velocity by mixing accelerated steam with water.

Since dynamic forces and, therefore, dynamic natural convection are independent of gravity, the heat sink can be located at a lower elevation than the heat source, reducing costs substantially.

2. Ejector-Condenser

One of devices realizing the idea of dynamical convection is an Ejector-Condenser (EC). Fig.1 shows a typical geometry of EC.

Steam first comes into the Laval Nozzle and speeds up to a high velocity. Next, in the Mixing Chamber (MC) it mixes with "cold" water that takes off its heat, mass, and kinetic energy. At the outlet of MC the resulting two-phase mixture gets a supersonic flow. Then, in the Diffusor the flow kinetic energy turns into potential form. As a result the EC pressure can exceed essentially initial steam and "cold" water pressures. Fig.1 shows also typical pressure profiles in EC at different values of return pressure.

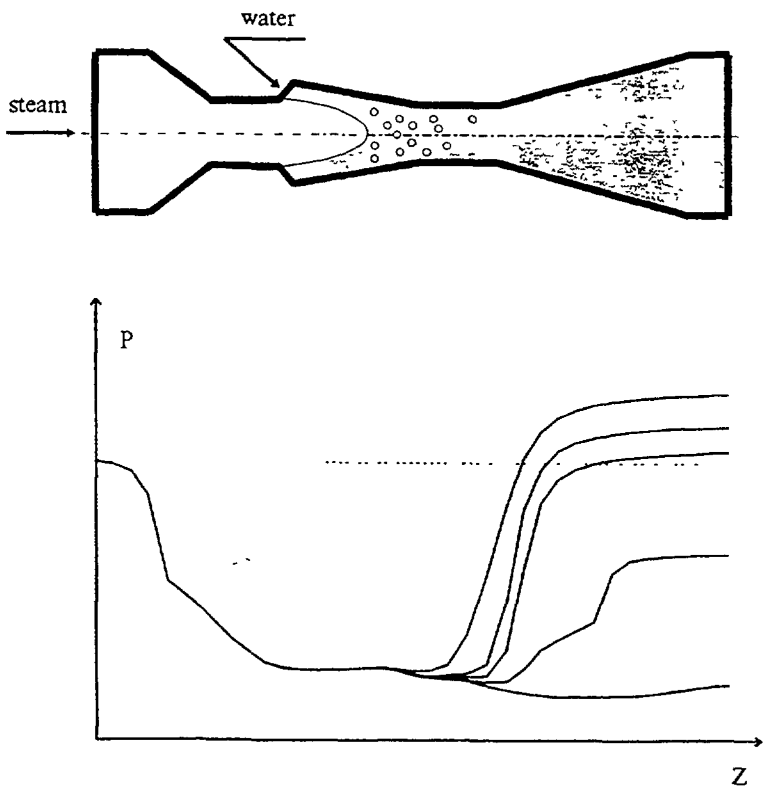

FIG. 1. Ejector-Condenser for PAHRSEC.

Presently there are two trends to use of EC in NPP Safety Systems:

- Development of high-pressure EC to supply water in reactor or in containment while accident conditions: [1], [2], [3] and others.
- Development of closed loops for heat removal from the 1st or the 2nd circuits as well as from the containment with EC as a pump. In that case EC in PAHRSEC should have the special properties:
- simple start-up (without bypass in MC)
- low EC pressure difference
- high "cold" water temperature (about 100 - 110 °C)
- a quite wide range of parameters for stable operation

3. PAHRSEC

In this paper some PAHRSEC study results for operating NPPs and new generation ones are presented.

Fig.2 shows the heat removal scheme for SG under accident conditions. The scheme "steam-liquid" has been tested as a most promising one for currently operating and new generation reactors.

Scheme "Steam-Steam" (S-S) **Scheme "Steam-Liquid" (S-L)**

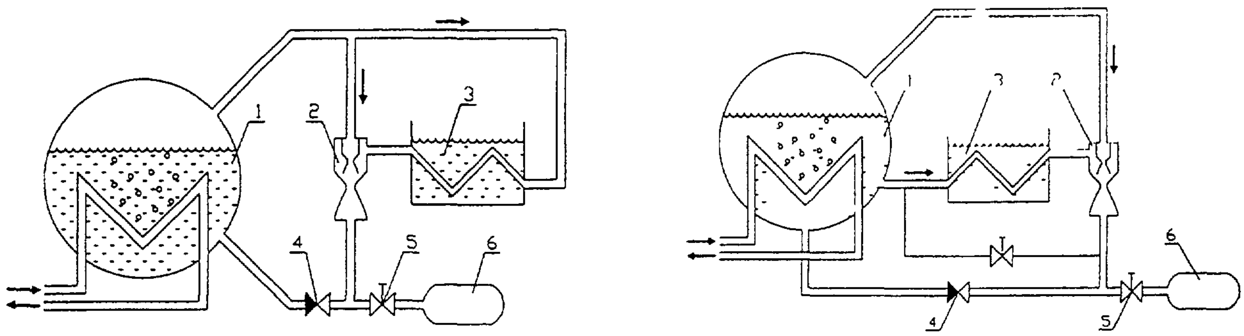

1 - Steame Generator (SG); 2 - Ejector-Condenser; 3 - Heat-Exchanger; 4 - Check Valve; 5 - Start-Up Valve; 6 - Start-Up Tank

FIG. 2. Heat removal from the steam generator under accident conditions.

PAHRSEC starts up as the valve 5 opens. Steam from SG (1) enters the EC nozzle (2) and "cold" water from SG (1) through HE (3) enters MC. After EC the resulting water, through the check valve (4), returns into SG. The ultimate heat sink is the HE water under atmosphere pressure. The analysis of PAHRSEC and its testing, presented below, have shown that PAHRSEC has the following properties:

- passive operation regime
- simplicity of passive start-up and capability to be restarted up repeatedly (as well as manually)
- short time interval between an accident and the beginning of heat removal
- maintaining stable operation over a wide range of SG parameters
- resistance to "strong" external disturbances such as the safety valve being opened
- capability to control (automatically or manually if necessary) its power for reliable cooling.

Again, the System is consistent with other safety systems and uses standard and operating equipment that is very important for its swift installation at reactors in service.

4. Experimental study

Fig.3 shows the started at ^{2} test facility with maximal heat removal of 3.5 MW. The facility has all main parts of a real PAHRSEC:

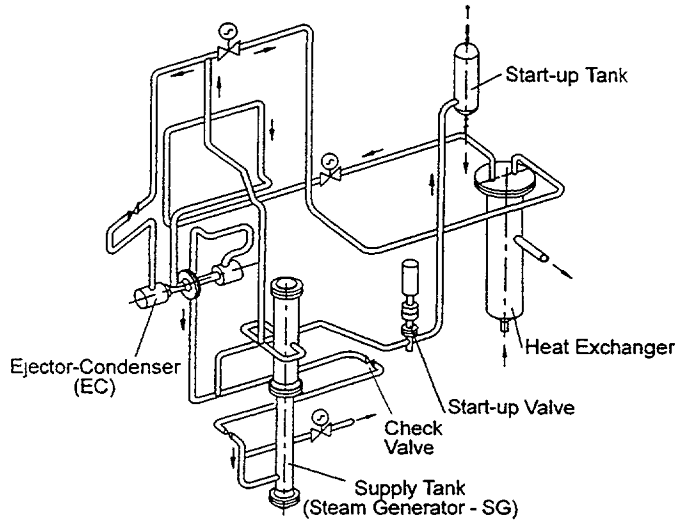

FIG. 3. PAHRSEC Test Facility and Ejector-Condenser of Medium Power.

- Supply tank. Its total height is 5.3 m and its volume is 0.5 m^3. There is a system of steam supply and removal of steam and liquid (not shown on Fig.3) which allows to simulate different emergrncy situations at real units (for example, in SG). Water level, pressure, and temperature are mesured in the tank. The maximal pressure and temperature in it can reach 9 MPa and 315 °C respectively.
- Ejector-Condenser. Its photograf is presented on Fig.3. That EC allows to remove heat from a heat source with power about 3.5 - 4 MW.
- Heat Exchanger (HE). It is 5 m high and 0.53 m in diameter. There are two pipe coils in the vessel, each is 80 m long. The total heat echange area is 21 m^2.
- Check valve. It is a typical one, located between EC and Supply tank.
- Start-up valve. An air-driven valve, installed in the start-up line. Its actuation time is 0.7 - 0.9 s.
- Start-up tank. It is 1.5 m high and 0.426 m in diameter.
- Data acquisition and processing system. It allows to monitor non-stationary slow and quick processes (the frequency of channel measurements is 2 Hz and 2 KHz for quick processes). It uses conventional primary transducers typical for thermal-physical experiments, and made on base of IBM PC AT. (A hardware of "CAMAC" standard is used as a communication means with the object.)

Some experimental results are presented on Fig.4-6.

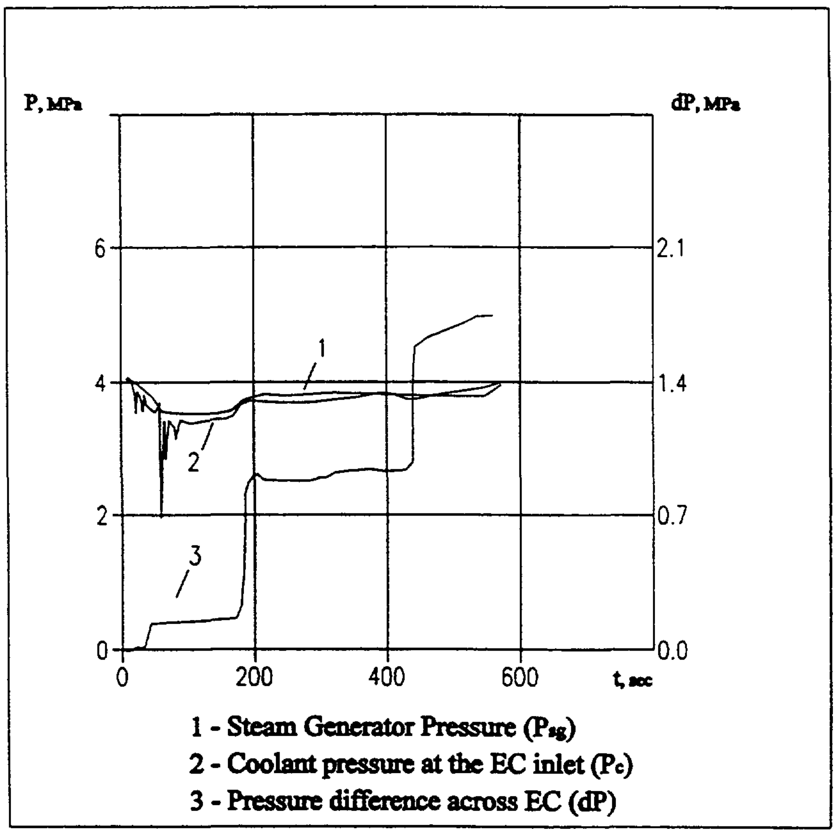

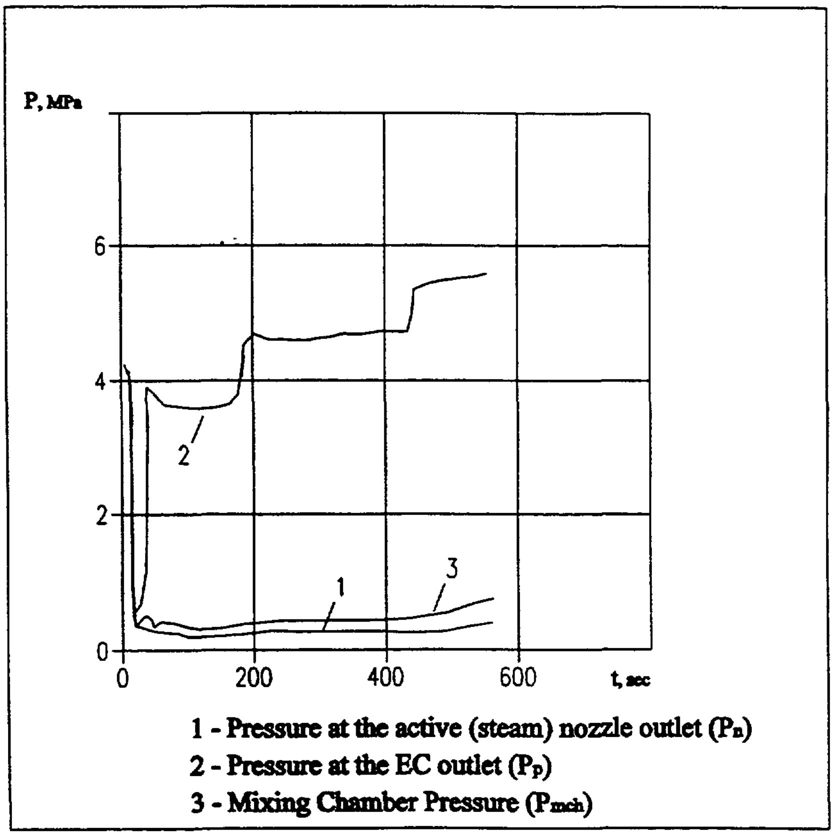

FIG. 4. Start-Up of EC and Determination of The Maximal Attainable Pressure Difference In PAHRSEC Circuit.

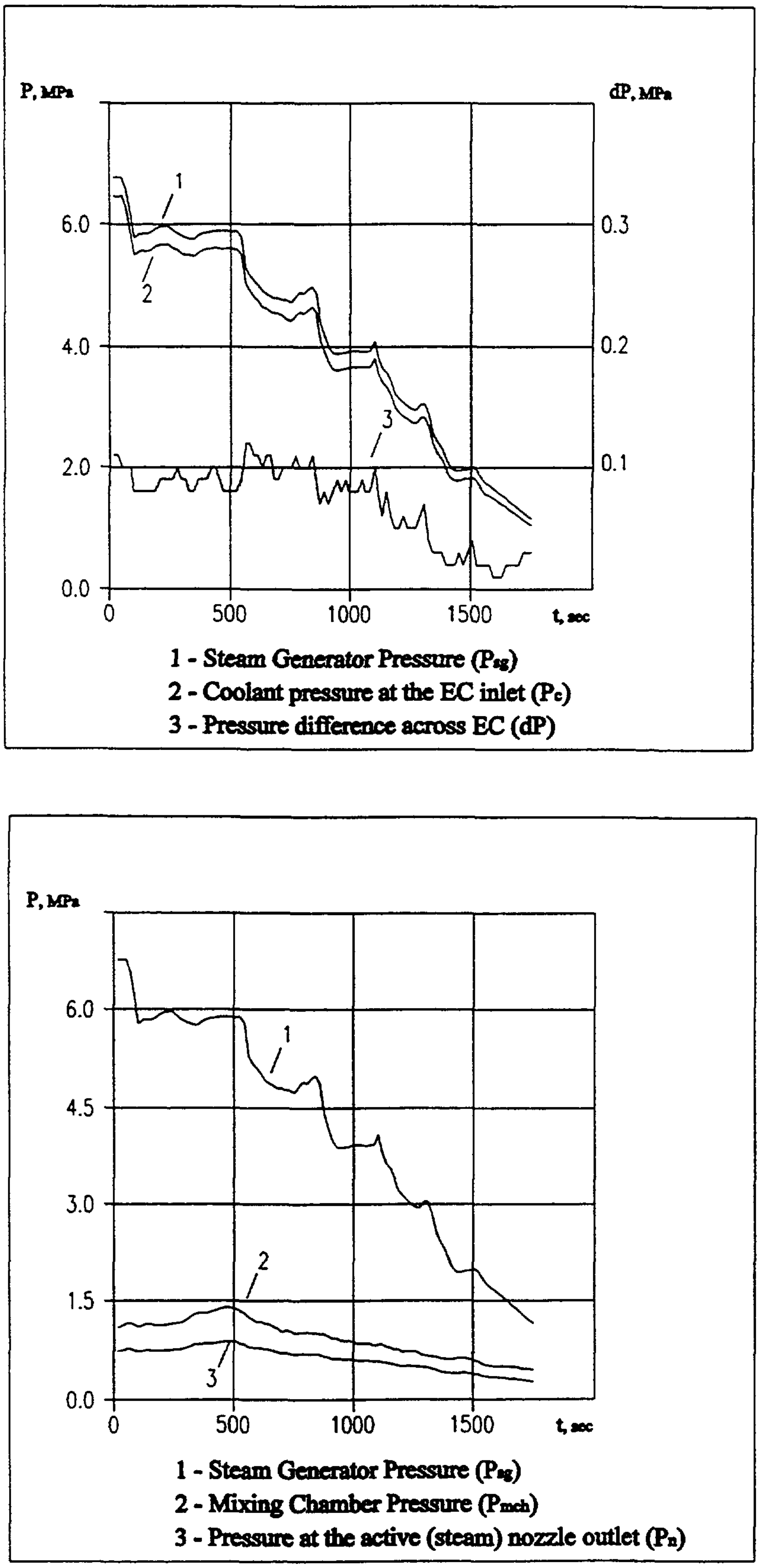

FIG.5. PAHRSEC Operation under "Rapid" Pressure Change in SG.

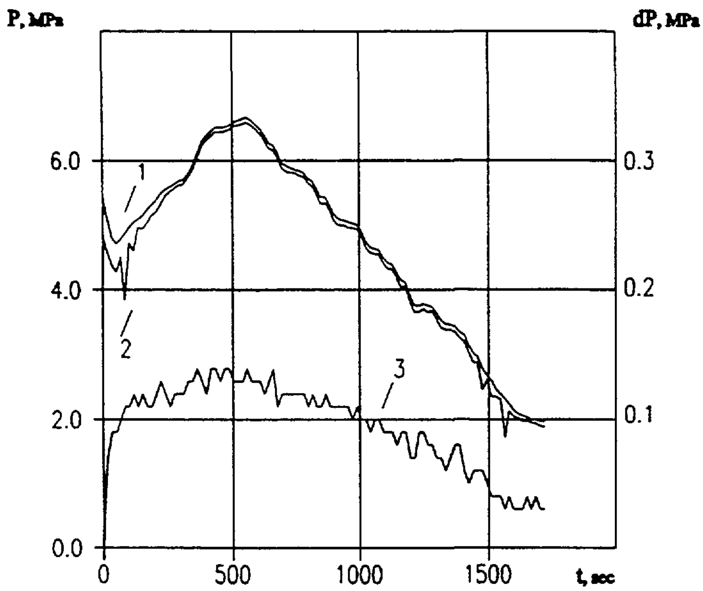

1 - Steam Generator Pressure (P_{sg})
2 - Coolant pressure at the EC inlet (P_c)
3 - Pressure difference across EC (dP)

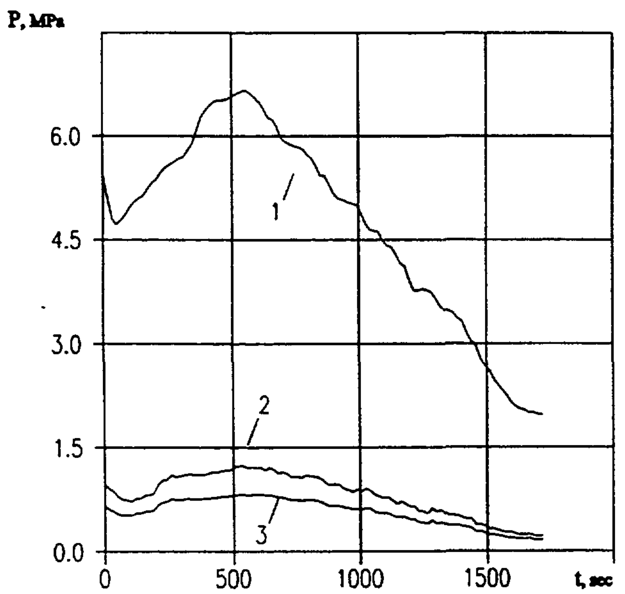

1 - Steam Generator Pressure (P_{sg})
2 - Mixing Chamber Pressure (P_{mch})
3 - Pressure at the active (steam) nozzle outlet (P_n)

FIG. 6. PAHRSEC Operation under "Slow" Pressure Change in SC.

Typical experimental curves of PAHRSEC start-up and of maximal EC pressure difference definition are presented on Fig.4. After the start-up valve opens the pressures P_p, P_n and P_{mch} drop. One can say that EC comes into operation if the pressures P_n and P_{mch} correspond to the saturation pressure at the mixing chamber temperature. One can see that EC start time is very short (3-5 s.). The start-up of the whole System occurs later and depends on the start-up tank volume. After the tank 6 fills out, the pressure behind EC becomes higher then that in the SG and this opens the valve 4. This is the way PAHRSEC starts up. It should be noticed again thatheat removal from SG begins just after the valve 5 opening and it is most intensive at this moment.

During one experiment, when time was about 200 s, 400 s, and 600 s (Fig.4) the hydraulic resistance behind EC was suddenly increased. Despite it, the System worked in a stable way and MC pressure did not change. The maximal EC pressure difference was higher than 1.5 MPa.

The PAHRSEC parameters behaviour while step-by-step SG pressure decrease is shown on Fig.5. In this case the System worked stabily in the range 1 - 7 MPa.

During the first 400 s of another experiment (Fig.6) the SG presure was being increased from 4.6 MPa to 6.8 MPa and then it was being decreased in a monotone way to 2 MPa. The System again worked stabily.

5. Installation of PAHRSEC at the 3rd and the 4th blocks of Novovoronezh NPP

VNIIAES (RINPO), EREC, GIDROPRESS and AEP Institutes have developed the technical requirements for PAHRSEC designe for WWER-440 NPP, where it was shown that:

- the System is compact and can be easily integrated with existing equipment
- it uses common technology: HE, piping, valves etc. are standard ones (the "steam-liquid" scheme has been chosen just from these reasonings)
- its cost is much lower relative to other safety systems of the same purpose

The calculations of "black-out" accidents for WWER-440 have been conducted using the code TRAC-PF1/MOD2. They showed that one PAHRSEC was sufficient to remove heat from one SG. The perameters behaviour when two PAHRSECs are put in to operation is shown on Fig.7. In about 2.8 hours (10^4 s) the system reaches a quasi-stationary regime when power of residual heat generation is equal to PAHRSEC heat removal power.

6. Full-scale 10 MW PAHRSEC

The full-scale experimental set (Fig.8) with N = 10 MW is intended for

- testing EC for WWER-440 PAHRSEC
- study of PAHRSEC behaviour under different accident conditions

The set design takes into account the requirements to meet while introducing at acting WWER-440, and the experience of running 3.5 MW PAHRSEC.

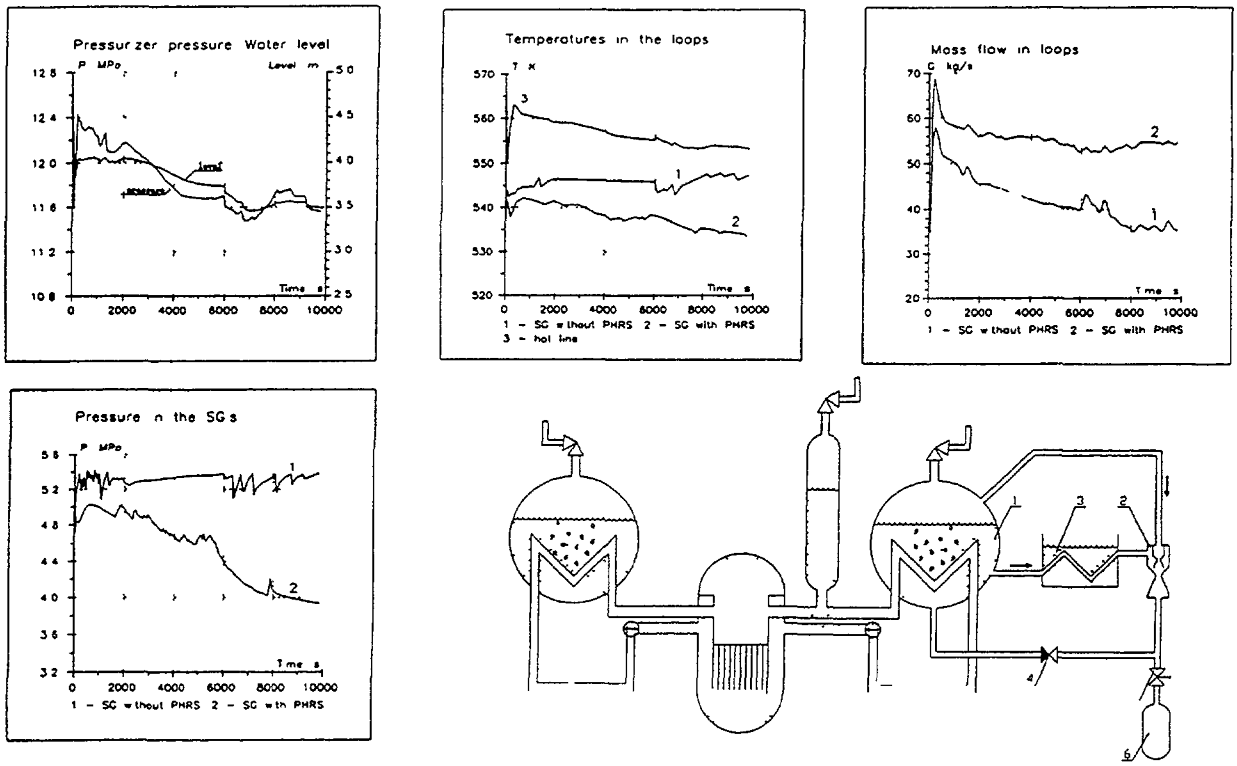

FIG. 7. WWER-440, "Black-Out", PAHRSEC-10 MW.

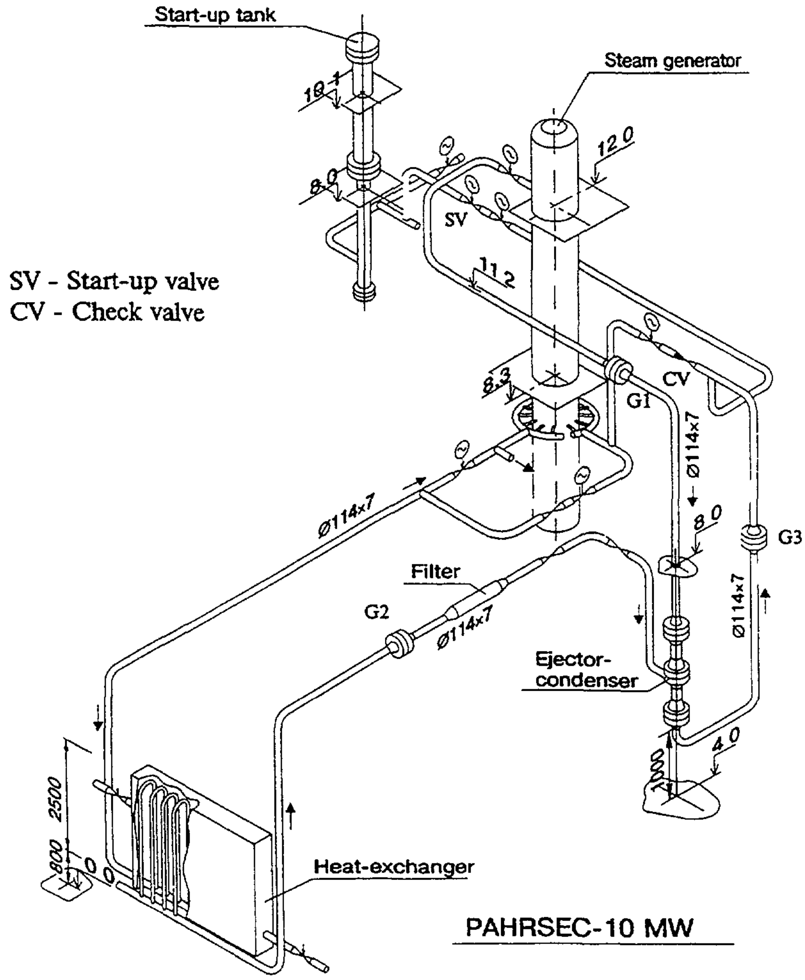

FIG. 8. PAHRSEC Test Facility of 10 MW.

Researches planned:

- start up of the System under rated SG parameters
- start up under off-design SG parameters
- repeat start-up
- operation under different disturbances
- determining the stable operation range
- heat removal under low (less than 1 MPa) SG pressure
- experimental and simulated founding serviceability of PAHRSEC in different accident conditions (black-out, SG's tube rupture, LOCA, etc.)

Fig.9 shows the 10 MW EC and Heat Exchanger. The whole 10 MW PAHRSEC is nearly ready, and its putting in service is going to be soon.

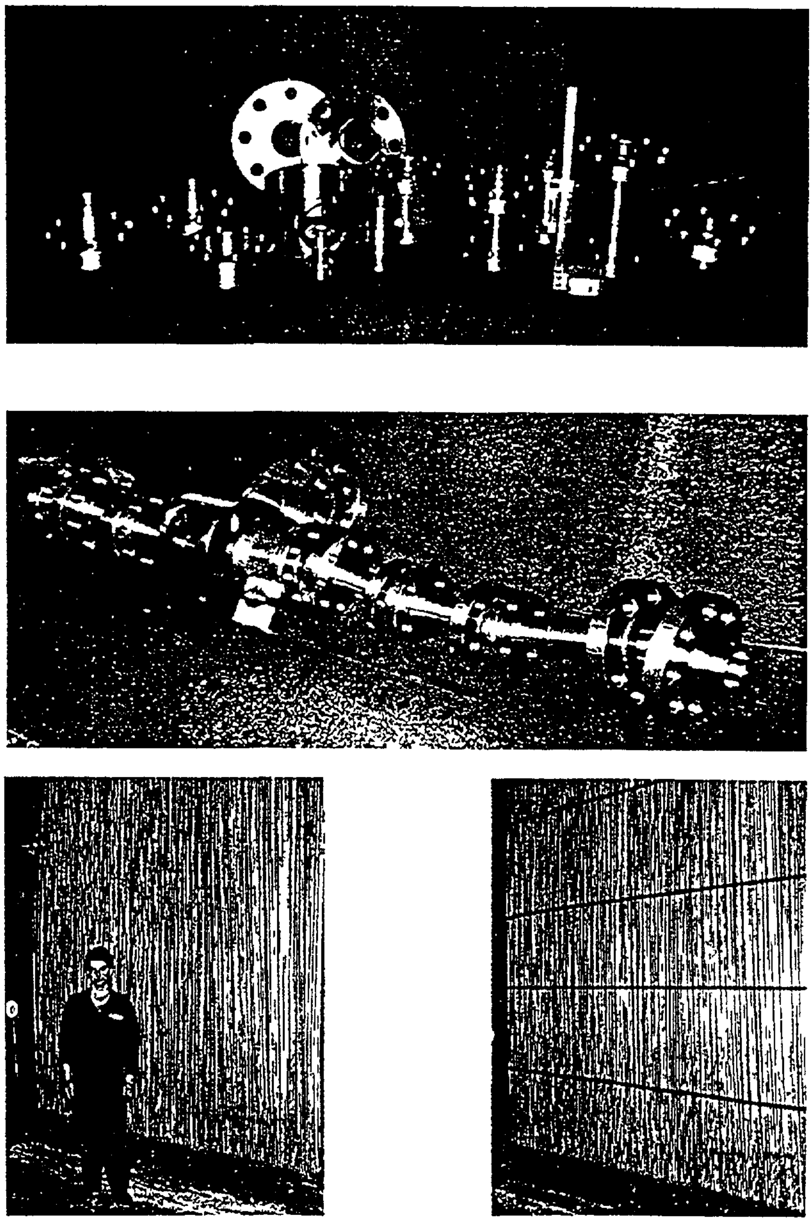

Fig 9 Ejector-Condenser and Heat-Exchanger for the Test Facility of 10 MW PAHRSEC

7. Future development of PAHRSEC

Fig.10 shows the scheme with gravitational start-up system. For that kind of EC a cylindric MC is needed. Fig.10 shows a general view of the EC. Its tests have been made and basic serviceability has been demonstrated.

PAHRSEC-2 scheme (Fig.11) has been proposed which has

- two joints with SG istead of three in "steam-liquid" scheme (Fig.2)
- stable operation under low SG pressure

PAHRSEC with Gravitational Start-Up System
(W. Reinsch)

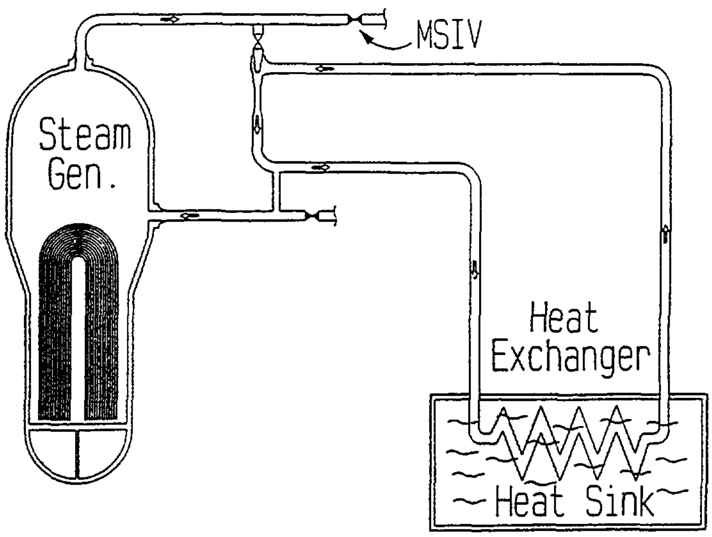

EC with Cylindric Mixing Chamber

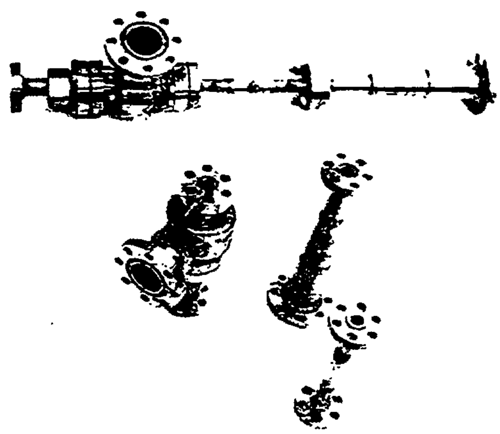

FIG. 10.

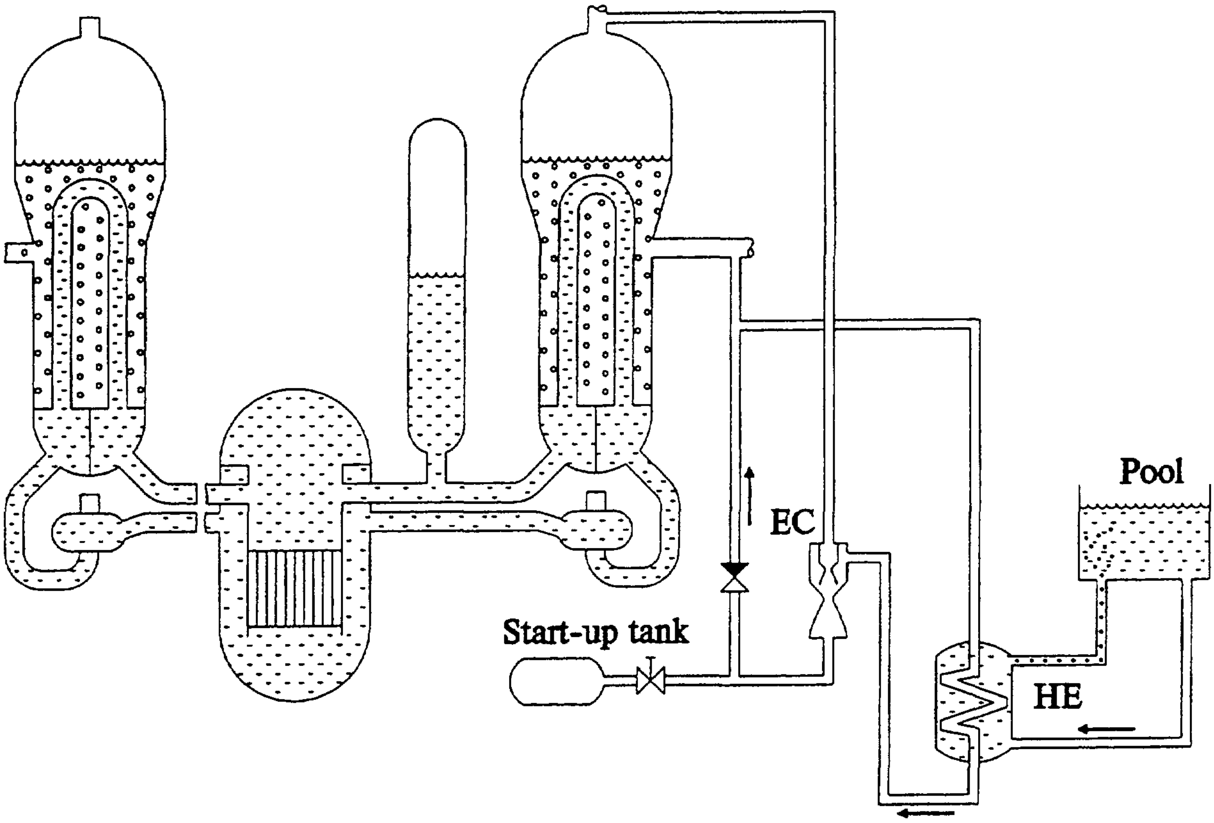

FIG. 11. PAHRSEC -2

8. PAHRSEC scheme for containment

Operation principle of the scheme on Fig.12 is the same as that for SG.
That scheme can work in two regimes:

- supply of water from the supply tank to the containment and decrease of pressure in it.
- heat removal and water circulation throughout the circuit: containment - air cooled heat exchanger - supply of "cold" water to EC - injection in containment.

Fig.12 shows also EC tested under low steam pressures 0.1 < P < 0.5 MPa. It should be mentioned that a system for water supply to containment by means of EC has been also studied in [2].

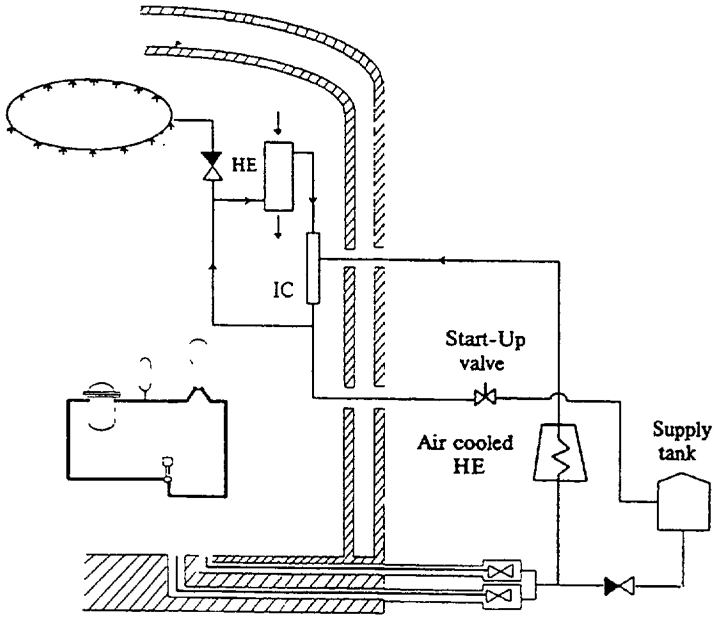

(a) Scheme of containment PAHRSEC for severe accidents

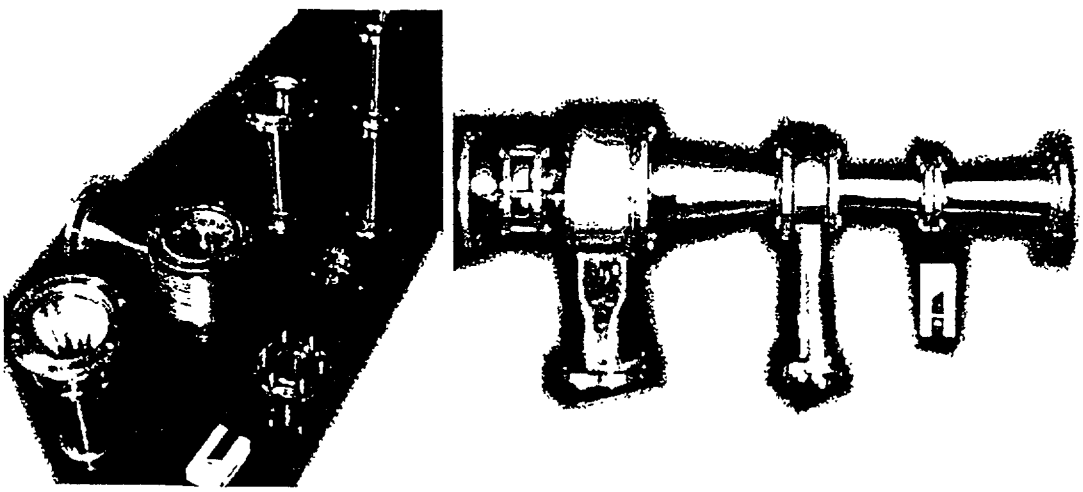

(b) EC designed for operation with low pressure steam

FIG. 12.

REFERENCES

1. G.Cattadore, L.Galbiati, L.Mazzocchi, P.Vanini, "A Single-Stage High-Pressure Steam Injector for Next Generation Reactors: Test Results and Analysis", European Two-Phase Flow Group Meeting. University of Hannover, Germany, 7 to 10 June, 1993.

2. T.Narabayashi and others, "Thermohydraulics Study of Steam Injector for Next Generation Reactor", Int. Conference on "New Trends in Nuclear System Thermohydraulics", May 30th - June 2nd, 1994 - Pisa, Italy, v.1, pp 653-661.

3. F.L.Carpentino and others, "The Safe Integral Reactor (SIR)", ABB Preprint.

AN EXPERIMENTAL STUDY ON THE BEHAVIOUR OF A PASSIVE CONTAINMENT COOLING SYSTEM USING A SMALL SCALE MODEL

D. SAHA, N.K. MAHESHWARI, D.K. CHANDRAKER,
V. VENKAT RAJ, A. KAKODKAR
Bhabha Atomic Research Centre
Bombay, India

Abstract

A Passive Containment Cooling System (PCCS) has been proposed for the Advanced Heavy Water Reactor (AHWR) being designed in India. The function of the system is the long term cooling of the reactor containment following Loss of Coolant Accident. The system removes energy released into the containment through Isolation Condensers immersed in a pool of water. An important aspect of IC working is the potential degradation of IC performance due to the presence of noncondensables. Tests have been conducted on a small scale model of PCCS with constant steam flow rate and steam flow rate simulating decay heat curve using air as noncondensable. The effect of variation of different parameters like the partial pressure of noncondensable has also been studied. The studies carried out within a limited range of values of different parameters have confirmed the efficacy of the separation of noncondensables and removal of energy released into the containment. This paper deals with the details of the test set up, the test procedure and results.

1.0 INTRODUCTION

Increasing awareness towards safety and the experience gained in the past have led to the incorporation of a number of passive safety systems in the new generation of nuclear reactors being designed. These systems depend on the natural laws of gravity, thermal-hydraulics and physics and do not require intervention of operators or use of externally actuated electrical or mechanical devices. One such system envisaged for long term containment cooling of advanced reactors following Loss of Coolant Accident (LOCA) is the Passive Containment Cooling System (PCCS). The purpose of the PCCS is to limit the containment pressure to a value below a predetermined level and to achieve a walk-away period without operator action. An analytical evaluation of different PCCS concepts indicates that the PCCS incorporating Isolation Condenser (IC) may be the best option [1]. PCCS with IC has been adopted for the Simplified Boiling Water Reactor (SBWR) [2]. It is proposed to incorporate a PCCS with IC in the Advanced Heavy Water Reactor (AHWR) being designed in India. An important aspect of IC functioning is the potential degradation of heat removal capability of IC due to the presence of noncondensables. Experimental data available on the performance of PCCS [3] is very meagre. In view of this an experimental programme to study and understand PCCS behaviour and performance is being carried out in phased manner. In the first phase experiments have been conducted on a small scale model to confirm the working principles of PCCS and to understand the various phenomena involved.

2.0 DESCRIPTION OF PCCS

A simplified diagram of the PCCS is shown in fig.1. The isolation condenser comprises of a large number of vertical tubes connected to horizontal cylindrical headers at the top and bottom. The IC is immersed in a large pool of water located at a high elevation as shown in the figure.

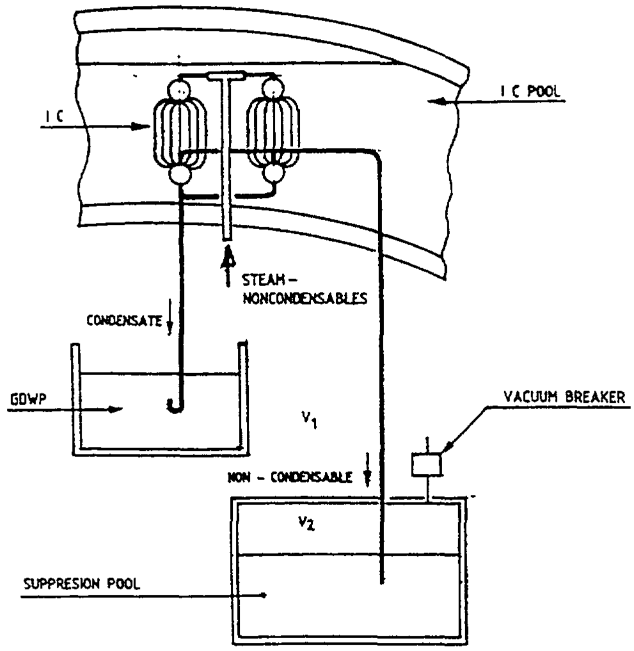

Fig.1 PASSIVE CONTAINMENT COOLING SYSTEM WITH ISOLATION CONDENSER

Steam-noncondensable gas mixture enters the IC from volume Vi (drywell) of primary containment following LOCA through a line which has no valve. Steam is condensed in IC and condensate flows by gravity to the Gravity Driven Water Pool (GDWP) from the bottom header of the IC. The noncondensables are led to the vapour suppression pool in volume V2 (wetwell) through a vent line submerged in water. Due to inflow of noncondensables into volume V2, the pressure of V2 increases. When the pressure in V2 exceeds the pressure in V1 by a preset value the vacuum breaker opens and noncondensables return to V1. When the differential pressure between V2 and V1 reduces to a preset value the vacuum breaker closes. The continued accumulation of noncondensables in IC causes degradation of the performance of IC causing pressure rise in V1. This may again cause the flow of noncondensables to V2, depending on the conditions. The PCCS is always available for containment heat removal. The differential pressure between the volumes V1 and V2 initially provides the driving head for the steam-gas mixture flow through the IC. The heat removal capability of PCCS is affected mainly by the flow path pressure loss, noncondensables inside the containment and heat transfer coefficients in the pool and IC.

3.0 TEST SET UP

Tests to study system response behaviour have been conducted on a small scale model of the PCCS (see fig.2), the volume scaling of the set up being approximately 1:3000. Elevation and hydraulic resistances could not be simulated in this small scale model. The configuration of IC has been simplified as shown in fig.2. The upflow tube is thermally insulated. The downflow tube inner diameter is 10 mm and length 300 mm. Instead of natural circulation, a small forced flow of water is maintained in the secondary side of IC. Air has been used as the noncondensable gas during the tests. The steam air mixture from volume V1 flows to IC steam box or upper header. The noncondensable gas vent line runs from IC water box or

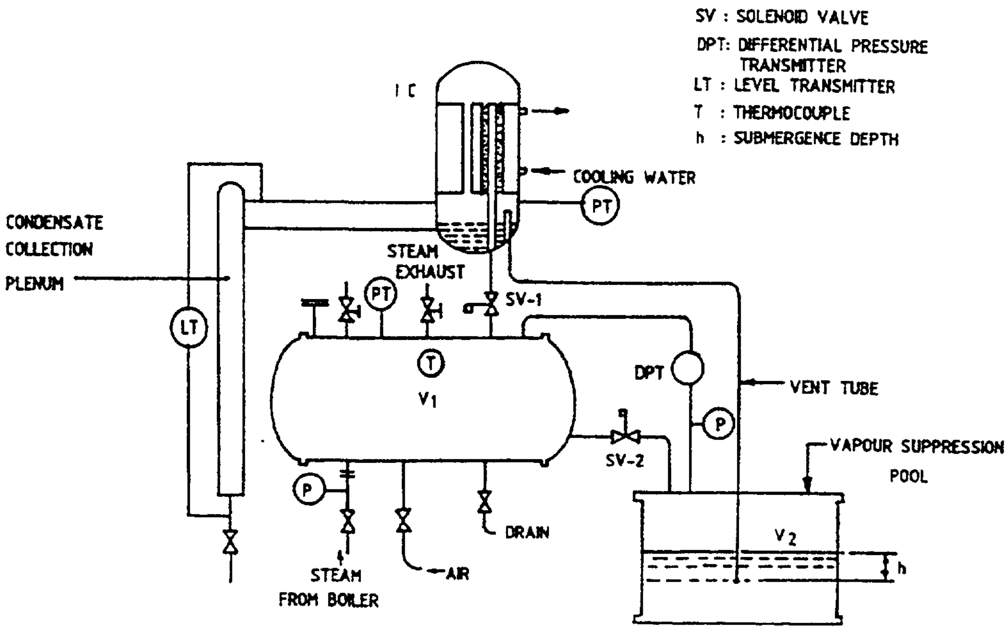

Fig. 2 EXPERIMENTAL SET-UP

lower header to suppression pool. The condensate from the IC water box flows to a condensate collection plenum which is vented at top to the gas space of the IC water box. The level of water in the plenum is maintained at an almost constant value using a valve in the drain line from the condensate plenum. Air is injected into volume V1 from a compressor and steam is introduced from a boiler.

The volume V2 is connected to the IC through the gas vent line. The vacuum breaker between the volumes V1 & V2 has been simulated by a solenoid valve and a transmitter provided for differential pressure measurement between the two volumes. Whenever the pressure of V2 exceeds the pressure of volume V1 by a specified amount, the solenoid valve opens and air flows back from volume V2 to V1. When the differential pressure reduces to a set value, the solenoid valve closes.

The pressures of volume V1, V2 & IC water box are measured by pressure transmitters. The level in condensate collection plenum is measured by a level transmitter. The temperature of volume V1 is measured at three different locations by thermocouples installed inside the vessel. Air partial pressure Pa in V1 is calculated as the difference between the total pressure Pt and steam saturation pressure. The flow of steam into the volume V1 is estimated approximately by the condensation rate of steam in the IC and condensation in V1 due to heat loss. Variation in steam flow rate into volume V1 is estimated by measuring pressure drop across a restriction in steam inlet line.

4.0 TEST CONDITION

Tests have been conducted under the following conditions.

i) By maintaining a constant steam flow into volume V1

ii) By varying steam flow rate into volume V1 as per decay heat curve. Variation of steam flow with time is depicted in Fig. 3

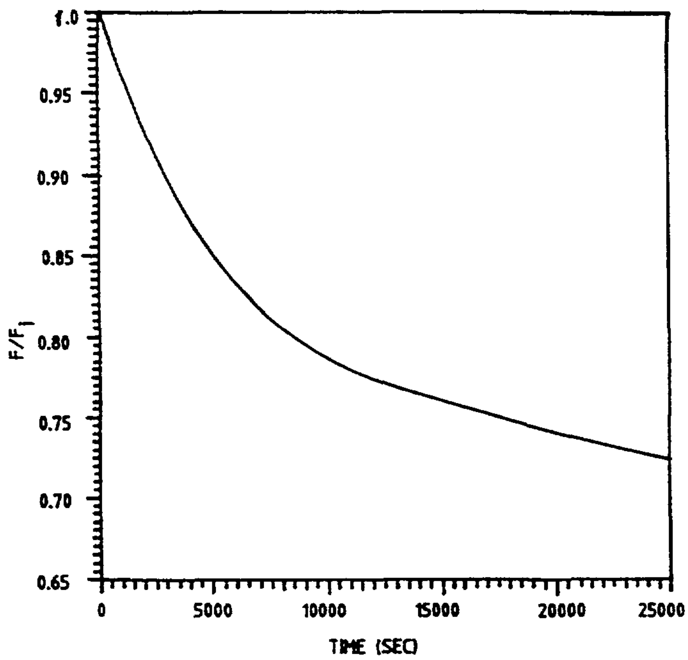

Fig. 3 VARIATION OF FLOW (F) WITH TIME

In both the above cases, initially volume V2 was maintained at atmospheric pressure. Steam flow rate into volume V1, air content and submergence depth of vent tube in suppression pool were varied during the tests.

5.0 TEST PROCEDURE

Volume V1 is initially isolated from IC and volume V2. Air was purged from volume V1 through exhaust line by supplying steam from boiler for a sufficiently long time. During this process, the V1 vessel also got heated up. After air was removed, the exhaust line was closed. The volume V1 was pressurised to initial air partial pressure by introducing air. Air line was then closed. Steam was then supplied to the volume V1 to achieve desired initial total pressure. The IC and volume V2 were maintained at cold atmospheric condition. Tests were initiated by opening the valve between volume V1 and IC. The valve in the steam inlet line was also opened simultaneously. Variable steam flow rate into V1 was achieved by operating the valve shown in figure 2. Heat loss from volume V1 was ascertained by maintaining constant pressure in this volume with through flow of steam and measuring the amount of condensate over a period of time.

6.0 RESULTS AND DISCUSSIONS

With constant steam input to volume V1, a number of experiments were conducted for different values of parameters of interest. Results of two such test runs are depicted in Figs. 4a and 4b. Fig. 4a represents a case with very low steam flow rate. In this case, because of initial high condensation rate in IC, V1 pressure first decreases and then increases with reduction in condensation rate in IC. Since the IC pressure exceeds the V2 pressure by an amount more than the submergence depth of vent tube, the vent tube water is driven out and air enters the volume V2. This causes the V2 pressure to rise. At about 3200 seconds water again enters vent tube and flow of air into V2 stops. Beyond this time no change in V2 pressure was observed. V1 pressure also remains almost unchanged since the energy removal rate of IC matches with the energy input rate. The tests were continued for about 10,000 seconds. Upto this time, no further change in the pressures of V1 or V2 was observed. Since V1 pressure was always higher than V2 pressure, during the test, the vacuum breaker simulator did not operate and there was no return of air from V2 to V1. IC water box pressure is also plotted in Fig. 4a.

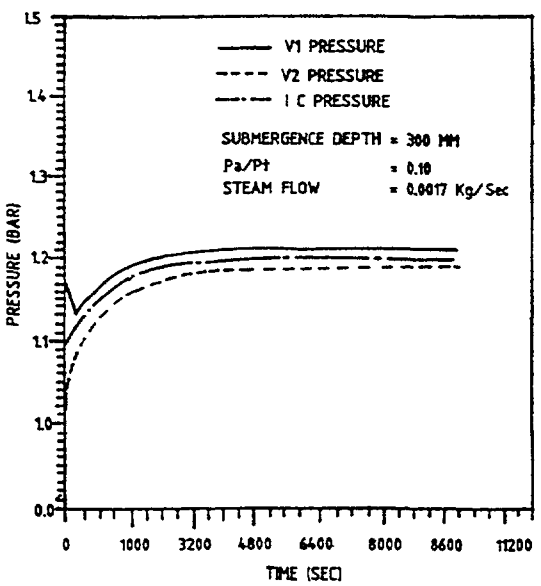

Fig. 4a PRESSURE TRANSIENTS WITH CONSTANT STEAM FLOW RATE

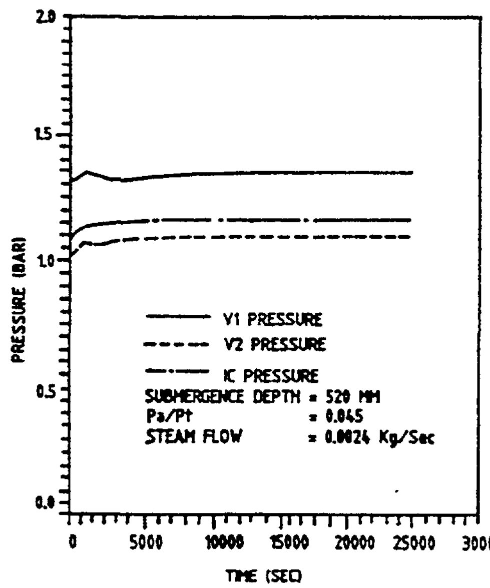

Fig. 4b PRESSURE TRANSIENTS WITH CONSTANT STEAM FLOW RATE

Fig. 4b depicts the results of another experiment with different values of parameters of interest. Because of higher steam flow rate the initial sharp decline of V1 pressure was not observed in this case. However, the subsequent trends of the pressure curves were observed to be the same as in the earlier case. Though the tests were conducted for a longer period (25,000 seconds) no decrease in V1 pressure was observed which is necessary for vacuum breaker simulator to operate. This indicates that there was no significant variation of IC heat removal rate during the test period.

Figs. 5a to 5e depict pressure transients in V1 and V2 for variable steam flow rate. It may be observed from fig. 5a that the pressure in V1 dropped below the pressure in V2 and the vacuum breaker opened (indicated by arrow in figure) at around 17,000 secs. and closed subsequently. The effect of increase in the initial amount of air in volume V1 can be ascertained by comparing figure 5b with 5a. In the case shown in 5b the vacuum breaker opened at around 15,000 seconds. However, pressures in both the volumes were found to be higher for higher initial air content. Due to limited periods over which the tests were conducted, subsequent vacuum breaker opening could not be obtained. Comparison of fig. 5a with fig. 5c reveals the effect of higher steam flow rate. From fig. 5c if can be observed that due to higher steam flow, pressure in V1 has increased considerably, but the pressure in V2 remains almost unaltered. Upto 20,000 sec vacuum breaker opening was not encountered. The effect of change in submergence depth is depicted in figs 5d and 5e. Increase in submergence depth led to an increase in V1 pressure. However, no significant change of V2 pressure was observed. For cases depicted in 5d and 5e vacuum breaker opening did not take place during the limited period for which the tests were carried out.

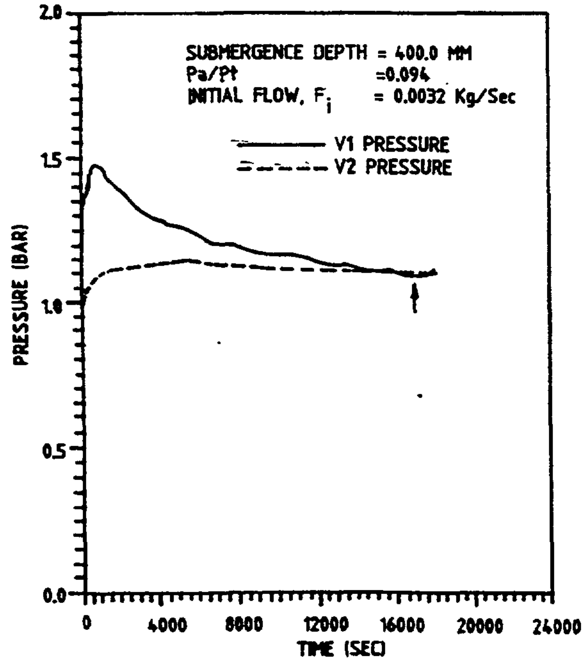

Fig. 5a PRESSURE TRANSIENTS WITH VARIABLE STEAM FLOW RATE

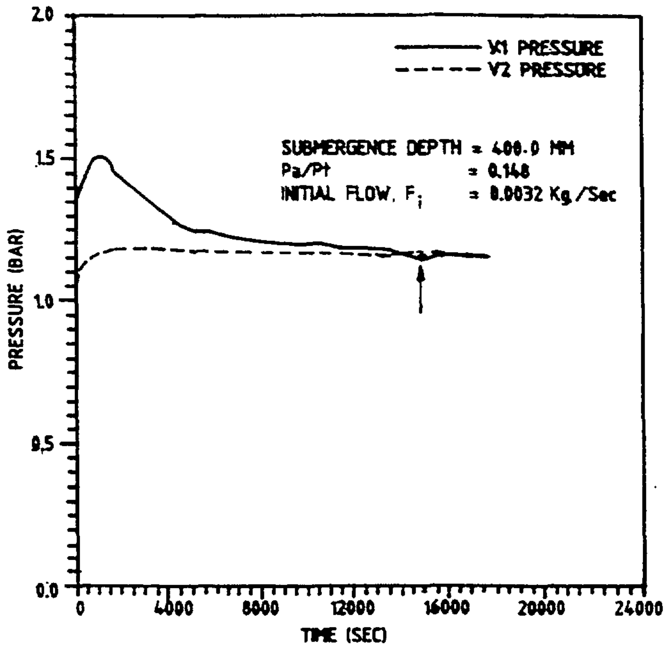

Fig. 5b PRESSURE TRANSIENTS WITH VARIABLE STEAM FLOW RATE

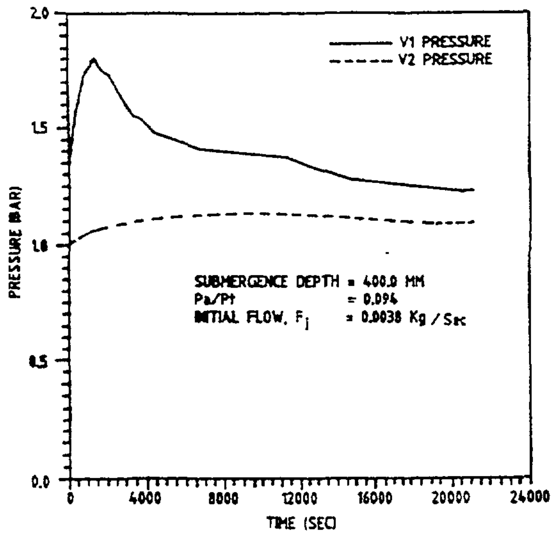

Fig. 5C PRESSURE TRANSIENTS WITH VARIABLE STEAM FLOW RATE

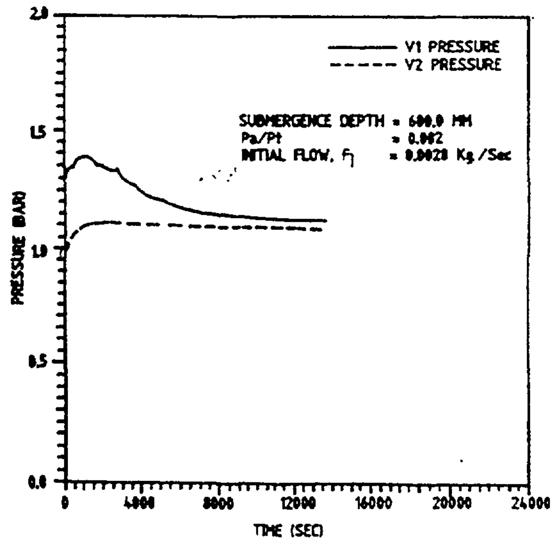

Fig. 5d PRESSURE TRANSIENTS WITH VARIABLE STEAM INPUT

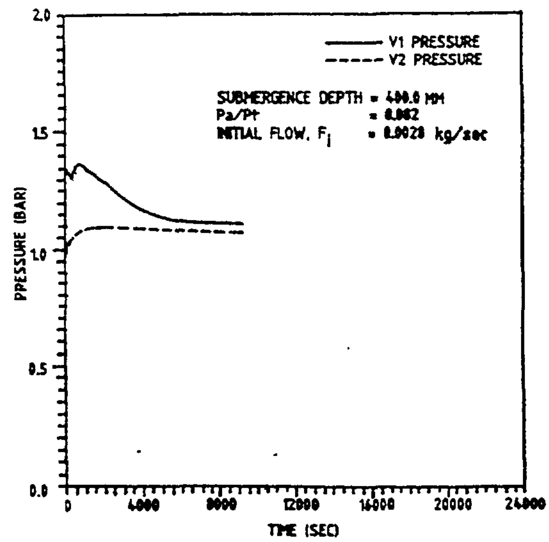

Fig. 5e PRESSURE TRANSIENTS WITH VARIABLE STEAM INPUT

7.0 CONCLUSIONS

1. The tests conducted over the limited range of values of different parameters have confirmed the efficacy of PCCS in separating the noncondensables and removal of energy released into the containment.

2. During experiments with constant steam flow rate, pressures in volumes V1 and V2 had attained almost a steady value after initial transients. Vacuum breaker did not open in this case since V1 pressure was always higher than V2 pressure.

3. During experiments with reducing steam flow rate (simulating decay heat curve) V1 pressure dropped below the pressure of volume V2 causing vacuum breaker to open. The reduction of V1 pressure can be attributed to the decrease in steam flow rate and improvement of IC performance.

ACKNOWLEDGEMENT

The authors gratefully acknowledge the help rendered by Shri M.L. Dhawan of RED, BARC. Thanks are also due to Instrumentation Section of RED.

NOMENCLATURE

F : Flow
Fi : Initial Flow
h : Submergence depth
Pa : Air partial pressure
Pt : Total pressure

REFERENCES

1. Hirohide Oikawa et al., "Heat Removal Performance Evaluation of Several Passive Containment Cooling Systems During Loss of Coolant Accident" J. of Nucl. Science & Technology, V 28, N10, Oct., 1991.

2. M. Brandani et al. "SBWR - Isolation Condenser and Passive Containment Cooling: An Approach to Passive Safety." Proceedings of IAEA TCM, IAEA-TECDOC-677, Rome, Sept. 1991.

3. Seliechi, Yokobori et.al. "System Response Test of Isolation Condenser Applied as a Passive Containment Cooling System." The 1st JSME/ASME Joint International Conference on Nuclear Engineering, Tokyo, November, 1991.

RESULTS OF SAFETY-RELATED COMPONENTS/SYSTEMS TESTS

(Session IV)
Part 2

Chairman

E.F. HICKEN
Germany

STEAM INJECTOR DEVELOPMENT FOR ALWR's APPLICATION

G. CATTADORI
SIET- Piacenza

L. GALBIATI, L. MAZZOCCHI
CISE Technologie Innovative - Segrate, Milan

P. VANINI, V. CAVICCHIA
R&D Department, Nuclear division,
ENEL , Rome

Italy

Abstract

Steam Injectors (SI's) can be used in Advanced Light Water Reactors (ALWR's) for high pressure makeup water supply; this solution seems to be very attractive because of the "passive" features of SI's, that would take advantage of the available energy from steam without introduction of any rotating machinery. In particular, SI's could be used for high pressure safety injection in BWR's or for emergency feedwater in the secondary side of evolutionary PWR's.

An instrumented Steam Injector (SI) prototype, operating at high pressures, has been built and tested. The experimental results confirm the capability of tested SI to operate at constant inlet water pressure (about 0.3 MPa) and inlet water temperature up to 50°C, with steam pressure ranging from 2.5 to 9 MPa (4.5-9 MPa at maximum inlet water temperature). The discharge pressure target (10% higher than steam pressure) was fulfilled in the operating range. It should be noted that the minimum operating limit can be lowered to 1.5 MPa with some modifications. To achieve these results an original double-overflow flowrate-control/startup system, patented by ENEL/CISE in 1993, has been used.

1. INTRODUCTION

A *Steam Injector* (SI) is a device without moving parts, in which steam is used as the energy source to pump cold water from a pressure lower than the steam to a pressure higher than the steam. In fact, a large amount of heat, available from steam condensation, can be partly converted into mechanical work useful for pumping the liquid. In this respect, SI can be regarded as equivalent to different devices, like turbine-driven pumps, where steam thermal energy is used to pressurize a liquid; in comparison to this kind of equipment, the main difference is that in SI all thermodynamic processes rely on direct contact transport phenomena (mass, momentum and heat transfer) between fluids, not requiring any moving mechanism.

The SI can be divided into the following regions:

a) steam nozzle, producing a nearly isentropic expansion and partially converting steam enthalpy into kinetic energy; it can be a sonic nozzle or, if a stronger expansion is required, a supersonic nozzle with the typical converging-diverging shape;

b) water nozzle, producing a moderate acceleration and distributing the liquid all around the steam nozzle outlet;

c) mixing section, where steam and water come into contact. Steam transfers to water heat (because of temperature difference), mass (because of the related condensation) and momentum (because of velocity difference). The final result is the complete steam condensation, with an outflowing subcooled liquid at relatively high pressure. The shape of the mixing section is usually converging, for reasons reported in [1];

d) diffuser, where the liquid kinetic energy at mixing section outlet is partially recovered producing a further pressure rise.

It should be noted that the arrangement of steam and water nozzles could be inverted, creating a circular water nozzle and an annular steam nozzle as reported in [2]. In another type of arrangement, [3], the annular water jet is accelerated both by central and outer steam jet. However, is authors' opinion that the central steam jet/outer liquid configuration should be more convenient because it minimizes the perimeter of the steam nozzle and avoids the direct contact between steam and mixing section walls; in this way viscous dissipations should be reduced.

SI's were used as feedwater supply devices in locomotives and in the Merchant Marine since World War II and are manufactured by a few companies for applications in food and paper industry. In nuclear field, several systems based on high-pressure steam-injectors were proposed in [1], [4], [5] and [6].

It should be noted that, with respect to nuclear systems, the attractiveness of SI's is quite evident, because a high pressure water supply can be essential to very important emergency functions (like emergency core cooling, feedwater supply for decay heat removal and so on) and usually a steam supply is easily available in power plants. Moreover, SI can be regarded to a great extent as a passive system, as it does not require any external energy supply or moving mechanical part.

However, commercially available SI's operate at "low" pressure (< 2 MPa). Moreover, no single-stage high-pressure steam injector is available from previous research programs undertaken in [4] and [5] (for application to a BWR). In [6], a high pressure SI has been developed for application to CANDU reactors but the maximum discharge pressure was limited at about 4 MPa. In [6] a single-stage high-pressure steam injector has been developed for application to the secondary side of a VVER-440 but the inlet liquid pressure was, basically, at the same pressure of the steam generator so that the pressure gain requested to the component was very limited.

In 1991, ENEL, the Italian Electricity Generating Board, which is engaged in a wide range of activities concerning ALWR's, decided to evaluate the applicability of a **single-stage SI** for a ALWR's application; so, CISE was charged to perform an SI development project in cooperation with ENEL itself. The results of this project can be found in [7]: tested SI operated with steam pressure ranging from 2.5 to 8.5 MPa, always fulfilling the discharge pressure target (10% higher than steam pressure), with inlet water temperature up to 37°C. However, in order to improve the SI performance (reducing, in particular, the steam consumption, see ch. 3.3) an additional optimization study on the injector design, was undertaken by CISE in cooperation with ENEL. The corresponding experimental activity was performed at SIET laboratories in 1994. Results are reported below.

2. EXPERIMENTAL SETUP

The test section used in the experimental activity was made of stainless steel (figure 1). As can be seen, on the basis of the results obtained in [7], two overflow openings (primary and secondary overflows) where realized on the mixing chamber in order to allow SI start-up and discharge flowrate control. The SI was tested at SIET laboratories where a steam-water test facility was designed and built. Figure 2 shows a schematic diagram of the experimental plant which supplies metered flows of steam and water to the test section and which includes equipment for controlling and measuring the thermalhydraulic parameters. An open loop including pumps, heat exchangers and a pressurizer (volume = 1 m^3) provided demineralized water to the SI at the required conditions; water flowrates up to 25 kg/s were available, with fluid pressure and subcooling controlled at the test section inlet. A line coming from an external boiler provided superheated steam up to 5 kg/s flowrate and 9 MPa pressure; liquid injection was used to control the steam temperature at the test section inlet. Open-system operation was straightforward, with the total discharge directed to condenser. The test section discharge pressure was varied by means a control valve. The following measurements were taken during the tests:

- ☐ inlet liquid and steam flowrates;
- ☐ inlet and outlet fluid pressures and temperatures;
- ☐ axial pressure profiles in the different SI components: steam nozzle, water nozzle, mixing section, diffuser (totally 60 measurement stations).
- ☐ primary and secondary overflow temperatures and flowrates.

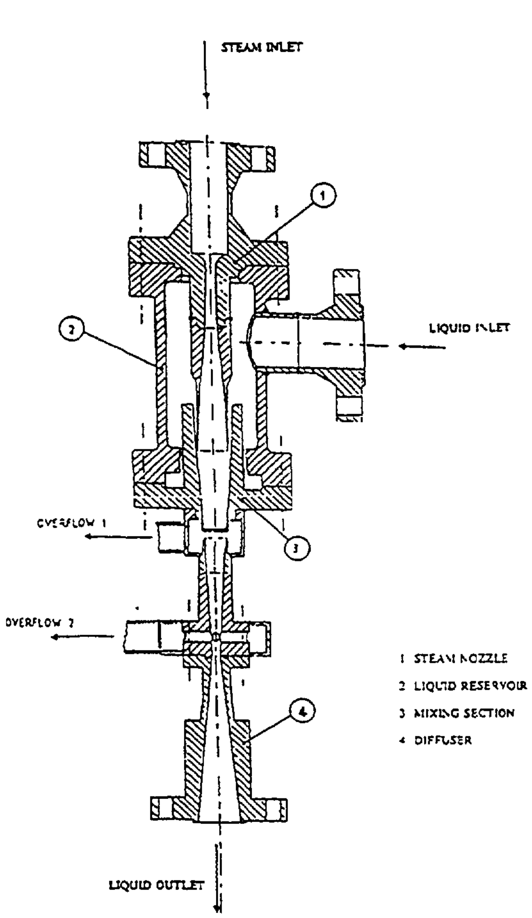

Figure 1 - Test section schematic

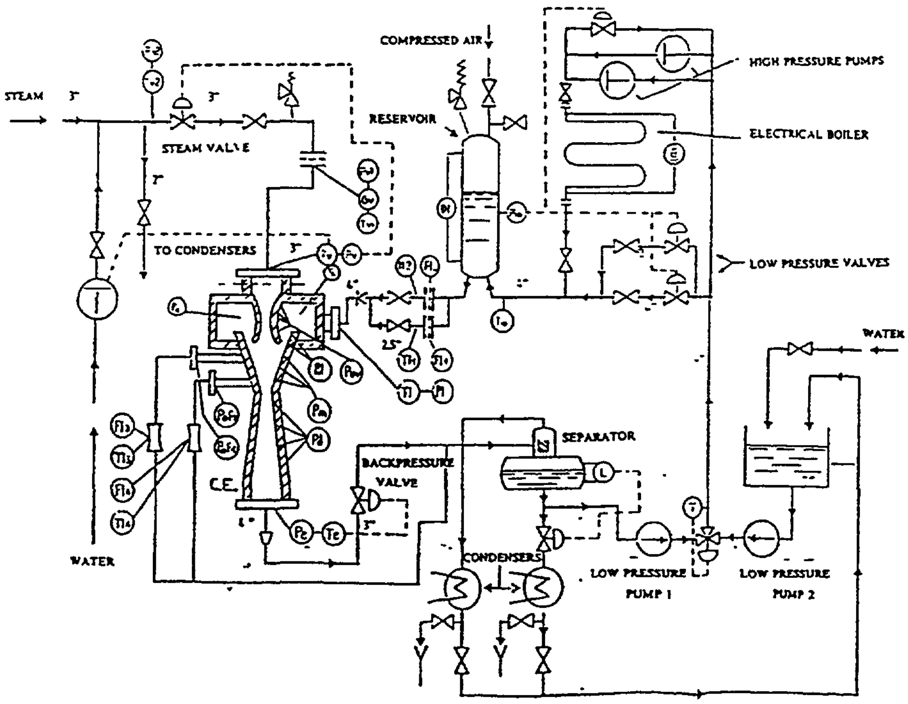

Figure 2 - Schematic of
the test facility

Flowrates were measured by means calibrated orifice plates (accuracy = 2% of reading). Temperatures and pressures were measured by K-type thermocouples (accuracy = 1°C) and by thin film-type pressure transmitters (accuracy = 0.1% FS), respectively.

3. TEST RESULTS AND DISCUSSION

3.1 Independent and dependent variables

There were four independent variables to be controlled or selected for each test run. These four can be described as:

- ☐ steam supply pressure;
- ☐ steam superheat;
- ☐ water supply pressure;
- ☐ water supply temperature.

To these four indipendent variables, concerning fluid conditions, it should be added:

- ☐ backpressure valve setting;
- ☐ OF2 valve setting (OF1 valve could be always closed after startup).

On the other hand, several dependent variables (for any given set of indipendent variables) were selected and measured.
They were:

- ☐ water supply flow rate;
- ☐ water/steam flow rate ratio (ω);
- ☐ steam nozzle pressures;
- ☐ mixing section pressures;
- ☐ primary and secondary overflow pressures/flowrates;
- ☐ diffuser pressures.
- ☐ discharge liquid pressure;
- ☐ discharge liquid temperature.

The range of the independent variables explored in the test program is shown in table I. As can be noticed, the tests were conducted in a wide range of steam pressure (2.5 MPa - 9 MPa). Steam superheat was varied (between 1-16°C). The inlet water pressure to the test section was kept constant at about 300 kPa. The inlet water temperature was varied from 15°C to 50°C. The reason for this was to check the injector expected performance degradation at increased water temperature.

Main dependent parameter variations are summarized in table II.

table I - RANGE OF INDIPENDENT VARIABLES

Steam supply pressure	2.5 - 8.9 MPa
Steam superheat	1 - 16 °C (max. steam quality = 1.06)
Water supply pressure	300 kPa
Supply water temperature	15 - 50 °C

table II - RANGE OF DEPENDENT VARIABLES

Inlet liquid flowrate	16-19 kg/s
Liquid-to-steam flowrate ratio (ω)	3-12
Discharge liquid pressure	2.8 - 9.8 MPa
Discharge liquid temperature	78 - 197 °C
Primary overflow pressure	77 - 476 kPa
Secondary overflow pressure	247 - 2994 kPa
Discharge flowrate	3.5 - 14.5 kg/s

3.2 Discharge pressure

The injector discharge pressure for the entire test series is summarized in figure 3. This figure shows the pressure at the diffuser outlet as a function of the injector inlet steam pressure. In figure 4, the axial pressure profile at maximum inlet steam pressure is shown (the profile is similar at lower supply steam pressures). It should be remembered that discharge pressure was fixed at an approximately constant value (10% higher than inlet steam pressure), in order to meet the specifications. Tested one-stage SI developed sufficient discharge pressure except when steam supply pressure was less than about 2.5 MPa. It should be noted that maximum inlet steam pressure could not be increased over 9 MPa because of limitations of the experimental facility. Actually, the component can develop sufficient discharge pressure even at higher inlet steam pressures (provided that steam condensation is complete).

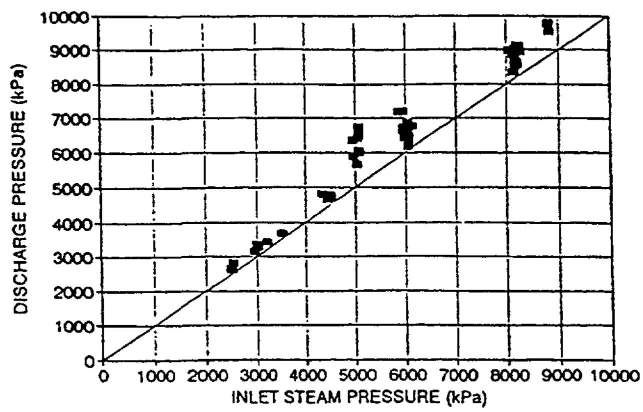

Figure 3 - SI discharge pressure: experimental results

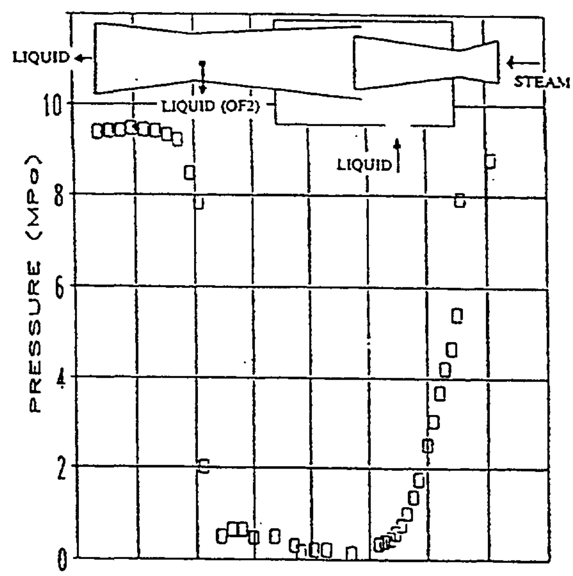

Figure 4 - Experimental pressure profile along the mixing section

3.3 Discharge Flowrate

Discharge flowrate is shown in Fig 5 at different inlet liquid temperatures It can be noted that discharge flowrate decreases when inlet liquid temperature increases

Figure 5 - Discharge Flowrate at different inlet liquid temperatures, OF2 optimal setting

□ Tl=27°C, ◘ Tl=42°C ■ Tl=50°C

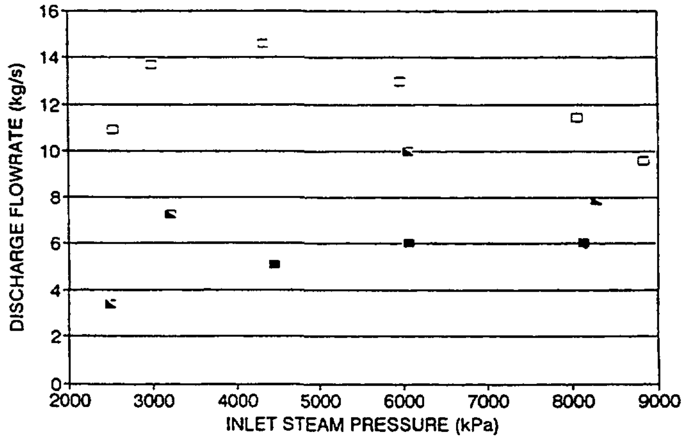

3.4 Steam Consumption

Steam consumption is an important parameter in order to evaluate the performance of an injector In particular specific steam consumption (Steam Rate, SR) can be defined as

$$SR=\frac{\Gamma_G}{(\Gamma_L-\Gamma_{OF2})}$$

where Γ_G and Γ_L are, respectively, the steam and liquid flowrates entering the SI and Γ_{OF2} is the liquid flowrate leaving the SI from secondary overflow

In figure 6 SR values at different inlet water temperatures and steam pressure are shown in case of optimized OF2 setting (Appendix 1, test series I, optimized data) It can be seen that SR increases with inlet steam pressure and inlet water temperature (test series II)

Figure 6 - Steam Rate (SR) at different temperatures, OF2 optimal setting

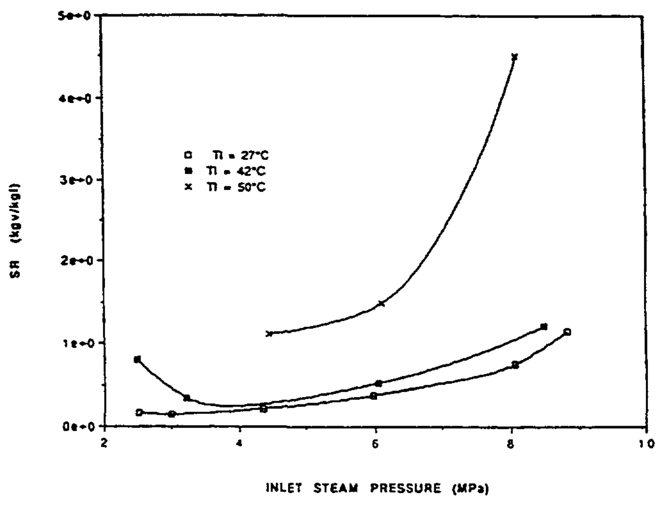

3.5 SI Characteristic

Figure 7 shows a typical SI characteristic (obtained using the procedure reported in App. I. test series III). The inlet steam pressure is 5 MPa and the inlet water pressure is 0.3 MPa. The inlet water temperature is 15°C. The characteristic is similar to that for a centrifugal pump: the discharge pressure drops as the discharge flow rate becomes larger and larger.

It should be noted that, in case of "low"-pressure injector, *without any overflow*, the injector performs as a positive displacement pump so that a constant flowrate is discharged against a range of backpressures, as noted in [8]. So, an SI can be regarded as a positive displacement pump at "low" pressures (where high mixing section area contraction ratios are not required and overflow is not necessary) and a centrifugal pump at "high" pressures (where secondary overflow spillage is needed).

Figure 7 - SI characteristic (P_{LO}=300 kPa, T_L=15°C, P_{GO}=5MPa)

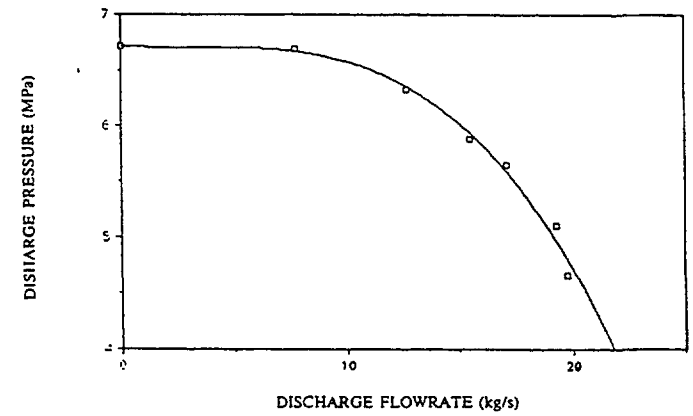

3.6 Liquid-to-Steam Flowrate Ratio

The liquid-to-steam flowrate ratio (ω) was ranging between 3 and 12. ω is a significant variable because the principle of operation of the SI relies on the steam being condensed by the water in the mixing section and producing vacuum. If the water/steam flow rate ratio is too low, the steam will not be completely condensed in the mixing section. On the other hand, according to available theories, the maximum pressure which can be developed by the injector decreases as the water/steam ratio increases. Thus for the best pressure performance, the injector should be operated at low water/steam ratio but not so low that the steam will not condense completely. The water/steam flow ratio for a test could be varied by changing the steam supply pressure to the injector: the lower limit, for which condensation can be complete, depending also on backpressure setting, was not found. In fact, as reported above, because of design limitation of the experimental facility, the inlet steam pressure could not be increased over 9 MPa.

3.7 Flowrate Spillage

The tested SI spills some of the water being pumped. In figure 8 spillage at constant inlet liquid pressure (300 kPa) and different temperatures is shown: inlet steam pressure being costant, spillage increases with temperature.

Figure 8 - OF2 spillage: temperature effects (P_{LO}=300 kPa)

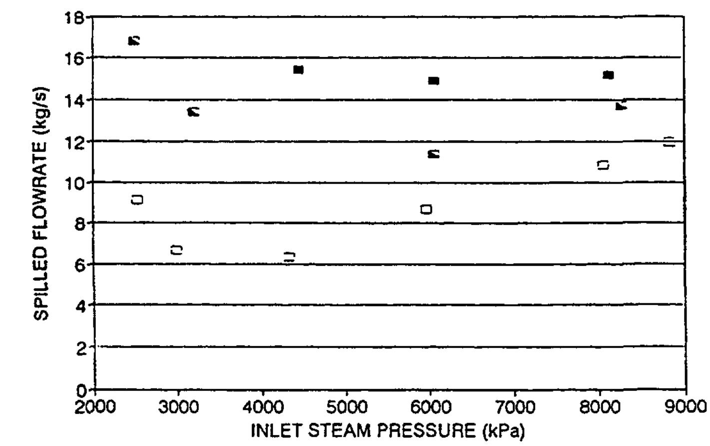

3.8 Low Quality Tests

Several tests (Test series IV) were performed at low-quality values of the steam entering the test section (down to x=0.28-29). The SI operated in a very good way. The steam nozzle expansion ratio decreased at low inlet steam quality. For this reason, the liquid suction in the mixing chamber decreased. Nevertheless, being the two-phase flow mass entering the steam nozzle higher than the mass of pure steam, the total mass entering the SI was found to be approximately constant at different inlet steam quality values. On the other hand, it has been found that the secondary overflow spillage tends to decrease at low steam quality, while discharge flowrate, as a consequence, has an opposite trend.

As far as SR is concerned, this parameter (if it is referred to the pure steam entering the SI) decreases at low quality tests in comparison to tests at x=1 or x>1. However, it is possible to introduce a further parameter, SRa, defined as the ratio between the steam nozzle outlet steam flowrate (Γ_{Ga}) and the net flowrate pumped by the steam injector (Γ_L - Γ_{OF2}):

$$SRa = \Gamma_{Ga}/(\Gamma_L - \Gamma_{OF2}).$$

The steam nozzle steam outlet flowrate can be derived assuming an isentropic expansion in the steam nozzle and calculating the steam quality x_a at the nozzle exit as:

$$x_a = (s_o - s')/(s'' - s')$$

where s_o is the specific entropy at steam nozzle inlet section and s', s" represent the specific liquid and steam entropies at steam nozzle outlet section, calculated at the pressure of the steam after the expansion in the nozzle. When SRa is calculated (Fig. 9), this parameter seems to be only slightly affected by any change of inlet steam quality (even if tends to decrease at low steam qualities). In fact, it has been found that the mass of steam at the mixing section inlet shows just a slight decrease at low inlet steam qualities. In conclusion, it can be said that, at low inlet steam quality, the injector performance is only slightly affected by the higher quantity of liquid entering the steam nozzle: SI performance depends on the actual steam flowrate after expansion and on the actual steam nozzle expansion ratio (which keeps approximately constant the total mass flowrate entering the injector)

Figure 9 - "Low" quality tests: modified steam rate (SRa)

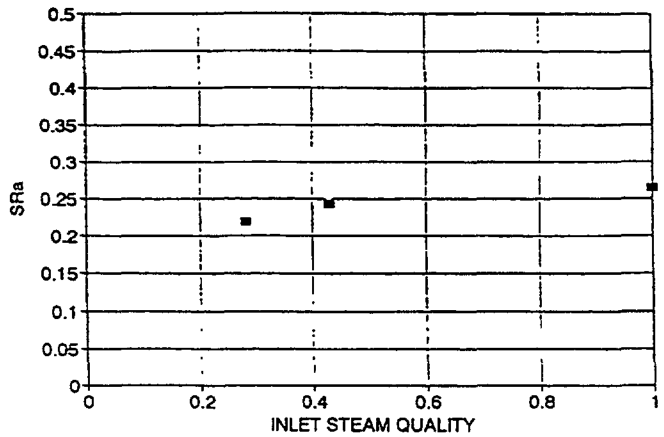

3.9 Modified Test Section

The main objective of the described tests was to minimize the steam consumption: indeed, at inlet liquid temperature of 37°C and at maximum inlet steam pressure (9 MPa), steam rate was reduced about 5 times in respect to [7].

However, if a higher steam consumption is accepted, SI operating range can be extended. In fact, using a modified test section (derived from the previous configuration by a reduction of the liquid nozzle area), several tests were performed at constant liquid pressure (about 300 kPa) and different inlet liquid temperatures (up to 42°C). SI operating range was wider (1.5-9 MPa) but, at the same time, steam rate was higher (about 2.2 at 9 MPa and T_L=27°C), figure 10.

Figure 10 - Modified test section: steam rate (SR) at different temperatures

□ Tl=27°C; ■ Tl=42°C

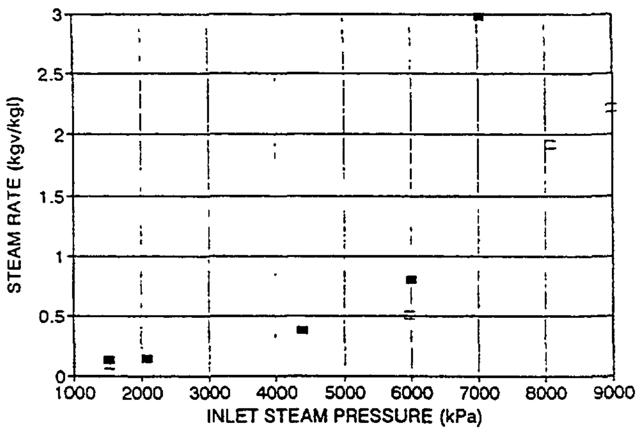

4. APPLICATION TO ALWR's

4.1 Application to BWR's

SI's can be used in BWR's in a high pressure coolant injection system. Using only reactor dome steam and steam pressure to actuate OF2 valve (see after), the SI system would be capable of drawing cold water from selected sources (e.g. the condensate storage tank) injecting this water into the reactor.

An automatic double overflow flowrate control/startup system can been envisaged using two valves, connected to OF1 and OF2 discharge lines. The OF1 line is provided for startup when the injector is full of water. Steam entering the injector would initially purge standing water in the mixing section and a steam/water mixture would flow through OF1 discharge line to the suppression pool for several seconds until a sufficient suction flowrate is established to enable full condensation of the steam in the mixing section and sufficient pressure is obtained to direct flow to the reactor vessel. As steady state flow has been established, the relief valve in the OF1 line will close due to the drop in the static pressure inside the mixing section, resulting from the acceleration of flow in the mixing section itself.

As regards the secondary overflow, a valve controlled by steam pressure could be inserted on OF2 line: in fact, optimal discharge flow through OF2 line depends on inlet steam pressure. This valve would tend to open at low inlet steam pressure, allowing a suitable liquid flowrate discharge: on the contrary, OF2 valve would be almost close at high inlet steam pressure.

An additional possibility would be to modulate the inlet liquid flowrate by means of a valve controlled by inlet steam pressure: in this case, at constant discharged liquid flowrate, water consumption would be reduced and operating range would be extended down to very low steam pressures.

Comparing the experimental results with the performance requirements specified in [1] for a 600 MWe BWR application, it can be derived that the present SI fully satisfy the above requirements in terms of pressure, with a scaling factor about 1:4 in terms of discharge flowrates.

4.2 Application to PWR's

SI's can be applied to the secondary side of PWR's. In this case, steam from the steam generators operating at a pressure ranging in the field of safety/relief valve opening set-point can be used to run a SI supplying feedwater back to the steam generators. Cold water could be taken from the demineralized water storage tank. As far as system automation is concerned, the same start-up/flowrate control system described in the previous paragraph could be used. A simulation with RELAP5/MOD2 has been performed, [9], to verify the expected performance of the SI taking into account the various interactions between this component and the secondary side of a PWR. The analysis has demonstrated the adequacy of SI in removing long term decay heat and preventing excessive heatup of the reactor coolant system. In particular, simulation results show that, assuming a 600 MWe PWR reactor (2 loops), the SI can operate till 12 days after scram (when its lower operating limit, 2.5 MPa, is reached). It should be noted that the present SI is characterized by a scaling factor about 1:1.5 (in terms of discharge flowrates) in respect to the full size component (designed for one loop).

5. CONCLUSIONS

The test results showed that CISE one-stage high-pressure SI can operate, at constant liquid pressure (about 0.3 MPa), with steam pressure ranging from 2.5 to 9.0 MPa and supply water temperature ranging from 15 to 50°C, providing water to a discharge fixed pressure about 10 percent higher than steam pressure.

It should be noted that:

- ☐ steam consumption is quite low and tends to increase with inlet liquid pressure and temperature and with steam pressure;
- ☐ the tested high-pressure SI spills some of the water being pumped (at least at constant supply water pressure). Spillage increases as the supply-water temperature increases;
- ☐ the high-pressure SI (due to secondary overflow spillage) can be regarded as a centrifugal pump.

REFERENCES

[1] CATTADORI, G., GALBIATI, L., MAZZOCCHI, L. & VANINI, P., Steam Injector Analysis and Testing. European Two-Phase Flow Group Meeting, The Royal Institute of Technology, Stockholm, Sweden (1992).

[2] FITZSIMMONS, G. W. Simplified Boiling Water Reactor Program. Steam Injector System. Final Report, GE-NE, GE FR 00876 (1990).

[3] NARABAYASHI, T., ISHIYAMA, T., MIYANO, H., NEI, H. & SHIOIRI, A. Feasibility and Application on Steam Injector for Next-Generation Reactor. 1st JSME/ASME Joint International Conference on Nuclear Engineering (1991) p. 23-28.

[4] NARABAYASHI, T., IWAKI, C., NEI, I., MIZUMACHI, W., SHIOIRI, A., Thermalhydraulics Study on Steam Injector for Next Generation Reactor. New Trends in Nuclear Systems Thermohydraulics (1994) p. 653-661.

[5] SUURMAN, S. Steam-Driven Injectors Act as Emergency Reactor Feedwater Supply, "Power", 3 (1986) 95.

[6] SOPLENKOV, K. Passive Heat Removal System with Injector-Condenser (PHRS-IC). Electrogorsk Research & Engineering Centre of Nuclear Plant Safety (1994).

[7] CATTADORI G., GALBIATI, L., MAZZOCCHI, L. & VANINI, P., A Single Stage High-Pressure Steam Injector for Next Generation Reactors: Test Results and Analysis, International Journal of Multiphase Flow, in press (1995)

[8] GROLMES, M.A. Steam-Water Condensing-Injector Performance Analysis with Supersonic Inlet Vapor and Convergent Condensing Section, ANL-7443 (1968)

[9] GALBIATI, L., MARTINI, R., Application of a high-pressure steam injector to the secondary side of a PWR. Report CISE-SPT-94-43 (1994)

NOMENCLATURE

A	cross sectional area
OF1	primary overflow
OF2	secondary overflow
T	temperature

Greeks

Γ	mass flowrate
ω	liquid-to-steam flowrate ratio

Subscripts

G	steam
L	liquid
OF2	secondary overflow
a	steam nozzle outlet, mixing section inlet
e	mixing section outlet, diffuser inlet
o	rest conditions

APPENDIX 1

TEST PROCEDURES AND TEST PROGRAM

The startup sequence in the tests was the following

a) at the startup both overflow valves and backpressure valve were opened,

b) water supply valve was opened first and most of the initial water flow was discharged through the overflow lines,

c) when the steam supply valve was opened, condensation began in the mixing section,

d) a strong vacuum developed in the mixing section and the primary overflow valve could be closed

At this point a performance optimization sequence was adopted

e) the OF2 valve was partially closed (avoiding any interferences with the flow developed in the mixing chamber),

f) the discharged backpressure could be increased by closing the backpressure valve till discharge pressure was 10% higher than inlet steam pressure At this point data from data acquisition system were recorded,

g) the OF2 valve was closed step by step (setting every time the backpressure valve to give discharge pressure always 10% more than inlet steam pressure) till stalling was reached

After every backpressure valve setting, data were recorded

Four test series were performed in testing program

Test series I Using the above startup-optimization sequence tests were performed at constant inlet liquid pressure (300 kPa) an temperature (27°C) for different inlet steam pressures

Test series II At constant inlet liquid pressure (300 kPa), water temperature was increased up to 50°C, using again the described startup-optimization sequence

Test series III Tests were performed and an SI "characteristic" (similar to that of a centrifugal pump characteristic) was derived using the following procedure inlet liquid pressure and temperature were fixed together with the inlet steam pressure Then, at different backpressure valve position, OF2 valve was gradually closed till stalling

Test series IV In order to investigate the SI behaviour in case of a two-phase mixture entering the steam nozzle some tests were performed with an inlet steam quality less than 1 (down to x=0 28) The above optimization sequence was also used in these tests

TESTS ON FULL-SCALE PROTOTYPICAL PASSIVE CONDENSERS FOR SBWR APPLICATION

P. MASONI
ENEA ERG FISS,
Bologna, Italy

A. ACHILLI
SIET,
Piacenza, Italy

P.F. BILLIG
GE Nuclear Energy,
San Jose, California, USA

S. BOTTI, G. CATTADORI, R. SILVERII
SIET,
Piacenza, Italy

Abstract

The Simplified Boiling Water Reactor (SBWR) is an evolutionary design in boiling water reactors. A key feature of the SBWR is the use of simple passive systems to respond to any type of design basis event (DBE). Two of these systems are the Passive Containment Cooling System (PCCS) and the Isolation Condenser System (ICS).

As a part of the SBWR design and U.S. certification program, GE and the Italian companies ANSALDO, ENEA, and ENEL are sponsoring a test program of full-scale, prototypical condensers for both ICS and PCCS, at full pressure, temperature and flow conditions. The PCC and IC full-scale prototypes were designed, and were manufactured by ANSALDO. The tests are performed by SIET at the Performance ANalysis and Testing of HEat Removal Systems (PANTHERS) facility. ENEA has the responsibility to co-ordinate the tests and to perform pre- and post-test analysis. Both the thermal and structural performance of the heat exchangers are measured in these tests at various conditions the units might experience in the SBWR. The test facility consists of two separate loops, one for the PCC testing, the other for the IC testing. At the time of writing this paper (April 1995), the PCC testing was completed and the facility preparation for the IC testing is in progress. The IC tests are scheduled to begin in June and to be completed by the end of 1995.

The paper gives a brief description of the PANTHERS experimental program aimed to demonstrate the thermal-hydraulic and structural performances of a full scale prototype of the PCC . Preliminary results of the experimental tests are given. These results show the thermal-hydraulic performance of the heat exchanger as a function of inlet pressure and of the air mass fraction for: some steady-state performance tests; for a test in which the water level in the PCC pool is allowed to drop and the PCC tubes to uncover and for a test with non-condensable gas build-up.

The experimental results are very satisfactory and show a very good repeatability. The structural design of the heat exchanger is very robust: the unit has survived ten LOCA cycles and more than 100 thermal-hydraulic performance tests.

In addition to the PCC results, a short description of the test objectives and the test matrix for the PANTHERS-IC testing is given.

1. INTRODUCTION

The Simplified Boiling Water Reactor (SBWR) is an evolutionary design in boiling water reactors (BWRs). The SBWR has been developed by an international design team from North

America, Europe, Mexico and Asia and led by the General Electric Company (GE). The design extensively uses the technology of operating BWRs, as well as new developments found in the Advanced BWR (ABWR). A key feature of the SBWR is the use of simple passive systems to respond to any type of design basis event (DBE) [1]. These systems utilize passive forces, such as gravity head, natural circulation, or naturally induced pressure differences, to operate.

One of these systems is the Passive Containment Cooling System (PCCS). The SBWR containment is similar to existing GE BWRs which have the reactor in a drywell region. The drywell is connected to a wetwell through submerged pipes in the suppression pool, a part of the wetwell. The PCCS consists of three Passive Containment Condensers (PCC) connected to the upper drywell gas space. During a postulated loss-of-coolant accident (LOCA) steam in the drywell is driven into the PCCS by the pressure difference between the wetwell and drywell in combination with the vacuum produced by condensation. The condensate flows down into the Gravity-Driven Cooling System (GDCS) pools in the drywell. The GDCS is another SBWR passive system which provides makeup to the reactor. Non-condensable gases, such as containment nitrogen, are separated in the PCC and vented to the wetwell through submerged pipes in the suppression pool. All piping on the PCCS contain no valves, which results in a complete passive operation.

Another important passive system is the Isolation Condenser System (ICS). Its main purpose is to limit the over pressure in the reactor system at a value below the set-point of the Safety Relief Valves, as a consequence of a main steam line isolation. Three condensers are submerged in a compartmentlized pool of water located in the reactor building and above the reactor containment. The primary side of the three Isolation Condensers (IC) are connected by piping to the reactor pressure vessel. Closed valves in each condensate return line prevent condensation during normal power operation of the plant. When operation of the IC system is required, the valves are opened, the condensate is returned to the reactor vessel by gravity, and the steam flows directly from the reactor to the condensers. The rate of flow is determined by natural circulation. Vent lines are provided on the IC to remove non-condensable gases (radiolytic hydrogen and oxygen) which may reduce heat transfer rates during extended periods of operation.

As a part of the SBWR design and U.S. certification program [2], GE and the Italian companies ANSALDO, ENEA, and ENEL are sponsoring a test program of full-scale, prototypical condensers for both ICS and PCCS, at full pressure, temperature and flow conditions. The two PCC and IC full-scale prototypes were designed, and manufactured by ANSALDO. ENEA has the responsibility to co-ordinate the tests conducted by SIET at the Performance ANalysis and Testing of HEat Removal Systems (PANTHERS) facility [3]. Both the thermal and structural performance of the heat exchangers are measured in these tests at various conditions the units might experience in the SBWR. The test facility consists of two separate loops, one for the PCC testing, the other for the IC testing.

At the time of writing this paper (April 1995), the PCC testing was completed and the facility preparation for the IC testing is in progress. The IC tests are scheduled to begin in June and to be completed by the end of 1995.

Both PCC and IC tests are conducted in accordance with the requirements of NQA-1/1a-1983 Quality Assurance Programme.

2. PCC TESTING

2.1. Test Objectives

The test objectives of the PANTHERS PCC Test Program are:

(a) Demonstrate that the prototype PCC is capable of meeting its design requirements for heat rejection. (*Component Performance*)

(b) Provide a sufficient database to confirm the adequacy of TRACG to predict the quasi-steady-state heat rejection performance of a prototype PCC , over a range of non-condensable flow rates, steam flow rates, operating pressures, and superheat conditions, that span and bound the SBWR range. (*Steady State Separate Effects*)

(c) Determine and quantify any differences in the effects of non-condensable build-up in the PCC tubes between lighter-than-steam and heavier-than-steam gases. (*Concept Demonstration*)

(d) Confirm that the mechanical design of the PCC is adequate to assure its structural integrity over a lifetime equal to that required for application of this equipment to the SBWR. (*Component Demonstration*)

2.2. Test Unit

The PCC is described in reference [3]. The full-scale PCC prototype consists of two identical modules, and the complete two-module assembly is designed for 10 MW nominal capacity, at the following conditions:

- Pure saturated steam in the tubes at 308 kPa absolute and 134 °C.
- Pool water at atmospheric pressure and 101 °C temperature.
- Fouling on secondary side of 9×10^{-5} °C/W-m^2.

The PCC design pressure is 759 kPa (gauge) and the design temperature is 171 °C.

2.3. Test Facility Description

The PANTHERS-PCC test loop (Figure 1) includes a pool tank in which the full-scale prototype of the two-module unit PCC is submerged in water. Figure 2 is a photograph of the PCC in the water pool. In the picture, the front wall and the roof of the pool are removed. The steel frame structure, visible around the PCC, holds in fixed position the pool instrumentation and the cables of the PCC instrumentation. The PANTHERS-PCC test loop is described in ref. [3-4].

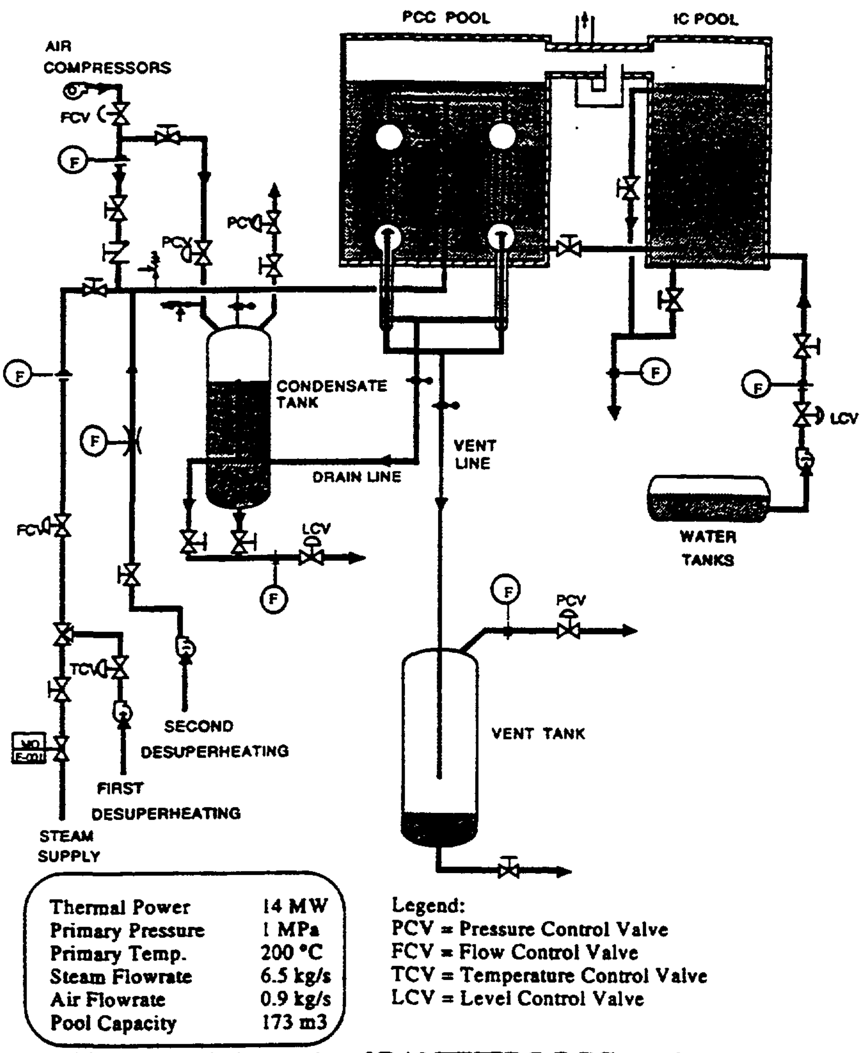

Figure 1 - Schematic of PANTHERS-PCC test loop

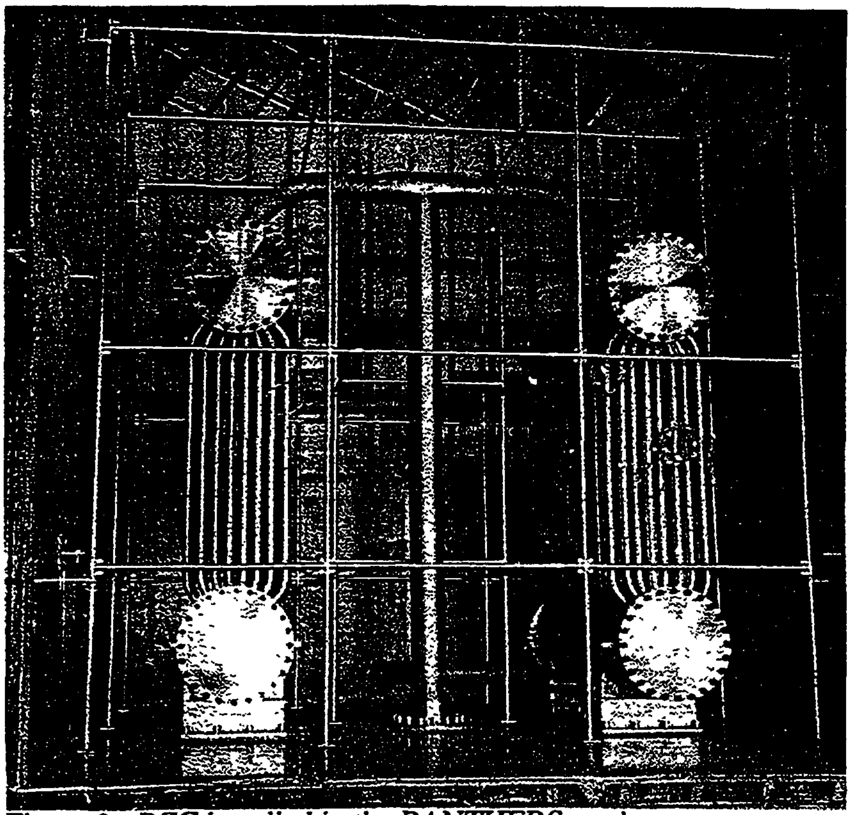

Figure 2 - PCC installed in the PANTHERS pool

The test loop elevations are full-scale relative to SBWR. The required power to test the full unit PCC is obtained using superheated steam from a power station adjacent to the PANTHERS facility.

Test facility process instrumentation is used to measure global mass and energy balances and to characterize the state of the test facility outside the condenser unit. Thermal-hydraulic performance instrumentation is provided to monitor the primary and secondary side heat transfer capability of the prototype and other pressure and temperature details of interest. Structural instrumentation is provided on the condensers to confirm design stress levels and monitor vibration frequencies. A summary of the instrumentation used to monitor the thermal-hydraulic performance and mechanical behavior of the PCC is given in ref. [3-4].

Wall thermocouples are brazed at 9 different axial levels on 4 PCC tubes. These instruments measure the differential temperature across the tube wall, to derive the local heat flux. This wall thermocouple instrumentation is useful to identify the length of the tube over which condensation occurs, when the PCC heat removal exceeds the thermal power of the supplied air/steam mixture.

2.4. Test Matrix

The majority of the PANTHERS PCC testing is steady-state performance testing. For these tests, the facility is placed in a condition where steam or air-steam mixtures are supplied to the PCC at a steady rate, and the condensed vapor and vented gases are collected. All inlet and outlet flows are measured. The vented gases are released to the atmosphere. Once steady-state conditions are established, data are collected for a period of 15 minutes. The time-averaged data are reported and analyzed. The table I shows the PANTHERS PCC Test Matrix in which the tests have been divided into groups described below.

- Test Group 1 is used to determine the baseline heat exchanger performance over a range of saturated steam flow rates without the presence of non-condensable gases. Test Group 1 data are compared with design requirements to meet Test Objective 1.
- Test Group 2 addresses the effect of superheat conditions in the inlet steam.
- Test Groups 3 through 6 are PCC steady-state performance tests with air/steam mixtures. As noted previously, the independent variables are steam mass flow rate, air mass flow rate, steam superheat conditions, and absolute operating pressure.

Table I - PANTHERS-PCC TEST MATRIX

Test Group	Test Conditions	Description
1	7	PCC steady-state performance; saturated steam
2	6	PCC steady-state performance; superheated steam
3	4 [a]	PCC steady-state performance; air/steam mixtures
4	7 [a]	PCC steady-state performance; air/steam mixtures
5	2 [a]	PCC steady-state performance; air/steam mixtures
6	18	PCC steady-state performance; air/steam mixtures
7	6	PCC performance; non-condensable build-up
8	3	PCC performance; pool water level effects
9	10	PCC component demonstration; LOCA cycles

[a] Each test is performed at five inlet pressures with fixed steam and air inlet flow rates

- Test Group 3 is used to compare heat rejection rates over a range of air flow rates to the saturated, steam-only condition determined from the pure steam series. Holding steam flow constant at near rated conditions, these tests yield the effect of air on the condensation process.
- Test Group 4 supplements Test Group 3, in that it defines condensation performance at the extremes of the SBWR air/steam mixture ranges, and at several intermediate points.
- Test Group 5 further supplements Test Group 4 by extending the effect of non-condensable gases over the superheated steam range.
- Tests included in Group 6 are lower priority tests. They supplement the previously identified tests by increasing the data density within the already established air/steam flow map.

The PANTHERS PCC test matrix includes transient tests which are used to establish non-condensable build-up effects and PCC pool water level effects. They are not intended to be systems transient tests.

- Test Group 7: six test conditions are specified in this Group. In these test conditions, steam is supplied at a constant rate, and steady-state conditions established. Air, helium, or air/helium mixtures are then injected into the steam supply, with the vent line closed, and the transient degradation in heat transfer performance is measured, as a function of the total non-condensable mass injected. Air is similar to nitrogen in molecular weight, and is heavier than steam. Helium is lighter than steam, and is expected to behave in a manner similar to hydrogen. Hydrogen can be present in the SBWR containment as result of radiolysis and reaction of the Zircaloy fuel cladding with reactor water. Test Group 7 data are evaluated to meet the requirements of Test Objective 3.
- Test Group 8. In these test conditions, steam and air/steam mixtures are supplied to the PCC , and steady-state conditions established, similar to the steady-state performance tests. In these tests, however, the water level in the PCC pool is allowed to drop and the PCC tubes to uncover as a result of boil off. Both the PCC pool level and the PCC heat rejection rate are monitored as a function of time.

Test Groups 1 through 5, 7 and 8 provide a database for TRACG qualification and meet Test Objective 2.

Component testing (structural tests) of the prototype PCC is performed using the same hardware and test facility. The component demonstration tests are conduct in a similar manner to the thermal-hydraulic testing. Structural data are collected during the thermal-hydraulic tests as well as the structural performance tests. The approach taken to address Test Objective 4 is to subject the equipment to a total number of pressure and temperature cycles in excess of that expected over the anticipated SBWR lifetime.

- Test Group 9: Simulated LOCA cycles are performed by pressurizing the PCC with steam, so that both the temperature and pressure effects of a LOCA are simulated. The PCC pool is at ambient temperature at the beginning of a test, but is allowed to heat up to saturation as each cycle proceeds. Each LOCA cycle lasts approximately 30 minutes. Ten cycles are performed.

3. TEST RESULTS

The testing was completed at the end of December 1994. At the time this paper is written (April 1995), the analysis of results is still in progress; we can only outline some preliminary conclusions.

- The thermal-hydraulic performance satisfies the design requirements for the PCC unit.
- The PANTHERS/PCC facility operation is "smooth". Steady state conditions are rapidly reached and kept.
- No unexpected phenomena have been detected.
- In the steady-state performance tests with pure steam (Group 1), the inlet pressure of the PCC is a dependent variable and increases quasi linearly with the steam mass flow rate. Figure 3 shows the experimental points and the regression line.
- In the steady-state performance tests with air/steam mixtures, the condenser efficiency decreases as the air mass fraction (ratio between inlet air mass flow rate and total inlet mass flow rate) increases. Figure 4 shows the experimental results for the tests with constant inlet steam mass flow rate and constant inlet pressure. While four of the tests are with saturated steam, one is with 20°C superheated steam: the effect of superheating is negligible. The condenser efficiency increases as the inlet pressure increases. Figure 5 shows the condenser efficiency as a function of the inlet pressure for tests with constant steam mass flow rate, at four different values of the air mass fraction. The figure shows also the results for tests with 20°C and 30°C of superheating. The effect of superheating is

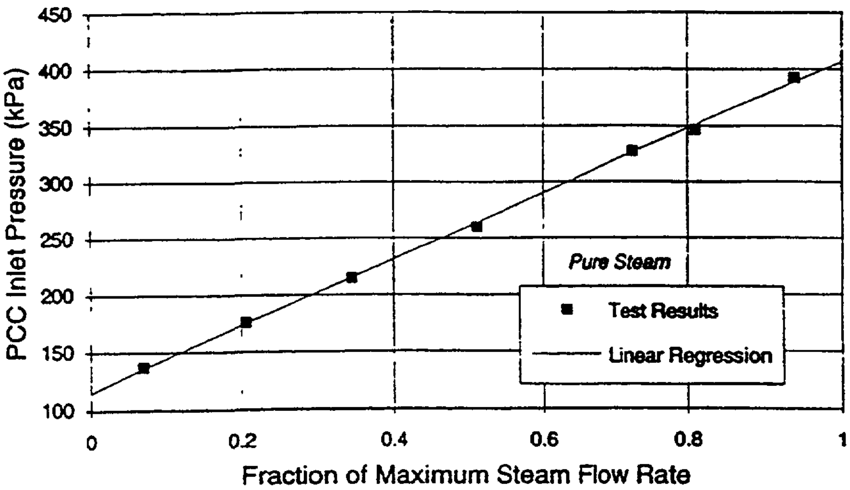

Figure 3 - Pure steam tests: PCC inlet pressure vs. steam flow normalized to the maximum steam flow rate

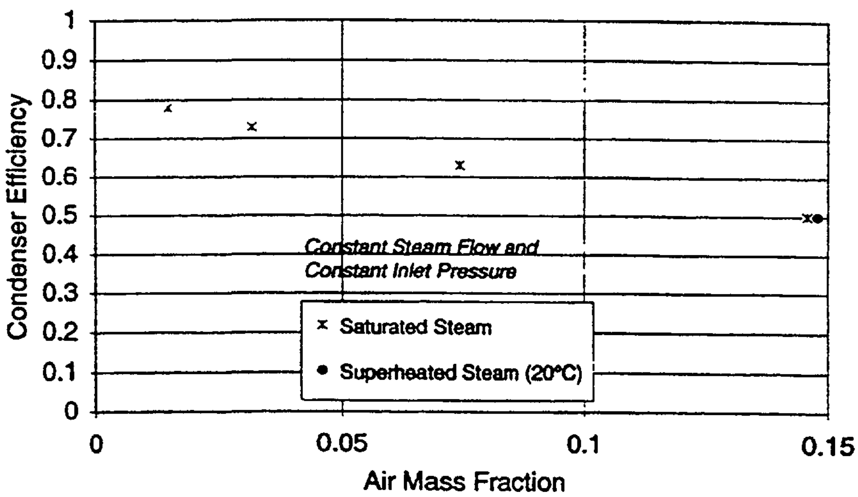

Figure 4 - Condenser Efficiency vs. air mass fraction at constant steam mass flow rate and constant inlet pressure

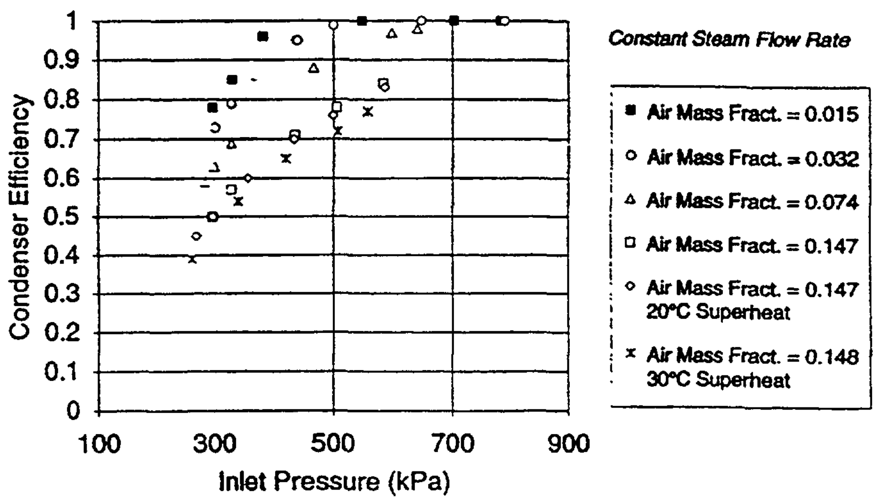

Figure 5 - Condenser efficiency vs. inlet pressure at different air mass fractions and constant steam flow rate.

again very small. The lower the air mass fraction, the lower the inlet pressure at which the efficiency approaches unity.

- Figure 6 shows the inlet pressure as a function of the IC pool water level in a test of Group 8 (slow transient test) with steam only. While decreasing the water level in the PCC pool, the inlet pressure decreases from the initial value to approximately 80 % the initial value, until the tube bundle starts to be uncovered. From this moment on, the pressure increases. Refilling the pool, the pressure follows the same trend, but with a small hysteresis. When the tube bundle was almost completely covered with water, the inlet pressure again reached its minimum and then followed the same values as when the level decreased. The PCC completely recovered its condensing efficiency.
- Figure 7 shows the effect of the air build-up in the condenser tubes (Test Group 7), in terms of tube wall ΔT (normalized to the initial values) as a function of time. After reaching steady state with steam only, air is slowly injected with a constant flow rate (Time ~1000 s) Because the venting is prevented, the air, heavier than steam, is accumulated in the bottom of the PCC. Tube wall ΔT is proportional to the local heat flux. It drops to zero when the portion of the tube where the thermocouples are located is filled with air, preventing any further condensation. The lower is the location of the wall thermocouple in the tube, the sooner the heat flux drops to zero.

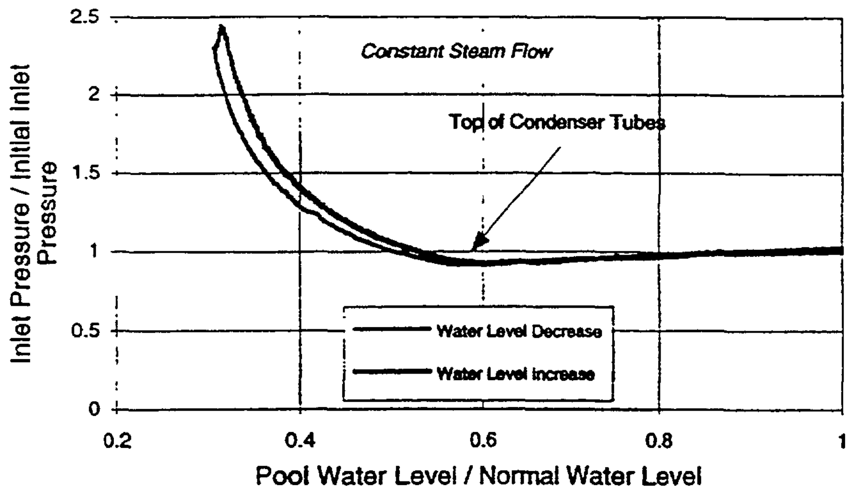

Figure 6 - Inlet pressure (normalized to the initial inlet pressure) vs. pool water level (normalized to normal water level)

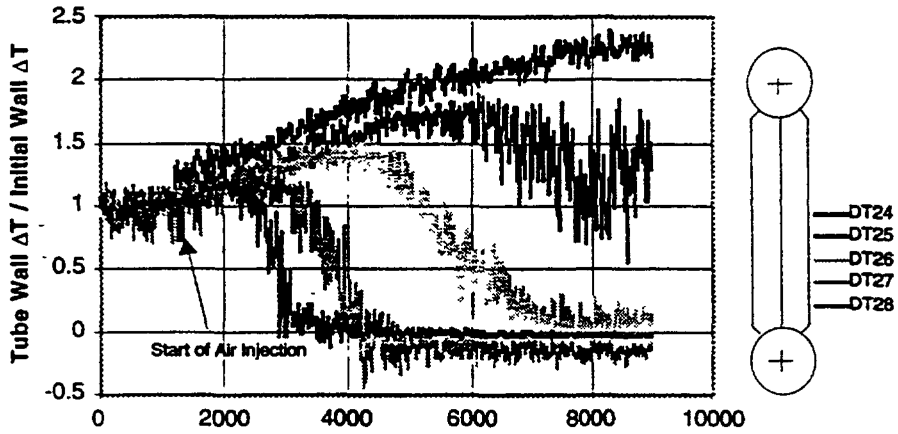

Figure 7 - Tube wall ΔT (normalized to the initial values) vs. Time, at different axial tube location, in an air build-up test

4. IC TESTS

4.1. Test Program Objectives

The test objectives of the PANTHERS-IC Test Program are:

1. Demonstrate that the prototype IC is capable of meeting its design requirements for heat rejection. (*Component Performance)*
2. Provide a sufficient data base to confirm the adequacy of TRACG to predict the quasi-steady heat rejection performance of a prototype IC , over a range of operating pressures that span and bound the SBWR range. (*Steady-State Separate Effects)*
3. Demonstrate the start-up of the IC unit under accident conditions. *(Concept Demonstration)*
4. Demonstrate the non-condensable venting capability of the SBWR IC design, and condensation restart capability following venting. *(Concept Demonstration)*
5. Confirm that the mechanical design of the IC is adequate to assure its structural integrity over a lifetime equal to that required for application of this equipment to the SBWR. (*Component Demonstration*)

The thermal hydraulic specific objectives are:

a) measure the steady-state heat removal capability over the expected range of the following SBWR conditions:
   - steam pressure
   - concentration of noncondensible gases
   - pool-side bulk average water temperature
   - pool-side water level
b) confirm that the vent lines and the venting strategy for purging non-condensable gases perform as required during IC operation.
c) confirm that tube-side heat transfer and flow rates are stable and without large fluctuations.
d) confirm that there is no condensation water hammer during the expected start-up, shutdown and operating modes of the IC.
e) confirm that the condensate return line performs its function as required during steady state and transient operation and that water level oscillations and condensation induced flow oscillations do not impair heat removal capacity
f) Measure the heat loss from the IC when it is in the standby mode, with the condensate drain valves closed
g) Measure the drain time for the IC upper plenum during the IC start-up transient.

The structural specific objectives are:

a) measure the temperature and the stress levels at the critical locations of the IC in all the test conditions
b) measure the vibration at critical locations on the IC resulting from flow and/or condensation.

c) verify through pre- and post-test non-destructive examination (NDE) of selected header/tube weld joints that a specified fraction of thermal cycles results in no excessive deformation, crack initiation or excessive crack growth rate
d) measure the stress levels at critical locations on the IC, resulting from flow and/or condensation induced vibration during expected periods of IC operation

4.2. Test Unit

The IC is described in ref. [3]. The full-scale IC prototype is one module of the two-module SBWR IC design. The single module is designed for 15 MW nominal capacity, at the following conditions:

- Pure saturated steam at 289 °C
- Pool water at atmospheric pressure and 100 °C
- Tubes plugged 5%
- Fouling factor on secondary side, 9×10^{-5} °C/W-m^2

The design pressure is 8.62 MPa and the design temperature is 302°C. The IC material is INCONEL 600.

Figure 8 shows the schematic of PANTHERS-IC test loop.

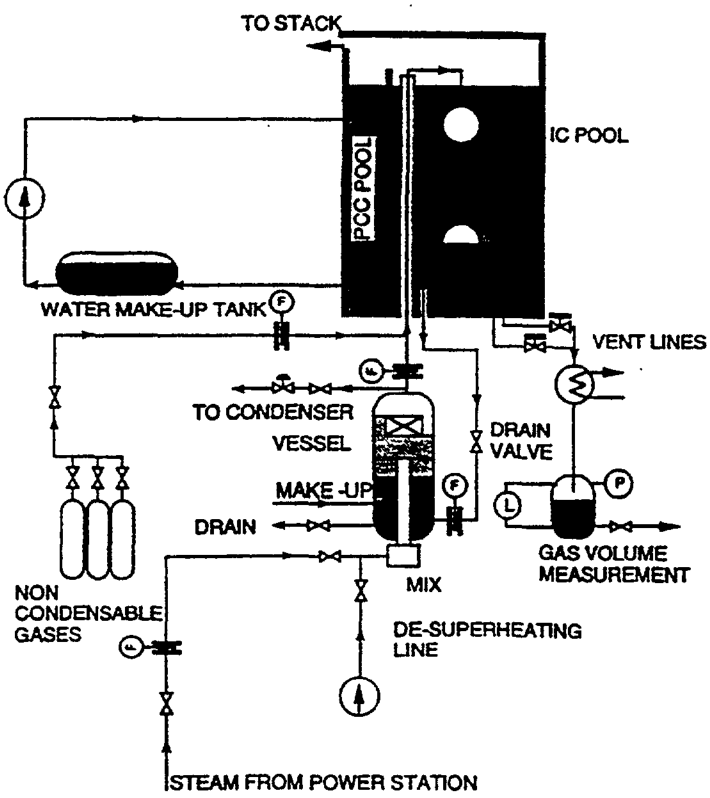

Fig. 8 - Schematic of PANTHERS-IC

4.3. Test Matrix

Seven types of tests are planned, three of which are structural tests. The majority of the thermal hydraulic IC tests are steady-state performance tests. The transient tests will be used to demonstrate the start-up of the IC under full-scale thermodynamic conditions. Table II shows the IC test matrix.

a) Test type 1: steady-state performance tests
These data will establish the IC heat rejection rate as a function of the inlet pressure.
In general, the procedure for the steady state tests will be as follows:
The steam vessel and IC will be purged of initial air. The IC pressure may be either

design pressure, or a lower value, depending on whether or not the test is also being used as a structural demonstration cycle. The IC is then placed in operation by opening the IC drain valve. Steam supply to the steam vessel is then regulated such that the vessel pressure stabilizes at the desired inlet value. Data will then be acquired for a period of approximately 15 minutes. At this point, the steam supply may be increased or decreased to gather data at a different operating pressure, or the test may be terminated. In all cases, flow into the IC will be natural circulation driven, as is the case for the SBWR.

b) Test type 2: start-up tests
These tests will be performed in much the same manner as the steady-state performance tests, but transient data will be recorded over the course of the experiment. The objective is demonstrate the start-up and operation of the IC in a situation comparable to a reactor isolation and trip. These tests will be performed with an initial pressure of 9.48 MPa, and, after the opening of the drain valve, the inlet pressure is stabilized at 8.618 MPa

c) Test type 3: non-condensable gas
Non condensable gas effects tests begin in a similar manner as he steady-state performance tests, until the pressure has been stabilized at the desired value. In this case, a mixture of air and helium will be injected into the IC supply line at a very low flow rate. The ratio of air to helium in the injected flow will be 3.6:1, simulating the composition of radiolytic gases. Gas injection will continue until the IC inlet pressure increases to 7.653 MPag. The lower IC vent is then opened, and the IC vented until pressure returns to the initial operating pressure, or stabilizes at an intermediate value. If the pressure has returned to the initial value, the test is terminated. If the inlet pressure has stabilized, the IC top vent will be opened, and the performance monitored until venting is complete, and the inlet pressure returns to the initial value. The test is then terminated.

d) Test type 4: pool water level
Water level tests also begin with the IC in stable operation at the desired initial inlet pressure. The IC pool water level is then reduced and the IC performance monitored. water level will be reduced until the pool level is at mid height of the condenser tubes, or the IC inlet pressure reaches 8.618 MPag (1250 psig) whichever comes first. The pool water level will then be increased to normal and the IC performance allowed to return to normal. The test is then terminated.

e) Test type 5: normal IC operation structural cycle.
This type of test is essentially representative of the cyclic duty expected of the IC as used in operation in the SBWR. The test is conducted in a very similar manner as a steady state performance test (test type 1) but the operating pressure is equal to the design pressure, 8.618 MPa and the initial pool water temperature is less than 32 °C. Thermal hydraulic tests can be qualify as a structural type 5 cycle if these limits are respected and the inlet pressure is held for 2 hours.

f) Test type 6: reactor heatup/cooldown without IC operation.
This type of test is essentially representative of the cyclic duty expected of the IC as used in stand-by mode in the SBWR. The test consists in a pressurization of the IC up to 8.618 MPag and in a cooldown and de-pressurization. The initial pool water temperature is less than 32 °C. Thermal hydraulic tests can be qualify as a structural type 6 cycle if these limits are respected.

g) Test type 7: Anticipated Transient Without Scram (ATWS) event simulation. The test is very similar to test type 5, the main difference being a rapid pressurization of the IC up to 9.480 MPa, before opening the drain valve.

Table II PANTHERS-IC TEST MATRIX

Test Cond. No.	No. of tests	Test Type	Inlet Pressure (MPa)
1	3	2	8.618
2	1	1	7.920
3	1	1	7.240
4	1	1	6.21
5	1	1	5.52
6	1	1	4.83
7	1	1	4.14
8	1	1	2.76
9	1	1	1.38
10	1	1	0.69
11	1	1	0.21
12	1	3	0.48
13	1	3	2.08
14	1	4	0.48
15	1	4	2.08
16	20	5	8.618
17	5	6	8.618
18	1	7	8.618

5. CONCLUSIONS

The PANTHERS experimental program has successfully tested a full-scale prototype of the PCC. Data from these tests are now being used in the certification work for the SBWR plant.

The broad selection of data allow analysts to study many applications of the PCC performance. data collected by PANTHERS-PCC are used to compare the heat removal from a prototype condenser with the SBWR design requirements. By using the steady-state tests with steam only, a correlation can be developed to derive the condenser performance at design conditions.

The database from the steady-state performance tests will be able to confirm the adequacy of computer codes, such as GE's TRACG, to predict the quasi-steady-heat rejection performance of a prototype PCC, over a range of non-condensable gas flow rates, steam flow rates, operating pressures, and superheat conditions, that span and bound the SBWR range. The transient tests can also provide data for computer code validation. For example, from one set of transient tests, analysts can determine and quantify any differences in the effects of non-condensable gas build-up in the PCC tubes between lighter than steam (helium) and heavier-than steam (air) gases. From tests where the pool water level was allowed to drop and partially uncover the tubes, the results can be used to study the performance of the heat exchanger with varying heat transfer surface area.

Results from structural tests demonstrate that the PCC is a very robust design. After ten LOCA cycles and over one hundred thermal performance tests, the unit emerged unscathed.

The final evaluations of the performance data from the PANTHERS-PCC are currently taking place; however, at present it appears that all the test objectives will be met.

In addition to the PCC test results, a short description of the test objectives and of the test matrix for the PANTHERS-IC testing has been given. Based on the PANTHERS-PCC experience, the authors are confident that the IC testing program will be successfully accomplished in the planned time.

REFERENCES

[1] UPTON, H. A., COOKE, F. E., SAWABE, J. K., 1993, "Simplified Boiling Water Reactor Passive Safety Features", Proc. of the 2nd ASME-JSME Nuclear Engineering Joint Conference ICONE 2, Vol. 1, (PETERSON, P.F., Ed.), San Francisco(CA) March 21-24 1993.

[2] Rao, A. S., 1993 "Simplifying the BWR" *ATOM* No 430, September/October 1993.

[3] Masoni, P., Botti, S., Fitzsimmons, G. W., 1993, "Confirmatory tests on full-scale condensers for the SBWR", Proc. of the 2nd ASME-JSME Nuclear Engineering Joint Conference ICONE 2, Vol. 1, (PETERSON, P.F., Ed.), San Francisco(CA) March 21-24 1993.

[4] Masoni, P., Bianchini, G., Billig, P.F., Botti, S., Cattadori, G., Fitch, J.R., and Silverii, R., 1995. "Tests on Full-scale Prototypical Passive Containment Condenser for SBWR's Application", Proc. of the 3rd ASME-JSME Nuclear Engineering Joint Conference ICONE 3, Kyoto (J) April 23-27, 1995

TESTING STATUS OF THE WESTINGHOUSE AP600

E.J. PIPLICA, J.C. BUTLER
Westinghouse Electric,
USA

Presented by L. Conway

Abstract

Westinghouse has developed AP600--a 600 MWe two-loop, advanced, simplified passive plant--in response to the Advanced Light Water Reactor Program sponsored by the Electric Power Research Institute and the U.S. Department of Energy.

The principal safety functions of primary coolant inventory, reactivity control, reactor residual heat removal, and fission product containment are accomplished with safety systems that are based on logical extensions of proven technology and rely on natural forces such as gravity, convection, and evaporation.

AP600 technology is supported by rigorous testing. The test programme is the single most visible portion of the AP600; it is a global effort, with the cooperation of the U.S. government (including the U.S. NRC), industry, and the academic world. With the completion of this programme, the AP600 has become the most thoroughly and rigorously tested reactor system in the world. The results have demonstrated the performance of the components and systems unique to the passive safety concept upon which the AP600 is based.

Westinghouse has developed AP600--a 600-MWe two-loop, advanced, simplified passive plant--in response to the Advanced Light Water Reactor Program sponsored by the Electric Power Research Institute and the U.S. Department of Energy see figure 1). The AP600 is currently scheduled to receive Final Design Approval from the U.S. Nuclear Regulatory Commission (NRC) in September 1996. In support of the design and the design certification review, the AP600 has undergone the most extensive test program ever conducted on a nuclear power plant design.

The overall AP600 plant design follows in the decades-long tradition of Westinghouse two-loop PWRs (see figure 2), which have consistently operated with average lifetime availabilities of 83 percent--significantly better than the U.S. national average.

AP600 passive safety systems simplify safety functions that have traditionally been provided by active safety systems (see figure 3). The principal safety functions of primary coolant inventory, reactivity control, reactor residual heat removal, and fission product containment are accomplished with safety systems that are based on logical extensions of proven technology and rely on natural forces such as gravity, convection, and evaporation.

Passive Residual Heat Removal

A natural circulation heat exchange loop connected to the reactor and located inside the containment transfers reactor heat to a water pool inside the containment, serving the same function as a conventional emergency feedwater system (see figure 4).

Passive Core Cooling System

A few simple valves are used to align and automatically actuate the passive safety systems (see figure 5). To provide high reliability, these valves are designed to actuate to their safeguards positions upon loss of power or upon receipt of a safeguards actuation signal. However, they are also supported by multiple, reliable power sources to avoid the possibility of unnecessary actuations.

The passive core cooling system (PXS) uses three passive sources of water to maintain core cooling through safety injection. These injection sources include the core makeup tank (CMT), the accumulators, and the in-containment refueling water storage tank (IRWST). These injection sources are directly connected via two nozzles for direct vessel injection (DVI) so that no injection flow will be spilled for the larger break cases. The CMTs inject at any RCS pressure, using gravity to provide injection flow. For larger leaks, additional water is provided by the accumulators, which inject water pressurized by compressed nitrogen at 700 psig. Long-term injection water is provided by gravity from the IRWST, which is designed for injection at atmospheric pressure. The automatic depressurization system (ADS) is composed of four stages to permit a relatively slow, controlled RCS pressure reduction. The ADS depressurizes the RCS to atmospheric pressure.

Passive Containment Cooling System

The AP600 steel containment vessel is a robust containment system that prevents radioactive releases to the environment and serves as the vehicle for heat transfer for reactor residual heat removal in the event of postulated accidents (see figure 6). Outside air is ducted by air baffles between the steel containment shell and the concrete building, cooling the vessel's outer surface by natural convection. In accident scenarios, this air-cooling is enhanced by draining water stored in a 400,000-gallon annular tank in the roof of the shield building onto the steel containment shell. This tank has sufficient water to providefor three days of cooling, after which time additional cooling water could be provided by operator action to maintain low containment pressure and temperature. But even if no additional water was provided at this time, air-cooling alone would be sufficient for continued public safety.

AP600 Test Program

AP600 technology is supported by rigorous testing. The test program is the single most visible portion of the AP600; it is a global effort, with the cooperation of the U.S. government (including the U.S. NRC), industry, and the academic world. With the completion of this program, the AP600 has become the most thoroughly and rigorously tested reactor system in the world. The results have demonstrated the performance of the components and systems unique to the passive safety concept upon which the AP600 is based.

The AP600 test program was initiated in 1985 with the overall objectives to provide design information to verify component designs, to simulate the AP600 thermal-hydraulic phenomena and behavior of the passive safety systems, to provide high quality, qualified data to validate the computer codes used in the Westinghouse safety analyses, and to support the U.S. NRC design certification review of the AP600. The AP600 test program was completed in 1994 and successfully achieved all of these objectives. The test results confirmed the exceptional behavior of the passive systems and were instrumental in facilitating code validations.

The AP600 tests can be grouped into three general categories:

Component Design Verification Tests: These tests confirmed the performance of AP600 design features.

Passive Containment Cooling System (PCS) Tests: These tests confirmed the operation of the PCS and helped validate the computer code modeling.

Passive Core Cooling System (PXS) Tests: These tests confirmed the operation of the PXS and were invaluable in the development and validation of computer code models.

Component Design Verification Tests
Component design verification tests were used to confirm performance of AP600 features associated with the use of canned motor reactor coolant pumps (RCPs) and top-mounted nuclear instrumentation.

Reactor Coolant Pump (RCP) Air and Water Flow Tests
Because the AP600 RCPs are attached to and take suction from the steam generator channelhead, an RCP air flow test was performed to observe the flow patterns in the steam generator channelhead (see figure 7). The test demonstrated that no adverse flow patterns that could affect pump performance will occur and established the pump hydraulic parameters. Water flow tests were also performed to verify the hydraulic performance.

High-Inertia RCP Rotor Test
To ensure that a large margin to departure from nucleate boiling (DNB) is maintained in the AP600 design following a complete loss of motor electrical power to the RCPs, a full-scale, high-inertia shaft using a stainless-steel-encased, depleted-uranium journal was constructed with bearing journals, radial bearings, and thrust bearings. This assembly was mounted on a shaft and placed in a dynamometer test stand. Water was circulated around the bearing and a motor was used to spin the shaft at pump-operation speeds (see figure 8).

The testing successfully demonstrated the design and construction of a full-scale encapsulated, depleted-uranium journal. The bearing journal, radial bearings, thrust bearings, and friction-dynamometer test rig operated smoothly with no significant vibration over the entire speed and load range. The test results demonstrated that a large margin to DNB will be maintained following a loss of power to the RCPs.

Incore Instrumentation System Test
This test investigated interference from the control rod drive mechanisms (CRDMs) on the fixed detector signal (see figure 9). A full-scale CRDM was operated next to a simulated fixed detector and the output signal was compared to the input signal.

The test results demonstrated that the AP600 incore instrumentation system will not be affected by electromagnetic interference from the CRDMs.

Reactor Internals Air Flow Test
A scaled model of the reactor vessel downcomer and bottom head was constructed of clear plastic to allow visualization of flow patterns in the vessel lower head (see figure 10). Flow tracers were injected to illustrate these flow patterns. The test was conducted at various flow rates to ensure that no flow anomalies/vortexes can occur in the AP600 vessel due to removal of bottom-mounted instrumentation.

This test demonstrated that there will be no abnormal flow distribution.

Passive Containment Cooling System (PCS) Tests
The operation of the AP600 ultimate heat sink using natural, passive safety systems has been confirmed by a comprehensive test program. This program included large-scale

integral testing of the passive containment cooling system (PCS). The PCS tests included the heated plate test, the integral PCS test, the air flow path resistance test, the large-scale heat transfer PCS test, the water distribution tests, and the wind tunnel tests.

Heated Plate Test

The initial data for and demonstration of the PCS heat and mass transfer processes that occur on the outer surface of the containment were obtained by experiments on a thick steel plate 2 ft. (0.61m) wide by 6 ft. (1.8m) tall that was heated on one side and had an evaporating water film and ducted air flow on the other side (see figure 11). The plate was heated to simulate the temperature of the containment wall that would occur in an actual plant following a postulated accident. The total plate-heating capacity installed was approximately 12,000 watts.

The resulting test data confirmed the calculational models for heat removal from the containment surface for both a wetted and dry surface. The test also showed that a stable water film can be easily formed and that even high air velocities would not strip water from the surface.

Integral PCS Tests

A 3-ft. (1-m) diameter by 24-ft. (7.3-m) high steel pressure vessel was built to simulate the entire PCS heat transfer processes occurring both on the inside and outside containment surfaces (see figure 12).

The steel pressure vessel was initially filled with one atmosphere of air and heated on the inside with dry steam. Three different steam inlet arrangements were used: one with a steam inlet near the top of the vessel to minimize air steam mixing; one near the bottom of the vessel to promote air steam mixing; and one where steam was uniformly introduced along the full height of the vessel during the test. The vessel was surrounded by a full-size cooling air flow path. The cooling air could be heated and humidified to simulate a full-range of expected conditions. The outer surface of the vessel was wetted by applying water to the top of the external surface.

This test demonstrated that even with the least effective steam inlet arrangement, the overall heat removal capability of the PCS met or exceeded analytical predictions. The dry heat transfer results of up to 40 psig confirmed the capability of the PCS to provide adequate cooling to maintain containment pressure below its design pressure when the initial water supply was used (within three days), and if no resupply occurred. There was sufficient heat removal even without external water, preventing containment failure following several accident scenarios.

Air Flow Path Resistance Test

A 1/6-scale replica of a 14 degree section of the entire PCS air flow path was constructed to quantity the air flow path resistance (see figure 13). This test resulted in the addition of two aerodynamic improvements to the air flow path--a rounded entrance into the air cooling annulus and rounded air baffle supports from the containment. The final air flow path resistance demonstrated was used in subsequent analyses.

Large-Scale Heat Transfer PCS Test

A 1/8-scale AP600 containment vessel was constructed to examine the performance of the PCS on a large computer code verification and to demonstrate that the code results were scalable (see figure 14). This vessel simulated the inside containment structures and volumes in order to achieve prototypical internal circulation patterns and air/steam mixture ratios, as well as a scaled external cooling air flow path. Instrumentation was installed to measure the vessel steel shell inner and outer wall temperatures at multiple locations, inside steam/air temperature, steam condensation rate, cooling air temperature rise, and cooling air velocity.

Testing was conducted for natural convection air-only cooling and forced convection with various degrees of water coverage on the outer vessel. Controlled steam flows were used to establish the test conditions providing internal pressures up to 40 psig. The results of the water distribution tests were used to establish water coverage on the vessel dome and walls, which ranged from full coverage to partial water coverage using a striping pattern. Cooling air flow rates were also varied to simulate the range of expected air flow velocities using both forced and natural convection. A condensation measuring system was used to measure internal steam condensation in these tests, focusing on both the external heat transfer mechanisms and the internal heat transfer mechanisms, effects of noncondensable, and transient conditions similar to those that may be encountered in a severe accident scenario. Testing demonstrated PCS heat transfer capability over a wide range of pressure, steam flow rate, and noncondensable gas conditions.

Water Distribution Tests

These tests provided a large-scale demonstration of the capability to distribute water on the steel containment dome outer surface and top of the sidewall for the entire range of expected water flow rates. The test apparatus is a full-sized, 1/8 sector of the AP600 containment dome (see figure 15).

Testing has been completed, and the results confirm the detailed design of the water delivery and distribution system.

Wind Tunnel Test

The AP600 wind tunnel tests were performed at the University of Western Ontario's boundary layer wind tunnel. Detailed scale models of the AP600 structures (see figure 16) were used in the test to simulate the structural details of the shield building air inlet and exhaust and surrounding buildings.

The tests demonstrated that wind will have no adverse impact on the natural convection-induced draft flow in the containment annulus. The tests also provided data that were used to assess baffle loadings under severe wind conditions.

Passive Core Cooling System (PXS)Tests

The test programs for the AP600 passive core cooling features included the passive residual heat removal heat exchanger (PRHR HX) test, the automatic depressurization system (ADS) test, the check valve test, the core makeup tank (CMT) test, the full-pressure, full-height integral test, and the long-term cooling integral systems test.

Passive Residual Heat Removal Heat Exchanger (PRHR HX) Test

This test characterized the thermal performance of the PRHR HX and the mixing behavior of the in-containment refueling water storage tank (IRWST), using prototypical PRHR HX tubing material, tube diameter, pitch, and length with the HX tubes located inside a scaled IRWST (see figure 17). The test conditions covered a full range of expected flow rates, including forced PRHR cooling and natural circulation flow rates by varying the pumped flow through the tubes.

This test was the largest of its kind and provided the data necessary to develop heat transfer correlations for vertical tube HXs.

Automatic Depressurization System (ADS) Test

The automatic depressurization system (ADS) tests were a full-sized simulation of the operation of the ADS function of the PXS and was conducted at ENEA's Vapore facility in Casaccia, Italy (see figure 18). The purpose of the tests was to confirm the design of the spargers, determine the dynamic effects on the IRWST structure, and confirm the operability of the ADS valves.

The tests demonstrated the successful performance of the sparger. These tests were performed over a range of water temperatures and water levels using steam flow rates greater than those anticipated in the actual transient. System performance was demonstrated over a wide range of plant conditions using a full-scale simulation of an ADS flow path.

Check Valve Test
Tests were conducted to demonstrate the capability of the passive safety injection check valves to open under low pressure differential conditions that exist during gravity drain injection (see figure 19). The tests used a hydraulic loop to determine the opening and operating differential pressure for each of the check valves.

Test results demonstrated the suitability of standard check valves for the passive safety injection functions.

Core Makeup Tank (CMT) Test
This test verified the gravity drain behavior of the CMT, the steam pressure balance piping over a full range of flow rates and pressures, and the operation of the tank level instrumentation, which acts as a control for the ADS. A 1/6-diameter and 1/3-height scale CMT was constructed and instrumented (see figure 20) to obtain the condensation rates within the tank to verify the analytical computer model. The test facility was designed to simulate the CMT operating modes over a wide range of conditions.

The CMT test did, in fact, evaluate the operation of the CMT over a full range of conditions and provided invaluable data for CMT computer code model development.

High-Pressure Integral Systems Test
A large-scale, full-height, full-pressure integral systems test was performed using the SPES test loop at the SIET facilities in Piacenza, Italy (see figure 21). The purpose of this test was to simulate the AP600 thermal-hydraulic phenomena and behavior of the passive systems following specified small-break loss-of-coolant accidents, steam generator tube ruptures, and steam line breaks. The test loop, known as SPES-2, was modified to represent the AP600 loop configuration and PXSs and included: two cold legs, one short leg per loop, CMTs, accumulators, PRHR HX, ADS, and DVI lines. A series of tests were performed to simulate high-pressure system interactions as the result of a loss-of-coolant, steam generator tube rupture, or steam line break accident.

Testing was completed in 1994. The tests covered a broad spectrum of break sizes, break locations, and system interactions. The test results have been used extensively to validate the computer codes and modes used in AP600 safety analyses.

Long-Term Cooling Integral Systems Test
The long-term cooling integral systems test simulated the operation of the PXS from ~300 psig, the transition to the natural convection post-accident, long-term cooling mode for the AP600, and demonstrated the operation of the long-term gravity makeup path from the IRWST and long-term core cooling via the natural circulation flow path from the flooded containment. The test used a scaled model made of stainless steel to simulate the reactor vessel, IRWST, CMT, RCS (including the pressurizer), and lower containment structure (see figure 22). Water was the working fluid, permitting direct modeling of the test with existing Westinghouse analysis codes. The core was simulated with electric heater rods scaled to match core decay heat.

The tests were performed at Oregon State University and completed in 1994. Since completion of the testing, the test results have been used to validate AP600 computer code modeling. The U.S. NRC, in recognition of the value of the test facility, has performed additional confirmatory testing.

Design Certification
On June 26, 1992, Westinghouse submitted the Standard Safety Analysis Report (SSAR) and Probabilistic Safety Study (PSS) to the U.S. NRC for review in support of the application for design certification. The SSAR includes a complete plant design minus the as-site and as-procured information. The PSS evaluates the AP600 design's risk to the public. It has also been used by the AP600 design team as a design tool, in that conclusions drawn from the preliminary PSS have been factored into the detailed design.

In November 1994 the NRC issued a draft safety evaluation report on the AP600 design. The NRC safety evaluation report (NRC SER) reported on the review of the design certification submittals by the NRC staff and by the Advisory Committee on Reactor Safeguards, a committee of independent experts from outside the NRC. NRC technical approval of the AP600 design, know as Final Design Approval, is expected in September 1996.

The successful completion of the AP600 test program has facilitated the design certification process and has culminated in a thoroughly tested design. The AP600 test program provides fundamental engineering data not only to support the licensing process leading to NRC design certification, but also to provide utilities with confidence in the innovative aspects of the AP600. The AP600 test program supports the licensing schedule leading to FDA in September 1996.

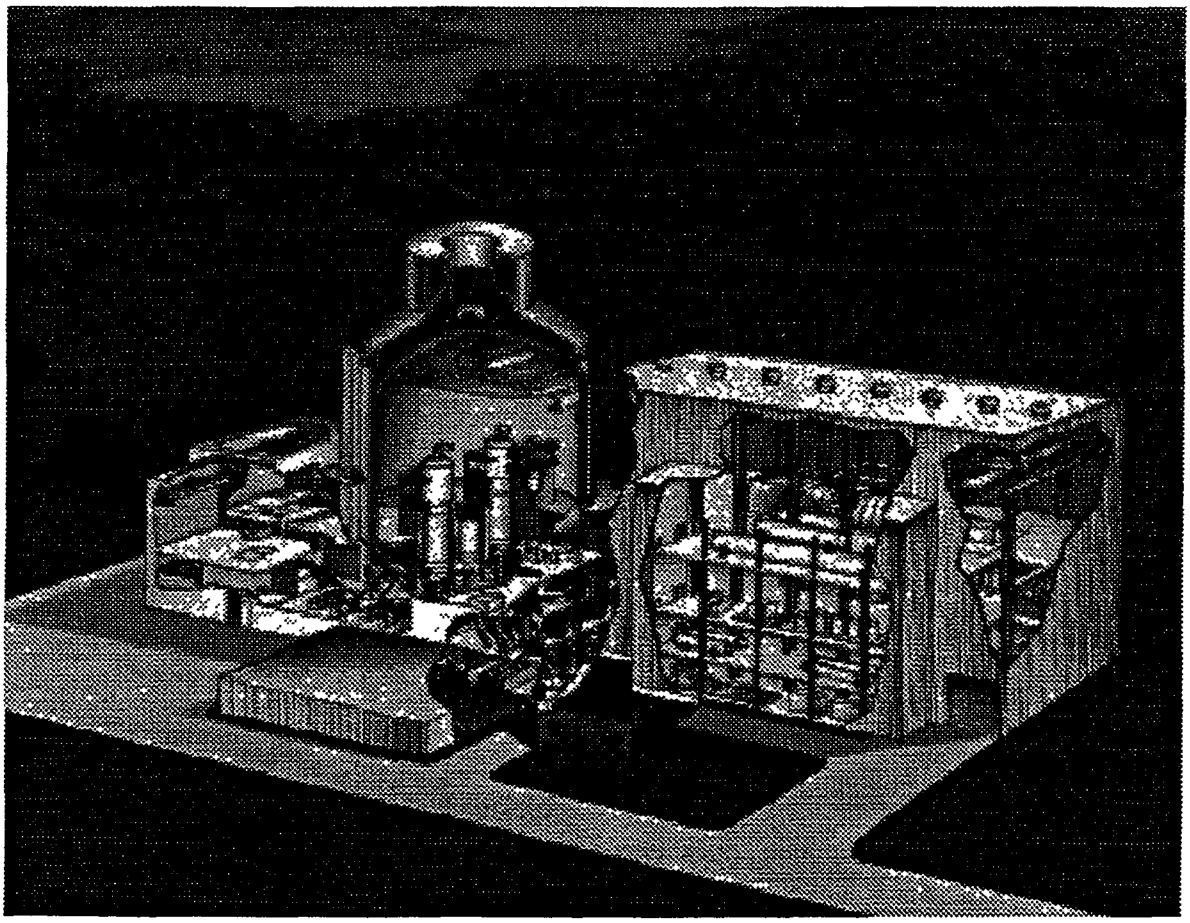

FIG. 1. AP600 - The new Westinghouse standard 600 MWe plant

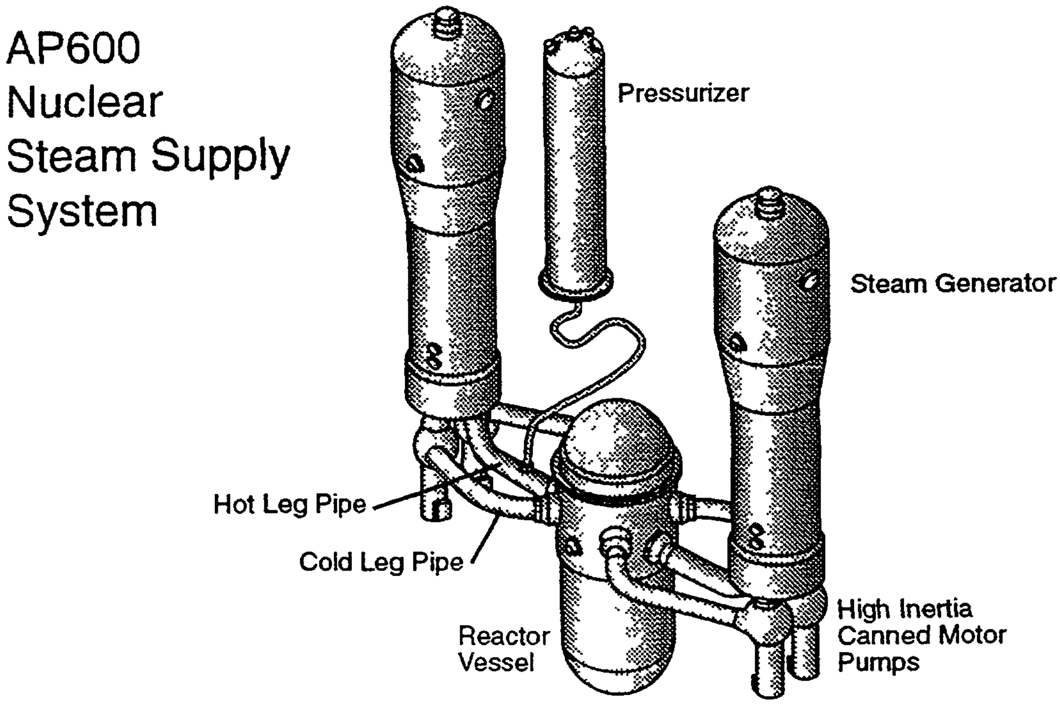

FIG. 2. AP600 nuclear steam supply system

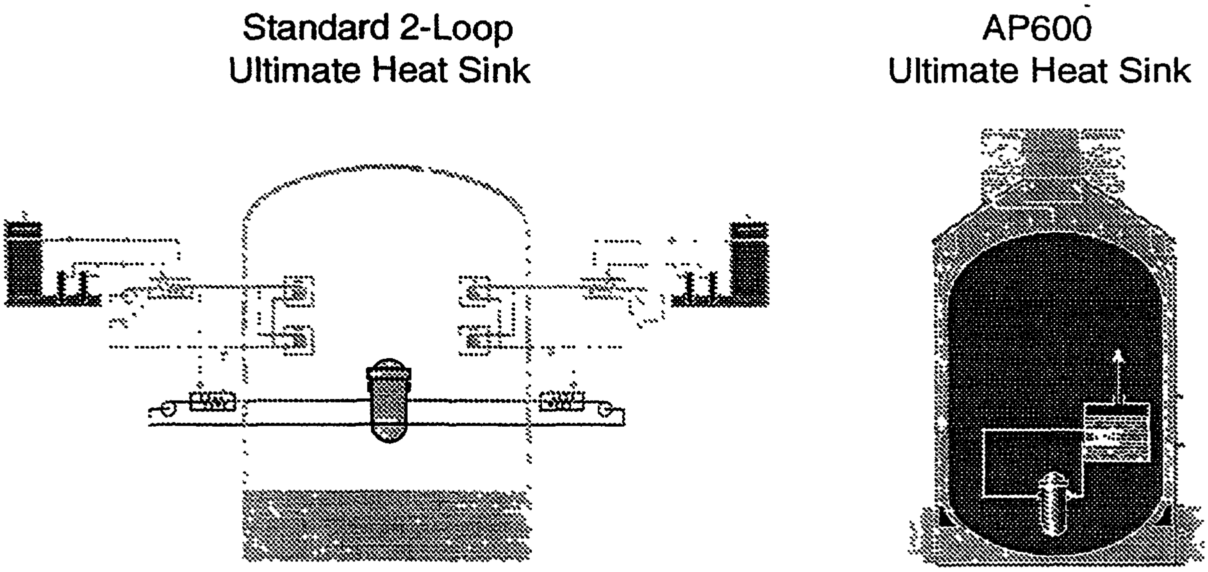

FIG. 3. AP600 simplified safety systems rely on natural forces

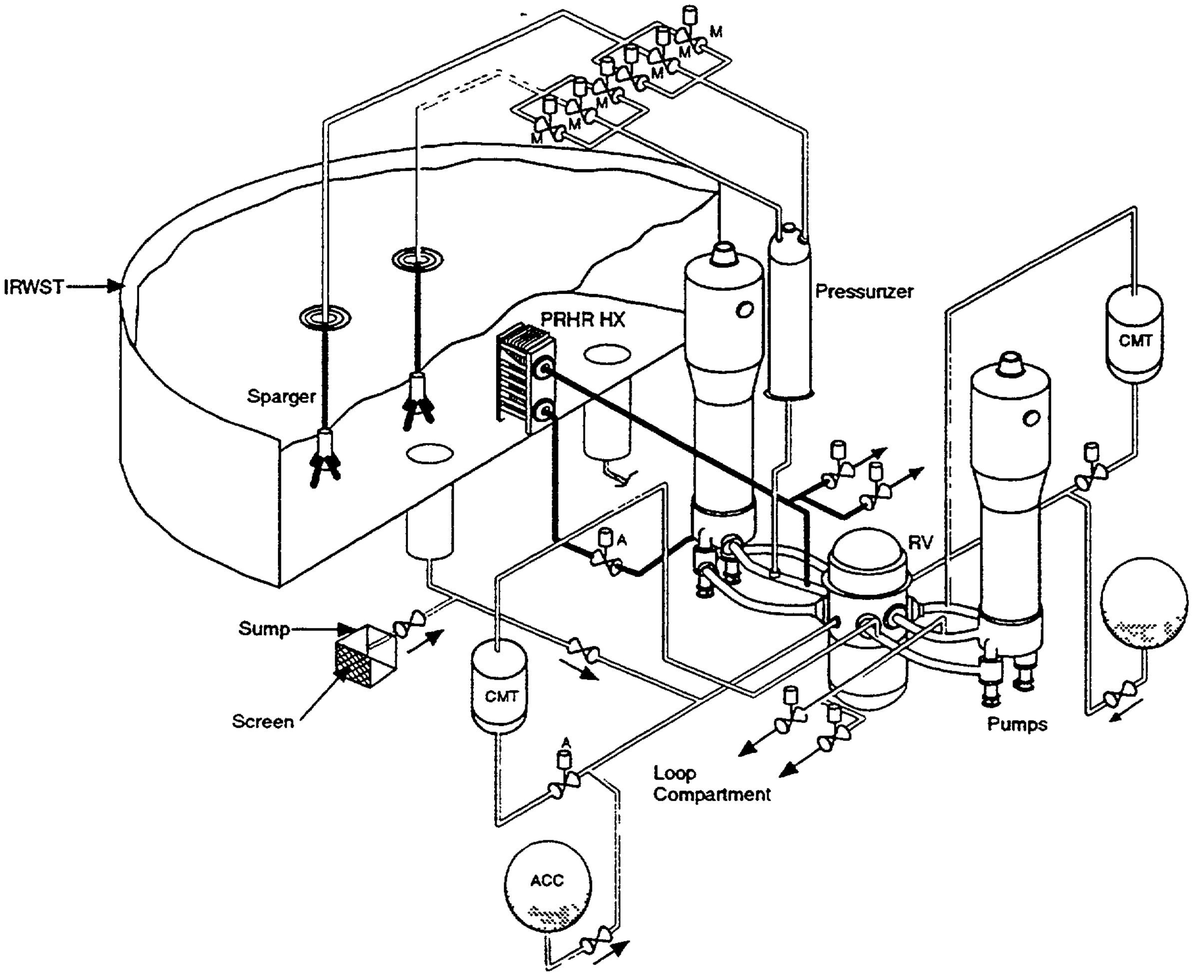

FIG. 4. Passive safety systems

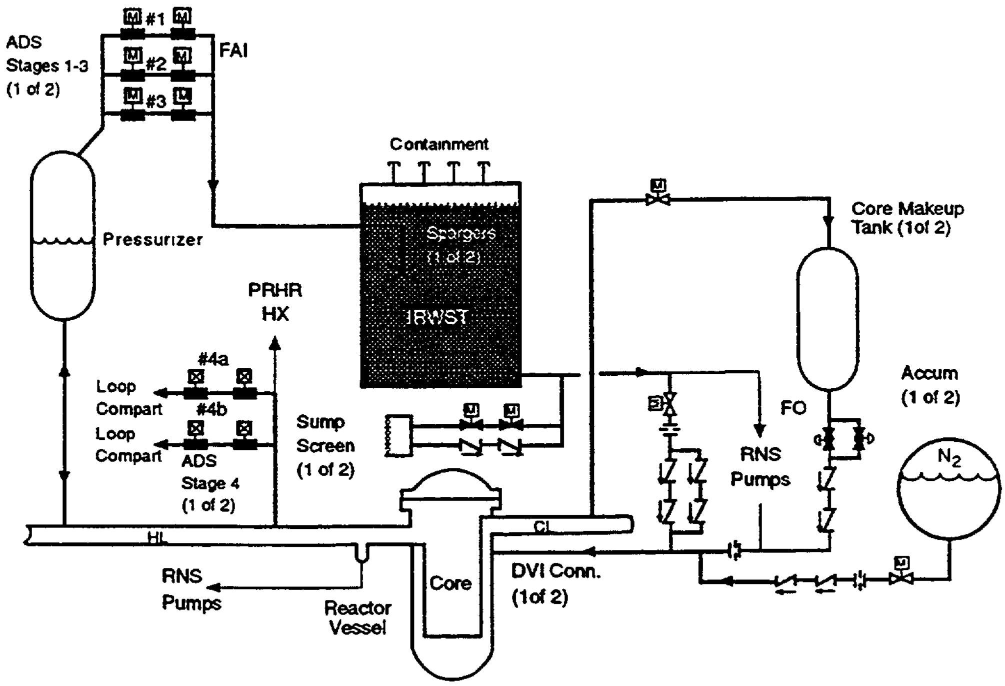

FIG. 5. AP600 - Passive core cooling systems

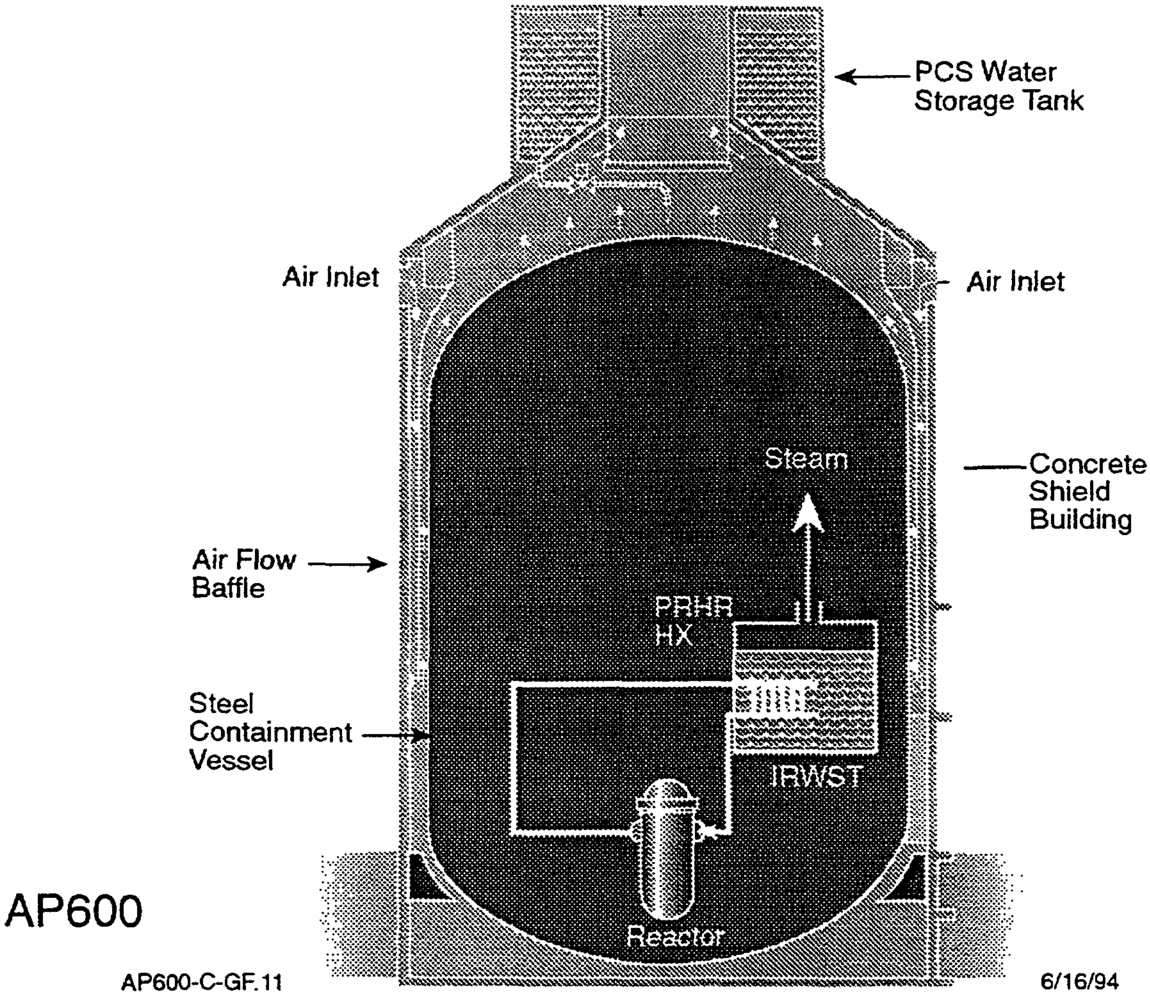

FIG. 6. AP600 - Passive containment cooling systems

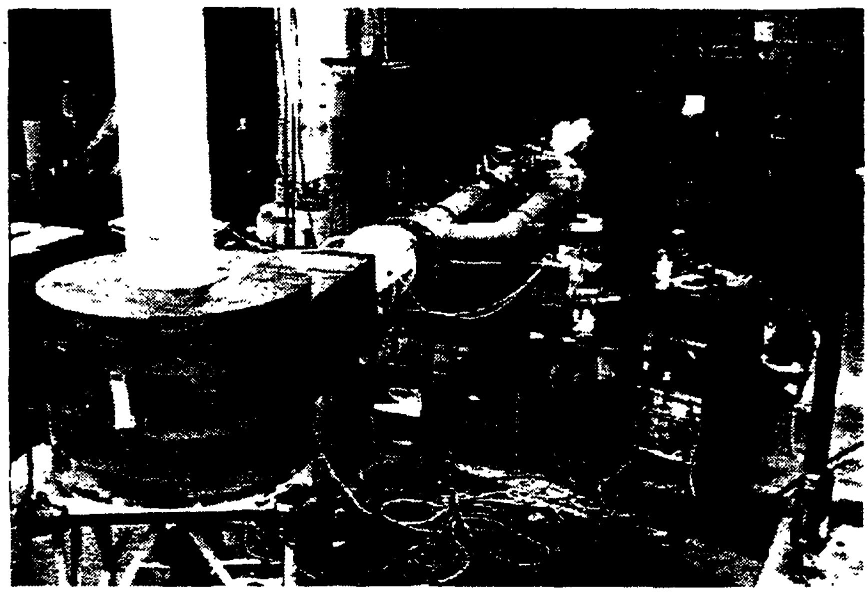

FIG. 7. AP600 reactor coolant pump sir and water flow tests

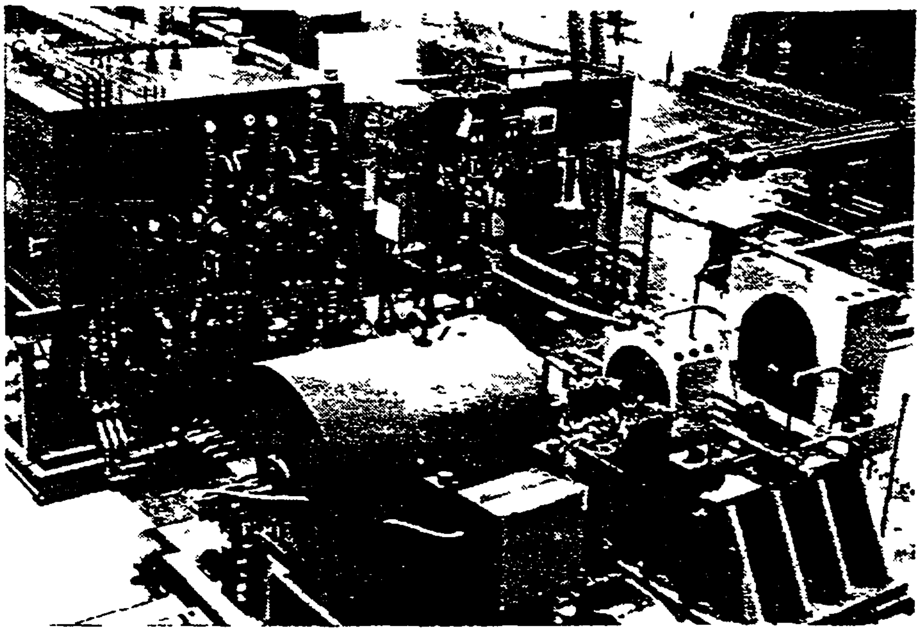

FIG. 8. AP600 high-inertia RCP rotor test

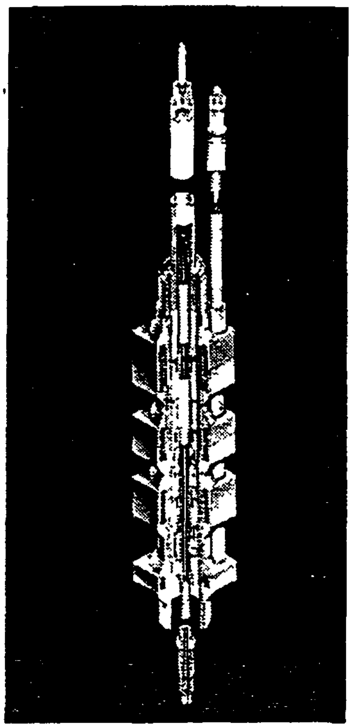

FIG. 9. AP600 incore instrumentation system test

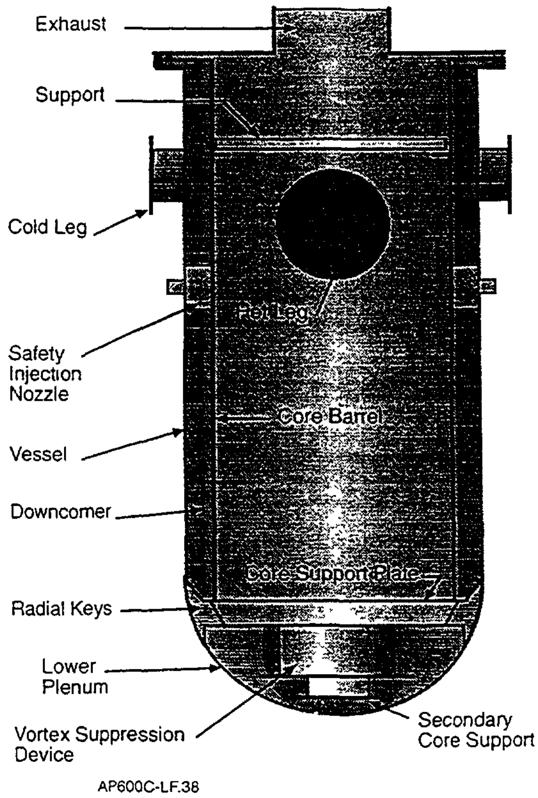

FIG. 10. AP600 reactor internals air flow test

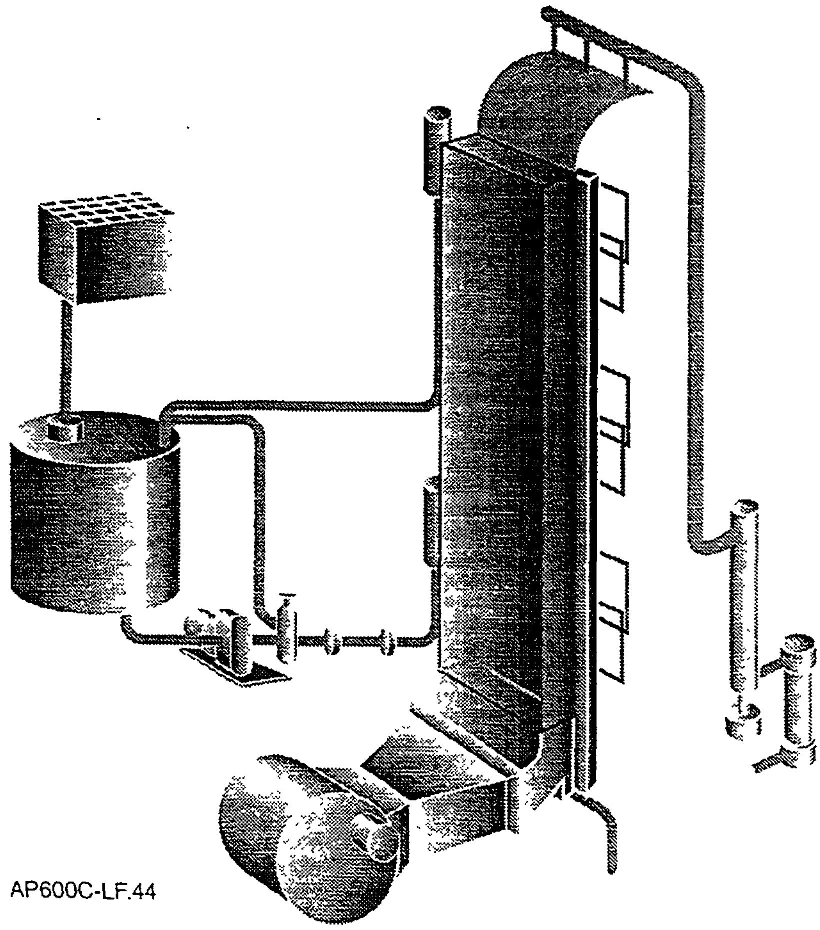

FIG. 11. AP600 heated plate test

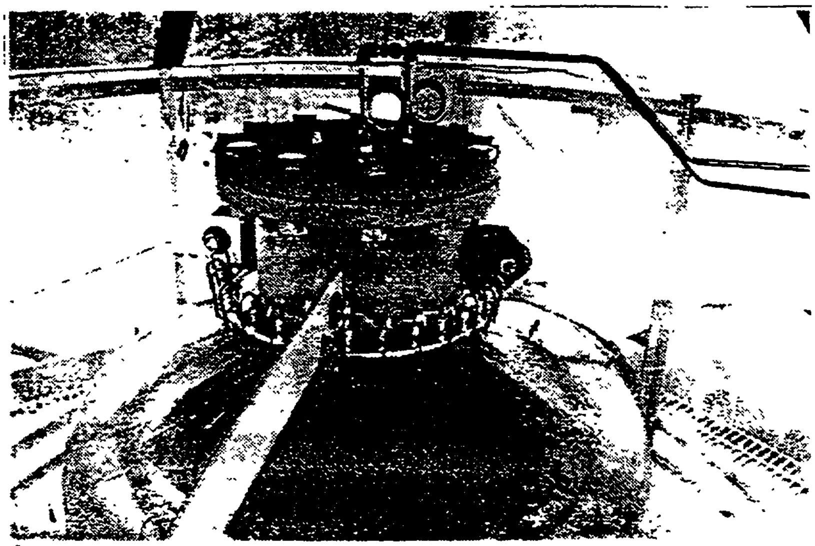

FIG. 12. AP600 integral PCS tests

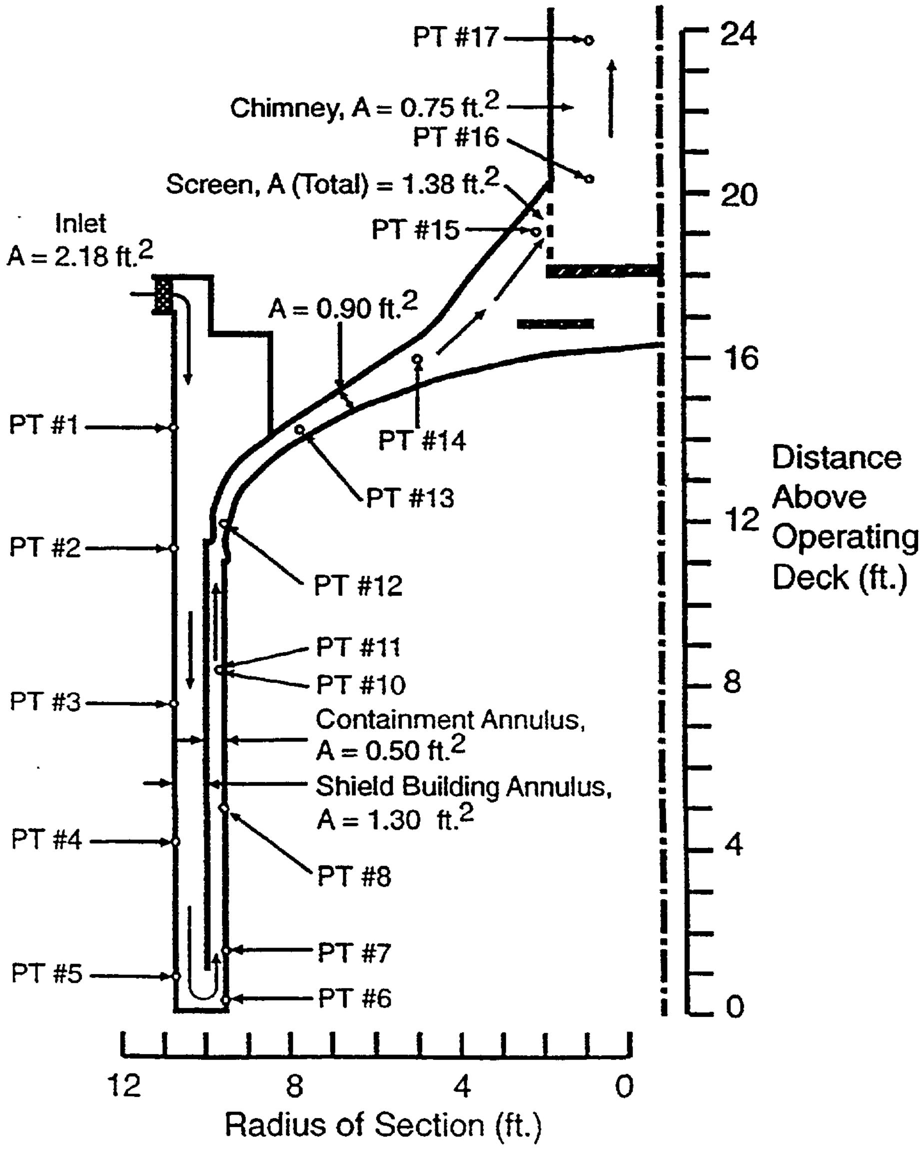

FIG. 13. AP600 PCS air flow path resistance test

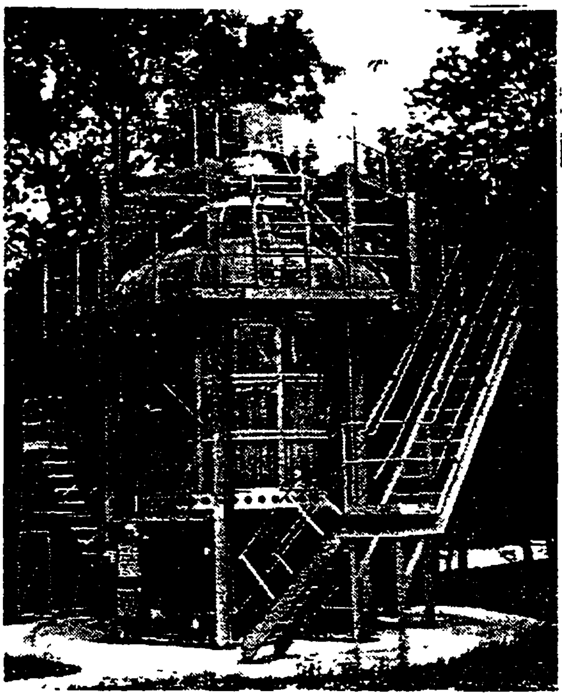

FIG. 14. AP600 large-scale heat transfer PCS test

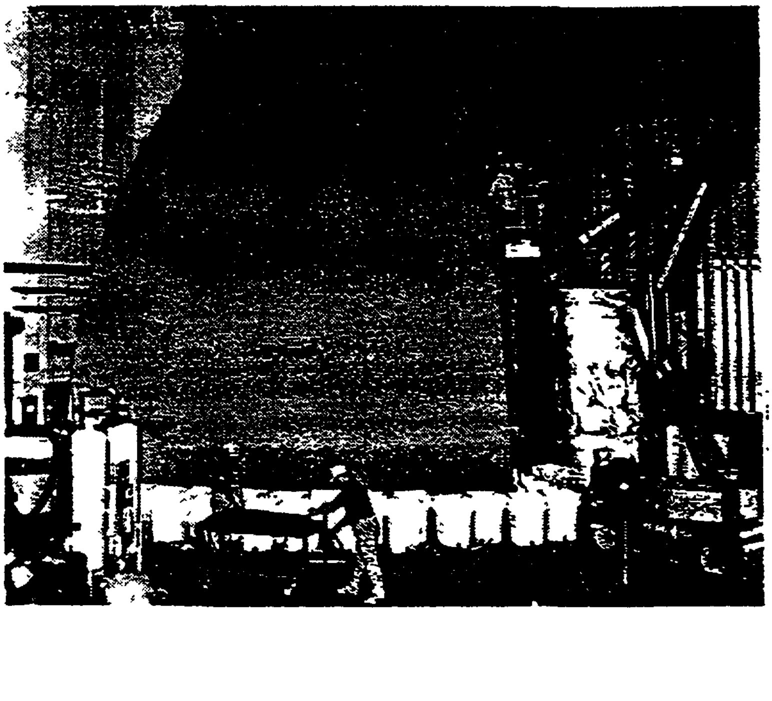

FIG. 15. AP600 water distribution tests

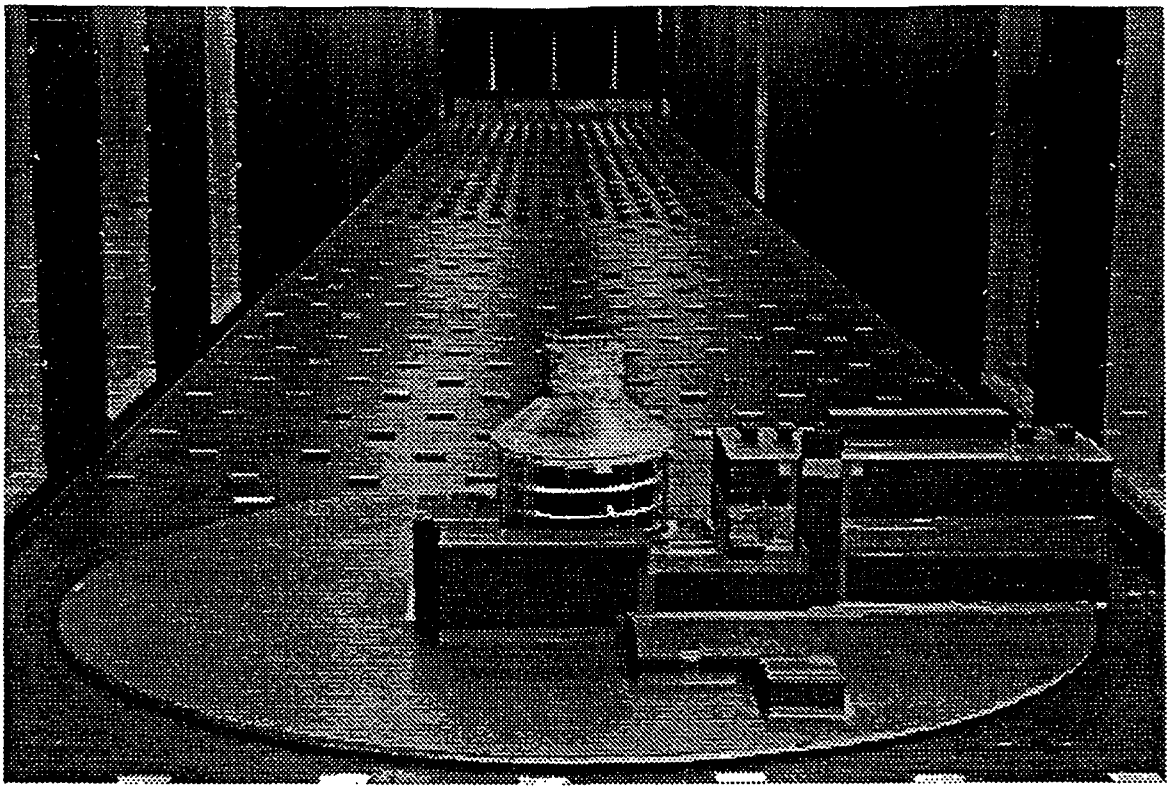

FIG. 16. AP600 wind tunnel tests

FIG. 17. AP600 passive residual heat removal exchanger test

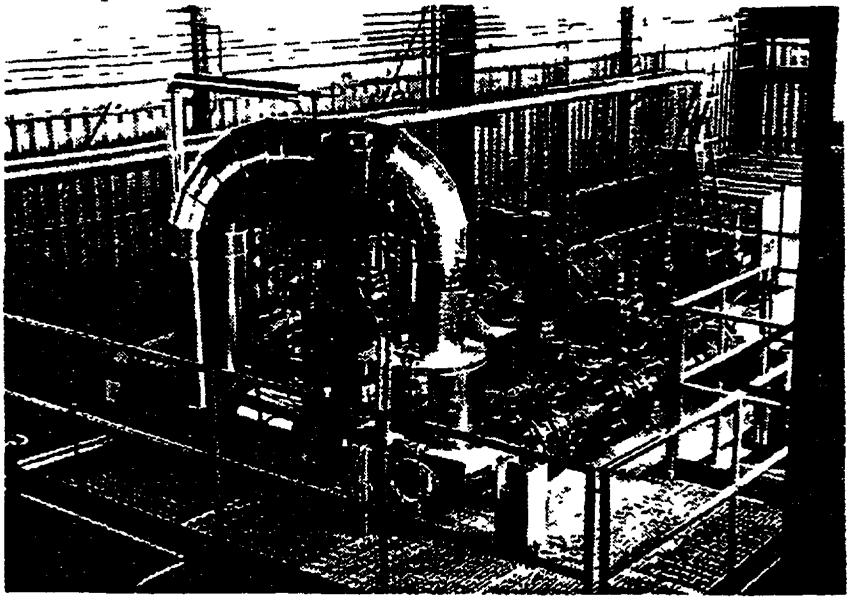

FIG. 18. AP600 automatic depressurization system test

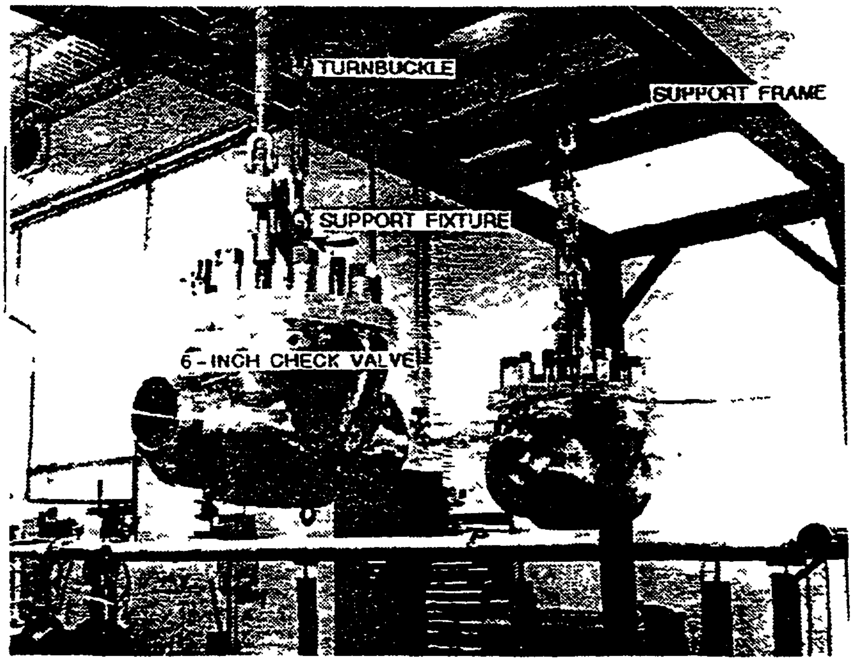

FIG. 19. AP600 check valve test

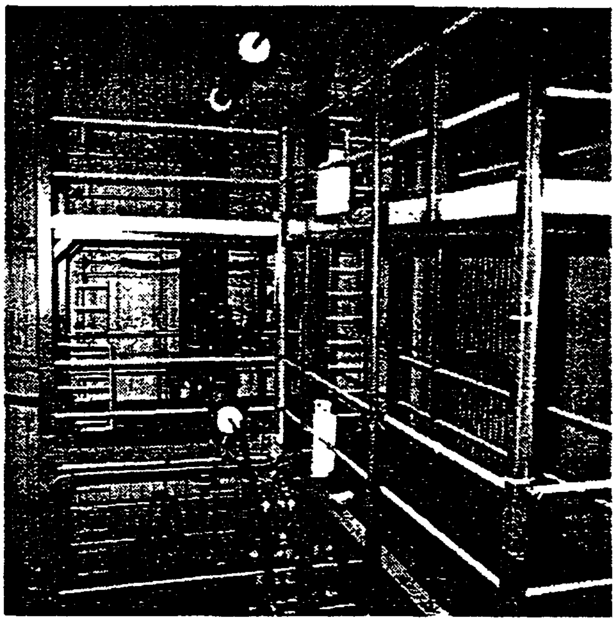

FIG. 20. AP600 core makeup tank test

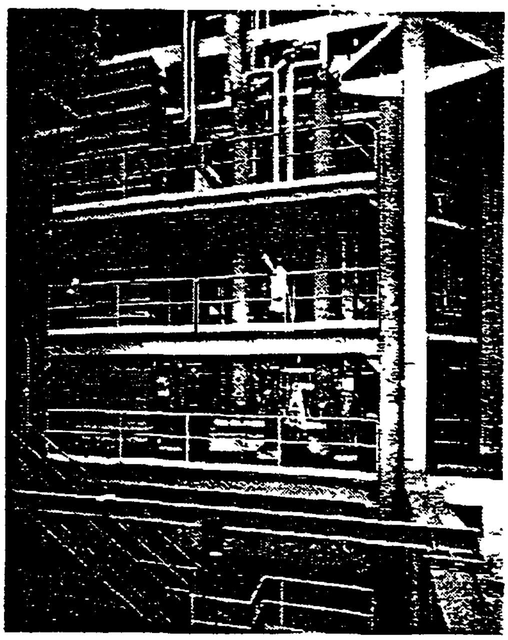

FIG. 21. AP600 full-pressure, full-height integral systems test

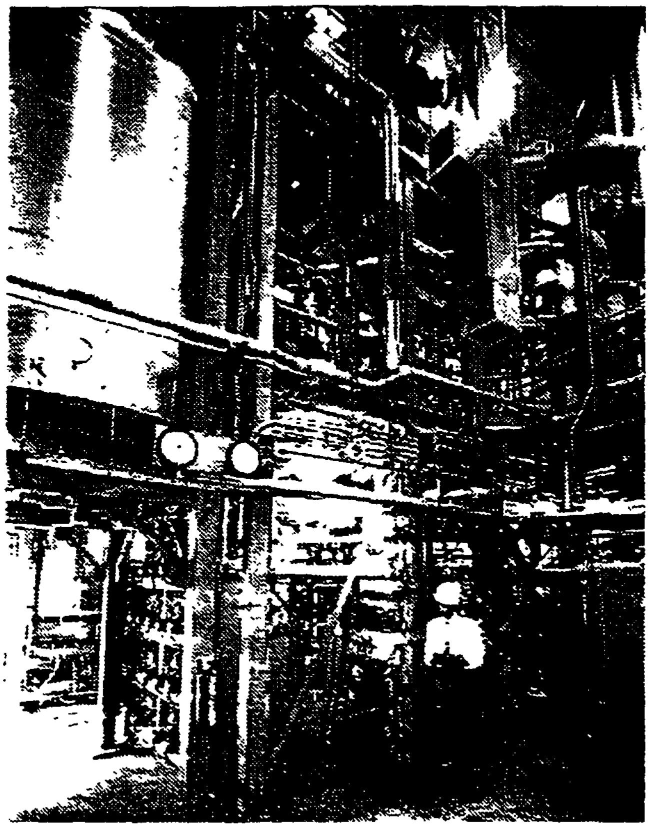

FIG. 22. AP600 long-term cooling integral systems test

TESTING FOR THE AP600 AUTOMATIC DEPRESSURIZATION SYSTEM

T. BUETER, L. CONWAY
Westinghouse Electric Corporation,
Pittsburgh, USA

P. INCALCATERRA, C. KROPP
ENEA C. R. Casaccia, Rome,
Italy

Abstract

The Automatic Depressurization System (ADS) of the Westinghouse AP600 reactor will be used to provide controlled depressurization of the reactor coolant system (RCS). This will, in turn, allow the initiation and long term operation of gravity driven cooling flow in the RCS. ADS tests were conducted at the VAPORE test facility in Casaccia, Italy through a Technical Cooperation Agreement between Westinghouse, ENEA, SOPREN/ANSALDO, and ENEL to produce data for the development and verification of computer codes to simulate the system. The test program also provided insights about the operation of valves supplied from various vendors that could be used in the AP600 ADS. The data gathered from the tests showed the ability of the ADS design to fulfill its function over the range of conditions expected in the AP600. The tests also demonstrated the abilities of gate and globe valves from several vendors to initiate and terminate an ADS blowdown as could be required in the AP600.

INTRODUCTION

The Automatic Depressurization System (ADS) in the Westinghouse AP600 Reactor will be used to provide staged depressurization of the reactor coolant system (RCS) to allow the initiation and continued long term gravity driven cooling flow to the RCS. The AP600 ADS design consists of 2 independent sets of ADS flow paths. Each of the flow paths consists of 4 separate stages. Each stage will contain 2 valves in series, an isolation valve and a control valve. Stages 1 through 3 are positioned at the top of the pressurizer. Stage 4 is connected to one of the two hot legs in the RCS loops. Each of the stages 1, 2, and 3 of the ADS will discharge through a sparger into the In-containment Refueling Water Storage Tank (IRWST), which will condense the steam discharge.

In order to test the design of the ADS and develop data for the development of computer codes that model the AP600 ADS, a full scale model of one of the ADS flow paths (stages 1, 2, and 3) was constructed at ENEA's VAPORE (VAlve and Pressurizer Operation Related Experiments) facility in Casaccia, Italy. The ADS tests were performed at VAPORE in three phases. The first phase, phase A, consisted of steam blowdowns performed to measure the steam condensation pressure pulses generated by the sparger. That testing was completed in 1992 and produced valuable data for the design of the IRWST structure as well as for the computer codes. Other papers have been published on this aspect of the ADS testing, and this paper will focus on the remaining phases of the testing.

The phase B testing was done through a technical cooperation agreement of Westinghouse, ENEA, SOPREN/ANSALDO, and ENEL to gather data on the ADS performance. The Phase B testing also was done to indicate the loadings that can be expected in the ADS piping, to gather data on the types of valves that could be used in the AP600 ADS, to gather data on the effects of the ADS blowdowns on the valves, and to benchmark the safety analysis computer codes. The phase B testing was further divided into two parts, B1 and B2. Phase B1 produced data with which to benchmark the computer codes used for the design certification of the AP600. Phase B2 showed the effects of the blowdown on the valves and gathered information about the various loads produced by the blowdown on the valves and piping of the ADS.

TEST FACILITY

The VAPORE test facility was originally designed to test safety valves for power plants. It has a 1400 ft^3 (39.6 m^3) PWR pressurizer and a discharge line at the top of the pressurizer for steam discharges through the valves and into an in-ground, reinforced concrete discharge tank. The pressurizer has a volume of about 40 m^3, and a design pressure and temperature of 19.7 MPa (about 2900 psig) and 365°C (625°F), respectively. There are 1.6 MW of electric heaters available to heat the water for a test at VAPORE. This facility met the needs of the tests of the ADS design, although some significant modifications were needed for the AP600 testing program.

Modifications were made to the discharge tank, including the addition of a prototypical sparger, and the ability to heat the condensing water in the tank to up to 100°C with superheated steam from the C. R. Casaccia district heating system. For the phase B testing the sparger was repositioned at a higher elevation in the pool, because the analyses from the Phase A part of the testing indicated the new position would allow the steam discharge to condense more quickly and reduce the loads on the tank walls.

A water line with two isolation gate valves was added at the bottom of the pressurizer, and a full size prototypical ADS loop was constructed. It was built to allow it to be connected to the steam discharge line or the water discharge line through the use of a common elbow/spool piece that had to be moved from the steam line to the water line (or visa versa) for a test.

The ADS loop at VAPORE consists of three stages of piping and valves. Each stage consists of a pair of valves, a gate valve upstream of a globe valve. The three stages are arranged in a loop as shown in Figure 1. The AP600 design calls for two redundant loops to be supported on top of the pressurizer. The fourth stage of the AP600 ADS which connects to the hot legs of the RCS, was not modeled at VAPORE.

PHASE B TESTING

The phase B1 testing was performed in the latter half of 1994. The tests were designed to produce flow regimes similar to those that the ADS on the AP600 would experience. That is, the phase B1 tests were designed to produce data that would bound the mass flow and quality of expected transients in the AP600. The tests showed that the ADS design was capable of performing its depressurization function as well as provided data for the validation of computer codes that could simulate the AP600 safety systems. The Phase B1 data also provided the responses of the sparger discharge pool to the revised elevation of the sparger.

The B1 tests were performed with only two 8-inch gate valves, stages 2 and 3, and one 4-inch globe valve, stage 1. The 8-inch globe valves in stages 2 and 3, and 4-inch gate valve in stage 1 were simulated with orifices in some of the tests to bound the data on the blowdown with all six of the valves installed. Some of the B1 tests were performed with no orifices installed to bound the maximum mass flow of the ADS loop.

The Phase B1 tests included several series. One test series consisted of blowdowns through only one stage, a gate/globe (orifice/valve for the B1 tests) pair in the ADS loop. Other tests called for the blowdown to go through 2 stages together, and other tests required 3 stages together.

The tests included blowdowns with 2 phase flow, i.e., flow from the bottom of the pressurizer through the liquid line. There were also tests with saturated steam through the steam discharge line in the top of the pressurizer. These two types of tests showed the influences of relatively large mass/small volumetric flows versus relatively small mass/large volumetric flows in the ADS and the discharge pool.

For all of these tests data was taken from approximately 130 locations in the VAPORE ADS piping and the sparger discharge pool. These data points included the temperatures and pressures before and after each of the valves, the temperatures and pressures in various positions on the discharge pool walls and in the immediate vicinity of the sparger. Typically, there were 43 pressure transducers, 10 pressure transmitters, 15 strain gages, 10 load cells, 9 accelerometers, 2 level transmitters, 1 ΔP cell, 3 valve position indicators, and 46 thermocouples in the set of instruments used on the ADS loop and in the sparger pool during a test.

For the Phase B2 tests, the ADS valves were also instrumented with a data acquisition system developed by ITI MOVATS. This system included instruments to measure the valve torque and thrust, the valve stem position and the movement of the valve spring pack at any point during the valve stroke.

Examples of the Phase B1 data for a blowdown from one of the tests is shown in Figures 2, 3, 4, and 5. Figure 2 shows the pressure and temperature of the fluid as it enters the ADS loop. As flow was initiated by opening the 12-inch gate valve used for isolation of the pressurizer, the rapid increase in temperature and pressure can be seen at the entrance to the ADS loop. The rather quick initial drop in the temperature shown in this figure at the beginning of the blowdown is a result of the cold water from the bottom of the pressurizer traveling through the piping (where the water discharge line was located). After the few seconds required for the plug of cold water to pass, the temperature increase in the blowdown fluid as it enters the ADS loop is evident.

The pressure in the piping before the ADS loop decreases as the blowdown progresses until the isolation valve is closed, when it levels off. The pressure and quality at the entrance of the ADS loop was controlled through the use of one of the 12-inch insolation gate valves, VLI-2, as a kind of orifice. The valve was left in a carefully measured, partially closed position in order to create a flow orifice to limit the mass flow. This also created a source of a pressure drop and flashing to steam in the saturated fluid. This use of the valve allowed for the input fluid quality to be varied to as much as 20%, while the mass flow was kept in the required range of the AP600 design.

Figure 3 shows the temperature and pressure in the middle of the ADS stage through which the blowdown traveled, in this case the 4-inch piping, stage 1. The rapid increase of the pressure and temperature correlates to the time of the opening of the 12-inch isolation valve plus a short time for the fluid to transit to the ADS loop. For this test, the flow area through the 12-inch gate valve, VLI-2, used to control the mass flow and quality, was slightly less than the flow area of any of the piping or valves in stage 1.

Figure 4 shows the pressure and temperature of the fluid in the 16-inch discharge line for the ADS loop. The data trace mimics those in the previous figure, albeit at a lower pressure due to the pressure drop through the ADS stage piping and valve and the increase in the size of the piping as the fluid exits the ADS loop. The time delay is slightly longer as the fluid had to travel completely through the loop before it arrived at the discharge line.

Figure 5 shows the discharge pool response to the blowdown from an instrument near the lower part of one of the sparger arms. The initiation of the discharge can be clearly seen in the temperature data. The pressure changes cannot be discerned, because they are so small. This is because the pressure increases only slightly as the condensing water remains subcooled with atmospheric pressure at the top of the pool. The water in the discharge pool very rapidly cooled the saturated, two phase fluid from the blowdown, causing the rapid local temperature increase in the fluid where the sparger arms were located.

Some of the Phase B1 tests required that the discharge pool be cold, i.e., less than 60°C, while others required that the discharge pool be at saturation temperature, 100°C. The hot pool tests were performed to gather data on the effects of the blowdowns on the discharge tank for those analyses where it is postulated that the pool may have been heated to saturation prior to the ADS initiation. The cold pool tests were performed to collect data on the expected usual operating conditions of the ADS.

As discussed earlier the cold pool tests showed that the ADS loop discharge was rapidly cooled, condensing the steam in the two phase flow, or completely condensing the saturated steam flow for the steam tests. The average temperature of the discharge pool after the test was increased nominally with the blowdown, usually 5°C to 10°C. In Figure 5, a higher overall temperature can be seen at the end of the test than was at the beginning of the test. This is a local, transient, effect seen immediately after a test was completed. After a relatively short time, the temperature of the pool reached equilibrium at a level 5°C to 10°C higher than it was before the test.

The Phase B2 tests were designed to examine the valves installed in the ADS loop at VAPORE. Gate valves and globe valves were designed, built by several different vendors, and installed in the test facility. Two of the gate valves and one globe valve used in the Phase B2 tests were used for the phase B1 tests as well. In the Phase B1 tests the valves were always used either in the fully open or fully closed positions, i.e., they were not opened or closed with a differential pressure across them.

In contrast, the Phase B2 tests were designed to test the ability of each valve to initiate and terminate an ADS blowdown at the various pressures expected to be seen in the AP600. One series of tests called for the initiation and termination of the blowdown flow with the globe valve in the ADS stage, i.e., a gate/globe valve pair. Another series of tests called for the initiation and termination of the blowdown flow with the gate valve in the stage. These tests were done in a range of pressures from approximately 400 psig (30 bar) to 2235 psig (154 bar) to cover the range of pressures for the AP600 ADS.

Figures 6, 7, 8 and 9 show some of the results from a typical Phase B2 blowdown test. In Figures 6 and 7, the data traces for the torque and thrust, respectively, applied to the 4-inch gate valve during a blowdown can be seen. This blowdown was initiated and terminated with the 4 inch gate valve. The "steps" in the torque signal as the valve closes are due to the effects of the fluid flow on the valve gate. That is, a static valve test would not show these characteristic plateaus in the torque during the valve stroke. In this test, as in all of the B2 tests, the ADS valve successfully initiated and terminated the flow through the ADS loop.

The maximum torque and thrust for the valve can be seen a few seconds after the beginning of the valve stroke, just before the torque and thrust drop from their maximum to their minimum.. The maximum torque is usually when the valve is in its seat, as is the case in Figure 6. The torque will reach a 0 point just after it starts to open as seen in the figure where the trace drops in a vertical line to the minimum value. The thrust trace in Figure 7 is similar in shape to the torque data, as the thrust would be expected to be. In some of the tests the valve thrust values did not follow the torque as closely as expected. The test valve operators had sufficient torque to open and close the valves, and it was expected that the thrust traces would all look the same as the torque traces. But, there were tests where this was not true. This was thought to be due to the design of the threads on the valve stem, the type of grease used, or the forces imposed by the fluid flow through the valve.

The valve was opened under the pressure of the fluid from the pressurizer, remained open for a few seconds, then closed. The valve was fully open at the point in the traces where an almost horizontal line can be seen in the data traces. Another increase in the torque and thrust occurred when the valve started to close again. The running values can be seen until the valve contacts the seat, at which point the gate is forced into the seat and the torque rises to its initial value. The torque is reduced slightly on the close stroke as the force of the fluid helps to close the valve. This can be seen at the peak at the end of the trace where the torque drops rapidly a few percent just after it reaches the peak.

Figures 6 and 7 can be compared to the fluid pressure upstream and downstream of the ADS loop in Figures 8 and 9, respectively, to see the relative fluid temperature and pressure at the various stages of the valves' operation. As with the Phase B1 tests the pressure in the ADS loop exhibits a rapid increase as the valve opened, peaks, then drops off as the valve was closed. The pressure upstream of the ADS loop steadily decreases as the pressurizer is drained. Again, there is a sharp, short lived decrease in the fluid temperature in the entrance to the ADS loop as the cold water from the bottom of the pressurizer passes past the entrance to the ADS loop.

Since one of the concerns with gate valves is the thermal binding of the gates in the seats, cold stroke tests were performed after each hot blowdown test, to show any significant changes in the torque or thrust required to operate a valve when it was allowed to cool down in the closed position.

The results of those tests showed that the torque and thrust required to unseat the gate of the valve after it had cooled were usually *lessened* after the valve had cooled in the closed position. In fact, after the valve had been allowed to cool from operating temperatures, then stroked one time, the opening torque and thrust were usually slightly higher on subsequent cold stroke tests. That is, for the first cold stroke the torque and thrust required to open the valve were usually less that what was required when the valve was hot. The torque and thrust values returned to their usual values on the second and third cold stroke tests. In all cases the torque and thrust required to open the valve were essentially the same when the valve was hot as when the valve was cooled in the closed position before it was opened.

SUMMARY

The ADS testing program performed at VAPORE produced data for the development and refinement of computer simulations of the AP600 ADS. The tests demonstrated the ADS design can successfully depressurize the AP600 RCS in a controlled manner for the range of pressures and fluid qualities that may be seen in the AP600. The phase B1 tests covered a range of combinations of flow paths that could be used if the ADS was called upon to depressurized the RCS. This phase of the testing also demonstrated the suitability of the submerged depth of the discharge tank sparger for the AP600 design. The phase B2 tests demonstrated the ability of gate and globe valves from a variety of vendors to successfully initiate and terminate a blowdown of the AP600 RCS. Phase B2 also covered a wide range of supply pressures to test the valves in conditions representative of the AP600.

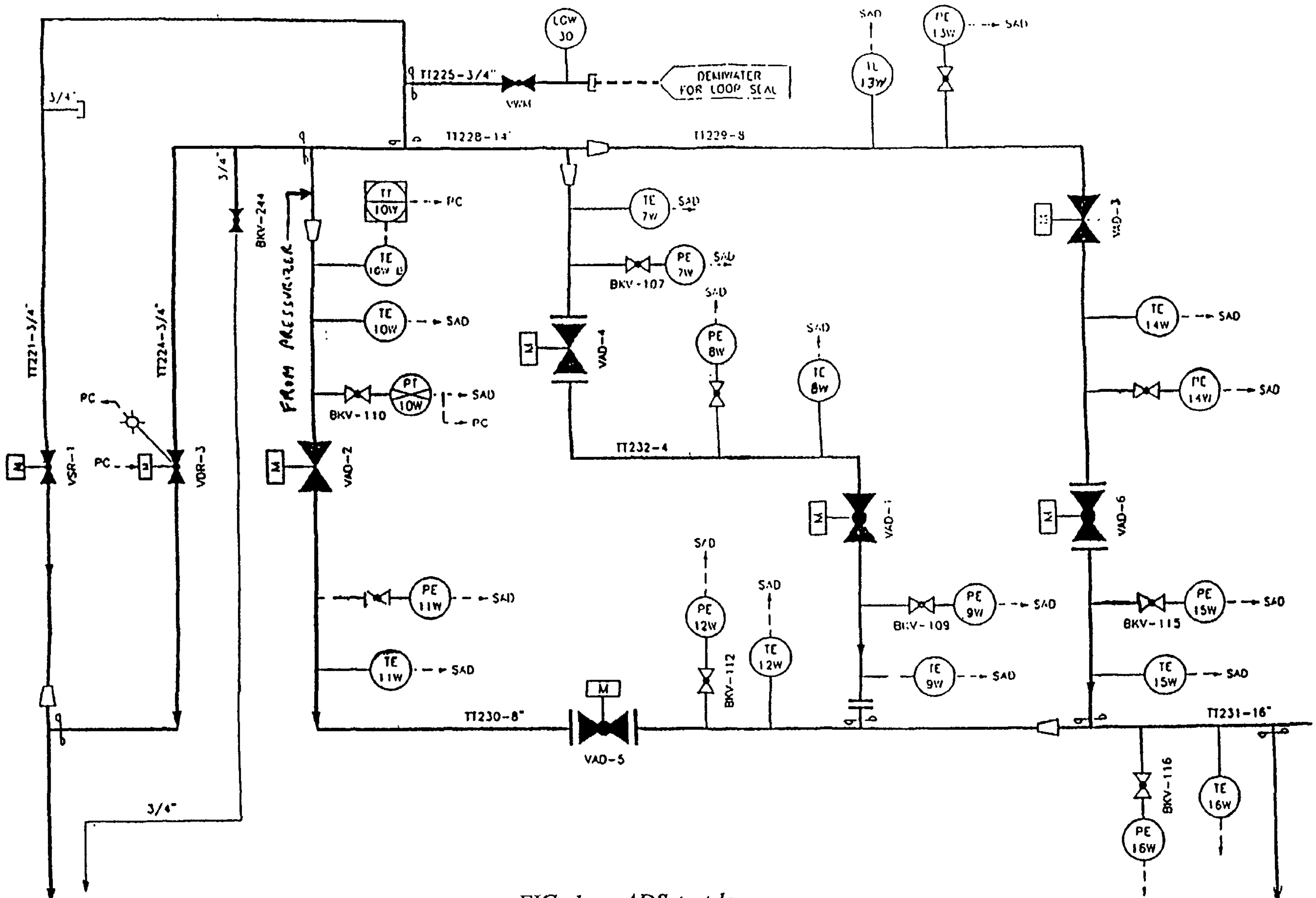

FIG. 1. ADS test loop

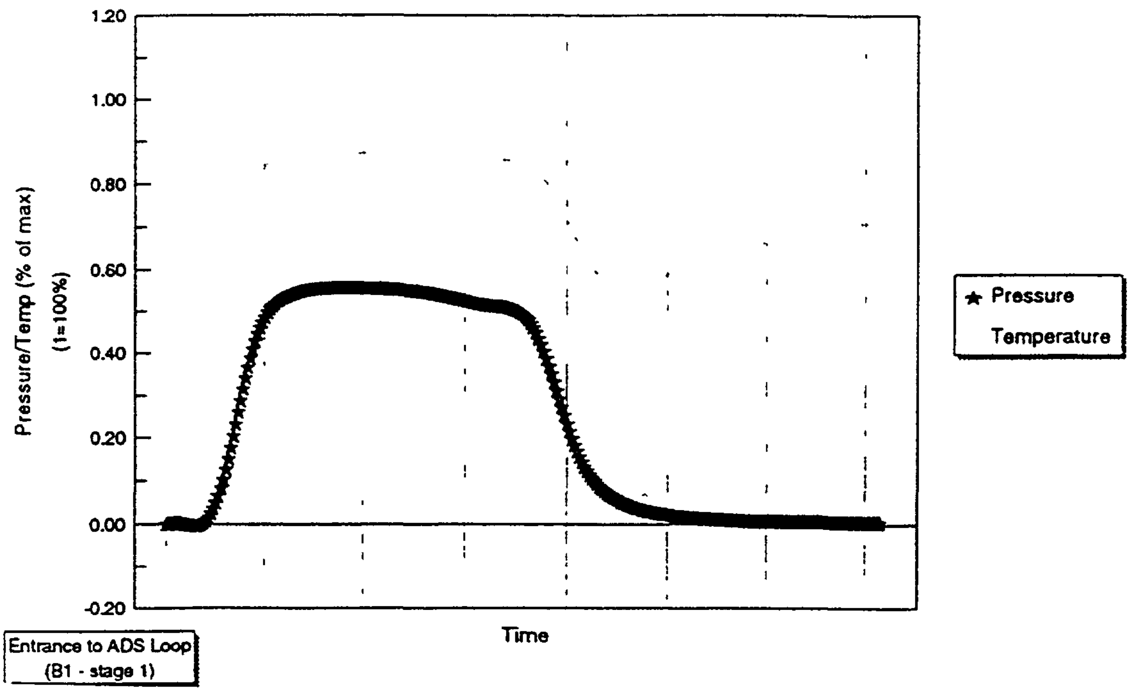

FIG. 2. Pressure and temperature at entrance to ADS loop

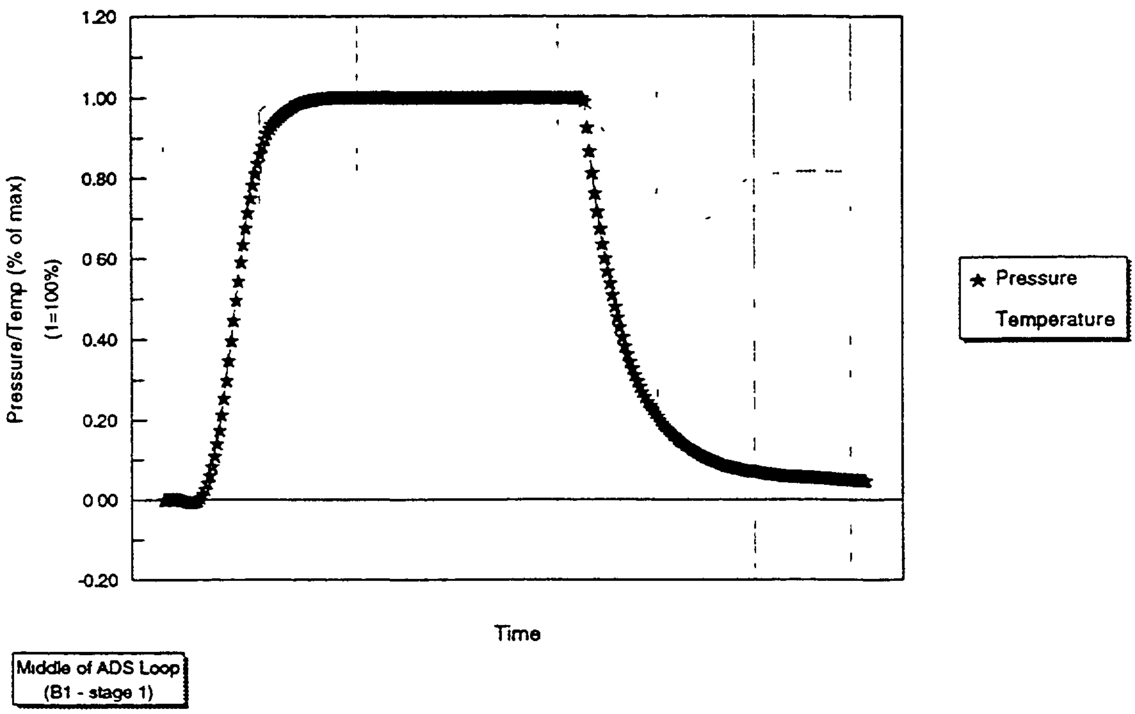

FIG. 3. Pressure and temperature at middle of ADS loop

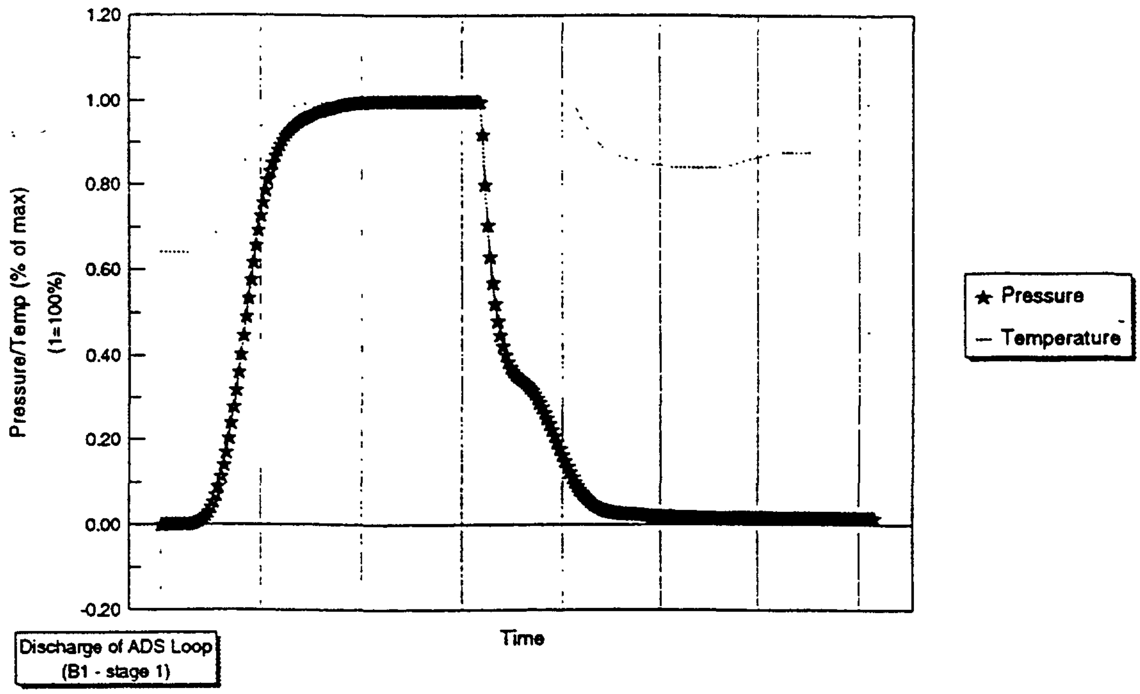

FIG. 4. Pressure and temperature at discharge of ADS loop

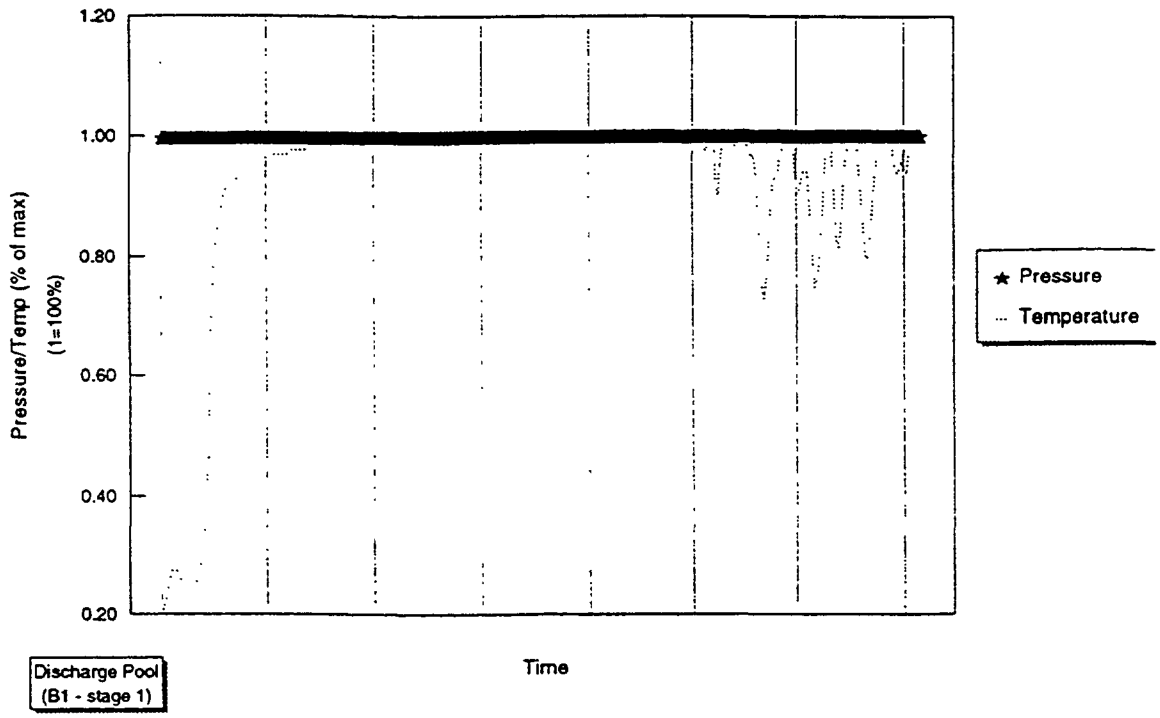

FIG. 5. Pressure and temperature in discharge pool

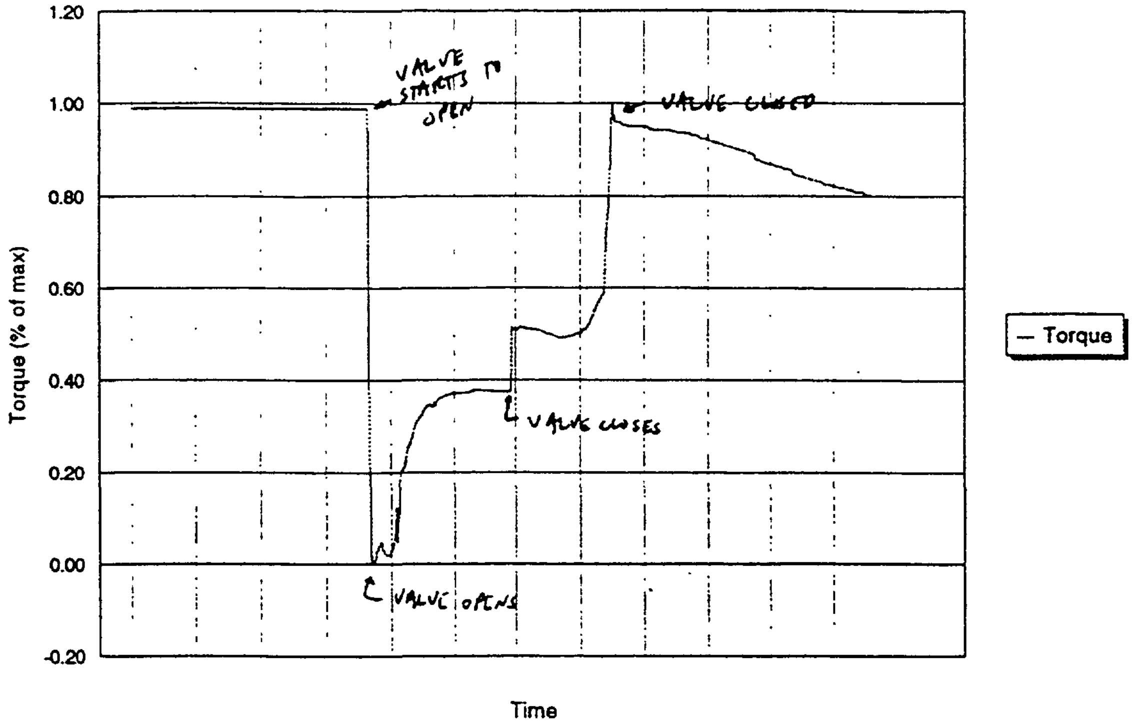

FIG. 6. *Torque applied to gate valve during blowdown*

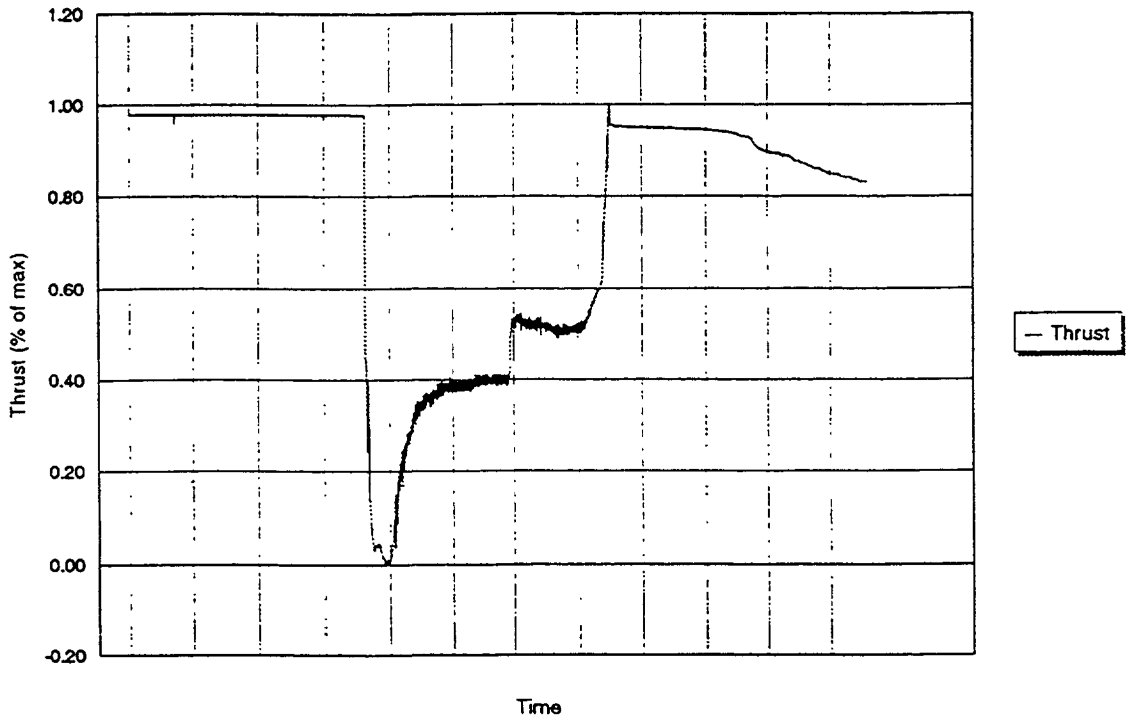

FIG. 7. *Thrust applied to gate valve during blowdown*

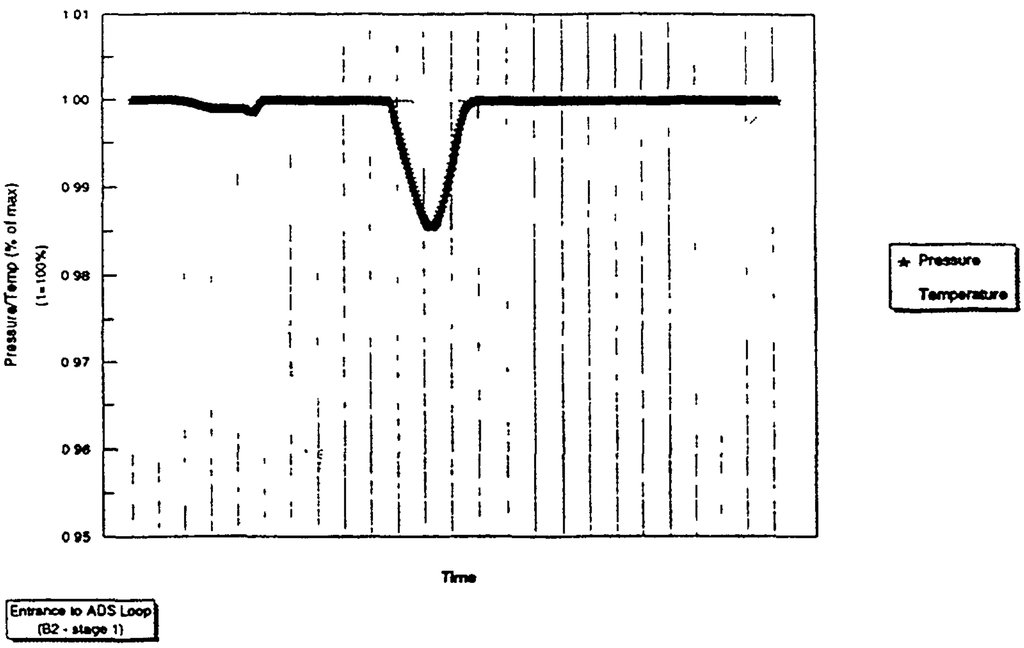

FIG. 8. *Pressure and temperature at entrance to ADS loop for phase B2 blowdown*

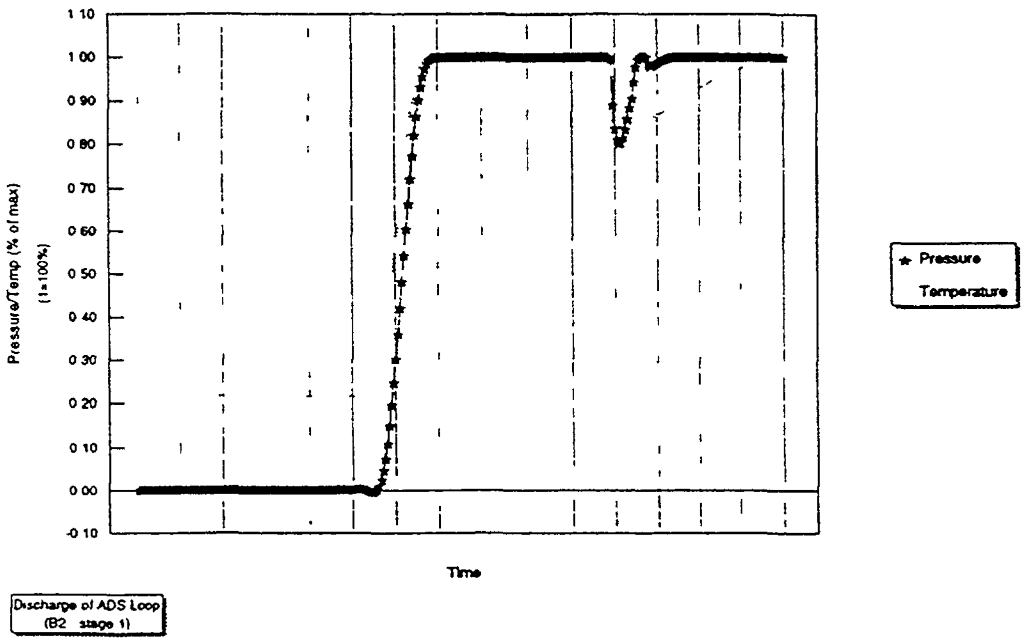

FIG. 9. *Pressure and temperature at discharge of ADS loop for phase B2 blowdown*

THE STUDY OF THE EFFECTIVENESS OF THE EMERGENCY CONDENSER OF THE BWR 600/1000 IN THE NOKO TEST FACILITY

E.F. HICKEN, H. JAEGERS, A. SCHAFFRATH
Forschungszentrum Juelich, ISR,
Juelich, Germany

Abstract

The BWR600/1000 is a new innovative passive boiling water reactor concept which is being developed by Siemens. The concept is characterized in particular by passive safety systems (i.e. four emergency condensers, four building condensers, eight passive pressure pulse transmitters, six gravity-driven core flooding lines, eight rupture disks arranged in parallel to the relief valves and two scram systems).

For experimental investigations of the effectiveness of the emergency condenser the NOKO test facility has been constructed at the Forschungszentrum Jülich in cooperation with Siemens. This project is sponsored also by the BMBF and some German Utilities. The test phase started in early 1995.

The NOKO facility has a maximum operating pressure of 9 MPa and maximum power of 4 MW for steam production. The emergency condenser consists of 8 tubes and is fabricated with original geometries and materials.

The objectives of the experiments are the study of the effectiveness of the BWR600/1000 emergency condenser under all expected conditions and (including non-condensibles), the use of the experimental data for computer code validation and model improvements.

Some results from the start-up phase will be given.

After finishing the emergency condenser test series several other components (e.g. building condensers and passive pressure pulse transmitters of the BWR600/1000) shall be tested in the NOKO facility. Because of the multi-purpose design of the NOKO test facility only few reconstructions are necessary for other designs.

1. Introduction

The BWR 600/1000 is a new innovative passive boiling water reactor concept which is being developed by Siemens. The concept is characterized in particular by passive safety systems (i.e. four emergency condensers, four building condensers, eight passive pressure pulse transmitters, six gravity-driven core flooding lines, eight rupture dishes arranged in parallel to the safety valves and two scram systems. For completeness fig. 1 and 2 show the design of the BWR 600/1000.

For experimental investigations of the effectiveness of the emergency condenser (and later for other components) the NOKO test facility has been constructed at the Forschungszentrum Jülich (KFA) in cooperation with Siemens, which was responsible for the detailed planning and for most components. This project is funded by the BMBF, some German Utilities, Siemens and KFA.

2. The NOKO Test Facility

The general design is shown in fig. 3. An electrical heater, which has been used before for in the HDR facility, produces a two-phase flow mixture, which is separated in the separator. The pressure vessel with an inner diameter of 0.5 m and a height of 12.7 m is mainly used to control the water level. Connected to the pressure vessel are the feed line and the down-pipe of the emergency condenser. Both pipes lead the headers; eight pipes are connected to the headers. For the simulation of the water pool the emergency condenser is placed within a vessel. This vessel, named condenser, contains 20 m^3 of water and can be operated up to 1 MPa. The heat removal from this condenser is evaporation of water. The steam is condensed in the condensation tank, which is used also as a water storage tank and as a depressurisation system for relief and safety valves. The heat removal from the condensation tank happens through a cooling loop which transfers the energy to a river or a cooling tower.

The power level of the electrical heater can be controled in 8 steps; the maximum pressure within the primary loop is 9 MPa.

The detailed planning of the test facility started in October 1993; in December 1994 the facility was running for a short time with 1.35 MW.

3. Instrumentation

In addition to the instrumentation used for operational purposes the test instrumentation is shown in fig. 4. As a result from start-up tests some more instruments, mainly mass flow instrumentation will be installed.

The accuracy of instrumentation will repeatedly be checked with calibrated instruments; the power of the electrical heater can be measured with an accuracy of 0.2 %.

4. Test Programme

Although not yet fixed we expect about 100 test runs within 1 year. The variables to be studied are power, pressure, pressure vessel level on the primary side, pressure, temperature and water level on the secondary side, length of down pipe and flow resistences in steam line and down-pipe. In addition, the mass flow through the emergency condenser in case of a flooded pressure vessel will be studied.

5. Results from Start-Up Tests

After the usual difficulties during the start-up period we can state that the electrical heater and the control systems operate appropriately. The recirculation pump is sensitive to subcooling due to requirements from the component protection system.

The instrumentation shows no difficulties. The heat up period is about 2-4 hours and the time for one test between 30 and 60 minutes.

In fig 5 and 6 preliminary date are shown. The solid curves show the expected values as calculated by the vendor. Both figures contain experimental data.

6. Future Tests

It is planned to test the passive pressure pulse transmitters, see fig. 7, in parallel to the emergency condenser.

Following the tests with the emergency condenser, the building condenser, fig. 8, will be tested.

Following these tests steam injectors, see fig. 9 are candidats for being installed in the NOKO facility.

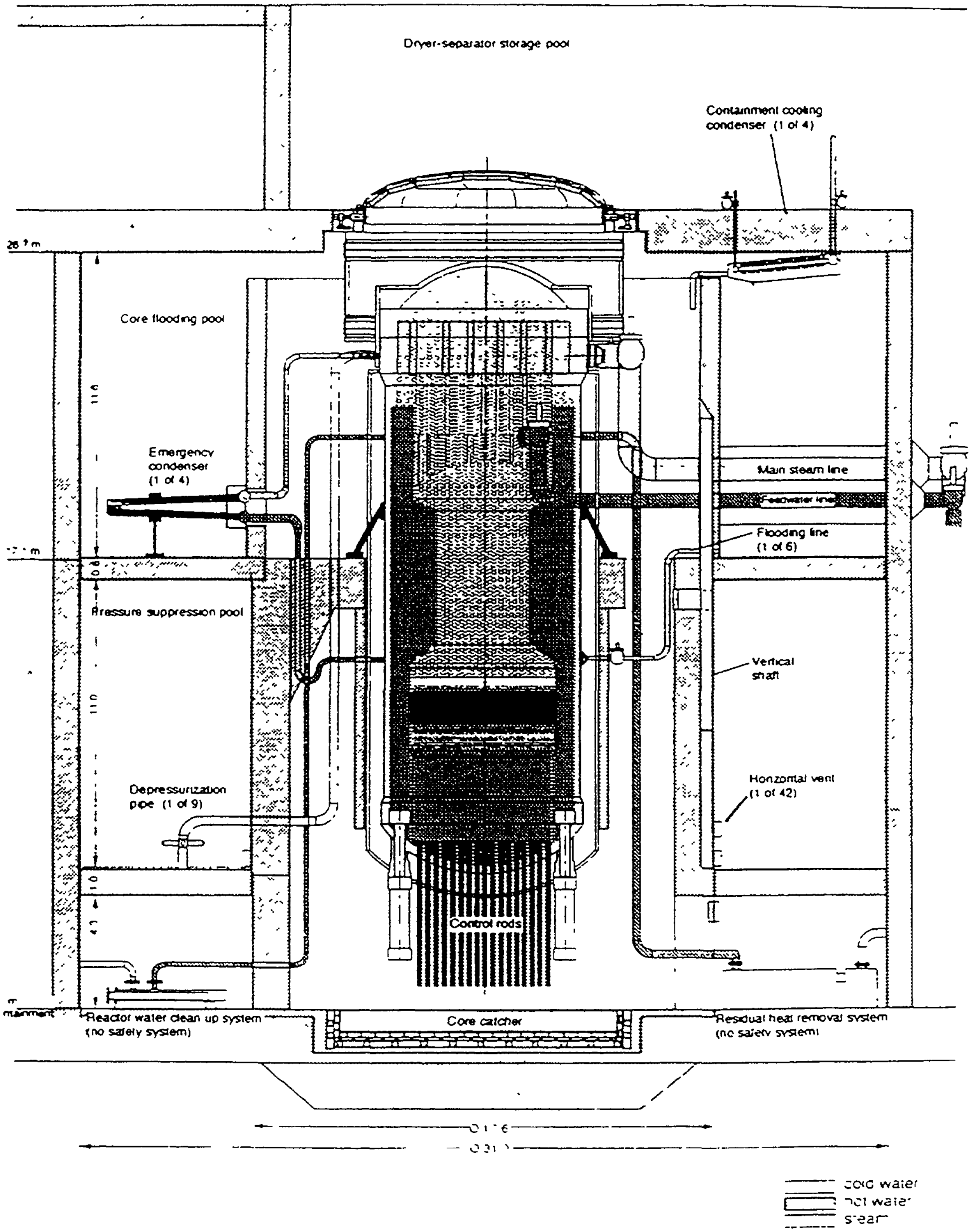

FIG. 1. BWR 600/1000 containment

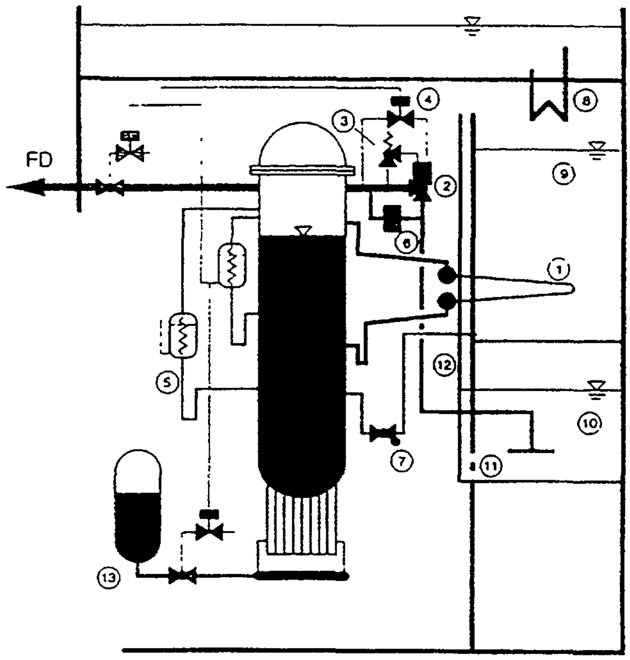

1 Emergency condenser (total of 4)
2 Safety-relief valve (total of 8)
3 Spring-loaded pilot valve
4 Diaphragm pilot valve
5 Passive pressure pulse transmitter
6 Rupture disk (total of 8)
7 Flooding line (total of 4)
8 Containment cooling condenser (total of 4)
9 Core flooding pool
10 Pressure suppression pool
11 Horizontal discharge vent
12 Vertical discharge shaft
13 Scram system

FIG. 2. BWR 600 - passive systems

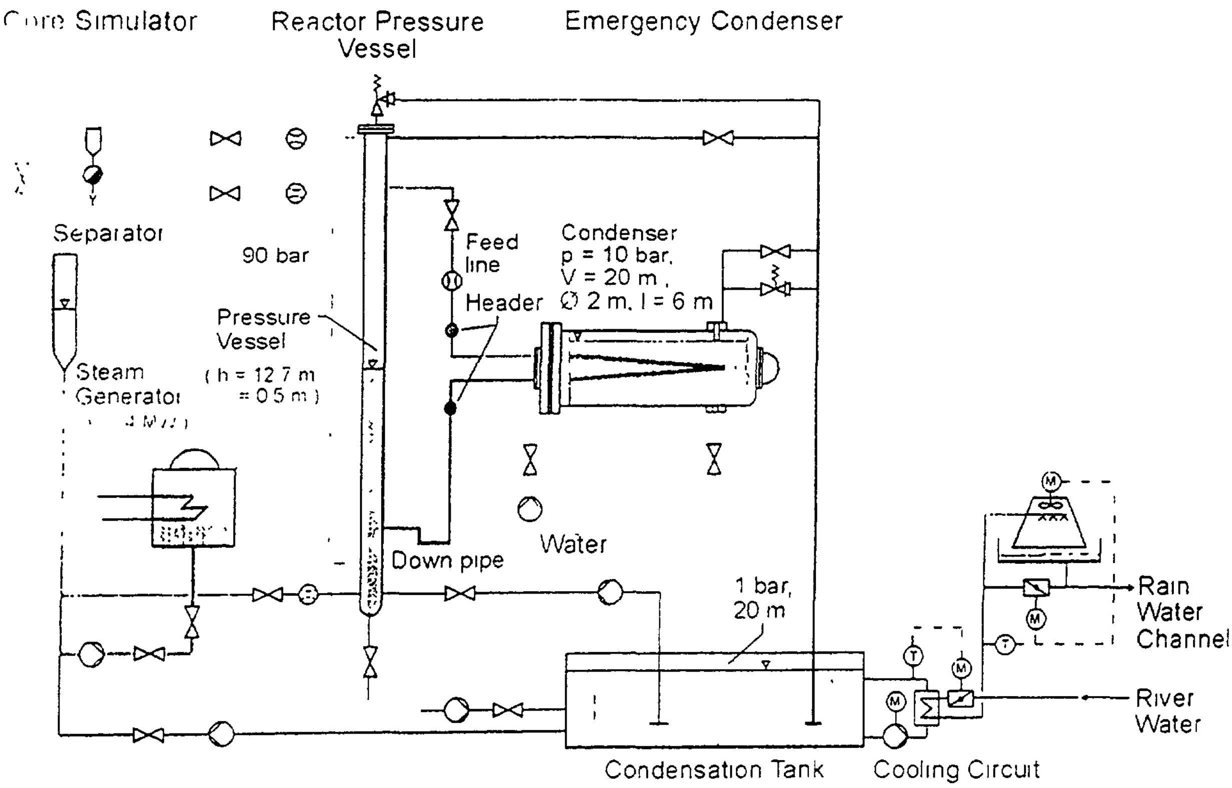

FIG. 3. General design of the NOKO test facility

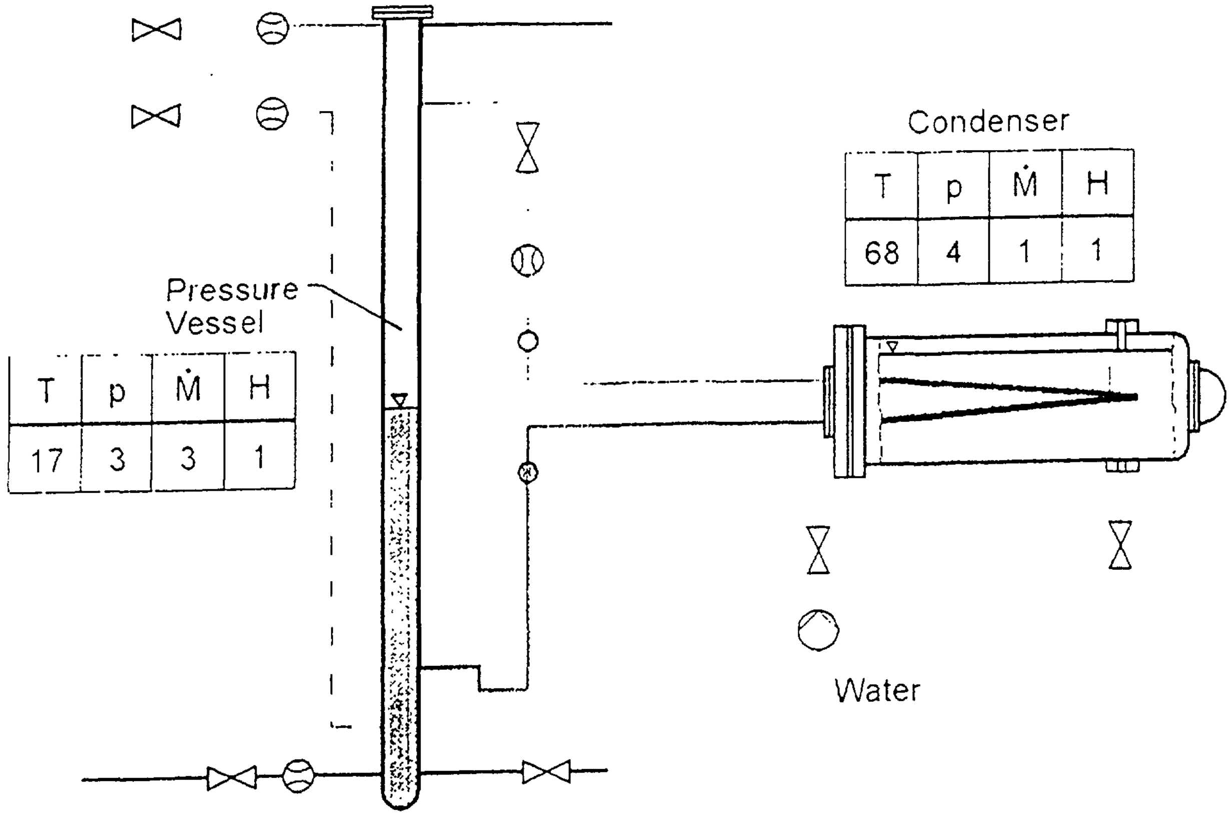

FIG. 4. Instrumentation scheme

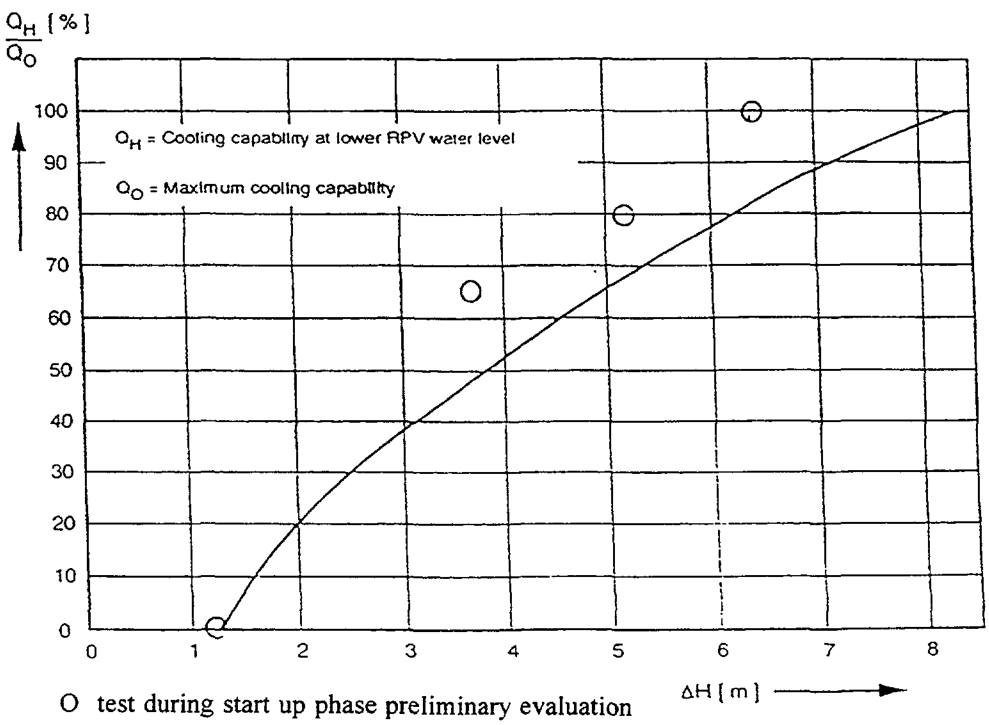

FIG. 5. SWR 1000 - emergency condenser. Cooling capability as a function of loss of water level in the RPV (ΔH in m)

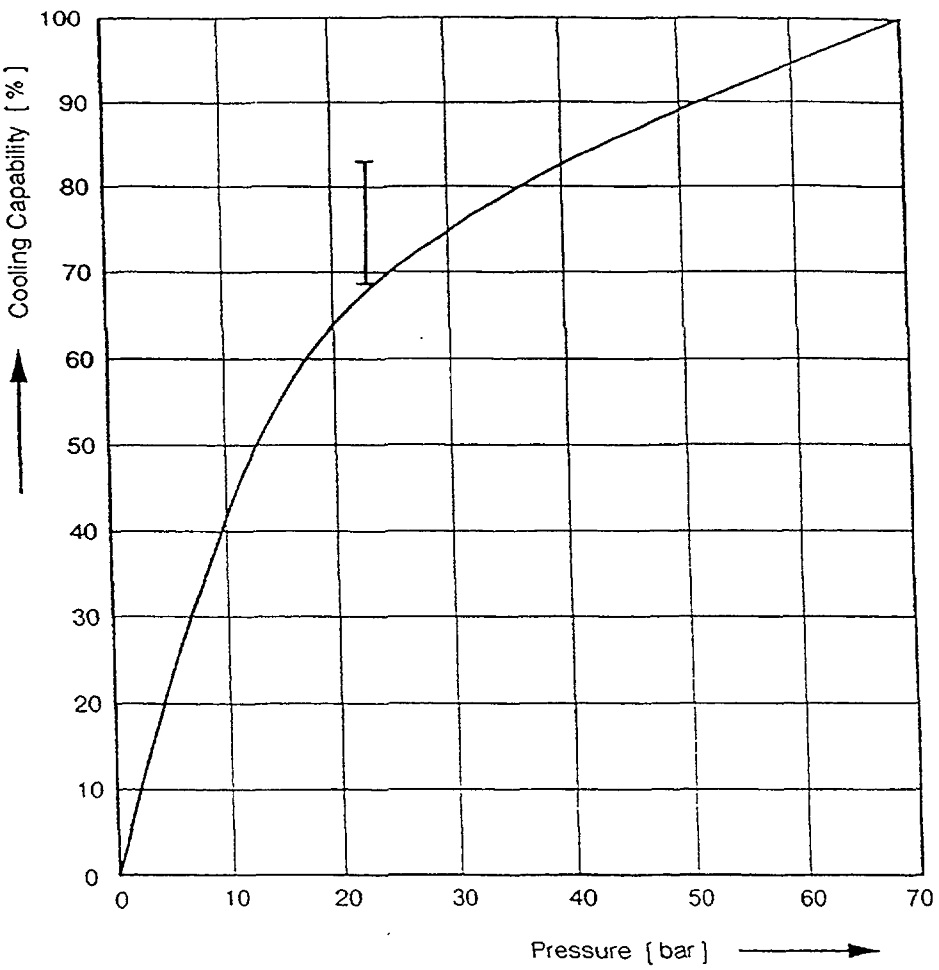

FIG. 6. *SWR 1000 - emergency condenser. Cooling capability as a function of pressure in the RPV*

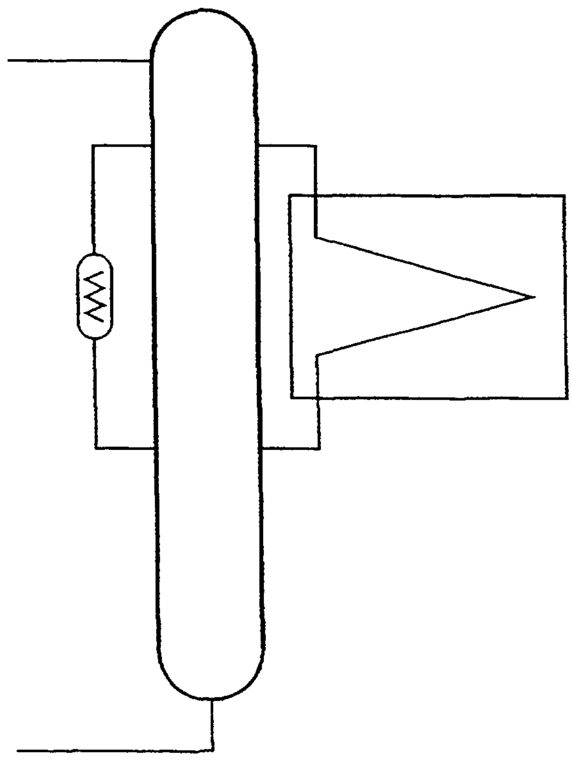

FIG. 7. *Passive pressure pulse transmitter*

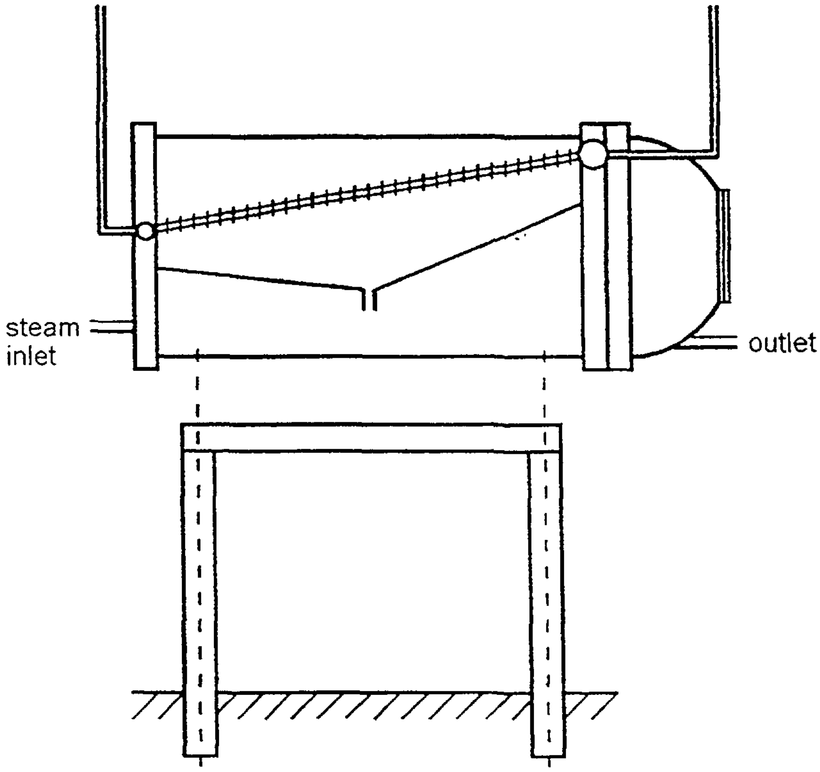

FIG. 8. Building condenser

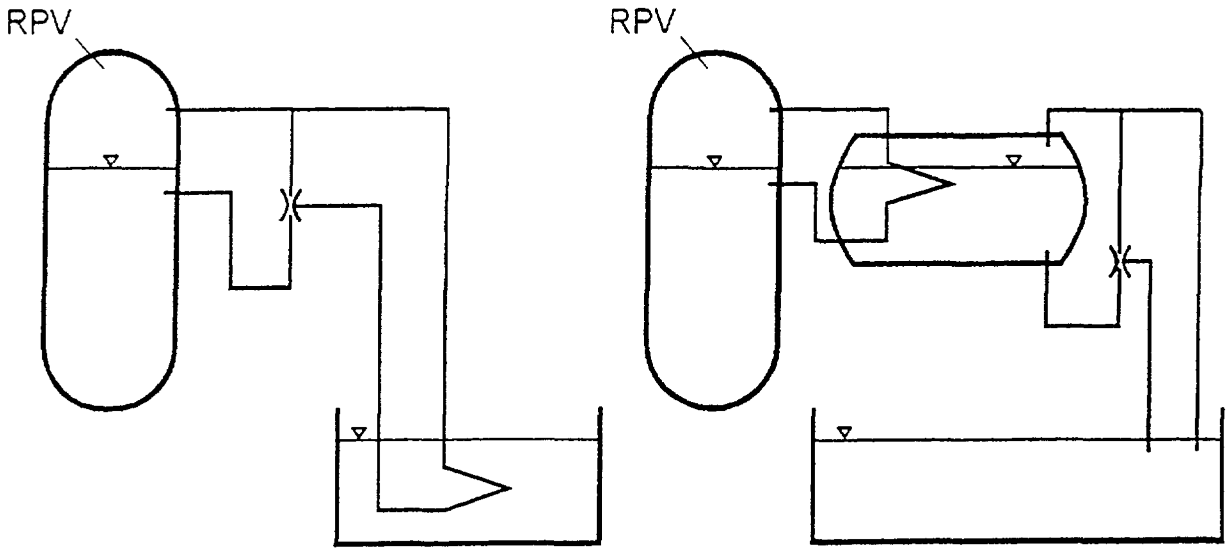

FIG. 9. Steam injectors

EXPERIMENTAL STUDY OF ISOLATION CONDENSER PERFORMANCES BY PIPE-ONE APPARATUS

R. BOVALINI, F. D'AURIA, G.M. GALASSI, M. MAZZINI
Dipartimento di Costruzioni Meccaniche e Nucleari,
Università degli Studi, Pisa, Italy

Abstract

The paper discusses an experiment performed in PIPER-ONE facility which simulates a General Electric BWR-6 with volume and height scaling ratios of 1/2200 and 1/1, respectively. The apparatus was properly modified to test the thermalhydraulic characteristics of an isolation condenser-type system. This system consists in an once-through heat exchanger, immersed in a pool with water at ambient temperature and installed at about 10 m above the core.

The analysis of a first test on isolation condenser behaviour, named PO-SD-8, performed in 1992 showed that the RELAP5 code predicts well the overall thermohydraulic behaviour, but discrepancies were identified in predicting local phenomena occurring in the pool and in the isolation condenser. Therefore a second test, (named PO-IC-2), has been performed with improved instrumentation.

The paper describes the results obtained in test PO-IC-2 and discusses the capabilities of the Relap5/Mod3.1 code.

1. INTRODUCTION

Innovative reactors (essentially AP-600 and SBWR) are characterized by simplification in the design and by the presence of passive systems for emergency core cooling. Experimental and theoretical researches are needed to qualify the new components introduced in the design and to characterize the thermalhydraulic scenarios expected during accidents. Available system codes are not retained suitable to evaluate the thermalhydraulic performances of the new systems, especially in case of long lasting transients evolving at low pressure /1/.

In the frame of the activities carried out at University of Pisa related to the analysis of thermalhydraulic situations of interest to the mentioned reactors (e.g. refs. /2/ and /3/), three series of experiments have been carried out utilizing the PIPER-ONE facility. They were aimed at the experimental investigation of the behaviour of systems simulating the main features of the Gravity Driven Cooling System (GDCS, first series of experiments, refs. /4/) and of the reactor pressure vessel Isolation Condenser (IC), (second and third series of experiments, refs. /5/ to /7/ and ref. /8/, respectively). At the same time Relap5/mod2 and mod/3 codes /9/, /10/ have been extensively applied as best estimate tools to predict the transient scenarios of both SBWR and AP-600 reactors (see also refs. /11/ and /12/).

PIPER-ONE is a General Electric BWR experimental simulator specifically designed in the early '80 to reproduce small break LOCA transient scenarios (e.g. refs. /13/ to /15/).

The above mentioned experiments were essentially devoted to a qualitative investigation of the thermalhydraulic conditions typical of the new components foreseen in the above reactors (essentially SBWR) and setting up a data base suitable for code assessment. The distortions that characterize PIPER-ONE hardware, in comparison with a scaled loop simulating SBWR, completely prevent applications of the measured data to reactor conditions: the core and downcomer heights, as well the distance between the Bottom of Active Fuel (BAF) and the IC top are important parameters not considered in the model.

On the other hand, Relap5/mod2 and mod3 are worldwide known codes developed at Idaho National Engineering Laboratory (USA). The aforementioned applications to innovative reactors scenarios emphasized the codes inadequacies in producing reliable results when system pressure attains values below 0.5 MPa. Numerical deficiencies, limited ranges of validity of the utilized correlations and lack of user experience (i.e. difficulty to develop a suitable code use strategy) are retained mostly responsible of this situation.

The purposes of the activity described in the present document, that is the direct follow up of the post-test evaluation of the previous IC experiment PO-SD-8, (ref. /7/), are essentially:

a) to give an outline of test results obtained during the high pressure part of the test PO-IC-2, also related to the study of the isolation condenser performance;
b) to evaluate the capabilities of the latest version of Relap5/mod3 code (i.e. version 3.1) in reproducing the experimental scenario, giving emphasis to the attempt of fixing the code limitations and the criteria for the optimal use of the code.
c) to demonstrate possible improvements in the latest code version with respect to the previous one especially in relation to condensation heat transfer.

In order to achieve these objectives the original Relap5/mod2 nodalization of the PIPER-ONE apparatus /16/, also modified to perform pre-test and post-test calculations of the test PO-SD-8 (e.g. refs. /7/ and /17/), was completely renewed. In particular, the number of nodes was roughly doubled also considering the available computer code capabilities. This nodalization was qualified by the calculation of the test PO-SD-8 and was used extensively for stability analysis in PIPER-ONE loop, (ref. /18/).

Some tens of sensitivity calculations were performed in the present context to identify some uncertain boundary conditions in the experiment (e.g. spatial distribution of heat losses to the environment) and to optimize the user choices, like the countercurrent flow limiting option in the annular region of steam separator to predict liquid deentrainment from the mixture flowing out from the core.

2. EXPERIMENTAL FACILITY

The PIPER-ONE apparatus is an integral test facility designed for reproducing the behaviour of BWRs in thermalhydraulic transients, dominated by gravity forces.

The ENEL BWR plant installed at Caorso (I) was formerly taken as the reference prototype in the design of the apparatus. The reactor is a General Electric BWR-4 plant, equipped with a Mark II containment, but it has some features of the latest GE design (e.g., 8x8 fuel rod assembly). The BWR-6 plant, equipped with 624 fuel bundles was assumed as reference for the first test carried-out on the PIPER-ONE facility, chosen by OECD-CSNI as ISP 21 /19/; then, the latter was used as reference plant for all the LOCA tests, which had already been performed.

The apparatus is constituted by the main loop, the ECCS simulators (LPCI/CS, HPCI/CS) and the systems simulating ADS, SRV and steam line, as well as the blow-down line.

Nine zones can be identified in the main loop: lower plenum, core, core bypass (outside the core), guide tube region, upper plenum, region of separators and dryers, steam dome, upper downcomer, lower downcomer and jet pump region.

The volume scaling factor is about 1/2200, while the core cell geometry and the piezometric heads acting on the lower core support plate are the same in the model and in the reference plant.

The heated bundle consists of 16 (4x4) indirectly heated electrical rods, whose height, pitch and diameter are the same as in the reference plant. The maximum available power is about 320 kW, corresponding to 25% of scaled full power of the reference BWR.

The one-dimensionality as well as the overall simplicity of the apparatus have to be highlighted; this is the direct outcome of the main objective of the research. In fact, the primary circuit was designed in such a way to have as far as possible:

- one dimensional cylindrical volumes (nodes in code calculations);
- connections between adjacent nodes clearly defined (geometric discontinuities, Venturi nozzles, orifices);
- lack of items (such as pumps and control systems) which can originate confusing situations in code calculations.

The instrumentation system has features consistent with the fundamental philosophy of the facility design. The data acquisition system can record 128 signals, with a frequency of up to 10 Hz for each signal.

As already mentioned, the facility hardware was modified by inserting the IC loop, which can operate at the same pressure of the main circuit (Fig. 1).

The main component of the isolation condenser loop is a heat exchanger consisting of a couple of flanges, that support 12 pipes, 22 mm outer diameter and 0.4 m long; it is immersed in a tank of 1 m^3 volume, containing stagnant water, located at 4th floor of the PIPER-ONE service structure. The heat exchanger is connected at the top and at the bottom respectively with the steam dome and the lower plenum of the main loop. In order to enhance natural convection inside the pool, a sort of shroud has been installed that divides the pool into two parts.

The isolation condenser loop is instrumented with a turbine flow-meter and a differential passive transducer on the hot side; a series of almost 30 thermocouples in various position of the IC and of the pool as shown in Fig. 2, complete the IC instrumentation.

Hardware restrictions preclude the possibility to have a system correctly scaled with respect to those provided for the new generation nuclear reactors, particularly the GE SBWR. This is evident from Table I, where relevant hardware data characterizing the isolation condenser loop installed in PIPER-ONE facility are compared with SBWR related data. In particular the item "ratio" of Table I demonstrates that the heat transfer area of isolation condenser in PIPER-ONE is roughly five times larger than the ideal value. The distance between bottom of the active fuel and the isolation condenser and the height of the core itself are two of the most important parameters differentiating PIPER-ONE from SBWR. These essentially prevents any possibility of extrapolating PIPER-ONE experimental data to SBWR.

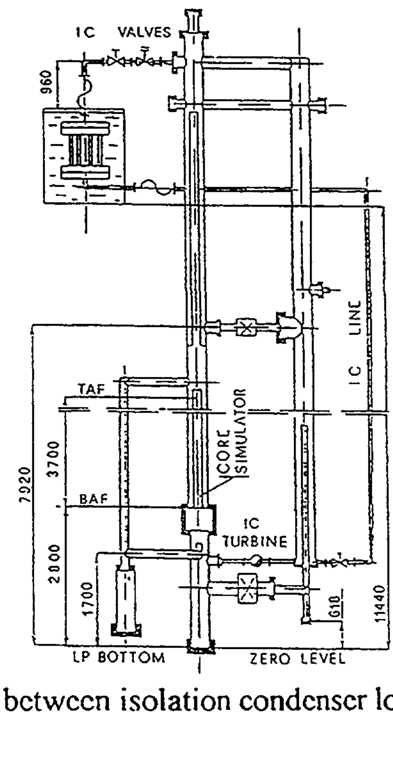

Fig. 1 - Connection between isolation condenser loop and PIPER-ONE loop.

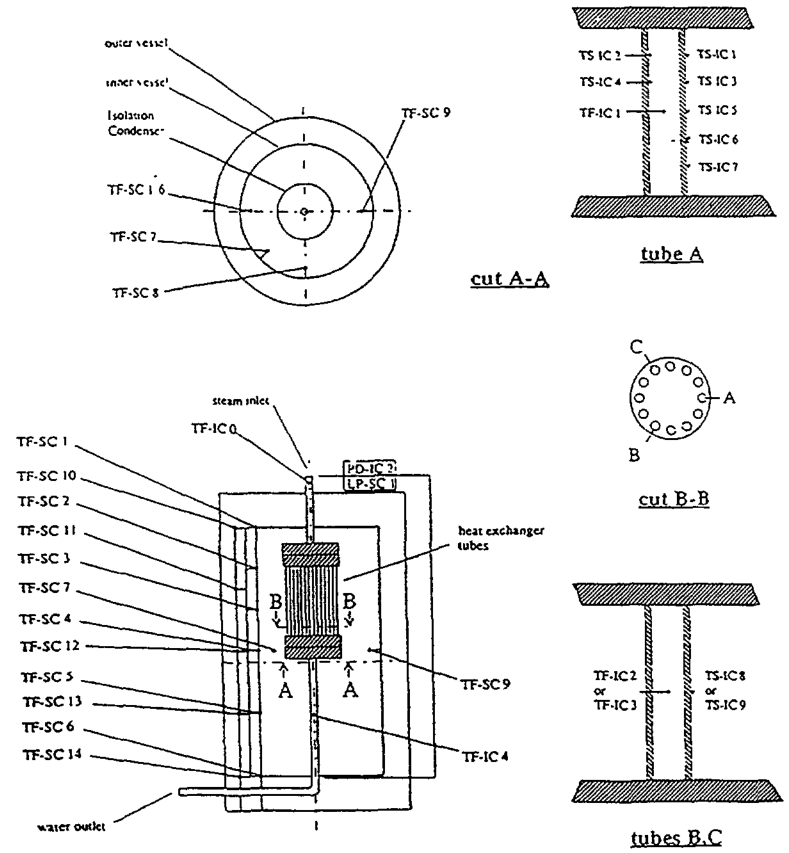

Fig. 2 - Sketch of isolation condenser pool with temperature measurement locations

Tab. I - Comparison between isolation condenser related data in PIPER-ONE and in SBWR.

	QUANTITY	UNIT	PIPER-ONE	SBWR (*)	RATIO (+) PIPER-ONE/SBWR	IDEAL (+) VALUE OF THE RATIO PIPER-ONE/SBWR
1	Primary system volume	m^3	0.199	595.	1/2990	1/2990
2	Core height	m	3.710	2 743	1 35/1	1/1
3	Maximum nominal core power	Mw	0.250	2000.	1/8000	1/2990
4	Value of 3% core power	Mw	0.041 (-)	60.	1/1463	1/2990
5	Ratio (3% core power) /primary system value	Mw/m^3	0.206	0.1	2.06/1	1/1
6	Isolation condenser heat transfer area (++)	m^2	0.301	184	1/610	1/2990
7	Isolation condenser heat transfer area over primary system volume	m^{-1}	1.512	0.31	4 9/1	1/1
8	Isolation condenser volume	m^3	0.0015	2 334	1/1556	1/2990
9	Isolation condenser volume over primary system volume	-	0 0075	0.0038	1.97/1	1/1
10	Isolation condenser heat transfer area over 3% core power	m^2/Kw	7.341	3 066	2 39/1	1/1
11	Height of isolation condenser top related to bottom of active fuel	m	8.64	24.75	1/2.86	1/1
12	Diameter of a single tube	m	0.020	0 0508	1/2.54	1/1
13	Thickness of a single tube	m	0.0023	0.0023	1/1	1/1

(+) non-dimensional
(++) only tube bundles
(*) IC data have been taken from reference /21/
(-) related to BWR6

3. TEST DESCRIPTION

The experiment comprises two phases characterized by different levels of heating power (40 and 75 kW, respectively, later indicated as phases A and B of the test). They correspond to the scaled value of the core decay power and to the capability of heat removal by the IC device, found in test PO-SD-8.

The test specifications foresaw constant heating power for 5÷10 minutes for both experimental phases, in such a way that quasi-steady state conditions could be reached by the main thermalhydraulic quantities (pressure, flowrates, collapsed levels, etc.).

In the test, the primary circuit was pressurized at the specified value by single-phase natural circulation; the heat source was provided by the core simulator and the structure heating system. Then, liquid was drained from the primary circuit for establishing the test specified liquid levels, roughly at steam separate top elevation. After some hundreds seconds of steady conditions, with heat losses compensated by the heating cables, the test started by supplying power to the core simulator and opening the valves of the IC loop.

As usual for the experiments in PIPER-ONE facility, the test was designed on the basis of pre-test calculations performed by Relap5/Mod3 code.

The initial and boundary conditions measured during the two phases of test PO-IC-2 are given in Tabs. II and III.

Tab. II - PIPER-ONE test PO-IC-2: initial conditions

PARAMETER	SIGN	UNIT	VALUE
LP pressure	PA-LP-1	MPa	5.1
LP fluid temperature	TF-LP-1	C	262.5
Core level	LP-CC-1	m	11.9
Downcomer level	LP-LD-1	m	11.9
IC line fluid temperature	TF-IC-1	C	17.5
IC pool fluid temperature	TF-SC-1	C	17.5

Tab. III - PIPER-ONE test PO-IC-2: boundary conditions

PARAMETER OR EVENT	TIME (s)
Test initiation	0.0
Power versus time	see Figs. 3 to 6
IC top valve opens	4.0
IC bottom valve opens	32.0
IC top valve closes	508.0
IC top and bottom valve open	602.0
IC top and bottom valve close	1106.0
End of test	1184.0

The most significant results measured during the phases A and B are reported in Figs. 3 to 6.

Figure 3 shows the different phases of the transient; when the core power is 40 kW, the primary pressure shows a slight decrease (0.3 MPa/min) demonstrating that the power exchanged through the isolation condenser is greater than supplied power. Roughly a steady condition is reached at 75 kW core power (phase B), with a decrease of primary pressure of only 0.02 MPa/min. According to the results of test PO-SD-8, the overall power removed by

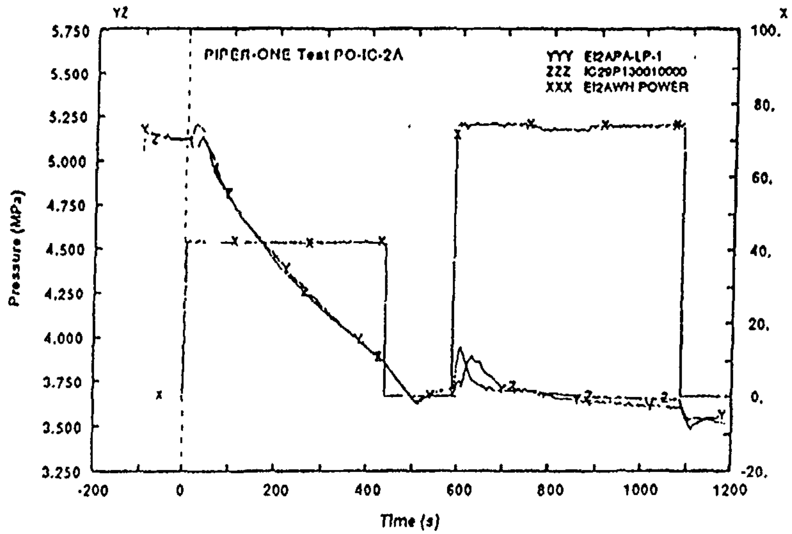

Fig. 4 - Measured and calculated trends of IC outlet mass flow rate

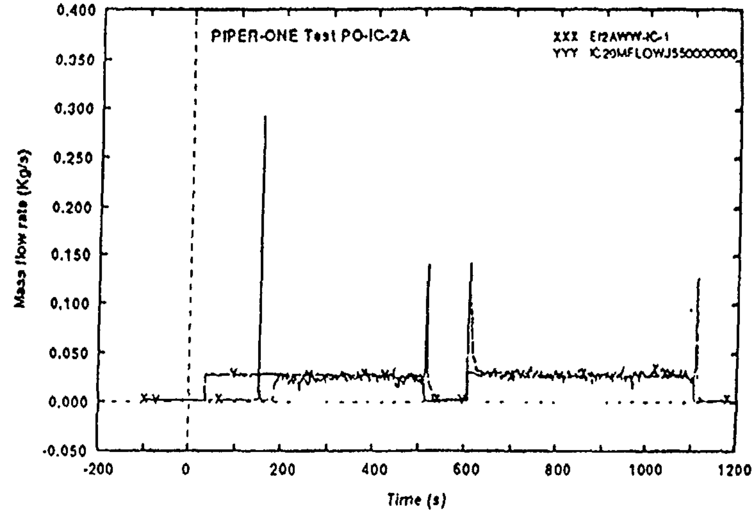

Fig. 6 - Measured and calculated trends of IC pool fluid temperature along the axis

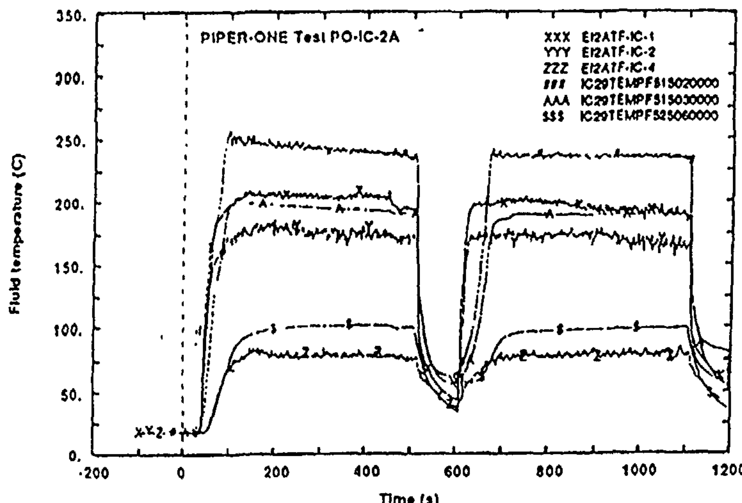

Fig. 5 - Measured and calculated trends of IC tubes fluid temperature along the axis

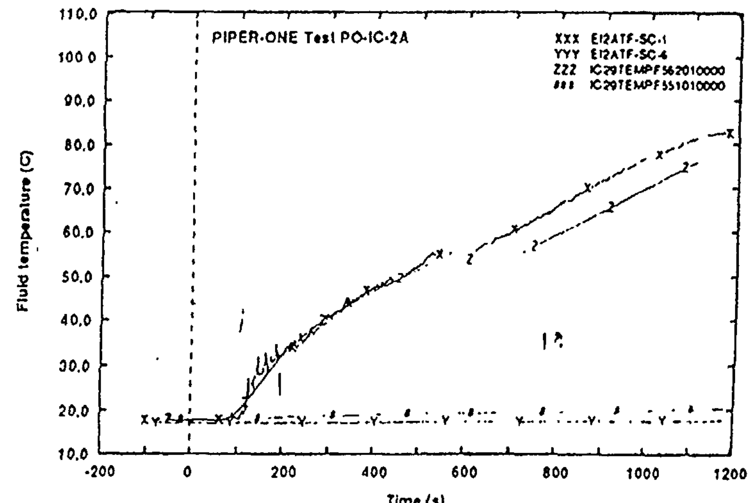

Fig. 3 - Measured and calculated trends of primary pressure and power

the isolation condenser is of the order of 80 kW, corresponding to an average heat flux of about 200 kW/m^2 in the considered conditions. The condensate mass flowrate, registered at the drain line (Fig. 4), appears quite constant along the two phases of the test (the turbine was initially blocked, but started to operate with about 3 minutes of delay from the opening of IC valve).

In Fig. 5, the fluid temperatures measured in three positions along the Isolation Condenser heat exchanger are compared with the steam temperature at IC inlet (equal to the saturation temperature corresponding to the primary system pressure); in particular, the bottom curve gives an idea of the subcooling conditions attained by the liquid exiting from the heat exchanger.

Finally, the curves in Fig. 6 essentially show the strong fluid temperature stratification in the pool: in the upper zone temperature increases up to about boiling conditions at test end, while the bottom part of the pool remains at ambient temperature during all the test (fluid temperature less than 20 °C).

4. RESULTS OF CODE APPLICATION

4.1 Adopted nodalization

The standard version of the Relap5/mod3.1 has been adopted as reference code in the present study; necessary adjustments of initial and boundary conditions, within the experimental uncertainty bands, have been done with this code version ("reference" code version) aiming at getting the "base calculation". The adopted standard version of Relap5/mod3.1 runs on an IBM RISC 6000.

Once the "base calculation" results have been obtained, previous code versions Relap5/mod2.5, Relap5/mod3 7J and Relap5/mod3 v80, running on Cray mainframe, IBM PC 486 and IBM RISC 6000 respectively, have been utilized, too.

The overall strategy of the performed analysis aimed at assessing the capabilities of the "reference" code version and at identifying possible improvements with respect to previous code versions; sensitivity calculations considering variations in the nodalization have been performed in this framework.

Additional objective of the analysis was to confirm the explanation given for the reasons of constant IC flow when core power is varied.

Considering the above objectives, the acquired experience in the use of the latest Relap5 code versions, the code user guidelines, (ref. /19/), and the criteria proposed in ref. /20/ for nodalization development and qualification, a new PIPER-ONE input deck has been developed.

The sketch of the new nodalization is shown in Fig. 7. Actually this has been developed in the frame of the BIP (Boiling Instability Program) proposal, (e.g. ref. /18/), and already used in that frame for planning of experiments.

The main difference with respect to the original nodalization (e.g. ref. /16/) lies in the number of nodes, that is now roughly three times larger. Moreover, the hardware modifications in the primary circuit of the facility have also been considered. In particular, the feedwater line has been added and the connection zone between downcomer and lower plenum and the region around the top of the separator have been slightly modified to better reproduce natural circulation in the reference reactor.

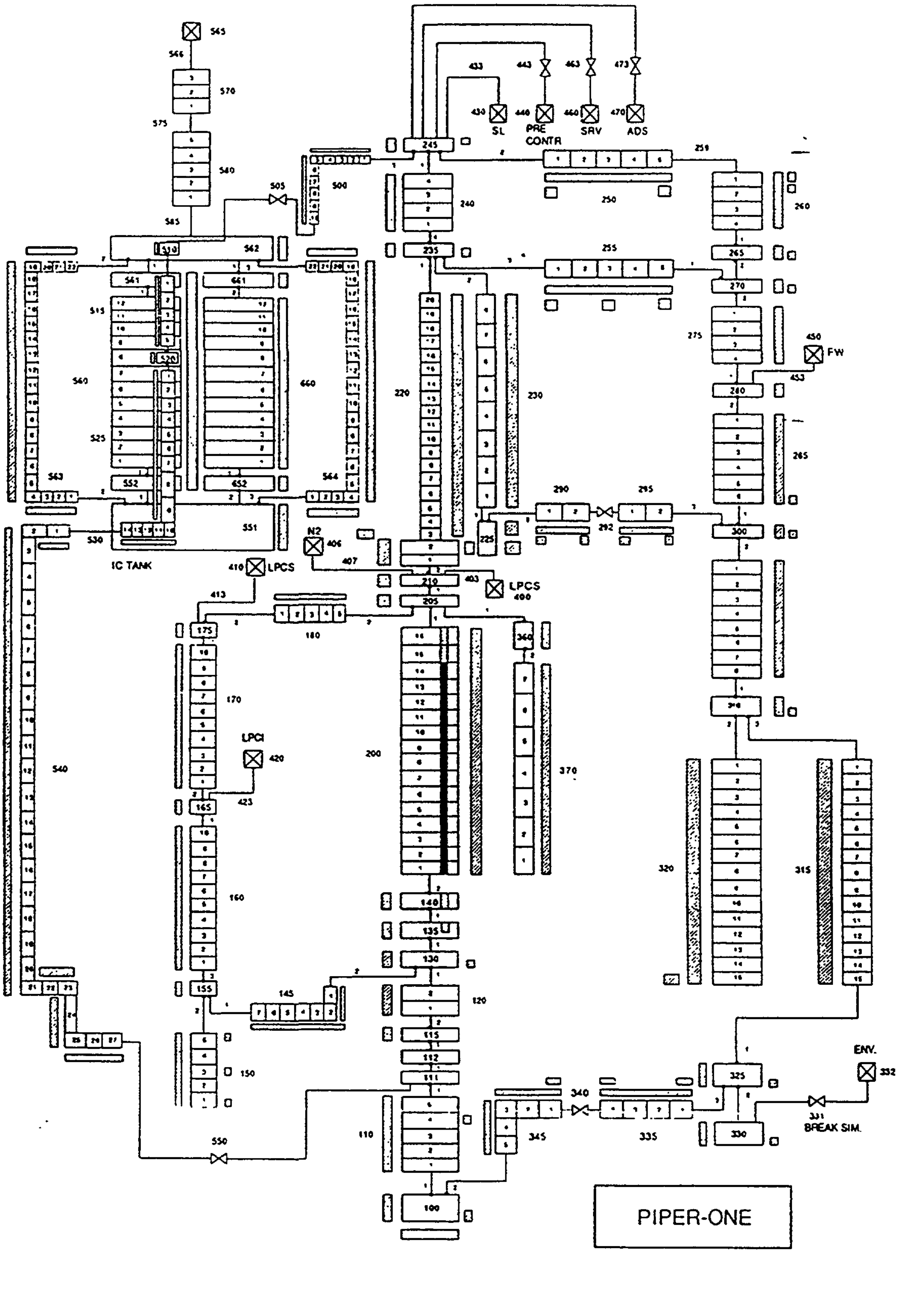

Fig. 7 - Nodalization of PIPER-ONE loop

4.2 Analysis of post-test results

The pre-test results /22/, that have been the basis for the design of the PO-IC-2 experiment, are not comparable with the actual data because of the differences between specified and actual values of the initial and boundary conditions. In particular, as already mentioned, the electrical power supply to the fuel rod simulator was limited to less than 100 kw.

For these reasons, three phases of the post-test analysis can be distinguished:

a. achievement of good comparison between calculated and predicted trends of available primary circuit data;
b. definition of a reference calculation on the basis of the above activity;
c. execution of a series of sensitivity calculations aiming at reaching the stated objectives.

In the frame of the analysis at item a., boundary and initial condition values related to the primary loop have been changed within the presumed experimental error bands, up to getting a satisfactory comparison between predicted and measured time trends in the primary circuit itself.

Once this process ended (this required a somewhat large effort because of the relative low power of the experiment), the reference calculation results were also compared with the experimental values in the IC system (phase b.).

The phase c. of the analysis consisted of five different steps (Tab. IV) aiming at the evaluation of:

3a) influence of code version;
3b) influence of selected initial/boundary condition values;
3c) user effects;
3d) nodalization effects;
3e) sensitivity of code results when a geometric/hydraulic relevant parameter is changed in the input deck.

4.2.1 Steady state calculations (Phase a)

As already mentioned, the main objective of the calculations was to match the primary circuit pressure trend.

Tab. IV - Documented calculations

GROUP	VARIED PARAMETER	EFFECT ON PREDICTED IC PERFORMANCE		
		(TS-IC-7) - (HTTEMP15050510)		
		100.s	300.s	1000.s
3a) INFLUENCE OF CODE VERSION	USED CODE VERSION			
	RELAP5/Mod3 1	-16 9	-17 1	-12
	RELAP5/Mod3V7J	-14 6	-0 1	-
	RELAP5/Mod3V80	-14 8	-0 4	-
	RELAP5/Mod2.5	-14 7	-14 8	-17 1
3b) INFLUENCE OF INITIAL AND BOUNDARY CONDITIONS	INITIAL AND BOUNDARY CONDITIONS	-16 9	17 1	-12
		-12 9	-13 3	-4 6
3c) USER EFFECT	IN/OUT FLOW TO IC CONTROL VOLUMES	-16 9	17 1	-12
		-16 7	-16 7	-11 8
		-16 9	-16 9	-11 4
		-16 9	-17.2	-
3d) NODALIZATION EFFECTS	MESH NUMBER OF IC PIPE WALL			
	10	-16 9	-17 1	-12
	20	-17 1	-17 5	-12 4
	NODE NUMBER OF IC PIPE AND CORRESPONDING INTERNAL POOL ZONE			
	5	-16 9	-17 1	-12
	10	-10 6	-14 6	-8 4
	IC PIPE MATERIAL THERMAL CONDUCTIVITY			
	STANDARD STEEL	-16 9	-17.2	-12
	STANDARD STEEL *2	-17.3	-17.5	-12.3
3e) CHANGES OF RELEVANT PARAMETERS	HEATED DIAMETER IN THE EXTERNAL SIDE OF IC PIPE WALL			
	0 005 m			
	0 1 m	-16 9	-17 1	12
	0 001 m	-43 7	-44	-37 3
		-3 0	3 4	0.3
	LP-VALVE CLOSURE AT 300 s IN THE TRANSIENT	-16 6	17.2	31 9

The initial condition at the assumed "time zero" in the experiment was achieved at zero core power and zero flows inside feedwater and steam lines and at core inlet; structures heating systems were active to compensate heat losses to environment.

The calculations was carried out changing:

- the fluid temperature around the loop
- the heat losses to environment
- the downcomer and core region levels
- the opening/closure time of IC valves

4.2.2 Reference calculations results (Phase b)

Three minor discrepancies are shown in the lower plenum pressure trend (Fig. 3):

- at the transient beginning, owing to the initial fluid temperature stratification not correctly considered in the code;
- during the interruption of electrical power given to the rods, mostly due to inadequate consideration of heat input to the fluid from the structures heating system;
- during the second part of the test as a consequence of the above mentioned cause.

It should be noted nevertheless a good agreement between the experimental and the calculate trends during the part of the test of main interest.

The mass flowrate across the IC is quite well predicted by the code (Fig. 4); the zero flow resulting from the turbine signal in the first 180 s is originated by a malfunction as already mentioned.

The fluid temperature at the inlet and long the IC axis are represented in Fig. 5. The agreement between measured and calculated trends is quite good.

The comparison of fluid temperatures at the IC outlet, (Fig. 6), confirms that the overall heat transfer to the pool is satisfactorily predicted by the calculation: this appears to be true also considering separately the tubes region (where both condensation and heat transfer to the pool from subcooled liquid take place) and the single tube region (where only heat transfer to the pool from subcooled liquid takes place).

The data in Fig. 8 show an overestimation of surface temperature by the code: this is true for all the surface temperatures. Considering that the overall power exchanged is quite well predicted, one can deduce a code error in predicting the heat transfer coefficient either in the inner surface, in the outer surface, either in both the surfaces. This conclusion is also supported by the observation that measured and calculated surface temperatures are very close when flowrate and exchanged power are nearly zero.

The good agreement between measured and calculated trends of pool temperature at different axial elevations (Fig. 9) constitutes an independent proof of the agreement in the overall exchanged power. Furthermore, the temperature increase in the pool results from Fig. 10: the smooth increase of fluid temperature in the pool leads to a smooth decrease of the temperature difference between tubes inner wall surface temperature and pool temperature itself. Removed power remain constant: this means an average increase of the overall heat transfer coefficient during the experiment.

4.2.3 Sensitivity calculations (Phase c)

Five main groups of calculations have been distinguished in Tab. IV, where the varied parameter ranges are reported, if applicable. In all cases six quantities have been selected to characterize the influence of the varied parameter:

- lower plenum pressure;
- IC tubes surface temperature (external side level 3);
- IC tubes internal fluid temperature (level 3);

- IC outlet fluid temperature;
- IC HTC inside tubes (level 3);
- IC HTC outside tubes (level 3).

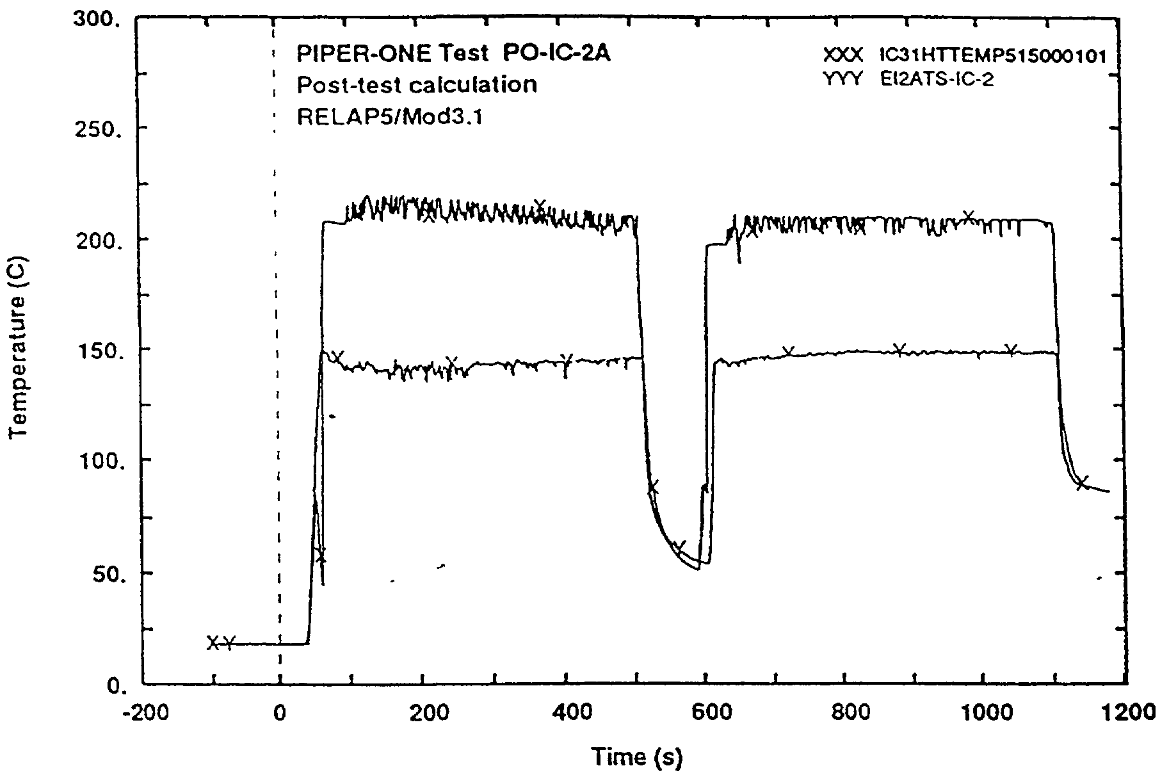

Fig. 8 - Trends of IC tubes internal surface temperature (top level)

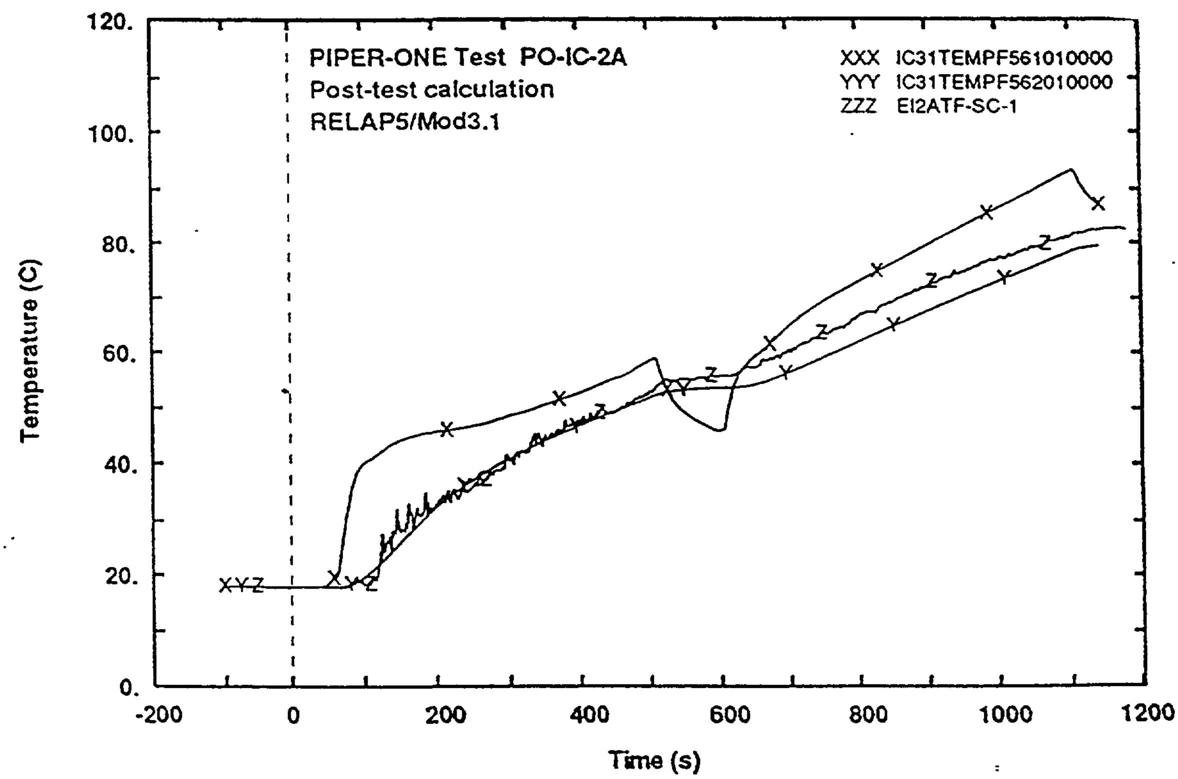

Fig. 9 - Trends of IC internal pool fluid temperature (top level)

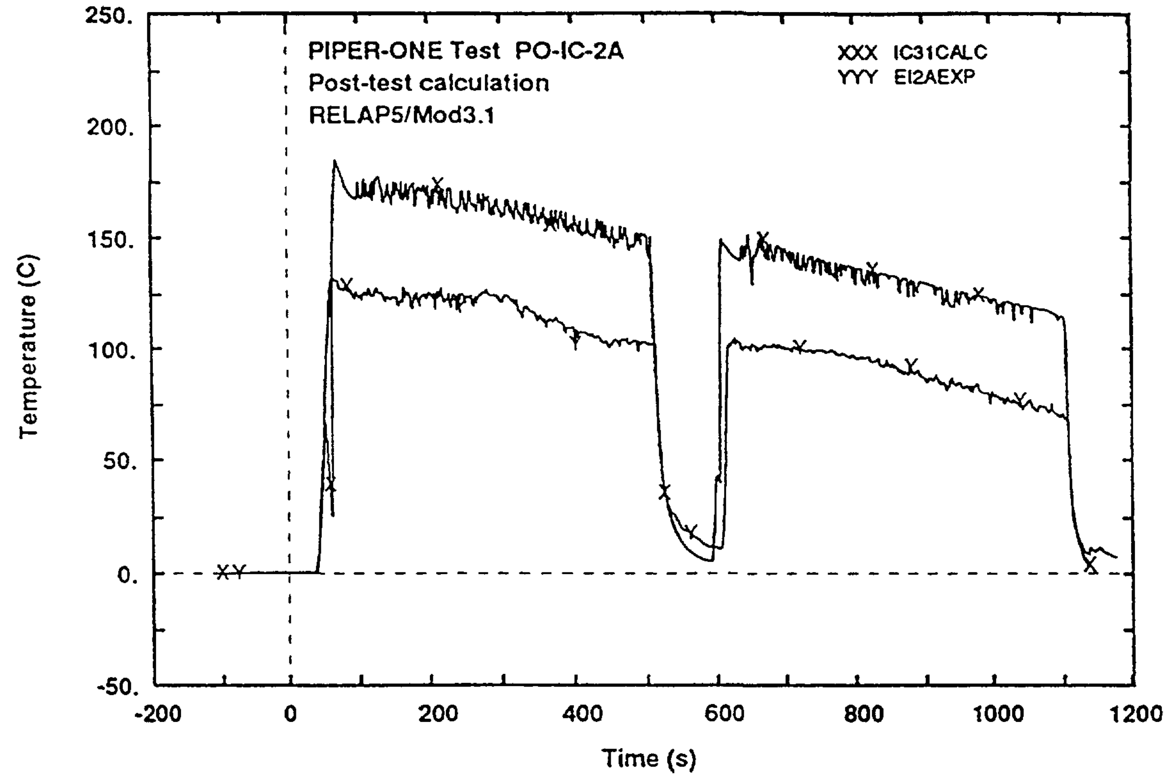

Fig. 10 - Trends of temperature difference between internal side of IC tubes and IC pool fluid (top level)

In the last part of Tab. IV, the differences between measured and calculated values of surface temperature in the lowest node of the IC tubes, are reported too. This is done at 100, 300 and 1000 s into the transient. It can be noted that in almost all the cases calculated outer surface temperature values are larger than measured values (the consideration about possible thermocouples "fin" effect should be made here, too). Assuming that heat transfer power and fluid temperature are the same in the experiment and in the calculation, it can be concluded that calculated HTC values are lower than in the experiment.

Primary pressure is not very much affected by code version, while the unphysical behaviour for fluid temperature, already noted in the analysis of the PO-SD-8 test (7J code version), appears in the application of V80 version of the code. Internal heat transfer coefficient is oscillating only in Relap5/Mod3.1.

A large number of boundary conditions has been varied: the influence of the considered changes cannot be retained relevant as far as the IC behaviour is concerned.

The studied nodalization effects include the increase in the number of conduction heat transfer meshes and the increase in the number of hydraulic nodes. The effects of these variations at a global level (primary circuit pressure) are negligible. However, local effects can be very important as shown by the inner wall surface temperature and by the heat transfer coefficient. Some calculations leads to the conclusion that heat transfer coefficient should be in someway connected with node dimensions. The change of the hydraulic diameter in the IC secondary side has a strong effect on the primary loop pressure and on the IC related quantities.

5. CONCLUSIONS

The present document reports the analysis performed with Relap5 in relation to the PIPER-ONE experiment PO-IC-2. The test is the follow-up of the similar experiment PO-SD-8 and aims at characterizing phenomena connected with the operation of isolation condenser in a geometric configuration typical for SBWR. The test studied was conducted at high pressure (around 5 MPa) to study code performance in this situation.

Conclusion can be drawn in relation to:

A) overall system performance;
B) thermalhydraulic phenomena inside the IC;
C) code capabilities;
D) effect of various changes in the calculation conditions.

It has been confirmed that a constant removed power characterizes the IC performance (item A)), whatever are the primary loop thermalhydraulic conditions. From the analysis of experimental data supported by specific code calculations, the reason why IC exchanged power remains constant when core power conditions are varied, has been made clear. This is a consequence of IC flowrate that is determined by the pressure difference created in the downcomer of the main loop that remains almost constant during the performed experiment. Constant IC flowrate means constant condensation length in the IC tubes and constant transferred power to the pool.

The shroud put in the pool was not effective in provoking natural circulation because of the high conductivity across its wall that led to fluid temperature stratification with the same characteristics in the inner and outer zones of the pool.

Heat transfer coefficients are several (3-7) times larger in the condensing zones of the IC tubes than in the single phase liquid region (item B)); the fluid pool temperature increase (up to 70 K) has a negligible role in this situation (high pressure steam). Liquid level in the IC remains almost constant when varying core power.

A new detailed nodalization of PIPER-ONE apparatus was adopted for this study. The standard version of Relap5/mod3.1 is able to catch the overall phenomenology during the four main periods of the experiment (item C)).

Discrepancies have been identified mainly concerning the IC tubes surface temperatures that are overestimated on the outer surface: this means underestimation by the code of the outer heat transfer coefficient provided that the overall exchanged power is well predicted. However the possible "fin" effect originated by thermocouples has not been considered in this conclusion. An unphysically high heat transfer coefficient is produced in the output by the code although apparently not used. During the period of power shut-off the code was not able to simulate the condensation shock occurring the in IC line.

An extensive series of sensitivity calculations has been carried out (item D)). These demonstrated:

* some improvements in the code results when passing from the earliest to the latest Relap5/mod3 code versions; however oscillations in condensation heat transfer value are much larger in the reference code version. Furthermore the transition logics from heat transfer mode 2 to 3 (and viceversa) could be improved;
* changes in the equivalent diameter of the pool side of the IC has an important effect on the calculation of the local quantities like heat transfer coefficient and temperatures;
* changes in nodalization can also have a noticeable effect as far as the calculation of the above mentioned quantities is concerned. The last item stressed the need to define some

relationship between the (condensation) heat transfer coefficient and the average node dimensions: this seems necessary to get reproducible results when condensation heat transfer is involved.

Further activity in this area includes the analysis of a companion experiment during which nitrogen gas was injected into the primary circuit and actually caused large degradation of the IC removed power.

REFERENCES

/1/ D'Auria F., Modro M., Oriolo F., Tasaka K.: "Relevant Thermalhydraulic Aspects of New Generation LWR's", CSNI Spec. Meet. On Transient Two-Phase Flow - System Thermalhydraulics, Aix-En-Provence (F), April 6-8, 1992.

/2/ D'Auria F., Galassi G.M., Oriolo F.: "Thermalhydraulic phenomena and code requirements for future reactors safety analysis", Int. Conf. on Design and Safety of Nuclear Power Plants (ANP) - Tokyo (J), October 25-29, 1992.

/3/ Andreuccetti P., Barbucci P., Donatini F., D'Auria F., Galassi G.M., Oriolo F.: "Capabilities of the RELAP5 in simulating SBWR and AP-600 Thermalhydraulic behaviour", IAEA Technical Committee Meet. (TCM) on Progress in Development and Design Aspects of Advanced Water Cooled Reactors, Rome (I), September 9-12, 1991.

/4/ Bovalini R, D'Auria F., Mazzini M.: "Experiments of Core Coolability by a Gravity Driven System performed in Piper-One Apparatus", ANS Winter Meeting, San Francisco (CA), November 10-15, 1991.

/5/ Bovalini R., D'Auria F., Mazzini M., Vigni P.: "Isolation Condenser performances in PIPER-ONE Apparatus", 1992 European Two-Phase Flow Group Meet. , Stockholm (S), June 1-3, 1992.

/6/ D'Auria F., Vigni P., Marsili P.: "Application of Relap5/Mod3 to the evaluation of Isolation Condenser performance", Int. Conf. on Nuclear Engineering (ICONE-2) - San Francisco (US), March 21- 24, 1993

/7/ Bovalini R., D'Auria F., Galassi G.M., Mazzini M.: "Piper-One research: the experiment PO-SD-8 related to the evaluation of isolation condenser performance. Post-Test analysis carried out by Relap5/Mod3-7J code", University of Pisa Report, DCMN - NT 200 (92), Pisa (I), November 1992.

/8/ D'Auria F., Galassi G.M:, Mazzini M., Pintore S.: "Ricerca Piper-One: specifiche dettagliate della prova PO-IC-2", University of Pisa Report, DCMN - NT 234(94), Pisa (I), Giugno 1994.

/9/ Ransom V.H., Wagner R.J., Trapp J.A., Johsen G.W., Miller C.S., Kiser D.M., Riemke R.A.: "Relap5/mod2 Code Manual - Vol. 1: code structure, systems and solution methods", NUREG/CR-4312 EGG 2396 - EGG Idaho Inc., March 1987.

/10/ Carlson K.E., Riemke R.A., Rouhani S.Z., Shumway R.W., Weaver W.L.: "Relap5/Mod3 code manual - volume II. User guide and input requirements", NUREG/CR-5535, June 1990.

/11/ D'Auria F., Oriolo F., Bella L., Cavicchia V.:"AP-600 Thermalhydraulic Phenomenology: A Relap5/mod2 Model Simulation", Int. Conf. on New Trends in Nuclear System Thermohydraulics - Pisa (I), May 30 - June 2 1994, Int. Top. Meeting on Advanced Reactor Safety - Pittsburgh (PA) April 17-21, 1994

/12/ Barbucci P., Bella L., D'Auria F., Oriolo F.: "SBWR thermalhydraulic performance: a RELAP5/MOD2 model simulation", 6th Int. Top. Meet. on Nuclear Reactor Thermalhydraulics, Grenoble (F), Oct. 5-8 1993

/13/ Bovalini R., D'Auria F., Di Marco P., Galassi G.M., Giannecchini S., Mazzini M., Mariotti F., Piccinini L., Vigni P.: "PIPER-ONE: a facility for the simulation of SBLOCA in BWRs", Spec. Meet. on Small Break LOCA Analyses in LWRs, Pisa (I), June 23-27 1985

/14/ Bovalini R., D'Auria F., Mazzini M., Pintore S., Vigni P.: "PIPER-ONE Research: overview of the experiments carried out", 9th Conf. of Italian Society of Heat Transport, Pisa (I), June 13-14 1991

/15/ Bovalini R., D'Auria F., Mazzini M., Pintore S., Vigni P.: "PIPER-ONE Research: Lesson learned", 9th Conf. of Italian Society of Heat Transport, Pisa (I), June 13-14 1991

/16/ D'Auria F., Fruttuoso G.:" OECD CSNI ISP 21, PIPER-ONE test PO-SB-7: post-test analysis performed at Pisa University by RELAP5/MOD2 code", University of Pisa Report, DCMN - RL 386 (89), Pisa (I), March 1989, OECD CSNI 2nd Workshop on ISP 21, Calci (I), Apr. 13-14 1989

/17/ D'Auria F., Galassi G.M., Mazzini M.: " PIPER-ONE research: specifications of PO-SD-8 experiment" (in Italian), University of Pisa Report, DCMN - NT 190 (92), Pisa (I), Jan. 1992

/18/ Ambrosini W., D'Auria F., Galassi G.M., Mazzini M., Virdis M: "Preliminary planning of BIP tests to be performed in Piper-One apparatus", University of Pisa Report, DCMN - NT 207 (93), Pisa (I), May 1993.

/19/ D'Auria F., Mazzini M., Oriolo F., Paci S.: "Comparison Report of the OECD/CSNI International Standard Problem 21 (PIPER-ONE Experiment PO-SB-7)", CSNI Report Nr. 162, Paris (F), Nov. 1989

/20/ Bajs T., Bonuccelli M., D'Auria F., Debrecin N., Galassi G.M.: "On Transient qualification of LOBI/MOD2, SPES, LSTF, BETHSY and KRSKO Plant nodalizations for RELAP5/MOD2 code", University of Pisa Report, DCMN - NT 185(91), Pisa (I), Dec. 1991

/21/ Brandani M., Rizzo F.L., Gesi E., James A.J.: "SBWR-IC & PCC System: an approach to passive safety", IAEA Technical Committee Meet. (TCM) on Progress in Development and Design Aspects of advanced Water Cooled Reactors, Rome (I), September 9-12, 1992

/22/ Bovalini R., D'Auria F., Galassi G.M., Mazzini M.: "Post-Test analysis of PIPER-ONE PO-IC-2 experiment by RELAP5/MOD3 codes", University of Pisa, DCMN Report, NT 254 (95), March 1995.

COMPUTER MODEL DEVELOPMENT AND VALIDATION

(Session V)

Chairman

A. LERIDON
France

ANALYSIS OF PACTEL PASSIVE SAFETY INJECTION TESTS WITH RELAP5 CODE

R. MUNTHER, J. VIHAVAINEN
Lappeenranta University of Technology,
Department of Energy Technology

J. KOUHIA
Technical Research Centre of Finland,
Nuclear Engineering Laboratory

Lappeenranta, Finland

Abstract

The gravity driven emergency core cooling (ECC) systems are utilized as important components of passive safety coolant systems of advanced reactors. Most of the published investigations have been primarily concerned with the presentation of new concepts, a few of their computational analysis and even fewer studies have been addressed to the experimental investigation of these systems.

PACTEL (Parallel Channel Test Loop) is an experimental out-of-pile facility designed to simulate the major components and system behavior of a commercial Pressurized Water Reactor (PWR) during different postulated LOCAs and transients /1/. The reference reactor to the PACTEL facility is Loviisa type VVER-440. The recently made modifications enable experiments to be conducted also on the passive core cooling. In these experiments the passive core cooling system consisted of one core makeup tank (CMT) and pressure balancing lines from the pressurizer and from a cold leg connected to the top of the CMT in order to maintain the tank in pressure equilibrium with the primary system during ECC injection. The line from the pressurizer to the core makeup tank was normally open. The ECC flow was provided from the CMT located at a higher elevation than the main part of the primary system. A total number of nine experiments have been performed by now.

A preliminary series of experiments with gravity driven core cooling was conducted with PACTEL facility in November 1992 /2/. The simulated transient was a small break loss-of-coolant accident (SBLOCA) with a break in a hot leg. In order to investigate this behavior more precisely, a second series of experiments with an improved instrumentation of the facility was performed in November 1993 with a small break in a cold leg. In these tests a rapid condensation of vapor interrupted the emergency core cooling flow several times. The tests indicated also that steam condensation in the CMT can prevent continuous ECC and even lead to partial core uncovery. The initiation of condensation and the thermal stratification in the CMT were found very difficult to model in the RELAP5 analysis of the experiments.
However, it should be underlined that these tests presented here are not directly applicable to the safety analyses of any suggested design, because of the major differences in the geometry between these concepts and PACTEL. Our objective has been only to simulate the gravity driven ECC and thus to enhance the understanding of the physical phenomena important in passive safety systems working with low differential pressures.

1. INTRODUCTION

Along with the normal evolution in LWR reactor designs several new interesting concepts have been presented. These ALWR designs aim at plant simplifications and safety and operability improvements. The principal tool being used to achieve a safer and simpler reactor is the use of passive system designs. Unfortunately, it is not easy to confirm that passive safety systems operate as intended under all the relevant conditions. More work is needed to evaluate the extent of improvements in safety which can be realized.

This paper provides the presentation of gravity driven emergency core cooling experiments with PACTEL, their analysis and discussion of the phenomena related to the experiments. The recently made modifications enable experiments to be conducted also on the passive core cooling. Firstly this paper describes the experimental facility, the modifications needed for Gravity driven ECC tests and test conditions. Secondly the RELAP5 represantation of PACTEL is described. Then the experimental results are compared to the calculational results. Finally conclusions are drawn both from the experiments and the their modelling with RELAP5.

2. PACTEL FACILITY

The PACTEL facility simulates the major PWR components and systems during small- and medium-size break LOCAs. The facility consists of a primary system, the secondary side of the steam generators, and emergency core cooling systems (ECCS). The reactor vessel is simulated by a U-tube construction including downcomer, lower plenum, core and upper plenum.

The facility is a volumetrically scaled model of the 6-loop VVER-440 PWR (The Finnish Loviisa plant being the reference) with three separate loops and 144 full-length, electrically-heated fuel rod simulators arranged in three parallel channels. The fuel rod simulators are heated indirectly.

The reference reactor has certain unique features differing from other PWR designs. The VVER-440 has six primary loops with horizontal steam generators. Due to the construction of the steam generators the driving head for the natural circulation in small break LOCAs is relatively small. The primary loops have loop seals in both the hot and cold legs. The loop seal is a U-shaped bend in the leg piping connecting the steam generator to the pressure vessel. It is interesting to note in the current context that the basic design of the VVER-440 reactor exhibits certain inherent safety features that are again found by the new designs. The reactor core has low power density and the primary circuit water inventory is large relative to the power. These characteristics ensure smooth behaviour in transient conditions.

Volumetric scaling (1:305) preserving the elevations has been applied in the PACTEL design. Maintaining system component heights and elevations is important for realistic simulation of small break and natural circulation transients. The main characteristics of the facility are presented in Table I.

Table I. Main characteristics of PACTEL facility.

Reference power plant	VVER-440
Volumetric scaling factor	1:305
Scaling factor for elevations	1:1
Number of primary loops	3
Maximum heating power	1 MW
Number of fuel rod simulators	144
Outer diameter of fuel rods	9.1 mm
Heated length of fuel rods	2420 mm
Axial power distribution	chopped cosine
Axial peaking factor	1.4
Maximum temperature of fuel rods	800 °C
Maximum primary pressure	8.0 MPa
Maximum operating temperature	295 °C
Maximum secondary pressure	4.65 MPa

3. PACTEL MODIFICATIONS AND TEST MATRICES FOR PASSIVE CORE COOLING EXPERIMENTS

The passive core cooling system used in the experiments consists of one core makeup tank and pressure balancing lines from the pressurizer and from a cold leg connected to the top of the core makeup tank in order to maintain the tank in pressure equilibrium with the primary system during injection. The line from the pressurizer to the core makeup tank is normally open. The core makeup tank is located above the reactor coolant loops and steam generators, so the motive force for injection is the gravity head, Figure 1. The makeup tank used limits the primary pressure to 5 MPa in the experiments. Since the PACTEL facility is not a model of any of the proposed passive ALWR designs, the modifications in the facility are intended only to simulate the gravity driven flow to the primary system. Neither automatic depressurization system (ADS) nor special valves are simulated. The primary system is depressurized from the pressurizer relief valve.

3.1 First series of experiments

The first stage of each experiment involved heating the facility to the proper temperature. Before the tests the core power was set to 80 kW corresponding to 1.8% of the 1375 MW thermal power of the Loviisa reactor. The fluid temperature and pressure reached a quasi steady state near 220 °C and 40 bars and at this point the pressurizer heater power was reduced to 2 - 4 kW. These conditions were maintained for about half an hour permitting the fluid to attain a more uniform temperature and allowing the heat losses through flanges and support structures to approach an equilibrium. The SG feedwater injection was adjusted manually to keep the water level in the SGs constant. Because of the large water inventory on the secondary side no fast automatic control was needed. Before each experiment, the CMT was filled to the top with water at a temperature and pressure of about 40 °C and 38 bar, respectively.

The experiments were started by opening the break simulation valve in hot leg number 1 at time t = 0s. Three different break sizes (Ø 2, 4 and 6mm) were used. Simultaneously with the break valve opening, the ECC line valve and the cold leg PBL valve were opened. The power of the pressurizer heaters was turned off. The first two tests, GDEØ1 and GDEØ2, were terminated when a rapid condensation of vapor in the CMT vapor space depressurized the CMT. Check valves prevented the collapsed vapor space in the CMT to be filled with liquid drawn from the ECC line. In order to investigate the flow restrictions in the ECC line the armature of the line was varied during the three first tests. Neither the primary system nor the secondary system were depressurized by the operator in the GDEØ1 and GDEØ2 tests.

In tests GDEØ3, GDEØ4, and GDEØ5 the secondary side valve was also opened. The primary system was depressurized in stages through the pressurizer relief valve before the anticipated CMT flow interruption in the GDEØ3 and GDEØ4 tests. For the large 6 mm (in dia.) break in the GDEØ5 test no extra depressurization was needed. These three tests were terminated when a thermal hydraulic status quo and a low pressure level was reached.The first series consisted of five experiments, Table II.

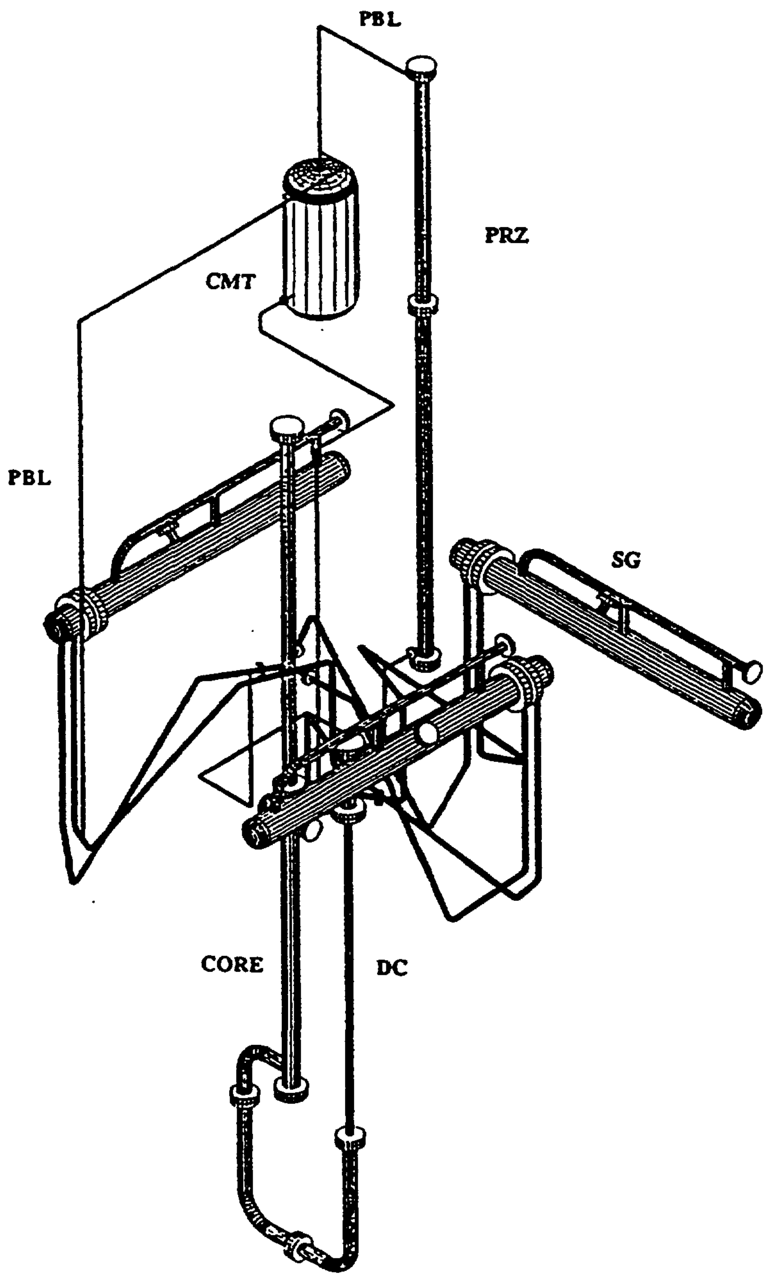

Figure 1. The passive ECC system of PACTEL.

TABLE II
TEST MATRIX/PHASE 1

DESCRIPTION	*FORESEEN PHENOMENA/AIMS*	*NOTES*
GDE01/ low power (< 80 kW) 2.0% (4 mm) hot leg break without ECC.	*Investigation of the blowdown process at low pressure.Gravity driven ECC effectiveness. Flow regimes. Phase separation and stratification. Condensation. Break flow. Coolant distribution.*	*for all of PCC-tests pressure = 40 bars. Steady-state initial conditions.*
GDE02/ 2.0% (4 mm) hot leg break with gravity driven ECC.	*As above.*	*Initial conditions as above. Minimized flow restricitions in the ECC line.*
GDE03/ 2.0% (4 mm) hot leg break Gravity driven ECC with sudden depressurization of primary system.	*Effect of primary side depressurization.*	*As above. Primary and secondary side depressurization. Optimized flow restrictions in the ECC line.*
GDE04/ 2.0 % (2 mm) hot leg break Gravity driven ECC with sudden depressurization of primary system.	*Effect of break area.*	*As above.*
GDE05/ 4.4% (6 mm) hot leg break. Gravity driven ECC	*As above.*	*As above. No depressurizations.*

3.2 Second series of experiments

The gravity-driven ECC behaviour was investigated more in the second phase of the tests with particular emphasis on break location, pressure reductions, reproducibility of the condensation manouvered experiments and system operation for the case of a small break LOCA. The major parameters and phenomena of concern during experiments are the break mass flow rate and the associated total primary coolant mass inventory, coolant distribution, different types and alternate paths of natural circulation in the loops, condensation and related heat transfer characteristics. For the second set of experiments the instrumentation of the facility was improved. In order to investigate the temperature stratification in the CMT ten thermocouples were installed to the upper part of the CMT, Fig 2. The water level in the CMT was measured with a pressure difference transducer. One loop of the three loop facility was isolated. When compared to the first series of experiments, the main differences are that the second series was carried out with two active loops, insulated PBLs and an improved instrumentation in the CMT.

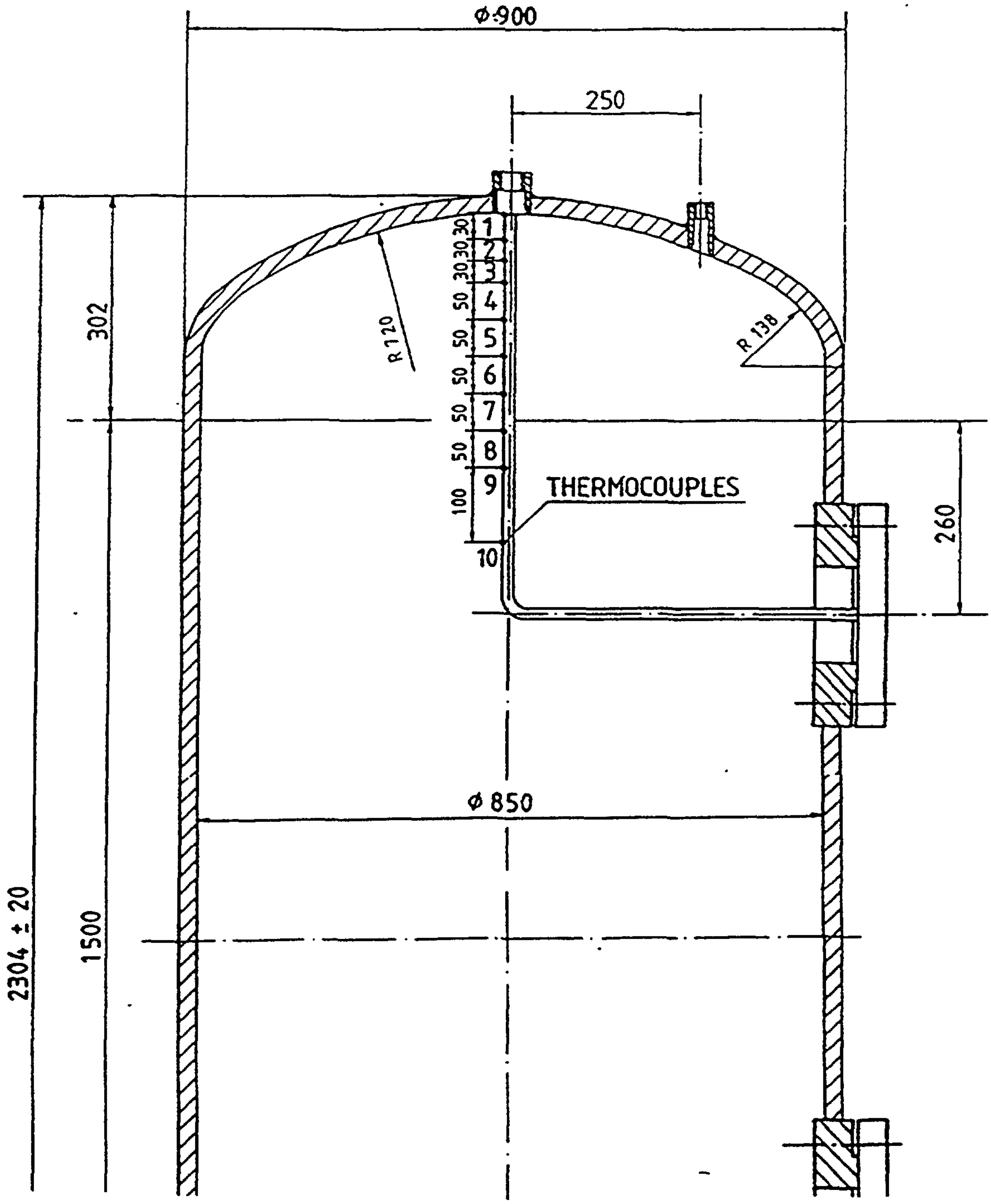

Fig. 2. Temperature measurement in the CMT tank.

The experiments were started by opening the break simulation valve in cold leg number 1 at time t = 0s. Two different break sizes (Ø 4 and 2mm) were used. Simultaneously with the break valve opening, the ECC line valve and the cold leg PBL valve were opened. The power of the pressurizer heaters was turned off. The first two tests, GDE11 and GDE12, were terminated by operator at t= 3000s. Neither the primary system nor the secondary system were depressurized by the operator in the GDE11 and GDE12 tests.

In test GDE13 the secondary side valve was also opened and the primary system was depressurized in stages through the pressurizer relief valve before the anticipated CMT flow interruption. This test was terminated at t=2000s by the operator.

For the small 2 mm (in dia.) break in the GDE14 test no depressurization was used. A high water level in the pressurizer was used in the initiation of the test in order to achieve circulation through the CMT in the early stage of the transient. The test was interrupted immediately after the condensation initiation at t=1170s. The second phase of the experiments was performed in November, 1993. The test matrix is presented in Table III.

Table III *Test matrix for the second series of passive core cooling experiments with the PACTEL facility.*

TEST MATRIX/PHASE II

TEST/ DESCRIPTION	*FORESEEN PHENOMENA/AIMS*	*NOTES*
GDE11 / low power (<80kW), 2.0% (4 mm) cold leg break with gravity driven ECCS.	*Gravity driven ECC effectiveness. Flow regimes. Phase separation and stratification. Condensation. Break flow. Coolant distribution. Investigation of the blowdown process at low pressure. Break location.*	*For all PCC-tests pressure = 40 bars. Steady-state initial conditions. No depressurization of the primary or the secondary system.*
GDE12 / 2.0% (4 mm) cold leg break with gravity driven ECCs.	*As above. Reproducibility.*	*As above. Initial conditions as well as possible same as above.*
GDE13 / 2.0% (4 mm) cold leg break with gravity driven ECCs. Sudden depres-suriza-tion of the primary system.	*Effect of depressurization.*	*As above. Depressurization of the primary and the secondary systems.*
GDE14 / 0.5% (2 mm) cold leg break with gravity driven ECCs.	*CMT natural circulation. Effect of break size.*	*As above without depressurizations. High pressurizer level at test initiation.*

4. THE RELAP5 REPRESENTATION OF PACTEL

A base RELAP5/Mod3 input deck for PACTEL was modified to include the gravity driven emergency core cooling system. The additions included the CMT and associated pressurizer and cold leg pressure balancing connections. The model was composed of 257 hydrodynamic volumes, 284 junctions, and 394 heat structures. Although this input served as a starting point for the calculations, many modifications were made to it during the course of the analysis. Revisions were made to the original model as new information became available and as input deficiences were discovered. Those modifications that were expected to have the most effect on these calculations, and the corresponding input changes are discussed next.

In the CMT, modelled as a cylinder, the effect of nodalization was investigated by changing the number of CMT nodes. These calculations showed that there was no significant difference between 2, 5 and 10 node CMT models for the overall CMT behavior. However, the amount of rapid depressurizations of the CMT varied between 2, 5 and 10 node models and none of the models corresponded to the amount or timing of the depressurizations in the tests. The results with a CMT modelled as a branch did not give any prediction for rapid pressure drops in the CMT. In the analysis of the first test series the presented calculations were made with 5 node model. For the calculations of the second series a 30 node model of the CMT was used. No condensation was then observed in the simulations.

The junctions between the cold legs and the downcomer, and between the upper plenum and the hot legs were at first modelled as crossflow junctions, but later modified as normal junctions in order to achieve realistic flow paths and water levels in the upper plenum and the upper part of the downcomer. The modelling of these junctions also had an effect on the heat loss distribution in the primary system and this way to the primary pressure when the coolant flow was near stagnation.

The subcooled discharge coefficient at the break was also varied for a better presentation of the leak mass flow of the experiments.

The nodalization schemes for both experimental series are presented in the Appendix I.

5. RELAP5 ANALYSIS OF THE FIRST TEST SERIES

The test results from the transients performed in the PACTEL loop were compared to computer simulations by the RELAP5/Mod3 program /3/. The actual starting steady state conditions in individual tests were used as input to the computer simulations. All the calculated transients began with the opening of the break valve. Also the ECC line valve and the cold leg PBL valve were opened simultaneously. Condensation of steam in the CMT was observed in all experiments.

In the calculation of the GDEØ1, there were five rapid pressure peaks against the measured one at 1860 s, Fig 3. The experiment was terminated after this. It was found that changing the maximum time step had an effect on the peak appearance. On the other hand, RELAP5 changed the flow chart from vertically stratified flow to bubbly flow in the CMT at the initiation of condensation. Also the pressure of the pressurizer, the ECC flow and the vapor content of the upmost CMT node increased at the condensation initiation.

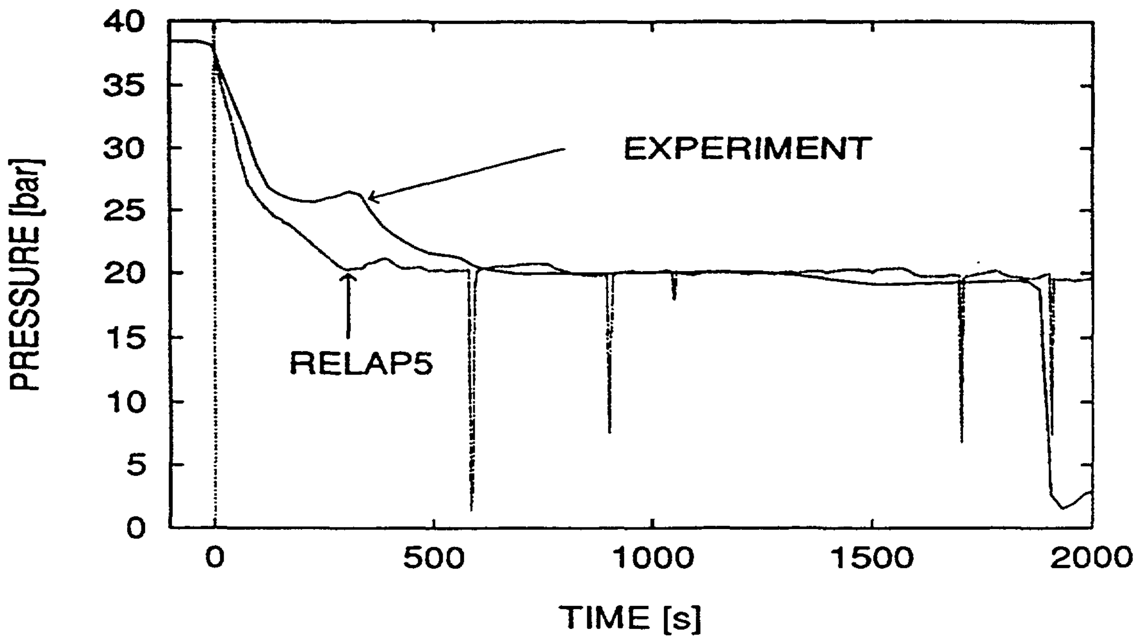

Fig. 3. The CMT pressure in GDEØ1

The best approximation for the condensation induced pressure peaks was achieved in the modelling of GDEØ3 experiment, where also the oscillatory period after the condensation was modelled, Fig 4. However, there were extra pressure peaks also here.

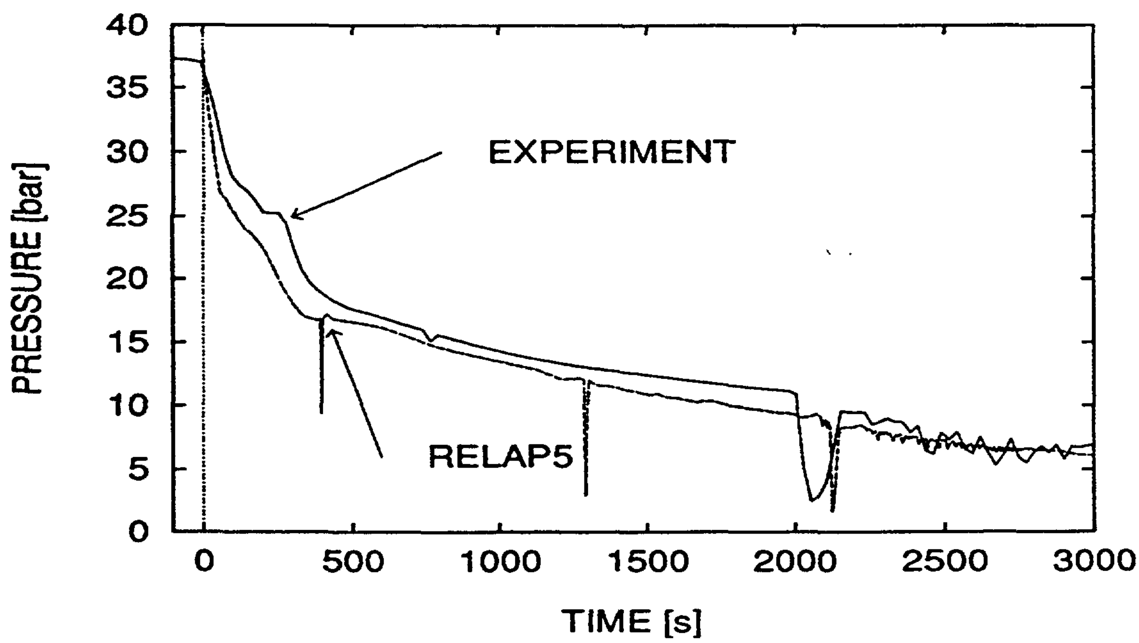

Fig. 4. The CMT pressure in GDEØ3

It was also found that the modelling of pressure losses in the PBLs had a significant effect on CMT depressurization behavior. Unfortunately no measured data was available for pressure losses in the PBLs. A sensitivity study on pressure losses in the cold leg PBL, pressurizer PBL, and the ECC line was performed and it was found that depressurization modelling was very sensitive especially for the value of pressure loss in the cold leg PBL.

6. RELAP5 ANALYSIS OF THE SECOND TEST SERIES

In the second series of experiments condensation behavior differed a lot from that observed in the preliminary tests. As the ECC flow in the first tests stopped totally several times because of rapid and very short condensations there was now only one condensation phase which lasted much longer. Good reproducibility was achieved in GDE11 and GDE12 test. The CMT pressures in GDE11 and GDE12 tests are shown in Fig. 5. In both experiments there was a condensation phase starting at about 1700s and lasting for 300s.

During the long condensation period in the GDE11 and GDE12 experiments the water level decreased to the top of core and even slightly below. The uncovery lasted only a short time and no significant heat-up in the core was found. In the GDE13 and GDE14 experiments no core uncovery was found.

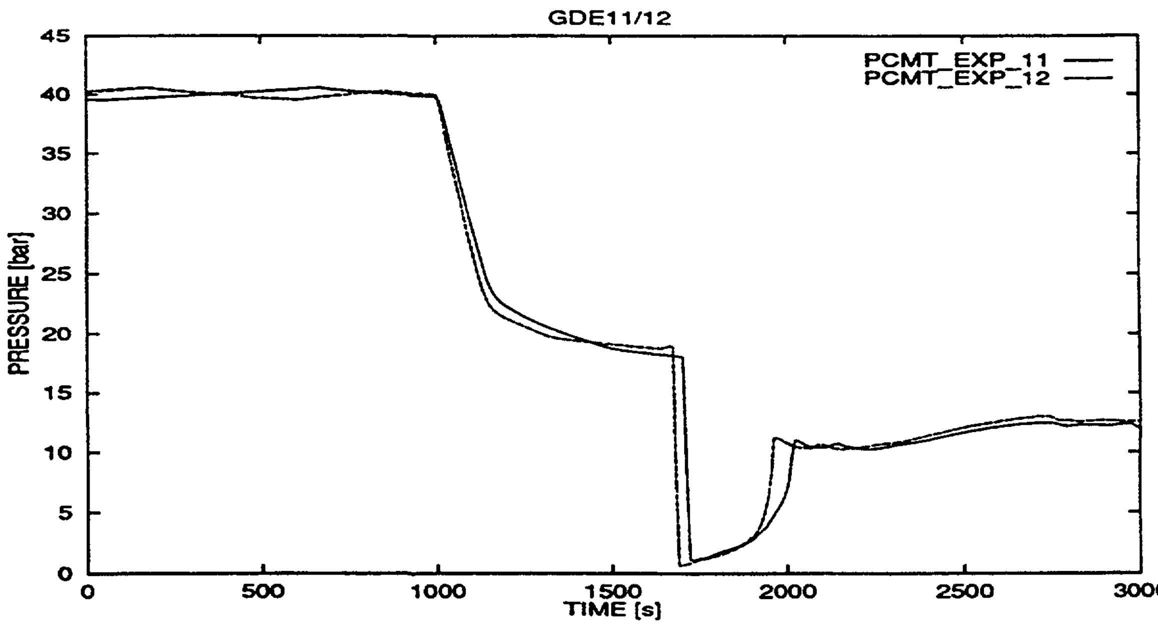

Fig. 5. The CMT pressures in GDE11 and GDE12 tests

In the RELAP simulation of the GDE11 experiment no condensation was observed. However, the overall modelling of the transient is rather good. Fig. 6 shows the measured and calculated CMT pressures in the GDE11 test. A thick 30 node model of the CMT was used in all simulations of the second series. With the thicker nodalization of the CMT a better presentation of temperature stratification in the CMT was achieved.

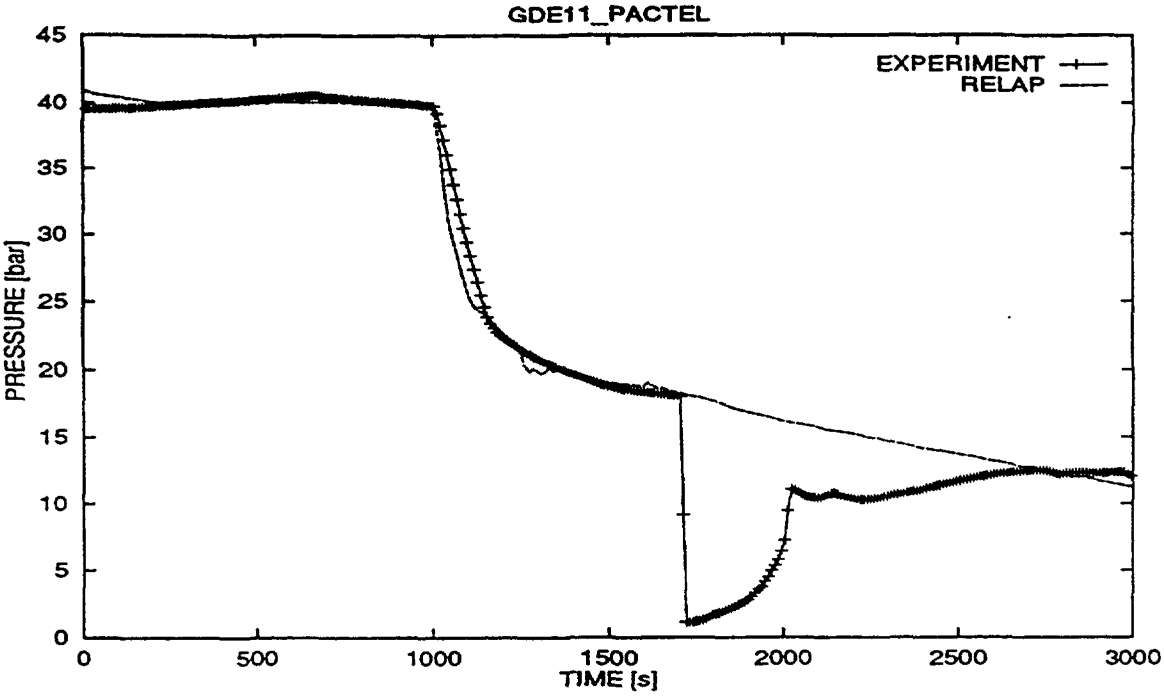

Fig. 6. Measured and calculated CMT pressures in GDE11 test

The operator activated primary system depressurization in stages affected to the total collapse of the vapour space, and in the GDE13 test there were three short condensations observed in the CMT, Fig. 7.

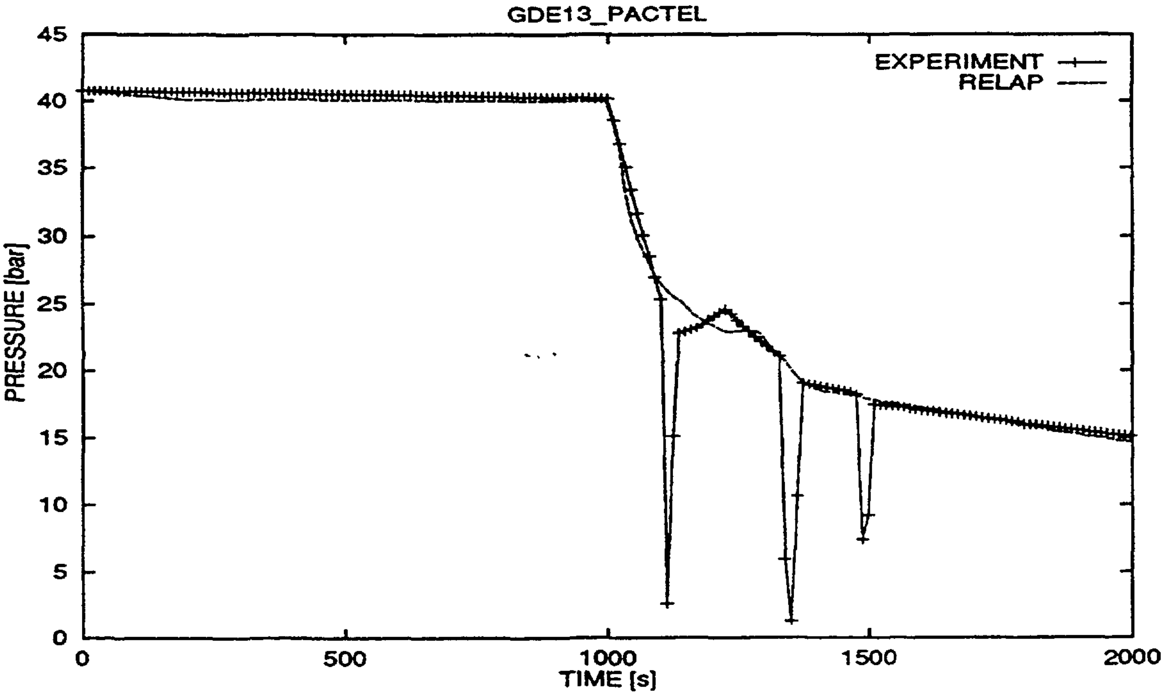

Fig. 7. Measured and calculated CMT pressure in GDE13

The first condensation was already at t = 1100s straight after the depressurization initiation. Similar period of short condensations were observed in the experiments of first series in both experiments with or without depressurizations.

A very steep vertical temperature gradient was formed inside the CMT in all tests. Fig. 6. shows that the temperature difference just before the condensation in the GDE11 experiment was 180 K in a water layer 0.15 m thick (the thermocouple numbering corresponds to that shown in Fig. 2.). The measured results are shown in Fig. 8. After the condensation at t= 1700s hot water is sucked to the CMT from the cold leg PBL mixing and filling the CMT. The CMT is repressurized after a new stratification of temperature is formed inside the CMT. With RELAP only the temperature stratification before condensation can be modelled, Fig. 9.

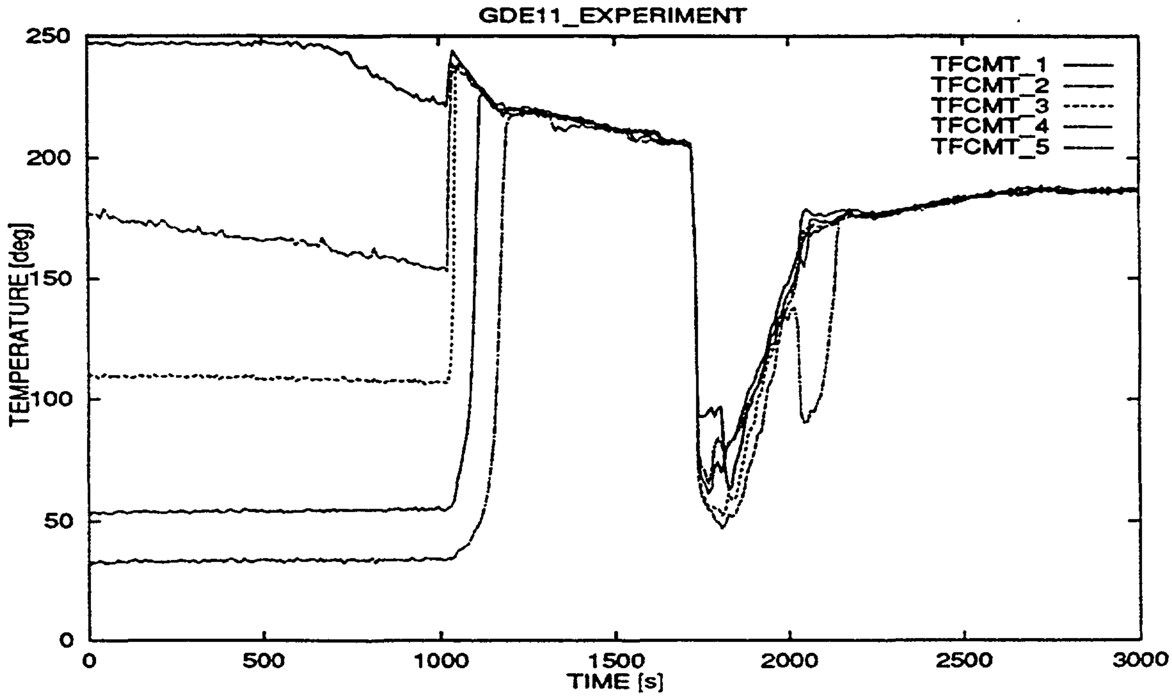

Fig. 8. Measured temperature distribution in the CMT at GDE11 test

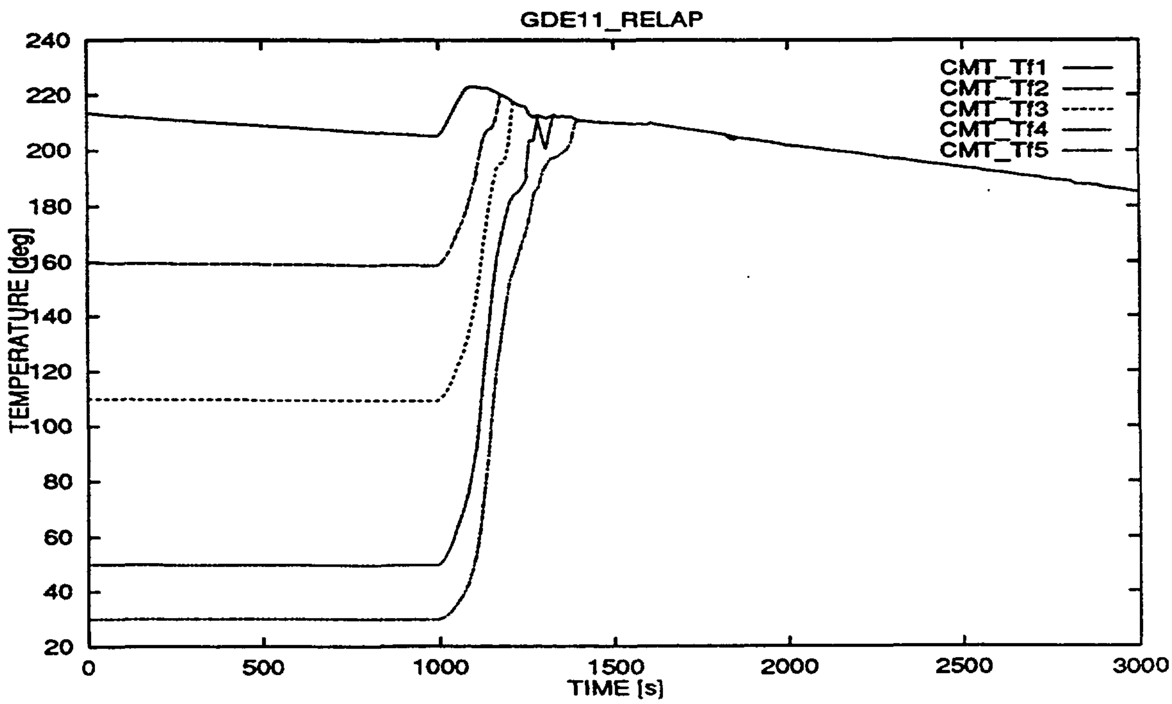

Fig. 9. Calculated temperature distribution in the CMT at GDE11 test

An effort for preventing the rapid condensation was done by carrying a thick, insulating level of hot water to the CMT with a natural circulation loop formed between the CMT and the primary system via the cold leg PBL and ECC line. For this reason the water level in pressurizer was set high and a small break size was chosen at the GDE14 test initiation. This natural circulation phase of the CMT was also in the ROSA-V/LSTF experiment /4/. With these preconditions a short natural circulation phase was then observed in the GDE14 experiment. However, this natural circulation phase was not effective enough to form a sufficient layer of hot water in the CMT. In PACTEL the total water volume above the CMT is small since there are horizontal steam generators.

7. CONCLUSIONS

No core uncovery was found in any of the tests of the first series. However, the emergency core cooling flow from the core makeup tank was stopped when rapid condensation collapsed the core makeup tank pressure. The tank repressurized rather quickly and the emergency core cooling flow was provided until the next condensation phase.

In the second series of experiments only two of the three loops of the facility were used as in the first series of experiments all the loops were active. The break was now located to the cold leg and two different break sizes were used. In one of the tests both the primary system and the secondary system were depressurized. In all the four experiments performed steam was flowing into the CMT and then later condensed to the cold water of the CMT. There were striking changes in the vertical temperature gradient of the CMT. It was experienced that condensation was then initiated easily by steam or water flow from the PBLs as the steep stratification in the CMT was broken. Especially the changes in water level in the pressurizer seemed to be responsible for most of the condensation periods.

We also simulated the both experimental series gravity driven core cooling experiments with RELAP5/mod3.1. The comparison of calculations and experiments show a good agreement both in magnitude and time of occurrence for most of the different physical events. The main observed discrepancy was due to limitations in the RELAP5 code to accurately predict rapid condensation in the CMT. The most critical aspect in the calculational results was that the appearance of condensation was dependent also on computational features, such as the time step and the nodalization.

From the results presented, we conclude that: 1) condensation modelling of the PACTEL experiments can not be satisfactorily achieved with the modelling capabilities of the current version of RELAP5. The forthcoming versions of the code should be equipped models where stratification and the possibility for the breaking of stratified layers can be evaluated. 2) the thermal hydraulic balance in the system is very sensitive and therefore experimental data should be used in the calculations whenever possible.

Condensation of steam in the CMT could be avoided with some technical arrangements in the test facility. However, even though improvements were made to gravity driven ECC systems, we cannot guarantee that computational models will provide accurate answers. Therefore, to build this confidence more experimental data has to be obtained and new computational models developed.

REFERENCES

/1/ T. Kervinen, V. Riikonen, J. Kouhia, "PACTEL, Facility for Small and Medium Break LOCA Experiments," Proceedings of ENC'90 Conference. European Nuclear Society, Lyon, France, September 23-28, 1990

/2/ Munther, R., Kalli, H., Kouhia, J., Kervinen, T. Passive core cooling experiments with PACTEL facility. ENS TOPNUX'93, Haag, Netherlands, April 25-28, 1993.

/3/ Munther, R., Vihavainen, J., Kalli, H., Kouhia, J., Riikonen, V., RELAP5 analysis of gravity driven core cooling experiments with PACTEL. ARS'94, INTL topical meeting on advanced reactor safety, Pittsburgh, USA, April 17-21, 1994. ISBN 0-89448-193-2.

/4/ T. Yonomoto, Y. Kukita, Y. Anoda, "Passive Safety Injection Experiment at the ROSA-V Large Scale Test Facility," Proceedings of the ANS National Heat Transfer Conference, p. 393, American Nuclear Society, Atlanta, Georgia, August 8-11, 1993.

APPENDIX: NODALIZATION SCHEMES FOR PACTEL GRAVITY DRIVEN CORE COOLING EXPERIMENTS

First series:

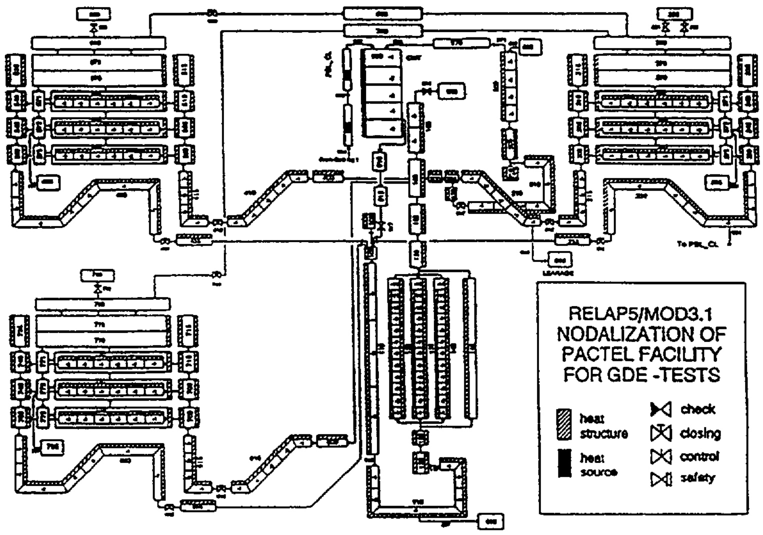

Second series:

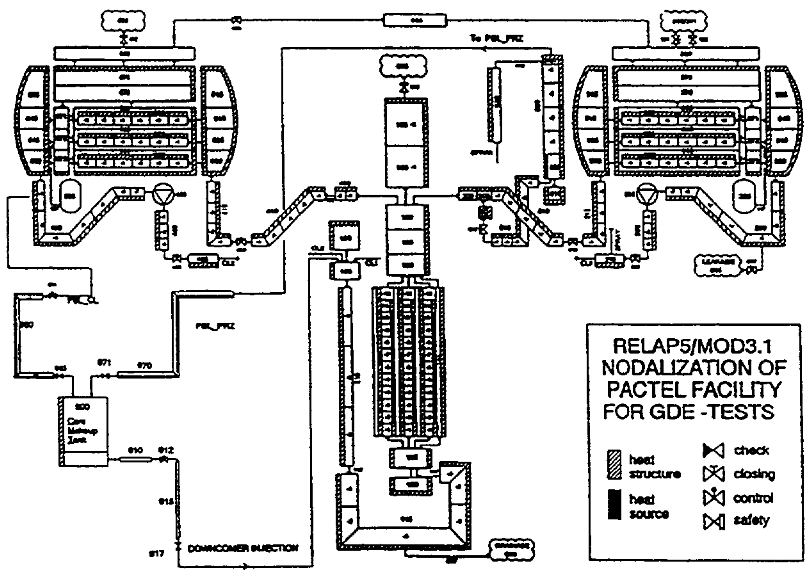

HEAT TRANSFER TO AN IN-CONTAINMENT HEAT EXCHANGER IN NATURAL CONVECTION FLOW: VALIDATION OF THE AEA TECHNOLOGY COMPUTATIONAL FLUID DYNAMICS CODE CFDS-FLOW3D

R. O'MAHONEY, J.N. LILLINGTON
AEA Technology, Winfrith Technology Centre,
Dorchester, United Kingdom

Abstract

Validation is presented of an appropriate computer code for modelling heat transfer from the containment atmosphere to an in-containment heat exchanger using new data from ENEL. This work has been carried out in collaboration with ENEL, CISE and ANSALDO. The study helps to identify conditions under which natural circulation induced by the heat exchanger does initiate. The Computational Fluid Dynamics (CFD) code CFDS-FLOW3D, developed by AEA Technology, has been used, initially in a 2-dimensional mode, to simulate the natural convection flow generated within a test vessel by an internal heat exchanger operating in a steam-air gas mixture. The model incorporates a calculation of the heat exchanger condensation rate based on local conditions. Calculational parameters have been identified which allow the transient timesteps to converge sufficiently but without using excessive CPU time. Results of pre-test calculations performed for 2 different geometrical configurations are presented. These calculations suggest that the heat exchanger will operate as intended and, at the design values of pressure and temperature, would exceed the planned test power by up to 28%. Post-test simulation results are presented for the first test performed. Good general agreement with major measured parameters is found and a possible explanation for the high upward velocity measured outside the heat exchanger exit is offered. The simulation underestimated the total condenser power by about 16%; this is believed to be due to underpredicting the steady state steam fraction in the vessel. CFDS-FLOW3D is found to be a suitable tool for simulating the details of complex buoyancy driven flows, including non-condensibles, in passive containment cooling applications. The code is sufficiently flexible to be able to represent correctly heat exchanger condensation effects and to be able to simulate the resultant natural convection flows in either 2-D or, if required, in 3-D.

1. INTRODUCTION

A characteristic feature of innovative advanced reactor designs is their reliance on passive safety systems and, in particular, natural convection to transport decay heat away under accident conditions. This approach results in slow heat-up rates thus avoiding the need for operators' intervention for an extended period.

In many current designs the route for decay heat removal from the core to the 'ultimate heat sink' is as follows:

1. Decay heat is removed from the core by natural circulation via the reactor coolant system (RCS) to a large condensing pool or tank, thence imparted to the containment atmosphere through evaporation,

2. The heat must then be transferred from the atmosphere in the interior of the containment to the exterior of the containment barrier and finally to the outside atmosphere (ie the ultimate heat sink).

There are two types of containments being considered in current designs. Steel containments, e.g. as in AP600, are attractive from the point of view of good heat transfer from the interior to the exterior but concerns have been expressed that these would not be sufficiently strong to meet European licensing requirements. Concrete containments are strong but they are poor heat conductors and heat exchangers will need to be introduced to transfer heat from the interior to the exterior.

The main purpose of this paper is to present the validation of an appropriate computer code for modelling heat transfer from the containment atmosphere to such a heat exchanger using new data from ENEL. This work has been carried out in collaboration with ENEL, CISE and ANSALDO. The study helps to identify conditions under which natural circulation induced by the heat exchanger does initiate.

2. HEAT EXCHANGER EXPERIMENTS

ENEL are evaluating the feasibility of a Passive Containment Cooling System (PCCS) applicable to a large dry double-barrier concrete containment. The internal heat exchangers are connected to external heat exchangers sited in large tanks of water above the containment and heat is transferred by evaporating water in natural circulation. The ENEL 1994 work programme involved a series of tests performed with a mock-up heat exchanger at 1:40 scale.

The technical design criteria include the following:

- the system is completely passive, both internal and external to the primary containment boundary,
- the system is able to maintain its performance for an indefinite period,
- the peak containment pressure should not exceed the containment design pressure for LBLOCA,
- the system performance should be such as to lower containment pressure to less than half the design pressure within 24 hours of the peak,

Passive operation of the PCCS is obtained by utilising natural convection of the relevant fluids, ie steam and non-condensables (air, hydrogen (for severe accidents)) in the containment atmosphere and water in pools as part of closed thermo-syphon systems.

ENEL are undertaking a programme of experimental tests to verify the behaviour of internal containment heat exchangers (HXs), both with respect to their heat transfer characteristics and also to the natural circulation of the steam-air mixture through the HX. The gas circulation and heat transfer will be strongly coupled. The gas velocities expected to be very low, less than 1m/s. An important aspect of the tests will be the identification of conditions under which the HX gas natural circulation does, or does not, initiate.

These tests are being performed at the CISE facility in Milan (figure 1); the first phase was carried out during late 1994 and early 1995. The tests are aimed to validate the HX design criteria, in particular:

- to verify the design correlation for HX behaviour as a function of the containment atmosphere composition and concentrations,
- to verify the HX behaviour as a function of the geometry of the chimney (height and outlet area),
- to identify the presence of any recirculating flow inside the chimney, as a function of the chimney bottom shape.

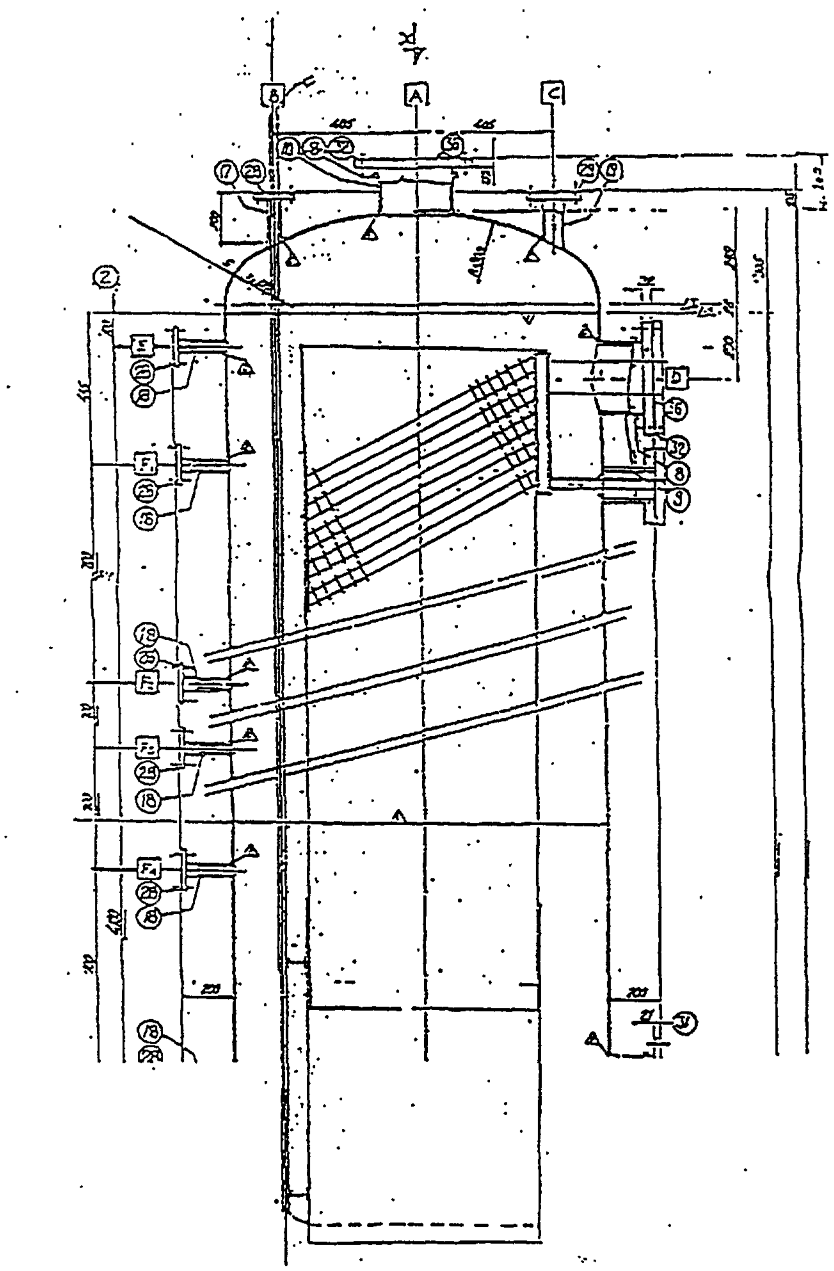

Figure 1. ENEL Heat Exchanger (HX) Test Section

Tests performed later in the experimental schedule will have objectives to:

- verify the effect of light non-condensable gases (eg hydrogen) on the HX behaviour,
- verify the HX behaviour as a function of geometrical design, eg different HX tubes and numbers of rows,

2.1. Heat Exchanger Facility

The heat exchanger experimental facility (figure 1) consists of an insulated vessel with a design pressure of 5 bar and design temperature of 150°C. The vessel is approximately 8m high and 1m internal diameter with a heated pool of water at the bottom. A 1:40 scaled heat exchanger, with a variable height chimney below it, is located near the top of the vessel. A circular screen is located just below the chimney bottom to allow the outlet flow area to be varied. During the tests the pool is heated producing evaporation; this pressurises the vessel and causes the air-steam mixture to circulate. The heat exchanger (HX) secondary side is connected in a closed loop to an external heat exchanger (ie a condenser) to control its temperature. The steam-depleted gas mixture exiting the HX will be heavier than the bulk gas mixture and will therefore tend to flow down the chimney and generate a natural circulation gas flow.

Data have been obtained by ENEL for a total of 6 tests; 4 with a 3m chimney configuration and 2 with a 5m chimney configuration.

3. PRE-TEST ANALYSIS

AEA pre-test analysis has concentrated on two aspects. Firstly, using correlations developed by HTFS [1,2,3], to predict the heat transfer performance of the HX under the design conditions of pressure and temperature and, secondly, using the computational fluid dynamics code CFDS-FLOW3D, to predict the gas mixture flow patterns at start-up and close to the predicted operating point. A prediction of the HX heat transfer performance can be used to confirm the applicability of the selected test conditions. The CFDS-FLOW3D analysis can be used to give confidence that the HX circulation flow will initiate and continue as intended.

Heat exchanger correlations developed by HTFS [1,2], adapted for condensation using the Reynolds-Colburn mass-transfer/heat transfer analogy, have been used to determine the HX condensation rate, and thereby the buoyancy driving force, as a function of the HX inlet velocity. Similarly, using the HTFS HX pressure drop correlation [3] together with an estimate of the additional losses, the total system frictional pressure drop has been determined as a function of inlet velocity. The buoyancy force and total pressure drop have been evaluated for design conditions of a saturated air-steam mixture at 2.6bar, HX inlet temperature of 109°C and HX secondary coolant temperature of 100°C with a 5m high chimney. The condensation buoyancy driving term decreases with increasing velocity while the total system pressure drop increases with increasing inlet velocity. The crossover of these curves indicates the predicted operating point of the system, approximately 0.275 m/s. This velocity corresponds to a total power transferred due to condensation of approximately 170% of the planned test power. Therefore, for these conditions, the HX should easily remove the design power and in practice the system would be expected either to reach a steady state at a lower gas temperature or, operate with a slightly higher secondary coolant temperature.

3.1. Predictions of Flow Patterns

A 2-dimensional CFDS-FLOW3D model has been created representing one half of the facility (using a plane of symmetry) for the first design configuration, ie with a 5m high chimney which has its outlet area reduced to ⅓ of the inlet area in order to maximise the outlet velocity. The CFDS-FLOW3D model is shown in figure 2. The initial conditions are the test design conditions together with zero flows. Steam is added to the bottom layer of cells at a rate equivalent to the net heat input to the water pool. Steam is removed from the gas mixture at the HX level inside the chimney at a rate determined from the HTFS correlations using the local conditions. These correlations have been added as user coding to CFDS-FLOW3D. The HX pressure drop calculation has been implemented in a similar manner.

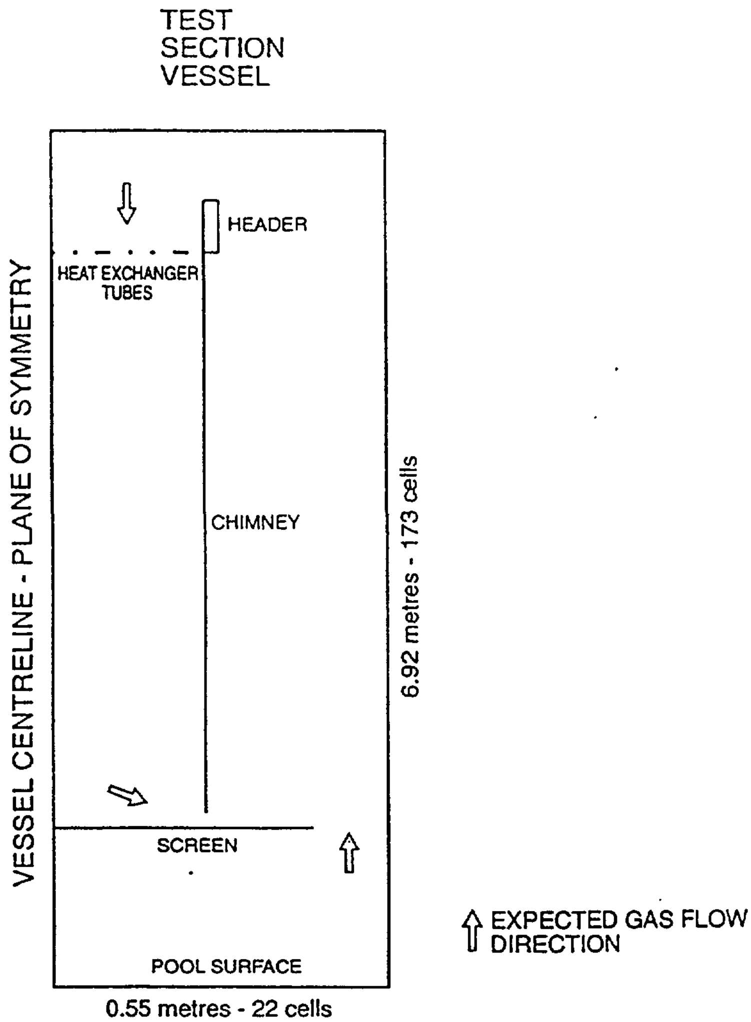

Figure 2. CFDS-FLOW3D Model of ENEL Heat Exchanger Test Section with 5m Chimney

A CFDS-FLOW3D calculation has been run, as a transient, for 45 seconds allowing the flows to develop from zero. Although the gas mixture was predicted to flow up the chimney towards the HX for a short initial period (4½ seconds), the flow quickly turned round as the local mixture density increased and the desired circulation pattern was established. The predicted velocity contours (figure 3) show the overall flow pattern; of particular interest are the high-

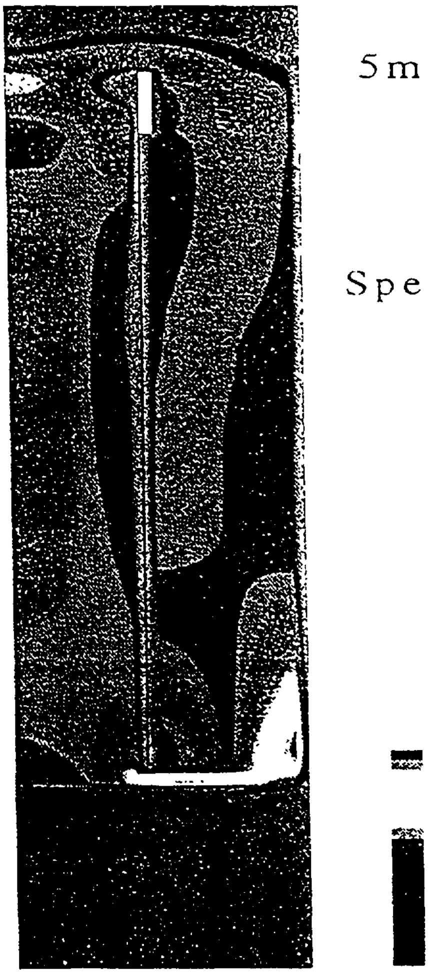

Figure 3. CEDS-FLOW3D Pre-test Predictions for 5m Chimney: Speed contours at 45 seconds

speed flow exiting the chimney bottom and the small 'dead' or low-speed region just inside the edge of the HX inlet. There is no sign of re-entrant or recirculating flow at the chimney outlet; the facility is therefore predicted to operate as intended, for these design conditions. The predicted gas temperature contours (figure 4) clearly show the colder gas inside the chimney exiting at the bottom and mixing with the warmer gas in the outer annulus. The predicted HX inlet velocity at 45 seconds was 0.26m/s and the predicted total power was 128% of the design power. Although lower than the power estimated by the previous analysis this still easily exceeds the design power.

Pre-test analysis using CFDS-FLOW3D was also performed for the second design configuration, ie with a 3m chimney which has its outlet area equal to the inlet area in order to maximise the potential of re-entrant flows. This analysis indicated that the test would proceed as intended, without re-entrant or recirculating flows at the chimney outlet, and that the HX power would exceed the design power. Post-test analysis of this configuration is described in the next section.

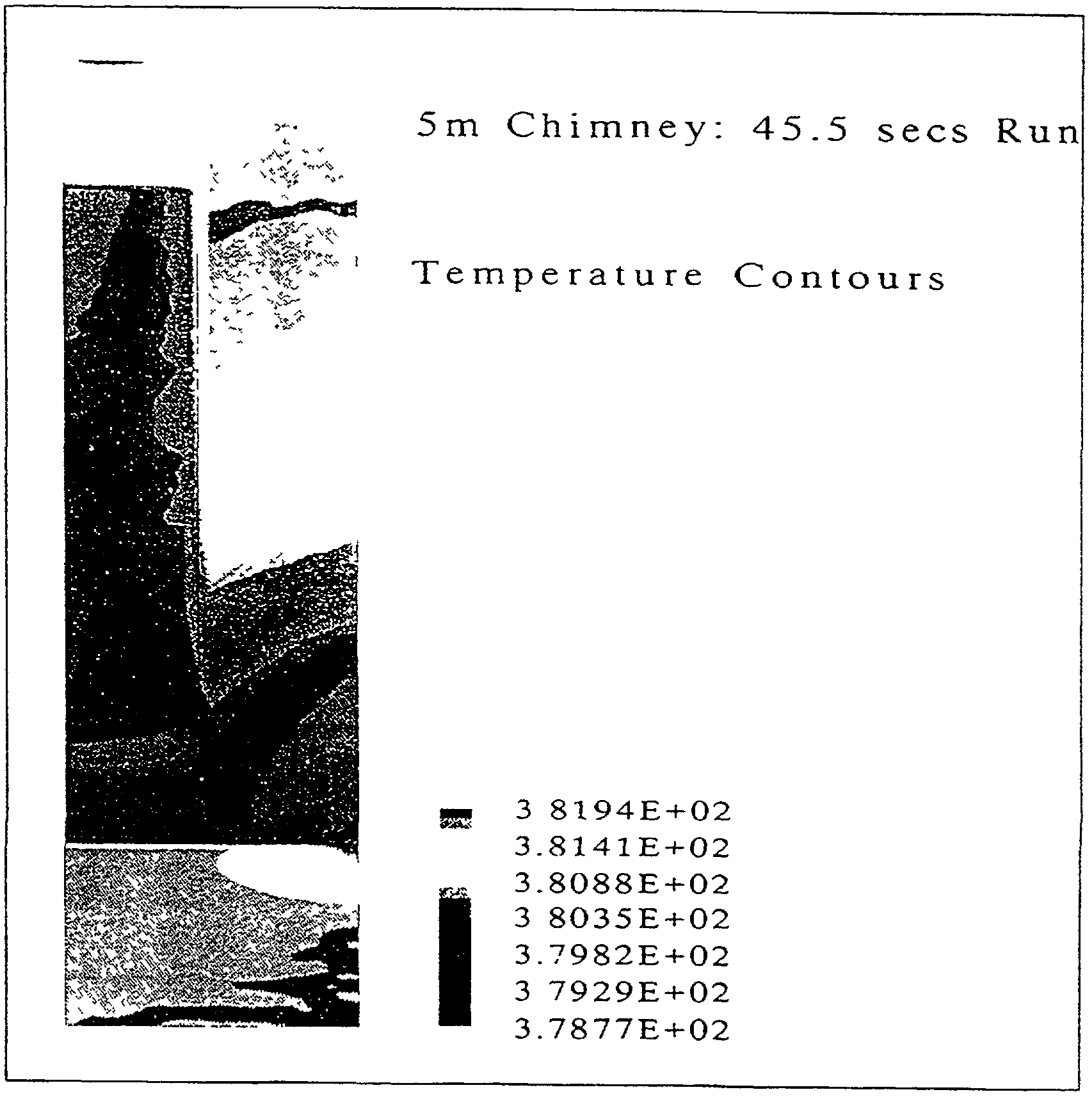

Figure 4. CFDS-FLOW3D Pre-test Predictions for 5m Chimney: Gas Mixture Temperature Contours at 45 seconds

4. POST-TEST ANALYSIS

Post-test analysis has been performed for the first test for which data were available, test 8a. The first stage of the analysis repeated the HTFS correlation prediction method of section 3 but using the actual test conditions. This enabled the HX inlet velocity to be estimated and the sensitivity to the assumed tube interface temperature to be identified. For the pre-test analysis the tube interface temperature was assumed to be 103°C, based on a secondary coolant temperature of 100°C plus a 3° temperature difference from the coolant to the gas-side tube interface. The actual test 8a data indicate that the tube interface temperature must lie between 103.25°C (secondary coolant temperature) and 106.93°C (HX gas mixture outlet temperature). If a tube interface temperature of 104.6°C (Tcoolant+1.25°) is assumed, then the correlation method of section 3 predicts that the system will operate at an inlet velocity of 0.21m/s and an HX condenser power of 101% of the design power with an HX outlet temperature of 107.08°C. This predicted power and outlet temperature agree very well with the measured values for this test; this tube interface temperature was therefore used in the second stage of analysis - the CFDS-FLOW3D simulation described below.

4.1. Simulations of Flow Patterns

A 2-dimensional CFDS-FLOW3D simulation of test 8a has been run, as a transient, for 133 seconds starting from zero flows. At 133 seconds the simulation was reasonably close to steady conditions as can be seen from the HX inlet velocity (figure 5) and HX condensation power (figure 6). The predicted condenser power at 133 seconds was 79.5% of the measured power and the inlet velocity was 0.168m/s. The 'sensible' heat transfer, ie the convective heat transfer in addition to the condensation heat transfer, predicted for these conditions by the HTFS correlation [1], is approximately 4.3% of the measured power. Thus the total power removed by the HX is predicted to be 84% of the measured power removed. The difference is likely to be due, at least in part, to a reduction in the predicted steam mass fraction of the gas mixture during the 133 seconds of the transient. This could probably be addressed in future simulations by choosing slightly different initial conditions for the transient.

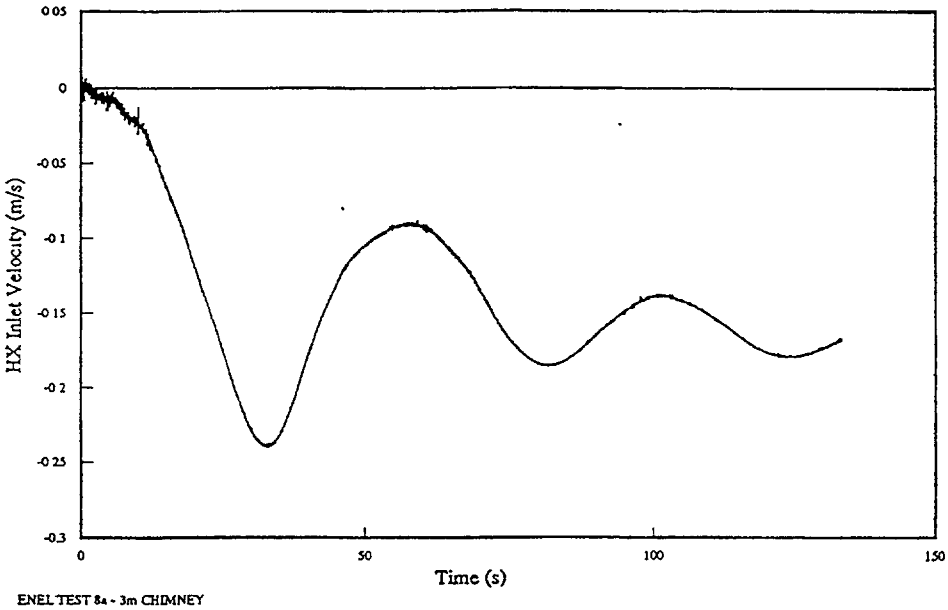

Figure 5. CFDS-FLOW3D Post-test Simulation for 3m Chimney, Test 8a: HX Inlet Velocity vs Time

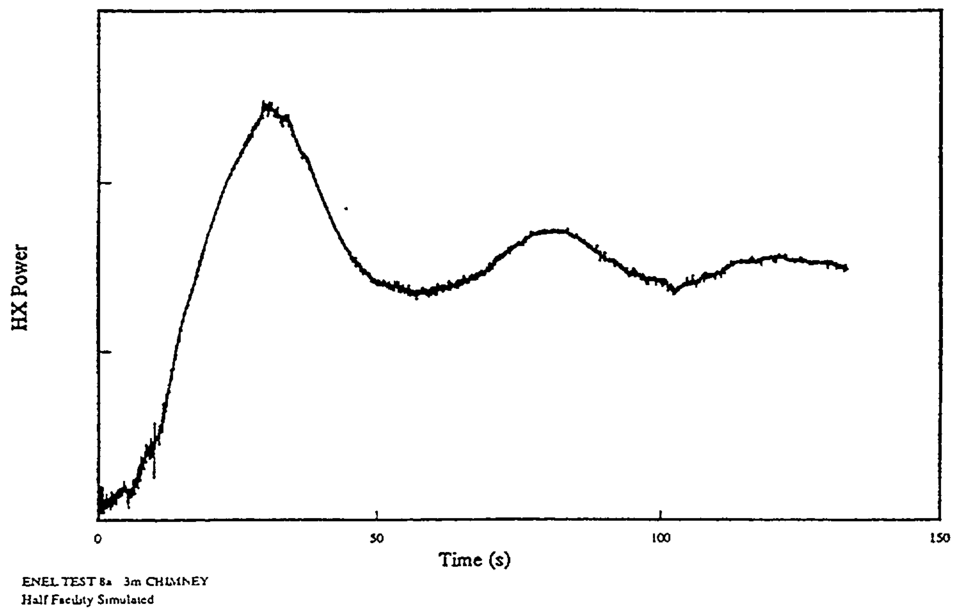

Figure 6. CFDS-FLOW3D Post-test Simulation for 3m Chimney, Test 8a: HX Condensation Power vs Time

The u-velocity contours (vertical velocity) and velocity vectors from the CFDS-FLOW3D simulation of test 8a (figures 7 & 9 respectively) show the rising gas mixture (+ve velocity) in the outer annulus and the falling gas mixture within the HX chimney. Of particular interest is the small region of high upward velocity (shown red) close to the outer wall above the edge of the screen. This region is close to the annulus gas velocity measurement point and its existence may, at least partly, explain the high annulus gas velocities measured for some tests. (Annulus gas velocities would, based on the respective flow areas, be expected to be slightly lower than those at the HX inlet).

The gas temperature contours (figure 8) show the cooling effect of the HX. The CFDS-FLOW3D simulation predicts an HX outlet gas temperature of 106.75°C and an HX gas inlet temperature of 108.55°C. These compare very well with the measured values.

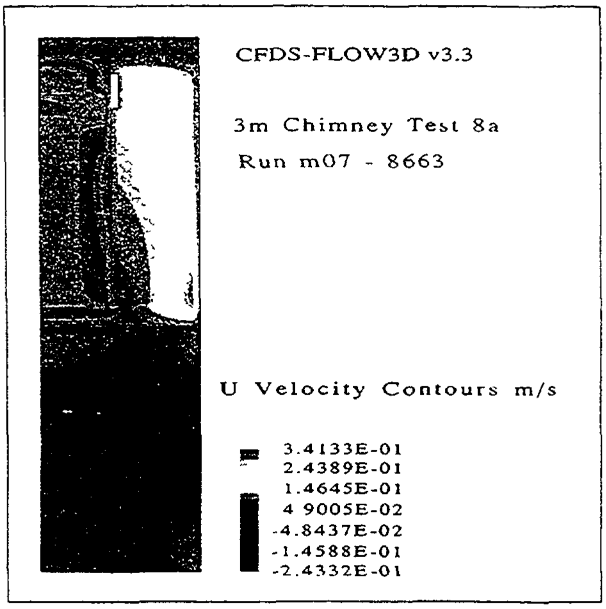

Figure 7. CFDS-FLOW3D Post-test Simulation for 3m Chimney, Test 8a: U-velocity (upward) Contours at 133 seconds

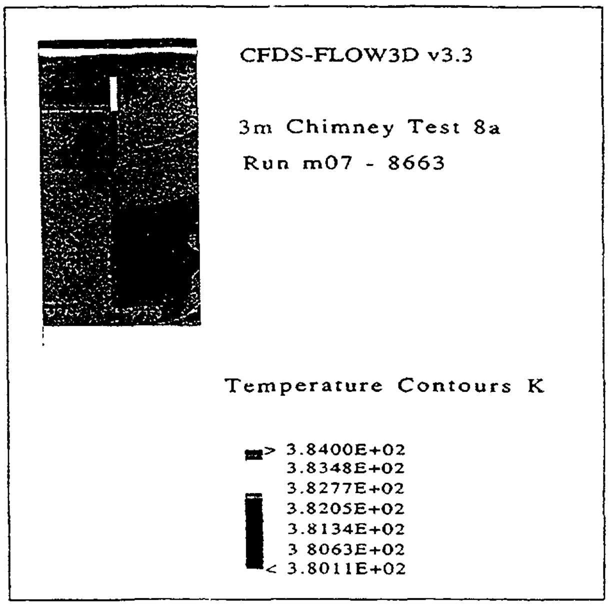

Figure 8. CFDS-FLOW3D Post-test Simulation for 3m Chimney, Test 8a: Gas Mixture Temperature Contours at 133 seconds

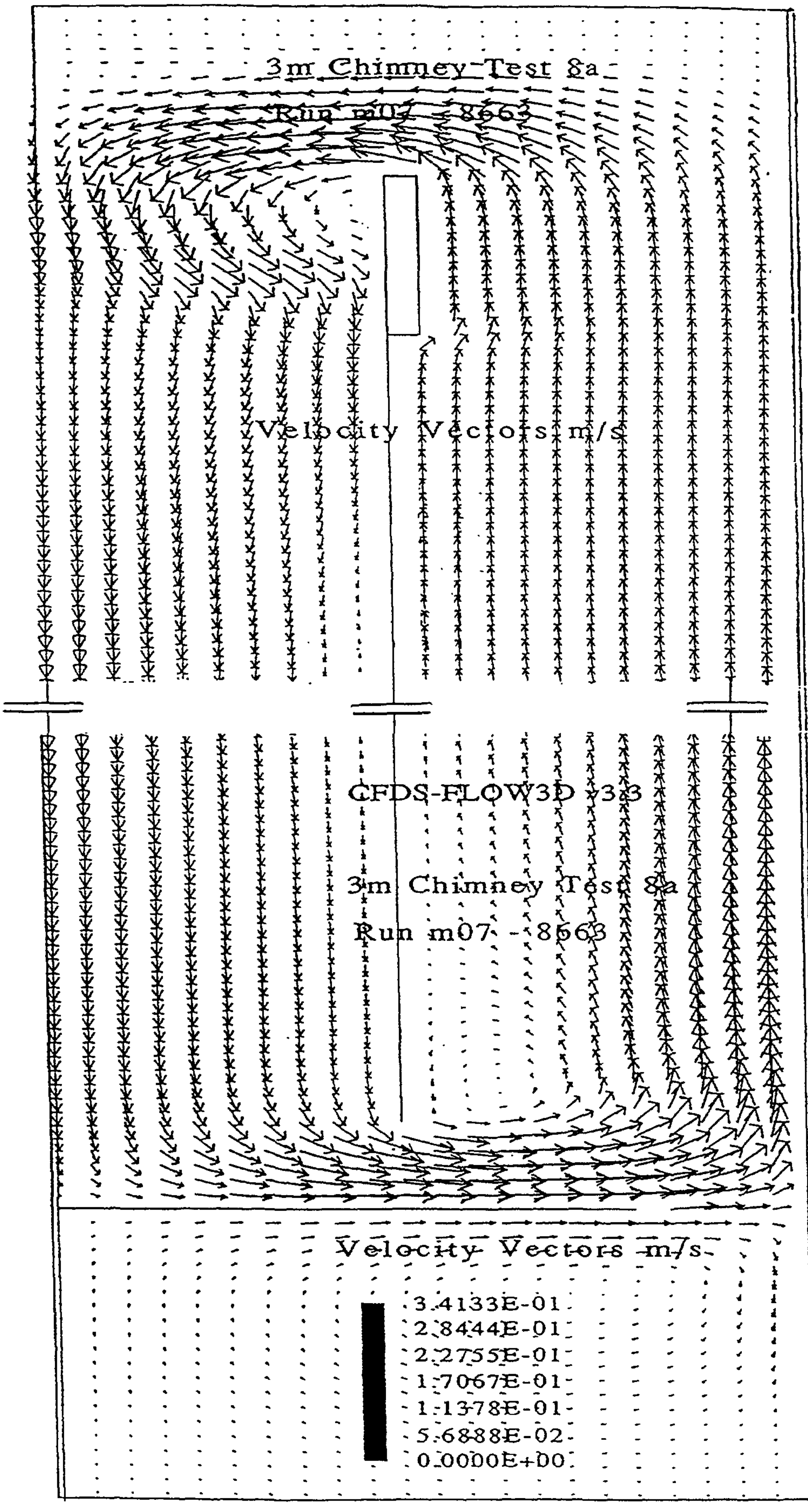

Figure 9. CFDS-FLOW3D Post-test Simulation for 3m Chimney, Test 8a: Gas Velocity Vectors at 133 seconds: HX Inlet & Chimney Outlet

5. SUMMARY AND CONCLUSIONS

1) Pre-test analyses were performed, including CFDS-FLOW3D predictions, for 2 of the tests; 1 test for each of the 2 chimney configurations that were to be used. These indicated that the tests would operate as intended and that the HX power was sufficient for the design conditions. The actual test data have confirmed these predictions.

2) Post-test analysis, including a CFDS-FLOW3D simulation, has been performed for the first test conducted, test 8a. The simulation is in good general agreement with major measured parameters and also offers an explanation for the high upward gas velocities measured in some tests. The simulation underestimated the total measured condenser power by about 16%; this is believed to be due to underpredicting the steady state steam fraction in the vessel.

The following findings relate to the capability of CFDS-FLOW3D for this analysis:

3) CFDS-FLOW3D is sufficiently flexible to allow correlations to be added to represent the HX condensation and the HX pressure drop. This is achieved by providing additional "user" subroutines written in fortran.

4) CFDS-FLOW3D is sufficiently flexible to represent the CISE facility geometry in either 2-D or, if required, in 3-D.

5) For the 2-D model used so far the code is relatively slow running, taking timesteps of up to 30ms. The post-test simulation of test 8a took 32 hours CPU time to calculate 133 seconds of transient on a SUN SPARCstation 10. It is thus just practical to compute a complete transient, approaching the steady state, without using a CRAY.

6) The CFDS-FLOW3D simulation has provided a detailed insight into the flow patterns likely within the test vessel and has provided a plausible explanation of otherwise unexpected results.

5.1. Further AEA Analysis of ENEL Data

The following future activities are planned:

- Perform post-test analyses of the remaining 5 tests for which data are provided.

In achieving these there will also be an aim to:-

- Further improve the running speed of the calculations - perhaps by spreading the condensation region.

- Move to a 3-Dimensional representation of the facility.

6. ACKNOWLEDGEMENTS

The authors acknowledge the support of the UK Department of Trade and Industry who funded this work. They also acknowledge fruitful technical discussions with P Vacchiani of CISE and V Cavicchia and P Vanini of ENEL who supplied the data.

REFERENCES

[1] Heat Transfer and Fluid Flow Service, Airside Heat-transfer Coefficients for Staggered and In-line Arrays of Finned Tubes, HTFS Handbook Paper AM1, Harwell, 1985.

[2] Heat Transfer and Fluid Flow Service, Fin Efficiency and Surface Effectiveness, HTFS Handbook Paper AM7, Harwell, April 1986.

[3] Heat Transfer and Fluid Flow Service, Airside Heat-transfer Pressure Drop for Staggered and In-line Arrays of Finned Tubes, HTFS Handbook Paper AM3, 1980.

ATHLET MODEL IMPROVEMENT FOR THE DETERMINATION OF HEAT TRANSFER COEFFICIENTS DURING CONDENSATION OF VAPOR IN HORIZONTAL TUBES

E.F. HICKEN, H. JAEGERS, A. SCHAFFRATH
Forschungszentrum Jülich ISR, Jülich, Germany

Abstract

Pre- and posttest calculations of the NOKO experiments shall be performed with the ATHLET code. ATHLET which is being developed by the Gesellschaft für Anlagen- und Reaktorsicherheit (GRS) mbH is intended to cover in a single code the entire spectrum of loss-of-coolant and transient accidents in Light Water Reactors (LWR).

The present work is sponsored by BMBF. The objectives are in detail:
- the modeling of the emergency condenser and the NOKO test facility,
- the improvement of the ATHLET condensation model to describe the condensation heat transfer of pure vapors and vapor/non-condensible mixtures in horizontal and inclined tubes in ATHLET
- pre- and posttest calculations of selected NOKO experiments.

The progress to date is that ATHLET and its pre- and postprocessors are installed on the IBM RISC workstation cluster of the Zentralinstitut für Angewandte Mathematik (ZAM) and DEC workstation of the institute. Furtheron an input data set for NOKO has been developed and first calculations have been performed.

As a first step for an ATHLET model improvement the present condensation model was analysed and a literature study was performed. The present ATHLET condensation model is only able to determine heat transfer coefficients for annular flow with turbulent or laminar films in vertical tubes. Therefore, the correlations of Nusselt and Carpenter & Colburn are used. During an ATHLET run, the heat transfer coefficients are determined by using both approaches and the maximum value is used for further calculation.

In the literature, condensation heat transfer in horizontal and slightly inclined tubes is discussed in the same manner. The flow conditions can be determined by using the flow chart of Tandon with the improvement of Palen (transition regime between annular and stratified flow). For every flow condition several empirical or semi-empirical correlations are available. In the first section of the tubes, the steam velocity is relatively high and there is a non-negligible influence of vapor shear on the condensate film and the heat transfer. During condensation along the tubes, the steam velocity and its influence on the heat transfer decreases.

For the determination of heat transfer coefficients during condensation in horizontal and inclinced tubes the stand-alone modul KONWAR (Kondensation in waagerecht und leicht geneigten Rohren) has been developed. After the input of actual geometry and flow parameters, the water steam properties are calculated by using ATHLET functions, which are linked to KONWAR. In a next step, the flow conditions are determined following by the calculation of the heat transfer coefficients.

1. Introduction

The BWR 600/1000 is a new innovative boiling water reactor concept which is being developed by Siemens. The concept is characterized in particular by passive safety systems; they are decribed in another paper. One of the important safety systems is the so-called emergency condenser. This safety system has to transfer decay heat from the vessel/core region to a heat sink in the containment, for the BWR 600/1000 concept into a large water pool.

Parameters influencing the effectiveness of the emergency condenser are the primary pressure in the pressure vessel, the pressure and temperature of the containment, non-condensibles and the geometrical design. The experimental data will be gained with the NOKO facility, which is described in another paper.

Pre- and posttest calculations of these tests shall be performed with the ATHLET code which has been developed and validated by the Gesellschaft für Anlagen- und Reaktorsicherheit (GRS) Germany. The Institute for Safety Research and Reactor Technology (ISR) of the Research Center Jülich (KFA) received the task from the BMBF to use the ATHLET code for the emergency condenser and - if necessary - improve or modify models. In specific, the tasks listed below are given.

- The modeling of the emergency condenser and the NOKO test facility,
- the improvement of the ATHLET condensation model to describe the condensation heat transfer of pure vapors and vapor/non-condensible mixtures in horizontal and inclined tubes in ATHLET
- pre- and posttest calculations of selected NOKO experiments.

2. The Physical Phenomena

Fig. 1 show schematically one pipe (out of 4 x 104 pipes in a BWR 600/1000) with an arbitarity water level inside. The length is about 10 m, the tube inside diameter 38.7 mm and the wall thickness 2.9 mm. The inlet steam velocity ranges from about 6 m/s at 7 MPa to about 20 m/s at 1 MPa; the outlet water velocities are up to 0.25 - 0.3 m/s. It is evident that depending on velocities and pressures differences flow characteristics of the condensate exist. Fig. 2 shows some possibilities. It should, however, be mentioned that - due to relatively thick tube wall - the main thermal resistance is with the metal wall.

The outside heat transfer mechanism is mainly boiling. Due to the relatively narrow bundle boiling from the lower branch of the tube may influence the boiling of the upper branch. In addition, larger bubbles may be formed and produce some unsteady behavior.

The temperature decrease inside the tube below the water level is also of interest because the density differences between the down-pipe and the pressure vessel determines the water level difference, see fig. 3.

The effectiveness of the emergency condenser in case of the existance of non-condensibles cannot be calculated with sufficient accuracy. For very low concentrations of non-condensibles these will be solved in the condensate and thus be removed from the emergency condenser. For higher concentrations non-condensibles will be accumulated within the tubes; the bend between down-pipe and reactor vessel may block the removal of the non-condensibles. It will be of interest which concentrations of non-condensibles will exist along the tubes.

It will also be studied if flashing inside the tubes due to pressure transients will influence the effectiveness.

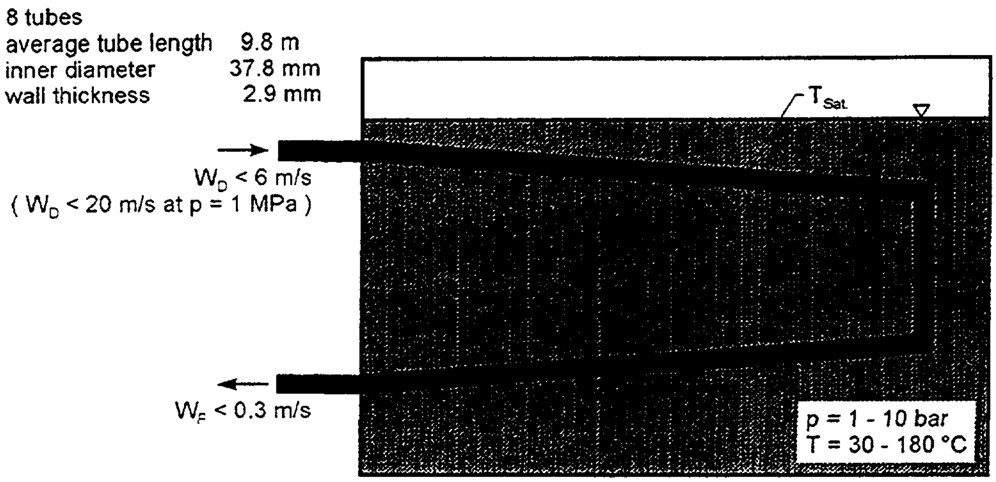

FIG. 1. NOKO tube characteristical operating conditions for 7 MPa.

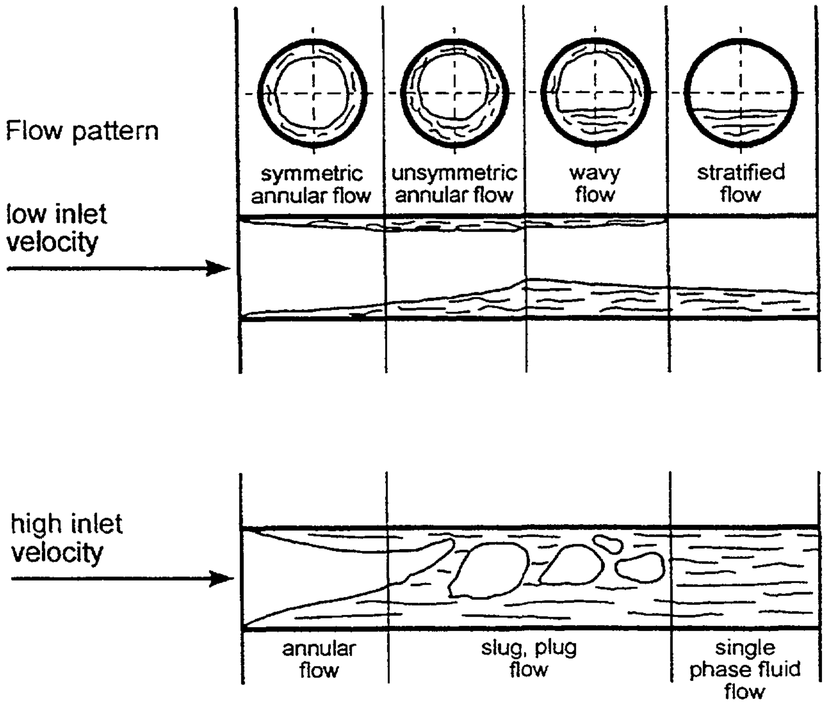

FIG. 2. Flow patterns occuring during condensation inside horisontal tubes.

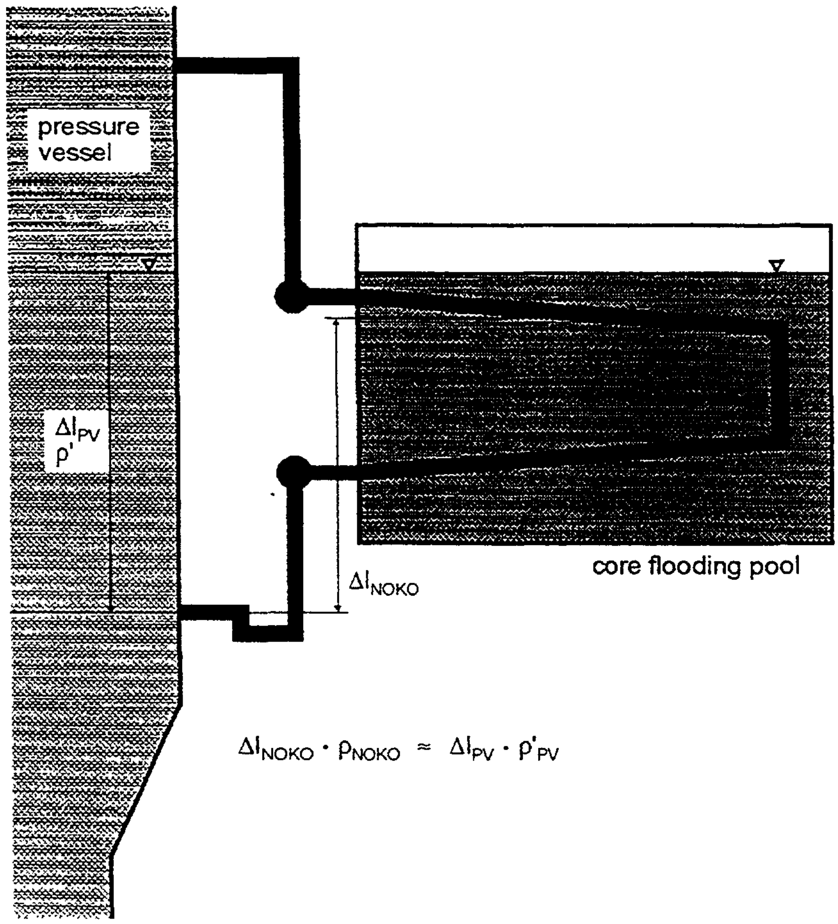

FIG. 3. Water level difference between emergency condenser and pressure vessel.

3. The Heat Transfer Package in ATHLET

The general aspects of the ATHLET code have been described elsewhere.

The heat transfer package in ATHLET is controlled by levels; level 1 is characterized by heat transfer from fluid to structures. Within this level 3 different modes, see fig. 4, are possible. Within each mode heat transfer coefficients will be determined by using different options. For the further calculation the maximum value will be used. It should be noted that experimental data for condensation inside tubes are mainly available for vertical tubes.

Fig. 5 shows a more detailed flow regime, as proposed by Tandon/Palen. In fig. 6 the different correlations are listed. For the emergency condenser these correlations will be tested. If they do not fit, model improvements would be necessary.

Fig. 7 shows flow regimes with the pressure and the power as parameter the which are expected in the emergency condenser.

It has not been decided which method will be used in case of non-condensibles inside the tubes. As a start the reduction of the inside heat transfer will be related to the decrease in the (steam) saturation temperature.

Mode	Fluid	Correlation	Mechanism
1	single phase liquid	Dittus-Boelter Mc Adams min	forced convection natural convection 20 W/m² K
5	two phase fluid	Chen Nusselt Carpenter-Colburn min	forced convection laminar film condensation turbulent film condensation 20 W/m² K
9	single phase steam	Hausen Dittus-Boelter Mc Eligot min	forced convection forced convection forced convection 10 W/m² K

FIG. 4. ATHLET heat transfer correlations of 'level 1'.

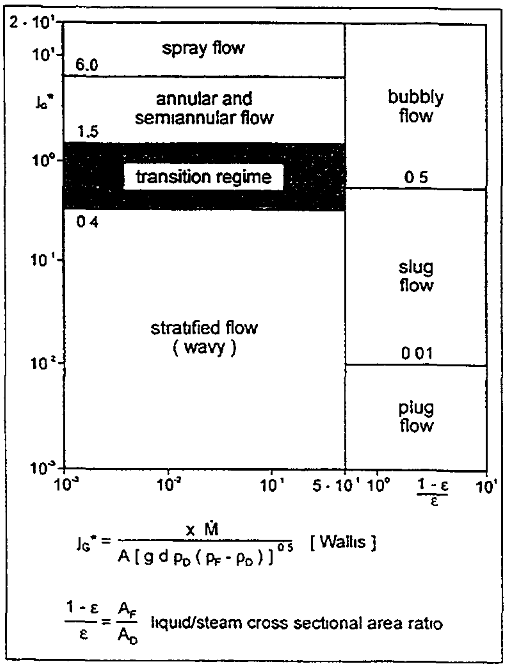

FIG. 5. Flow regime map for condensation inside horizontal tubes according to TANDON.

Flow pattern	Fluid	Correlation
Spray flow	two	Solimann
annular and semiannular flow	phase	Nusselt, Kosky & Staub, Akers, Carpenter & Colburn, Chen, Kruzihlin, Baehr
stratified flow	fluid	Jaster & Kosky, Rufer & Kezios
bubbly, slug, plug flow		Brebber
	steam	Hausen, Dittus-Boelter
	water	Sieder-Tate, Dittus-Boelter

FIG. 6. Correlations which will be tested for NOKO calculations.

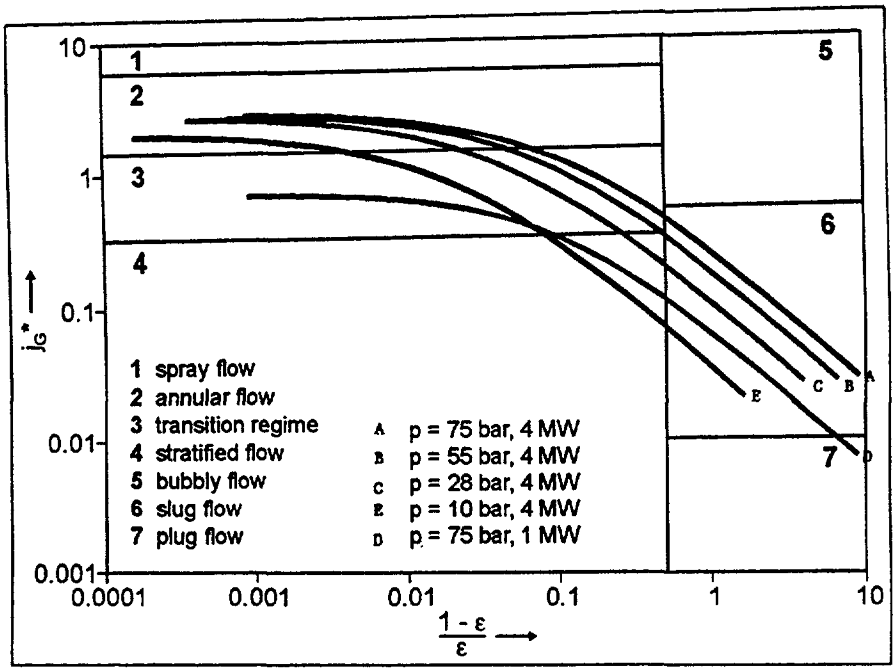

FIG. 7. Flow regimes inside the NOKO tubes.

4. ATHLET Modeling of the NOKO-Facility

Fig. 8 and 9 show the nodalisation of the NOKO facility. It includes 3 thermofluiddynamic systems, 60 network-objects, constisting of 280 nodes and 240 junctions, 60 heatslabs and special components (e.g. pump, heat exchanger, electrical heater). All control systems can be simulated.

A special nodalisation has to be used for the "secondary" side of the condenser, see fig. 10, due to the recirculation flows.

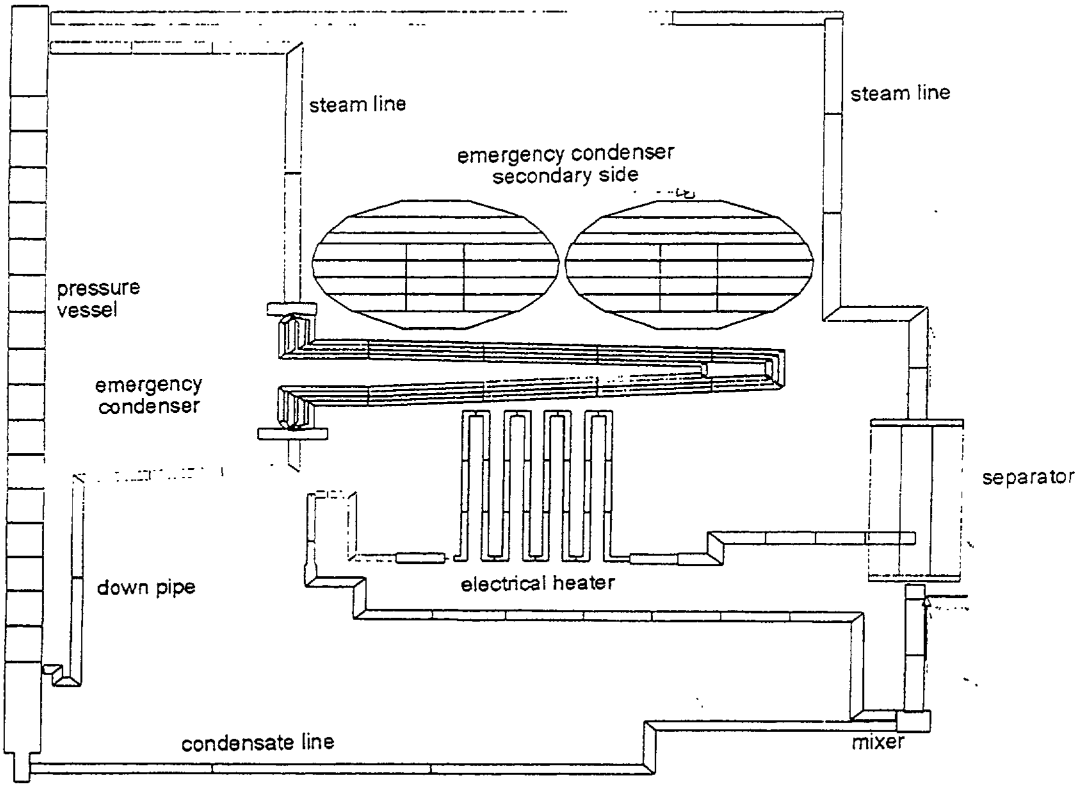

FIG. 8. NOKO nodalisation scheme.

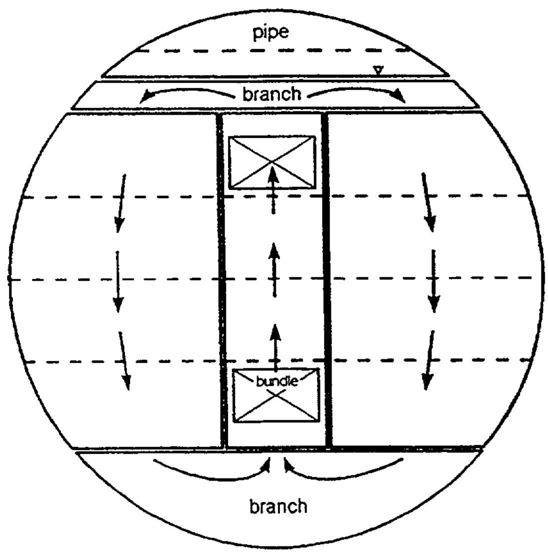

FIG. 9. Nodalisation scheme of NOKO secondary side.

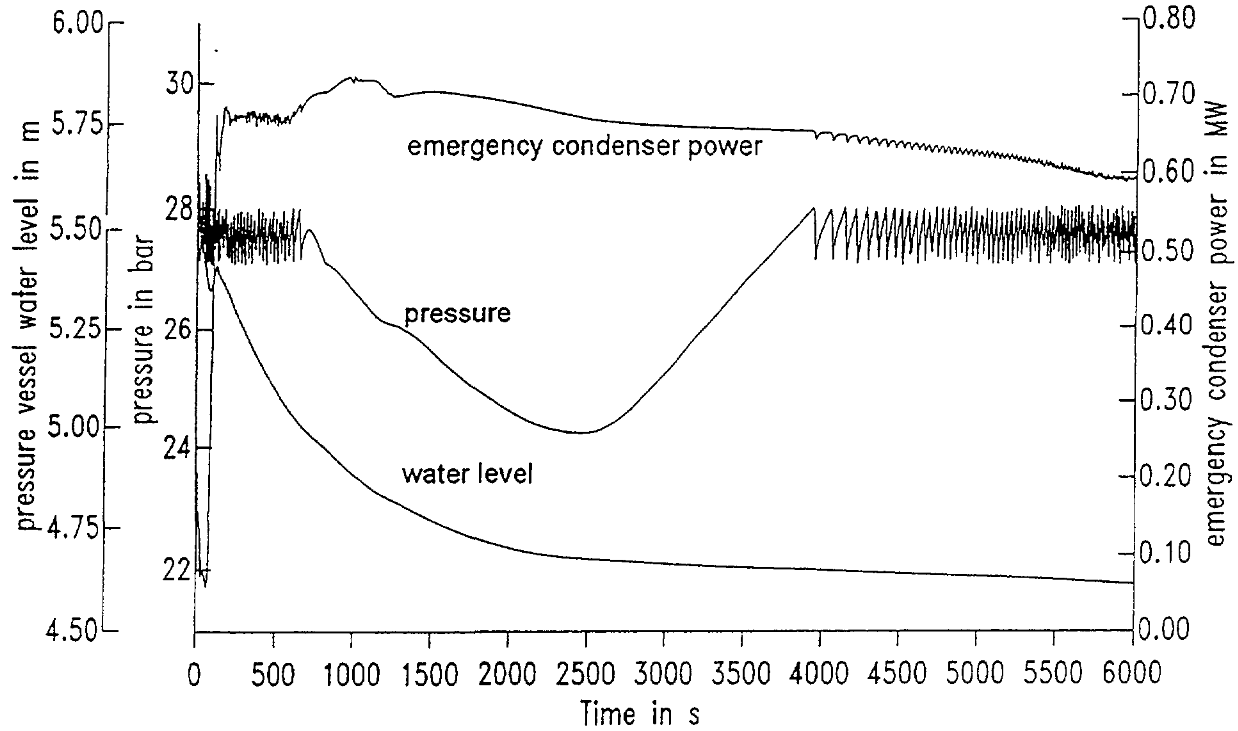

FIG. 10. Emergency condenser power, water level in pressure vessel and pressure (4 tubes, M_D = 0.3 kg/s, p = 28 bar).

5. Some Results from Calculations

In the following, an ATHLET run at 2.8 MPa pressure is discussed, see fig. 11. During the calculation, 4 emergency condenser tubes are open. The pressure in the system is fixed by the control system, the water level decrease is specified by the user in the input data set. During the decrease of the water level, heat is removed to the condenser secondary side. At nearly 800 s, the removed heat is larger than the energy supplied by the steam and the pressure decreases. The increase of the emergency condenser power at 800 s results from the uncoverage of the control volumes behind the tube bends. In the horizontal part of a U-tube, the increase of heat transfer surface caused by water level decrease is much stronger than in the tube bend. After heatup of the emergency condenser secondary side (see T6 - T8 in Fig. 11) and the increase of the fluid temperature at the end of the tubes with time, the emergency condenser power slowly decreases and, at 3500 s, the amount of condensate reaches the amount of steam again. In Fig. 11, the temperature distribution in the emergency condenser is shown. The temperature measurement positions T1 - T4 are located inside the bundle (T1 = inlet, T2 = before tube bend, T3 = after tube bend, T4 = outlet). The saturation temperature in the different control volumes identify uncoverage. After total condensation of the steam, the fluid subcools. The degree of subcooling is influenced by the temperature outside the bundle and the degree of its uncoverage. On the secondary side of the emergency condenser, there is a temperature increase with a gradient of 0.01 K/s.

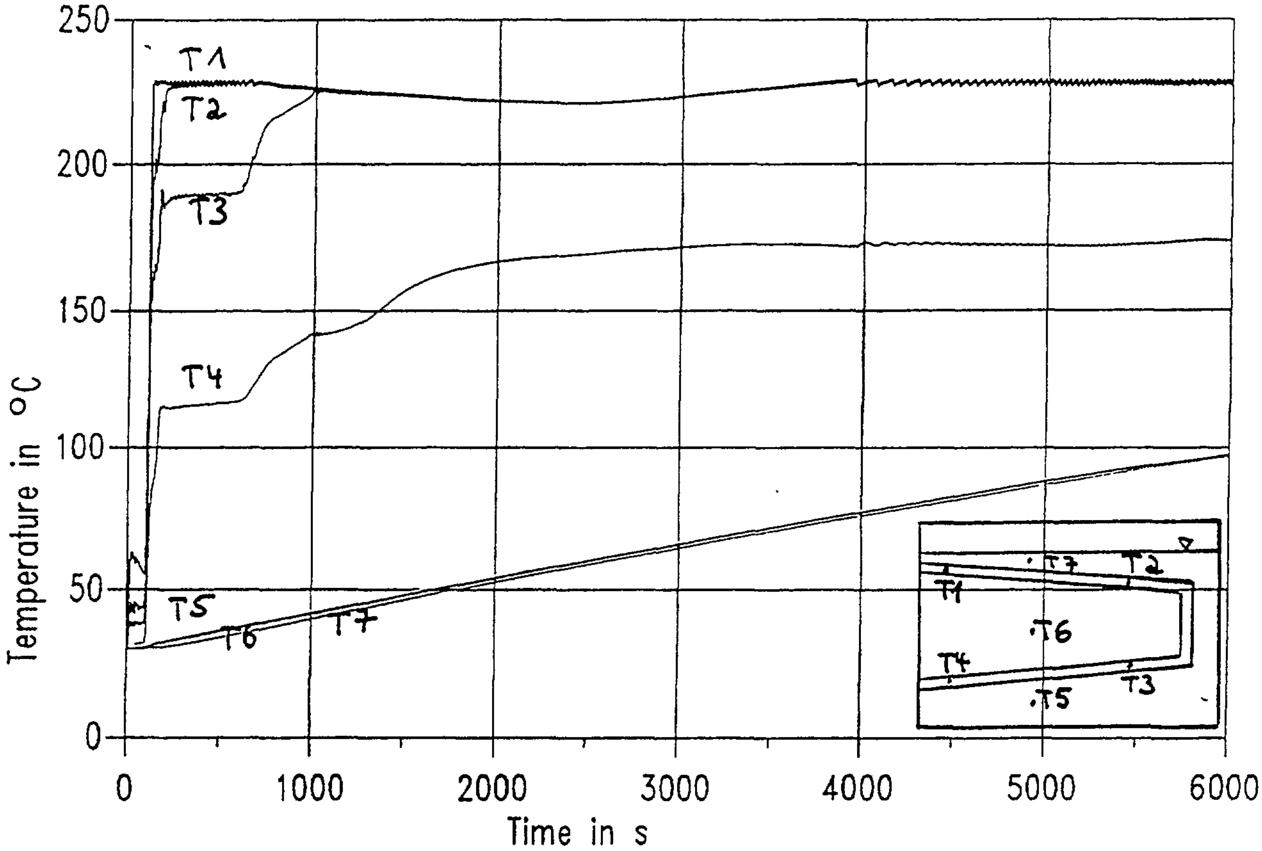

FIG. 11. Temperatures emergency condenser.

RELAP5/MOD3 PRE-TEST PREDICTIONS FOR THE SPES-2 1" C. L. BREAK TEST S01613

A. ALEMBERTI, C. FREPOLI, G. GRAZIOSI
ANSALDO Nuclear Division,
Genoa, Italy

Abstract

SPES-2 is a full height, full pressure experimental facility scaled 1/395 respect to the Westinghouse AP600 plant. The SPES-2 facility designed and operated by SIET in Piacenza is the evolution of the previous existing SPES-1 facility. The SPES-2 test matrix provides a complete set of experiments from Cold Leg break accidents to Steam Generator Tubes Ruptures and Main Steam Line break. The SPES-2 test program is performed under the technical cooperation agreement among ENEL, ENEA, ANSALDO and WESTINGHOUSE.
In the frame of the SPES-2 activities ANSALDO carried out pre-test calculations for the facility as well as comparisons with full plant behaviour to support the facility scaling criteria.
SPES-2 calculations were made using a noding developed by ANSALDO for the Relap5/mod3/V80 code.
Experiment S01613 was the last test of the SPES-2 test matrix, a 1" break on the Cold Leg bottom performed with a total of three PRHR tubes instead of the normal SPES-2 configuration where only one tube is used to simulate one of the two scaled AP600 PRHR heat exchangers.
The main purpose of this test was to investigate the facility response when an overcooling capability is provided to the primary system.
The paper presents first the Relap5/mod3 noding for the SPES-2 facility with highlights on particular aspects of the nodalization used for the simulation.
Then a comparison between experimental data and pre-test calculations is performed to show the agreement between pre-test predictions and experimental data.
The code results shows that Relap5/mod3, when the noding is carefully tuned on the facility using the informations provided by hot and cold shakedown as well as some of the previous transient tests, is able to predict the facility response for the main parameters of the transient.
A brief comparison between the pre-test predictions made for test S00401 (1" Cold Leg Break test with one PRHR tube) and test S01613 is also presented to analyze the different response of the facility when an overcooling capability is provided to the primary system.

INTRODUCTION

The paper presents a comparison of the pre-test prediction made by ANSALDO using RELAP5/Mod3/V80 with SPES-2 test data for transient S01613, a 1" C.L. break made with 3 PRHR tubes.
The SPES-2 noding developed by ANSALDO was tested first against cold and hot shakedown tests and tuned to obtain a current reproduction of the SPES-2 primary pressure losses, primary and secondary heat losses etc. Once the first SPES-2 experimental results were available modification to the noding were made to better simulate the facility behaviour and also results from full 3-D simulations were used to improve the RELAP5 response [4].
The above work leaded to the SPES-2 noding presented in Figure 1.
The agreement between pre-test prediction and experimental data for test S01613 was very good and it will he discussed in the following.
Then a comparison between the calculated data for this test and the 1" C.L. break with 1 PRHR tube is performed. Final conclusions are then provided.

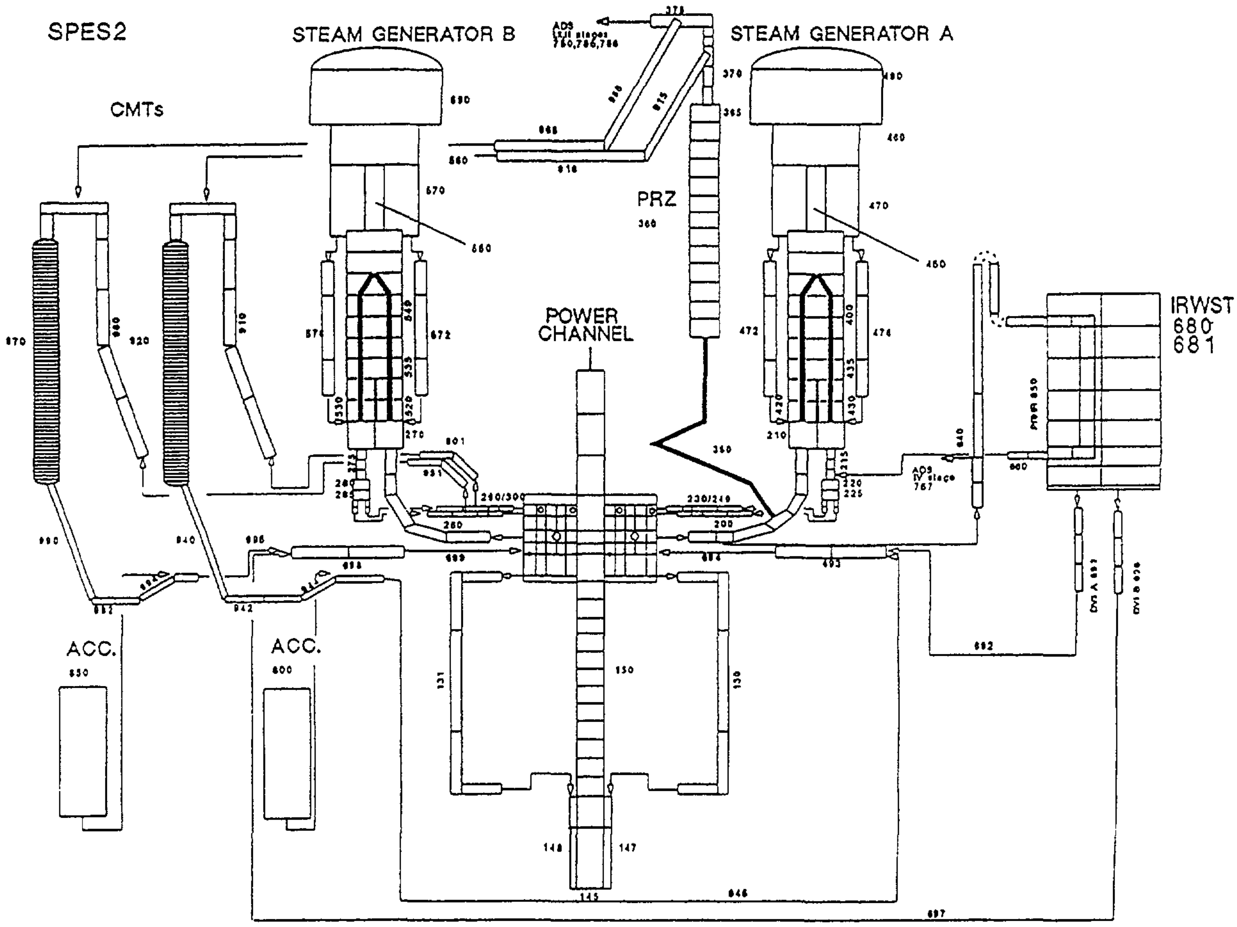

Figure 1 - SPES-2 Relap5/mod3 noding

S01613 PRE-TEST CALCULATION AND EXPERIMENTAL DATA COMPARISON

Figure 2 presents the primary side pressure behaviour. The agreement between the experimental data and the pre-test prediction is very good. After a phase of fast primary pressure decrease oscillations in RCS pressure take place due to an unstable natural circulation phenomena while a constant and slow primary pressure decrease takes place due to the PRHR heat exchange.
When CMT injection switch from single to two-phase flow in the balance line (shown by CMT injection increase in Figure 3 and 4) the primary pressure decrease is affected due to the lower entalphy of the flow entering the core.
First stage ADS timing is well calculated by the code as it is shown in Figure 2 by the sudden decrease of the primary pressure.
Figure 3 and 4 shows the decrease of the CMT injection flow in the first phase of the transient due to the CMT heat-up and a consequent decrease of the head available for injection until the CMT Cold Leg Balance Line flow is in single phase conditions. As the Balance lines flow become two-phase the CMT injection increases. However the CMT injection is not very stable as in other transients [1], [2] due to the presence of slugs in the balance line. The code was able to compute in the correct way the above phenomenology.
Figure 5 presents the break flow comparison showing a very good agreement between predictions and experimental data.
Figure 6 is a comparison of the pressurizer level. The pressurizer level decrease in the first part of the transient is well predicted, being conditioned by the primary mass loss. The pressurizer level increase at the end of the transient due to ADS valves opening is well calculated by the code while the subsequent pressurizer draining is qualitatively predicted with a short time delay.

Figure 7 and 8 presents the PRHR mass flow and PRHR inlet-outlet temperatures comparison.
PRHR mass flow oscillations frequency is well predicted while the amplitude is higher in the prediction respect to experimental data. The average value is any-way very close to experiment.
PRHR inlet temperature is obviously well predicted while the strong PRHR outlet subcooling is also calculated of the correct amount.

Relap5 pre-test predictions and S01613 exp. data

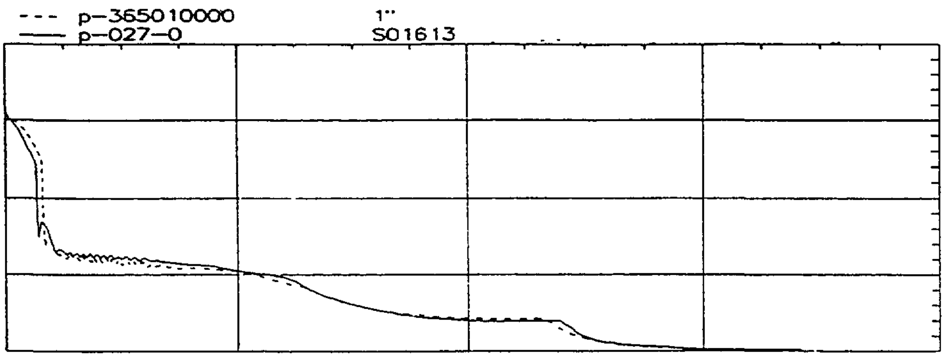

Figure 2 — pressurizer pressures

Relap5 pre-test predictions and S01613 exp. data

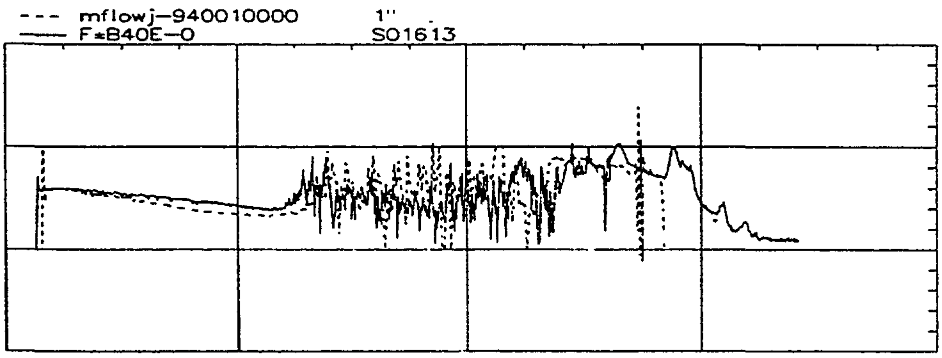

Figure 3 — CMT B injection flows

Relap5 pre-test predictions and S01613 exp. data

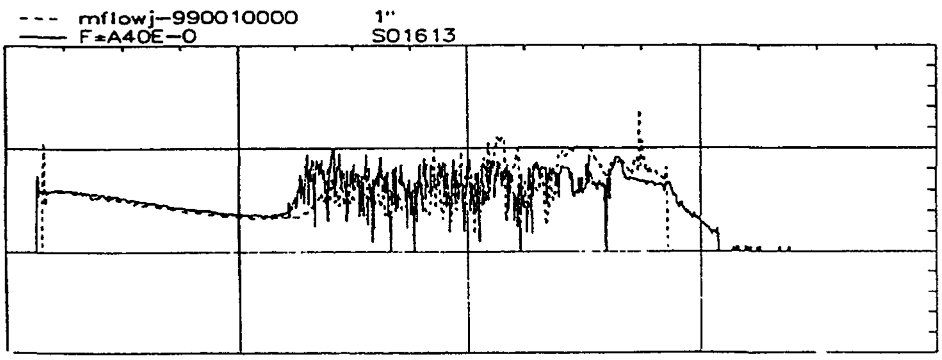

Figure 4 — CMT A injection flows

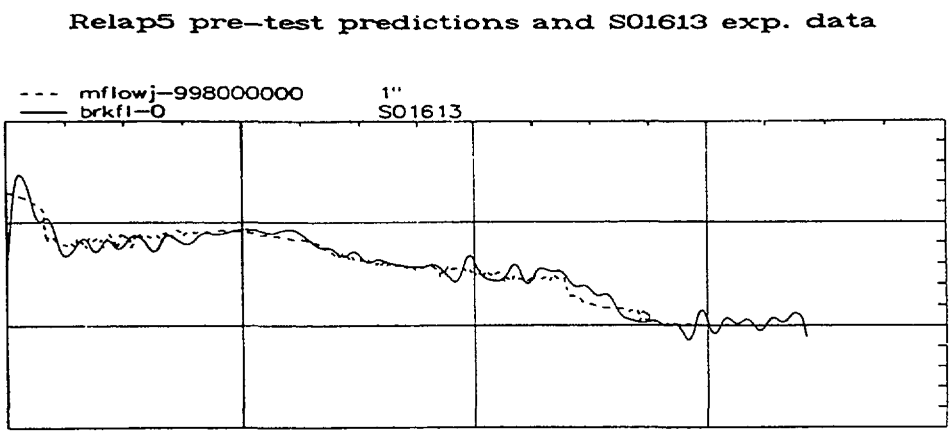

Figure 5 — Break mass flows

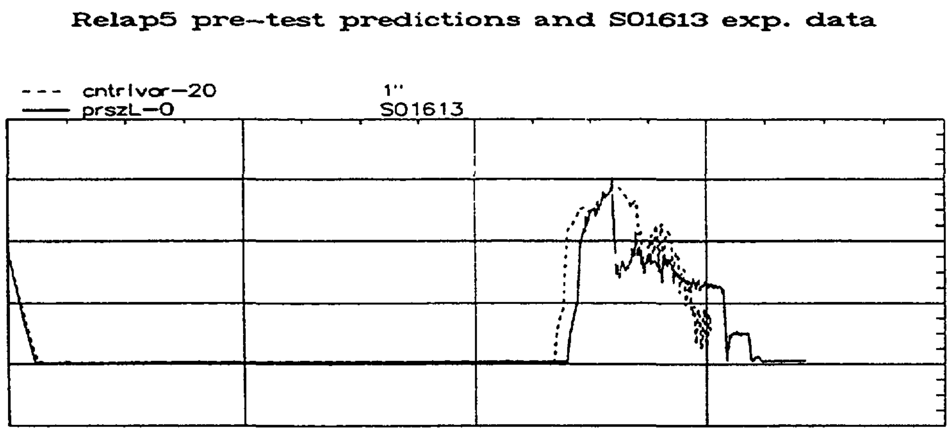

Figure 6 — Pressurizer levels

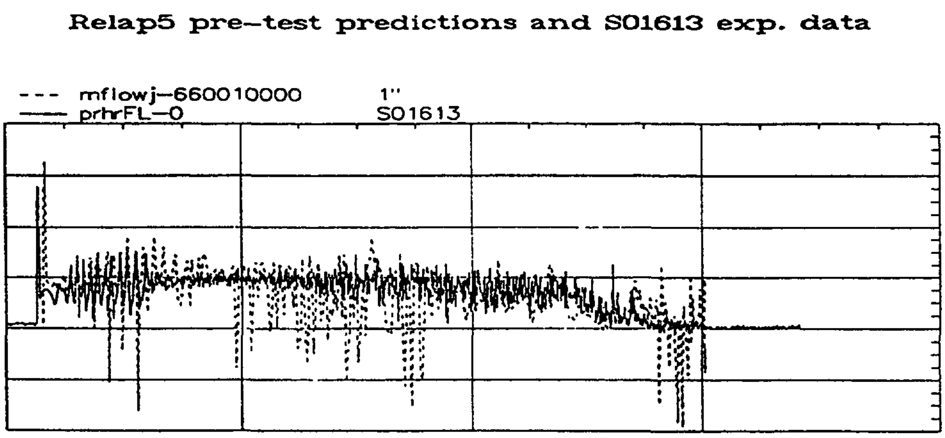

Figure 7 — PRHR mass flows

Relap5 pre-test predictions and S01613 exp. data

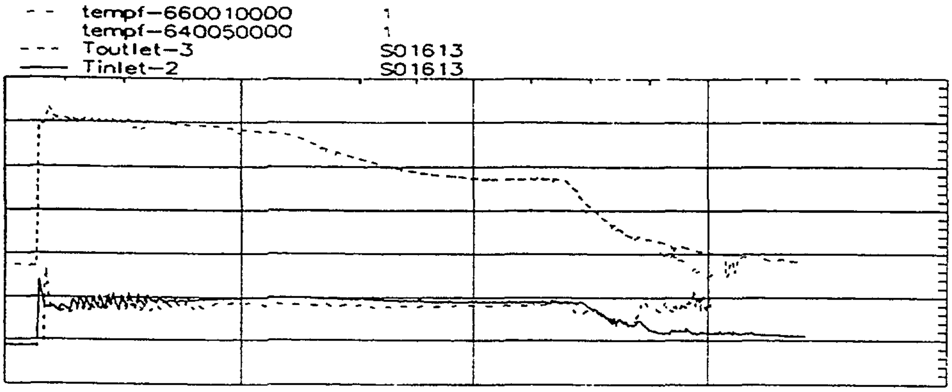

Figure 8 — PRHR inlet and outlet temperatures

Relap5 pre-test predictions and S01613 exp. data

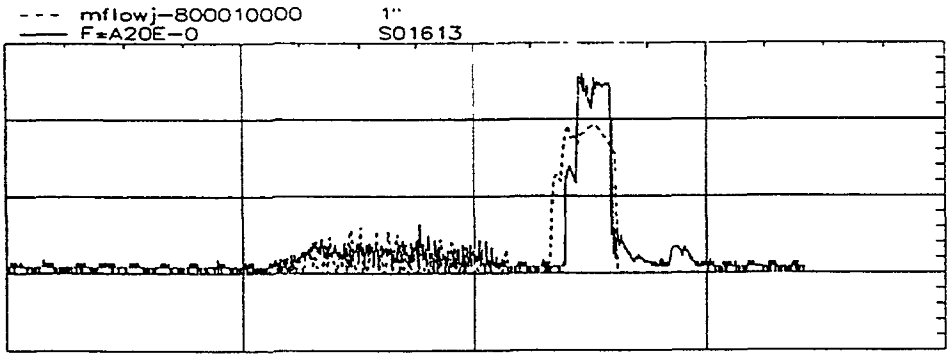

Figure 9 — Accumulators injection flows

Relap5 pre-test predictions and S01613 exp. data

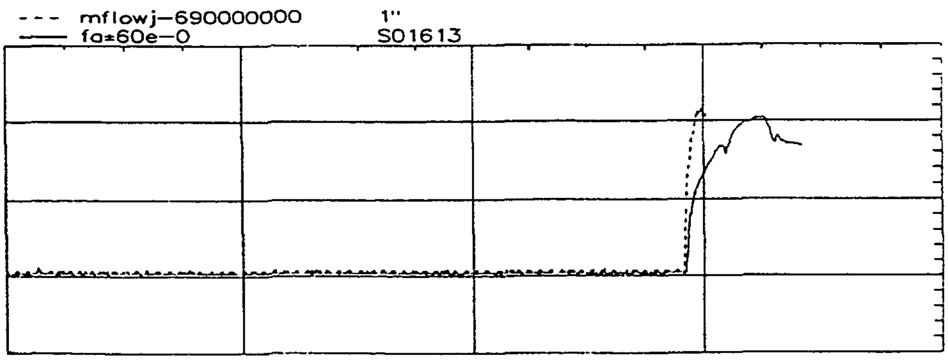

Figure 10 — IRWST injection flows

Figure 5 compares the accumulator behaviour. The injection flow is small until ADS opening takes place, the qualitative behaviour and effects of second stage opening is correctly calculated by the code.
Figure 10 presents the IRWST injection flow comparison. Timing is very well calculated while some difference is present in the injection behaviour.

COMPARISON OF RELAP5 PREDICTIONS FOR SPES-2 TEST S01613 AND TEST S00401

A comparison of the RELAP5 results for the 1" C.L. break tests with one (S00401) and three (S01613) PRHR tube is here briefly presented.
Figure 11 presents the primary pressure behaviour. As can be seen the primary pressure value is reduced when three PRHR tubes are used in the PRHR due to the overcooling capability of the PRHR. However main phenomenologies of the two transients are very similar note that the first stage ADS timing is not strongly affected.
This is confirmed by the break flow comparison presented in Figure 12. Since the two break flows are very similar the RCS residual mass is very close in the two runs so that also CMT level (Fig.13) as well as CMT injection flow (Figure 14) are not influenced by the PRHR overcooling capability.
Accumulators flows (Figure 15) shows some difference in the peak value but the injection behaviour is the same as well as starting and end time.
IRWST injection timing (Figure 16) is close between the two transients.
PRHR mass flows (Figure 17) shows as higher tendency of the run with 3 PRHR tubes to oscillations while PRHR inlet outlet temperatures are affected obviously by the higher cooling capability due to the greater heat exchange area.
PRHR inlet temperature is affected by the saturation pressure difference while outlet temperature is lower in the case with 3 PRHR tubes.
The difference is anyway limited due to the already low value reached also in the case of only 1 PRHR tube.
The main phenomenologies predicted by the code during the two transients were the same and also quantitative values does not change greatly due to the overcooling capability of the PRHR heat exchanger.

Comparison of Relap5 prediction for test S00401 and S01613

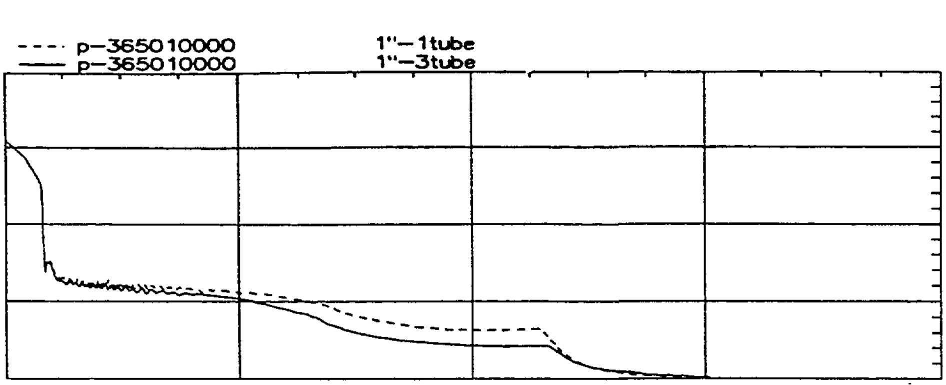

Figure 11 — pressurizer pressures

Comparison of Relap5 prediction for test S00401 and S01613

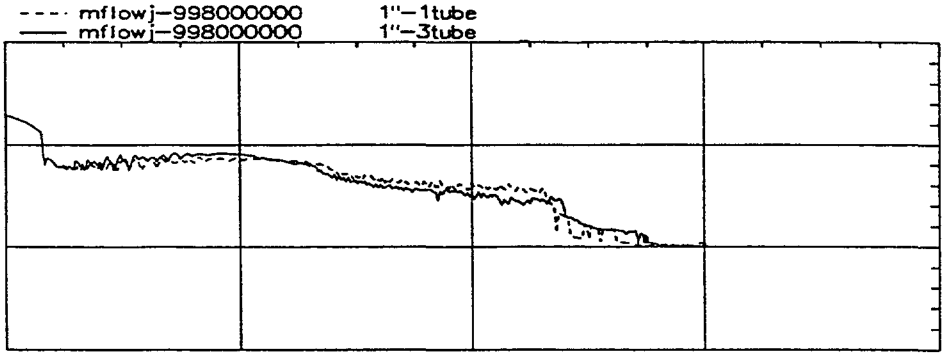

Figure 12 — Break mass flows

Comparison of Relap5 prediction for test S00401 and S01613

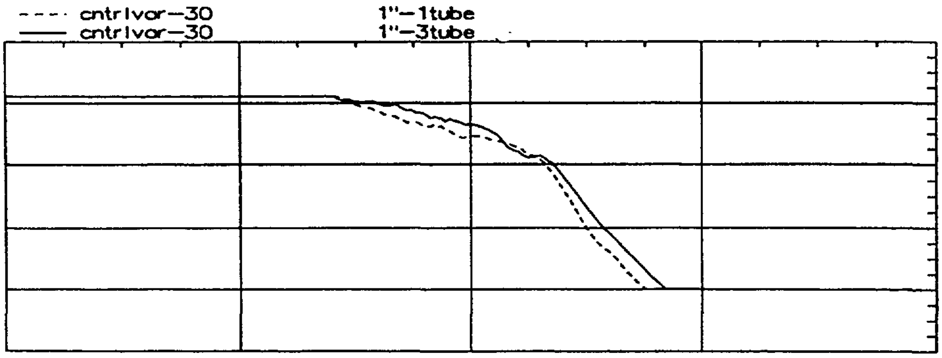

Figure 13 — CMT B levels

Comparison of Relap5 prediction for test S00401 and S01613

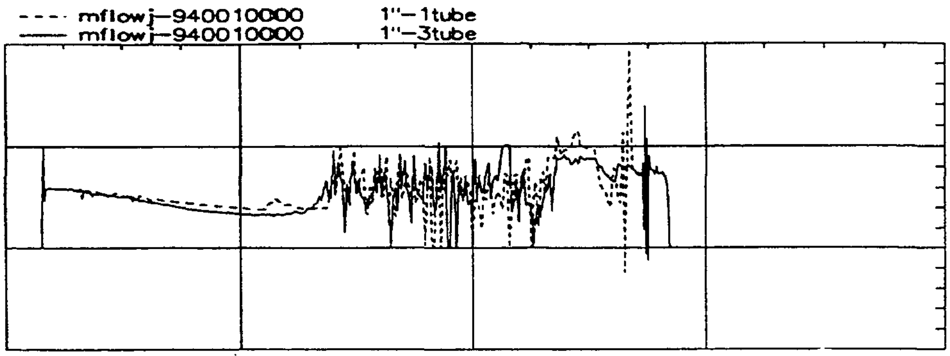

Figure 14 CMT B injection mass flows

Comparison of Relap5 prediction for test S00401 and S01613

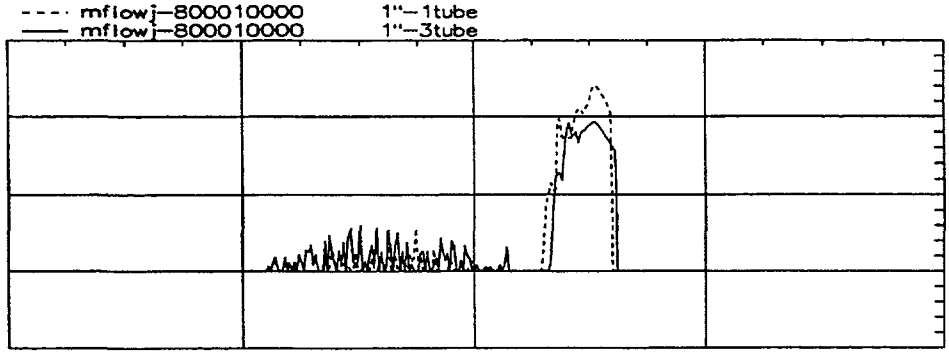

Figure 15 — Accumulators injection mass flows

Comparison of Relap5 prediction for test S00401 and S01613

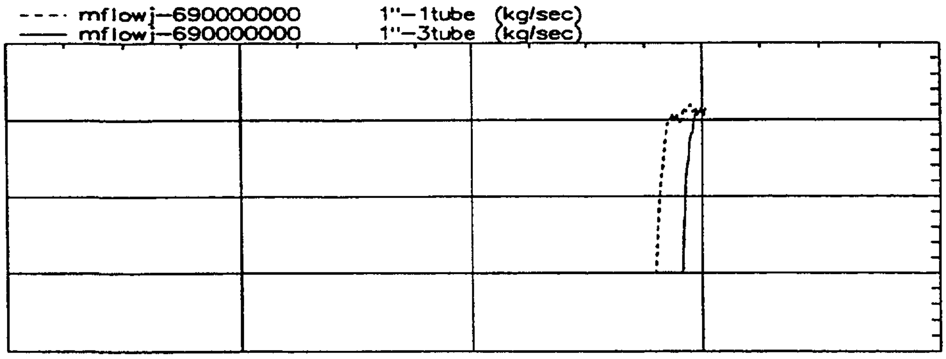

Figure 16 — IRWST injection mass flows

Comparison of Relap5 prediction for test S00401 and S01613

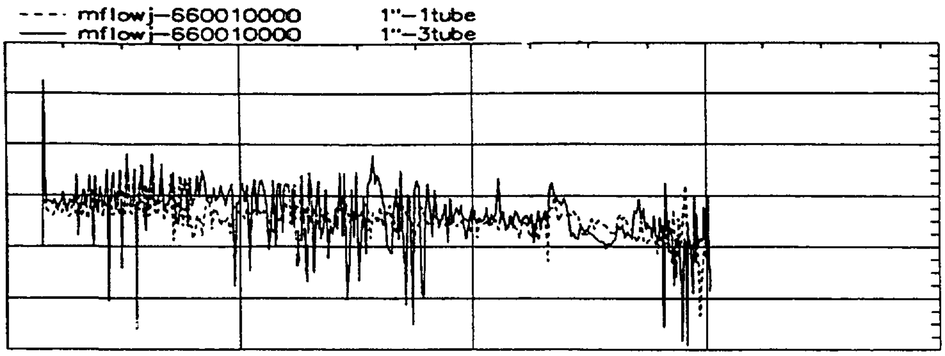

Figure 17 — PRHR mass flows

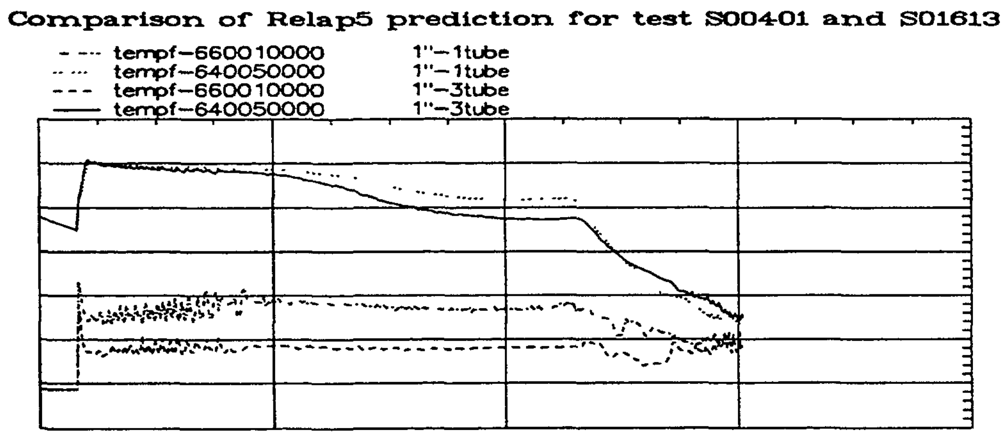

Figure 18 — PRHR inlet and outlet temperatures

CONCLUSIONS

A comparison between RELAP5/mod3/V80 pre-test predictions made by ANSALDO and 1" SPES-2 C.L. break with three PRHR tubes has been presented.
The results indicate that all phenomenologies of the transients were captured by the code. Qualitative and quantitative values of pressure, injection flows, temperatures etc. were very well predicted by the code.
A comparison has also been presented between code results for 1" C.L. break with one and three PRHR tubes.
The comparison shows that the response of the facility is slightly influenced by the PRHR overcooling capability. Main phenomenologies remain the same while timing of the events is very close in the two cases.

REFERENCES

[1] Alemberti A., Frepoli C., Graziosi G. 1994
SPES-2 cold leg break experiments: Scaling approach for decay power, heat losses compensation and metal heat release.
International Conference - New Trends in Nuclear System Thermohydraulics - Pisa, May 30th-June 2nd

[2] Alemberti A , Frepoli C., Graziosi G. 1994
Comparison of the SPES-2 pre-test predictions and AP600 plant calculations using RELAP5/mod3
International Conference - New Trends in Nuclear System Thermohydraulics - Pisa, May 30th-June 2nd

[3] M. Bacchiani, C.Medich, M.Rigamonti (SIET) - L.E. Conway (Westinghouse)
SPES-2, AP600 Integral System Test - Inadvertent ADS opening and Cold Leg Break Transients
International Conference - Pittsburgh Pa April 17-21 ARS-94

[4] Alemberti A., Frepoli C., Graziosi G. 1994
SPES-2 RELAP5/mod3 noding and 1" cold leg break test S00401
22nd Water Reactor Safety information Meeting- Washington D.C. October 24-26 '94

DEVELOPMENT AND INITIAL VALIDATION OF FAST-RUNNING SIMULATOR OF PWRs: TRAP-2

E. BREGA
ENEL-ATN

C. LOMBARDI, M. RICOTTI, R. SORDI
Department of Nuclear Engineering,
Polytechnic of Milan

Milan, Italy

Abstract

Fast running computer programs with versatile, user-friendly, interactive features are very useful for the design and operation of nuclear reactors. TRAP-2 tailored to AP600 reactor belongs to such a category.

The main simplifying hypotheses are the incompressible but thermally expandable fluid and the homogeneous/thermal equilibrium approach for two-phase flow. Distributed parameter components and lumped parameter components are adopted to describe the whole circuit. The first ones are solved by the Method of Characteristics. The system is modelled by several circuits in parallel including primary loops and safety circuits: the analysis of the first ones proceeds by implicit method, while that of the latter ones by explicit method.

Either a zero-dimensional or a mono-dimensional approach is available for neutron kinetics: the solution is obtained at the end of the thermohydraulic time step. Several nested iterative procedures are adopted to find the relevant parameters in a fixed time and space grid. Heat exchangers are solved iteratively between primary and secondary side, while the pressurizer is described by a two-fluid two-phase model. In quasi stagnant conditions the primary circuit can be collapsed in a two separate phase volume, while maintaining the current models for safety circuits: this increases substantially the computation speed of the program, at present ranging from 15 times to about 1 the real time on PC.

Validation of the program is in progress. Satisfactory comparisons have been obtained with RELAP results of safety transients of a passive reactor. Other comparisons with experimental data are being performed regarding SPES transient tests for the AP600 system.

1. INTRODUCTION

The analysis of any reactor concept concerns two aspects: safety and operability. Remaining within the framework of a pressurized light water concept, here we consider PWRs, both of conventional and advanced design. Safety aspects in relation to large loss of coolant accidents (LOCA) would appear thoroughly studied and documented: complex computer programs are available for a complete description of these accidents. On the other hand in any reactor system, "slow" accidents are more important than previously supposed, both for the delayed triggering of the protection system, especially when of "passive" nature, and the higher effect on the transient of the dynamic behaviour of many components in view also of their control system.

As far as operability is concerned, the analysis of different operating conditions, particularly start-up and stability behaviour, may yield important information about reactor flexibility.

These considerations had led us to the conclusion that a simple but complete computation model for plant transients might be a useful tool for both parametric studies during design activity and on-line simulation, when the reactor is in operation.

The slowness of the transient to be analyzed and the limited production of steam inside the primary circuit allowed us to adopt the hypotheses suitable for an incompressible fluid, and in particular to disregard the sound speed effects. Moreover, two-phase flow is taken into account in a simplified manner, by applying the same equations adopted for the liquid phase, corrected for the increased specific volume.

When the plant is in quasi stagnant configuration in the primary circuit, such as in very low flow rate/power condition, a single volume-two fluid model is adopted to simulate the primary circuit including the vessel, maintaining the current models for the safety systems. This assumption substantially simplifies and accelerates the computation.

This model has been implemented in several computer programs tailored for different reactor systems, such as AP600, conventional PWRs, PIUS [1], MARS [2] and ISIS [3].

This paper is devoted to a synthetic description of the model [4] and to its first validation activity concerning comparisons with the experimental safety transients obtained in SPES [5] facility for AP600 and with RELAP transients obtained for the safety analysis of the MARS reactor.

2. BASIC THERMOHYDRAULIC MODEL

The thermohydraulic model is based on the general conservation equations of mass, momentum and energy, and on the constitutive laws to close the system.

The circuit is assumed monodimensional and described by a series of constant cross section ducts, in which the fluid flows along the axis direction. Then convection and diffusion in the other two directions are taken into account by means of an integration process, which implies the adoption of two constitutive equations for the diffusive terms in energy and momentum balance, i.e. for the heat flux and the friction factor.

The fluid is incompressible but thermally expandable. Its density is only a function of enthalpy, assuming the pressure value at saturation condition (this hypothesis can be easily removed in the future).

Two phase flow, when present, is treated according to the homogeneous model with equal steam and water velocities at thermal equilibrium. The presence of separated steam and water zones, such as in the pressurizer and the steam generator dome is described by mass and energy balance equations applied to each zone, disregarding the momentum balance equation but using a Bernoulli type equation for pressure loss evaluation.

The overall reactor system (primary, secondary and safety circuits) are characterized by a number of parallel circuits, which are coupled hydraulically and/or thermally and may function in natural convection. To describe correctly their functioning and their activation (when applicable) a detailed and precise spatial distribution of their relevant parameters, such as density, pressure, boron concentration, is needed. This yields to consider distributed parameter components in the case of pipes, reactor channels and heat exchangers. By assuming constant the cross section of each component, or subcomponent in which the actual component has been divided, one obtains:

Mass $$\Omega\frac{\partial \rho_m}{\partial t}+\frac{\partial \Gamma_m}{\partial z}=0 \tag{1}$$

Boron $$\Omega\frac{\partial \rho_m C_b}{\partial t}+\frac{\partial \Gamma_m C_b}{\partial z}=0 \tag{2}$$

Energy $$\rho_m\frac{\partial h_m}{\partial t}+\frac{\Gamma_m}{\Omega}\frac{\partial h_m}{\partial z}=\frac{q''\Pi_h}{\Omega} \tag{3}$$

Momentum $$\frac{1}{\Omega}\frac{\partial \Gamma_m}{\partial t}+\frac{1}{\Omega^2}\frac{\partial}{\partial z}\left(\frac{\Gamma_m^2}{\rho_m}\right)=-\frac{\partial p}{\partial z}-\rho_m g\cos\vartheta-f\frac{2\Gamma_m|\Gamma_m|}{D_e\Omega^2\rho_m} \tag{4}$$

In two-phase flow the above quantities are substituted by those obtained by the homogeneous model with equal steam and water velocities.

The circuit plena do not require such a detailed description, because the intense turbulence here existing justifies the hypothesis of a complete fluid mixing, thus disregarding any information about spatial distribution of the relevant parameters. Then a lumped parameter treatment is applicable, integrating the balance equations within the volume. For instance this implies an instantaneous and homogeneous mixing of all boron contained inside the volume, which is opposite to the distributed parameter case, where its value shifts rigidly without any mixing between the inlet and outlet sections (piston behaviour).

In lumped parameter components the outlet-inlet pressure drop is obtained by the "mechanic" energy equation (Bernoulli type), valid for incompressible fluids, which leads to an ordinary derivative system. This subdivision in several distributed parameter components with constant cross section requires the presence of connecting areas, which allow sudden variation of the cross section. For these special components mass and "mechanic" energy equations are solved, neglecting the inertia and the head terms, while considering the friction term through a number of kinetic heights, given by the usual hydraulic resistance handbooks.

The constitutive relationships concerning the friction factor and the heat transfer coefficient or the heat flux are function of the local conditions of the fluid. The correlations are derived by the literature and the main ones are detailed in Table I (SI units).

In the heat exchangers, including the steam generator, the heat flux is calculated by assuming constant, within each time step, the thermoydraulic data of one fluid, when calculating the evolution of the other and viceversa. In natural convection heat exchangers, the procedure may be iterated, within the same time step.

A special component is the accumulator, which is pressurized with inert gas and injects water in the primary circuit, when its pressure falls below the accumulator one. A rather simple model describes the transient of the inert gas pressure versus the injected flow rate. In this case an iterative procedure is adopted within each time step to take into account the counterpressure determined in the primary circuit by the injected fluid.

3. REACTOR CORE MODELS

The reactor core model presents three aspects: channel thermohydraulic, fuel rod behaviour and neutron power kinetics.

From a thermohydraulic viewpoint the core may be approximately described as a bundle of separate channels, each containing one fuel element. With their different power inputs, these channels have also slightly different flow rates in order to satisfy the boundary condition in obtaining the same core pressure drop. During transient conditions a steam-water mixture may be obtained in the hottest channel and this would imply a slightly higher asymmetry in channel flow rate distribution and above all a "void" generation, which involves a negative reactivity feedback. A thorough description of this thermohydraulic configuration is really too complicated for our program aims and so a simplification has been adopted.

TABLE I - MAIN CORRELATIONS INCLUDED IN CURRENT TRAP-2 VERSION.

AUTHORS	CORRELATION	APPLICATION FIELD
(analytic)	$f = \frac{16}{Re}$	internal laminar flow
SELANDER	$f = \left[3.8 \log\left(\frac{10}{Re} + 0.2\frac{\varepsilon}{D_e}\right)\right]^{-2}$	internal turbulent flow
(analytic)	$Nu = 4.36$ (for uniform th.flux) $Nu = 3.66$ (for uniform temper.)	forced convection, laminar flow
DITTUS-BOELTER	$Nu = 0.023\, Re^{4/5}\, Pr^{n}$ (heated n=0.4; cooled n=0.3)	forced convection, single-phase turbulent flow (liquid or vapour)
CHURCHILL-CHU	$Nu = \left\{0.60 + \frac{0.387\, Ra^{1/6}}{\left[1 + (0.559/Pr)^{9/16}\right]^{8/27}}\right\}^{2}$	free convection, single-phase external flow (liquid)
ROHSENOW	$q'' = \mu_l\, h_{fg}\left[\frac{g(\rho_l - \rho_v)}{\sigma}\right]^{1/2}\left(\frac{c_{p,l}(T_w - T_{ls})}{0.013\, h_{fg}\, Pr_l}\right)^{3}$	free convection, external flow, nucleate boiling
JENS-LOTTES	$q'' = \frac{e^{(4p/6.2)}}{(25)^4}(T_w - T_{ls})$	two-phase and subcooled flow

The reactor core is described through a single power channel representing the core average channel. This is viewed as a "pipe" with constant cross section, and a power input derived from the fuel rod subroutine. However at the end of each time step and maintaining the already calculated core boundary condition constant, the parallel channel behaviour is determined out of line. Three channels are examined, each representative of those of the central, intermediate and peripheral zone respectively. In this way, a more precise temperature and void distribution can be calculated to determine reactivity feedback data. This out-of-line calculation follows an iterative procedure to correct the flow rate of each channel at the same overall flow rate and in order to converge to the same pressure drop.

The fuel rod temperature distribution is described in the radial direction. The cross section is divided into five annular zones: three in the fuel zone, one in the gap and one in the cladding, and their temperatures are the unknowns. The general Fourier equation was solved by referring to these five temperatures. The boundary conditions are: the power generated in each zone, which is proportional to its area (deriving from the neutron kinetic subroutine), the coolant temperature and the corresponding heat transfer coefficient. In conclusion, five linear algebraic equations are obtained, the solution of which yields the desired temperature distribution and thus the thermal power transferred to the coolant.

The thermal conductivities and specific heats of zircaloy and uranium oxide are taken as temperature dependent, while their density is assumed constant. Gap conductivity is assumed to be burn-up and linear power dependent and so an empirical correlation based on a rather complex fuel performance model was developed.

The neutron power is calculated out-of-line at the end of each time step; the resulting value is the power input for the calculation of the fuel rod temperature distribution in the following time step. The reactivity is calculated as the sum of five terms due to: fuel temperature (Doppler), moderator temperature, moderator density, moderator voids, boron coolant concentration. Each one is calculated by multiplying the corresponding parameter variation with respect to a reference condition by a given input value (reactivity coefficient), which can be a function of the parameter itself.

The neutron kinetic equations (Nordheim-Fuchs) are written for six delayed neutron groups and solved by the simplified Runge-Kutta method, according to the procedure indicated in ref.[6]. The solution can be optionally obtained either by this zero dimension approach or by a monodimensional one. Obviously in the latter case the above procedure is different in the sense that the thermohydraulic parameter effect is calculated directly on neutron cross sections instead of on the overall reactivity. However, the experience gained during the tests showed that the monodimensional solution coincides practically with the zero dimensional one in the "slow" transients. The solution is obtained by a shorter time step then the one used in the thermohydraulic part of the program. Therefore the neutron kinetic integration is carried out with constant input data throughout the whole thermohydraulic time step.

4. NUMERICAL SOLUTION

The differential equations are discretized by subdividing the space and the time in given finite intervals. The time grid is in general fixed, but it can be varied along the transient, while the space grid is fixed. An option foresees a variable space grid, based on the length run by the fluid in each time step: this procedure is apt to describe fast transients with low axial numerical diffusion, but it is time consuming when the flow rate falls to very low values in any single circuit.

The solution is obtained through the "Method of Characteristics", which seems efficient in reducing numerical diffusion along the fluid pattern.

The multiple circuits solutions are coupled by implicit ("on-line") or explicit ("out-of-line") method in time advancement. Those solved with the first method, which in the present program can be two, are the primary loops, while all the safety systems and the secondary side are coupled explicitly. For on-line circuits, an iterative procedure is set up: starting from given flow rate and pressure values in a reference cross section of one selected circuit, the thermohydraulic parameters of the fluid are calculated along all its possible patterns and finally the pressure in the starting cross section is obtained. This value must be equal to the initial one within a given convergence error, otherwise the flow rate is modified accordingly. The starting cross section is the connecting point between the pressurizer surge line and the primary circuit. This pressure is determined through an iterative procedure between the pressurizer and the circuit pressure. In conclusion, a number of nested iterative procedures are to be solved, i.e.: first and second circuit coupling parameters, pressurizer and first circuit pressure, primary and secondary circuits inside heat exchanger for heat flux, first circuit flow rate.

The out-of-line circuits, typically the emergency cooling systems, are solved at the end of each time step, keeping constant their boundary conditions i.e. the thermohydraulic conditions of the connecting points with the primary circuit.

When the transient reaches a quasi stagnant condition in the primary circuit, low flow rate and power, an important simplification is adopted. All the primary circuits, including the reactor vessel, are collapsed in a single volume, where all the existing liquid and steam are collected in two separate zones. The enthalpy is uniform in the zone and is obtained by weighing the previous values in each component by their corresponding masses. On the contrary, the safety systems maintain their geometry and are solved without any change in the procedure. The transient behaviour of the two zone volume is calculated by a model similar to that already adopted for the pressurizer.

The control system is modelled by detailing the function of the various controllers, which can be proportional, integrative or derivative. In the present version the main controlled quantities are indicated in Fig. 1 and refer to: pressure and liquid level into pressurizer and steam generators, core fluid temperature, grid load.

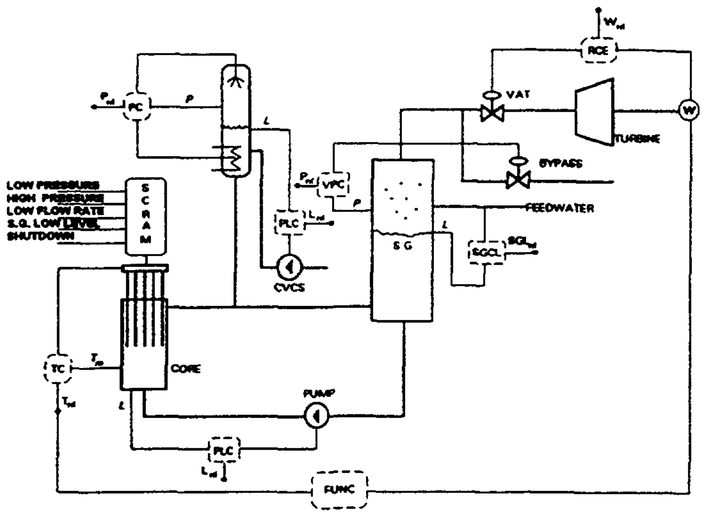

Fig. 1: TRAP-2 set of controls for a standard PWR.

5. TRAP-2 PROGRAM CAPABILITIES

The transient analyses performable by TRAP-2 program are listed in Table II. The modular structure of the implemented model allowed us the generation of different programs for each reactor configuration (AP600, PIUS, MARS, ISIS), with particular attention to the characteristic components of each one.

TABLE II - AVAILABLE ANALYSES IN CURRENT TRAP-2 VERSION.

Accident transients	*Operational transients*	*Stability analysis*
- Station Blackout - Depressurization - Boron Dilution - Steam Line Break - Loss of Feedwater - Steam Generator Tube Rupture - Control Failure (1 control or more) - Small Break LOCA - Loss of Pump supply (1 pump or more)	- Hot and Cold Shutdown - Start-up - Load Following	- Superposition of disturbances on critical plant parameters (different amplitude and frequency)

Both the input data file and the analysis set up file (ASCII format) are easily modifiable by the user so that parametric studies are supported. The output data are in column ASCII format and any graphic program can import and plot the results. A synoptic diagram of the circuits shows the main parameter values during the transient.

TRAP-2 is written in FORTRAN and developed on personal computers under MS-DOS/Windows operative system. The dimension of the executable files is less then 1 Mbyte. The program runs on PC and the transients are usually executed with time steps of about 100 ms; the CPU time required, depending on the type of analysis and the nodalization besides the time step, ranges from almost the real time to one order of magnitude.

6. TRAP-2 VALIDATION

ENEL has started to validate TRAP-2 computer program by means of comparisons with experimental data and a further validation activity is in progress by comparing it with a reference program.

6.1. SPES-2 2" LOCA accident.

An experimental program has been commissioned by Westinghouse in cooperation with ANSALDO, ENEA and ENEL to support the design certification for AP600. SPES-2 is an experimental facility made in SIET with the overall objectives to simulate the AP600 thermalhydraulic behaviour, in particular referring to the passive systems.

The SPES-2 test facility nodalization as simulated by TRAP-2 program is reported in Fig. 2. The circuits are subdivided in 93 components, with a total number of 628 sections (belonging to distributed parameter comps.) plus 14 volumes (belonging to lumped parameter comps.). The simplified nodalization corresponding to the stagnation model is shown in Fig. 3 (460 sections plus 4 volumes).

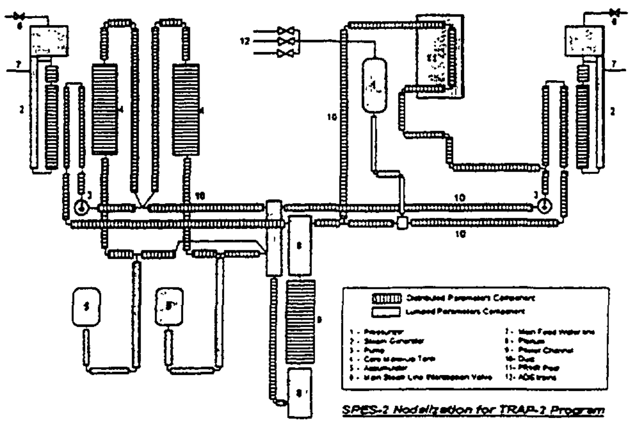

Fig. 2: TRAP-2 nominal nodalization.

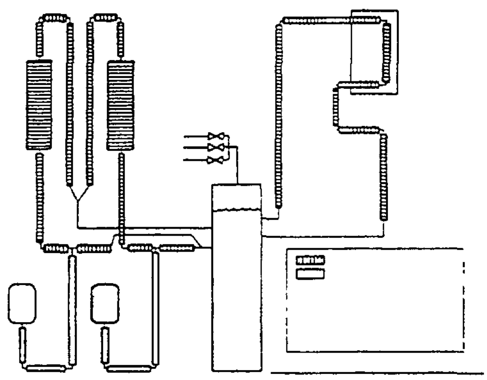

Fig. 3: stagnation model nodalization.

The TRAP-2 program is currently hosted on a PC586/66 MHz and the dimension of the executable file is 960 Kbytes. The CPU time needed in this case ranges from 15 time the real time to about 5 and is obviously dependent on the time step. The time interval used during the accident simulations here reported is 25 ms, shorter than the usual one.

The test of SPES-2 considered for the initial TRAP-2 validation simulates a 2" cold leg break of AP-600; the break is located between the cold leg to CMT balance line and the pressure vessel.

The system, initially at nominal conditions, undergoes a slow depressurization owing to loss of coolant, which is opposed by the pressurizer heaters action as long as the liquid level into the pressurizer is greater then the heaters cut-off threshold. When the system pressure reaches the limit of activation of the reactor trip on low pressure, the signal is sent to the Steam Generators. After 2 s the SG isolation valves are closed. After about 4 s the power channel heaters are reduced at 20% of nominal power and start to follow the SCRAM curve. Since this instant the pressure slows down more rapidly because the SG exchanged power is greater than the residual power given to the fluid from the channel heaters. During a short period this unbalance is reversed and causes a small rise of the pressure, together with the circuit flow rate reduction due to the RCP trip.

The activation of the CMTs and of the PRHR system cools down the primary fluid, so opposing to the pressure rise and maintaining the system pressure practically constant for few minutes.

We resolve to proceed with the TRAP-2 stagnation fluid model after the primary flow rate has reached its natural convection value, sufficiently low to justify a dramatic simplification of the simulation. This passage allows a noticeable computation time reduction without lack of accuracy for the passive safety systems.

The CMTs cooling flow rate increases, due to the entrance of some steam in the rising ducts toward the tanks, and then a slow pressure descent starts. The injection of the accumulator fluid at room temperature begins when the system pressure is under the intervention threshold: this event does not modify the pressure descent because it reduces substantially at the same time the natural convection into the CMT loops. The CMT is described with a distributed parameter duct, and this prevents to calculate the actual water level. Therefore, the first train of ADS valves opens at a fixed time, thus leading to a sensible augmentation of the depressurization trend; the subsequent increase of the accumulators flow rate stops finally the circulation in the CMT loops.

The result of this first level of validation seems satisfactory as far as the system pressure is concerned. However, a more rapid pressure descent in the first part of the simulation in comparison with SPES-2 data leads to an anticipation of the SCRAM signal and of the subsequent activation of CMTs and PRHR loops, while a higher accumulators flow rate causes a steeper decreasing slope after ADS activation. The first type of discrepancy is probably due to an incorrect evaluation of the circuit heat losses for their insufficient knowledge, the second one to an underestimation of the stagnation model in predicting the exact value of the pressure at the connection of the DVI line with the pressure vessel. The LOCA flow rate follows the pressure behaviour and fits quite well the mean value of the experimental data.

Other differences between TRAP-2 prediction and experimental data are referred to the CMT flow rates when the steam-water mixture reaches the inlet of the riser duct of the two loops: TRAP-2 depicts an analogous behaviour for both, i.e. a lower flow rate and a sudden reduction when the accumulators start to inject their own fluid, while SPES-2 data show a delayed flow rate peak of one CMT with respect to the other. Even this is caused by the approximation used by the stagnant model: a lack of simulation of the primary circuit components (cold and hot legs, steam generators, pumps, pressurizer, downcomer), of the consequent circuit asymmetry and of particular flow conditions (stratified and countercurrent flow regimes) give incorrect predictions on pressure and flow distribution.

Finally, the comparison of the PRHR behaviour shows a certain difference in the initial and mean flow rate and in the outlet temperature, probably caused by the absence of heat losses in the connecting pipes (unknown) and by a lower value of the calculated heat transfer coefficient with respect to the real one.

6.2. MARS Steam Line Break accident.

TRAP-2 program has been utilized by ENEA-RIN for a further analysis of the MARS project safety features [7]. The main safety evaluation has been carried out with RELAP5/mod2.5 program and the availability of these results allows us a validation of TRAP-2 with a best-estimate code.

The 600 MWth MARS (Multipurpose Advanced Reactor Inherently Safe) one single loop reactor relies on a totally inherent and passive safety concept. The key issue of residual heat evacuation in case of accident is solved through a completely passive Emergency Core Cooling System (ECCS) which consists of two independent circuits based on natural circulation triggered by passive check valves, which are activated by the primary pump trip. Each train consists of:

- an ECCS Primary Loop directly connected to the pressure vessel at the same pressure as the primary system;
- an ECCS Secondary Loop at the same temperature and pressure as the ECCS Primary Loop;
- a tertiary Pool and Condenser Loop consisting of a water reservoir (Pool) at the ambient temperature and pressure and an air-condenser connected to the pool.

The MARS nodalization as used by TRAP-2 (version /2M especially devoted to MARS system) is sketched in Fig. 4 and is the same utilized by RELAP (91 nodes). The set of transients performed includes Station Blackout, Steam Generator Tube Rupture and Steam Line Break [8].

The TRAP/RELAP validation is still in progress: in this paper we report two graphs as an example, referring to the initial period (400 s on a computed total of 7000 s) of Steam Line Break accident. The first (Fig. 5) relates to the core flow rate, the second (Fig. 6) to the thermal power exchanged between the ECCS Loops: the comparison is really good apart a

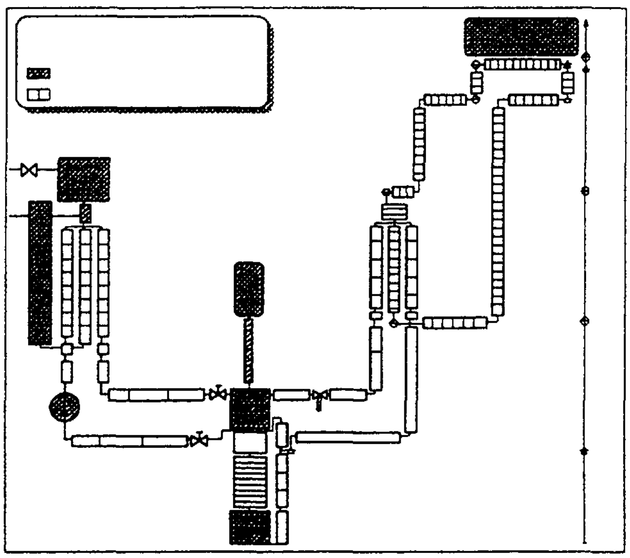

Fig. 4: TRAP-2 nodalization of MARS reactor.

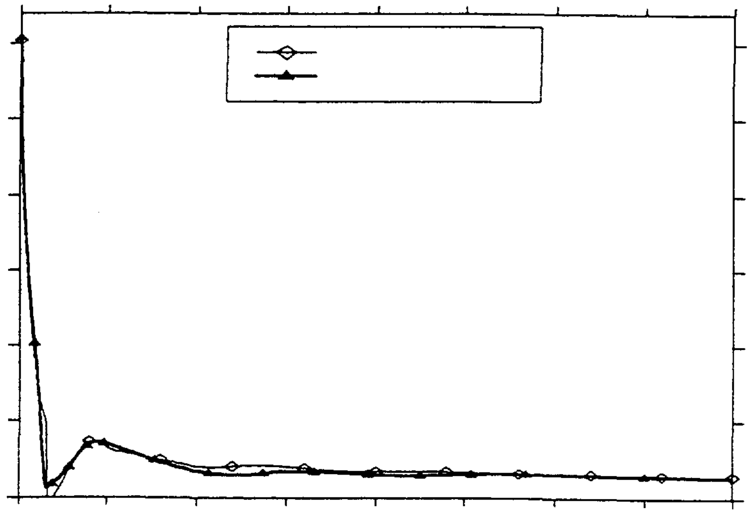

Fig. 5: TRAP/RELAP comparison on MARS SLB accident.

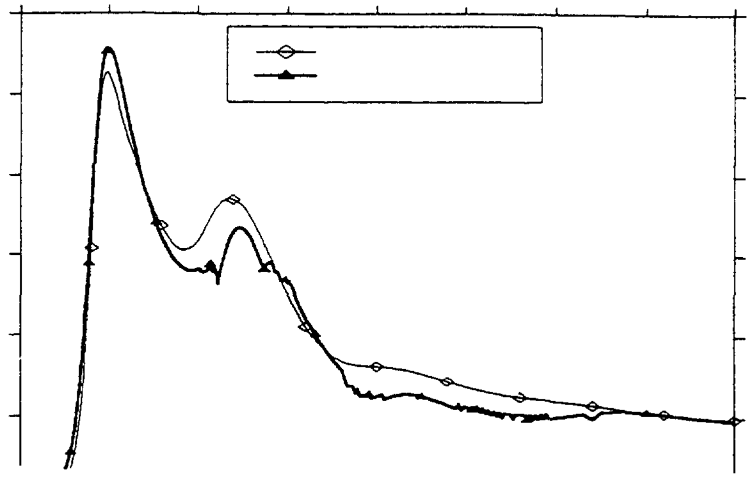

Fig. 6: TRAP/RELAP comparison on MARS SLB accident.

slight discrepancy in the power due to a different evaluation of the heat transfer coefficient in such a low flow condition.

The transients were performed on a PC586/66 MHz with a time step of 100 ms, requiring a CPU time of 1.1 second per simulated second.

7. CONCLUDING REMARKS

A fast running program easily tailored to several reactor systems belonging to PWR concept has been presented.

It showed to be versatile, user-friendly and useful for parametric studies concerning safety and operability. The first validation effort shows its numerical consistence, and a satisfactory agreement with a best-estimate program and experimental tests.

This result allows us to proceed in the validation together with a further refinement of the model, always retaining the initial hypothesis to disregard sound speed effects.

NOMENCLATURE

SYMBOLS		*GREEKS*	
c_p	specific heat at constant pressure	ε	roughness
C_b	boron concentration	μ	dynamic viscosity
D_e	equivalent diameter	ρ	density
f	friction factor	σ	superficial tension
g	gravitational acceleration	Γ	mass flow rate
h	specific enthalpy	ϑ	inclination angle
Nu	Nusselt number	Π_h	heated perimeter
p	pressure	Ω	cross section area
Pr	Prandtl number	*INDEXES*	
q''	superficial heat flux	fg	latent heat of evaporation
Ra	Rayleigh number	l	liquid
Re	Reynolds number	ls	liquid at saturation
t	time	m	mixture
T	temperature	w	wall
z	spatial abscissa	v	vapour

REFERENCES

[1] BABALA, D., HANNERZ, K., Pressurized water reactor inherent core protection by primary system thermohydraulics, Nucl.Sci. & Eng. **90** (1985) 400-410.

[2] CAIRA, M., CUMO, M., NAVIGLIO, A., "Energy security: alternatives to Oil", MARS nuclear plant: an Italian proposal for an 'inherent safety' nuclear reactor, US DOE and Italian MICA meeting, Argonne, Illinois, USA (1988).

[3] CINOTTI, L., DAFANO, D., Contributi italiani al nucleare di 2° generazione: il sistema ISIS, Energia Nucleare **1** (1990) 48-58.

[4] RICOTTI, M., TRAP: modello per analisi di sicurezza e operabilità di PWR convenzionali e di nuova concezione, applicazioni e approccio neurale alternativo, PhD Thesis, Polytechnic of Milan, Milan (1993).

[5] RIGAMONTI, M., SPES-2: the full height full pressure Italian test facility simulating AP600 plant, main results from the experimental campaign, these Proceedings.

[6] CHAO, Y., ATTARD, A., A resolution of the stiffness problem of reactor kinetics, Nucl.Sci. & Eng. **90** (1985) 40-46.

[7] ENEA-Nuclear Energy Division, MARS project: Safety Evaluation Report of MARS Reactor (RVS), MT.GLM.15 (1994).

[8] VETTRAINO, F., RICOTTI, M., SORDI, R., "ICONE-3 International conference on nuclear engineering", Dynamic response of MARS reactor under design basis accident conditions, Kyoto, Japan (1995).

HEAT AND MASS TRANSFER PHENOMENA IN INNOVATIVE LIGHT WATER REACTORS

W. AMBROSINI, F. ORIOLO
Università degli Studi di Pisa,
Dipartamento di Costruzioni Meccaniche
e Nucleari, Pisa

G. FRUTTUOSO, A. MANFREDINI
THEMAS s.r.l., Pisa

F. PAROZZI, M. VALISI
ENEL-ATN, Milan

Italy

Abstract

The paper describes the work performed in the development and the application of models for predicting heat and mass transfer phenomena relevant in innovative LWRs. Film condensation and falling film evaporation are addressed comparing model predictions with separate effect experimental data. Development of models for non-equilibrium code application is also discussed.

1. INTRODUCTION

Heat and mass transfer phenomena play an important role in innovative light water reactors, being at the basis of some passive safety features designed to mitigate postulated accident consequences.

Passive containment cooling, in particular, is one of the key issues in innovative reactors that has contributed to the new interest for these phenomena in the nuclear field. In fact, some passive reactor containments are conceived to allow for decay heat removal by means of a combination of condensation onto a inner heat transfer surface and convection-radiation or convection-evaporation on the outer surface. AP600 [1] and SBWR [2] plant concepts are relevant examples of this strategy of containment cooling, asking for a better understanding of heat and mass transfer phenomena.

In consideration of the requirement to maintain these plants in safe conditions for a very long period (three days or even more) after a postulated accident, with no operator action or external intervention, the need is felt for an improved knowledge of the involved phenomenology, in order to achieve models capable to predict the behaviour of reactor plants during such long lasting transients with a reasonable accuracy.

As a consequence, the enlargement of the available data base on evaporation and condensation in the presence of noncondensable gases has been the target of experimental investigations carried out by different organizations (see e.g., refs. [3], [4], [5], [6] and [7]). These studies involve both separate effect and integral test facilities and are aimed at achieving a better knowledge of the capabilities of passive cooling systems.

On the basis of these new data, models available in the literature can be reconsidered and assessed to ascertain their capabilities in providing quantitative estimates of the related heat and mass transfer rates. Both heat transfer and fluiddynamic aspects are involved in this respect, the greatest interest being on falling film evaporation and filmwise condensation. Moreover, the way to account for the presence of noncondensable gases in the prediction of heat and mass transfer rates in other conditions, as pool evaporation or condensation, requires an improvement with respect to previously adopted models.

It must be also emphasized that besides the interest that heat and mass transfer phenomena have for passive reactor concepts, they are relevant also for present commercial nuclear power plants in many operating situations. In particular, during some beyond-DBA conditions, a degraded performance of the active safeguards can make passive heat removal mechanisms to turn out as the ultimate possibility for mitigating accident consequences.

In the present work problems related to heat and mass transfer in innovative reactors and in code applications are reviewed collecting material partly produced in the frame of a cooperation between the University of Pisa, ENEL and THEMAS s.r.l., partly developed independently by the University. The common feature connecting the presented applications is the adoption of the heat and mass transfer analogy for predicting evaporation or condensation in conditions of interest for light water reactors.

In the following, after short notes about the treatment of heat and mass transfer phenomena in the mentioned analogy, evaporation of falling water film, filmwise condensation and general thermal non-equilibrium modelling problems will be discussed.

2. PHYSICAL BASIS OF THE MODELS

2.1 Modelling Heat and Mass Transfer Phenomena

Whenever at an interface between two phases of a multicomponent mixture evaporation or condensation occur, the mass transfer is accompanied by a simultaneous heat transfer. This characteristic makes heat and mass transfer processes very peculiar in the class of phenomena governed by diffusion of chemical species.

A simple energy balance (or jump condition) at the immaterial surface separating the phases (interface) is used to put a relation between the heat flux and the specific evaporation-condensation rate (cfr. e.g., [8])

$$\sum_{k=1}^{2}\left(q''_{k.int} + G_{k.int}\, h_{k.int}\right) = 0 \tag{1}$$

This equation, together with the mass jump condition

$$\sum_{k=1}^{2} G_{k.int} = 0 \tag{2}$$

puts a relation between the heat exchanged by convection between each phase and the interface and the related mass transfer, stating that no mass transfer can occur without a corresponding heat transfer.

In the presence of noncondensables in the gaseous phase the evaporation-condensation rate depends on the resistance within the boundary layer located at the interface, in which the major changes in the concentration of the components occur. In this narrow region close to the interface, the multi-D continuity equations can be combined with the Fick's law of diffusion, to give the overall mass conservation equations. For a two-component mixture made of vapour and a noncondensable gas these equations are

$$\frac{\partial \rho_v}{\partial t} + \vec{\nabla}\cdot(\rho_v \vec{w}) = \mathcal{D}_{vn}\nabla^2\rho_v \tag{3}$$

$$\frac{\partial \rho_n}{\partial t} + \vec{\nabla}\cdot(\rho_n \vec{w}) = \mathcal{D}_{vn}\nabla^2\rho_n \tag{4}$$

Restricting to one-dimensional steady processes in the proximity of a plane interface permeable only to the vapour and orthogonal to the y Cartesian coordinate and assuming perfect gas behaviour for the two components and constant pressure, some well known results can be easily obtained from the above equations (cfr. e.g., [9], [10]):

- whenever vapour diffusion occurs from or toward the interface, an advection fluid velocity is generated, given by the relationship

$$w = \frac{\mathcal{D}_{vn}}{\rho_n}\frac{\partial \rho_n}{\partial y} \tag{5}$$

which is the result of the condition that the noncondensable gas has zero net flow across the interface;

- because of the superposition of diffusion and transport, given the partial pressures of the vapour in the bulk fluid and at the interface, the specific mass transfer rate has a logarithmic form

$$G_{v.int} = \frac{\mathcal{D}_{vn}}{\delta_m}\left(\rho_v + \frac{\mathcal{M}_v}{\mathcal{M}_n}\rho_n\right)\ln\left(\frac{p - p_v}{p - p_{v.int}}\right) \tag{6}$$

- assuming that the partial pressure of the vapour at the interface, where phase change occurs, is equal to the saturation pressure at the local temperature, the mass transfer rate is finally linked to liquid phase conditions.

In the above equation (6), the thickness of the boundary layer is needed to calculate the mass transfer rate. To this purpose it is noted that in two dimensions equation (3) for an incompressible fluid can be written as

$$\frac{\partial \rho_v}{\partial t} + w_x\frac{\partial \rho_v}{\partial x} + w_y\frac{\partial \rho_v}{\partial y} = \mathcal{D}_{vn}\left(\frac{\partial^2 \rho_v}{\partial x^2} + \frac{\partial^2 \rho_v}{\partial y^2}\right) \tag{7}$$

By comparing this equation with the energy equation for a fluid with negligible frictional heating

$$\frac{\partial T_g}{\partial t} + w_x\frac{\partial T_g}{\partial x} + w_y\frac{\partial T_g}{\partial y} = \alpha_g\left(\frac{\partial^2 T_g}{\partial x^2} + \frac{\partial^2 T_g}{\partial y^2}\right) \tag{8}$$

the well known analogy between heat and mass transfer is established, allowing to relate the boundary layers for heat and mass transfer.

For our purposes, this analogy puts a correspondence between the dimensionless groups adopted in the semi-empirical correlations to be used for heat and mass transfer (cfr. [11]):

$$Nu_g = \frac{H_{conv}L}{k_g} \quad\leftrightarrow\quad Sh = \frac{K_m L}{\mathcal{D}_{vn}} \tag{9}$$

$$Pr_g = \frac{\nu_g}{\alpha_g} \quad\leftrightarrow\quad Sc_g = \frac{\nu_g}{\mathcal{D}_{vn}} \tag{10}$$

As a result, assuming a dependence of heat transfer coefficient on $Pr^{0.33}$, the following formulation is obtained for the mass transfer constant [12]

$$K_m = \frac{\mathcal{D}_{vn}}{\delta_m} = \frac{H_{conv}}{\rho_g C_{pg}}\left(\frac{Pr_g}{Sc_g}\right)^{\frac{2}{3}} \tag{11}$$

Finally, since the interfacial heat fluxes in equation (1) can be expressed as a function of the interfacial temperature, the energy jump condition resulting after substitution of (6) can be taken as an implicit definition of this variable [13], [14]

$$\sum_{k=1}^{2} q''_{k.int}(T_{int}) + K_m \lambda \tilde{\rho}_v \ln\left(\frac{p - p_v}{p - p_{sat}(T_{int})}\right) = 0 \quad (12)$$

where the phasic interfacial heat fluxes are evaluated using appropriate heat transfer coefficients.

Due to the nonlinearity of the diffusive expression of mass transfer rate, iterative techniques are needed to solve the above equation, unless lower level approximations with, eventually, correction factors [15] are retained sufficient for particular purposes.

2.2 Modelling Falling Film Phenomena

When a liquid film falls down an inclined surface, a velocity field is established within its thickness which depends on fluid properties, flow rate per unit perimeter and boundary conditions. The liquid film Reynolds number, defined as

$$Re_{lf} = \frac{4\,\Gamma}{\mu} \quad (13)$$

is generally used for discriminating between the possible flow regimes. In particular [see e.g., 11]:

- for $Re_{lf} < 30$, a laminar film with a smooth interface is generally reported;
- for $30 < Re_{lf} < 1800$, superficial waves are observed although the film is still laminar;
- for $Re_{lf} > 1800$ the falling film is completely turbulent.

The Nusselt theory [16] can be adopted for evaluating the thickness of laminar-smooth falling liquid films. In the presence of interfacial shear, the relation between the film thickness and the flow rate per unit perimeter is the following:

$$\Gamma = \frac{g \cos\theta\, \rho_l (\rho_l - \rho_g)\, m^3}{3\, \mu_l} + \frac{\rho_l\, m^2\, \tau_i}{2\, \mu_l} \quad (14)$$

Depending on the value of the interfacial shear stress, τ_i, various flow regimes may be identified, ranging from complete downflow, to reverse flow (flooding) conditions.

A more compact way to express the same result is the following

$$m_l^+ = \frac{\sqrt{2}}{2} Re_{lf}^{0.5} \quad (15)$$

where

$$m_l^+ = \frac{m\, w^*}{\nu_l} \quad (16)$$

and

$$w^* = \sqrt{\frac{\tau_c}{\rho_l}} \qquad \tau_c = \frac{2}{3}\tau_w + \frac{1}{3}\tau_i \quad (17)$$

having the form of relations often adopted for annular flow in pipes (see e.g., [17]).

The above formulations hold for a steady and smooth laminar film in the absence of mass transfer. In the case of evaporation or condensation, it is assumed that the effect of mass transfer on the velocity field inside the film is negligible. Moreover, the relationship between the constant film thickness and flow rate obtained in the absence of mass transfer are used to represent the relation between the local values of the same variables when mass transfer occurs.

Under these assumptions, the change along the surface in the film flow rate due to mass transfer is given by:

$$\frac{d\Gamma}{dz} = - G_{v.int} \quad (18)$$

In the classical treatment of the condensation of a pure vapour by Nusselt, the above equation, together with (14) (in which the shear stress is neglected) is used to obtain a relationship for the derivative of the film thickness

$$m^3 \frac{dm}{dz} = \frac{\mu_l\, k_l\, (T_{sat} - T_w)}{\rho_l\, (\rho_l - \rho_v)\, g\, \lambda} \quad (19)$$

adopted to calculate the film thickness at the bottom end of the surface. On the basis of equation (18) a more complicated expression is reached in the present work accounting for the presence of noncondensable gases (see Sect. 5).

The value of the film thickness is needed to determine the thermal resistance between the interface and the wall. In the classical Nusselt theory, the equivalent conductance of the liquid film is due only to heat conduction

$$H_{lf} = \frac{k_l}{m} \quad (20)$$

When the effective heat transfer coefficient between the bulk fluid and the wall owing to the combined effect of convection and mass transfer must be derived, the averaged values of film thickness and interfacial and wall temperatures are used to give:

$$H_{eff} = H_{lf} \frac{T_{int} - T_w}{T_g - T_w} \quad (21)$$

It is reported that the application of the Nusselt theory leads to underestimate the effective heat transfer coefficients. The reason is that both waviness and turbulence actually reduce the equivalent thickness to be considered in equation (20) and contribute to reduce the diffusion boundary layer.

The stability of the falling film has been an interesting subject of research since the pioneering work by Kapitsa [18]. In particular, theoretical and experimental evidence has been reported supporting the following conclusions:

- a liquid film falling down a vertical plate is unstable at all the Reynolds numbers, i.e. superficial waviness is always present; surface inclination has a stabilizing effect [19];
- condensation tends to stabilize the liquid film, while evaporation has the opposite effect (see e.g. [20]);
- the structure of waviness is rather chaotic and at sufficiently high Reynolds number consists of large *roll waves* riding over a thin smooth substrate (see e.g., [21], [22]).

The effect of turbulence and waviness on heat transfer is not specifically addressed in the models described hereafter and will be matter of further studies. Anyway, in the presence of noncondensable gases these effects are often second order ones.

3. FALLING FILM EVAPORATION

3.1 Experimental set up

A facility has been built at the University of Pisa to investigate the evaporation of falling water films in conditions typical of the AP600 Passive Containment Cooling System.

As known, the containment system of this innovative reactor consists of a steel safety envelope located inside a concrete building (Figure 1) in which natural circulation flow paths exist for the external air in order to cool down the steel surface by convection and radiation after a postulated accident. Water tanks are also provided for spraying water on the outer steel surface, thus enhancing removal of decay heat by falling film evaporation.

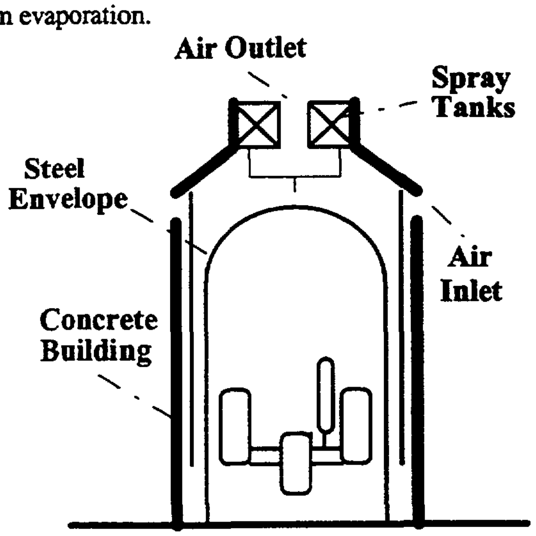

Figure 1 - Sketch of AP600 Containment System

The experimental facility (Figure 2), designed considering the conditions occurring during loss of coolant accident scenarios [23]. consists of a AISI 304 L flat plate (2 x 0.6 x 0.022 m.). supported by a metallic frame. The surface underwent a preparation by sandblasting and by a spray painting of about 0.3 mm of metallic zinc, in order to make uniform the thermal emissivity of the wall and to reproduce the mean surface characteristics of the containment shell of AP-600.

The supporting frame allows for a rotation of the plate up to 90 degrees with respect to the vertical axis, so that the behaviour of liquid films can be analyzed using different inclinations of the surface; situations occurring in the elliptical containment dome can be so reproduced. To simulate the heating of the containment wall that would occur in an actual plant following a postulated accident, the test plate is heated from the back using 100 modular electric heaters (195 x 95 mm.), subdivided into three different electrically

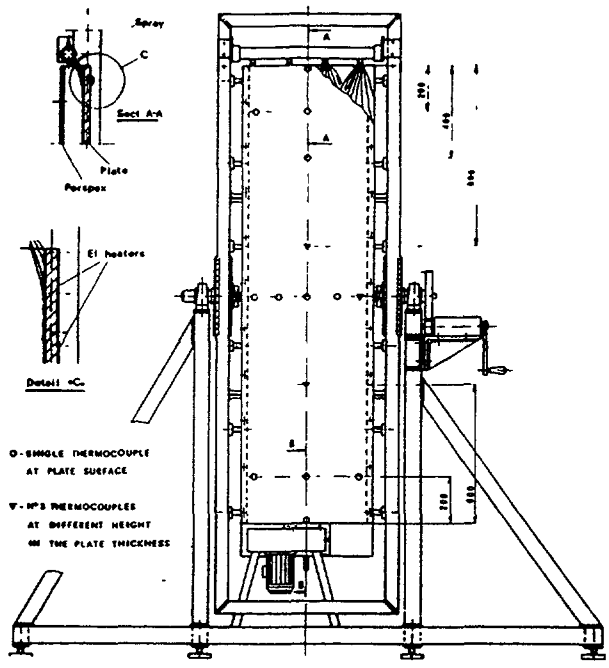

Figure 2 - Facility for film evaporation tests

equilibrated groups. The total heating capacity installed is approximately 36 kW and is supplied by three PID regulated electric generators with a maximum voltage difference of about 50 $V_{a.c.}$. The electric power supplied to the heating resistances is measured with an on-line electronic wattmeter.

A Plexiglas baffle plate, located at a distance of 10 cm from the plate, faces the surface along which the liquid film flows. Air from an axial fan flows up through the duct: the fan has a variable speed motor drive that allows varying air speed from 0.5 to 10 m/s.

Cooling water is preheated with electric resistances up to a selected temperature and is supplied at a prescribed rate to some interchangeable sprays nozzles. The spray system is provided with a centrifugal pump; the cooling water flow rate can be regulated with a by-pass flow path with related valves. The measurements of the following thermofluid-dynamic variables can be performed in the apparatus:

- inlet and outlet liquid film temperatures:
- temperatures within the plate thickness;
- film thickness;
- water and air flows;
- electrical power supplied to the system;
- average temperature and humidity of air flow.

All the measurements of test parameters are recorded and processed on a personal computer.

3.2 Correlation of first results

During the last year, the facility was subjected to a complete revision, comprising the displacement of the structure in a more convenient location and acquisition of new instrumentation. Therefore, the results here presented are those obtained in a previous shakedown campaign [24].

Three series of tests have been run during the shakedown of the facility:

1. tests for characterizing the plate from the point of view of temperature distribution and heat losses;
2. tests for evaluating the heat transfer capabilities in dry conditions (no water film);
3. tests for evaluating the heat transfer capabilities in wet conditions (with water film).

During the first series, the needed information on the plate behaviour during heating was achieved; the heat losses were also estimated for further use in data processing.

The data collected in the second series of tests should represent containment cooling by natural circulation of air between the baffle and the steel envelope. A good agreement could be obtained between data and a semi-empirical correlation for heat transfer in a short duct ($2 < L/D_h < 20$) [9]:

$$Nu / Pr^{0.33} = 0.023 \left[1 + (D_h/L)^{0.7} \right] Re^{0.8} \quad (22)$$

For low Reynolds numbers, anyway, the convective heat transfer for the dry plate surface appeared to be conservatively underpredicted by the correlation.

The series of data with falling water film was correlated making use of the heat and mass transfer analogy. Adopting Eq. (22) for heat transfer in dry conditions, the corresponding relation for mass transfer is:

$$Sh / Sc^{0.33} = 0.023 \left[1 + (D_h/L)^{0.7} \right] Re^{0.8} \quad (23)$$

The experimental value of the Sherwood number is calculated on the basis of the observed evaporation mass velocity, G_v.

In turn, G_v should be determined on the basis of the experimental values of injected and collected water during each test. Since the measurement chains for measuring the injected and collected mass flow rates were not yet qualified, an energy balance was adopted to infer the evaporation rate on the basis of the power supplied to the plate and of the measured film internal energy variation from inlet to outlet.

Thus, two different estimates of the evaporation rate were obtained:

- a *maximum value*, calculated assuming that the difference between the power fed to the plate and the variation of the liquid film sensible heat represents the evaporation power;
- *a Best Estimate (BE) value*, obtained taking into account theoretical predictions of the heat losses and of the power exchanged by convection from the film surface to the external air.

The values of both maximum and best estimate values of the dimensionless group $Sh/Sc^{0.33}$ have been reported in Figure 3 . It can be noted that:

- maximum and best estimate data appear very close to each other, confirming the adequacy of the adopted approach to infer evaporation data;
- BE data are well represented by the relationship reported in Eq. (23) for short tubes, although in agreement with a similar research by Westinghouse [25] an overall underprediction seems to be obtained by the theoretical estimates.

As the above described results demonstrated the reliability of the heat and mass transfer analogy for describing evaporation phenomena, this approach was taken as a basis for setting up a more complete model obtained reviewing and improving relationships previously developed for the FUMO code [26]. In this model, the laminar-smooth film relationships (see Sect. 2) have been adopted for calculating the film thickness and an estimate of the film temperature evolution along the plate is obtained with the following energy balance equation

$$C_{pl} \Gamma \frac{\partial T}{\partial z} = q''_w - q''_{conv} - G_v \left(h_{v,sat} - h_l \right) \quad (24)$$

where the evaporation rate is evaluated according to Eq. (6). The following formulation is adopted for temperature profile in the film thickness.

$$T(y,z) = C_0(z) + C_1(z)\, y + C_2(z)\, y^2 \quad (25)$$

where the functions C_0, C_1 and C_2 can be found on the basis of the boundary conditions and of an integral form of the energy balance equation (24).

These relationships are then solved in axial meshes in which the plate has been subdivided, adopting an iterative technique for estimating the interfacial temperature. Despite of the simplicity of the models adopted for film fluiddynamics, a good performance in predicting the evaporation rate in the first performed tests has been obtained (Figure 4).

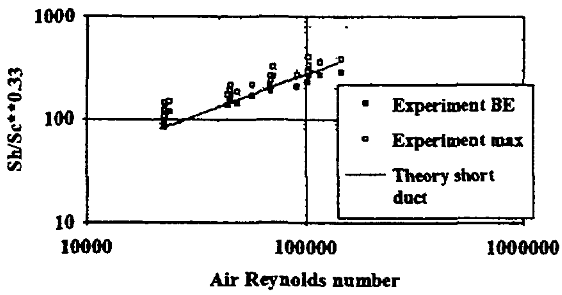

Figure 3 - Correlation of first data for wet tests

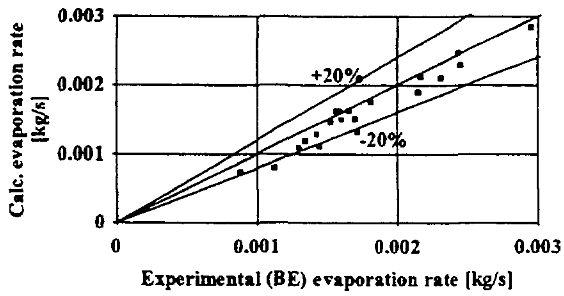

Figure 4 - Calculated vs. experimental evaporation rates

4. FILM CONDENSATION

4.1 Considered experimental data

The SBWR reactor is equipped with a passive containment cooling system capable to remove decay heat after postulated accidents [2].

In particular, two different systems are introduced to accomplish with this function:

- the isolation condenser system (IC);
- the passive containment cooling system (PCC).

The first one consists of a loop connected with the reactor pressure vessel containing a condenser submerged in an external water pool; it is intended to allow for reactor depressurization by directly condensing the vapour produced in the core. On the other hand, the PCC circuit is connected to the dry-well atmosphere and contains a separate condenser, also submerged in an external pool.

Although the function of the two systems is nearly the same, their ranges of application and the operating conditions are different. In particular, the IC performs decay heat removal by condensing pure vapour at high pressure conditions, while the PCC system has to cope with the problem of noncondensable gases present in the containment atmosphere and operates at far lower pressures.

Both systems have been the subject of interesting experimental researches aimed at providing data on the SBWR plant accident behaviour during their operation (see e.g. [4], [5], [6] and [7]). In particular, the data provided by the PANTHERS experimental program [6] are used in the present paper for validating models for the prediction of heat and mass transfer in filmwise condensation conditions.

The program is part of a more general experimental effort including also downscaled tests for the study of blowdown (GIST) and PCCS performance (GIRAFFE and PANDA) [27], [28]. In this frame, PANTHERS tests supply information on full-scale behaviour, making use of prototypical condensers for both IC and PCCS.

Notwithstanding the wide knowledge existing in the nuclear field about condensers, the full-scale experimental investigation is justified by the peculiarities of the design of IC and PCCS. In particular, in the case of PCC the most challenging modelling aspect is the operation of the condenser with considerable fractions of noncondensable gases. The main objective of the tests is to confirm the adequacy of the design of both apparatuses in meeting the requirements for use in SBWR.

Figure 5 shows a sketch of the PCCS configuration of the PANTHERS facility installed at SIET in Piacenza. It consists of the following main parts:

- the PCCS two-module unit submerged in a pool tank;
- piping for injecting vapour or vapour-air mixtures at prescribed conditions of flow rate, pressure and temperature;
- a condensate tank in which liquid from the condenser is drained; during tests pressure in this tank is maintained equal to the pressure of the inlet mixture;
- a vent tank, maintained at a pressure lower than the inlet mixture, to which noncondensable gases from the condenser outlet are purged;
- a water make-up system to restore the required level in the condenser pool.

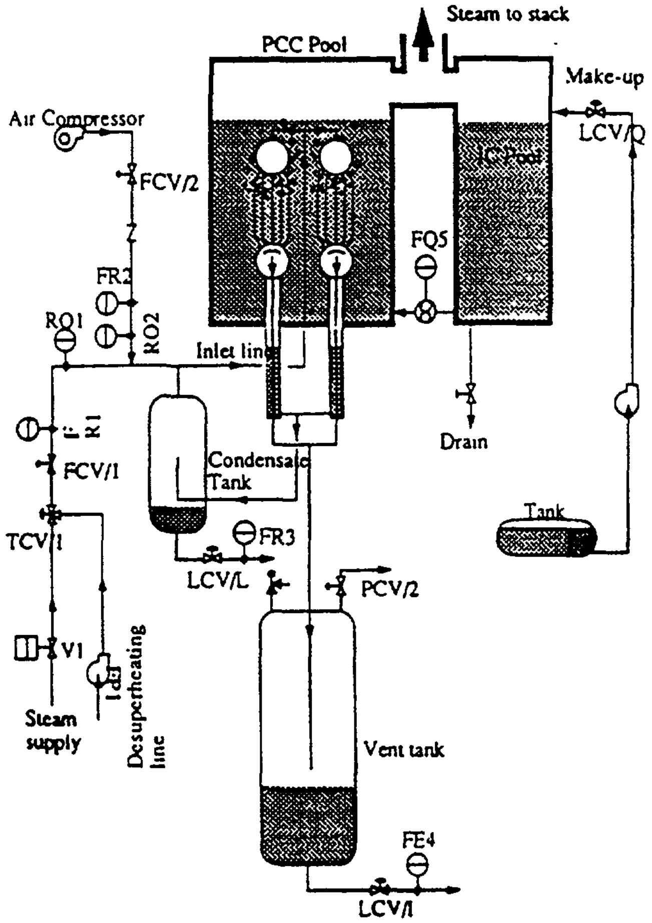

Figure 5 - Sketch of the PANTHERS Facility in the PCCS configuration [from Ref. 6]

The loop elevations are the same as in SBWR; in particular, the position of the pool levels and of the loop seal in the drain line have been kept as in the reactor.

The required power to feed vapour in the test rig is supplied by a nearby power station. A maximum of 6.0 kg/s of steam at 17 MPa and 540 °C can be obtained.

The tests considered in the present work are related to PCCS performance. They have been carried out by injecting known flow rates of vapour and air into the prototype condenser and measuring the corresponding condensate flow rate in steady-state conditions.

To quantify the effect of the noncondensable gas on the capability to suppress steam, a condensation efficiency is defined by the relationship [6]

$$\text{Efficiency} = \frac{\text{Condensate Flow Rate}}{\text{Inlet Steam Flow Rate}} \tag{26}$$

which is one of the most interesting data to be predicted by models.

4.2 Model characteristics and performance

In consideration of the ongoing experimental program, a cooperation started between ENEL, THEMAS s.r.l. and University of Pisa to set up and qualify a component model for IC and PCCS. The objective of the activity was to acquire experience in the simulation of condensation phenomena in the presence of noncondensable gases in order to set up models for long term analysis of the accident behaviour of SBWR.

The ICONA (Isolation CONdenser Analysis) program was then conceived as a numerical component model to be validated as a stand-alone module. The main characteristics of the code are the following:

- mixture balance equations for mass and energy are solved in control volumes;
- allowance for an arbitrary number of noncondensable gases is made;
- thermal equilibrium between liquid, vapour and gases is considered;
- control volumes are connected by junctions through which homogeneous flow is assumed;
- allowance is made for countercurrent flow conditions at junctions;
- a full range heat transfer package is adopted and a cubic coarse-mesh algorithm is used for treating heat conduction in plane, cylindrical and spherical structures;
- phase separation in volumes is allowed to simulate water pools;
- a semi-implicit numerical method is adopted to solve balance equations.

Filmwise condensation is dealt with in the code by the heat and mass transfer analogy. A steady-state energy balance equation is written for the film assuming the form

$$H_{lf}\left(T_{int}^{w}-T_{w}\right) \qquad (27)$$

$$= H_{g}\left(T_{g}-T_{int}^{w}\right) + K_{m}\,\lambda\,\tilde{\rho}_{v}\ln\left(\frac{p-p_{sat}(T_{int})}{p-p_{v}}\right)$$

which expresses that the heat flux transferred by the liquid film to the wall is equal to the summation of the two contributions due to convection and condensation [13]. This is equivalent to assuming no variation in the sensible heat of the liquid film along the structure.

The convective heat transfer coefficients are evaluated according to classical single phase convection relationships. The difference between the gas and the film velocity is taken into account for calculating the gas Reynolds number entering the heat transfer correlations.

The film thickness is evaluated in each hydraulic mesh in consideration of the calculated liquid film flow rate by the Nusselt theory, with allowance for interfacial shear (equation 14).

Equation (27) is then solved iteratively for the interfacial temperature. Then, an overall condensation heat transfer coefficient is evaluated by the relationship

$$H_{cond} = H_{lf}\frac{T_{int}-T_{w}}{T_{g}-T_{w}} \qquad (28)$$

This heat transfer coefficient is finally used to define the convective boundary conditions of the condenser structures.

In the simulation of the considered PCCS tests, the ICONA code has been used with six axial nodes to represent the condenser pipes and two nodes for the steam and water boxes. The external pool, the condensate drainage line and the external tanks have been also represented.

The performance of the code has been evaluated comparing the calculated condensation efficiency with the experimental values. Figure 6 reports the results obtained in this comparison for the available data points. The agreement between the calculated and the experimental efficiency is remarkable, also considering the limitations of the adopted numerical frame and the simplicity of the nodalization.

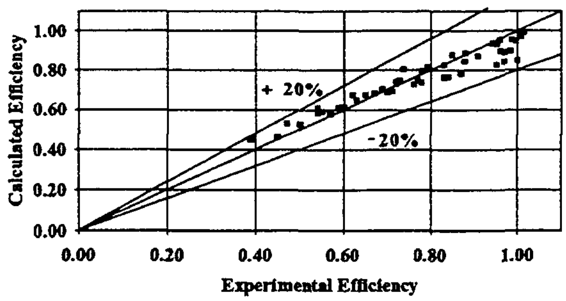

Figure 6 - Overall model performance for PCCS tests

Figure 7 and Figure 8 report the same information in the form of the ratio between the calculated and the experimental efficiencies as a function of test pressure and air molar fraction. Some clear trends can be noted:

- the efficiency tends to be slightly overestimated at low pressure and underestimated at high pressure;
- the spread around unity is increasing with increasing air fractions.

The first observation reflects the tendency of the model to slightly underestimate the slope of the efficiency curve as a function of pressure. The second is partly due to the fact that with a higher noncondensable fraction a lower efficiency is generally obtained, thus enhancing the relative error of the calculation.

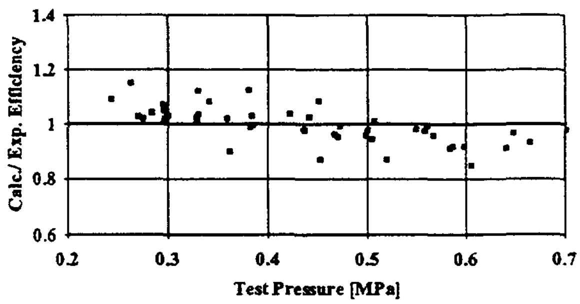

Figure 7 - Model performance versus test pressure

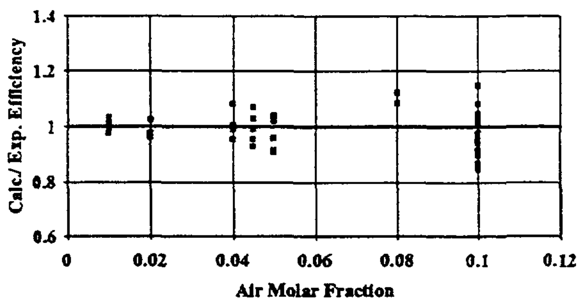

Figure 8 - Model performance versus air molar fraction

The above results must also be considered taking into account that the experimental data are preliminary. More decisive conclusions will be obtained on the basis of the final data release.

5. NON-EQUILIBRIUM CODE APPLICATIONS

It is well known that the treatment of heat and mass transfer is of particular concern in codes for the thermal-hydraulic analysis of nuclear power plants when thermal non-equilibrium is adopted. In fact, with respect to the older equilibrium models, the separate mass and energy balance equations require the explicit definition of terms for mass and heat transfer between the phases.

In the presence of noncondensable gases, the evaluation of evaporation and condensation can be performed by means of diffusion approaches as those outlined in the previous sections. In the thermal-hydraulic module of the aerosol transport code ECART [29] this approach has been used to treat pool interfacial heat and mass transfer and wall condensation.

ECART (ENEL Code for Analysis of Radionuclide Transport) [30] is based on a mechanistic approach to vapour and aerosol phenomenology and is aimed at unifying reactor coolant and containment system analysis, representing the current state-of-the-art of LWR severe accident aerosol codes. The code has been developed by ENEL with the support of Synthesis, Themas, University of Pisa, and Politecnico of Milano. Most of model development and validation actions related to this computer code were partially sponsored by the European Commission in the frame of safety research programs since 1989. Through an agreement between ENEL and EdF and joint research actions on LWR severe accident studies, EdF started a significant financial and technical contribution to the development and validation of ECART, that became of ENEL and EdF common property.

ECART mainly consists of three phenomenological sections: one for vapour and aerosol phenomena, one for the chemistry, and one section dedicated to thermal-hydraulics. The latter has been recently developed in order to be directly coupled with the other two sections and to supply them with the boundary conditions required for a realistic evaluation of the physical phenomena, with reference to a steam-water-noncondensable gas mixture, in conditions that are expected during radionuclide release and transport.

The main characteristics of the thermal-hydraulic module are summarized as follows:

- the model makes use of separate balance equations for mass and energy in the liquid pool and in the gas atmosphere;
- thermal equilibrium is assumed within the pool and the atmosphere;
- up to nine noncondensable gases can be modelled, chosen among the most important ones for severe accidents and source term experiments;
- control volumes are connected by junctions through which homogeneous flow is assumed;
- allowance for countercurrent flow at junctions is made by proper correlations; models for critical flow are also included;
- a full range heat transfer package is adopted and a cubic coarse-mesh algorithm is used for treating heat conduction in plane, cylindrical and spherical structures;
- phase separation in volumes is allowed to simulate water pools with the related scrubbing effects;
- a semi-implicit numerical method is adopted to solve balance equations.

The interfacial heat and mass transfer terms appearing in balance equations are calculated combining approaches adopted in the FUMO containment code [31] with an updated treatment of interfaces. At present, interfaces are considered at the two locations of the pool surface and of the condensate film on heat structures facing the atmosphere.

In the former case, due to the presence of noncondensable gases, the interfacial temperature is determined making use of a linearized diffusive approach included in the energy jump condition across the pool surface:

$$H^{ps}_{l.int}(T_l - T^{ps}_{int}) = H^{ps}_{g.int}(T^{ps}_{int} - T_g) + H^{ps}_{pv.int}(T^{ps}_{int} - T_{sat}(p_v)) \tag{29}$$

where

$$H^{ps}_{pv.int} = \frac{\lambda}{p - p_v} K_m \left[\rho_v + \frac{\mathcal{M}_v}{\mathcal{M}_n}\rho_n\right]\frac{dp_{sat}}{dT} \tag{30}$$

and $H^{ps}_{l.int}$ and $H^{ps}_{g.int}$ are convective heat transfer coefficients calculated assuming natural convection on a flat horizontal plate.

The last term at the R.H.S. of Eq. (29) represents the heat flux corresponding to mass transfer

$$q''_{v.int} = H^{ps}_{pv.int}(T^{ps}_{int} - T_{sat}(p_v)) \tag{31}$$

defined as positive for evaporation and negative for condensation. An intuitive criterion to establish the conditions for evaporation and condensation as a function of the vapour partial pressure in the bulk atmosphere is readily obtained from the above equation.

A similar approach is adopted in the case of steady condensation on vertical walls, using the Nusselt theory for film dynamics and considering the effect of noncondensable gases. The balance equation required to calculate the evaporation rate involves now the wall temperature

$$\frac{k_l}{m}(T_w - T^w_{int}) = H^w_{g.int}(T^w_{int} - T_g) + H^w_{pv.int}(T^w_{int} - T_{sat}(p_v)) \tag{32}$$

where $H^w_{pv.int}$ is evaluated from a formulation similar to Eq. (30). As the condensation rate depends on the film thickness in a more complicate way than in the case of condensation of pure vapour, the use of Eq. (18) leads to a more complicate relation for film thickness derivative than expressed by Eq. (19)

$$m^2\frac{dm}{dz} = a\frac{b + c\,m}{d + e\,m} \tag{33}$$

where m is the film thickness and a, b, c, d and e are constants depending on fluid properties and heat exchange conditions. A double analytical integration of Eq. (33) over the whole length of the cooling surface allows the evaluation of the total condensation rate and of the average values of film thickness and heat transfer coefficient.

The above relationships need a thorough qualification on the basis of separate effect experimental data to be assessed. A preliminary verification of their adequacy was obtained in the first shakedown tests of the code in which a pressurization transient in the Caroline Virginia Tube Reactor (CVTR) containment simulator was analyzed [32].

Figures 9, 10 and 11 report the results obtained by the stand alone version of the code. Although they must be considered preliminary, it can be noted an overall agreement which depends critically on the formulations adopted for heat and mass transfer.

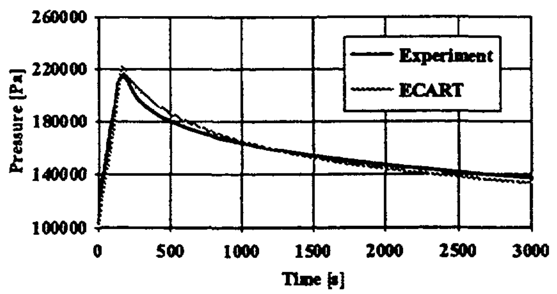

Figure 9 - CVTR test No. 3: containment pressure

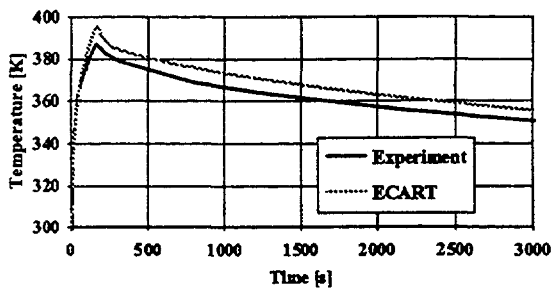

Figure 10 - CVTR test No. 3: upper compartment temperature

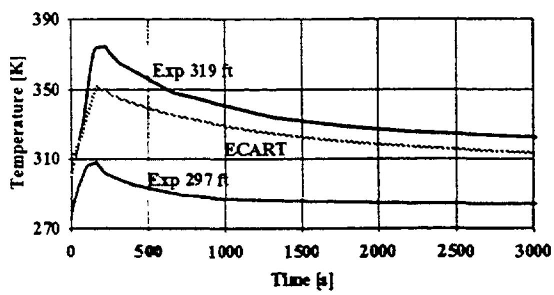

Figure 11 - CVTR blowdown test: lower compartment temperature

6. CONCLUSIONS

In the present paper works performed in relation to heat and mass transfer phenomena have been collected in the attempt to attain an organic presentation of data and modelling techniques.

Although the discussion was mainly focused on innovative reactor features, it is clearly understood that the validity of the conclusions reached is general and hold for a wider spectrum of applications.

The above reported results point out the adequacy of the heat and mass transfer analogy for the evaluation of heat and mass transfer in nuclear reactors. It is remarkable to note that very simple models, mostly proposed in the first half of the century, have the capability to catch the main features of delicate phenomena as evaporation and condensation in the presence of noncondensable gases in a large range of parameters.

Subtle aspects of the related physics require to be furtherly investigated to provide more reliable predictions of heat and mass transfer rates. It is the case of film and vapour-gas mixture fluiddynamics, particularly in relation to the effect of superficial waves and film disruption, which have been neglected in the present treatment.

The agreement obtained between experiments and predictions is nevertheless encouraging to progress along the same line of thought.

REFERENCES

[1] H.J. Bruschi and T.S. Andersen "The Westinghouse AP600: the leading technology for proven safety and simplicity", IAEA TCM Meeting on Progress in Development and Design of Advanced Water Cooled Reactors, Rome (I), September 9-12, 1991

[2] R.J. Mc Candless, A.S. Rao, C.D. Sawyer "SBWR - Simplifications in plant design for the 90's" IAEA TCM on Progress in Development and Design Aspects of Advanced Water Cooled Reactors, Rome (I), September 9-12, 1991

[3] F.E. Peters, A.T. Pieczynski, M.D. Carelli "Advanced Passive Containment Cooling Experimental Program", International Conference on New Trends in Nuclear System Thermohydraulics, May 30-June 2, 1994, Pisa, Italy

[4] H. Nagasaka, K. Yamada, M. Katoh and S. Yokobori "Heat removal tests of isolation condenser applied as a passive containment cooling system", 1st JSME/ASME Joint International Conference on Nuclear Engineering, November 4-7, 1991, Keio Plaza Hotel, Tokyo, Japan

[5] S. Yokobori, H. Nagasaka, T. Tobimatsu "System response test of isolation condenser applied as a passive containment cooling system", 1st JSME/ASME Joint International Conference on Nuclear Engineering, November 4-7, 1991, Keio Plaza Hotel, Tokyo, Japan

[6] P. Masoni, S. Botti, G.W. Fitzsimmons "Confirmatory Tests of Full-Scale Condensers for the SBWR", ASME, March 1993

[7] F. D'Auria, P. Vigni, P. Marsili "Application of

RELAP5/MOD3 to the evaluation of Isolation Condenser performance", Int. Conf. on Nuclear Engineering (ICONE-2), San Francisco (US), March 21-24
[8] N.E. Todreas and M.S. Kazimi "Nuclear Systems" Vol. I-II, Hemisphere Publishing Corporation, 1990
[9] F. Kreith "Heat Transfer Principles" (in Italian), Liguori Editore, Napoli 1974
[10] R.B. Bird, W.E. Stewart, E. N. Lightfoot "Transport Phenomena", John Wiley & Sons, 1960
[11] A. Bejan "Heat Transfer", John Wiley and Sons, 1993
[12] J.G. Collier "Convective Boiling and Condensation." McGraw-Hill Book Company, 1972
[13] A.P. Colburn and O.A. Hougen "Design of Cooler Condensers for mixture of vapours with non-condensing gas", Ind. Engng. Chem., 26, 1178-82, 1934
[14] D. Butterworth, G.F. Hewitt "Two-Phase Flow and Heat Transfer", Oxford University Press, 1979
[15] H.J.H. Brouwersand A.K. Chesters "Film models for transport phenomena with fog formation: the classical film model", Int. J. Heat Mass Transfer, Vol. 35, No. 1, pp. 1-11, 1992
[16] W. Nusselt "Surface condensation of water vapour". Z. Ver. dt. Ing. 60 (27), 541-546; 60 (26) 569-575
[17] W. Ambrosini, P. Andreussi and B.J. Azzopardi "A physically based correlation for drop size in annular flow". Int. J. Multiphase Flow, Vol. 17, No. 4, 1991, pp. 497-507
[18] P.L. Kapitsa - Zh. Eksper. Teoret. Fiz. 18, 3, 1948
[19] T.B. Benjamin "Wave formation in Laminar Flow Down an Inclined Plate", J. Fluid Mech., 2, 554, 1957
[20] G. Kocamustafaogullari "Two-Fluid Modelling in Analyzing the Interfacial Stability of Liquid Film Flows", Int. J. Multiphase Flow Vol. 11, No. 1,1985, pp. 63-89
[21] T.D. Karapantsios And A.J. Karabelas "Surface Characteristics of Roll Waves on Free Falling Films", Int. J. Multiphase Flow. Vol. 16, No. 5, pp. 835-852, 1990
[22] C.E. Lacy, M. Sheintuch and A.E. Dukler "Methods of Deterministic Chaos Applied to the Flow of Thin Wavy Films", AIChE Journal, Vol. 37, No. 4, pp. 481-489, 1991
[23] A. Manfredini, F. Mariotti, F. Oriolo and P. Vigni "A facility for the evaluation of heat flux from a plate cooled by a water film, with counter-current air flow" 11th National Congress on Heat Transfer of the UIT, Milano (I), June 24-26 1993
[24] W. Ambrosini, A. Manfredini, F. Mariotti, F. Oriolo, P. Vigni "Heat Transfer from a Plate Cooled by a Water Film with Counter-Current Air Flow", International Conference on 'New Trends in Nuclear System Thermohydraulics', Pisa, May 30-June 2, 1994
[25] T. Van De Venne, E. Piplica, M. Kennedy And J. Woodcock "The Westinghouse AP600 Passive Containment Cooling Test and Analysis Program." ANP '92 Congress, Tokyo, October, 25-29, 1992
[26] A. Manfredini, M. Mazzini, F. Oriolo, S. Paci "Validazione dell'efficacia dello spruzzamento esterno del contenimento in impianti nucleari a maggiore sicurezza passiva." 8th National Congress on Heat Transfer of the UIT, Ancona, June 28-29, 1990
[27] A.S. Rao, J.R. Fitch, and P.F. Billig "Safety Research for the SBWR", The 20th Water Reactor Safety Meeting, Bethesda, MD, 1992
[28] F. Magris, A. Villani, C. Medich and M. Bolognini "Design and Experimental Verification of Isolation Condenser and Passive Containment Cooler for SBWR", International Conference on Design and Safety of Nuclear Power Plants, 1992
[29] F. Oriolo, W. Ambrosini, G. Fruttuoso, F. Parozzi, R. Fontana "Thermal-Hydraulic Modelling in Support to Severe Accident Radionuclide Transport", International Conference on 'New Trends in Nuclear System Thermohydraulics', Pisa, May 30-June 2, 1994
[30] R. Fontana, E. Salina and F. Parozzi "ECART (ENEL Code for Analysis of Radionuclide Transport). Definition of the code architecture and construction of the aerosol and vapour transport module", ENEL Report. No. 1019/2, 1991 (unpublished work)
[31] A. Manfredini, M. Mazzini, F. Oriolo, S. Paci "The FUMO code: Description and Manual" (in Italian) - Università di Pisa, Dipartimento di Costruzioni Meccaniche e Nucleari, RL 416 (89), 1989
[32] R.C. Schmitt, G.E. Bingham, J.A. Norberg "Simulated design basis accident tests of the Carolinas Virginia Tube Reactor containment" Idaho Nuclear Corporation, Final Report IN 1403, Prepared for U.S.A.E.C, Contract No. AT(10-1)-1230, 1970

NOMENCLATURE

Roman Letters

C_p	specific heat at constant pressure	[J/(kg K)]
C_0	temperature profile coefficient	[K]
C_1	temperature profile coefficient	[K/m]
C_2	temperature profile coefficient	[K/m^2]
D_h	hydraulic diameter	[m]
$\mathcal{D}_{vn}$	vapour diffusion coefficient	[m^2/s]
G	mass velocity	[kg/(m^{2}s)]
h	fluid specific enthalpy	[J/kg]
H	heat transfer coefficient	[W/(m^2 K)]
k	thermal conductivity	[W/(m K)]
K_m	mass transfer coefficient	[m/s]
L	length	[m]
m	film thickness	[m]
$\mathcal{M}$	molecular weight	
Nu	Nusselt number	

p	pressure	[Pa]
Pr	Prandtl number	
q"	heat flux	[W/m^2]
Q	power	[W]
Re	Reynolds number	
Sc	Schmidt number	
Sh	Sherwood number	
T	temperature	[K]
w	fluid velocity	[m/s]
w^*	shear velocity	[m/s]
x	space coordinate	[m]
y	space coordinate within the film	[m]
z	space coordinate along the plate	[m]

Greek Letters

α	thermal diffusivity	[m^2/s]
Γ	mass flow rate per unit perimeter	[kg/(m s)]
δ_m	thickness of mass transfer boundary layer	
θ	inclination angle with respect to downward vertical	
λ	latent heat of evaporation	[J/kg]]
μ	dynamic viscosity	[kg/(m s)]
ν	kinematic viscosity	[m^2/s]
ρ	density	[kg/m^3]
$\tilde{\rho}_v = \rho_v + \frac{\mathcal{M}_v}{\mathcal{M}_n}\rho_n$		[kg/m^3]
τ_c	characteristic shear stress	[Pa]
τ_i	interfacial shear stress	[Pa]
τ_w	wall shear stress	[Pa]

Subscripts

cond	condensation
conv	convective
eff	effective
g	gas-vapour mixture
int	interfacial value
k	k-th phase index
l	liquid
lf	liquid film
n	noncondensable gas
sat	saturation
v	vapour
w	wall

Superscripts

ps	pool surface
w	wall
+	dimensionless value

Abbreviations

BE	Best Estimate
EdF	Electricitè de France
ENEL	Italian Electricity Board
IC	Isolation Condenser
LOCA	Loss Of Coolant Accident
PCCS	Passive Containment Cooling System
PID	Proportional Integral Derivative
R.H.S.	Right Hand Side

APPLICATION OF THE UMAE UNCERTAINTY METHOD IN ASSESSING THE DESIGN AND THE SAFETY OF NEW GENERATION REACTORS

F. D'AURIA, G. FRUTTUOSO, G.M. GALASSI,
S. GALEAZZI, F. ORIOLO
University of Pisa, Pisa

L. BELLA
ENEL CRT, Pisa

V. CAVICCHIA, E. FIORINO
ENEL ATN, Rom

Italy

Abstract

The present paper deals with the problem of uncertainty evaluations in the predictions of transient behaviour of nuclear power plants by complex thermalhydraulic system codes. This is relevant to the design and the safety assessment of nuclear reactors.

The UMAE (Uncertainty Methodology based on Accuracy Extrapolation) methodology, recently proposed by the University of Pisa is briefly outlined and the main results are summarized.

Emphasis is given in the paper to the application of the method in the domain of advanced reactors; in this frame a few results obtained from the analysis of Spes-2 (AP-600 simulator) data are discussed.

1. INTRODUCTION

Evaluation of power plant performance during transient conditions has been the main issue of safety researches in the thermalhydraulic area carried out all over the world since the beginning of the exploitation of nuclear energy for producing electricity, e.g. [1] and [2].

A huge amount of experimental data have been obtained from the operation of test facilities simulating the behaviour of nuclear plants. Several complex system codes have been developed and qualified that allow the characterization of plant transient performance, ref. [3].

In the last few years uncertainty methodologies have been proposed to evaluate the errors in the prediction of transient scenarios outcoming from the use of the system codes, refs. [4] and [5]. The error quantification is a necessary step to prove the safety of the existing plants and to optimize the design and the operation.

The UMAE (Uncertainty Methodology based on Accuracy Extrapolation) has been recently developed at the University of Pisa and fully applied to the calculation of error bands in the time trends of relevant thermalhydraulic quantities in PWR following a typical small break Loss of Coolant Accident, ref. [6]. The use of the UMAE requires the availability of a qualified computer code and of relevant experimental data obtained in properly scaled simulators, refs. [7] and [8].

The objective of the present paper is to propose a framework for the application of the UMAE to the AP-600, with main regard to the deterministic evaluation of the safety margins during anticipated incident conditions. This requires, among the other things, the availability of specific experimental data like those obtained or being obtained by the Spes-2, the Rosa-V and the OSU experimental programs. Such data can be combined, as far as similar phenomena are concerned, with those available from facilities simulating current generation PWR.

To this aim, an outline of the mentioned uncertainty methodology is part of the paper and the results of the application of a few steps are discussed. These essentially include the independent qualification of the adopted computer code with the demonstration that the error in predicting the so-called relevant thermalhydraulic aspects is within acceptable limits. The analyses performed in relation to experimental data available from the AP-600 simulator Spes-2, ref. [9], are utilized hereafter, ref. [10].

2. BASIS AND DEVELOPMENT OF THE UMAE

The fundaments of the methodology have been discussed in previous papers, e.g. refs. [11] and [12] and can be drawn from the considerations 1 to 6 below, related to the test facilities and the codes. It is assumed that both of these are representative of the actual state of the art: i.e. facilities are "simulators" of a reference LWR and codes are based on the "six balance equations model" and must be intended as generically "qualified", ref. [3].

1. The direct extrapolation of experimental data is not feasible; nevertheless, the time trends of significant variables measured during counterpart tests in differently scaled facilities are quite similar: this fact must be exploited.
2. Phenomena and transient scenarios occurring in larger facilities, being nearly constant the other conditions (e.g. design criteria, quality of instrumentation, etc.), are more close to plant conditions than those recorded from smaller facilities.
3. "Qualified" codes are indispensable tools to predict plant behaviour during nominal and off-nominal conditions.
4. The confidence in predicting a given phenomenon by the code, must increase when increasing the number of experiments analyzed dealing with that phenomenon.
5. The uncertainty in the prediction of plant behaviour cannot be smaller than the accuracy resulting from the comparison between measured and calculated trends for experimental facilities; furthermore, accuracy (uncertainty) must be connected with the complexity of the facility (plant) and of the considered transient.
6. The effects of user and of nodalization must be included in the methodology.

The basic idea is to get the uncertainty from considering the accuracy. The main problems to achieve this are connected with the availability of experimental data that must be 'representative' of plants, with the quantification of accuracy and with the justification of any relationship between accuracy obtained in small dimensions loops with accuracy of the plant calculation, i.e. uncertainty.

The use of data base from counterpart and similar tests in Integral Test Facilities was of large help in this context, with main reference to the last mentioned problem. In particular, similar tests are those experiments performed in differently scaled facilities that are characterized by the occurrence of the same thermalhydraulic phenomena; counterpart tests are similar tests where boundary and initial conditions are imposed following a scaling analysis.

Two main aspects have been considered at a preliminary level to judge the realism of the accuracy extrapolation ref. [6]: from the experimental side, the design of the facilities, the boundary and initial conditions of the experiments, the suitability of the instrumentation, the quality of the recorded data have been evaluated together with the similarity of the phenomena; from the code side, the general qualification process, the capability to simulate the relevant phenomena identified, the qualification of the nodalization and of the code user have been independently assessed.

Several parameters of geometric or thermohydraulic nature can be used, in principle, to derive uncertainty from accuracy values; furthermore, the use of a unique parameter is preferable to minimize the possibility of counterfeiting information from the available data base. The selected parameter should constitute a link between the experimental data and the data foreseeable in the plant in the case of occurrence of the conditions of interest, it must be representative of the involved phenomena at a global scale (i.e. the equivalent diameter in the core simulators is representative of thermalhydraulic phenomena in the core but does not affect substantially pressure behaviour during a depressurization transient), it must take into account the present status of the technology (i.e. the height of the facilities or the initial pressure might not be suitable parameters because they are nearly the same in the different facilities and in the reference plant).

Several parameters fulfil the above requirements, nevertheless the volume of the facility or, in dimensionless form, the ratio between primary system fluid volumes in the facilities and in the reference plant was selected as 'extrapolation' parameter.

The situations depicted in Figure 1 are expected from using such an approach ref. [11]. The volume scaling ratio is reported on the horizontal axis; this quantity actually varies by four orders of magnitude from the smallest facility to the plant ref. [12]. The shaded area represents the range of facilities, the smallest one and the largest one are characterized by a volume roughly 2000 times and 50 times, respectively, lower than that of a 1000 MWe plant. On the vertical axis the generic quantity Y and the ratio Y_E/Y_C (experimental over calculated value) are represented where Y is the value of any quantity that is relevant in a given transient.

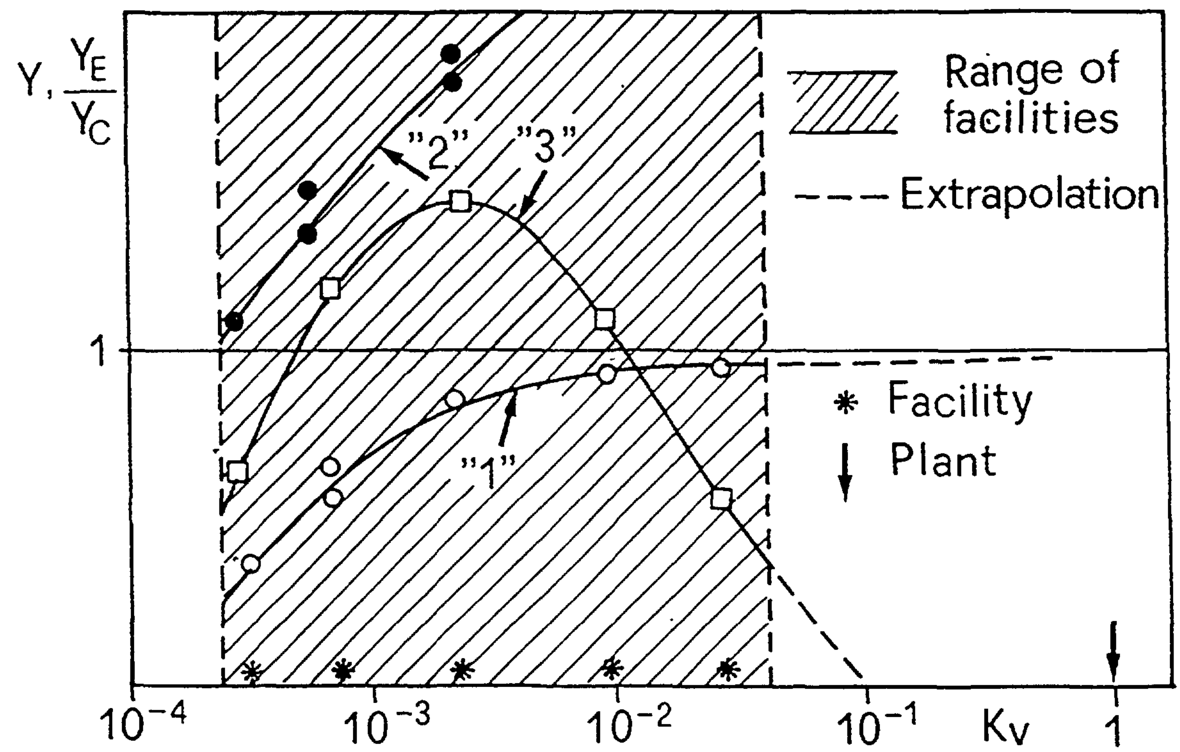

Figure 1 - Possible trends resulting from scaling analyses

2.1 UMAE flow diagram

The use of calculated and measured data related to counterpart and similar tests, especially with the help of the code, directly led to the achievement of quantities connected with the uncertainty. "Dispersion bands" and "extrapolated" plant behaviour were previously defined and evaluated ref. [6].

The UMAE procedure aims at calculating the uncertainty and, although making use of the same above-mentioned data base, involves the rationalization of the various steps including the use of statistics in order to avoid or minimize the expert judgement at the various levels.

Generic experiments in integral facilities and related calculations other than counterpart and similar tests, can be processed by the UMAE, provided the availability of data base related to a reasonable set of individual phenomena that envelope the key phenomena foreseeable in the selected plant scenario.

A simplified flow-diagram of the UMAE is reported in Figure 2. The way pursued to evaluate the data base and the conditions to extrapolate the accuracy are synthesized hereafter.

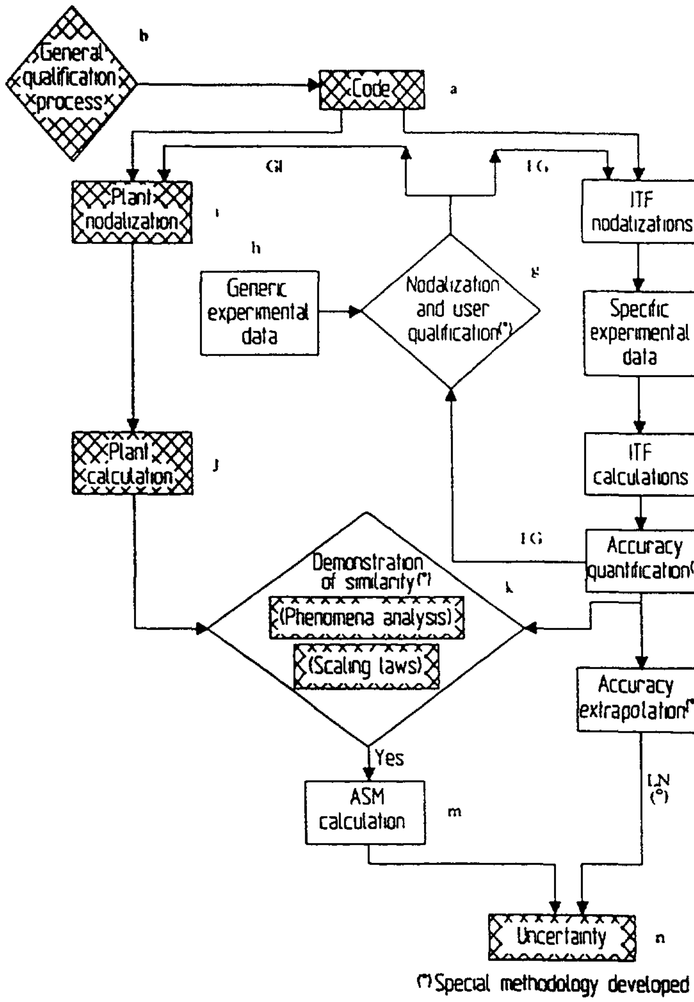

(Dashed blocks represent blocks that are common to UMAE and CSAU)

Figure 2 - Simplified flowsheet of UMAE.

2.1.1 Evaluation of the Specific Data Base

The specific data base is constituted by the signals recorded during the considered experiments and by the results of the code calculations. Each test scenario (measured or calculated) should be divided into 'Phenomenological Windows' (Ph.W). In each Ph.W. 'Key Phenomena' (K.Ph) and 'Relevant Thermalhydraulic Aspects' (RTA) must be identified. K.Ph characterize the different classes (e.g. small break LOCA, large break LOCA, etc.) of transients and RTA are specific of the assigned one; K.Ph are always applicable; the definition of RTA for small break LOCA in PWR has been done in ref. [8]. K.Ph and RTA qualitatively identify the assigned transient; in order to get quantitative information, each RTA must be characterized by 'Single Valued Parameters' (SVP, e.g. minimum level in the core), 'Non-Dimensional Parameters' (NDP, e.g Froude number in hot leg at the beginning of reflux condensation), 'Time Sequence of Events' (TSE, e.g . time when dryout occurs) and 'Integral Parameters' (IPA, e.g. integral or average value of break flowrate during subcooled blowdown).

2.1.2 Accuracy Extrapolation (block "l")

If the following conditions are fulfilled, accuracy in predicting SVP, NDP, IPA and TSE can be extrapolated, ref. [13]:

- the design scaling factors of the involved facilities are suitable;
- the test design scaling factors of the involved experiments are suitable;
- the experimental data base is qualified;
- the nodalizations and the related users are qualified;
- RTA are the same in the considered experiments if counterpart or similar tests are involved; otherwise, the same RTA can be identified in different experiments;
- RTA are well predicted by the code at a qualitative and a quantitative level;
- RTA are the same in the plant calculation 'facility K_V scaled' and in the experiments; parameters ranges (SVP, NDP, TSE and IPA), properly scaled, are also the same. This must be interpreted in different ways depending upon the availability of counterpart tests;
- in the plant calculation 'realistic conditions' Ph.W and K.Ph are the same as in the considered experiments; SVP, NDP, TSE and IPA may be different: reasons for this are understood.

The extrapolation of accuracy is achieved with reference to the above mentioned parameters through the use of the statistics ref. [14]. The ratios of measured and calculated values of SVP, NDP, TSE and IPA are reported in diagrams like that shown in Figure 1 assuming that they are randomly distributed around the unity value. This is also justified by the huge number of variables affecting the considered ratios. In this way 'mean accuracy' and '95th percentile accuracy' are derived that are applicable to the plant calculation. The measurement errors, the unavoidable scaling distortions and the dimensions of the facility are directly considered.

It should be noted that only one calculation, performed with a qualified Analytical Simulation Model (ASM in Figure 2), is necessary to get the reference plant scenario. The ASM is qualified in the frame of the block "k" of Figure 2; the final part of the qualification process, ref. [15], essentially derives from comparing RTA of the plant calculation with those obtained in the experimental facilities during the same accident situations. Qualitative and quantitative accuracy evaluation steps are used in this frame, ref. [16]. The "extrapolated accuracy" values are superimposed to the reference plant trends to get the final value of uncertainty.

3. APPLICATION OF THE UMAE TO THE LICENSING PROCESS

The procedures aiming at the evaluation of the uncertainty in codes predictions of Nuclear Plants related scenarios (herein called uncertainty methodologies) have as main output error values. These can be at a given time, either error bands to be superimposed to a "base" value, either ranges of variation of the assigned quantity, either limit values (boundary value approach).

The Peak Cladding Temperature following dryout of the surface of the fuel rods is the most important quantity to be predicted in safety or licensing calculations. The result obtained from the application of the UMAE procedure is outlined hereafter ref. [6].

The UMAE has been applied so far to the uncertainty evaluation in a small LOCA assumed to occur in the Krsko Westinghouse plant installed in Slovenia. The plant is a two loop 630 Mwe PWR. The considered transient is originated by a rupture in the cold leg between the pump and the vessel; the break area is about 5% of the cross section area of the main pipe. Scram, isolation of secondary side and pump trip are foreseen during the transient; failure of high pressure injection systems is assumed, while accumulators are supposed in operation. The calculated transient is stopped before allowing the intervention of low pressure injection systems.

The result concerning the rod surface temperature trend in the core region when the maximum temperature is predicted, is given in Figure 3. The calculated error bands are superimposed. The PCT during both the dryout periods is calculated with an error of the order of 100 K.

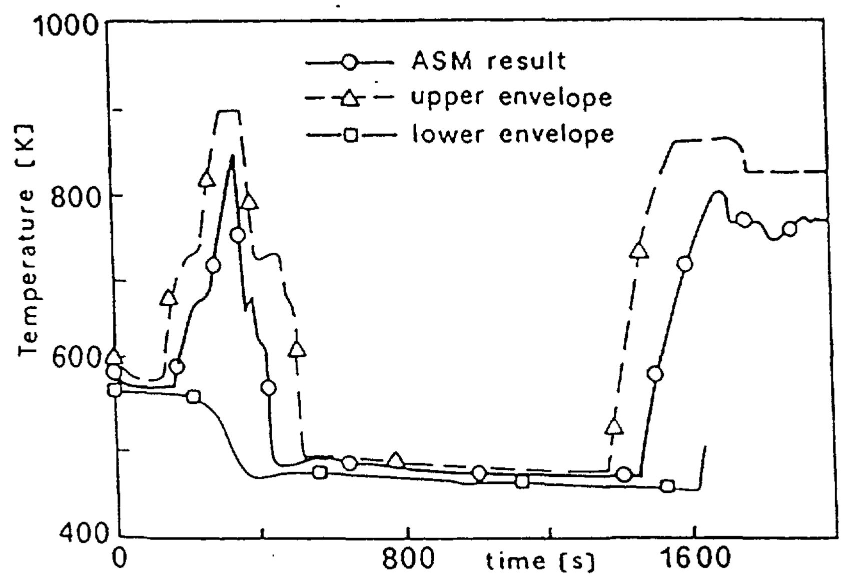

Figure 3 - Uncertainty resulting from ASM calculation of a Small Break LOCA in the KRSKO Westinghouse plant.

Another application of the UMAE was dealt with a data base including experiments in separate effect facilities, ref. [17]; this led to an error for the PCT of about 270 K in a thermalhydraulic scenario different from what previously considered.

Two safety/licensing indications can be outlined:

1) all Design Basis Accident simulations, either from experimental facilities either from the use of best-estimate codes, led so far to PCT (where applicable) in the range 500-1000 K; so the addition of uncertainties in the range 100-300 K still keeps the rod surface temperature values well below the safety limit (1473 K); this leaves some margin for possible changes of plant operating conditions;
2) a no-dryout situation is shown as the most acceptable code calculation result in Figure 3. This comes out from time uncertainty values for the dryout start and for the rewet occurrence and constitutes a typical bifurcation.

The final remark here is that the application of uncertainty methodologies within the DBA area, should lead to sufficiently reduced error bands for PCT; e.g. an error ± 700 K obtained from uncertainty study could be useless testifying deficiencies either in plant design either in the methodology/code itself. The former possibility should be excluded, with present knowledge, within the DBA boundaries.

4. USE OF DATA RELEVANT TO AP-600

In order to apply the UMAE to reactor calculations, the availability of a qualified code and of "relevant" experimental data is needed; "relevant" experimental data must be obtained from suitable facilities and directly related to transient scenarios of interest in the plant. Furthermore, codes can be fully qualified when the comparison of predicted results with "relevant" data is successfully made (see also before).

Most of the thermalhydraulic phenomena important for new reactors are also important for present generation reactors, although the ranges of parameters can be different. A comprehensive evaluation of the differences between present and new generation reactors can be found in ref. [18] as far as thermalhydraulic phenomena are concerned. As a result of the above investigation, most of the experience gained in qualifying system codes on the basis of situations of interest in present generation reactors can be used for next generation reactors. However specific testing is also requested: the behaviour of the Core Make-up Tanks (CMT), of the Passive Residual Heat Removal (PRHR) heat exchanger, etc., must be experimentally qualified in integral and separate effect test facilities (ITF and SETF); the system code capability in predicting the resulting scenarios should also be demonstrated.

In this framework, specific programs started in different organizations, e.g. Spes-2, Rosa-V, OSU in relation to AP-600 and Panthers, Panda, Toshiba, Piper-one (see ref. [19] for this last case) in relation to SBWR.

A few steps of the overall code assessment and uncertainty evaluation processes carried out with reference to the application of the Relap5 code to Spes-2 experiments, are discussed.

4.1 Spes-2 2" cold leg break test scenario

The Spes-2 facility reproduces all the main zones of the AP-600 primary circuit. A sketch of this can be seen in Figure 4, see also ref. [20].

The analyzed event is a small break LOCA, originated by to a 2" break in the AP600, in one of the cold legs in the loop not connected to the pressurizer. This test, No. 3 of the SPES-2 Tests Matrix, assumes the actuation of all passive Engineered Safety Features, with the exception that the area of one of the 4th stage SPES-2 ADS valves has been reduced, to simulate the failure to open of one AP600 4th stage ADS valve. Conversely, the active systems (i.e. the normal RHR and the CVCS) are assumed not to operate.

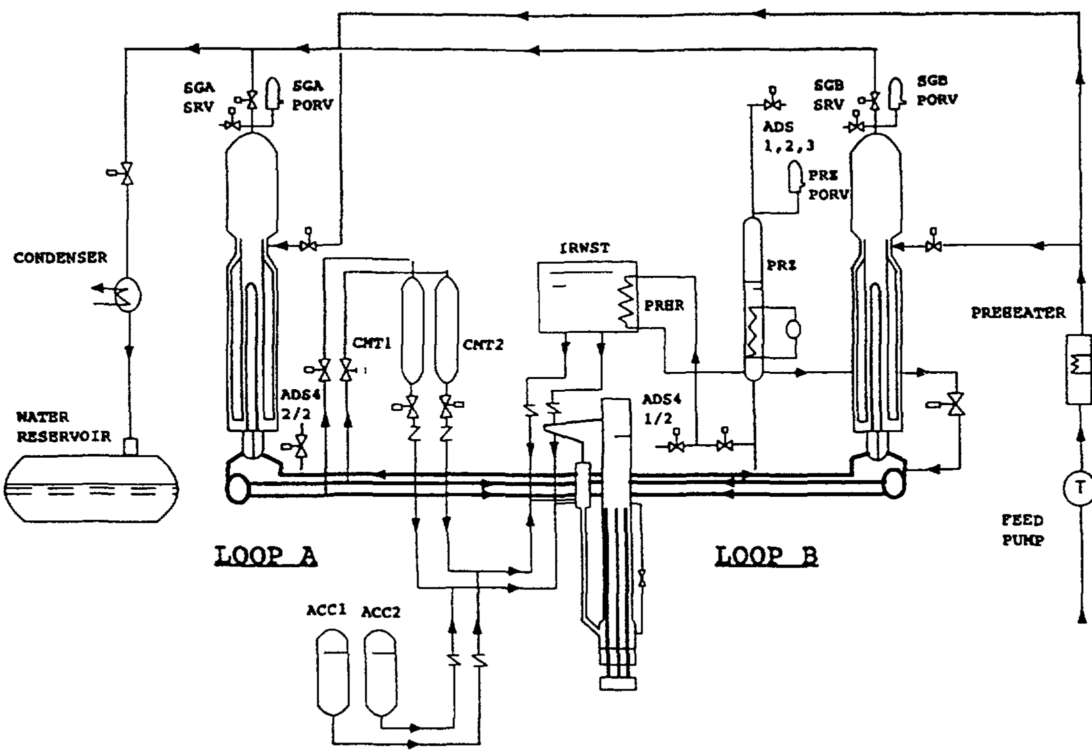

Figure 4 - Simplified flow sheet of SPES-2 facility

From a qualitative point of view the following phenomena occur:

- After the break device is opened, the primary pressure drops to the reactor trip set point and the main steam line isolation valves are closed, causing a slight increase of SG pressure. The heater rod power is controlled to match the scaled AP600 decay power, with an extra contribution to compensate for the heat losses. The compensation power is switched off when the first stage ADS opens.
- When the pressure reaches the "S" signal setpoint, the main feedwater is isolated, the RCPs are switched off, inducing a small "bump" in the primary pressure and the PRHR and CMTs isolation valves are opened.
- The RCS cools down to the same temperature of the secondary side and the coolant becomes saturated; in this period the primary and the secondary pressures are of course the same.
- As long as the primary circuit inventory allows, water is circulated through the cold leg, the balance line and the CMT discharge line. In this period the CMT remains filled with water, although coolant mass is added to the primary circuit, since less dense water from the RCS is substituted with denser water from the CMT. Once the siphon breaks, the CMTs start to empty, causing a significant jump in their injection flow.
- When the CMT level falls to the proper setpoint, the ADS valves open, depressurizing the RCS and allowing the accumulators to inject. Since the accumulators and the CMTs share the same injection line, CMTs injection is reduced in this period.

  When the accumulators empty, the CMTs continue to provide coolant to the RCS, at an increased rate.
- At the proper CMT level, the 4th ADS stage is actuated, reducing the RCS pressure to a very low value, close to the atmospheric pressure, and allowing stable coolant injection from the IRWST.

4.2 Overview of code results

A detailed nodalization has been developed for the Spes-2 facility including all the geometrical details (Figure 5), see also ref. [21].

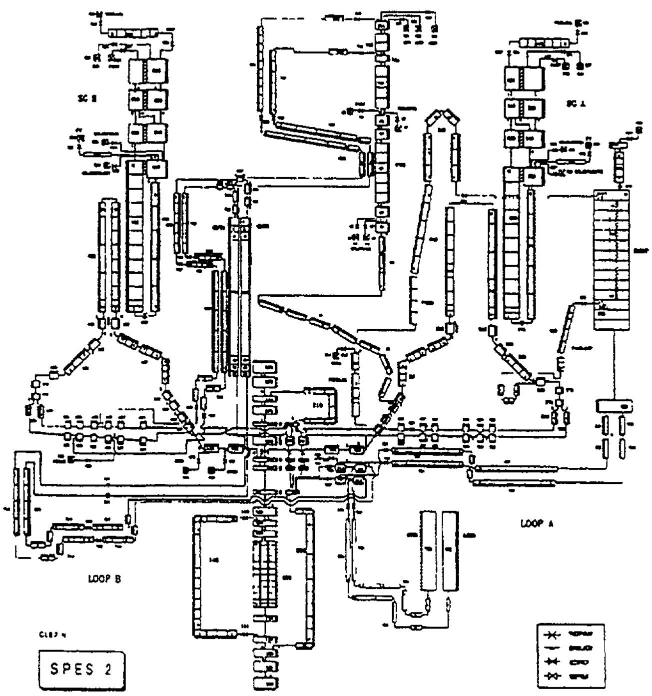

Figure 5 - Nodalization of the SPES-2 facility for the RELAP5/MOD2.5

The analysis of the 2" Cold Leg Break Test has been performed assuming the initial conditions measured on the facility. The calculated and the experimental event timings are in good agreement.

The agreement between calculated and experimental break flow is good as long as subcooled blowdown occurs through the break. After, while in the calculation a sharp decrease in the mass discharge happens at about 550. s, testifying a mixture quality transition of the flowrate at the break, experimental results do not evidence this phenomenon, and the break flow reductions occurs later, when the 1st stage ADS valve opens, resulting both in system depressurization and in mass drawing towards the pressurizer, with a related coolant diversion from the break.

Phenomenological differences between experiment and calculation again appear during the accumulator injection phase: bypass of injected liquid occurs in the calculation, whereas accumulator injected mass is essentially bleed through the ADS valves during the test.

The trends of the primary and secondary pressure versus time are shown in Figure 6: the agreement with the measurements is good. The slight underprediction of the secondary pressure is due to inaccuracies in the evaluation of the heat losses.

Mainly due to the very good prediction of the primary pressure, both the hot and cold

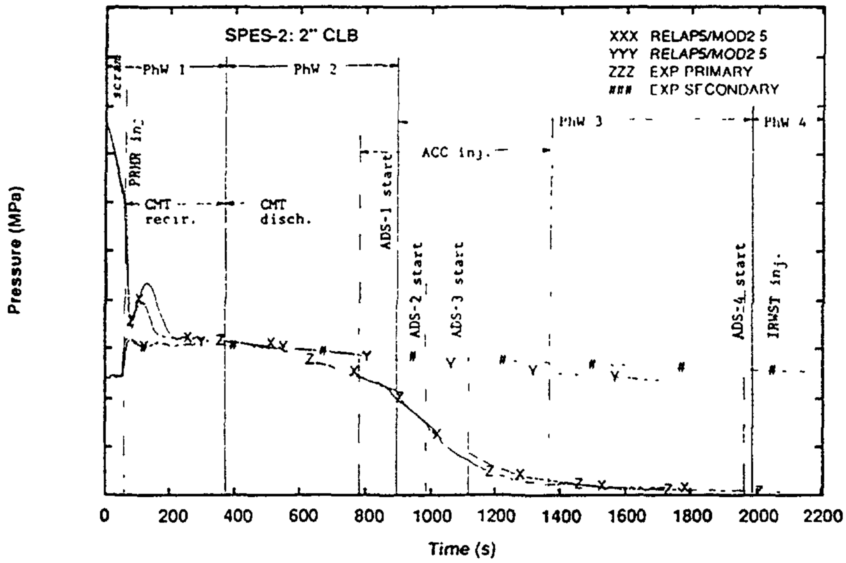

Figure 6 - SPES-2 test # 3: Primary and SGs secondary side pressure

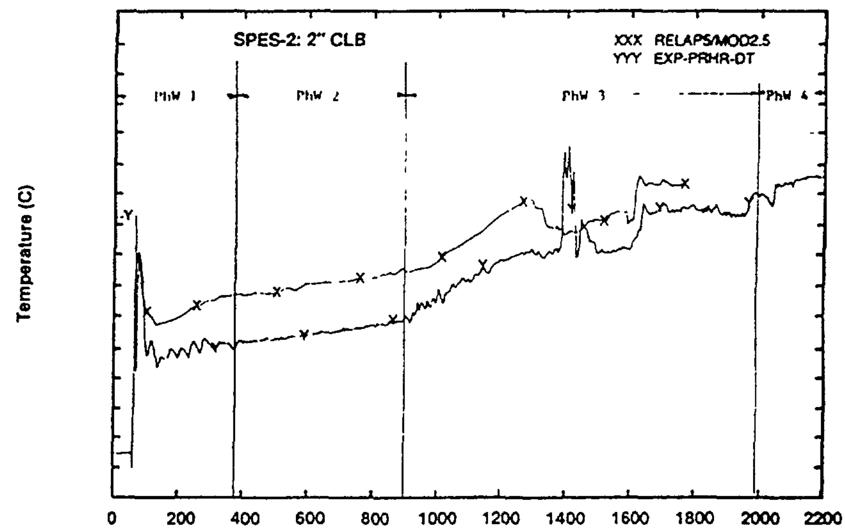

Figure 7 - SPES-2 test # 3: Fluid temperature jump across the PRHR

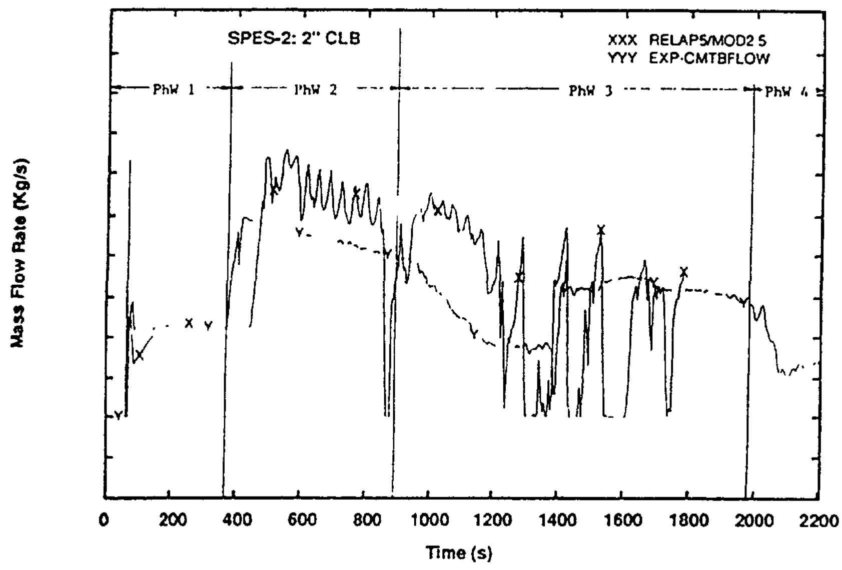

Figure 8 - SPES-2 test # 3: Discharged flow rate from CMT B

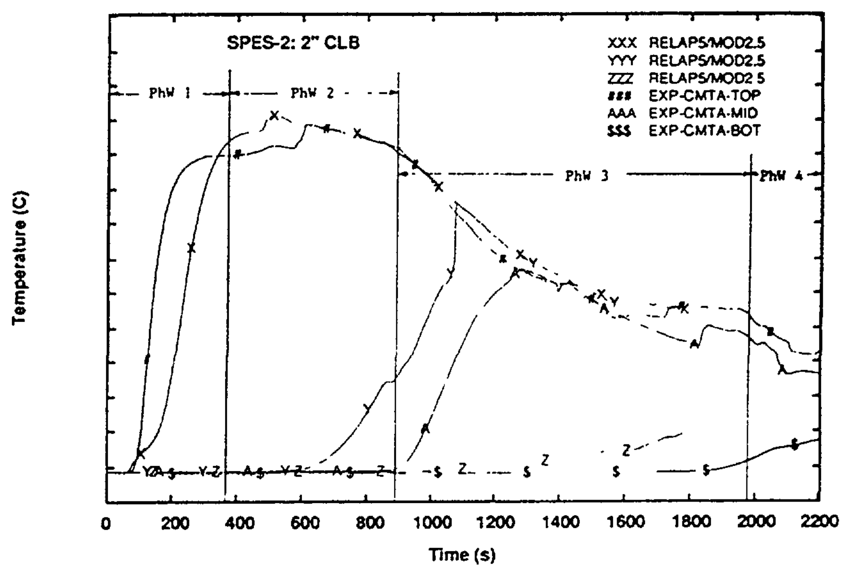

Figure 9 - SPES-2 test #3: Fluid temperature at various elevations in CMTA

legs temperatures are very well predicted. The main events during the test are also shown.

Figure 7 plots the difference between the outlet and the inlet PRHR temperatures. A difference as large as 40° C can be observed: in fact, while the PRHR inlet temperature (essentially the hot leg temperature) is very well calculated, the outlet temperature is overpredicted, resulting in an underprediction of the heat exchanger performance.

Figure 8 presents the discharge flow from the CMT connected to the same cold leg where the break is located; the discharge flow from the other CMT is qualitatively similar.

The CMT flow during the recirculation period is correctly predicted, although a delayed inception of the CMT emptying phase (by less than 100 s) is calculated and the related flow is somehow overpredicted.

A substantial thermal stratification is observed in the CMTs, which is slightly underpredicted by the SPES-2 model (Figure 9).

The "spikes" in the calculated discharge flow, which are not as much evident in the experiment, are due to sudden condensation phenomena in the CMTs.

The accumulator injection, whose onset is predicted within 100 s and whose flow is very well predicted, reduces the draining from the CMTs, although not as much as predicted.

The overall prediction of the CMT mass balance is good enough to allow to predict the 1st and the 4th ADS stage openings with an error of 20 and 220 s, respectively.

The ADS flow rate (stage 1-2-3) is plotted in Figure 10, while Figure 11 presents the differential pressure across the pressurizer. In the two figures, a large water suction from the RCS to the PRZ is evident, which allows a large ADS discharge flow.

The parameters more directly related to the AP600 plant safety are the heated rod temperatures and the core differential pressure (which allows a more direct calculation/measurement comparison than the core level).

The heated rod temperatures are predicted with very good accuracy. In agreement with the experiment, no dry-out has been calculated to occur.

The pressure drop across the core is shown in Figure 12: the calculation matches very well the measured value, allowing to deduce a good prediction of the vessel water inventory.

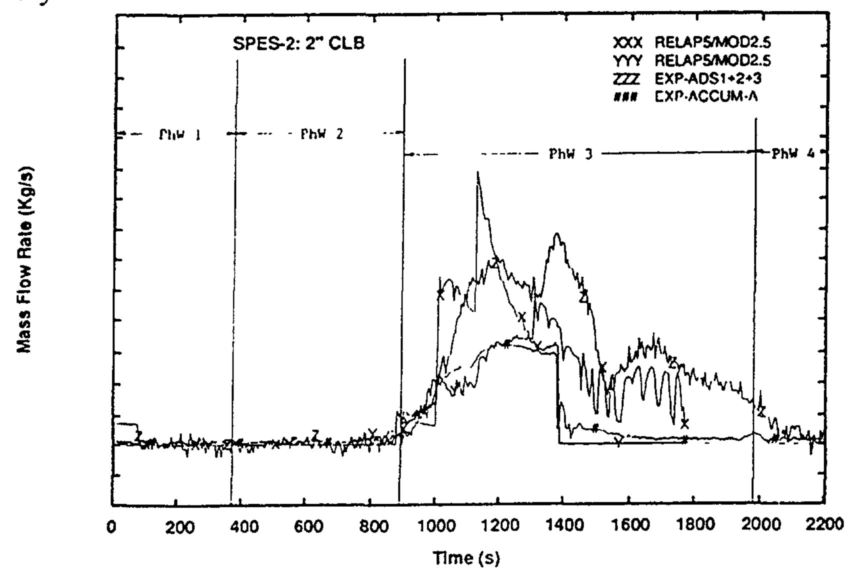

Figure 10 - SPES-2 test # 3: Discharged flow rate from ADS valves 1,2,3 and Accumulator

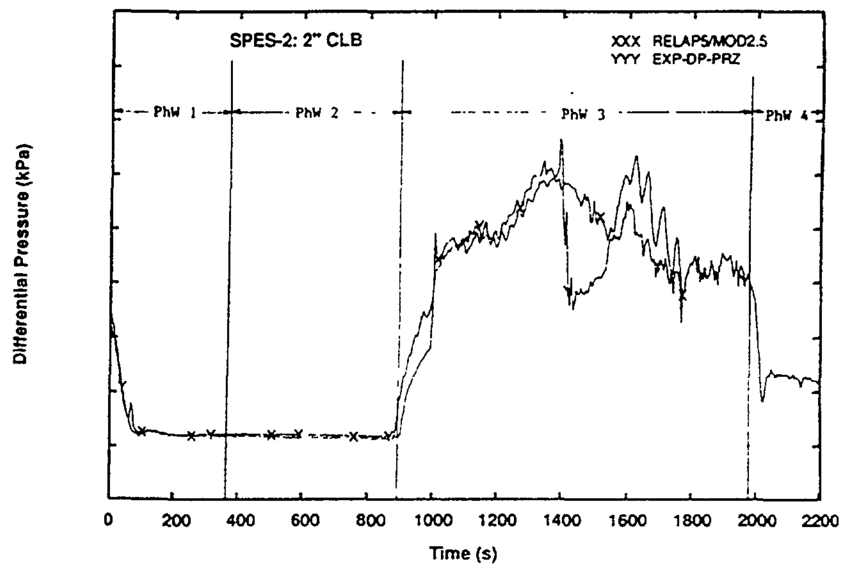

Figure 11 - SPES-2 test # 3: Pressurizer differential pressure

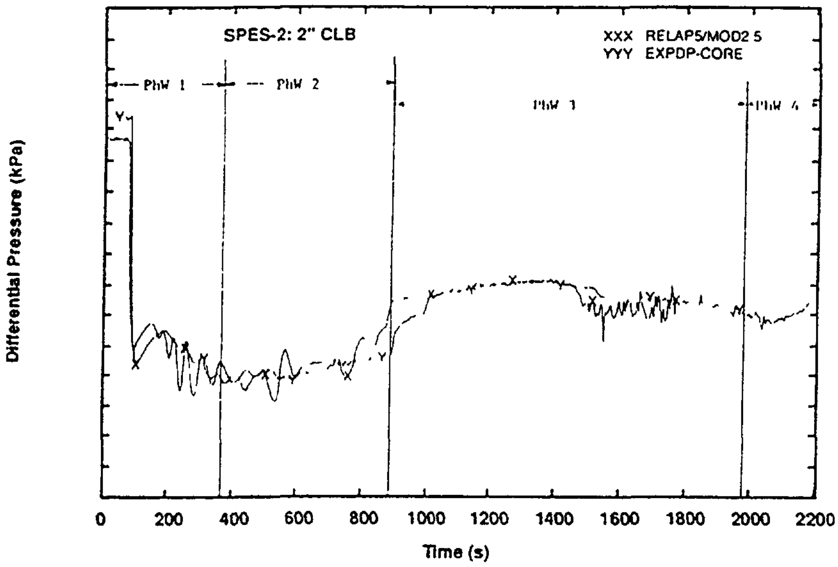

Figure 12 - SPES-2 test # 3: Core differential pressure

4.3 Qualitative and quantitative accuracy evaluation

In order to evaluate qualitatively the accuracy following the procedure mentioned in sect. 2, the transient has been subdivided into 4 phenomenological windows; more than 30 RTA have been identified which are characterized by around 70 NDP, IPA, SVP and TSE.

The Ph.W and the agreement between measured and calculated trends of the RTA can be seen in Table 1.

Table 1 - Agreement between calculated and experimental RTA in SPES-2 test # 3

Phenomenological Window (PhW)	Relevant Thermalhydraulic Aspect (RTA)	Time Sequence Event (TSE)		Single Valued Parameter (SVP)		Non-Dimensional Parameter (NDP)		Integral Parameter (IPA)	
SUBCOOLED BLOWDOWN PHW1	Pressurizer emptying	Discharge time (s)	E					$\int_{\text{Time}=0}^{\text{Time of PRZ level}=0} \text{Break flow}$	E
		SCRAM time (s)	F						
	Primary System Pressure behaviour	Pump Trip time (s)	R	PS-SS pressure difference at 250 s (MPa)	E				
		Pump Coastdown duration (s)	M						
		Peak Width (s)	M			Peak Pressure to initial pressure ratio	R		
	Secondary System Pressure behaviour	FW closure time (s)	E						
		SL closure time (s)	E						
		Time of first pressure peak (s)	E	Pressure increase at the first peak (MPa)	R				
	Break flow							$\int_{\text{Time}=0}^{\text{End of PhW1}} \text{Break flow}$	R
	CMT Behaviour	Drain valve (DV) opening time (s)	E						
		End of recirculation mode in CMT_A (s)	M					$\int_{\text{DV opening time}}^{\text{DV opening time}+250\text{s}} CMT_A \text{ flow}$	R
		End of recirculation mode in CMT_B (s)	R					$\int_{\text{DV opening time}}^{\text{DV opening time}+250\text{s}} CMT_B \text{ flow}$	E
	PRHR behaviour	Time of valve opening (s)	R	Average subcooling at the PRHR HX inlet between 250 and 500 s	E	$\dfrac{\int_{\text{Time of valve opening}}^{\text{End of PhW}} \text{PRHR power}}{\int_{\text{Time of valve opening}}^{\text{End of PhW}} \text{Core power}}$	NE	$\int_{\text{Time of valve opening}}^{\text{End of PhW1}} \text{PRHR flow}$	R
				Average subcooling at the PRHR HX outlet between 250 and 500 s	M				
	In vessel fluid stratification			Subcooling at DC bottom (DC outlet) at 500 s	E				

Legend: E Excellent R Reasonable M Minimal
U Unqualified NE Not Evaluated

Table 1 - Agreement between calculated and experimental RTA in SPES-2 test # 3 (Cont'd)

Phenomenological Window (PhW)	Relevant Thermalhydraulic Aspect (RTA)	Time Sequence Event (TSE)		Single Valued Parameter (SVP)		Non-Dimensional Parameter (NDP)		Integral Parameter (IPA)	
CMT DISCHARGE MODE PHW2	PRZ pressure	Time when PS pressure equals SS pressure (s)	R	Average PS-SS pressure difference during the PhW2	E				
	SG SS behaviour			Average SG_A pressure in the PhW2	R				
				Average SG_B pressure in the PhW2	R				
	In vessel fluid stratification			Subcooling at DC bottom (DC outlet) at 750 s	E				
				Subcooling at DC bottom (DC outlet) at the end of PhW2	R				
	Break Flow							$\int_{\text{Start of PhW2}}^{\text{End of PhW2}} \text{Break flow}$	M
	CMT behaviour	Time when first CMT starts discharging (s)	R	CMT_A level 200 s before ADS1 actuation	R			$\int_{\text{Start of discharging mode}}^{\text{End of PhW2}} CMT_A \text{ flow}$	M
		DT between CMT_A and CMT_B times of start discharge occurrence	M	CMT_B level 200 s before ADS1 actuation	E			$\int_{\text{Start of discharging mode}}^{\text{End of PhW2}} CMT_B \text{ flow}$	R
	PRHR behaviour			Average subcooling at the inlet between 600 and 850 s	E	$\dfrac{\int_{\text{Start of PhW2}}^{\text{End of PhW2}} \text{PRHR power}}{\int_{\text{Start of PhW2}}^{\text{End of PhW2}} \text{Core power}}$	NE	$\int_{\text{Start of PhW2}}^{\text{End of PhW2}} \text{PRHR flow}$	E
				Average subcooling at the outlet between 600 and 850 s	M				
	ACC behaviour	Time of ACC_A start(s)	R					$\int_{\text{Start of discharge}}^{\text{End of discharge}} ACC_A \text{ flow}$	R
		Time of ACC_B start (s)	R					$\int_{\text{Start of discharge}}^{\text{End of discharge}} ACC_B \text{ flow}$	R
	Primary System behaviour	Time of minimum mass (s)	M	Minimum mass (kg)	E	Total CMT discharged mass/PS mass at the end of PhW2	M		
						Minimum mass/initial mass	E		
ADS1 START TO IRWST INTERVENTION PHW3	Primary System and Secondary System behaviour			Average ΔP/Δt in PS in the period between the PhW3 start and 1250. s(MPa/s)	R				
				Average ΔP/Δt in PS in the PhW3 (MPa/s)	NE				
				Minimum mass in the PS in the period between PhW3 start and 1250. s (kg)	R				
	Break flow					Ratio between K and initial PS mass	NE	$\int_{\text{Start of PhW3}}^{\text{Start of PhW3 + 250 s}} \text{Break flow}$	M
								$K = \int_{\text{Start PhW3}}^{\text{End of PhW3}} \text{Break flow}$	NE
	ADS behaviour	ADS-1 intervention time (s)	R			Ratio between the sum of the ADS flow integrals and the break flow integral	NE	$\int_{\text{Start of PhW3}}^{\text{End of PhW3}} \text{ADS-1 flow}$	NE
		ADS-2 intervention time (s)	R			Ratio between the sum of the ADS flow integrals and the initial PS mass	NE	$\int_{\text{Start of PhW3}}^{\text{End of PhW3}} \text{ADS 2 flow}$	NE
		ADS-3 intervention time (s)	R					$\int_{\text{Start of PhW3}}^{\text{End of PhW3}} \text{ADS 3 flow}$	NE
		ADS-4 intervention time (s)	M					$\int_{\text{Start of PhW3}}^{\text{End of PhW3}} \text{ADS 4 flow}$	NE
	ACC behaviour	End of ACC-A liquid discharge (s)	R			Ratio between the sum of ACC flow integrals and initial PS mass	NE		
		End of ACC B liquid discharge (s)	R						
	CMT behaviour					Ratio between the sum of CMT flow integrals and initial PS mass	NE	$H = \int_{\text{Start of CMT discharge phase}}^{\text{End PhW3}} \text{CMTA + CMT flow}$	NE

Legend: E Excellent R Reasonable M Minimal

U Unqualified NE Not Evaluated

Some discrepancies can be noted in the comparison between measured and calculated trends, but a good positive overall qualitative judgement allowed us to perform the subsequent step, e.g. the quantitative accuracy evaluation.

The application of the FFT based method, ref. [16] gave the results shown in Table 2. It should be noted that the overall accuracy value is within the limit 0.4 that has been fixed for the acceptability of a calculation, ref. [6].

Table 2 - Average accuracy for parameters selected for FFT application and global accuracy of the code calculation

PARAMETER	AA	I/WF
DP-CORE	0.32	25.5
DP-PRZ	0.63	24.2
DP-SGADC	0 46	15 8
F_A01P	0 35	21 4
F_A40E	1 51	26 0
F_A80E	1 29	18 6
F_B20E	0 70	20.2
F_B40E	1 48	23 8
IF030P	0 20	27 4
IF040P	2 51	13 9
INTF_005	0 10	60 5
P-027P	0 09	29 5
P-A04S	0 26	26 4
T-A03PL	0 07	27.6
T-A401E	0 20	161
T-A420E	0 53	24 4
T-A82E	0.59	22.2
T-A83E	0 40	27 1
T-B401E	0 19	98 0
T-B420E	0 20	22.9
TW020P87	0 10	33.3
GLOBAL ACCURACY	**0.40**	**29.1**

5. CONCLUSIONS

The UMAE methodology has been presented that allows the calculation of uncertainty in the predictions of off-normal conditions in nuclear reactors by thermalhydraulic system codes. Essentially, the uncertainty is derived from the extrapolation of accuracy obtained by comparing measured and calculated variables trends that are relevant to the assigned accident scenario. The use of data from counterpart tests, was of large help in developing the concepts at the basis of the methodology.

One complete example of application of the UMAE to a small break LOCA in PWR has been given. In that case dryout is foreseen and peak cladding temperature, including the error of the order of 100 K, remains well below the licensing limits.

The main peculiarity of the UMAE is the direct exploitation of the huge experimental data base now available from integral test facilities: this is strictly necessary and is retained suitable to characterize any foreseeable accident scenario in Light Water Reactors. Moreover, all the aspects contributing to the uncertainty are taken into consideration: the user effect, the nodalization qualification, the errors in introducing boundary and initial conditions, the intrinsic capabilities of the code in predicting the phenomena of interest, are fully included in the final evaluation of the error bands.

Few additional biases to be included in the final value of uncertainty that are not fully considered by the UMAE, have been identified in the frame of the present research although not discussed in this paper. Among these, the potential occurrence of important multidimensional phenomena represents a critical issue if only codes based on one-dimensional models are available: experimental data from specific facilities should be used to accertain the codes capabilities in this connection.

The application of the UMAE to situations relevant to the new generation reactors, and in particular AP-600, seems feasible once data from differently scaled facilities have been analyzed. It should be noted that most of the experience gained in the analysis of transients in present reactor configuration can be directly utilized: specifically, in the considered small break LOCA case a large number of RTA are the same in PWR and AP-600 scenarios.

REFERENCES

[1] CSNI Group of Experts. 1989. "Thermohydraulic of Emergency Core Cooling in Light Water Reactors", Report No. 161, Committee on the Safety of Nuclear Installations.

[2] US-NRC 1989. "Compendium of ECCS Research for Realistic LOCA Analysis", NUREG-1230, U.S. Nuclear Regulatory Commission.

[3] D'Auria F. 1987a. "Experimental Facilities and System Codes in Nuclear Reactor Safety", Int. Seminar State of the Art on Safety Analyses and Licensing of Nuclear Power Plants, Varna (BG).

[4] D'Auria F., Leonardi M., Glaeser H., Pochard R. "Current status of methodlogies evaluating the uncertainty in the prediction of thermal-hydraulic phenomena in nuclear reactors", Int. Symposium on "Two-Phase Flow Modelling and Experimentation", Roma (Italy), October 9-11, 1995.

[5] Boyack B.E., Catton I., Duffey R.B., Griffith P., Katsma K.R., Lellouche G.S., Levy S., Rohatgi U.S., Wilson G.E., Wulff W., Zuber N. 1990a - "An overview of the code scaling, applicability, and uncertainty evaluation methodology", J. Nuclear Engineering and Design Vol. 119.

[6] D'Auria F., Debrecin N., Galassi G.M. 1994. "Outline of the Uncertainty Methodology based on Accuracy Extrapolation (UMAE)", CSNI Workshop on Uncertainty Evaluation, London (UK).

[7] D'Auria F., Debrecin N., Galassi G.M. 1993a. "Application of RELAP5/MOD2 system code to small break LOCA counterpart experiments in PWR simulators", IX Brazilian Meet. on Reactor Physics and Thermalhydraulics, Caxambu, Minas Gerais (BRA).

[8] D'Auria F., Ferri R., Vigni P. 1993. "Evaluation of the data base from the Small Break LOCA Counterpart tests performed in PWR Experimental Simulators", 11th Conf. of Italian Society of Heat Transport, Milan (I).

[9] Alemberti A., Frepoli C., Graziosi G. "SPES-2 col leg break experiments: Scaling approach for decay power, heat losses compensation and metal heat release", Proc. New Trends in Nuclear System Thermohydraulic 1, 679-687 (1994), Pisa, (Italy)

[10] D'Auria F., Fruttuoso G., Oriolo F., Bella L., Cavicchia V., Fiorino E. "SPES-2: AP600 Integral Test Facility Results: Confirmatory Plant Behaviour and Relap5/Mod2.5 Code Assessment", ICONE - 3, The Third Int. Conf. on Nuclear Engineering, Kyoto (J), April 23-27, 1995

[11] Bovalini R., D'Auria F. 1993. "Scaling of the accuracy of Relap5/mod2 Code", J. Nuclear Engineering and Design, vol 139 Nr. 1.
[12] D'Auria F., Karwat H. 1989. "OECD CSNI State-Of-the-Art-Report on thermalhydraulics of Emergency Core Cooling Systems - Review of the Operation of Experimental Facilities", University of Pisa Report, DCMN - NT 138(89), Pisa (I).
[12] Bovalini R., D'Auria F., Galassi G.M. 1993. "Scaling of complex phenomena in System Thermalhydraulics", J. Nuclear Science and Engineering.
[13] Bovalini R., D'Auria F., De Varti A., Maugeri P., Mazzini M. 1992. "Analysis of Counterpart Tests performed in BWR Experimental Simulators", J. Nuclear Technology, Vol. 97 Nr. 1.
[14] Belsito S., D'Auria F., Galassi G. M. "Application of a Statistical model to the evaluation of Counterpart Test data base", J. Kerntechnik, Vol 59 Nr 3, 1994
[15] Bonuccelli M., D'Auria F., Debrecin N., Galassi G.M. 1993. "A methodology for the qualification of thermalhydraulic codes Nodalizations", 6th Int. Top. Meet. on Nuclear Reactor Thermalhydraulics, Grenoble (F).
[16] D'Auria F., Leonardi M., Pochard R. 1994a. "Methodology for the evaluation of thermalhydraulic codes accuracy", Int. Conf. on New Trends in Nuclear System Thermalhydraulics, Pisa (I).
[17] D'Auria F., Faluomi V., Aksan S.N. "A proposed Methodology for the Analysis of a Phenomenon in Separate Effects and Integral Test Facilities", Int. Conf. on New Trends in Nuclear System Thermohydraulics - Pisa (I), May 30 - June 2 1994
18] D'Auria F., Modro M., Oriolo F., Tasaka K. "Relevant Thermalhydraulic Aspects of New Generation LWR's", CSNI Spec. Meet. On Transient Two-Phase Flow - System Thermalhydraulics, Aix-En-Provence (F), Apr. 6-8, 1992, J. Nuclear Engineering & Design, Vol 145, Nrs. 1&2, 1993
[19] D'Auria F., Vigni P., Marsili P. "Application of RELAP5/MOD3 to the evaluation of Isolation Condenser performance", Int. Conf. on Nuclear Engineering (ICONE-2) - San Francisco (US), March 21- 24, 1993
[20] Bacchiani M., Medich C., Rigamonti M. "SPES-2 AP600 Integral System Test: Inadvertent ADS opening and Cold Leg Break Transients" ARS 1994 Int. Topical Meeting on Advanced Reactors Safety, APril 17-21, Pittsburgh, PA
[21] D'Auria F., Fruttuoso G., Galassi G.M., Oriolo F. "Post-test calculation of SPES-2 experiment No. 3 by Relap5/Mod2.5 code", Università degli Studi di Pisa, DCMN Report, NT 241 (94), Ottobre 1994.

LIST OF PARTICIPANTS

Allen, P.J.	AECL Sheridan Park Research Community 2251 Speakman Dr. Mississauga, Ontario L5K 1B2, Canada
Alloggio, G.	ENEL-ATN Via Monfalcone, 15 20132 Milano, Italy
Artaud, C.J.	Gamma-Metrics San Diego, CA, USA
Aujollet, P.	Centre d'etudes de Cadarache CEA/DRN/DER/SIS Batiment 211 C.E.N. Cadarache B.P. 1, 13108 - Saint-Paul-Lez-Durance, France
Bandurski, T.	Paul Scherrer Institut CH-5232 Villigen PSI, Switzerland
Banergee, S.	Consultant to NRC Washington D.C. 20555, USA
Bedrossian, G.C.	Comision Nacional de Energia Atomica Avda. del Libertador 8250 1429-Buenos Aires, Argentina
Billig, P.F.	G.E. Nuclear Energy Advanced Boiling Water Reactor Program 175 Curtner Ave., M/C 781 San Jose, CA 95125, USA
Bredikhin, V.	Research Institute of Nuclear Power Plant Operations, (VNIIAEA, RINPO) Moscow, Russian Federation
Bregaenel, E.	Area Attivita' Nucleari - Gruppo Nucleare di Milano Via Monfalcone 15, 20132 Milano, Italy
Budylin, B.V.	Minatom RF 109180, Staromonethy, 26 Moscow, Russian Federation

Cattadori, G.	SIET Via Nino Bixio, 27 29100 Piacenza, Italy
Cavicchia, V.	ENEL-ATN Viale Regina Margherita 137 00198 Roma, Italy
Choi, Y.S.	Korea Electric Power Corporation 103-16, Moon Jee Dong Yu Song Ku, Dae Jeon, Rep. of Korea
Cleveland, J.	Division of Nuclear Power, IAEA Wagramerstrasse 5 P.O. Box 100 A-1400 Vienna, Austria
Conway, L.E.	Westinghouse Electric Corp. P.O. Box 355 Pittsburgh PA 15230, USA
Curca-Tivig, F.	Siemens AG KWU NA-T Koldestrasse 16 91050 Erlangen, Germany
D'Auria, F.	Universita' Degli Studi di Pisa Departimento di Costruzioni Meccaniche e Nucleari Via Diotisalvi, 2 I-56126 Pisa, Italy
Delnero, G.	ANPA Via Vitaliano Brancati 48-00144 Rome, Italy
El-Bassioni, A.A.	U.S. Nuclear Regulatory Commission Washington D.C. 20555, USA
Eltawila, F.	Nuclear Regulatory Commission Washington D.C. 20555, USA
Erbacher, F.J.	Forschungszentrum Karlsruhe Institut fuer Angewandte Thermo- und Fluiddynamik Postfach 3640 D-76021 Karlsruhe, Germany
Fernandez, A.	EDF- SEPTEN 12-14, Avenue Dutriévoz 69628 Villeurbanne - Cedex, France

Ferreli, A.	ANPA Via Vitaliano Brancati 48-00144 Rome, Italy
Fiorini, G.L.	Centre d'etudes de Cadarache (CEA) DRN/DER/SIS 13108 St. Paul Les Durance Cedex, France
Fiorino, E.	ENEL, Rome Viale Regina Margherita 137 I-00198 Rome, Italy
Fornaciari, P.	ENEL, Nuclear Energy Division Viale Regina Margherita, 137 00198 Rome, Italy
Franks, S.M.	NE-45 Advanced Light Water Reactors Division Office of Nuclear Energy U.S. Department of Energy Washington D.C. 20585, USA
Galbiati, L.	CISE, Technologie Innovative V. Reggio Emilia, 39 20090 Segrate (Milano), Italy
Gaspari, G.	SIET Via Nino Bixio, 27 29100 Piacenza, Italy
Graziosi, G.	ANSALDO Nuclear Division Corso Perrone 25 16161 - Genova, Italy
Hicken, E.F.	Forschungszentrum Juelich ISR, D-52425 Juelich, Germany
Hittner, D.	FRAMATOME Tour Fiat Cedex 16 92084 Paris la Defense, France
Hoeld, A.	Gesellschaft fuer Anlangen- und Reaktorsicherheit (GRS) mbH Forschungsgelände Walter-Meissner-Strasse D-85748 Garching, Germany
Hsii, Y.	U.S. Nuclear Regulatory Commission Washington D.C. 20555, USA

Hutchings, G.	Scottish Nuclear Ltd. 3 Redwood Crescent, Peel Park East Kilbridge, G74 5PR Scotland, United Kingdom
Kim, B.S.	Korea Electric Power Corporation 103-16, Moon Jee Dong Yu Song Ku, Dae Jeon, Rep. of Korea
Kropp, C.	ENEA Via Anguillarese 301 00060 - S.M. di Galeria (Rome), Italy
Kwon, Y.M.	Korea Atomic Energy Research Institute (KAERI) System Safety Analysis Dept. P.O. Box 105, Yousung Taejeon, 305-600, Rep. of Korea
Kymäläinen, O.J.	IVO International Oy Rajatorpantie 8, Vantaa 01019 IVO, Finland
Leridon, A.M.	Chef du SCC Centre d'etudes de Cadarache (CEA) DER/SCC/DIR - BAT 727 13108 St. Paul Les Durance Cedex, France
Lillington, J.	Safety and Performance Services Dept. 240/A32, AEA Technology, Winfrith Dorchester Dorset DT2 8DH, United Kingdom
Lombardi, C.	Politechnico di Milano Via Ponzio, 34/3 20133 Milano, Italy
Lyu, T.-H.	WANO Tokyo Centre 2-11-1 Iwatokita, Komae Tokyo 201, Japan
Malave, M.	Nuclear Regulatory Council C/ Justo Dorado, 11 Madrid 28040, Spain
Manfredini, A.	Universita' Degli Studi di Pisa Via Diotisalvi, 2 I-56126 Pisa, Italy

Mansani, L.	ANSALDO Corso Perrone 25 16161 - Genova, Italy
Marella, G.	ANPA Via Vitaliano Brancati 48-00144 Rome, Italy
Martinelli, R.	ENEA Via Anguillarese 301 00060 - S.M. di Galeria (Rome), Italy
Mazzocchi, L.	CISE, Technologie Innovative V. Reggio Emilia, 39 20090 Segrate (Milano), Italy
Mcpherson, G.D.	U.S. Nuclear Regulatory Commission Washington D.C. 20555, USA
Medich, C.	SIET Via Nino Bixio, 27 29100 Piacenza, Italy
Monti, R.	ANSALDO Corso Perrone 25 16161 - Genova, Italy
Munther, R.K.	Lappeenranta University of Technology P.O. Box 20 Fin-53851 Lappeenranta, Finland
Noviello, L.	ENEL-ATN Viale Regina Margherita 137 I-00198 Rome, Italy
Orazi, A.	ANPA Via Vitaliano Brancati 48-00144 Rome, Italy
Oriolo, F.	Universita' Degli Studi di Pisa Via Diotisalvi, 2 I-56126 Pisa, Italy
Orsini, M.	ANSALDO Corso Perrone 25 16161 - Genova, Italy

Palavecino, C.	Siemens AG Berliner Strasse 295-303 63067 Offenbach 111, Germany
Palma, A.	Politechnico di Milano Via Ponzio, 34/3 20133 Milano, Italy
Parozzi	ENEL-ATN Via Monfalcone, 15 20132 Milano, Italy
Pedersen, T.	Division of Nuclear Power, IAEA Wagramerstrasse 5 P.O. Box 100 A-1400 Vienna, Austria
Proto, G.	ANSALDO Corso Perrone 25 16161 - Genova, Italy
Py, J.-P.	FRAMATOME Tour Fiat Cedex 16 92084 Paris la Defense, France
Reinsch, A.W.	Southern California Edison 5000 Pacific Coast Highway San Clemente, CA 92672, USA
Ricotti, M.	Politechnico di Milano Via Ponzio, 34/3 20133 Milano, Italy
Rigamonti, M.	SIET Via Nino Bixio, 27 29100 Piacenza, Italy
Saha, D.	Bhabha Atomic Research Centre Reactor Safety Division Hall No. 7, BARC, Trombay Bombay 400 085, India
Saltos, N.T.	U.S. Nuclear Regulatory Commission Washington D.C. 20555, USA
Sandrelli, G.	ENEL-ATN Via Monfalcone, 15 20132 Milano, Italy

Scandola,	SIET Via Nino Bixio, 27 29100 Piacenza, Italy
Shugars, H.	Gamma-Metrics San Diego, CA, USA
Silveri, R.	SIET Via Nino Bixio, 27 29100 Piacenza, Italy
Soplenkov, K.I.	Research Institute of Nuclear Power Plant Operation, (VNIIAEA, RINPO) 25 Ferganskaya St. Moscow, Russian Federation
Sordi, R.	Politechnico di Milano Via Ponzio, 34/3 20133 Milano, Italy
Tarantini, M.	ENEA ERG FISS Via Martiri di Monte Sole, 4 40129 Bologna, Italy
Tavoni, R.	ENEA - Energy Department Via Martiri di Monte Sole, 4 I-40129 Bologna, Italy
Trubkin, Y.	Electrogorsk Research Engineering Center (EREC) 6, Bezymiannaya St. Electrogorsk, Moscow Region 142530, Russian Federation
Valisi, M.	ENEL-ATN Via Monfalcone, 15 20132 Milano, Italy
Vidard, M.L.	EDF-SEPTEN 12-14, avenue Dutriévoz 69628 Villeurbanne Cedex, France
Zero, S.	FRAMATOME Tour Fiat Cedex 16 92084 Paris la Defense, France